



# EUROENGEOL ATHENS 2020

## Editors

V. P. MARINOS

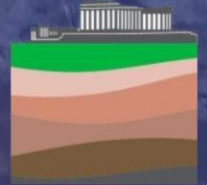
C. LOUPASAKIS

C. SAROGLOU

N. DEPOUNTIS

G. PAPATHANASSIOU

**3<sup>RD</sup> EUROPEAN REGIONAL CONFERENCE OF  
THE INTERNATIONAL ASSOCIATION FOR  
ENGINEERING GEOLOGY & THE ENVIRONMENT**



**Leading to Innovative  
Engineering Geology Practices**

**VOLUME 1  
Extended Abstracts  
Proceedings**

Organised by the National Group of Greece of IAEG



# EUROENGEO ATHENS 2020

Leading to Innovative  
Engineering Geology Practices

## EDITORS



**Vassilis P. Marinos**

Chairman of the Conference  
Vice President of IAEG for Europe  
Assistant Professor National Technical University of Athens, Greece



**Constantinos Loupasakis**

Co-Chairman of the Conference  
President of Greek NG of IAEG  
Associate Professor National Technical University of Athens, Greece



**Charalampos Saroglou**

Co-Chairman of the Conference  
Secretary of Greek NG of IAEG  
Dr. Engineering Geologist National Technical University of Athens, Greece



**Nikos Depountis**

IAEG NG of Greece  
Assistant Professor University of Patras, Greece



**George Papathanassiou**

IAEG NG of Greece  
Assistant Professor Aristotle University of Thessaloniki, Greece



## ORGANIZING COMMITTEE

**Vassilis P. Marinou**

Chairman of the Conference-Vice President of IAEG for Europe

**Constantinos Loupasakis**

Co-Chairman of the Conference- President of Greek NG of IAEG

**Charalampos Saroglou**

Co-Chairman of the Conference – Secretary of Greek NG of IAEG

**Georgios Stoumpos**

Secretary of the Conference – NG of IAEG

**Andreas Kaplanidis**

Treasurer of the Conference – NG of IAEG

**Nikos Depountis**

IAEG NG of Greece

**George Papathanassiou**

IAEG NG of Greece

**Stratis Karantanellis**

IAEG NG of Greece – YEG Chair

**Rafiq Azzam**

President of IAEG – Germany

**Faquan Wu**

Secretary of IAEG – China

**Eugene Vosnesensky**

Vice President of IAEG for Europe- Russia

**Louise Vick**

Chairman of YEG of IAEG-Norway



## ADVISORY COMMITTEE

**Ferentinou Maria**

Representative of IAEG NG of South Africa

**Fleurisson Jean – Alain**

Treasurer of IAEG-France

**Giordan Daniele**

President of Italian NG of IAEG

**Hutchinson Jean**

Vice President of IAEG for N. America

**Johnson Doug**

Vice President of IAEG for Australasia – IAEG NG of New Zealand

**Kazilis Nikos**

IAEG NG of Greece

**Kuroschi Thuro**

Representative of IAEG NG of Germany

**Reeves Helen**

Representative of IAEG NG of UK

**Stavropoulou Maria**

IAEG NG of Greece

**Ulusay Resat**

Editor in chief of BOEG- President of ISRM-IAEG NG of Turkey

**Verhoef Peter**

Representative of IAEG NG of Nederland

**Vlachopoulos Nikos**

Representative of IAEG NG of Canada

**Waeber Julien**

Representative of IAEG NG of USA

**Zangerl Christian**

Representative of IAEG NG of Austria





# SCIENTIFIC COMMITTEE

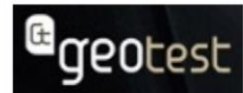
Abolmasov Biljana  
Alexiadou Chara  
Ann Williams  
Azzam Rafiq  
Baynes Fred  
Benardos Andreas  
Bozzano Francesca  
Burns Scott F.  
Christaras Vassilis  
Cohen-Waeber Julien  
Dahal Ranjan Kumar  
Delgado Carlos  
Depountis Nikos  
Dong, Jia-Jyun  
Evelpidou Niki  
Giordan Daniele  
Gkanas Athanassios  
Gkouvailas Alkis  
Huiming Tang  
Hutchinson Jean  
Jang Bo-An  
Kaplanidis Andreas  
Kazilis Nikos  
Kiril Angelov

Kontoes Charalampos  
Kosović, Ivan  
Koukis George  
Kuroschi Thuro  
Lawrence James  
Lekkas Efthimios  
Lollino Giorgio  
Loupasakis Constantinos  
Marinos Paul  
Marinos Vassilis  
Mark Eggers  
Mavrouli Olga  
Mazzanti Paolo  
Murphy Bill  
Ngan-Tillard Dominique  
Nikolaou Nikolaos  
Nomikos Pavlos  
Nomikou Paraskevi  
Oliveira Ricardo  
Papathanassiou George  
Papoutsis Ioannis  
Paraskevopoulou Chrysothemis  
Parharidis Isaak  
Perleros Vassilis

Rozos Dimitrios  
Sabatakakis Nikos  
Saroglou Charalampos  
Simeon Abam Tamunoene Kingdom  
Stavropoulou Maria  
Steiakakis Manolis  
Stoumpos George  
Torok Akos  
Tsagaratos Paraskeyas  
Tsiambaos Georgios  
Tsifoutidis Georgios  
Ulusay Resat  
Vassilakis Manolis  
Verhoef Peter  
Vick Louise  
Vilneuve Marlene  
Vlachopoulos Nikos  
Vosnesensky Eugene  
Wasoski Janusz  
Wu Faquan  
Yiouta-Mitra Paraskevi  
Zangerl Christian



## Thank you to our SPONSORS



## Under the auspices



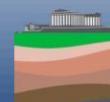
HELLENIC REPUBLIC  
MINISTRY OF INFRASTRUCTURE AND TRANSPORT

## Endorsed by



EUROENGEО ATHENS 2020

Leading to Innovative Engineering Geology Practices







**Professor Simon Loew**

Chair for Engineering Geology, Department of Earth Sciences ETH, Zurich, Switzerland

02

*The biggest challenges in landslide hazard analysis and mitigation*



**Dr. Dominique Ngan-Tillard**

Assistant Professor, Delft University of Technology, Faculty of Civil Engineering and Geosciences, Netherlands

03

*Engineering geology applied to archaeology at risk across the Dutch plain and archives*



**Professor Christian Zangerl**

University of Natural Resources and Life Sciences, Department of Civil Engineering and Natural Hazards, Institute of Applied Geology, Vienna, Austria

04

*Investigation, monitoring and modelling of landslides*

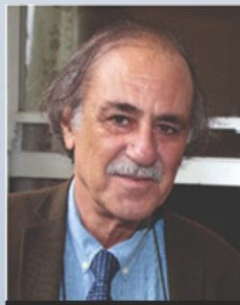


**Professor D. Jean Hutchinson**

Queen's University, Department of Geological Sciences and Geological Engineering, Kingston, Ontario, Canada

06

*The importance of ground truthing  
Engineering Geology innovations for  
Rock Slope stability management*



**Professor Reşat Ulusay**

Hacettepe University and Middle East Technical University (METU), Department of Geological Engineering, Ankara, Turkey

07

*Standardization and future trends in rock characterization and testing in geo-engineering*



**Dr. Helen Reeves**

Senior Associate Director for Engineering Geology, Jacobs, Tunnelling & Ground Engineering, Leeds, UK

08

*Can engineering geologist contribute to international agendas & fundamental societal challenges?*

**Professor Kuroschi Thuro**

Chair of Engineering Geology,  
Technical University Munich, Germany

**09**

*Hazard assessment and monitoring of  
landslide prone areas in Medellín,  
Colombia*

**Professor Eugene A. Voznesensky**

Lomonosov Moscow State University,  
Department of Engineering & Environmental  
Geology, Russia

**11**

*Characterization and Behaviour of Soils:  
Actual Objectives and Requirements*

**Adjunct Professor Jonny Sjöberg**

Luleå University of Technology,  
Department of Rock Mechanics and Rock  
Engineering, Sweden General Manager,  
Itasca Consultants AB, Sweden

**13**

*Engineering Geology for Civil and  
Mining Engineering — Case Examples  
from Sweden*

**Dr. Janusz Wasowski**

Senior geologist at CNR-IRPI (National  
Research Council - Institute for  
Geo-hydrological Protection), Bari, Italy

**14**

*Recent advances in Remote Sensing  
for use in Engineering Geology*

**Professor Neil Dixon**

Professor of Geotechnical Engineering in the  
School of Architecture, Building and Civil  
Engineering at Loughborough University, UK

**15**

*Delivering sustainable infrastructure:  
Global challenges, geosynthetic solutions  
and counting carbon*



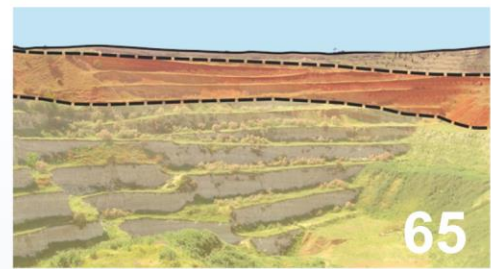
# THEMES



16



52



65



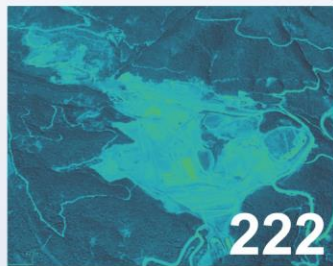
78



127



134



222



251



258



267

Theme 1 - Characterisation and Behaviour of Soils and Rocks.....	16
Theme 2 - Environmental Engineering Geology.....	52
Theme 3 - Advances in Site Investigation for Engineering Geology.....	65
Theme 4 - Engineering Geology for Engineering Works.....	78
Theme 5 - Engineering Geology for Urban Environment.....	127
Theme 6 - Analysis and Mitigation of Geo-hazards.....	134
Theme 7 - Recent Advances in Geomatics and Remote Sensing for use in Engineering Geology.....	222
Theme 8 - Engineering Geology and Cultural Heritage Protection.....	251
Theme 9 - Engineering Geology for the Society.....	258
Theme 11 - Marine Engineering Geology.....	267

**EUROENGEIO ATHENS 2020**

Leading to Innovative Engineering Geology Practices

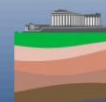




# TABLE OF CONTENTS

<b>KEYNOTES .....</b>	<b>1</b>
The biggest challenges in landslide hazard analysis and mitigation .....	2
<i>Simon Loew</i>	
Engineering geology applied to archaeology at risk across the Dutch plain and archives .....	3
<i>Dominique Ngan-Tillard</i>	
Investigation, monitoring and modelling of landslides .....	4
<i>Christian Zangerl, Klaus Voit, Christina Rechberger, Christine Fey, I Putu Krishna Wijaya</i>	
The importance of ground truthing Engineering Geology innovations for Rock Slope stability management .....	6
<i>Jean Hutchinson</i>	
Standardization and future trends in rock characterization and testing in geo-engineering .....	7
<i>Reşat Ulusay</i>	
Can engineering geologist contribute to international agendas & fundamental societal challenges? .....	8
<i>H.J. Reeves, S Bricker</i>	
Hazard assessment and monitoring of landslide prone areas in Medellín, Colombia .....	9
<i>Kurosusch Thuro, John Singer, Moritz Gamperl, Tamara Breuninger, Bettina Menschik</i>	
Characterization and Behaviour of Soils: Actual Objectives and Requirements .....	11
<i>Eugene A. Voznesensky</i>	
Engineering Geology for Civil and Mining Engineering — Case Examples from Sweden .....	13
<i>Jonny Sjöberg</i>	
Recent advances in Remote Sensing for use in Engineering Geology .....	14
<i>Janusz Wasowski</i>	
Delivering sustainable infrastructure: Global challenges, geosynthetic solutions and counting carbon .....	15
<i>Neil Dixon</i>	
<b>THEME 1 - CHARACTERISATION AND BEHAVIOUR OF SOILS AND ROCKS .....</b>	<b>16</b>
Classification of Tunnel Surrounding Rock Mass under High In Situ Stress .....	17
<i>Ning Liang, Faquan Wu</i>	
European soil classification system based on cone penetration test (CPT) results .....	19
<i>Lovorka Librić, Meho Sasa Kovačević</i>	
Internal erosion study of wide grading loose soil based on microscopic pore distribution .....	21
<i>Yanzhou Yin, Yifei Cui, Chaoxu Guo, Yao Jiang</i>	
Deep and remote monitoring approaches of large slope instabilities in Upper Graveglia Valley (Ligurian Apennine, Italy) .....	23
<i>Daniilo Godone, Paolo Allasia, Marco Baldo, Davide Notti, Giorgio Lollino, Francesco Faccini, Franco Marco Elter, Federico Mantovani, Flavio Poggi</i>	
Sandstone Intact Rock Strength. The use of compressive strength parameters for large tunnel design. A focus on the comparison between uniaxial and triaxial laboratory tests .....	25
<i>Lorenzo Paolo Verzani, Giordano Russo</i>	
Implications for TBM performance based on rock mass observations for the Blue Lias Formation .....	27
<i>Sarah Sissins, Dr. Chrysothemis Paraskevopoulou</i>	





The effect of schistosity on the uniaxial compressive strength of metamorphic rocks of northern Greece .....	29
<i>Athanasia X. Liouka, Thomas Makedon, Anastasios Tsikrikis</i>	
An IoT-enabled interactive platform for visualization and analysis of regional-scale groundwater system .....	31
<i>Chuen-Fa Ni, I-Hsien Lee, Yun-Chen Yu, Wei-Ci Li</i>	
A laboratory study on the brittle-ductile transition of four calcitic rocks .....	33
<i>Anastasios Tsikrikis, Maria Tzilini, Theodosios Papaliangas, Vassilis Marinou</i>	
Deformation stages of schists under uniaxial compression .....	35
<i>Dimitrios Kotsanis, Pavlos Nomikos, Dimitrios Rozos</i>	
Evaluation of crack initiation stress of Volakas marble specimens in uniaxial.....	37
<i>Dimitrios Kotsanis, George Papantonopoulos, Pavlos Nomikos</i>	
A Discretized Clay Shell Model (DCSM) for evaluating the effective stress coefficient of clayey sandstone permeability .....	39
<i>Pin Lun Tai, Jia Jyun Dong</i>	
Investigation of time-dependent stress relaxation behaviour in rock materials .....	41
<i>Dr. Chrysothemis Paraskevopoulou</i>	
Effect of pore size on electro pulse drilling of rock.....	43
<i>Nawnit Kumar, Xiaoli Liu</i>	
Geoengineering characterization of Lyulyakata limestone quarry, NE Bulgaria .....	44
<i>Temenuga Georgieva, George Ajdanijsky, Fanny Descamps, Jean-Pierre Tshibangu</i>	
Comparison of roughness indices on chalk and sandstone fractures .....	45
<i>Marie-Laure Wattier, Sara Vanduycke, Françoise Bergerat, Paul Wertz, Samir Mohammad, Jean-Pierre Tshibangu</i>	
The Quest for Rock Site Characterization for the Greek National Seismic Network .....	47
<i>Olga-Joan Ktenidou, Faidra Gkika, Christos Evangelidis</i>	
Liquefaction estimates at different earthquake magnitudes in the coastal area of Kato Achaia, Greece with the use of CPT .....	48
<i>Vasileios Boumpoulis, O. Kontopidis, Nikolaos Depountis, Nikolaos Sabatakakis</i>	
The effectiveness of Blastability Quality System on rock slopes. A case study in a landslide restoration .....	50
<i>Maria Chatziangelou, Costas Anagnostopoulos</i>	
<b>THEME 2 - ENVIRONMENTAL ENGINEERING GEOLOGY .....</b>	<b>52</b>
Dating of fault movements and earthquake recurrence near hard infrastructure .....	53
<i>K.V. Kanavou, D.C. Athanassas, V. Mouslopoulou, X. Aslanoglou, K. Stamoulis</i>	
Comparative life cycle assessment for shallow slope failure stabilization techniques .....	55
<i>Dominic Leal, Mike G Winter, Richard Seddon, Ian M Nettleton, Jan Marsden</i>	
Estimation of the sediment yield in earth-fill dams with the use of the Revised Universal Soil Loss Equation .....	57
<i>Maria Michalopoulou, Nikolaos Depountis, Katerina Kavoura, Nikolaos Sabatakakis</i>	
Rock material reutilization from tunnel excavation with reference to long tunnel structures .....	59
<i>Klaus Voit, Erik Kuschel, Christian Zangerl</i>	
Numerical assessment of groundwater flow and transport in fractured rocks: Benchmark cases for concepts of DFN, ECPM, and Hybrid approaches .....	61
<i>Yun-Chen Yu, I-Hsien Lee, Chuen-Fa Ni</i>	
Decadal change in land use and land cover pattern and river dynamics in Indrawati River, Central Nepal .....	63
<i>Kumud Raj Kafle, Kevin Bajracharya, Simrik Bhandari, Benju Shrestha</i>	



An experimental study to improve permeability and cleaning efficiency of oil contaminated soil by plasma blasting .....64  
*Bo-An Jang, Hyun-Sic Jang, Ahhyeon Kim, Injoon Baek*

**THEME 3 - ADVANCES IN SITE INVESTIGATION FOR ENGINEERING GEOLOGY ..... 65**

Layer interpolation with tomographic aid .....66  
*Juan Chavez-Olalla*

Project, site and deliverables management systems integration for ground investigation projects .....68  
*Alkis Gkouvailas, Michael Blakely, Emmanouil Zervas, Tania Santiapillai, Maryse Buot*

Variability of penetration rates (PRs) during open-hole drilling for different geological formations in Doha, Qatar .....70  
*Alkis P. Gkouvailas, Dafni E. Sifnioti, Julian Ashley, Francesco Barbagli, Maryse Buot*

Temperature and rock slope stability: a multi-sensor site monitoring network .....72  
*Ondřej Racek, Jan Blahůt, Filip Hartvich*

Subsoil litho-technical reconstruction via multivariate geostatistical tools .....74  
*Giovanna Vessia, Diego Di Curzio*

Geomechanical evaluation of an abandoned chalk mine using in-situ measurements .....76  
*Temenuga Georgieva, Fanny Descamps, Sara Vandycke, George Ajdanlijsky, Jean-Pierre Tshibangu*

**THEME 4 - ENGINEERING GEOLOGY FOR ENGINEERING WORKS ..... 78**

The effectiveness of willow poles for shallow slope failure stabilisation .....79  
*Mike G Winter, Ian M Nettleton, Richard Seddon, Jan Marsden*

The effectiveness of electrokinetic geosynthetics for shallow slope failure stabilization .....81  
*Ian M Nettleton, Richard Seddon, Mike G Winter, Jan Marsden*

The effectiveness of fibre reinforced soil for shallow slope failure stabilization .....83  
*Richard Seddon, Mike G Winter, Ian M Nettleton, Jan Marsden*

Forensic examination of critical special geotechnical measures .....85  
*Mike G Winter, Ian M Nettleton, Michelle Duffy-Turner, Gillian Butler, Philip Liew*

Assessment of slope stability by monitoring change of tensile force of anchor .....87  
*Oil Kwon, Jonghyun Lee, Byungsuk Park, Jahe Jung*

A Soil Improvement Methodology for a Shallow Tunnel Excavated in Extremely Weak Clay: A case study from Turkey .....88  
*Arif Emre Kaan Gündoğdu, Aslı Can, Kemal Acar, Candan Gökçeoğlu*

Proposed Engineering Measures and Analysis of Tunnel Portal Excavated in Paleo-Landslide Deposits (Bahce – Nurdag Tunnel, Turkey) .....90  
*Yunus Emre Özyürek, Aslı Can, Kemal Acar, Candan Gökçeoğlu*

A probabilistic approach to deal with uncertainty in tunneling .....92  
*Antonios Skolidis, Dr. Chrysothemis Paraskevopoulou, Dr. Vassilis Marinos*

Evaluation of Collapsed Zone in T24 Tunnel (Ankara-İstanbul High Speed Railway Project, Turkey) .....94  
*Ebu Bekir Aygar, Candan Gokceoglu*

Tunnel Collapse Due to the Insufficient Umbrella System: A Case Study from Turkey .....96  
*Ebu Bekir Aygar, Candan Gökçeoğlu*

Predicting uniaxial compressive strength of evaporitic rocks from Abu Dhabi, United Arab Emirates-Phase I with unit weight values .....98  
*Hasan Arman, Osman Abdelghany, Ala Aldahan*

Some empirical equations for estimating grout take amount: A case study from Turkey .....100  
*Ali Kayabasi, Candan Gokceoglu*





Engineering Geological Assessment of the Louziki dam site suitability, Chalkidiki, Greece .....	102
<i>Antriana Gkorani, Thomas Makedon, Vassilis Marinos, Vasileios Christaras</i>	
Site evaluation for the tunneling with an approach of engineering Geomorphology in Nepal .....	104
<i>Ranjan Kumar Dahal, Manita Timilsina, Shuichi Hasegawa</i>	
Rock mass excavatability assessment in tunnelling based on GSI. The case of Tempí tunnels in Greece.....	106
<i>Athina Tsirogianni, Charalampos Saroglou</i>	
Geotechnical Block Model (GBM) of Olympias Mine Using Q Classification System .....	107
<i>N. Grendas, E. Vagkli, M. Yumlu, G. Gkekas, D. Bogas</i>	
A study of biocementation implementation methods for embankment foundation soil .....	109
<i>Muhammad U. Safdar, Maria Mavroulidou, Mike J. Gunn, D. Purchase, Ian Payne, Jonathan Garelick</i>	
D8 motorway landslide: largest construction accident in recent Czech history .....	111
<i>Jan Blahůt, Josef Stemberk, David Mašín, Jan Klimeš, Filip Hartvich, Josef Rott, Jan Balek, Petr Tábořík, Michal Kusák</i>	
Compactability and permeability of clay-gravel composites: a laboratory evaluation.....	113
<i>Yang Lu<sup>2</sup>, Sihong Liu, Yonggan Zhang</i>	
Engineering Geological in-situ Investigation of the Tanahu HPP Powerhouse Cavern, Nepal .....	114
<i>M. R. Pokharel, E. Schnäcker</i>	
The Effect of the Horizontal-Vertical Stress Ratio on the Deformations at the T3 Tunnel (Çorum, Turkey) Entrance Section.....	116
<i>Anil Atakan, Murat Yılmaz, Atiye Tuğrul, Bora Arslan, Cemal Samur</i>	
Water level variation and slope stability analysis in a pit lake.....	118
<i>Emmanouil Steiakakis, G. Syllignakis, M. Galetakis, D. Vavadakis</i>	
Stability Assessment of Fractured Dolomite and Marl Rock Masses in a Tunnel.....	120
<i>Ákos Török, Péter Görög, László Rózsa</i>	
A visual and laboratory estimation of the Hoek-Brown constant $m_i$ for two marbles .....	121
<i>Anastasios Tsirikis, Trevor G. Carter, Vassilis Marinos</i>	
The Application of Advanced Numerical Models in Capturing Complex Rockmass Behaviour.....	123
<i>Ioannis Vazaios, Anastasios Stavrou</i>	
Engineering Geological detailed aspects impacting on the foundation and watertightness of the Julius Nyerere HPP Main RCC Dam, in Tanzania .....	125
<i>Nikolaos Kazilis, Maria Kazili</i>	
<b>THEME 5 - ENGINEERING GEOLOGY FOR URBAN ENVIRONMENT .....</b>	<b>127</b>
Engineering geological mapping of Moscow megacity area: from geological maps to georisk maps .....	128
<i>Olga Eremina, Irina Kozliakova</i>	
Engineering geological evaluation for urban land use planning and engineering construction within a database environment, a case study for the city of Thessaloniki, Northern Greece .....	129
<i>Aliki Kokkala, Vassilis Marinos, Vasileios Christaras, Konstantinos Voudouris</i>	
I.S.G.E.: An Integrated Spatial Geophysical & Geotechnical Evaluation tool based on fuzzy logic .....	131
<i>Christos Orfanos, Konstantinos Leontarakis, George Apostolopoulos, Ioannis E. Zevgolis</i>	
Assessment of Earthquake Induced Liquefaction Risks in the Hills of The Rohingya Refugee Camp Area, Cox's Bazar, Bangladesh for Sustainable Development .....	133
<i>A.T.M. Shakhawat Hossain, T. Dutta, M.E. Haque, M.H. Sayem, H. Imam, M. Khatun, S.J. Jafrin, P.A. Khan, M. Hasan</i>	



<b>THEME 6 - ANALYSIS AND MITIGATION OF GEO-HAZARDS.....</b>	<b>134</b>
The Kosova landslide in Bosnia and Herzegovina .....	135
<i>Mike G Winter, Sarah J Reeves, Senad Smajlović, Gurmel Ghataora, Džella Šehić, Haris Zejnić</i>	
Probabilistic rainfall thresholds for debris flow warning in Scotland .....	137
<i>Mike G Winter, Flora Ognissanto, Luke A Martin</i>	
Investigation of land subsidence due to the overexploitation of the aquifer at the Amyntaio basin, Greece.....	139
<i>Ploutarchos Tzampoglou, Constantinos Loupasakis</i>	
Prehistoric rock slides in Dagestan (Caucasus, Russia): Justification of their seismic triggering by slopes' stability back analysis.....	141
<i>Alexander Strom, Igor Fomenko, Vladislav Tarabukin, Oleg Zerkal</i>	
Assessing land subsidence phenomena with SAR Interferometry techniques and hydrogeological data in the Thriassio plain .....	143
<i>Agavni Kaitantzian, Constantinos Loupasakis, Issak Parcharidis</i>	
Rainfall thresholds for forecasting shallow rainfall-induced landslides in western Greece .....	145
<i>Spyridon Lainas, Nikolaos Depountis, Nikolaos Sabatakakis</i>	
Investigation of tectonized limestones in western Lefkada Island with field and laboratory testing and back-analyses of co-seismic landslides .....	147
<i>Vasilis Kallimogiannis, Charalampos Saroglou, G. Palantzas</i>	
Geohazard evaluation in central Nepal Himalaya with focus on landslide .....	149
<i>Prem Bahadur Thapa</i>	
Long-term rockslope monitoring and rockfall prediction .....	150
<i>Miloš Marjanović, Biljana Abolmasov, Marko Pejić, Jelka Krušić</i>	
Fault influence zones assessment and its accounting in site investigations .....	152
<i>Olga Barykina, Oleg Zerkal, Ernest Kalinin</i>	
Bayesian probabilistic back-analysis and run-out prediction of landslides: a case study in the Heifangtai, Gansu Province, China .....	154
<i>Peng Zeng, Xiaoping Sun, Tianbin Li, Rafael Jimenez</i>	
Soil Liquefaction evidences during the November 26th 2019 Durres Earthquake, Albania .....	156
<i>Shkëlqim Daja, Besnik Ago, Çerçis Durmishi, Shaqir Nazaj, Arjol Lule, Neritan Shkodrani</i>	
Roadmap to an early warning system in a large landslide near Tbilisi, Georgia .....	157
<i>Klaus Keilig, Markus Bauer, Peter Neumann, Kurosch Thuro</i>	
Earthquake - induced landslides in the island of Lefkada triggered by the November 17, 2015 event and assessment of landslide susceptibility .....	159
<i>Aglaia Matsakou, Vassilis Marinos, George Papathanassiou, Sotirios Valkaniotis, Athanasios Ganas</i>	
Locating-allocating emergency response services facilities considering landslide susceptibility assessments .....	161
<i>Anastasios Balampanis, Paraskevas Tsangaratos, Constantinos Loupasakis, Constantinos Athanassas</i>	
Implementing a novel ANN ensemble model based on machine learning models for landslide susceptibility mapping .....	163
<i>Paraskevas Tsangaratos, Anastasios Balampanis, Constantinos Loupasakis</i>	
Assessing the shrink swell potential of Highways England's geotechnical assets .....	165
<i>Jack Randall, Dr Christopher Power, James Codd</i>	
Investigation of the Kafireas Mountain landslide, in Evia Island, Greece .....	166
<i>Vasilis Perleros, A. Kalos, D. Georgiou, Paul Marinos</i>	
Forest Fires' impact on Landslide Susceptibility Assessment.....	168
<i>Constantinos Nefros, Constantinos Loupasakis, Gianna Kitsara</i>	



2D and 3D dynamic numerical modelling of seismically induced rock slope failure .....	170
<i>Anne-Sophie Mreyen, Emilie Lemaire, Hans-Balder Havenith</i>	
Development of a web-based landslide inventory map of Attica Region, Greece .....	172
<i>Nikolaos Tavoularis, Panagiotis Argyrakis, George Papathanassiou, Athanasios Ganas</i>	
A Probabilistic Approach for Mapping the Hazards Posed by Coseismic Landslides .....	174
<i>Mingdong Zang, Shengwen Qi</i>	
A landslide in bentonitic clays in Paphos, Cyprus .....	175
<i>Michael Bardanis, Evagelia Ioannou</i>	
Development of a low cost geosensor network for detection and monitoring of rainfall induced landslides in soil .....	176
<i>Dr. John Singer, Prof. Dr. Kurosch Thuro, Moritz Gamperl, Tamara Breuninger, Dr. Bettina Menschik</i>	
Vulnerability of road infrastructure exposed to earthquake-induced landslides: a case study from Lefkada island, Greece .....	178
<i>Sotirios A. Argyroudis, George Papathanassiou, Sotiris Valkaniotis, Vassilis Marinos, Mike G Winter</i>	
Projecting landslide susceptibility under Climate Change. The case of Eastern Pelion, Greece .....	180
<i>Aikaterini-Alexandra Chrysafi, Ioanna Iliá, Paraskevas Tsangaratos</i>	
The tsunami component of the Hellenic Plate Observing System (HELPOS) research infrastructure .....	182
<i>Marinos Charalampakis, Nikos Kalligeris, George Drakatos, Akis Tselentis</i>	
Tsunami risk assessment in the framework of the GEORISK project.....	184
<i>Marinos Charalampakis, Akis Tselentis, George Drakatos</i>	
Earthquake-generated tsunami hazard assessment for the Ionian Islands.....	186
<i>Marinos Charalampakis, George Drakatos, Christos Evangelidis</i>	
Spatial characteristics of a deep-seated gravitational slope deformation case in Taiwan: insights from long-term, multiple types of geodetic surveys .....	188
<i>Pai Chiao Lo, Ya Chu Chiu, Tai Tien Wang, Wei Lo</i>	
Engineering geological study of rockfall phenomena and instability analysis in Proussos Dipotama site, Central Greece, using terrestrial LIDAR and UAV platforms .....	190
<i>Maria Dandika, Vassilis Marinos, Efstratios Karantanellis, George Papathanassiou, Thomas Makedon</i>	
Study on mechanism of loess landslide induced by train vibration combined with water .....	192
<i>Yuanjun Xu Jiading Wang, Tianfeng Gu</i>	
The effect of suction on differential weathering and stability of soft rock cliffs on the example of Zenta Bay cliff (Split, Croatia) .....	193
<i>Ana Raič, Nataša Štambuk Cvitanović, Goran Vlastelica</i>	
Investigation of deep geohazard sites with seismic and ambient noise methods, combined with 3D Geomodelling .....	195
<i>Hans-Balder Havenith, Lena Cauchie, Anne-Sophie Mreyen</i>	
Detecting early landslide phenomena after wildfires through UAV-photogrammetric mapping .....	197
<i>Aggelos Pallikarakis, Georgios Deligiannakis, Ioannis Papanikolaou</i>	
Prediction of Karst susceptibility combining GIS based modeling and Remote Sensing data analysis .....	199
<i>Mirko Vendramini, Walter Giulietto, Fabrizio Peruzzo, Attilio Eusebio</i>	
A multi-instrument and multidisciplinary landslide assessment: The case of Monesi Landslide, Ligurian Alps (NW Italy).....	200
<i>Davide Notti, Aleksandra Wrzesniak, Niccolò Dematteis, Piernicola Lollino, Nunzio Luciano Fazio, Francesco Zucca, Daniele Giordan</i>	
Geological Control on Large-scale Landslide in the Central Nepal Himalaya .....	202
<i>Bikash Phuyal, Prem Bahadur Thapa</i>	





Stochastic approach for karst risk assessment of a motorway project.....	203
<i>Fabrizio Peruzzo, Walter Giulietto, Mirko Vendramini, Attilio Eusebio</i>	
Rockfalls occurrence administration along with the road network: an operative methodology for local standardized management in alpine territory .....	204
<i>Daniele Giordan, Martina Cignetti, Danilo Godone, Davide Bertolo, Marco Paganone</i>	
State of knowledge delineation of Deep-seated Gravitational Slope Deformation impact on anthropic elements: the Western Italian Alps case .....	206
<i>Martina Cignetti, Danilo Godone, Francesco Zucca, Davide Bertolo, Daniele Giordan</i>	
Slope protection respectful of natural resources and landscape thanks to earth retaining system.....	208
<i>Steve Gruslin, Domenico Nola</i>	
Slope Stability Hazards Evaluation of Dammam Formation West of Karbala Governorate-Middle of Iraq: Case study .....	210
<i>A. Jaffar H.A. Al-Zubaydi</i>	
Comparing high accuracy tLiDAR and UAV-derived point clouds for change detection in two semi-mountainous Mediterranean catchments in Central Evia island, Greece .....	212
<i>Simoni Alexiou, Georgios Deligiannakis, Aggelos Pallikarakis, Ioannis Papanikolaou, Emmanouil Psomiadis, Klaus Reicherter</i>	
Liquefaction phenomena triggered by the March 2021, Thessaly, Greece seismic sequence.....	214
<i>George Papathanassiou, Sotiris Valkaniotis, Athanassios Ganas, Riccardo Caputo</i>	
Effect of temperature on the evolution of post-earthquake landslides .....	216
<i>Marco Loche, Luigi Lombardo, Ali P. Yunus, Filippo Catani, Hakan Tanyaş, William Frodella, Xuanmei Fan, Gianvito Scaringi</i>	
Real-time monitoring of landslides with the use of inclinometer and GNSS instrumentation .....	218
<i>Nikolaos Depountis, Katerina Kavoura, Nikolaos Sabatakakis, Panagiotis Argyrakis, Kostas Chousianitis, George Drakatos</i>	
Assessing the effect of the coefficients of restitution on rockfall trajectory .....	220
<i>Pavlos Asteriou</i>	
<b>THEME 7 - RECENT ADVANCES IN GEOMATICS AND REMOTE SENSING FOR USE IN ENGINEERING GEOLOGY .....</b>	<b>222</b>
Investigation of the swelling/shrinkage phenomenon with the use of Earth Observation techniques in Nicosia, Cyprus.....	223
<i>Ploutarchos Tzampoglou, Dimitrios Loukidis, Niki Koulermou</i>	
An Integrated Object-Based Analysis with UAV Imagery and Machine Learning for site-specific Mass Movement Assessment .....	225
<i>Efstratios Karantanellis, Vassilis Marinos, Emanuel Vassilakis, Basile Christaras</i>	
InSAR in monitoring of underground civil works in urban areas. Case of Glòries square, Barcelona .....	227
<i>Joan Botey i Bassols, Pierre Gerard, Enric Vázquez-Suñé, Michele Crosetto, Anna Barra</i>	
Engineering Geological Appreciation and Monitoring of Rockfall's Dynamic, Based on Multi-Temporal UAV and LiDaR Surveys in "Apothikes" Area, Santorini Prefecture, Greece .....	229
<i>Ioakeim Konstantinidis, Efstratios Karantanellis, Vassileios Marinos, George Papathanassiou</i>	
Engineering geological appreciation on landslide and rockfall phenomena and monitoring using LiDAR and UAV platforms in a case site at Perivoli, Greece .....	231
<i>Apostolos Azas, Vassilis Marinos, Efstratios Karantanellis, George Papathanassiou</i>	
Landslide Susceptibility Assessment under seismic motion surveys: A case in Melissoyrgoi, Epirus .....	233
<i>Pinelopi Sotiriou, Vassilis Marinos, Efstratios Karantanellis, George Papathanassiou</i>	



Landslide Change Detection Based on Multi-Temporal Digital Elevation Models of Ropoto, Central Greece .....235  
*Athanasia Vassou, Vassilis Marinos, Efstratios Karantanellis, S. Valkaniotis, George Papathanassiou*

Integrating 3D point clouds and machine learning for intelligent rock slope environments development .....237  
*Ioannis Farmakis, David Bonneau, D. Jean Hutchinson, Nicholas Vlachopoulos*

Automated 3D rock discontinuity surface mapping and characterization: Not a plane segmentation problem .....239  
*Ioannis Farmakis, Efstratios Karantanellis, Nicholas Vlachopoulos, Vassilis Marinos*

Rockmass characterization and evaluation of rock fall potential based on traditional and SfM-based methods .....241  
*George Papathanassiou, Adrian Riquelme, Theofilos Tzevelekis, Evaggelos Evaggelou*

Results of comprehensive monitoring activities on Umka landslide, Belgrade, Serbia .....243  
*Biljana Abolmasov, Uroš Đurić*

New ground truth and space borne data for the verification of land subsidence occurring at the coastal zone of Athens, Greece .....245  
*Agavni Kaitantzian, Constantinos Loupasakis, Ploutarchos Tzampoglou, Issak Parcharidis*

Rock strength of a rock cliff evaluated through infrared thermography .....247  
*Marco Loche, Gianvito Scaringi, Jan Blahůt, Maria Teresa Melis, Antonio Funedda, Stefania Da Pelo, Ivan Erbi, Giacomo Deiana, Mattia Alessio Meloni, Fabrizio Cocco*

Lithological discrimination using aster images in the coastal mountain chain of the Lampa sector, Santiago, Chile .....249  
*Vidal V. Raúl, Arriagada S. Hernán, Péndola R. Daniel, Arotaipe Q. Rosmery*

**THEME 8 - ENGINEERING GEOLOGY AND CULTURAL HERITAGE PROTECTION .. 251**

Structural analysis of Rock slopes, using UAV & LiDAR, in the Archaeological site of Delphi, Greece .....252  
*Kyriaki Devlioti, Basile Christaras, Vassilis Marinos, Konstantinos Vouvalidis, Silvana Fais*

Rehabilitation methods of Victorian Tunnels in the UK .....254  
*Cameron Atkinson, Dr. Chrysothemis Paraskevopoulou, Richard Miller*

Parametric simulations on the stability conditions of the masonry wall of Chandakas .....256  
*Nikolaos Antoniadis, Michaela-Maria Karathanou-Nicholaidi, Constantinos Loupasakis*

**THEME 9 - ENGINEERING GEOLOGY FOR THE SOCIETY ..... 258**

Investigating the impact of Geological Uncertainty in Cost Overruns of Tunnelling Projects .....259  
*Georgios Boutsis, Dr. Chrysothemis Paraskevopoulou*

Socio-economic impacts of landslides in Pelion district, Greece .....261  
*Garyfalia Konstantopoulou*

From post-disaster landslides inventory to open landslides data .....263  
*Biljana Abolmasov, Miloš Marjanović, Uroš Đurić, Jelka Krušić*

Landslide activity affected by sludge basin water: a 40-year history assessed by interdisciplinary research .....265  
*Filip Hartvich, Petr Tábořík, Jan Klimeš, Jan Blahůt, Ondřej Racek, Josef Stemberk, Jan Balek*

**THEME 11 - MARINE ENGINEERING GEOLOGY ..... 267**

Investigation to soil-pile interaction in open-ended piles installed in soft soils .....268  
*M.Sc. Moritz Anton Loreth, Univ.-Prof. Dr.-Ing. habil. Sascha Henke*

**Author Index ..... 269**



## KEYNOTES





## The biggest challenges in landslide hazard analysis and mitigation

Simon Loew<sup>1</sup>

<sup>1</sup>Chair of Engineering Geology, ETH Zurich, Switzerland, [simon.loew@erdw.ethz.ch](mailto:simon.loew@erdw.ethz.ch)

Landslides cause about 20'000 fatalities per year on earth, and several billion of US\$ of direct annual costs from landslide damage. Substantial costs could be reduced, and many fatalities avoided if we could properly assess the hazard potential and reliably predict the occurrence of very rapid landslides. Landslide hazard is not universally defined but strongly related to landslide velocity, kinetic energy and mobility. This lecture gives an overview on how landslides in rock develop through geological time, and the major controls and drivers of landslide velocity. Laboratory and field observations give new insights into how landslides in rock slopes develop during thousands of years through micro- and macro-crack propagation and coalescence under subcritical stress conditions driven by diverse cyclic loads. New field monitoring systems allow to capture the corresponding very slow (micro- to millimeter per year) slope processes. The transition from a “stable slope” to a “marginally stable slope” and an “actively unstable” landslide is transitional in nature and only conceptually defined. Landslide velocity is strongly influenced by the landslide type, i.e. the materials involved, their states, boundary conditions and motion mechanisms. In most rocks, relative small changes in velocity occur as a function of state, i.e. pore pressure, temperature, strain and stress. This stands in contrast to velocity variations in response to changing boundary conditions, like loss of toe confinement, and a related change in motion mechanism, e.g. when toppling transitions into sliding, and sliding transitions into granular flow. Such changes in motion mechanism are often catastrophic events, but their potential and timing are difficult to assess reliably with current methodologies. New ideas for the assessment and mitigation of such hazardous events are presented and illustrated with field examples from the Great Aletsch Glacier Valley in the Swiss Alps.



## Engineering geology applied to archaeology at risk across the Dutch plain and archives

Dominique Ngan-Tillard<sup>1</sup>

<sup>1</sup>*Delft University of Technology, Netherlands, [d.j.m.ngan-tillard@tudelft.nl](mailto:d.j.m.ngan-tillard@tudelft.nl)*

The Netherlands has signed the Valetta convention for in-situ preservation of buried archaeology in 1992. The only sites which can be excavated for an archaeological investigation are those which would lose their archaeological value due to human or natural activities. Other sites have to be preserved in the subsurface for future generations. As estimating threats on buried archaeology remains difficult, the better safe than sorry approach prevails and more sites are excavated than needed.

Threats to buried heritage in a lowland, soft soil, densely populated country like the Netherlands are multiple, especially in the context of climate change and energy transition. Archaeological remains can be separated from their context or reduced to crumbles and lose any archaeological value during the excavation of underground spaces, works for the foundation of line infrastructures and buildings, or dredging for land reclamation or coastal protection. Land cultivation with heavy machinery also remoulds settlements buried at shallow depths and contribute to the erosion of these sites. Earthquakes induced by gas extraction in the North of the country fissure monumental buildings and might endanger the stability of emblematic elevated mounds where inhabitants have protected their living quarters from raising water from Neolithic times. Flooding from both the sea and the rivers remains the highest threat for the above ground heritage in the western Netherlands. Buried sites can be affected by rapidly changing ground water levels, as well as chemistry, and excessive drought periods. At a few occasions, human activities have been a chance for archaeology. For example, sand winning for coastal protection has helped to reveal the lost world of the North Sea.

Engineering geology contributes to the preservation of the (buried) heritage by promoting a multi-disciplinary approach in archaeological fieldworks. The combination of remote sensing, geophysics, geotechnical ground investigation, multi-scale observations of archaeological soils, physical modelling, and numerical simulations, has helped to discard some threats, quantify others and design protection measures when needed. The toolbox developed to assess the impact of line infrastructure loading and piling is explained in the keynote. The strategy adopted to evaluate risks of collapse of steep slopes under seismic and machine loadings applied to highly heterogeneous man-made mounds is exposed. And a pilot project aiming to reconstruct digitally damaged megaliths is presented.

Non-invasive X-ray imaging techniques commonly used in geosciences are extremely well suited to the study of both archaeological soils and artefacts. In multiple cases, they have brought insight into the provenance, manufacture, use, and/ or state of conservation of archaeological artefacts, especially when images were analysed with the mindset of an engineering geologist. For example, when encased cuneiform tablets under the custody of the Near East Institute of the Netherlands were scanned with the prime aim of revealing the texts hidden under the clay envelopes, a large number of negative imprints of plant fibres were discovered and related to an early sign of human manipulation of clay properties for the production of durable air dried objects.

To conclude, archaeology offers engineering geologists valuable case studies for testing and evaluating in a scientific way newly developed techniques and algorithms for modelling of soil and rock behaviors subjected to diverse loadings and boundary conditions. In return, engineering geology shares its know-how to estimate risk on buried archaeology, design remedial measures. It can also reveal unforeseen soil related aspects for collections of artefacts left unexploited in depots for decennia.

## Investigation, monitoring and modelling of landslides

Christian Zangerl<sup>1</sup>, Klaus Voit<sup>1</sup>, Christina Rechberger<sup>1</sup>, Christine Fey<sup>1</sup>, I Putu Krishna Wijaya<sup>1</sup>

<sup>1</sup>University of Natural Resources and Life Sciences, Vienna, Department of Civil Engineering and Natural Hazards, Institute of Applied Geology, Peter Jordan-Strasse 82, 1190 Vienna, Austria,  
[christian.j.zangerl@boku.ac.at](mailto:christian.j.zangerl@boku.ac.at)

Landslides are among the most widespread natural hazards on earth and they are particularly important in mountainous countries causing billions of euros in damages each year. Landslides occur in a wide variety of geological and geomechanical contexts and as a response to various loading and triggering processes. They are often associated with other major natural disasters such as earthquakes, floods and volcanic eruptions. The great variety of different types of landslides requires a flexible classification system, comprehensive process analyses, different investigation and monitoring methods, and process-adapted mitigation strategies. Literature offers a large number of different classification schemes for landslides, comprising one, which is widely accepted internationally and proposed by Varnes (1978) as well as Cruden & Varnes (1996), and recently adapted by Hungr et al. 2014. In principal, the classification is based on the type of material (i.e. rock and soil) and the type of movement (i.e. falls, topples, slides, spreads, flows, and new slope deformation). Furthermore, the system also includes a subdivision into different classes of movement velocity.

This contribution primarily focusses on deep-seated landslides ranging in velocities from extremely slow to extremely rapid, affecting entire valley slopes and reaching volumes of millions of m<sup>3</sup>. Concerning slowly moving landslides, if active or reactivated over longer periods of time, they can adversely affect settlements and infrastructure such as high- and railway lines, reservoir dams, pressure pipes, pipelines, and settlements due to differential and localised displacements of the ground surface and subsurface. Even for very slow movements the damage can be considerable and the life-cycle of man-made structures can be reduced, accompanied with a great economic loss. In some cases, there is also the danger of total slope failure with acceleration to high velocities and the transition to a flow-type like movement process, causing in the worst case dramatic consequences. Reactivation of ancient/pre-existing landslides or internal slabs is frequently observed and can be triggered by various factors comprising e.g. reservoir infilling or drawdown, toe erosion by flooding, extreme precipitation and snow melt, construction of a cut slope, or loading the slope in the upper area.

Based on detailed investigations of several slow and rapid moving landslides (e.g. from Austria and Indonesia) this contribution presents a synthesis of the major outcomes and fundamental processes as well as the experience obtained from the application of a large bundle of in-situ investigation, monitoring and numerical modelling methods. Extensive investigation campaigns over decades increased the state of knowledge about deep-seated landslides considerably. In particular insight was gained about geometry, kinematics, temporal deformation behaviour, hydrogeology factors and geomechanical characteristics. Recently, major improvements have been made concerning the successful application of terrestrial and airborne based remote sensing methods (ALS, TLS, InSAR, GB-InSAR, UAV) to measure 2D/3D slope deformations and to develop high-resolution digital terrain models for mapping and geometrical model design. Furthermore, advanced numerical modelling techniques allow the investigation of hydro-mechanical coupled slope processes such as initial formation and sliding mechanisms as well as the spatial-temporal development of slope stability.





Thus an improved level of knowledge on past events in connection with an increased process understanding and well-designed monitoring and early warning systems, spatial planning and technical measures is the key to minimize the hazards and risks associated with these types of landslides.

## REFERENCES

- Cruden DM, Varnes DJ (1996) Landslide Types and Processes. In: Turner AK, Schuster RL (ed) Landslides: investigation and mitigation (Spec. Rep. 247), National Academy Press, Washington D.C., pp 36-75.
- Varnes DJ (1978) Slope Movement Types and Processes. In: Schuster RL, Krizek RJ (ed) Landslides-Analysis and Control, Special Report 176 (2), Washington D.C. (National Academy of Sciences), pp 11-33.
- Hungr O, Leroueil S, Picarelli L (2014) The Varnes classification of landslide types, an update. Landslides 11:167–194.



## **The importance of ground truthing Engineering Geology innovations for Rock Slope stability management**

Jean Hutchinson<sup>1</sup>

<sup>1</sup> Queen's University, *Department of Geological Sciences and Geological Engineering, Kingston, Ontario, Canada, [hutchinj@queensu.ca](mailto:hutchinj@queensu.ca)*

Our ability to understand and assess natural rock slope stability is being transformed by the increasing availability of high quality remotely sensed data. This provides an unprecedented amount of detailed information about the surface of potentially unstable slopes. The trend is to toward applying automated approaches to assessing slope geometry and stability condition, given the high quality and increasing availability of this data. We must, however, keep in mind the geological setting in addition to the changing geometry, and develop geologically-possible conceptual models of the possible failure mechanisms that may be acting on the slope. There is a constant feedback loop between observations, refinement of the failure model and understanding of the slope stability. The analysis of data for two sites will be included in this discussion to illustrate these concepts.

## Standardization and future trends in rock characterization and testing in geo-engineering

Reşat Ulusay<sup>1</sup>

<sup>1</sup>*Hacettepe University, Geological Engineering Department, 06800 Beytepe, Ankara, Turkey,*  
[resat@hacettepe.edu.tr](mailto:resat@hacettepe.edu.tr)

In geo-engineering practice in rocks, rock engineering models developed depend on the input data such as boundary conditions, the properties of rock material and rock mass. Their correct evaluation frequently requires laboratory and in-situ tests, supplemented with a high degree of experience and judgement. In addition to rock engineering methodologies, the input from engineering geology is absolutely a fundamental for correct characterization of rocks and rock masses. This paper emphasizes the need and importance of standardization of rock characterization and testing methods within the context of the ISRM Suggested Methods (SMs) and introduces main future trends in rock characterization and testing.

The complexity of modern rock engineering practice suggests that there are some issues requiring further investigations and developments in characterization and experimental methods which may also lead to generation of new ISRM SMs. Determination of the strength and deformability for "difficult rocks", such as soft rocks and block-in-matrix rocks (BIMROCKS), is an important issue in geo-engineering. Due to their complex heterogeneity and mechanical variability, the correct characterization and determination of geomechanical properties of BIMROCKS are quite challenging issues.

There are many issues in rock dynamics testing requiring further investigations, such as shear strength of rock joints under dynamic loads, assessment of mechanical and physical causes of the rate effects on the rock strength and failure pattern etc. A database of true 3-axial test results, verification of constitutive relationships, more incorporation with acoustic emission and micro-seismic measurements etc. would be important. The behaviour of anisotropic and jointed rocks under true triaxial stress conditions should also be experimentally investigated more thoroughly and application of this method in highly stressed environments at great depths for predicting and prevention of rock bursts would be useful. Although the use of non-destructive and non-contact methods for field geotechnical characterization of rock masses has been receiving great attention, they also need standards and/or SMs. By considering the increasing interest in TBMs and deep borings, some improvements on determination of excavability and borability parameters and preparation of associated SMs are also some of the near future expectations

The long-term maintenance and preservation of man-made historical and modern rock structures become important issues in geo-engineering. Although they are well-known issues, quantitative evaluation methods are still lacking. Available test methods can be used for the purpose. However, disintegration of rocks during laboratory tests, in which weather conditions are simulated, occurs faster than the natural processes in situ, and they are also insufficient to provide experimental data for constitutive and mechanical modeling. Therefore, the development of new and/or modification of the existing experimental methods to solve this problem are needed. Guidelines for laboratory procedures to detect damage thresholds and petroleum geomechanics related laboratory tests will be the important developments expected in this area in the near future. The idea of potential uses for in-space resources and the striking similarities between the rocks on Earth and Mars, such as layered rock masses, jointing, weathering effects and some slope stability problems, indicate that the next generation of rock mechanics discipline would see the development and progress of extra-terrestrial rock mechanics.





## Can engineering geologist contribute to international agendas & fundamental societal challenges?

H.J. Reeves<sup>1</sup>, S Bricker<sup>2</sup>

<sup>1</sup>Jacobs, Tunnelling & Ground Engineering, Leeds, UK, [Helen.Reeves@jacobs.com](mailto:Helen.Reeves@jacobs.com)

<sup>2</sup>British Geological Survey, Keyworth, Nottingham, UK

When hominids chose a particular pebble to make a tool on the basis of its material properties, they used geological knowledge. Applied geology, hence, has a had long history. Geological knowledge has increased through the centuries through the developments in mining, initially for flint and later for metals, and through its use in major construction with regard to foundations and building materials. But much of this knowledge was localised and restricted to families or guilds until the invention of printing that enabled it to be communicated and shared cheaply and widely. Hence, when William Smith (the father of engineering geology of the modern world) started his career there was known geological knowledge that enabled him to observe and recognise strata that could be ordered, by the fossils, which assisted in his creation of the first geological map of England and Wales in 1815. William Smith's expertise in draining land, stabilising landslides and planning canal routes amply demonstrates his ability to create, and apply, the 3D geological model that is a prime requisite in modern engineering geological practice.

For the engineering geological professional there has never been a more exciting time to apply and communicate these fundamental geological and engineering geological skills. With international agendas, such as the UN Development Frameworks (Sendia Framework for Disaster Reduction, Sustainable Development Goals & Paris Climate Change Agreement), relating to the interaction of environment processes with human activities and behaviour that address the significant challenges affecting society. As well as the increased investment and development, across the globe, in large-scale transport and energy infrastructure programmes (e.g., High Speed rail, energy storage and waste disposal) required to meet the increasing global population and demands for more environmentally sustainable infrastructure delivery. There is now an increased demand on the use of the subsurface, especially in cities, for the provision of resources (e.g., water, heat, minerals), as a platform for infrastructure and as an environment that supports life and well-being. As a result, it is increasingly important that the engineering geological profession highlights, communicates and publicises, more widely beyond our profession, the fundamental engineering geological skill sets and tools that are being applied to help contribute to the better understanding, use and regulation of the subsurface. This is vital to make sure that governments understand the significant contribution our profession makes to these agendas and ensures the future funding to support education and training in the engineering geological profession is maintained.

## Hazard assessment and monitoring of landslide prone areas in Medellín, Colombia

Kuroschi Thuro<sup>1</sup>, John Singer<sup>4</sup>, Moritz Gamperl<sup>2</sup>, Tamara Breuninger<sup>3</sup>, Bettina Menschik<sup>5</sup>

<sup>1</sup>Chair of Engineering Geology, Technical University Munich, Germany, [thuro@tum.de](mailto:thuro@tum.de)

<sup>2</sup>AlpGeoRisk Munich, Germany, [singer@alpgeorisk.de](mailto:singer@alpgeorisk.de)

<sup>3</sup>Chair of Engineering Geology, Technical University Munich, Germany, [moritz.gamperl@tum.de](mailto:moritz.gamperl@tum.de)

<sup>4</sup>Chair of Engineering Geology, Technical University Munich, Germany, [tamara.breuninger@tum.de](mailto:tamara.breuninger@tum.de)

<sup>5</sup>Chair of Engineering Geology, Technical University Munich, Germany, [sellmeier@tum.de](mailto:sellmeier@tum.de)

Early warning of landslide events plays a central role in risk analysis. In the last century, more than half a million families in the tropical Andes region were affected by shallow landslides, mostly caused by heavy rainfall. Especially the region Antioquia with its capital Medellín (2.5 million inhabitants in 2017), Colombia, suffered a large number of deaths. Over 200,000 people there currently live in informal settlements exposed to this natural hazard. A comprehensive early warning system would offer a sustainable alternative to the currently costly and hardly feasible resettlement measures of the city administration.

In developing and emerging countries, a correlation between precipitation and the number of events is usually applied for risk analysis and the prediction of landslides. In addition, previous studies for the Medellín region have produced GIS-based susceptibility studies, which will be included in the project. In the presented project Inform@Risk, which is financed by the German Federal Ministry of Education and Research within the framework of the CLIENT II programme, the Leibniz University Hannover (LUH), the German Aerospace Center Oberpfaffenhofen (DLR), the Technical University Deggendorf (THD) and two companies - the firm AlpGeorisk in Unterschleißheim and the Expert Office for Aerial Image Evaluation and Environmental Issues (SLU) in Munich - are involved in addition to the Technical University Munich (TUM). The cooperation on site is carried out with all responsible municipal authorities and URBAM, a department of the University EAFIT, which is intensively involved in the urban development of Medellín.

TUM and AlpGeorisk are developing a combined, automated system that integrates a monitoring system and a stability analysis model (Fig. 1). The intended monitoring system will be assembled from low-cost sensors such as Time Domain Reflectometry sensors, inclination sensors, extensometers and piezometers in order to offer a financially attractive approach to early warning in developing and emerging countries. The current data of the monitoring system will be continuously fed into the process model. Sensitivity analyses on critical parameters such as precipitation and seismicity are carried out in the model. In combination with time series analyses from the data of the monitoring system, threshold values for the critical parameters will be determined as a function of the deformation rates and the stability analysis. The validated model can then be used for forward modelling to estimate the potential effects of heavy precipitation and earthquakes on the stability of the slopes in the Aburra valley.

The combination of a sensor-based early warning system (Fig. 2) and a combined stability analysis will contribute to the early warning of landslides in the Medellín region, which could also be applied to other areas in the tropical Andes.

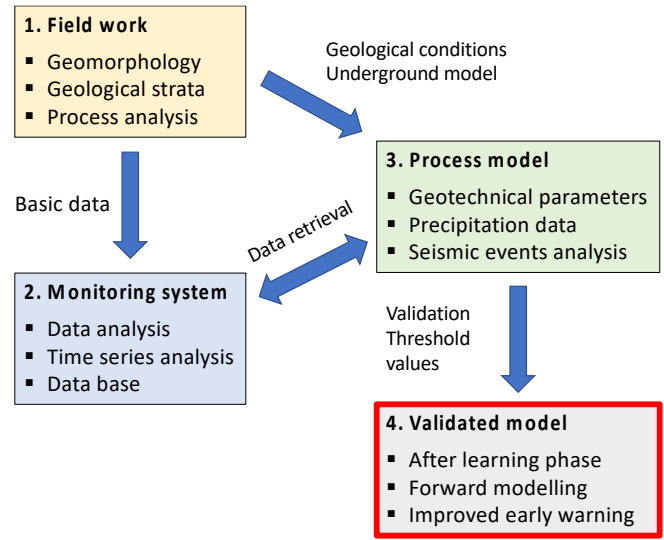


Figure 1. Strategy of a validated process model for a coupled early warning system.

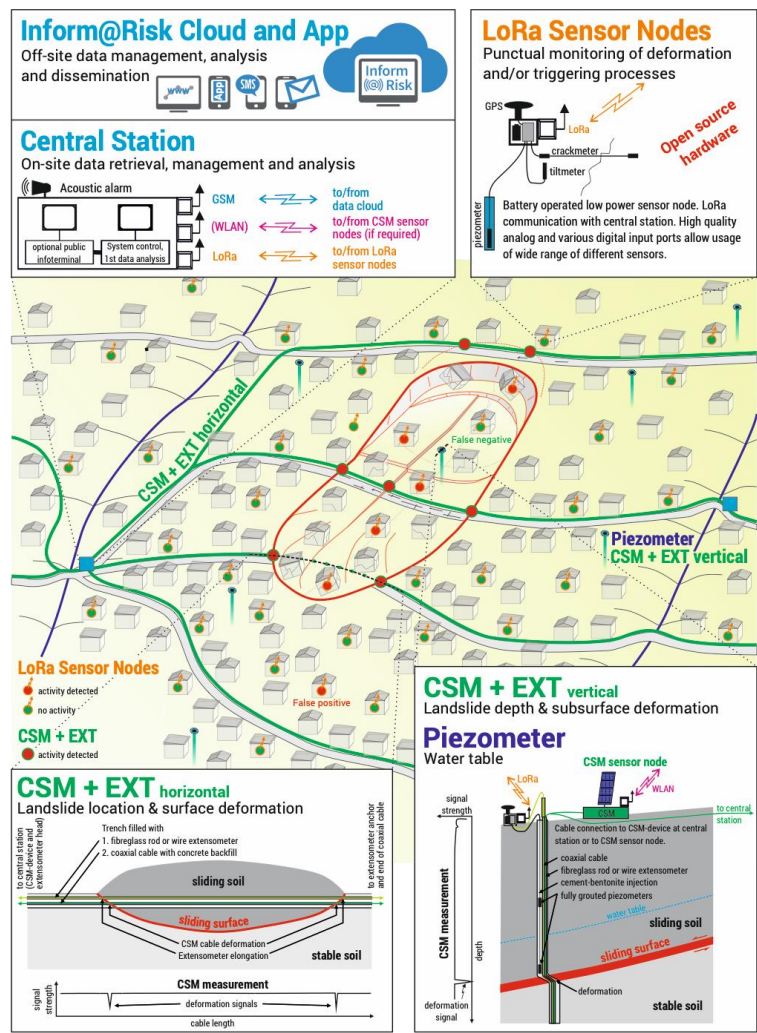


Figure 2. Schematic layout of the proposed landslide early warning system for informal settlements. Red dots: activity detected by sensor.



## Characterization and Behaviour of Soils: Actual Objectives and Requirements

Eugene A. Voznesensky<sup>1</sup>

<sup>1</sup>Professor, Lomonosov Moscow State University, Russia, [arnoldych@gmail.com](mailto:arnoldych@gmail.com)

### 1. From Babylon to Coulomb: main milestones in the history of geotechnics.

The very beginning of construction as a type of human activity started as soon as humans studied to dig and make stone instruments. The most ancient material evidences of simplest structures are 8-12 thousand years old. The earliest remaining structures are known in Egypt, India, Cyprus, Malta, Ireland. They demonstrate the considerable development of human construction ability already 4-5 thousand years ago. Ancient people had a general concept of slope stability in various soils, they built dams, canals and retaining walls. Architectural and engineering principles, developed by antic cultures, had been summarized in «De architectura libri decem» by Vitruvius (1<sup>st</sup> century BC) – the encyclopedic state-of-the-art of that time presenting all the knowledge and technology related to any human engineering activity. Works of Euclid, Archimedes and Philo of Byzantine (3<sup>rd</sup> century BC) had the major impact on the future progress in foundation calculations and soil behaviour, though telling nothing about it yet. Next milestone – appearance of official regulations of the responsibility for the quality of construction. The first known were Hammurabi laws in Babylon (1728-1686 BC), a detailed Code of building laws of the Chinese Song empire (1103), Egyptian building instructions (1204) and several French treatises of 16-17<sup>th</sup> centuries. Those documents, based exclusively on a summary of accumulated experience, gave rise to codes of practice in all countries. Initial understanding of soil properties and their implementation into calculations of foundations occurred only in 18<sup>th</sup> century, whereas the history of their application includes 4 main stages. The first – pre-classic – coincides in general with 18<sup>th</sup> century and was characterized by the development of empiric theories of soil lateral pressure based on the ideas about the stable angle of “natural slope” and specific gravity of reclaimed soils. Second – the birth of classic soil mechanics in works by S.A. Coulomb and others. Third stage – completion of classic soil mechanics development was related to the important experimental studies of sands and theoretical approaches. And the 4<sup>th</sup> stage – appearance of the modern experimental soil mechanics on its classic basis approximately 100 years ago.

### 2. Modern soil mechanics and its objectives.

So, where we have arrived now? Firstly, nowadays there is a technical feasibility of construction at any place on land and offshore and on any soils. For modern technology situation “impossible to build” do not exist, it is a question of costs solely. Secondly, humanity is facing the problem of overpopulation in cities and transportation collapses. These lead to construction of high-rise buildings and vast involvement of underground space and requires the understanding of deep soils and aquifers behaviour. And thirdly, foundations of all critical facilities are designed numerically with specialized software packages implementing various models of soil behavior. These models are based on state equations of modern soil mechanics and require experimental determination of parameters unknown in classic soil mechanics. This caused the development of new field and laboratory advanced soil testing methods which, in turn, have to account for such particular qualities of soil behaviour that were never considered in classic soil mechanics as excessive for its basic tasks. Some of them are discussed here.

**2.1.** Soils demonstrate an expressed non-linearity of their stiffness related to shear strain range (Burland, 1989; Clayton, 2011). This non-linearity is already well-pronounced in the strain range  $10^{-6}$ – $10^{-5}$  meaning that soil stiffness measured by conventional methods is underestimated for facilities like properly designed locks, retaining walls, tunnels and other structures, usually experiencing strains below  $10^{-3}$ . Because of these effects

shear strains are subdivided into very small (below  $10^{-6}$ ), small ( $10^{-6}$ - $10^{-3}$ ) and larger ranges. This pattern of soil behavior is accounted for in several models like HSSmall, Hardin and Drnevich, etc. Determination of these model's parameters in the small strain range requires high-precision instruments like local strain gauges, bender elements, local pore pressure probes. Resonant column and triaxial testing with local strain measurements and bender elements are generally suitable to determine soil small-strain stiffness parameters.

**2.2.** Local measurements led to understanding that for such accuracy in soil testing pore water cannot be considered incompressible – that was a very good assumption for classic mechanics' solutions. But in reality, e.g., in triaxial testing, pore pressure varies from maximum at the center of a specimen to the ends, and the difference between these values, related to the migration of infinitely small amounts of water driven by pressure gradient, depends on specimen size and permeability. This implies that strain rate is an important limiting factor in soil testing: shearing with open drainage does not necessarily mean “drained” conditions, whereas dynamic undrained testing with high frequency prevents correct pore pressure measurements.

**2.3.** During straining soil passes into instability zone. Soil strain instability is a pre-critical state well before failure, associated with the start of breakage or softening of interparticle contacts, rearrangement of pore space and increasing the strains rate. Point of instability reached at the strains below 0.01 can be described in terms of stress ratio, unique for a given soil and test boundary conditions. A technique for this point identification have been recently developed. This phenomenon gives evidence of failure preparation and also provides a new instrument for more reliable control of soil masses stability.

**2.4.** Since soils are non-linear materials in the whole possible range of their strains, the latter cannot be related to the applied stresses by a single state equation. This leads to the necessity of a set of such equations for different stages of deformation until failure and takes us to various models of soil behaviour. A correct distinction between stages of deformation is a key to adequate mathematic description of the processes, and needs identification of a threshold strain values separating those stages. The smallest measured threshold strain has the order of  $10^{-7}$  and marks a temporary invertible stiffness decrease and slow relaxation effects due to loss of direct contacts between some particles at the displacements of 1-4 nanometers, typical for van-der- Waals forces distance. The second threshold strain is a start of stiffness degradation and for various clays and sands it has the order of  $(2\div 8)\cdot 10^{-5}$ , sometimes up to  $5\cdot 10^{-4}$  depending of the type of soil structure. Third is a threshold strain of the start of pore pressure generation with the order of  $(1.4\div 10)\cdot 10^{-4}$  at the displacements of first  $\mu\text{m}$  – comparable with the size of the smallest particles in soils due to their separation and transmittance of their weight to pore fluid. Finally, the strain at the point of instability has the order of  $(2.5\div 8)\cdot 10^{-3}$  and marks the completion of pore space transformation and development of shear zones before failure.

### **3. Conclusion: actual requirements in soil behavior studies.**

Present state of knowledge requires the incorporation of new effects and regularities of soil behaviour in the instruments of soil mechanics. At the moment applied soil models, not very simple already, incorporate many assumptions and simplifications. They can be improved by addition of correct state equations properly describing the observed phenomena. Besides this, issues requiring intense studies and sometimes re-evaluation of existing procedures include, but are not limited to, determination of overconsolidation parameters of soils for deep foundations and excavations, soil strength parameters in dynamic loading, properties and classification of vastly spread technogenic soils and other. Our time is a new loop in geotechnical technology development.



## Engineering Geology for Civil and Mining Engineering — Case Examples from Sweden

Jonny Sjöberg<sup>1</sup>

<sup>1</sup>*Itasca Consultants AB, Luleå, SWEDEN, [jonny@itasca.se](mailto:jonny@itasca.se)*

Geological conditions are, in general, quite favorable for tunneling and mining in Sweden. Most of the bedrock is Precambrian, igneous and metamorphic, with fairly high strength and stiffness. Obviously, faults, weakness zones, and areas of poor rock and/or soil-like conditions also exist, and knowledge of the engineering geology is of critical importance for optimized tunneling and mining activities. This keynote lecture presents a number of case studies from both the civil and mining industry, in which engineering geology played a vital role, as follows:

- *Episyenite rock — challenges for design of metro tunnels*  
During the design work for new metro tunnels in the Stockholm area, episyenite rock was encountered, with partly very soft and weak rock. Significant efforts were required to adapt the design for tunneling through this rock volume.
- *Large-scale structures and their influence on mining-induced ground displacements*  
Sublevel cave mining result in caving and ground deformations on the hangingwall side of the orebodies, but how does this interact with pre-existing large-scale deformation zones? This was investigated through 3D numerical modeling with explicit representation of material removal and mechanical behavior of the rock mass and the structures.
- *The curious case of clay zones in a sublevel caving mine*  
An example of the presence of fairly large clay-weathered zones in an otherwise strong and hard rock mass in an underground mine is presented, including analysis of their effect on the large-scale rock mass behavior.
- *Geochemical effects on rock — example from a dam*  
The geochemistry of rocks and the effect on weathering and degradation is illustrated through a case study from a hydropower dam.
- *Can one have "too good rock"? — examples from an open pit mine*  
Large-scale pit slope stability is of vital importance for the safety and economics of an open pit operation. But what if your rock is so good that no signs of failure are apparent, and thus nothing to validate analysis against? The approach for design of the overall pit slopes for such as case is presented.





## Recent advances in Remote Sensing for use in Engineering Geology

Janusz Wasowski<sup>1</sup>

<sup>1</sup>*CNR - IRPI, National Research Council – Research Institute for Geo-hydrological Protection, Bari, Italy,*  
[j.wasowski@ba.irpi.cnr.it](mailto:j.wasowski@ba.irpi.cnr.it)

New and emerging remote sensing technologies e.g., very-high-resolution (sub-meter), optical and radar satellite constellations, progress and increase in applications of digital photogrammetry prompted by the recent availability of relatively easy-to-use techniques such as Structure from Motion (SfM) combined with the recent unprecedented surge in acquisitions of cm-dcm-resolution images by UAV (Uninhabited Aerial Vehicles), or simply drones, as well as by aerial and terrestrial laser scanners (LiDAR systems), allow producing detailed (“engineering scale”) topographic maps and digital surface models (DSM). Drones are becoming an important tool also for rapid inspections of difficult-to-access sites (e.g., high mountains) or for remote observations of dangerous sites (e.g., unstable slopes and active landslides). Moreover, very-high-precision (mm-cm) measurements of ground surface displacements (e.g., due to landsliding, subsidence, settlements) and infrastructure deformations (e.g., highways, dams) can be obtained by exploiting advanced space borne synthetic aperture radar (SAR) differential interferometry (DInSAR) techniques. The outstanding though still not fully exploited potential of DInSAR lies in the possibility of delivering multi-scale (from regional-scale to site-specific) deformation monitoring thanks to satellite wide-area coverage and regular schedule with high revisit frequency (days), while preserving adequate spatial resolution and millimetre precision of measurement.

The review of the engineering geology literature indicates a growing uptake of remotely sensed information, with an increasing trend particularly evident in the last two decades. Indeed, there already exists the capability of rapidly delivering high quality remotely sensed data that are useful (and possibly cost-effective) for many practical applications. This is perhaps most clearly demonstrated by the operational uses of remote sensing techniques in mining (e.g., for monitoring stability of slopes in open-pit mines) and in petroleum industries (e.g., for monitoring and management of ground instability in oil/gas producing fields). With specific reference to this 3rd European Conference of IAEG and its Main Topics, we can state that the new tools and techniques of earth surface remote sensing are capable to produce useful information for a variety of engineering geology fields ranging from the Characterisation and Behaviour of Soils and Rocks to the multidisciplinary socio-economic domains such as the Analysis and Mitigation of Geo-hazards or Engineering Geology and Cultural Heritage Protection.

It is recognized, however, that engineering geologists and geotechnical engineers may not be sufficiently familiar with rapidly evolving remote sensing technologies. Therefore, close multi-disciplinary collaborations are needed to fully exploit the enormous quantities of information the advanced space- and air-borne remote sensing can now offer. For example, our profession can benefit from collaborations with experts in advanced processing and interpretation of digital imagery.



## **Delivering sustainable infrastructure: Global challenges, geosynthetic solutions and counting carbon**

Neil Dixon<sup>1</sup>

<sup>1</sup>*Professor, School of Architecture, Building and Civil Engineering at Loughborough University, UK,*  
[n.dixon@lboro.ac.uk](mailto:n.dixon@lboro.ac.uk)

Our planet is experiencing unprecedented change: Population is increasing, resources are being depleted and the climate is changing. The global challenge is to provide an acceptable standard of living for all without using up natural resources and causing irreparable damage to the planet's climate. The United Nations programme *Transforming our world: the 2030 Agenda for Sustainable Development* establishes 17 Sustainable Development Goals, which are guiding the decisions taken by nations and organisations. Critical aspects include: ensuring availability and sustainable management of water and sanitation for all; building resilient infrastructure to promote inclusive and sustainable industrialization; making cities and human settlements inclusive, safe, resilient and sustainable; and ensuring sustainable consumption and production patterns. Each country and region face specific challenges in pursuit of sustainable development. A key driver for changing behaviour is climate change. At the 2015 United Nations Climate Change Conference, Paris, a global agreement by 196 parties was made to set a goal of limiting global warming to less than 2 degrees Celsius compared to pre-industrial level by controlling anthropogenic greenhouse gas emissions. This agreement, despite the United States of America withdrawing, is being used in many countries to establish policies and adopt practices that deliver sustainable development.

Against this backdrop of international agreements and goals, use of geosynthetics has the potential to play a prominent role in providing solutions that help to deliver the vision of global sustainable development. The lecture will discuss drivers to challenge and change the way critical infrastructure is delivered and will address how geosynthetics can play a key role in reducing carbon emissions and dealing with the consequence of climate change. As an example, it will detail a framework for calculating embodied carbon of construction solutions that incorporate geosynthetics, present case studies of its use, including comparison of solutions, and highlight the common pitfalls of such analyses.



## **THEME 1 - CHARACTERISATION AND BEHAVIOUR OF SOILS AND ROCKS**

## Classification of Tunnel Surrounding Rock Mass under High In Situ Stress

Ning Liang<sup>1</sup>, Faquan Wu<sup>2</sup>

<sup>1</sup>Key Laboratory of Shale Gas and Geoengineering, Institute of Geology and Geophysics, Chinese Academy of Sciences, University of Chinese Academy of Sciences, Innovation Academy for Earth Science, CAS, China; [liangning@mail.iggcas.ac.cn](mailto:liangning@mail.iggcas.ac.cn)

<sup>2</sup>Shaoxing University, China, [wufaquan@mail.iggcas.ac.cn](mailto:wufaquan@mail.iggcas.ac.cn)

### Backgournd

In most of the China railway tunnel construction, "Code for design on tunnel of railway" (TB10003-2005), issued by PRC Ministry of Railways in 2005, currently plays an important guiding role on tunnel rock mass classification at design stage. Unlike well predicting on rock mass classification in shallow project after excavation, there are great change of rock mass parameters and structure in deep tunnels. The traditional code for design suffers challenges and new phenomenons or factors should be considered. A further discussion on the surrounding rock mass classification is carried out with the example of the deeply buried Guanshan railway tunnel section under high in situ stress about 31.35 MPa and at the depth of 795m.

**Table 1. Preferred Structural Plane Parameters in a tunnel section**

ID	Dip direction (°)	Dip angle (°)	Space (cm)	Trace length (cm)	Normal density (m <sup>-1</sup> )	Average radium (m)
J <sub>1</sub>	60	80	12.3	74	8.1	0.47
J <sub>2</sub>	251	34	16.1	137	6.2	0.873
J <sub>3</sub>	210	70	10.2	46	9.8	0.293

### Methods

The Rock Mass Rating (RMR) System is a geomechanical classification system for rocks, developed by Z. T. Bieniawski between 1972 and 1973. It combines the most significant geologic parameters of influence and represents them with one overall comprehensive index of rock mass quality. In SMRM, the relationship of elastic modulus of rock mass and Rock Mass Rating (RMR) Classification can be defined as (Bieniawski, Z.T., 1973, 1979, 1989):

$$\begin{aligned}
 RMR &= \frac{1}{2}(E_m + 100) & E_m > 10GPa \\
 RMR &= 40 \lg(E_m) + 10 & E_m < 10GPa
 \end{aligned}
 \quad (1)$$

According to academic documents and many engineering projects, it proves that RMR well fits the rock mass classification of "Code for design on tunnel of railway" (TB10003-2005). Therefore we could calculate the degraded E of rock mass and RMR, affected by stress field change after the excavation disturbance, to adjust the rock mass classification based on SMRM.

Without the consideration of fissure water pressure, elastic modulus ratio of rock mass in SMRM can be defined by (Wu Faquan, 1993):





$$\frac{E_m}{E} = \begin{cases} \frac{1}{1 + \frac{32(1-\nu^2)}{\pi(2-\nu)} \sum_{p=1}^m \lambda \bar{a}^2 \sin^2 \delta} & \text{under pressure} \\ \frac{1}{1 + \frac{32(1-\nu^2)}{\pi(2-\nu)} \sum_{p=1}^m \lambda \bar{a} [(2-\nu) \cos^4 \delta + \sin^2 \delta]} & \text{under tensile} \end{cases} \quad (2)$$

where:  $E$  (MPa) and  $\nu$  are elastic modulus and Poisson's ratio of rock mass respectively;  $m$  is the number of structure plane;  $E_m$  is the elastic modulus of structure plane  $m$ ;  $\lambda$  (1/m),  $\bar{a}$  (m) are the normal density and radius of structure plane  $m$ ;  $\delta$  is the included angle of stress direction or survey line and normal direction of structure plane  $m$ .

**Results**

In the condition of all possible combination sets of the three preferred structure planes after excavation, the elastic modulus ratio of rock mass presents strong anisotropy and degradation. In different directions, the elastic modulus of rock mass fluctuate obviously. The phenomenon of strong anisotropy and degradation of elastic modulus proves to the degradation of rock mass quality, easy to occur deformation and failure.

**Table 2. Rock Mass Classification based on SMRM**

Rock type	J1+J2	J1+J3	J2+J3	J1+J2+J3
Max. of $E_m/E$	0.714	0.669	0.720	0.010
Min. of $E_m/E$	0.031	0.030	0.016	0.003
Max./Min. of $E_m/E$	23.409	22.026	45.904	3.722
Mean of $E_m/E$	0.287	0.373	0.319	0.005
Standard Deviation of $E_m/E$	0.198	0.186	0.247	0.001
Coefficient of Variation of $E_m/E$	69.0%	49.7%	77.4%	27.9%
RMR	54.613	54.457	28.016	<20
Rock Mass Classification	III	III	IV	V

**Conclusion**

There is no certain relationship between degradation and anisotropy of rock mass. The rock mass was good of level II before excavation. However, during excavation, the structure plane in rock mass will develop and the cohesive force will lost dramatically. The state of rock structure made great effect on the rock mass quality. According to the SMRM analysis, in the different developed structure plane combinations, such as J1+J2, J1+J3, J2+J3 and J1+J2+J3, the corresponding rock mass classifications are not the same, such as III, III, IV and V respectively.

Based on the SMRM, the rock mass classification could be carried out, considering the affecting by different structure plane combinations and development. And the matched engineering treatment measures will be put into effect properly.

**REFERENCES**

WU Faquan, 1993. Principle of statistic rock mass mechanics. Wuhan. China University of Geosciences Press.  
 Bieniawski, Z.T., 1973. Engineering classification of jointed rock masses. Trans. S.Afr. Inst. Civ.Eng.15, 335-344  
 Bieniawski, Z.T., 1979. The geomechanics classification rock engineering applications. Proc. 4th Int. Congr. Rock Mech., ISRM, Montreux, vol.2, 41-48  
 Bieniawski, Z.T., 1989. Engineering rock mass classification.: Jhon Wiley & Sons. New York, 272 p

## European soil classification system based on cone penetration test (CPT) results

Lovorka Librić<sup>1</sup>, Meho Sasa Kovačević<sup>1</sup>

<sup>1</sup>University of Zagreb, Faculty of Civil Engineering, Croatia, [lilibric@grad.hr](mailto:lilibric@grad.hr), [msk@grad.hr](mailto:msk@grad.hr)

### Introduction

European soil classification system for engineering purposes was developed according to EN ISO 14688-2:2018 in order to increase the quality, safety, reliability, efficiency, compatibility, and communication between experts in the field of geotechnics (Kovačević and Jurić Kačunić, 2013; Kovačević et al., 2018). For soil classification, laboratory testing of particle size distribution of soil and consistency limits should be carried out. Cone penetration test (CPT) is a simple, quick and economic test that enables obtaining continuous data on soil by depth. The basic principle of the CPT is pushing a specially designed probe into the ground at a controlled rate, with constant measuring of the penetration resistance at the tip of the probe ( $q_c$ ) and friction of the probe sleeve ( $f_s$ ), activated upon pushing of the probe between the sleeve and the surrounding ground. Soil classification, i.e. determining soil profile and identifying separate layers of the soil, represents one of the most important applications of cone penetration test (CPT) in geotechnical engineering. Soil parameters used in laboratory classifications are relatively well-connected to mechanical behaviour of soil (Kovalrvić, et al., 2019). For all parameters, correlations with CPT results have been developed based on available research and literature (Librić et al., 2016).

### Methods

Robertson (2009) suggests using  $I_c$  to prepare statistical correlations of CPT results and physical-mechanical properties of soil whenever possible. New local correlations were developed between soil behaviour type index  $I_c$  and percentage of fine particles  $FC$ , liquid limit  $w_L$  and plasticity index  $I_P$  for the following locations: Biđ-Bosut Field irrigation canal, Ilok port, Krsišće landslide, Mirogoj landslide and Krematorij landslide. The researched locations cover the entire area of northern Croatia. A summary database of 216 pairs of laboratory testing and CPT results was created. Two neural networks were developed: *netFC* for predicting the percentage of fine particles  $FC$  and *netwlp* for predicting the liquid limit  $w_L$  and plasticity index  $I_P$  (Reale et al., 2018). Verification of new correlations and developed neural networks (*netFC* and *netwlp*) using the database for northern Croatia was carried out on the example of Veliki vrh landslide. The database consists of 19 pairs of laboratory testing and CPT results.

### Results

The comparison of the application of new correlations and neural networks on the Veliki vrh landslide shown that the obtained regression values of measured and predicted  $FC$ ,  $w_L$  and  $I_P$  were significantly high ( $R > 0.98$ ). The difference between average absolute errors between new correlations and neural network was extremely small (0.73% for  $FC$ , 1.09% for  $w_L$  and 0.47% for  $I_P$ ). The very good efficiency of soil classification according to European soil classification system (ESCS) is achieved with new correlations (74%), whereas slightly better efficiency was achieved with neural networks (89%). Given that the Veliki vrh landslide is also located in northern Croatia, the existing database was supplemented with additional 19 samples, totalling 235 pairs of results of laboratory and CPT testing. New correlations with accompanying regression values and appropriate soil behaviour index  $I_c$  ranges were developed (Table 1).

**Table 1. New correlations for soil classification using CPT testing in the territory of northern Croatia**

Correlation	R	$I_c$
$FC = 6.8673 \cdot I_c^2 + 18.057 \cdot I_c - 43.277$	0.9676	1.402 – 3.389
$w_L = 18.334 \cdot I_c^2 - 67.079 \cdot I_c + 86.631$	0.9029	2.126 – 3.389
$I_p = 16.109 \cdot I_c^2 - 65.783 \cdot I_c + 79.428$	0.8607	2.126 – 3.389

### **Conclusion**

From an engineering perspective, the insignificant difference between the average absolute error of the prediction of percentage of fine particles  $FC$ , liquid limit  $w_L$  and plasticity index  $I_p$  between the new correlations and neural networks, justifies the application of the new correlations on the territory of northern Croatia and strongly confirms that soil type behaviour index  $I_c$  should be used to modify the empirical correlations that change depending on soil type and that  $I_c$  should be used to prepare statistical correlations whenever possible. Development of soil classification procedures based on results of cone penetration test can be achieved by development of neural network and software support for direct connection of test results with particle size distribution and consistence limits which are used in standard soil classifications. European soil classification system based on CPT results, applied to new projects in the future, will enable their further development.

### **REFERENCES**

- Kovačević, M. S., Gavin, K., Reale, C., Librić, L., Jurić Kačunić, D., 2019, Developing correlations between the soil fines content and CPT results using neural networks, Proceedings of the XVII ECSMGE-2019, Reykjavik, 244
- Kovačević, M. S., Jurić-Kačunić, D., 2014, European soil classification system for engineering purposes, *Građevinar*, 66 (9), pp. 801-810
- Kovačević, M. S., Jurić-Kačunić, D., Librić, L., Ivoš, G., 2018, Engineering soil classification according to EN ISO 14688-2:2018, 70 (10), pp. 873-879
- Librić, L., Jurić-Kačunić, D., Kovačević, M. S., 2017, Application of cone penetration test (CPT) results for soil classification, *Građevinar*, 69 (1), pp. 11-20
- Reale, C., Gavin, K., Librić, L., Jurić-Kačunić, D., 2018, Automatic classification of fine-grained soils using CPT measurements and Artificial Neural Networks, *Advanced Engineering Informatics*, 36 (2018), pp. 207-215
- Robertson, P.K., 2009, Interpretation of cone penetration tests - a unified approach, *Canadian Geotechnical Journal*, 49 (11), pp. 1337-1355



## Internal erosion study of wide grading loose soil based on microscopic pore distribution

Yanzhou Yin<sup>1,2</sup>, Yifei Cui<sup>3\*</sup>, Chaoxu Guo<sup>4</sup>, Yao Jiang<sup>1</sup>

<sup>1</sup>Key Laboratory of Mountain Surface Process and Hazards/Institute of Mountain Hazards and Environment, Chinese Academy of Sciences, China

<sup>2</sup>University of Chinese Academy of Sciences, China

<sup>3</sup>State Key Laboratory of Hydrosience and Engineering, Tsinghua University, China,  
[yifeicui@mails.tsinghua.edu.cn](mailto:yifeicui@mails.tsinghua.edu.cn)

<sup>4</sup>Fujian Academy of Building Research, Fujian Key Laboratory of Green Building Technology, China

\*Corresponding author

Wide grading loose soil (WGLS) is the main constituent part of hillslope deposits formed after earthquake in mountain areas. The spatial distribution of pore structure provides hydraulic conditions for the migration of fine particles during rainfall infiltration. When a considerable number of fine particles are eroded from upper soil layer, fine particles were observed to accumulate in a certain layer of the slope toe and form a relatively impermeable layer. Subsequently, shallow failure or debris flow will be initiated from this layer as a result of increasing pore pressure and the reduction of effective stress. Despite a large number of previous researches using macro-scale methods such as traditional seepage test, mid-scale flume test, and centrifuge test to study the process of fine migration, strategies for understanding the migration characteristics and mechanics of fines in this soil based on micro scale are still challenging. Therefore, in the present study, WGLS samples were firstly collected from the Subao River Basin, near Leigu Town in Sichuan Province, China. The samples were then scanned by scanning electron microscope (SEM) to obtain the 2D images of microscopic pore structure. Statistical analyses were performed on pore size distribution. In addition, the discrete element method (DEM) coupling lattice Boltzmann method (LBM) was used to analyze the effect of pore diameter distribution based on those 2D images on the migration of fines. The drag force calculation method of single particle and rebound boundary were adopted to solve the interaction between particles and fluid. The number ratios of pores with different sizes were set according to the pore size distribution curve. Compared with the traditional well graded soil, such as loess data with pore size distribution in accordance with normal distribution with the single peak at 13.5  $\mu\text{m}$ , WGLS samples give the bimodal peak distribution at 12  $\mu\text{m}$  and 72  $\mu\text{m}$ . Affected by the ratio of pore diameter and particle, jamming was likely to occur at the position where the pore diameter was small. With the increase of small-sized pores, the number of fine particles eventually trapped increase. The ratios of this value to the number of initial particles were 0.0089, 0.0293, 0.0383 at 0.26 s for the three samples. Pore pressure calculated from numerical simulation indicated that pore jamming increased the water pressure difference between the pore inlet and outlet and increased the fluid flow velocity through the surrounding pores. This result indicated a high probability of subsequent slope failure. In conclusion, the increase in the number of small-sized pores led to the pores being easily blocked. However, the flow field was beneficial to reduce the probability of jamming. This research is of significance for explaining the shallow layer damage of coarse-grained soil and the anti-seepage design of earth-rock dam.





## REFERENCES

- Guo, C., and Cui, Y., 2020, Pore structure characteristics of debris flow source material in the Wenchuan earthquake area. *Engineering Geology*, 267, 105499
- Cui, Y., Jiang, Y., and Guo, C. 2019, Investigation of the initiation of shallow failure in widely graded loose soil slopes considering interstitial flow and surface runoff. *Landslides*, 16(4), 815-828
- Cui, Y., Zhou, X. J., and Guo, C. X., 2017, Experimental study on the moving characteristics of fine grains in wide grading unconsolidated soil under heavy rainfall. *Journal of Mountain Science*, 14(3), 417-431
- Guo, X., Cui, P., Li, Y., Zhang, J., Ma, L., and Mahoney, W.B., 2015, Spatial features of debris flows and their rainfall thresholds in the Wenchuan earthquake-affected area. *Landslides*, 13(5), 1215-1229
- Cui, P., Guo, C., Zhou, J., Hao, M., and Xu, F., 2014, The mechanisms behind shallow failures in slopes comprised of landslide deposits. *Engineering Geology*, 180, 33-44
- Yin, Y., Cui, Y., Liu, D., and Lei, M., 2019, Study on Microscopic Process of Fine Particle Migration in Loose Soil. *Advanced Engineering Sciences*, 051(004), 21-29 (in Chinese with English abstract)

## Deep and remote monitoring approaches of large slope instabilities in Upper Graveglia Valley (Ligurian Apennine, Italy)

Danilo Godone<sup>1</sup>, Paolo Allasia<sup>1</sup>, Marco Baldo<sup>1</sup>, Davide Notti<sup>1</sup>, Giorgio Lollino<sup>1</sup>, Francesco Faccini<sup>2</sup>,  
Franco Marco Elter<sup>2</sup>, Federico Mantovani<sup>2</sup>, Flavio Poggi<sup>3</sup>

<sup>1</sup>CNR-IRPI, Institution, Italy, [danilo.godone@irpi.cnr.it](mailto:danilo.godone@irpi.cnr.it), [paolo.allasia@irpi.cnr.it](mailto:paolo.allasia@irpi.cnr.it), [marco.baldo@irpi.cnr.it](mailto:marco.baldo@irpi.cnr.it),  
[davide.notti@irpi.cnr.it](mailto:davide.notti@irpi.cnr.it), [giorgio.lollino@irpi.cnr.it](mailto:giorgio.lollino@irpi.cnr.it)

<sup>2</sup>DISTAV, University of Genova, Italy, [francesco.faccini@unige.it](mailto:francesco.faccini@unige.it), [franco.elter@unige.it](mailto:franco.elter@unige.it),  
[kurgioserver@gmail.com](mailto:kurgioserver@gmail.com)

<sup>3</sup>Regione Liguria, Institution, Italy, [flavio.poggi@regione.liguria.it](mailto:flavio.poggi@regione.liguria.it)

Landslides in mountain environment are frequent and constitute one of the main issues among natural hazards. The recognition of processes characterizing slope, and particularly large, slope instabilities deserve a multidisciplinary approach in order to better comprehend their dynamic. The new techniques, e.g. remote sensing, have allowed, in recent years, to develop reliable methodologies to identify these phenomena, which can present different degrees of hazard and therefore of risk for the inhabited areas and infrastructures. On the other hand, the update of conventional technique, e.g. deep measurement, may improve the knowledge of the phenomena by a different point of view, thus assuring a comprehensive analysis.

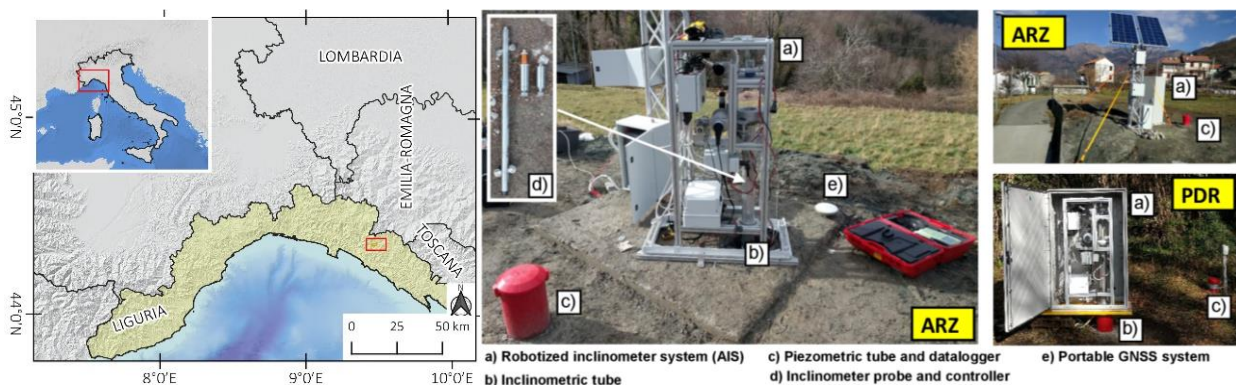


**Figure 1. Study area location and AIS instrumented sites**

The investigated phenomenon is located in Upper Graveglia Valley (Liguria, Northwestern Italy) and involves several roads, infrastructures and the hamlets of Arzeno (ARZ) and Prato di Reppia (PDR) - Genova Province (Figure 1). The area is classified as “very high geomorphological hazard area” by different planning regulations and well known in the scientific community (e.g. Brandolini et al, 2007). Since 2018 a monitoring network was set up with the aim of measuring surficial and deep displacements in order to plan mitigation action and improve its understanding. In the hamlets geo-gnostic activity was carried out and 2 inclinometers and 2 piezometers (coupled) were installed. In, approximately, the first two years an automatic inclinometer system (AIS) - which is described in details in Allasia et al, 2018 - was firstly installed in the ARZ borehole, as the site was considered the most active one and closer to the settlements. Then since January 2020, when the site kinematic was clearly established, the AIS was moved to the PDR one, where, previously, quarterly manual measurement were carried out. The AIS provided high frequency (2 measurements/day) measurement of the deep displacement. In addition to the deep-seated measurements, to make a robust crosscheck, a periodic GNSS monitoring, with the same frequency of manual inclinometer one, was planned with 2 benchmarks located in proximity to the boreholes and a third one located in the upslope sector (Passo del Biscia) of the landslide. In

order to reconstruct the past behaviour of the landslide, PS-InSAR time series covering the timespan 1992-2014, was analysed (Béjar-Pizarro et al. 2017). In January 2019 a helicopter-borne LiDAR survey of the area was carried out for a better three-dimensional description of the whole site, too.

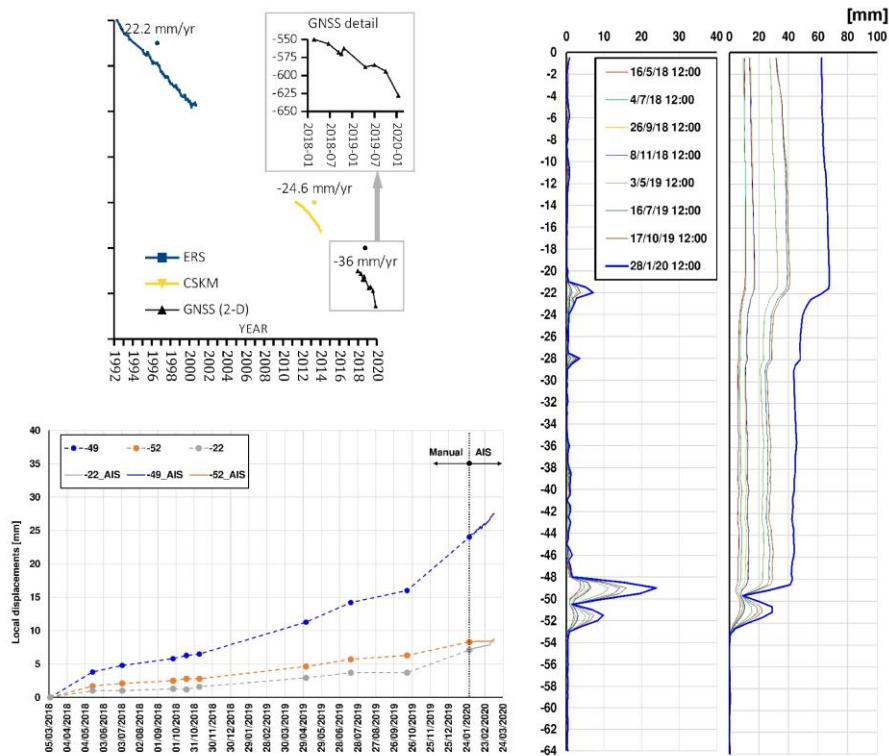


**Figure 2. Results of different approaches in PDR site: instrumental cross check (top left), inclinometer time series (bottom left), inclinometer local and cumulated displacements (right)**

The analysis of “historical” PS-InSAR data and the current monitoring datasets are in good agreement resulting in an average displacement of 27 mm/year for the investigated period. Moreover, surficial and deep measurements provide the same order of magnitude thus confirming the importance of an integrated approach in order to provide reliable results (Figure 2). Concerning the use of AIS, it provided an added value as it allowed to intensify deep measurements frequency and assure a better description of landslide behaviour. In the investigated case the main sliding surface was located at -49 meters and according to these preliminary observations an acceleration trend is observable.

**REFERENCES**

Allasia, P., Lollino, G., Godone D., Giordan D., 2018. Deep displacements measured with a robotized inclinometer system. Proceedings of the 10th International Symposium on Field Measurements in Geomechanics, Rio de Janeiro, Brasil, July 2018

Béjar-Pizarro, M., Notti, D., Mateos, R.M., Ezquerro, P., Centolanza, G., Herrera, G., Bru, G., Sanabria, M., Solari, L., Duro, J. and Fernández, J., 2017. Mapping vulnerable urban areas affected by slow-moving landslides using Sentinel-1 InSAR data. Remote Sensing, 9(9), p.876

Brandolini, P., Canepa G., Faccini, F., Robbiano, A., Terranova R. 2007. Geomorphological and geo-environmental features of the Graveglia Valley (Ligurian Apennines, Italy). Geografia Fisica e Dinamica Quaternaria. 30. 99-116

## Sandstone Intact Rock Strength. The use of compressive strength parameters for large tunnel design. A focus on the comparison between uniaxial and triaxial laboratory tests

Lorenzo Paolo Verzani<sup>1</sup>, Giordano Russo<sup>1</sup>

<sup>1</sup>GEODATA Engineering, Italy, [lpv@geodata.it](mailto:lpv@geodata.it), [grs@geodata.it](mailto:grs@geodata.it)

A complex hydropower project, with many underground structures, requires lot of investigations and studies for a whole understanding of the rock mass proprieties and behaviours during construction. A recent large underground project in Andean Cordillera, offers opportunity for a focus on the comparison between the laboratory data obtained from uniaxial and triaxial compressive tests on sandstone samples, with main reference to the Hoek-Brown failure criterion. The availability of tens of confined compressive strength tests ( $\rightarrow \sigma_{ci}$ ) on sandstone and their analysis through many rupture envelopes are of interest for a better understanding on the results of the laboratory data, possibly affected by different behaviour of the rock samples when tested through the unconfined compressive test ( $\rightarrow$  UCS). The sharp difference between the Hoek-Brown strength criterion parameter  $\sigma_{ci}$  and the UCS parameter is shown.

The intact rock strength is a parameter that strongly influence the characterization of the rock mass with a direct consequence on tunnelling design. Bewick et Al. (2015) and Kaiser (2016) focused on the conceptual difference between UCS and the Hoek-Brown parameter  $\sigma_{ci}$  derived by fitting in the main stresses plane the results of triaxial compressive tests. Moreover, the same Authors recommended the basic reference to  $\sigma_{ci}$  while indicating the Hoek-Brown failure envelope for the design. By the analysis of the data obtained from the Lab tests, some differences have been observed among the sandstone samples collected close to river area and those collected deeper inside the slope, to investigate the cavern area (Figure 1).

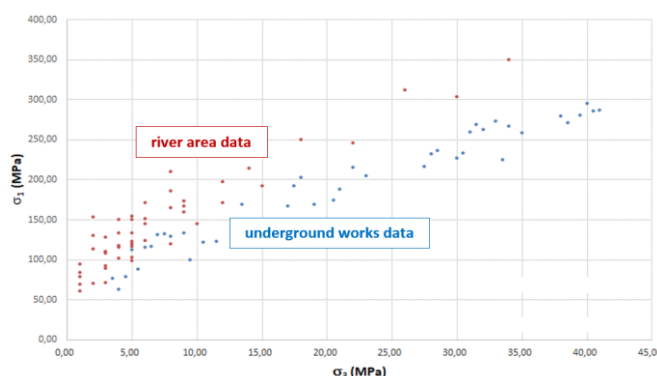


**Figure 1. Triaxial Test Data from different project areas**

The UCS data have a too high range of variability (~10 to 65 MPa), since many factors as the failure mechanism and testing procedure significantly affects the strength-values. By the comparison between the results of the compressive strength obtained from the UCS and the Triaxial tests ( $\rightarrow \sigma_{ci}$ ) a clear difference is observed ( $UCS \ll \sigma_{ci}$ ). Moreover, considering the different trends  $\sigma_1/\sigma_3$  obtained from the samples collected in different sites (river area and underground structures), the triaxial data have been analysed separately.

N. 91 triaxial tests are available, according to the Hoek-Brown failure-criterium, the intact rock parameter “ $m_i$ ” (material constant) and “ $\sigma_{ci}$ ” (compressive strength,  $\sigma_3=0$ ) are thus calculated (RocLab, by Rocscience).

### River area

- N. 50 TX-tests ( $1 < \sigma_3 < 34$  MPa)



- $m_i$  18 (14-22)
- $\sigma_{ci}$  90 (70-110) MPa.

Underground work sectors

- N. 41 TX-tests ( $4 < \sigma_3 < 41$  MPa)
- $m_i$  23±1 (22-24)
- $\sigma_{ci}$  65 (50-80) MPa.

The average  $\sigma_{ci}$  value, between 90 MPa and 65 MPa, is the value obtained from the analysis of all the n. 91 TX-tests plus one sound and representative UCS value (Figure 2):

- $m_i$  18.5
- $\sigma_{ci}$  77.8 MPa.

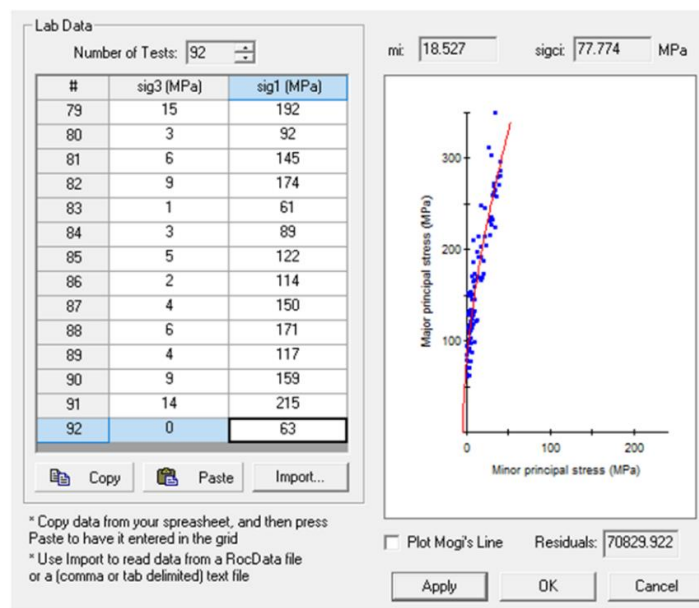


**Figure 2. Triaxial Test Data from different project areas.**

In the frame of the discussed data analysis, we observe that the values of the rock mass strengths ( $\sigma_c$  and  $\sigma_{cm}$ ) obtained with the average value of UCS=30MPa without a Disturbance Factor ( $D=0$ ), are close to those obtained applying the Disturbance Factor ( $D=1$ ) with  $\sigma_{ci}=65$ .

**REFERENCES**

Hoek, E., Carranza Torres C., Corkum B., 2002 Edition. Hoek-Brown failure criterion.

Hoek, E. and Diederichs, M. S., 2005. Empirical estimation of rock mass modulus. Internal Journal of Rock Mechanics and Mining Sciences 43 (2006): 203–215.

RocLab 2007 Rocscience Inc. Rock mass strength analysis using the Hoek-Brown failure criterion. User's Guide.

Kaiser P. K., December 2008. Rock mechanics challenges in underground construction and mining. ACG Australian Centre for Geomechanics, Volume No.31.

Bewick R.P., Amann F., Kaiser P. K., Martin C. D., ISRM Congress 2015 Proceedings. Symposium on Rock Mechanics. ISBN:978-1-926872-25-4. Interpretation of UCS test results for engineering design.

Kaiser P. K., 2016. Challenges in rock mass strength determination for design of deep underground excavations. Laurentian University, ISRM.

McQuarrie N., Horton B.K., Zandt G., Beck S., Decelles P., 2005. Lithospheric evolution of the Andean fold-thrust belt, Bolivia, and the origin of the Central Andean Plateau. Tectonophysics. 399. 15-37.

## Implications for TBM performance based on rock mass observations for the Blue Lias Formation

Sarah Sissins<sup>1</sup>, Dr. Chrysothemis Paraskevopoulou<sup>2</sup>

<sup>1</sup>Graduate Engineering Geologist, Jacobs, United Kingdom, [sarah.sissins@jacobs.com](mailto:sarah.sissins@jacobs.com)

<sup>2</sup>Assistant Professor, School of Earth and Environment, University of Leeds, UK,  
[c.paraskevopoulou@leeds.ac.uk](mailto:c.paraskevopoulou@leeds.ac.uk)

The Blue Lias Formation (BLI) is characterized by its layered rock mass, comprising of very strong limestone, interbedded with weak mudstone and shales (Hobbs et al. 2012). The differences in strength presents a challenge for tunnelling performance prediction, mistakes adversely affecting both time and costs (Paraskevopoulou and Benardos, 2013). This study aims at characterizing the rock mass, identifying implications for Tunnel Boring Machine (TBM) performance. Hinkley Point C (Figure 1.a) marine works was motivation for focusing on the BLI of the Bristol Channel Basin. The study provides a holistic methodological approach to be followed in the case of predicting TBM performance in similar heterogenous, layered rock masses.

The approach taken is two-fold. Firstly, the BLI is characterized by evaluating geotechnical properties and mechanical behaviour based on fieldwork observations (Figure 1.b) and laboratory testing results (Figure 1.c). Fieldwork was carried out in three localities, across S. Wales and Somerset. Secondly, the results are assessed with regards to TBM performance, with a focus on penetration rate, which is the distance mined during continuous boring (m/hr). TBM penetration rate is assessed by applying suitable pre-existing empirical models (Table 1). However, currently no models address the issue of parameter selection for heterogenous rock masses comprising of layers with different rock strengths (Marinos, 2019). Within this study, a bespoke weighting system proportional to the percentage of limestone present in the face is proposed.

The field and laboratory testing confirm the expected strength difference between the mudstone / shale and limestone, where the limestone is generally strong to very strong and the mudstone is very weak to strong, which is challenging for tunnelling performance prediction. A summary of the laboratory testing and rock mass classification results is given in Table 2. From results and relevant literature, geological (Figure 1.d) and geotechnical (Figure 1.e) models are developed, and four ground types (GTs) determined, distinguished primarily by GSI and limestone percentage (Table 2). The distinguishable geological members with the BLI are allocated GTs (Figure 1.e). Implications of findings for TBM performance are assessed, with a focus on penetration and utilization rate. The outcomes vary according to the model (Figure 1.g1), for the Hassanpour (2009) model the anticipated penetration rate decreases with increased limestone in the face, as expected. Whilst for other models, penetration rate is found to be insensitive to ground type, limited instead by machine restrictions. GT4 has the lowest Utilization (U-)values (Figure 1.g2), given the weaker rock mass requiring more support. For a 50m excavation the U-value does not vary much (between 42.5 to 45%), showing that stress has a greater influence than UCS for this model. At higher stresses (e.g. 200m), the effect of UCS variation is notably more pronounced.

Finally, the presented research work can be used as a guide to give a good indication and an approach to assess TBM performance in heterogeneous rock masses reducing the risk of cost and time overruns. There is a gap in the literature for a more complex method to be developed, which should be verified by laboratory cuttability tests.

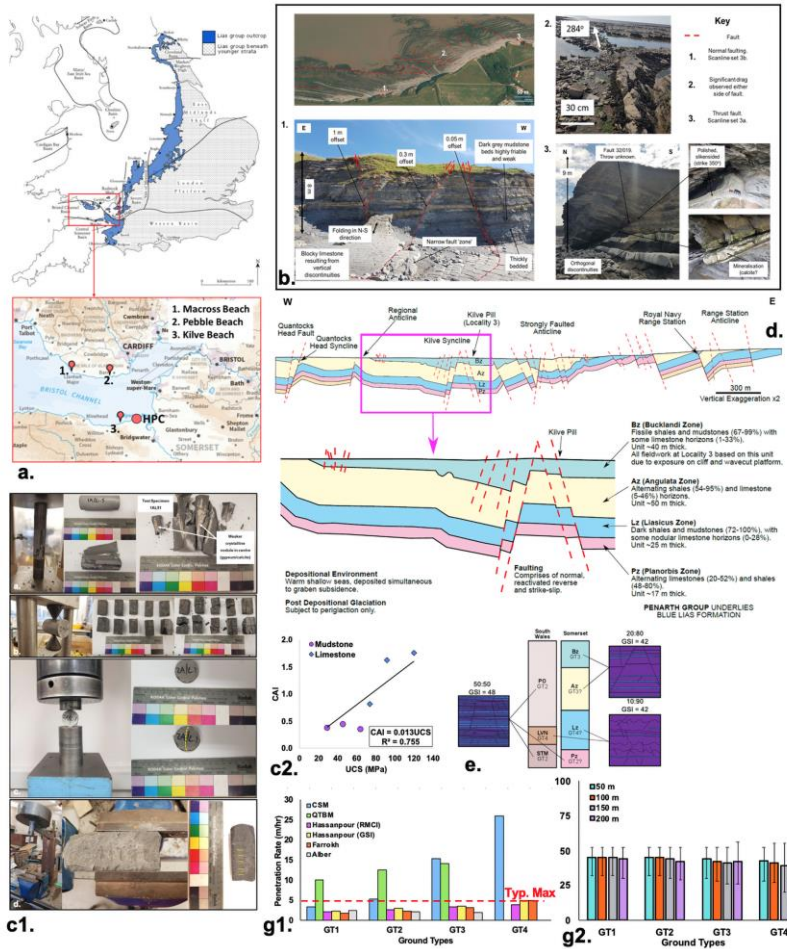


**Table 1. Penetration Rate (PR) Models**

Penetration Rate (PR) Model & Geotechnical Input	Empirical Formula	Advantages	Limitations and Comments
Farrakh (2013)	$PFR = 5 \times 10^{-17} + 0.0003 \cdot RQD + 0.533 \cdot CAI + 0.0008 \cdot UCS$	Simple. Based on a large data set. Considers rock mass and abrasivity. In this model UCS is the most controlling parameter.	Joint spacing and condition not considered. The statistical correlation seems overly simplistic.
RBD, CAI, UCS	$PFR = \frac{RQD \cdot CAI \cdot UCS}{1000}$	Simple input parameters (easily obtained). Model developed based on tunnel in layered dark shales, grey shales and argillaceous limestone with jointing characteristics.	Lack of acknowledgment of varying strength between layers for determination of the UCS input value. Limited dataset from Nowsood water conveyance tunnel.
Hassanpour et al. (2009)	$PFR = \frac{RQD \cdot CAI \cdot UCS}{1000}$	Simple input parameters (easily obtained). Model developed based on tunnel in layered dark shales, grey shales and argillaceous limestone with jointing characteristics.	Lack of acknowledgment of varying strength between layers for determination of the UCS input value. Limited dataset from Nowsood water conveyance tunnel.
UCS, RQD or GSI	$PFR = \frac{RQD \cdot CAI \cdot UCS}{1000}$	Simple input parameters (easily obtained). Model developed based on tunnel in layered dark shales, grey shales and argillaceous limestone with jointing characteristics.	Lack of acknowledgment of varying strength between layers for determination of the UCS input value. Limited dataset from Nowsood water conveyance tunnel.

**Table 2. Geotechnical design parameters based of GTs**

Ground Type	Type 1 (GT1)	Type 2 (GT2)	Type 3 (GT3)	Type 4 (GT4)
<b>Schematic Representation</b> (see Table 16 for descriptions)				
<b>Key Parameters with ranges given in [] (values in red have been estimated based on engineering judgement)</b>				
UCS <sub>max</sub> [MPa]	106 [80-152]	106 [80-152]	39-101 [7-3]	39-101 [7-3]
UCS <sub>min</sub> [MPa]	15 [4-7]	15 [4-7]	1-54 [1-7]	1-54 [1-7]
UCS <sub>avg</sub> [MPa]	72-142 [9-7]	61 [4-103]	9-63 [2-7]	5-59 [1-6]
BTS [MPa]	12 [10-15]	12 [10-15]	10 [9-11]	10 [9-11]
BTS [Mdst] [I]	5 [4-7]	5 [4-7]	5 [1-7]	1 [1-7]
BTS [MPa] Weighted Average	11 [9-14]	9 [7-11]	6 [3-8]	2 [0.5-8]
CAI [-] Weighted Average	1.6 [0.3-1.8]	1.0 [0.3-1.8]	0.6 [0.3-1.8]	0.5 [0.3-1.8]
RQD [%]	95 [90-100]	90 [80-100]	82.5 [68-97]	25 [0-50]
GSI [-]	80 [55-95]	48 [45-50]	42 [35-48]	33 [25-40]
Q [-]	4.85 [3-6.7]	2.4 [1.8-3]	1.9 [1.8-3]	n/a
RMR [-]	61-77 [7-5]	48-67 [5-5]	34-67 [5-4]	n/a
Discont. Spacing [m]	0.10-4.30 [0.72]	0.01-4.30 [0.53]	0.01-1.99 [0.22]	n/a
JRC [-]	8-10	0-10	0-10	n/a
Discont. Persistence [m]	0.04->100	0.04->100	0.05->100	n/a
<b>Determined Parameters (derived using Rocdata of Rocscience for tunnel depth of 50 m)</b>				
UCS <sub>rock mass</sub> [MPa]	10	3	1	0.4

Figure 1. a) Lias Group and position of field localities (modified Simms et al. 2004) and BGS (2015); HPC=Hinkley Point C; b) Field work at Locality 3; c) Lab Testing and results; d) Geological model; e) Geological stratigraphy and corresponding to Ground Types and g) Penetration rate and Utilization rate results

**REFERENCES**

Hassanpour, J., Rostami, J., Khamsehchiyan, M. and Bruland, A. 2009. Developing new equations for TBM performance prediction in carbonate-argillaceous rocks: A case history of Nowsood water conveyance tunnel. *GEOMECH ENG.* 4(4), pp.287–297.

Hobbs, P.R.N., Entwisle, D.C., Northmore, K.J., Sumbler, M.G., Jones, L.D., Kemp, S., Self, S., Barron, M. and Meakin, J.L. 2012. Engineering Geology of British Rocks and Soils-Lias Group. *BGS Internal Report.*, p.323.

Marinos, V. 2019. A revised, geotechnical classification GSI system for tectonically disturbed heterogeneous rock masses, such as flysch. *B ENG GEOL ENVIRON.* 78(2), pp.899–912.

Paraskevopoulou, C., Benardos, A. 2013. Assessing the construction cost of tunnel projects. *Tunnelling and Underground Space Technology Journal*, 38(2013), 497–505.

## The effect of schistosity on the uniaxial compressive strength of metamorphic rocks of northern Greece

Athanasia X. Liouka<sup>1</sup>, Thomas Makedon<sup>1</sup>, Anastasios Tsirikis<sup>1</sup>

<sup>1</sup>Aristotle University of Thessaloniki, Greece, [acliouka@geo.auth.gr](mailto:acliouka@geo.auth.gr), [thomas@geo.auth.gr](mailto:thomas@geo.auth.gr), [tsirikika@geo.auth.gr](mailto:tsirikika@geo.auth.gr)

### **Background**

The Uniaxial Compressive Strength (UCS) of metamorphic rocks with layered or banded structure, foliation or schistosity is affected by the direction of loading in respect to the orientation of these structural features. The design of many small as well as large scale construction works depends on the strength parameters and it is therefore essential that this effect is considered. Well known failures such as the Malpasset dam failure in France (1959) in which the orientation of the gneiss' schistosity contributed to the failure are examples of the poor understanding of this effect. Metamorphic rocks are abundant in Northern Greece affecting the majority of major construction works. The majority are gneisses, schists and marbles of Paleozoic and Mesozoic age.

### **Methods**

The Uniaxial Compression Test is used to derive the compressive strength by applying axial load to an intact unconfined cylindrical specimen. It represents the maximum compressive stress ( $\sigma_c$ ) that the specimen can sustain at failure under zero confining stress. The present paper contains results for samples of metamorphic rocks collected from locations of Serbo-Macedonian and Circum-Rhodope zones. More specifically gneiss and greenschist samples, slightly to moderately weathered were from Stavros and Agios Pavlos, Thessaloniki. The samples were cut in pairs for the conduction of the tests perpendicular and parallel to the observed schistosity. The tests were carried out according to ASTM D2938 - 95 in the Laboratory of Geomechanics, Department of Environmental Engineering, International Hellenic University.

### **Results**

Figure 1 shows the test results for two specimens from a greenschist sample from Agios Pavlos. The specimens were cut and loaded parallel and perpendicular to the schistosity respectively. The measured unconfined compressive strength of the specimens was 116,17 MPa and 174,39 MPa respectively (strength reduction 33,4%). The total number of tested samples was 6. On average, there was a 48,8 % reduction in gneiss' strength and a 33,3% reduction in schist's strength when they were loaded parallel to the observed schistosity (Table 1 includes results from 4 samples).

The diagrams axes represent axial stress (MPa) and axial strain (D/l, %) respectively. Initially, the curves are concave upwards, as some pores and small cracks in the rock close. The UCS is the peak value of the diagram, where the sample fails.

**Table 1: Test results for the UCS of the sample pairs tested**

SAMPLE PAIRS	LOCATION	WEATHERING	UCS (MPa)		REDUCTION %
			Specimen 1 (Parallel)	Specimen 2 (Perpendicular)	
1	Agios Pavlos	Moderate	78,56	120,83	34,9
2	Agios Pavlos	Slight	116,17	174,39	33,4
3	Agios Pavlos	Slight	119,77	174,39	31,3
4	Stavros	Moderate	77,58	151,61	48,8



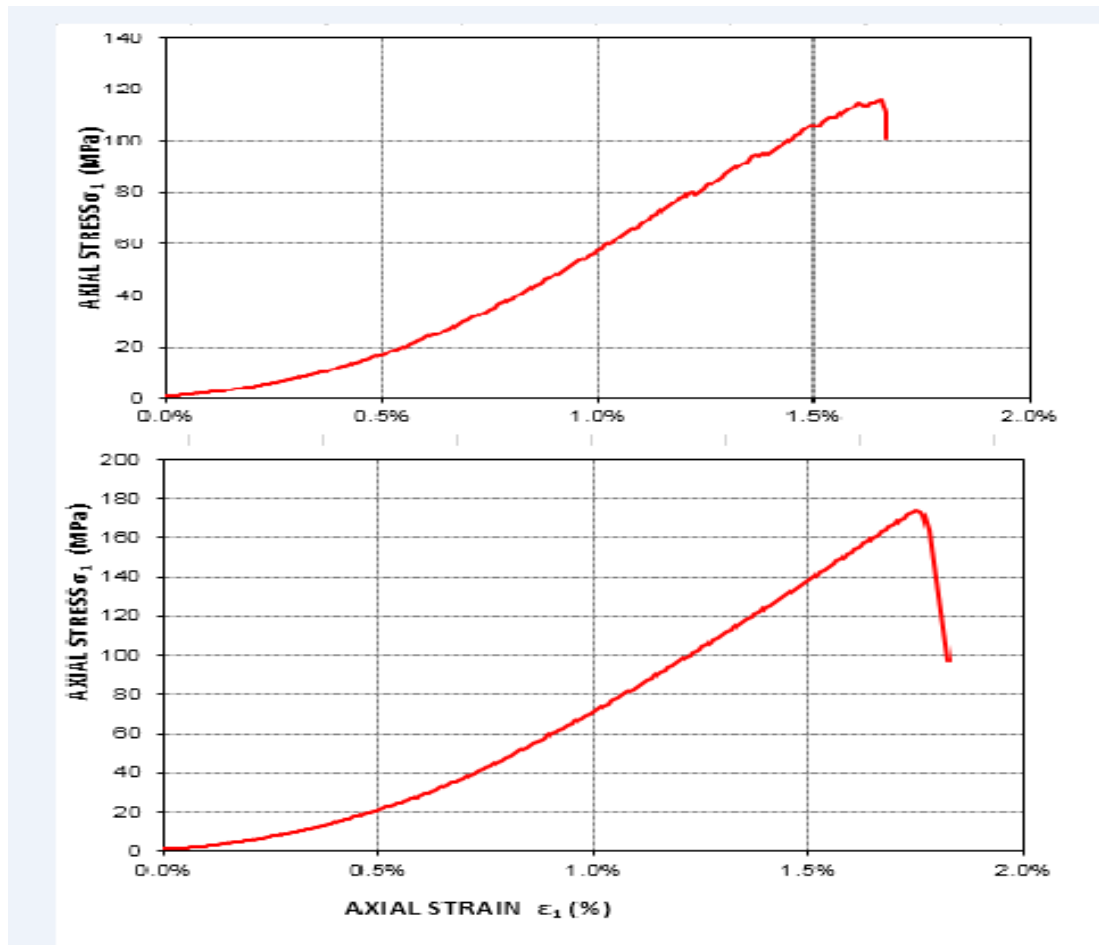


Figure 1. Stress – strain diagrams for sample pair 2

**Conclusions**

Although a relatively small number of samples was tested there is a clearly observed decrease in uniaxial compressive strength ranging between 31,31 % and 48,8% for specimens loaded parallel to the observed schistosity.

Sample pairs 1 and 4 present different degrees of weathering and the respective results suggest that a combination of the degree of weathering with the orientation of schistosity should be further investigated. From the tested samples there is an observed indication that weathering affects the reduction of strength as expected.

**REFERENCES**

ASTM (2002). Standard Test Method for Unconfined Compressive Strength of Intact Rock Core Specimens  
 P. Londe, The Malpasset dam failure, Engineering Geology, Volume 24, 1987, Pages 295--329  
 C.A. Ozturk, E. Nasuf , Tunneling and Underground Space Technology 37 (2013), Pages 45–54  
 N. Turk, W.R. Dearman, A correction equation on the influence of length to diameter ratio on the uniaxial compressive strength of rocks, Engineering Geology, Volume 22, Issue 3, 1986, Pages 293-300

## An IoT-enabled interactive platform for visualization and analysis of regional-scale groundwater system

Chuen-Fa Ni<sup>1</sup>, I-Hsien Lee<sup>2</sup>, Yun-Chen Yu<sup>1, 3</sup>, Wei-Ci Li<sup>1</sup>

<sup>1</sup>Graduate Institute of Applied Geology, National Central University, Taiwan (ROC),

[nichuenfa@geo.ncu.edu.tw](mailto:nichuenfa@geo.ncu.edu.tw), [yuyc@iner.gov.tw](mailto:yuyc@iner.gov.tw), [wiki70170@gmail.com](mailto:wiki70170@gmail.com)

<sup>2</sup>Center of Environmental Studies, National Central University, Taiwan (ROC), [sfdff327@gmail.com](mailto:sfdff327@gmail.com)

<sup>3</sup>Institute of Nuclear Energy Research, Atomic Energy Council, Executive Yuan, Taiwan (ROC),

[yuyc@iner.gov.tw](mailto:yuyc@iner.gov.tw)

Accurate assessment of groundwater resources relies on sufficient measurements and efficient analysis tools for implementations. The integrated measurement technologies and multidisciplinary knowledge for groundwater have enhanced the understanding of dynamics in groundwater systems. With the advantages of computer sciences and web service, the web platform provides an excellent open environment for groundwater investigations. However, most groundwater relevant web platforms are mainly focusing on data visualization. The data (points, polylines, and polygons) and pre-analysis results (i.e., the figures) overlap a street map to indicate the location of interests and quantify the influenced regions of groundwater hazards. Such a one-way interaction framework has significantly limited the implementations of measurement data and groundwater relevant applications. The study aims to develop an on-line web-based platform for groundwater data visualization, temporal and spatial data analysis, mesh generation, real-time flow modeling. IoT-enabled monitorings allow the platform to conduct real-time simulations and visualization. The study integrates multiple program languages such as Java, C, Python, and FORTRAN to bridge the data flow and on-line visualization. The interactive real-time web environment enables users to screen temporal and spatial measurements on the web map, conduct on-line data analyses, and develop numerical groundwater models. With efficient databases and numerous modules for data analyses and modeling, the platform allows users to share data and develop collaborative activities. The built-in analysis tools can also improve the efficiency of groundwater management and decision-making processes.

Figure 1 shows the framework of the platform. The platform enables users to screen temporal and spatial measurements on the web map, conduct on-line data analyses, and develop numerical groundwater models. With multiple databases and numerous modules real-time data analyses and modeling, the platform allows users to share data and develop collaborative activities (see Figure 2).

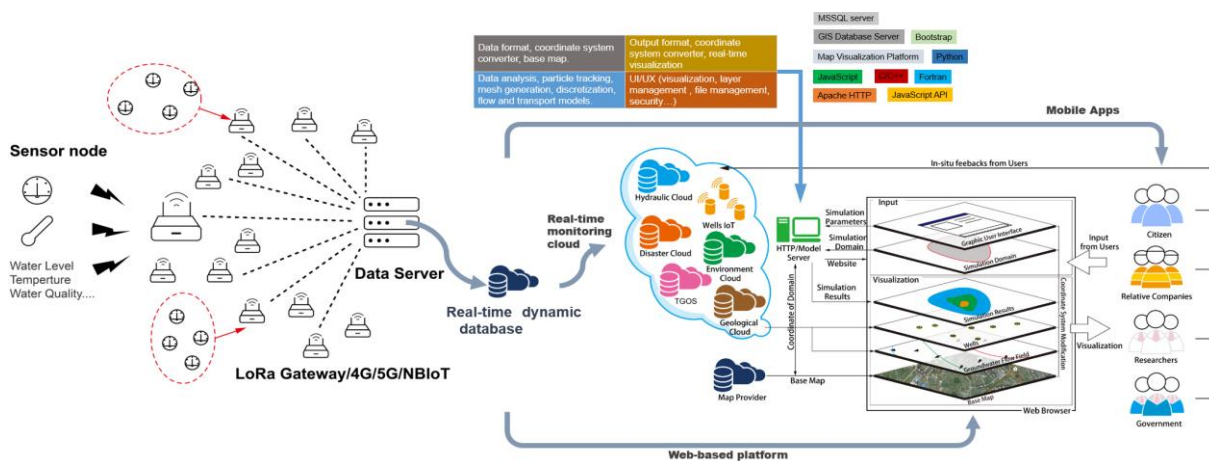


Figure 1. The framework of the platform

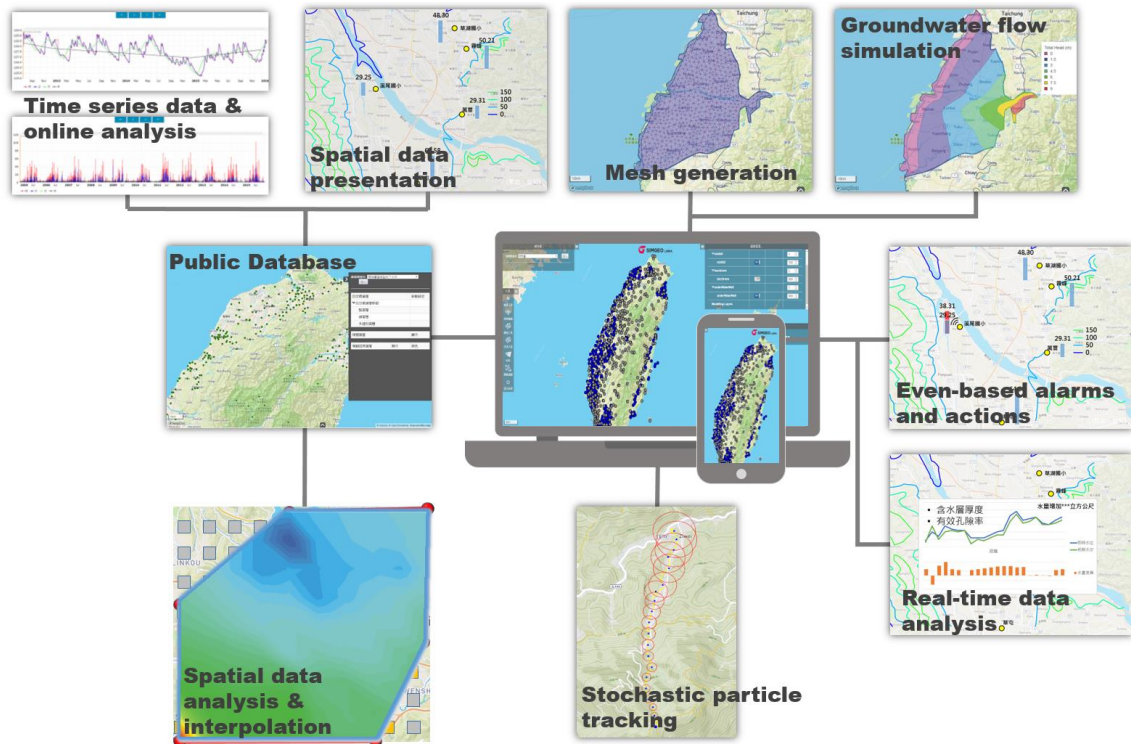


Figure 2. The developed features for on-line visualization and analysis of the groundwater system

**Acknowledgments**

This research is supported by the Ministry of Science and Technology (MOST), Taiwan ROC (Contracts MOST 107-2116-M-008-003-MY2, 108-2625-M-008-007-, and 108-2116-M-008-004-).

## A laboratory study on the brittle-ductile transition of four calcitic rocks

Anastasios Tsikrikis<sup>1</sup>, Maria Tzilini<sup>2</sup>, Theodosios Papaliangas<sup>2</sup>, Vassilis Marinos<sup>1</sup>

<sup>1</sup>Department of Geology, Aristotle University of Thessaloniki, Greece,

[tsikrika@geo.auth.gr](mailto:tsikrika@geo.auth.gr), [marinosv@geo.auth.gr](mailto:marinosv@geo.auth.gr)

<sup>2</sup>Department of Environmental Engineering, Hellenic International University, Greece,

[martzil@gmail.com](mailto:martzil@gmail.com), [tpapaliag@gmail.com](mailto:tpapaliag@gmail.com)

### **Background**

The brittle-ductile transition, is usually related to the strength of rocks. For instance, in silicate rocks under compression, the transition from brittle to ductile failure in a wide range of rock types is defined by  $\sigma_1 = 4.4\sigma_3$ , where  $\sigma_1$  and  $\sigma_3$  are the principal stresses, for silicate rocks and somewhat higher for carbonate rocks (Mogi, 2007). Zuo et al (2015) related the transition pressure  $\sigma_3$  to the ratio of the uniaxial compressive strength  $\sigma_c$  to the uniaxial tensile strength  $\sigma_t$  and the friction coefficient  $\mu$ . The aim of this laboratory study was to examine the strength and deformation behavior of four calcitic rocks, under conventional triaxial compression and to determine experimentally the principal stress ratio  $\sigma_1/\sigma_3$  at the brittle-ductile transition.

### **Experimental Procedure**

Four low porosity calcitic rocks, including two marbles, namely “Tranovaltos Marble” (TM) and “Kavala marble” (KM) and two crystalline limestones, “Mesaio limestone” (ML) and “Giannitsa Limestone” (GL) were tested in triaxial compression, according to ASTM D7012 - 14A, using an 4000kN INSTRON servo-controlled compression testing machine. 55 cylindrical samples 54 mm x108 mm were deformed dry, at a constant displacement rate of  $5 \times 10^{-5} \text{ s}^{-1}$  in a conventional NX Hoek triaxial cell at room temperature and confining pressures ranging from 5 to 70 MPa. Twelve additional samples were tested in uniaxial compression.

**Table 1: Physicomechanical properties of investigated rocks**

Rock type	Tranovaltos White marble	Kavala marble	Mesaio Limestone	Giannitsa Limestone
Dry density (kg/m <sup>3</sup> )	2717	2627	2621	2682
Open porosity (%)	0.15	0.16	0.25	0.75
Uniaxial compr. strength (MPa)	93.0	63.0	74.6	80.8

### **Results**

The results are presented as axial strength vs. confining pressure ( $\sigma_1 - \sigma_3$ ) diagrams in Figure 1. The values of the Hoek and Brown criterion constants  $m_i$  and  $\sigma_{ci}$ , determined from the triaxial data sets in the range of confining pressure between zero and the brittle-ductile transition (Hoek and Brown, 2018), using the Rocdata software (Rocscience Inc.), are also shown in the same figure. The fitted envelopes shown in the brittle field of the figure are based on the Hoek and Brown criterion, using the above values of  $m_i$  and  $\sigma_{ci}$ . The ratio of confining pressure at the brittle-ductile transition to uniaxial compressive strength ranged approximately from one third (KM) to one (GL). However, the stress ratio  $\sigma_1/\sigma_3$  at the transition is nearly the same and equal to 5.7 for the four rocks investigated. This value is in close agreement with the results published by Fredrich et al. (1990) for four well-known carbonate rocks and in line with Mogi's suggestion for carbonate rocks, i.e. higher than the value of 4.4 proposed for silicate ones.

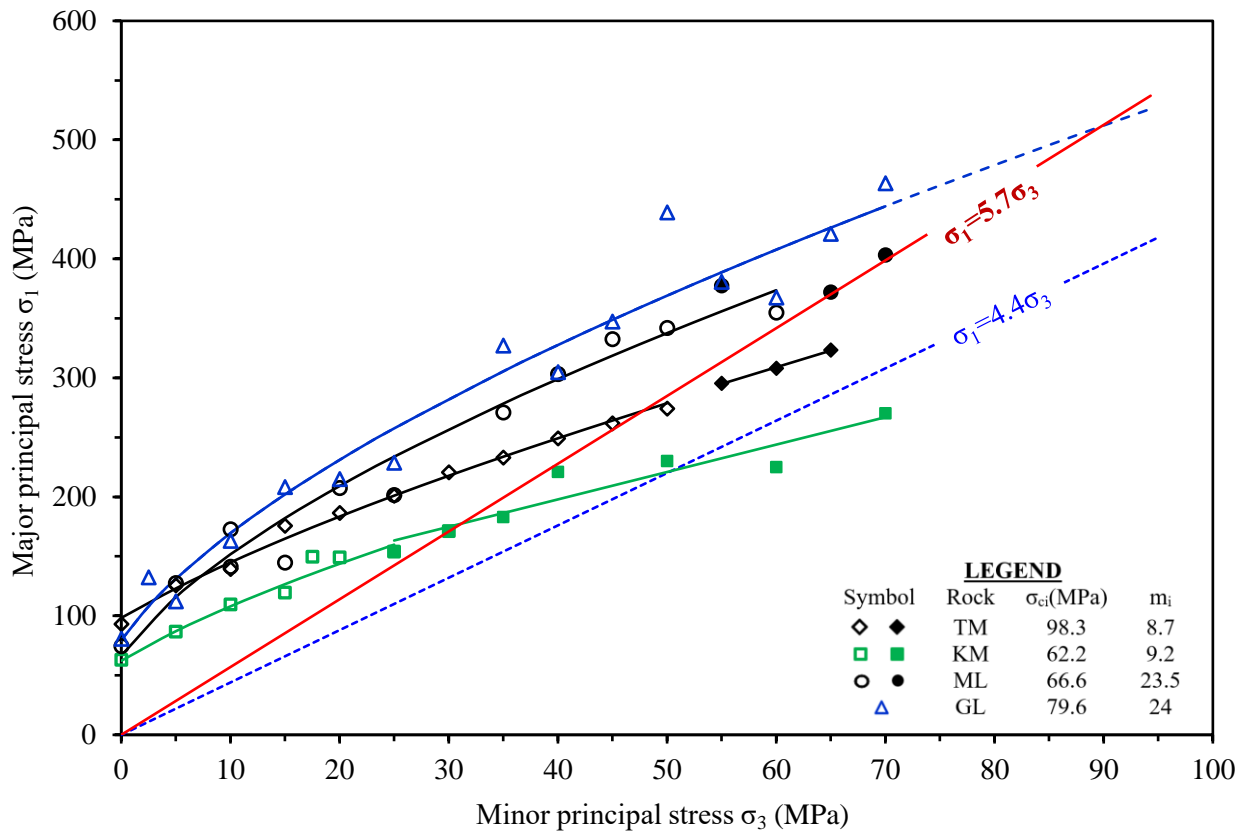


**Figure 1. Axial stress – confining pressure diagrams. Open symbols represent brittle behaviour and closed symbols ductile behaviour. The red line ( $\sigma_1 = 5.7 \sigma_3$ ) represents the common brittle-ductile line**

**Conclusions**

Our results suggest that the brittle-ductile transition of low porosity calcitic rocks occurs at confining pressures less than the uniaxial compressive strength and a principal stress ratio  $\sigma_1/\sigma_3$  nearly the same and approximately equal to 5.7.

**REFERENCES**

Fredrich, J. T., Evans, B. and Wong, T.F., 1989, Micromechanics of the brittle to plastic transition in Carrara Marble. J. Geophys. Res. 94, 4,129-4,145.

Hoek E., Brown E.T., 2018, The Hoek–Brown failure criterion and GSI – 2018 edition. Journal of Rock Mechanics and Geotechnical Engineering, 11, 445-463.

Mogi K., 2007, Experimental rock mechanics. London, UK. Taylor and Francis.

Zuo, J.P., Liu, H., Li, H., 2015, A theoretical derivation of the Hoek-Brown failure criterion for rock materials. Journal of Rock Mechanics and Geotechnical Engineering, 7(4):361-6.





## Deformation stages of schists under uniaxial compression

Dimitrios Kotsanis<sup>1</sup>, Pavlos Nomikos<sup>1</sup>, Dimitrios Rozos<sup>1</sup>

<sup>1</sup>*School of Mining and Metallurgical Engineering, National Technical University of Athens, Greece,*

[dkotsanis@metal.ntua.gr](mailto:dkotsanis@metal.ntua.gr), [nomikos@metal.ntua.gr](mailto:nomikos@metal.ntua.gr), [rozos@metal.ntua.gr](mailto:rozos@metal.ntua.gr)

The objective of this study is the determination of the various stages of deformation of schists under uniaxial compression. Since the fundamental work of Brace et al. (1966) and Bieniawski (1967), it is generally accepted that the experimental stress-strain curves of uniaxial compression tests up to the ultimate strength (UCS) can be distinguished into four sections corresponding to different stages of rock deformation. The initial section corresponds to the closure of pre-existing microcracks (stage I). When the majority of these microcracks are closed the rock can be roughly considered to behave as an elastic material (stage II). The end of stage I is defined as crack closure stress level (Ccc).

The onset of dilatancy delimits the beginning of the stable cataclastic phase (stage III). The tensile microcracks, which initiate at this stage, propagate mainly parallel to the direction of the applied load. The stress level associated with the beginning of this stage is defined as the crack initiation stress (Cci). With the increase of the applied load, new microcracks initiate and propagate while at the same time new and old microcracks coalesce and interact at oblique angles to the applied loading direction. The stress level where unstable crack growth begins is defined as crack damage stress (Ccd).

A total of eleven schist specimens, prepared from samples obtained from various locations of the Southeast Attica, Greece, were subjected to uniaxial compression. All specimens were cored normal to the schistosity plane. The axial load and the axial and lateral deformations were measured and recorded throughout the tests. The various deformation stages are determined by characteristic inflection points of the axial and volumetric stiffness curves obtained from the measured deformations, as suggested by Eberhard et al. (1998).

According to the tests results, the intact schists of the study area are of medium to very high strength with UCS values ranging from 20 to 133 MPa. In terms of their deformability, the Young modulus (E) ranged from 8 to 42 GPa.

Applying simple linear regression models for the whole dataset (Figure 1), it was found that strong correlations exist between the characteristic stress thresholds and the ultimate strength (UCS). Regardless of the physical properties of the tested samples, the average crack closure stress ratio ( $C_{cc} / UCS$ ) is equal to 0.37, while the crack initiation stress ratio ( $C_{ci} / UCS$ ) and crack damage stress ratio ( $C_{cd} / UCS$ ) are found to be 0.43 and 0.95, respectively.

The results of this work can be considered as an important contribution to the understanding of the mechanical behavior of schistose rocks which outcrop in the study region. The empirical equations, regarding the relationship between the characteristic stress thresholds and the ultimate strength, are applicable over a wide range of stresses and characterized by very strong coefficients of determination ( $R^2$ ).

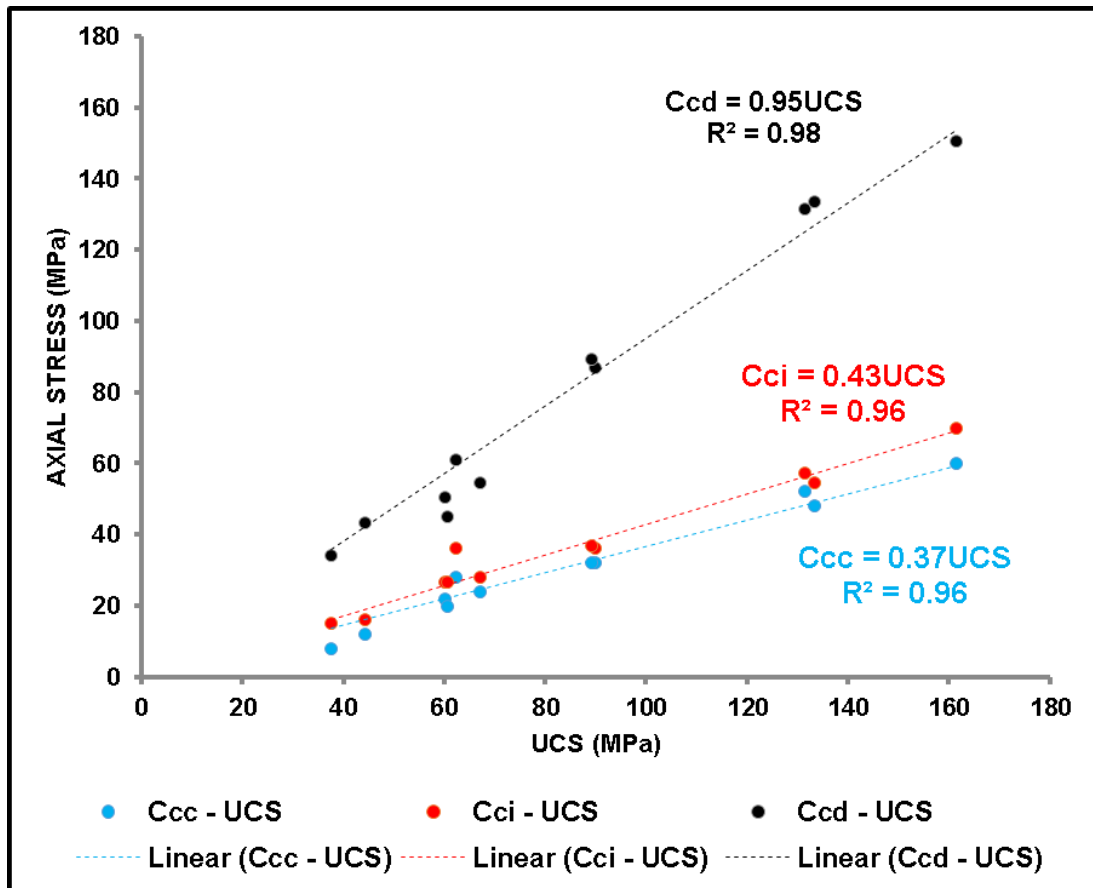


Figure 1. The relationship between ( $C_{cc}$ ), ( $C_{ci}$ ) and ( $C_{cd}$ ) with ultimate strength (UCS)

## REFERENCES

- Bieniawski, Z.T., 1967, Mechanism of brittle fracture of rock, part II – experimental studies. International Journal of Rock Mechanics and Mining Sciences & Geomechanics Abstracts, v.4(4), pp. 407 – 423
- Brace, W.F., Paulding, B., and Scholz, C., 1966, Dilatancy in the fracture of crystalline rocks. Journal of Geophysical Research, v.71(16), pp. 3939 – 3953
- Eberhardt, E., Stead, D., Stimpson, B., and Read, R.S., 1998, Identifying crack initiation and propagation thresholds in brittle rock. Canadian Geotechnical Journal, v35(2), pp. 222 – 233

## Evaluation of crack initiation stress of Volakas marble specimens in uniaxial

Dimitrios Kotsanis<sup>1</sup>, George Papantonopoulos<sup>1</sup>, Pavlos Nomikos<sup>1</sup>

<sup>1</sup>National Technical University of Athens, Greece,

[dkotsanis@metal.ntua.gr](mailto:dkotsanis@metal.ntua.gr), [geopous@metal.ntua.gr](mailto:geopous@metal.ntua.gr), [nomikos@metal.ntua.gr](mailto:nomikos@metal.ntua.gr)

### Introduction

Several studies in low porosity brittle rocks have concluded that fracture process characteristics of rock under stress can be divided into four stages based on the stress–strain behaviour displayed through axial and lateral deformation measurements during uniaxial compression laboratory tests. The scope of this investigation is to estimate the crack initiation stress of the Greek marble variety “Volakas” which is a fine grained, high porosity crystalline rock that is found in northern Greece.

### Methodology

We use three methods for comparison reasons. The first method relies on lateral strain measurements and it was proposed by Lajtai (1974) who suggested that the crack-initiation stress could be established by defining the onset where the lateral strains deviated from linearity. In order to identify this deviation we used the moving point regression technique described by Eberhardt et al. (1998), which uses the first derivative of the curve to highlight any slope or rate changes.

The second method is based on the volumetric strain and was developed by Eberhardt et al. (1998). They suggested that the crack-initiation stress could be marked on the volumetric stiffness curve by the transition from a regular region, which suggests the linear elastic area, to a more irregular region with or without a break in the curve slope.

The third method to establish the crack initiation stress is the Lateral Strain Response (LSR) method proposed by Nicksiar and Martin (2012). According to this method the desired stress value is found by plotting the difference between the measured lateral strain and the linear reference line as a function of axial stress (Figure 1). The maximum of this difference is taken as the onset of crack initiation.

### Results

In order to estimate the crack initiation stress, five marble specimens were subjected to uniaxial compression tests according to the ISRM suggested methods. For each specimen the axial and lateral strains were measured using LVDTs and also the volumetric strain was calculated and plotted versus axial stress. In Figure 1 the normalized axial stress (i.e. the axial stress normalized to the peak strength of the specimen) is plotted versus the axial, radial and volumetric strains for Volakas-1 specimen. In table 1 the results of our laboratory analysis are given. Besides the crack initiation stress,  $\sigma_{ci}$ , the compressive strength and the crack closure stress,  $\sigma_{cc}$ , of each specimen are given in order to evaluate the results. Crack closure stress is marked at the point that the axial stiffness curve plotted against axial stress starts to become horizontal on average. It is observed that the strength results are consistent with small standard deviation and COV%. The stress values for crack closure and crack initiation are more dispersed though with almost double for the former and almost triple COV% for the later. It is also noticed that the crack initiation stresses estimated with the Eberhardt et al. and LSR methodologies are well below the estimated crack closure stress.



**Table 1. Compressive strength and crack initiation stress according to three methods, for “Volakas” marble**

Specimen	Strength (MPa)	$\sigma_{cc}$ (MPa)	$\sigma_{ci}$ (MPa) (Lajtai)	$\sigma_{ci}$ (MPa) (Eberhardt et al.)	$\sigma_{ci}$ (MPa) LSR
Volakas-1	168	66	75	35	52
Volakas-2	151	49	87	28	51
Volakas-3	162	70	77	36	44
Volakas-4	161	60	86	27	39
Volakas-5	146	65	70	28	54
Average	158	79	31	48	62
St. dev.	9	7	4	7	8
COV%	5.7	9.0	13.5	13.7	13.1

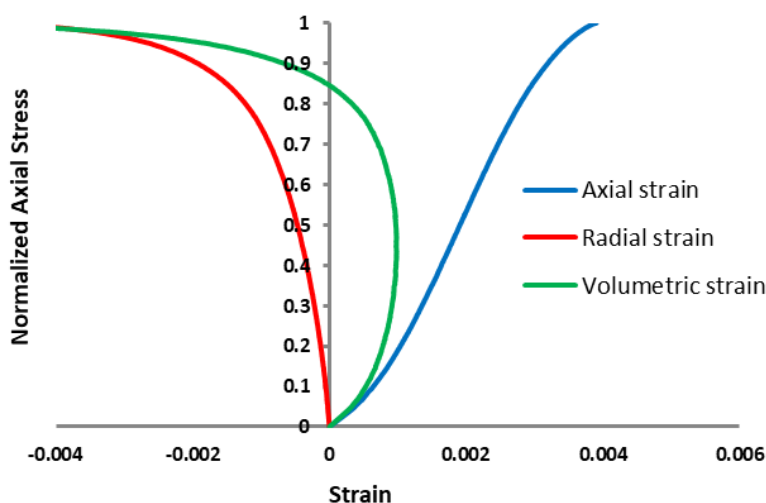


**Figure 1. Normalized axial stress versus axial, radial and volumetric strain plots for Volakas-1 specimen in UCS.**

**Conclusion**

It is clear from the above table that crack initiation stress cannot be estimated or even approximated for this type of marble. Each one of the methods used gave consistent results comparing between the samples but completely different results compared to the other methods. This wide variation of results should be attributed to the high porosity of this rock.

**REFERENCES**

Eberhardt, E., Stead, D., Stimpson, B. and Read, R.S., 1998, Identifying crack initiation and propagation thresholds in brittle rock. *Canadian Geotechnical Journal*, v. 35, pp. 222–233.

Nicksiar, M. and Martin, C. D., 2012, Evaluation of Methods for Determining Crack Initiation in Compression Tests on Low-Porosity Rocks, *Rock Mechanics and Rock Engineering*, v. 45, pp. 607–617.

Lajtai, E.Z., 1974, Brittle fracture in compression. *International Journal of Fracture Mechanics*, v. 10 pp. 525–536.

## A Discretized Clay Shell Model (DCSM) for evaluating the effective stress coefficient of clayey sandstone permeability

Pin Lun Tai<sup>1</sup>, Jia Jyun Dong<sup>2</sup>

<sup>1</sup>Institute of Applied Geology, National Central University, Taiwan, [ncu996002019@gmail.com](mailto:ncu996002019@gmail.com)

<sup>2</sup>Graduate Institute of Applied Geology, National Central University, Taiwan, [jjdong@geo.ncu.edu.tw](mailto:jjdong@geo.ncu.edu.tw)

The permeability of burial rocks at petroleum reservoir attracts great attentions of petroleum industry. For the projects of groundwater storage, carbon dioxide sequestration, nuclear repositories, or extraction of geothermal, the rock permeability is essential parameter for fluid flow simulation. As one of the most important aquifers, the permeability of sandstones are extensively measured and thoroughly studied. However, the influence of pore pressure on the fluid flow characteristics of clayey sandstones under different confining pressure is still unclear and controversial. The well known Clay shell model (CSM) depicts the influence of clay fraction, as well as the modulus ratio between sand grains and clays, on the effective stress coefficient  $\alpha$ . The CSM yield a constant effective stress coefficient  $\alpha$  irrespective of confining and pore pressure, which is contradictory to experimental results. This study accounts for the stress dependent modulus of clay on the CSM. With the discretization scheme, the different modulus of clay along the pore radius can be determined. The proposed discretized clay shell model (DCSM) predicts the pore radius variation under different confining and pore pressure. Together with Hagen-Poiseuille equation and Darcy law, the confining and pore pressure dependent effective stress coefficient  $\alpha$  can be determined via a responded surface method. Our model predicts  $\alpha$  within the range of measured ones for clayey sandstones. We illustrate the difference of predicted permeabilities using CSM and DCSM for a hypothetical case (Figure 1) with hydrostatic (<0.5 km) and abnormal high pore pressure (>1.5 km).

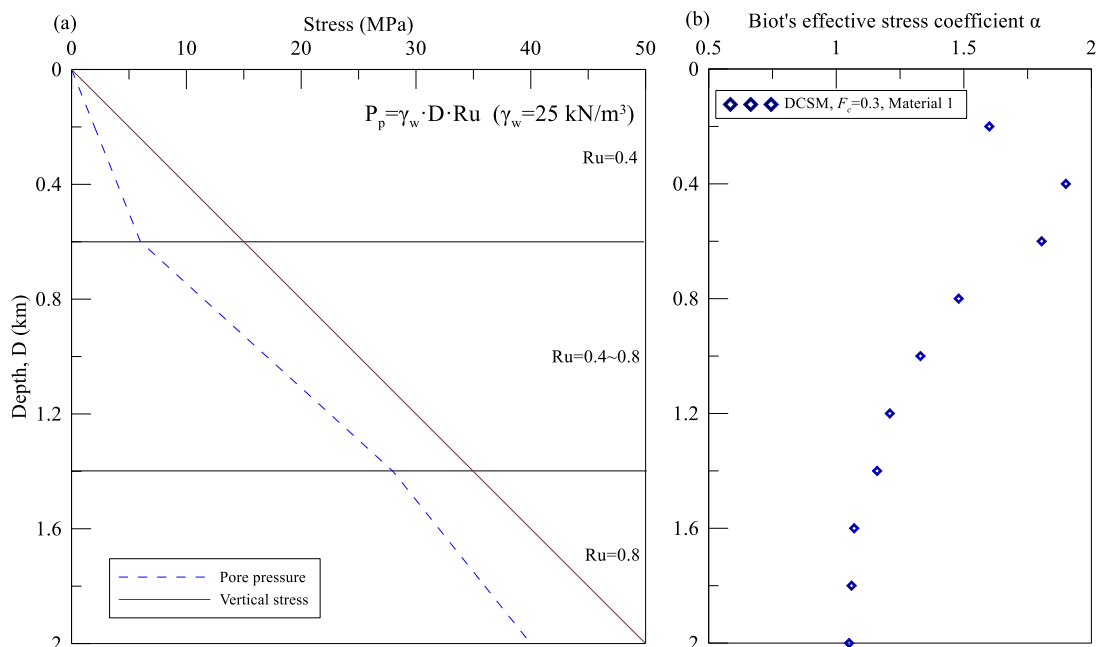
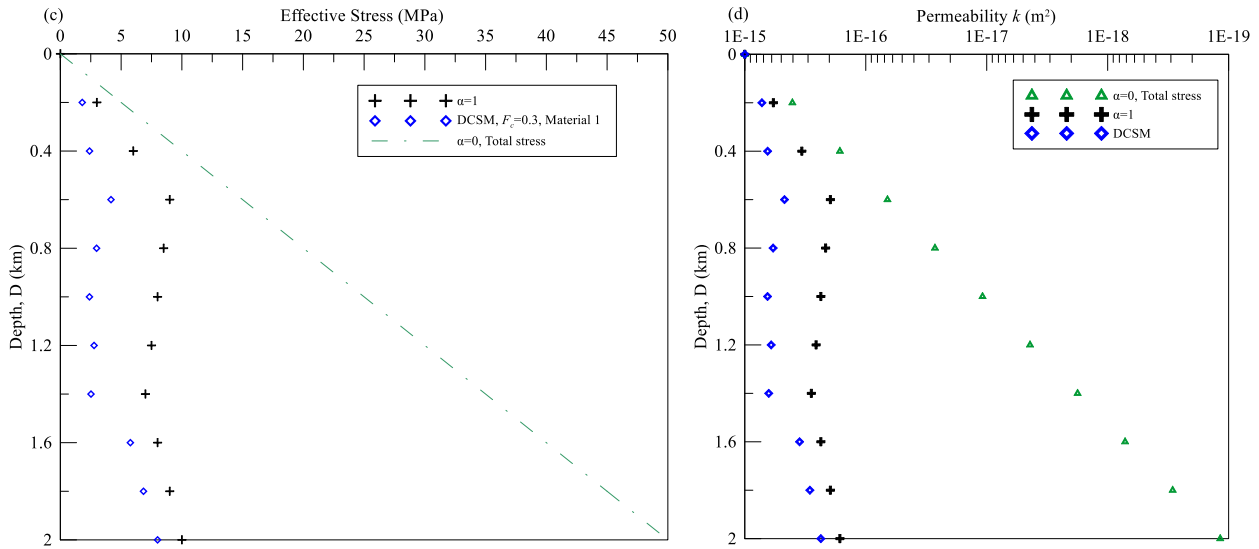


Figure 1 (a) Synthetic case that excess pore pressure increased with burial depth. (Assume the average of total unit weight of formation is  $5 \text{ kN/m}^3$ )





**Figure 1 (b) The effective stress coefficient  $\alpha$  changed with burial depth determined by DCSM ( $F_c = 0.3$ , material 1); (c) The prediction of effective stress by DCSM, and condition of  $\alpha = 1$  and 0. (d) The prediction of permeability using different  $\alpha$ .**

The effective stress coefficient  $\alpha$  increased with increasing depth at shallow, hydrostatic portion, and declined with increasing depth when the depth greater than 0.5 km. When the pore pressure approaches to the litho-pressure, the  $\alpha$  will approach to 1 when the depth reaches to 2km. The predicted permeability of rocks shallower than 0.5 km will be 2.5 times larger than the ones assumed  $\alpha = 1$ . When the depth increased from 0.5 km to 1 km and to 2 km, the predicted permeability using DCSM will increase to 3 times and decreased to 1.2 times larger than the ones predicted using  $\alpha = 1$ . The differences are mainly dominated by the combination of pore pressure and confining pressure, which changing significantly with depth is an abnormal high pore pressure zone existed.

## Investigation of time-dependent stress relaxation behaviour in rock materials

Dr. Chrysothemis Paraskevopoulou<sup>1</sup>

<sup>1</sup>Assistant Professor, School of Earth and Environment, University of Leeds, UK,

[c.paraskevopoulou@leeds.ac.uk](mailto:c.paraskevopoulou@leeds.ac.uk)

It has been observed that conventional design approaches in geotechnical design neglect the long-term time-dependent response of the ground. Time-dependent phenomena (ie.. creep, strength-degradation, swelling etc.) can take place wither in series or even act simultaneously. It is paramount thus to investigate and examine their behaviour characteristics separately (Paraskevopoulou et al. 2015). This work focuses on time-dependent stress relaxation which is defined as stress decrease while at least one principal strain is constrained and remains constant over time (Paraskevopoulou, 2016). Paraskevopoulou et al. (2017) have observed that there are three distinct stages during stress relaxation of rock materials shown in Figure 1.a. More specifically, when the axial deformation is kept constant the stress relaxes with a decreasing rate, this period is defined as the first stage of stress relaxation (R<sub>I</sub>). At the end of this stage the stress decrease approaches a constant rate which marks the transition to the second stage (R<sub>II</sub>). The third stage of relaxation (R<sub>III</sub>) follows where no further stress relaxation is measurable. Stress relaxation has been observed in various rock materials (Figure 1.b.) and it varies in terms of maximum stress decrease and relaxation time (duration). Stress relaxation is also sample geometry sensitive as observed by Perras et al. (2017).

This paper investigates the stress relaxation behaviour of Thornhill Sandstone through a lab testing series (Figure 1.c). The testing is conducted in the RMEGG Lab at the University of Leeds and both UCS (Baseline) and stress relaxation testing. The UCS testing was conducted in 12 cylindrical samples followed the ISRM guideline (Figure 1.d) and was used as Baseline to determine strength thresholds of UCS and CI values. Paraskevopoulou et al. (2018) approach was adopted to define the modified UCS\* by determining the relation between UCS<sup>B</sup> and CI values derived from the baseline testing (Figure 1.e). The modified UCS\* was used for determining the driving stress-ratio (stress level at which the axial strain remains constant). Stress relaxation testing was conducted in 12 cylindrical samples (examples are shown in in Figure 1.f) following the Paraskevopoulou et al. (2017) proposed testing methodology. The stress relaxation testing results (Figure 1.g) varied in terms of relaxation time from a few hours up to a day. The tests were terminated after the stress decrease has reached an asymptote. The Maximum stress relaxation observed on this type of sandstone varied from 1 MPa to 10 MPa shown in Figure 1.h. where the Driving Stress ratio is normalized to the UCS<sup>B</sup> derived from the Baseline testing ( $\sigma/UCS^B$ ). However, when the Driving-Stress ratio ( $\sigma/UCS^*$ ) is normalized to the modified UCS\* it gives a better fit (Figure 1.i). Finally, the proposed equation:

$$\text{MaxStress} = 0.2013e^{3.4(\sigma/UCS^*)} \text{ where } UCS^* = 2.35 CI$$

can be used to predict the maximum stress relaxation (decay) for Thornhill sandstone. It is suggested to follow this approach for various rock materials and produce more databases that can be used by practitioners as a first tool to estimate stress relaxation behaviour.

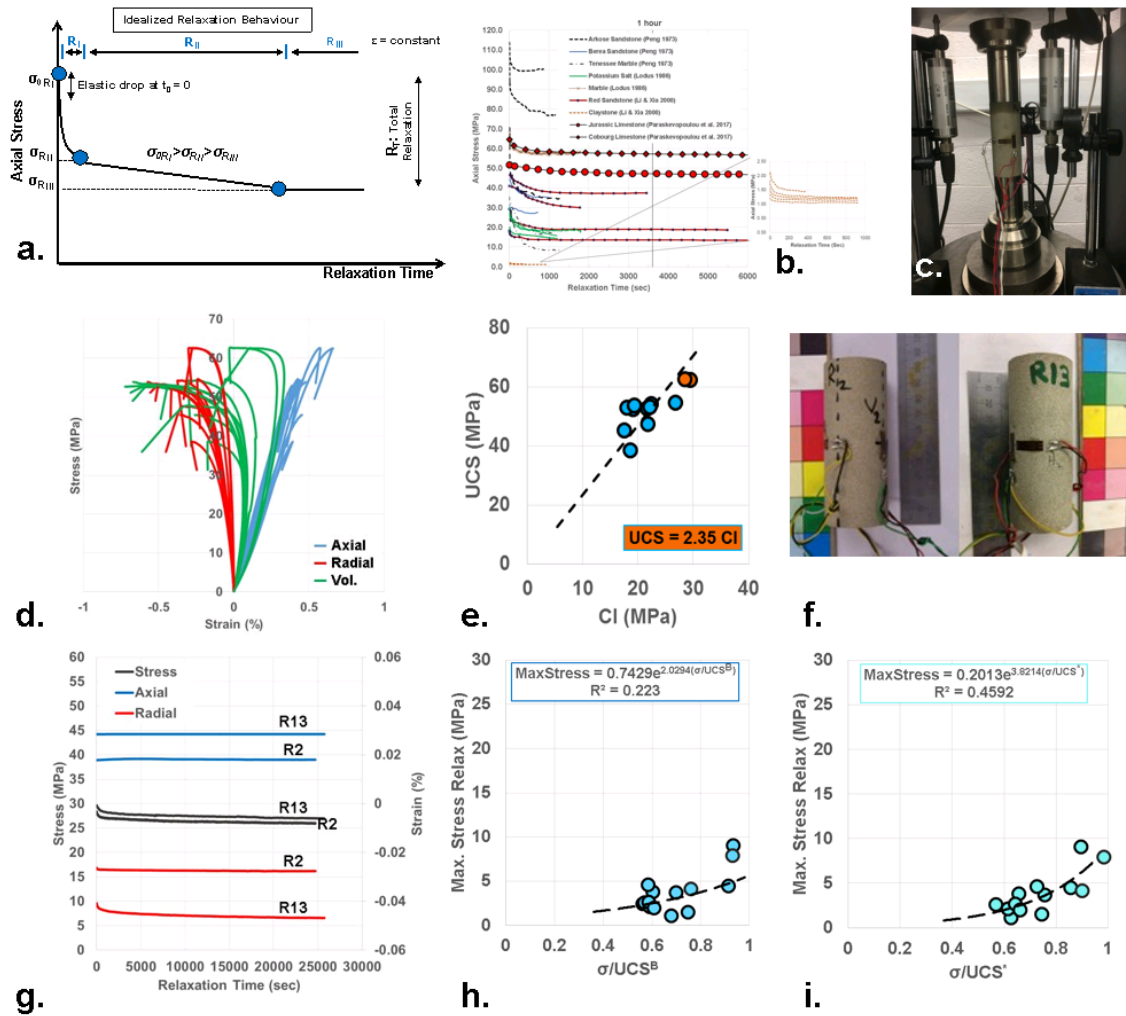


Figure 1. a) 3 stages of SR (Paraskevopoulou et al. 2017); b.) SR data of various rock types (modified after Paraskevopoulou et al. 2017); c) Equipment and Testing set up; d) Stress-strain response of TS samples tested in UCS conditions; e) Relationship between UCS and CI for TS determined from Baseline (UCS) testing; f) TS samples R2 and R13; g) SR testing results of R2 and R13; h) Max SR to Driving Stress-Ration normalized to UCS - Baseline; and g) Max SR to Driving Stress-Ration normalized to UCS – Modified, (where SR: Stress Relaxation)

**REFERENCES**

Paraskevopoulou, C. 2016. Time-dependency of rock and implications associated with tunnelling, PhD Thesis. In: Queen’s University Publications. Canada.

Paraskevopoulou, C., Perras, M., Diederichs, M.S., Amaan, F., Loew, S., Lam, T., 2015. Observations for the long-term behaviour of carboniferous limestone rocks based on laboratory testing. In: Proceedings of the EUROCK 2015, Austria.

Paraskevopoulou, C., Perras, M., Diederichs, M.S., Amann, F., Loew, S., Lam, T., Jensen., M. 2017. The three stages of stress-relaxation - Observations for the long-term behaviour of rocks based on laboratory testing. Journal of Engineering Geology, 216, 56-75(2017).

Paraskevopoulou, C., Perras, M., Diederichs, M.S., Loew, S., Lam, T., Jensen., M. 2018. Time-dependent behaviour of brittle rocks based on static load laboratory testing. Geotechnical & Geological Engineering, 36, 337-376(2018).

Perras, M.A., Haedener, P., Leith, K., Loew, S., Paraskevopoulou, C., 2017. Influence of sample geometry on constant strain relaxation tests. In: PRF 2017: Progressive Failure and Long-term Strength Degradation of Brittle Rocks ISRM Conference, Switzerland.



## Effect of pore size on electro pulse drilling of rock

Nawnit Kumar<sup>1</sup>, Xiaoli Liu<sup>2</sup>

<sup>1</sup>*The State Key Laboratory of Hydro-Science and Engineering, Tsinghua University, Beijing 100084, China,*  
[kumarn10@mails.tsinghua.edu.cn](mailto:kumarn10@mails.tsinghua.edu.cn)

<sup>2</sup>*The State Key Laboratory of Hydro-Science and Engineering, Tsinghua University, Beijing 100084, China,*  
[xiaoli.liu@mail.tsinghua.edu.cn](mailto:xiaoli.liu@mail.tsinghua.edu.cn)

Electro pulse drilling has huge prospects in deep bore wells and horizontal fracking. The mechanism of electro-pulse drilling of rocks is based on the fact that the dielectric strength of rocks is less than the dielectric strength of the insulating liquid. When a high voltage pulse is applied across the rock in the presence of an insulating liquid, a discharge channel is formed inside the rock which creates shock waves leading to the destruction of the rock media. Considering the heterogeneous nature of rocks, this paper addresses the need to identify the factors influencing its dielectric strength.

It has been found that dielectric strength is attributed to the breakdown of air or gases present in the pores of rocks. This study hypothesizes that the size and shape of pores highly influence the breakdown strength of a rock. To simulate this effect, the electric field on different shapes and sizes of pores was observed numerically. Due to the application of an electric field, the air inside the void is polarized, and a local electric field is created inside the void. When the strength of the local electric field is more than the dielectric strength of the void, an electron avalanche is formed due to which a plasma channel is created inside the void. As the electric field is increased, the plasma channel grows, which creates shockwaves leading to tensile failure of cavities. This process continues until a path for a complete breakdown of the rock is formed between the electrodes.

When energy released is plotted against pore sizes varying between 0.5nm to 1mm under the same voltage pulses, a logarithmic pattern was obtained. When shock wave pressure is plotted against pore size, an inversely proportional relationship was observed. In the case of irregularly shaped voids, the distance along the electric field is the governing factor. When the electric field strength was 50kV/cm, shock waves of 16.3Mpa were observed in pore size of 2um, while with an increase in pore size, shock wave pressure reduced considerably. For a given pore size, the breakdown strength of a rock decreases with an increase in pore density. However, for the same porosity, the breakdown strength increases with a decrease in pore density. It was also observed that for rocks having the same porosity but with different permeability, breakdown strength increased with permeability. Thus the relationship between voids and dielectric strength showed that pore shape, size, and density influence the dielectric strength of rocks.

### REFERENCES

- Yudin, A. S., et al. (2019). "Electrical discharge drilling of granite with positive and negative polarity of voltage pulses." *International Journal of Rock Mechanics and Mining Sciences* 123.
- Zhang, R.-Q., et al. (2017). "Discharge characteristics of high voltage pulses inside rocks with increasing their applied number." *AIP Advances* 7(11).
- Blunt, M. J., et al. (2013). "Pore-scale imaging and modelling." *Advances in water resources* 51: 197-216.
- Clarkson, C. R., et al. (2016). "Nanopores to megafactures: Current challenges and methods for shale gas reservoir and hydraulic fracture characterization." *Journal of Natural Gas Science and Engineering* 31: 612-657.

## Geoengineering characterization of Lyulyakata limestone quarry, NE Bulgaria

Temenuga Georgieva<sup>1</sup>, George Ajdanlijsky<sup>2</sup>, Fanny Descamps<sup>3</sup>, Jean-Pierre Tshibangu<sup>4</sup>

<sup>1</sup>Faculty of Engineering, UMONS, Belgium, [TemenugaDimova.Georgieva@umons.ac.be](mailto:TemenugaDimova.Georgieva@umons.ac.be)

<sup>2</sup>Faculty of Geology, University of Mining and Geology, Bulgaria, [g.ajdanlijsky@mgu.bg](mailto:g.ajdanlijsky@mgu.bg)

<sup>3</sup>Faculty of Engineering, UMONS, Belgium, [Fanny.DESCAMPS@umons.ac.be](mailto:Fanny.DESCAMPS@umons.ac.be)

<sup>4</sup>Faculty of Engineering, UMONS, Belgium, [Katshidikaya.TSHIBANGU@umons.ac.be](mailto:Katshidikaya.TSHIBANGU@umons.ac.be)

With its production of several million tons per year the Lyulyakata open pit limestone quarry, located in NE Bulgaria, is the main raw material supplier for soda ash and cement production in the area. The expansion of the quarry in-depth and its long-term sustainable development require an assessment of the possible slope instabilities that are closely controlled by the geological and geomechanical properties of the deposit.

The quarry is developed in thick-bedded Lower Cretaceous bio- to lithoclastic and micrite limestone, as the latter prevail. Because it is located into a NE limb of Devnya anticline, part of the core of Hitrino-Devnya swell of the North-Bulgarian dome (the Moesian Platform), the rock mass is disintegrated by a set of normal faults.

To define the rock mass structure and the potential modes of slope instabilities mass mesoscale structural measurements were performed before and after blasting works. An orthogonal joint system formed by one bedding controlled sub-horizontal (N55°/12°) and two sub-vertical, oblique to maximum principal stress direction (conjugate shear), joint sets with orientation N262°/83° and N183°/83° was determined. The joint sets are systematic with spacing between 0.5 m and 1.0 m and form a prismatic rock mass structure. Commonly the blasting works do not form discontinuities with other characteristics.

The analyses of the potential block instabilities showed that the occurrence of structurally controlled failures in the quarry is unlikely. However, a sliding plane and wedge failure would be the possible predominant failure types if the slope angle reaches 70-75°. They could result in a case of abrupt slope direction changes and opening of the vertical joints, which act as tension cracks. Toppling is less likely to take place.

Geomechanically the micrite and bio- to lithoclastic limestones are characterized by unconfined compressive strength (UCS) and tensile strength (UTS) tests. The UCS of the bio- to lithoclastic limestone ranges between 24 MPa and 28 MPa while its UTS is between 3 and 5 MPa. In contrast, the micrite samples demonstrate UCS between 98 MPa and 151 MPa. The UTS predominantly varying from 6 MPa to 9 MPa. The moderate strength of the bio- to lithoclastic limestone is explained by its porosity of over 20 % whereas the micrite limestone (porosity 8 %) exhibits a high strength due to its better cementation. The Rock Mass Rating (RMR<sub>89</sub>) analysis revealed that the massif is classified as Good quality. Only at the near-surface level, due to the impact of the weathering processes, a Fair quality could be expected.

The high strength value of the dominant in the quarry micrite limestone and the geometry of the typical for it structural blocks, controlled by lithology and regional geology stress regime, could be used as favorable features for the sustainable extension of the quarry. Following the orientation of the natural rock mass fragmentation from the pit slope will contribute to its sustainable further development.





## Comparison of roughness indices on chalk and sandstone fractures

Marie-Laure Wattier<sup>1</sup>, Sara Vandyscke<sup>2</sup>, Françoise Bergerat<sup>3</sup>, Paul Wertz<sup>4</sup>, Samir Mohammad<sup>5</sup>,  
Jean-Pierre Tshibangu<sup>1</sup>

<sup>1</sup>UMONS, Belgium, [marie-laure.wattier@umons.ac.be](mailto:marie-laure.wattier@umons.ac.be)

<sup>2</sup>FNRS, UMONS, Belgium, [sara.vandyscke@umons.ac.be](mailto:sara.vandyscke@umons.ac.be)

<sup>3</sup>CNRS, Sorbonne Universités UPMC Univ Paris06, France, [francoise.bergerat@sorbonne-universite.fr](mailto:francoise.bergerat@sorbonne-universite.fr)

<sup>4</sup>SA Carrières Feidt, Luxemburg, [pw@stones.lu](mailto:pw@stones.lu)

<sup>5</sup>UMONS and ULB, Belgium, [Samir.Mohammad@ulb.ac.be](mailto:Samir.Mohammad@ulb.ac.be)

The characterisation of roughness on natural rock fractures can be used to assist in the management of rock structures or underground works, but also to refine flow models used in applications such as oil production, water production, or underground fluid injection. The analysis of roughness on natural rock fractures has been widely explored for igneous rocks, but much work is still required to characterize sedimentary rocks, which present a vast range of lithologies and microstructures. In addition, studies often focus on the large scale (rock mass scale, metric or above), while some numerical models may benefit from a deeper understanding of small-scale roughness (centimetric scale or less). This study focuses on small-scale roughness via widely used statistical and fractal parameters. To represent typical hydrocarbons reservoirs or aquifer rocks, a selection of three Cretaceous chalks from the North-West European Basin and one Lias sandstone were studied.

Chalk samples were collected in Harmignies (Belgium), at Cap Blanc-Nez and Arras (France); the Luxemburg sandstone in Ernzen, Luxemburg. UCS and porosity were measured: sandstone (UCS=54MPa, Ø=18%), Obourg formation white chalk (6MPa, Ø=43%), Blanc-Nez chalk (UCS=19MPa, Ø=23%), Arras chalk (UCS=7MPa, Ø=43%).

Fracture samples were subdivided in 30x30mm square grids, each numerised with a laser device mounted on an X-Y cross-motion table. The resulting surfaces, with Z elevation points measured with +/-30µm accuracy (X-Y steps of 172µm), were processed to issue four classic roughness parameters: Ra (asperities height), Z2 (RMS value), fractal dimensions Dyard (yardstick method) and Dvar (semi-variogram method). A series of lab-generated surfaces were also analysed with the same method. They were produced by fracturing 40x40mm cores by means of either Brazilian tensile test or by shear test. Globally, the results presented are compiled from 3D topographic surface acquisition of about 350 scans.

**Table 1.**

		Mean Dyard	Mean Dyard	Mean Z2
Lab-generated	Chalk	1.0064	1.315	0.62
	Sdst	1.0047	1.356	0.34
Natural	Chalk	1.0033	1.277	0.35
	Sdst	1.0080	1.361	0.46

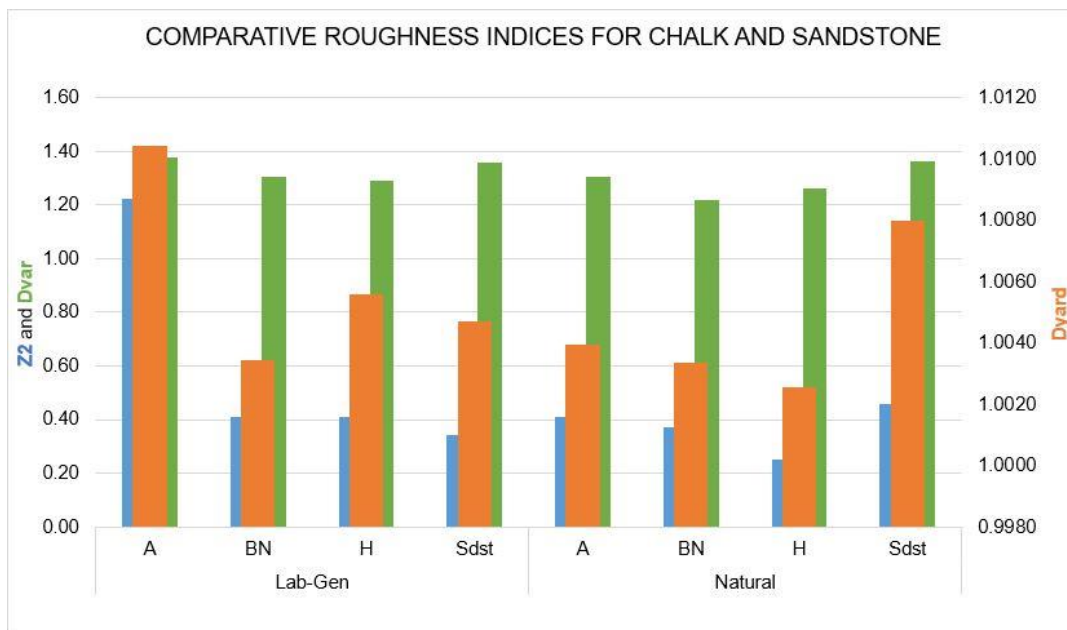


**Figure 2. Comparative roughness indices Z2, Dvar and Dyard for three chalks and a sandstone, natural fractures and lab-generated fractures.**

Roughness indices are in accordance with samples visual observation. Parameters Z2 and Dyard correlate well, while Dvar seems to express variations. The average asperities height Ra showed inconclusive results. While lab-generated fractures in shear or tensile mode tend to produce rougher surfaces than what is observed in the field on natural fractures, some disparities can be found, notably for the sandstone, for which alteration processes may have enhanced surface roughness over time. Within chalk samples, fault surfaces are rougher than joint surfaces for the chalk samples coming from Cap Blanc-Nez and Harmignies, however for surfaces collected in Arras, joint surfaces are rougher than the very smooth faults.

In conclusion, the same roughness characterisation process was successfully applied with use of fractal dimensions Dvar and Dyard, and statistical Z2 onto two very different lithologies: a sandstone and three chalks issued from different formations. The computations reveal differences, which not only distinguish the clastic, grainy and rougher sandstone from the chalk, but also highlight disparities between the chalks themselves.

**REFERENCES**

Bandis, S., Lumsden, A., Barton, N., 1983, Fundamentals of rock joint deformation, International Journal of Rock Mechanics, Mining Sciences and geomechanics, Vol 20, Iss 6, pp. 249–268

Belem, T., Homand-Etienne, F., Souley, M., 1997, Fractal analysis of shear joint roughness, International Journal of Rock Mechanics, Mining Sciences, Vol 34, Iss 3–4, pp.130.e1-130.e16

Chen, Y., Liang, W., Lian, H., Yang, J., and Nguyen, V.P., 2017, Experimental study on the effect of fracture geometric characteristics on the permeability in deformable rough-walled fractures, International Journal of Rock Mechanics & Mining Sciences, Vol 98, pp.121-140

Liu, X.G., Zhu, W.C., Yu, Q.L., Chen, Li, 2017, Estimation of the joint roughness coefficient of rock joints by consideration of two-order asperity and its application in double joint shear tests, Engineering Geology, Vol 220, pp.243–255.



## The Quest for Rock Site Characterization for the Greek National Seismic Network

Olga-Joan Ktenidou<sup>1</sup>, Faidra Gkika<sup>1</sup>, Christos Evangelidis<sup>1</sup>

<sup>1</sup>*Institute of Geodynamics, National Observatory of Athens, Greece, [olga.ktenidou@noa.gr](mailto:olga.ktenidou@noa.gr)*

### **Background**

The broadband seismic network of the National Observatory of Athens covers most Greek territory, mainland and island, with 50 broadband seismic stations. These are generally characterized as rock, without any in-situ site measurement of shear-wave velocity profiles or estimation of the stations' seismic response through recordings. Considering that: 1. today's sophisticated ground-motion models require a robust estimate of region-specific (rather than generic or borrowed) characterization of reference rock conditions; 2. today's strong-motion databases require more sophisticated, data-derived (rather than inferred) site metadata, and include broadband sensor data in addition to accelerometric data to better represent rock recordings; 3. Greek-provenance recordings represent a significant part of European data in global databases yet are poorly characterized, there are many good reasons that better site characterization of this network's stations has now become imperative. Moreover, stations up to now considered as rock were recently shown by the authors to exhibit significant variability and atypical seismic response with respect to their generic classification. Hence, the question of reference-station conditions becomes crucial.

### **Methods**

In-situ-characterization campaigns impose unattainable time/budget constraints, so we implement alternative approaches using the recordings themselves. We use the traditional empirical approach known as the horizontal-to-vertical spectral ratio (Lermo and Chavez-Garcia, 1993), and a more recent approach using ground-motion model residuals, namely the systematic deviation of a site compared to the average prediction. We also test the sensitivity of the results in terms of directional dependence following the approach of Ktenidou et al. (2016).

### **Results-Conclusion**

The computed transfer functions indicate that the response within what is classified by design codes as class A may vary, and even exhibit directional dependence (i.e., sensitivity of response to orientation). Results are compiled for future reference, hoping to aid in the quest for a more harmonized and data-driven site characterization throughout Greece.

### **REFERENCES**

- Ktenidou O.-J., F.J. Chávez-García, D. Raptakis and K.D. Pitilakis (2016). 'Directional dependence of site effects observed near a basin edge at Aegion, Greece'. Bull. Earthq. Eng. 14, 623-645.
- Lermo, J., and F.-J. Chávez-García (1993). Site effect evaluation using spectral ratios with only one station, Bull. Seism. Soc. Am. 83 1574-1594.

## Liquefaction estimates at different earthquake magnitudes in the coastal area of Kato Achaia, Greece with the use of CPT

Vasileios Boumpoulis<sup>1</sup>, O. Kontopidis<sup>1</sup>, Nikolaos Depountis<sup>1</sup>, Nikolaos Sabatakakis<sup>1</sup>

<sup>1</sup>University of Patras, Department of Geology, Greece, [geo11086@upnet.gr](mailto:geo11086@upnet.gr)

### **Introduction**

Cone Penetration Test (CPT) is an in-situ test that is used to determine the soil profile and stratigraphy and calculate the physical and mechanical properties of the penetrated soil. One of the most significant applications of this test, is the assessment and evaluation of the soil's liquefaction, through the continuous measurement of the soil parameters. The CPT results are more consistent and repeatable and allow a more detailed definition of soil layers than other in situ test (Youd and Idriss, 2001), compared with the SPT tests which are performed every 1,5-2 m in depth. As a result, CPT are used in the evaluation of the soil's liquefaction with a great success.

The methodology for the assessment of liquefaction from CPT tests, requires the calculation of the Factor of Safety ( $F_s$ ) against liquefaction, which is defined as the ratio between the Cyclic Resistance Ratio (CRR) and the Cyclic Stress Ratio (CSR),  $F_s = \text{CRR} / \text{CSR}$ . CRR is the strength of soil and the resist to liquefaction and CSR is the seismic demand. If  $F_s \leq 1$ , the soil layer is liquefiable and if  $F_s > 1$ , the soil layer is characterized as non-liquefiable (Seed and Idriss, 1971).

The current research focuses on the estimation of soil liquefaction in the coastal area of Kato Achaia, Greece, (Figure 1a) where some liquefied hot spots occurred after an earthquake of  $M_w = 6.4$  that struck Greece on the 8<sup>th</sup> of June in 2008 (Margaris et al, 2010, Batilas et al, 2014). Even though several damages in buildings and infrastructures were recorded in the wider area after the earthquake event, no serious damages were recorded in the coastal area of research, probably, due to its sparse residential development. For this reason, this research is important because it investigates the potentiality of liquefaction in the Kato Achaia coastal zone and therefore can provide to the local authorities all the necessary information for any potential risk may occur in future construction activities.

### **Methods and field investigation**

The liquefaction potentiality was estimated by performing eleven (11) CPT's in the field. The methodology that was used for the calculation of the CRR and CSR ratios, is the one that has been suggested by Youd and Idriss (2001). The factors of safety were calculated for three different earthquake scenarios: a)  $M_w = 7.5$  and  $a_{\max} = 0.24g$ , b)  $M_w = 6.5$  and  $a_{\max} = 0.24g$  and c)  $M_w = 6.4$  and  $a_{\max} = 0.18g$  which is the actual earthquake that struck Greece in 2008 caused by a right-lateral strike-slip vertical fault (Margaris et al, 2010).

### **Results**

The results of the CPT showed that the area has two (2) potentially liquefied soil layers, the first at a depth of 3.50-6.00 m and the second at a depth of 8.20-12.30 m. These soil layers are classified as potentially liquefied, since the soil behavior type  $I_c$  is less than 2.6, while layers with  $I_c > 2.6$  are classified as non-liquefied, because the soil is mainly clayey. Below, in a chart showing the average values of the safety factor for each test in relation to the depth of the soil layer, are presented the results of CPT's (Figure 1b).

**Conclusion**

Three different scenarios were examined for the liquefaction potentiality in the Kato Achaia coastal zone:

- The first extreme earthquake scenario with  $M_w=7.5$  and  $a_{max}=0.24g$ , proved to be the worst scenario since all soil layers estimated with a  $FS<1$ . This is a scenario with a very low probability to occur, as the faults in the surrounding area have a limited potential to earthquakes of  $M_w=7.5$ .
- The second scenario, with  $M_w=6.5$  and  $a_{max}=0.24g$ , and a high probability to occur had again a  $FS<1$ . However, below the depth of 10m the scenario seems to become more favorable since the  $FS$  was estimated as  $FS>1$ .
- The third scenario, representing the earthquake event of 2008, with  $M_w=6.4$  and  $a_{max}=0.18g$  proved to be a favorable scenario as nearly all soil layers estimated with a  $FS>1$ , apart from a few sparse zones located very close to the liquefied hot spots that had been observe after the earthquake.

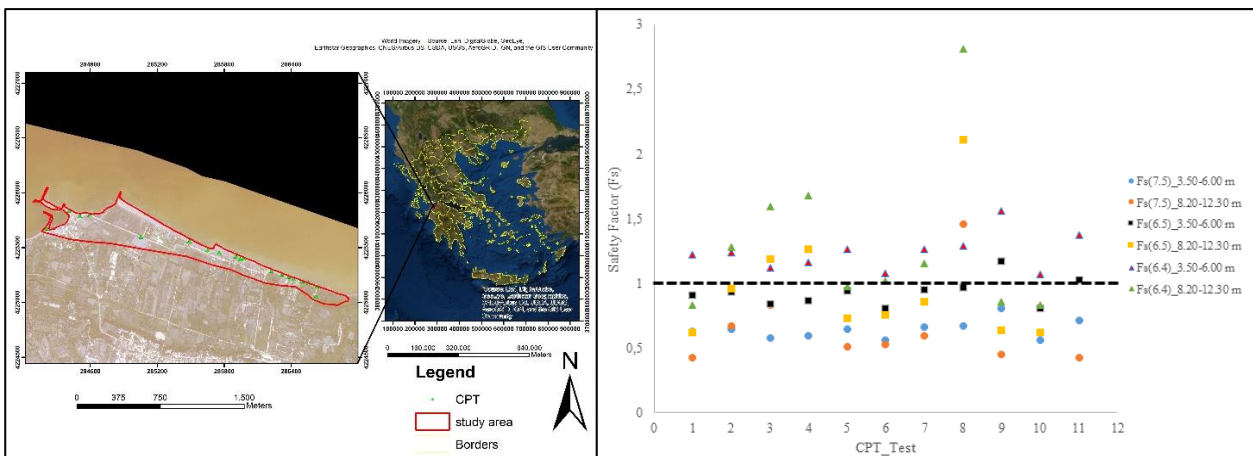


**Figure 1: a) Study area and b) Results of Cone Penetration Tests (Safety factors for liquefaction)**

All results prove that the CPT investigation method is accurate for detecting liquified areas and if a similar earthquake had struck with  $M_w=6.5$  and a higher acceleration than  $a_{max}=0.24g$ , the damages would be more serious and liquefaction more severe.

**Acknowledgment**

This research is co-financed by Greece and the European Union (European Social Fund- ESF) through the Operational Programme «Human Resources Development, Education and Lifelong Learning 2014-2020» in the context of the project “Integrated research of coastal vulnerability in Western Greece with remote sensing, engineering geology and in situ measurements” (MIS 5047163).”

**REFERENCES**

Batilas A, Pelekis P, Vlachakis V, Athanasopoulos G (2014) Soil Liquefaction/Non Liquefaction in the Achaia-Ilia (Greece) 2008 Earthquake: Field evidence, Site Characterization and Ground Motion Assessment. Inter J Geoengineering Case Hist 2(4):270-287. <http://dx.doi.org/10.4417/IJGCH-02-04-03>

Margaris, B., Athanasopoulos, G., Mylonakis, G., Papaioannou, C., Klimis N., Theodulidis N., Savvaidis A., Efthymiadou V. and Stewart P.J. (2010). The 8 June 2008 Mw6.4 Achaia–Elia, Greece Earthquake: Source Characteristics, Ground Motions, and Ground Failure. Earthquake Spectra, Volume 26, No. 2, pages 399–424.

Seed, H. B., and Idriss, I. M. (1971). “Simplified procedure for evaluating soil liquefaction potential.” *Journal of the Soil Mechanics and Foundations Division*, 1971, Vol. 97, Issue 9, Pg. 1249-1273.

Youd, T. L. and Idriss, I. M. (2001). Liquefaction resistance of soils: summary report from the 1996 NCEER and 1998 NCEER/NSF workshops on evaluation of liquefaction resistance of soils. Journal of geotechnical and geoenvironmental engineering, Volume 127 Issue 10.



## The effectiveness of Blastability Quality System on rock slopes. A case study in a landslide restoration

Maria Chatziangelou<sup>1</sup>, Costas Anagnostopoulos<sup>2</sup>

<sup>1</sup>Aristotle University of Thessaloniki, Greece, [mcha@ndr.com.gr](mailto:mcha@ndr.com.gr)

<sup>2</sup>International Hellenic University, [kanagnos@cie.teithe.gr](mailto:kanagnos@cie.teithe.gr)

There are small differences between the variables of the rock mass classification systems, but for this reason the same rock mass may be differently classified by the engineers. This can cause changes in the parameters for the foundations designing. Blastability Quality System's role is the combination of the different classical classification systems quickly in situ, that the engineers can use them at the same time, so as they minimize the differences of their estimations.

The Blastability Quality System (BQS) is based on Rock Mass Rating (RMR) and Geological Strength Index (GSI). The significance of this paper is the evaluation of the use of BQS on rock slopes in practice.

A landslide, which took place in Northern Greece, is used for our investigation.

The landslide is placed in Thassos Island in a tectonic active fault damage zone of gneiss and sandstone and it was triggered after intense and continuous rain in July 2018. The BQS is used in order to describe the landslide's mechanism and to decide the appropriate restoration.

The results of the BQS description are combined with the results of the Slope Mass Rating Classification (SMR) because the SMR had been devised and relied on RMR in order the classification can be applied on slopes. The qualified characteristics are used to classify the rock mass according to BQS and to SMR. The final results of classification methods BQS and SMR are similar. It is significant that the both estimates are really close. So, the BQS can effectively be used as a combinational classification system and result to the appropriate support measure.

The design of the appropriate support needs to consider the rock mass quality in details. For this reason, the rock mass is divided in four areas with different appearances, which they are separately classified. According to the results, the upper stratum of the rock mass is good quality and the lower stratum is medium quality. The decision about the installation of the support measures mainly depends on the lower stratum, where quality of the rock mass is the worst. Accordingly, if the lower stratum is supported effectively, it assures the main percent of stability.

The support measures cannot stop the movement of the fault, but they can follow the movement and absorb the energy and deformation. For this reason, the support measures need to be flexible and not rigid. Considering the presence of the active fault and the rock mass quality, the appropriate restoration can be a flexible system with gabions and benches which follow the geometry of the potential critical sliding cycle so, it can absorb the fault movement during future earthquakes. The cracked small wedges can be prevented from sliding by wire mesh. In addition to all of them, a drainage system and toe ditch need to drive the water of the rainfall out of the slope.

### REFERENCES

- Ajoy., Gh. & Akhilesh, J., 2012, *Blasting in Mining – New Trends*. Taylor & Francis, CRC Press, 150 p.
- Bieniawski, Z.T., 1989, *Engineering Rock Mass Classifications*, Wiley, New York.
- Bieniawski, Z.T., 1993, *Classification of Rock Masses of Engineering: The RMR System and Future Trends*, Rock Testing



and Site characterization, Elsevier, pp. 553-573.

Chatziangelou, M. & Christaras, B., 2017, A New Development of BQS (Blastability Quality System) for closely Spaced Formations. *Journal of Geological Resource and Engineering*, David Publishing, pp. 24-37.

Christaras, B. & Chatziangelou, M., 2014, Blastability Quality System (BQS) for using it, in bedrock excavation. *Structural Engineering and Mechanics*, Technopress, v.51, no. 5, 823-845.

Coppola, L., 2018, *Hydrogeological Instability in cohesive soils: Techniques for Prediction, Prevention and Control*, Springer, 281 p.

Hocking, G., 1976, A method for distinguishing between single and double plane sliding of tetrahedral wedges. *Int. Journal of Rock Mechanics & Mining Science*. v.13, pp. 225-226.

Hoek, E., Brown, E.T., 2019, The Hoek – Brown failure criterion and GSI – 2018 edition. *Journal of Rock Mechanics and Geotechnical Engineering II*, pp. 445-463.

Hoek, E., Marinos, P., Benissi, M., 1998, Applicability of the geological strength index (GSI) classification for very weak and sheared rock masses. The case of the Athens Schist Formation. *Bull eng Geol Env*, v. 547, pp. 151-160.

Kluger, M., Moon, V., Jorat, Eh., Kreiter, S., 2020, Rainfall threshold for initiating effective stress decrease and failure in weathered tephra slopes. *Landslides*, [https://doi.org/ 10.1007/s10346-019-01289-2](https://doi.org/10.1007/s10346-019-01289-2).

Loupasakis C., Konstantopoulou, G., 2007, A Failure Mechanism of the fine Neogene Formations: An Example from Thasos, Greece, *Landslides: Journal of International Consortium of Landslides*, Springer, v. 4, no. 4, pp. 351-355.

Marinos, V., Marinos, P., Hoek, E., 2005, The geological strength index: applications and limitations. *Bulletin of Engineering Geology and the Environment*, v. 64, pp. 55-65.

Marinos, P., Marinos, V., Hoek, E., 2007, Geological Strength Index (GSI). A characterization tool for assessing engineering properties for rock masses. *Proceedings International Workshop on Rock Mass Classification for Underground Mining*, Mark, *Pakalnis and Tuchman*, Information Circular, pp. 87-94.

Markland, J.T., 1972, A useful technique for estimating the stability of rock slopes when the rigid wedge sliding type of failure is expected. *Vol.19: Imperial College Rock Mechanics Research Report*, pp. 1-10.

Romana, M. Tomas, R., Seron, J.B., 2015, Slope mass Rating (SMR) geomechanics classification: thirty years review. In: *Proceedings – International Symposium on Rock Mechanics*, Quebec, Canada. *ISRM Congress*, v. 10.

Wu, F. & Wang, S., 2001, Strength theory of homogeneous jointed rock mass. *Geotechnique*, No.9, v. 51, pp. 815-818.



## THEME 2 - ENVIRONMENTAL ENGINEERING GEOLOGY



## Dating of fault movements and earthquake recurrence near hard infrastructure

K.V. Kanavou<sup>1</sup>, D.C. Athanassas<sup>1</sup>, V. Mouslopoulou<sup>2</sup>, X. Aslanoglou<sup>3</sup>, K. Stamoulis<sup>3</sup>

<sup>1</sup>*School of Mining and Metallurgical Engineering, NTUA, Greece, [kanavouv@mail.ntua.gr](mailto:kanavouv@mail.ntua.gr);*

*[athanassas@central.ntua.gr](mailto:athanassas@central.ntua.gr)*

<sup>2</sup>*National Observatory of Athens, Greece, [vasiliki.mouslopoulou@noa.gr](mailto:vasiliki.mouslopoulou@noa.gr)*

<sup>3</sup>*Department of Physics, University of Ioannina, Greece, [xaslanog@uoi.gr](mailto:xaslanog@uoi.gr); [kstamoul@cc.uoi.gr](mailto:kstamoul@cc.uoi.gr)*

### Introduction

Hard infrastructure serving urban and suburban areas is likely to be affected by large-magnitude ( $M > 6$ ) earthquakes, particularly in seismically active areas like Greece. Constraining the number and attributes of the active seismic sources by providing the engineers information on the of dimensions, slip-size and timing of the past large earthquakes in the vicinity of major technical works (such as tunnels, dams, mines, etc.), may be vital for their safety and longevity. However, as fault-slip accumulation is a highly variable process that spans various timescales (Mouslopoulou et al., 2009), it is important to provide chronometric constraints that derive from numerous earthquake-cycles. Slip rates on exhumed fault scarps are typically estimated by terrestrial cosmogenic nuclides (TCN);  $^{36}\text{Cl}$  for carbonate rocks and  $^{10}\text{Be}$  and  $^{26}\text{Al}$  for silicate rocks (Benedetti and van der Woerd, 2014). TCN accumulate on the rock surfaces through interactions with incoming cosmic rays over time and their concentration measures how long a fault surface lies above (or near) the ground surface. The individual exhumation events are identified on a fault scarp through the measurement of TCN (Figure 1) (e.g., Benedetti and van der Woerd, 2014; Mouslopoulou et al., 2014). An alternative and potentially effective method of dating the exposure duration of rock surface is based on the optically stimulated luminescence (OSL) signal from silicate minerals native to the rock itself, such as quartz and feldspar. Typically, OSL dating determines the time elapsed since the last exposure of mineral grains to daylight (Athanassas and Wagner, 2016; Stamoulis et al., 2017). However, in this study we attempt to use this method in “converse mode” and estimate the time elapsed since the exhumation of fault surface to daylight, based on the fact that light penetrates slightly into the rock surface and may reset OSL of quartz to a depth of a few millimeters (depending on the rock’s opacity) (e.g. Sohbaty et al., 2012; Sohbaty et al., 2018). This work describes the first attempt to test and refine the OSL methodology as a tool for numerically dating paleoearthquakes on carbonate scarps. As a case study, we used a fault from the eastern Corinth Rift in Greece and in particularly, the Psatha Fault, a structure of known late-Pleistocene (~16 ky) seismic history (Mouslopoulou et al., in prep.) which provides a unique opportunity to compare (and calibrate) the OSL methodology.

### Method

More than 80 samples were collected from nearly vertical fault escarpments (e.g. Psatha fault). The fault scarps were sampled in 10cm intervals, extracting limestone tiles with dimensions 5 cm wide, 15 cm long and 3 cm thick. A portion from the samples was processed at the Archaeometry Center of the University of Ioannina. Successive layers of rock were peeled off in 0.02 mm intervals by mechanical abrasion. Material from each layer passed through sieves and the portion  $< 63 \mu\text{m}$  was collected and chemically treated for quartz extraction. The samples were treated with 5ml HCl (8% w/w) to remove carbonates, 5ml H<sub>2</sub>O<sub>2</sub> (30% w/w) to remove organic residuals. Polymineral fine grains (4-11  $\mu\text{m}$ ) were collected through suspension and settling. Purified quartz grains were placed on small stainless discs for OSL measurement by applying the SAR protocol (Murray and Wintle, 2000).

**Results and conclusion**

Figure 2 illustrates a typical growth curve, and the associated decay curve, of a quartz sample extracted from the fault scarp. Despite the unusual material processed (carbonate rock), the sample demonstrates an OSL behavior typical of quartz which contains trapping centers where the charge is stable over geological period and is capable of producing luminescence signal. If we consider an average dose rate of 0.2-0.3 Gy/ka for a carbonate rock, the estimated OSL age is well younger than the formation age of the limestone. Given the sub-superficial position of the aliquot in relation to the fault surface, these preliminary measurements imply that the quartz has been partially lending credibility to our initial assumptions. Currently, efforts are made to generate an “OSL versus depth” profile. Comparison of the ongoing exposure-OSL measurements with the independent TCN chronology (Mouslopoulou et al., in prep), will enable testing and calibration of this new methodology against a well-established slip history.

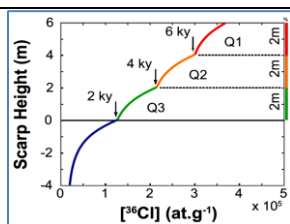


**Figure 1.** Numerical model of <sup>36</sup>Cl concentration profile on a carbonate fault scarp (Benedetti and van der Woerd., 2014). This model illustrates the <sup>36</sup>Cl concentration that was produced by three earthquake events. We observe that as the height increases, the <sup>36</sup>Cl concentration in the samples increases due to their exposition in cosmic ray for longer period in contrast with these samples, beneath the surface, where the rate accumulation decreases exponentially.

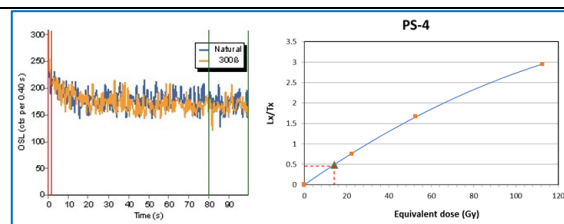


**Figure 2.** Typical OSL decay (left) and growth curve of quartz (right) for a sample from the Psatha fault. The decay curve represents the luminescence signal of quartz in the sample as a function of stimulation time while the growth curve represents the corrected OSL signal (Lx/Tx) as a function of the laboratory dose. Through the interpolation of the Ln/Tn ratio (natural signal), the equivalent dose can be calculated (red dotted line).

**REFERENCES**

Athanassas, C.D., Wagner, G.A. 2016, Geochronology beyond radiocarbon: optically stimulated luminescence dating of paleoenvironments and archaeological sites. *Elements*, v. 12, pp. 27-32

Benedetti, L., van der Woerd, J. 2014, Cosmogenic nuclide dating of earthquakes, fault and toppled blocks. *Elements*, v.10, pp.357-361

Mouslopoulou, V., Moraetis, D., Benedetti, L., Guillou, V., Bellier, O., Hristopoulos, D., 2014, Normal faulting in the forearc of the Hellenic subduction margin: Paleoearthquake history and kinematics of the Spili Fault, Crete, Greece. *Journal of Structural Geology*, v. 66, pp. 298-308, doi: 10.1016/j.jsg.2014.05.017

Mouslopoulou, V., Walsh, J.J., Nicol, A., 2009, Fault displacement rates on a range of timescales. *Earth and Planetary Science Letters* v. 278, pp. 186-197, <https://doi.org/10.1016/j.epsl.2008.11.031>

Mouslopoulou et al. (in prep), The late-Pleistocene slip history on the Psatha Fault, eastern Corinth Rift, as constrained by <sup>36</sup>Cl TCN dating. To be submitted in *Journal of Structural Geology*

Murray, A.S. & Wintle, A.G.2000, Luminescence dating of quartz using an improved single-aliquot regenerative-dose protocol. – *Radiation Measurements*, v. 33, pp. 57-73

Sohbati R., Jain M., Murray A., 2012, Surface exposure dating of non-terrestrial bodies using optically stimulated luminescence: A new method. *Icarus* 2 v. 21, pp. 160-166

Sohbati, R., Liu, J., Jain, M., Murray, A., Egholm, D., Paris, R., Guralnik, B. 2018, Centennial-to millennial-scale hard rock erosion rates deduced from luminescence-depth profiles. *Earth and Planetary Science Letters*, v. 493, pp. 218–230.

Stamoulis K.C., Tsodoulos I., Papachristodoulou C., Ioannides K.G. 2017, Paleoseismology: Defining the seismic history of an area with the use of the OSL dating method. *Proceedings of the 4th Workshop on new aspects and perspectives in nuclear physics*. Ioannina, May 5-6, 201



## Comparative life cycle assessment for shallow slope failure stabilization techniques

Dominic Leal<sup>1</sup>, Mike G Winter<sup>2</sup>, Richard Seddon<sup>3</sup>, Ian M Nettleton<sup>4</sup>, Jan Marsden<sup>5</sup>

<sup>1</sup>Formerly TRL Limited now Atkins, United Kingdom, [dominic.leal@hotmail.co.uk](mailto:dominic.leal@hotmail.co.uk)

<sup>2</sup>Formerly TRL Limited now Winter Associates, United Kingdom, [mwinter@winterassociates.co.uk](mailto:mwinter@winterassociates.co.uk)

<sup>3</sup>Formerly Coffey Geotechnics now Jacobs, United Kingdom, [richard.seddon@jacobs.com](mailto:richard.seddon@jacobs.com)

<sup>4</sup>Coffey Geotechnics, United Kingdom, [ian.nettleton@coffey.com](mailto:ian.nettleton@coffey.com)

<sup>5</sup>Formerly Highways England, United Kingdom, [geotechnicsteam@highwaysengland.co.uk](mailto:geotechnicsteam@highwaysengland.co.uk)

Work to evaluate the effectiveness of innovative geotechnical repair techniques for slopes was commissioned by Highways England. The techniques are the planting of live willow poles (Winter et al. (2018)), Fibre Reinforced Soil (FRS) (Seddon et al. 2018) and Electrokinetic Geosynthetics (EKG) (Nettleton et al. (2018)). These techniques were used in place of conventional approaches in order to reduce the overall impact of various challenges including environmental constraints (habitat and visual), access and utility constraints, and the need to reduce the scale and/or cost of traffic management and delays.

In addition to the technical efficacy of the techniques estimates of the carbon impacts of four remedial techniques were made. A notional 25° highway slope, 10m high and 100m wide for failure depths of 1m and 2.5m was assumed to be stabilized for the assessment. In addition to the willow pole planting, FRS and EKG techniques, a Granular Rock Fill Replacement control was also assessed. These were compared using a cradle-to-site life cycle assessment. Five life cycle steps were defined and assessed, from the acquisition and processing of each installation's constituent materials, through to the construction of the final product – a stabilised slope.

A cradle-to-site Life Cycle Assessment (LCA) boundary was adopted (using the cut-off approach), as opposed to a full cradle-to-grave assessment. This approach was adopted for a number of reasons. Firstly, each of the techniques has different maintenance requirements, occurring in uneven time frames. Secondly, the expected lifetimes and end-of-life scenarios for each technique vary in ways that would not allow for a balanced comparison within equal time frames. Data was compiled from a number of representative sources and where possible was selected for UK specific values. Transport was calculated using tonne.km factors for a range of delivery vehicles, depending on the material and scenario. All transport was calculated for two-way (full outward-empty return) journeys.

This study aimed to provide a range of general estimates, and as the slope under assessment was hypothetical, it did not have a real-world location. As a consequence, the transport impact calculations are based on assumed low-medium-high distances for transport impact calculations. The functional unit of analysis of the assessment was the ability of each technique to stabilise 1m<sup>2</sup> of failed slope; results are given in Figure 1 and total carbon for the entire failure are given in Figure 2.

It was found that at both failure depths, and for all transport cases, the greatest environmental impact was for the Granular Rock Fill Replacement. At 1m and 2.5m failure depths this technique resulted in an impact of 51 to 174 kgCO<sub>2</sub>e/m<sup>2</sup> of failed slope respectively, depending upon the transport distance assumed. Willow Poles had the least impact, resulting in 4 to 12 kgCO<sub>2</sub>e/m<sup>2</sup> of failed slope respectively. For the 2.5m failure depth EKG was the second best performing technique (EKG was not assessed for the 1m failure depth scenario), with an impact of around 14 kgCO<sub>2</sub>e/m<sup>2</sup>. FRS had an impact ranging between 16 and 35 kgCO<sub>2</sub>e/m<sup>2</sup>. For techniques requiring large quantities of materials and movements of these materials across substantial

distances (e.g. Granular Rock Fill Replacement and Willow Poles), it was found that transportation accounts for more than half of the total impact. A more complete treatment is given by Leal et al. (2018, 2020).

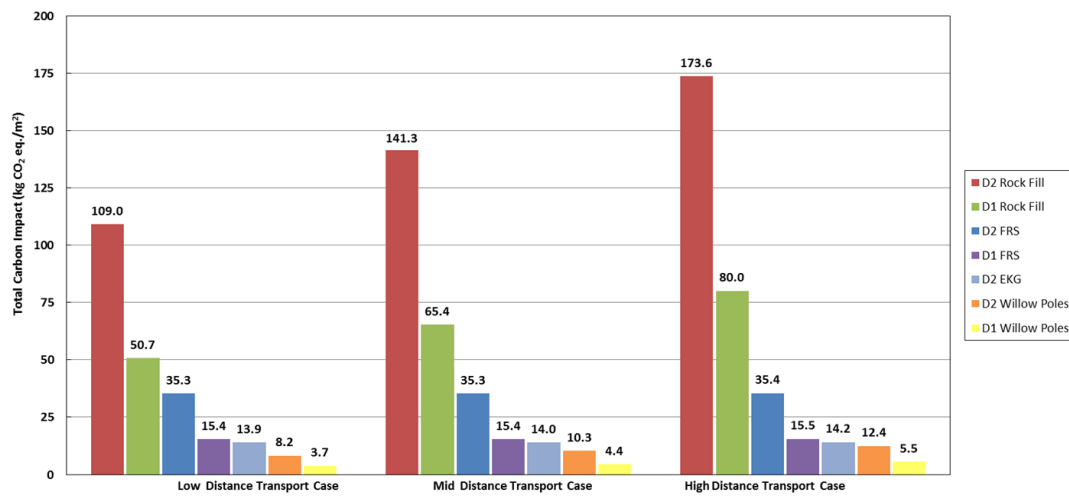


Figure 1. Areal impact comparison (D1 corresponds to a failure depth of 1m, and D2 to a failure depth of 2.5m).

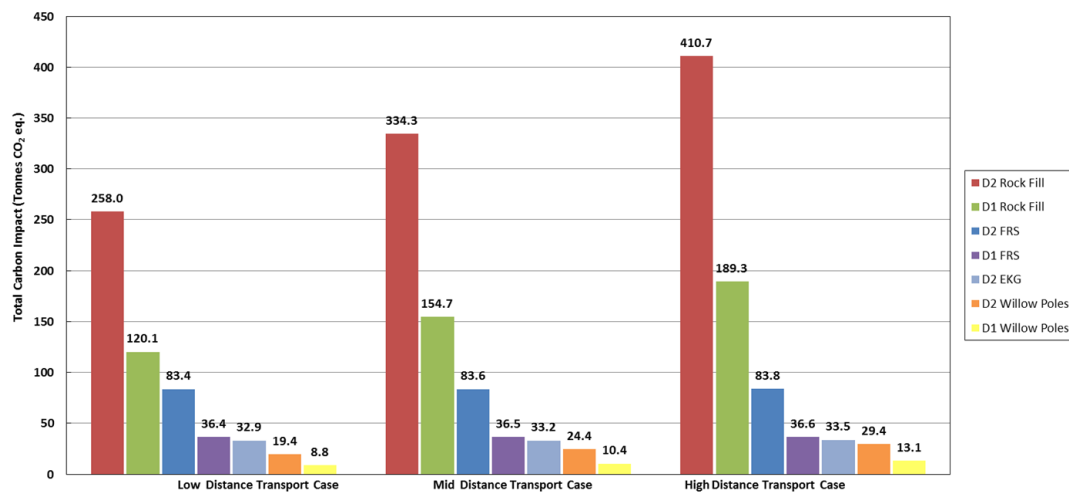


Figure 2. Total impact comparison (D1 corresponds to a failure depth of 1m, and D2 to a failure depth of 2.5m).

**REFERENCES**

Leal, D., Winter, M. G., Seddon, R. and Nettleton, I. M. 2018. Innovative geotechnical repair techniques: comparative life cycle assessment. PPR 889. TRL, Wokingham.

Leal, D., Winter, M. G., Seddon, R. and Nettleton, I. M. 2020. A comparative life cycle assessment of innovative highway slope repair techniques. *Transportation Geotechnics*, 22, 1-8.

Nettleton, I. M., Seddon, R. and Winter, M. G. 2018. Innovative geotechnical repair techniques: effectiveness of electrokinetic geosynthetics. PPR 890. TRL, Wokingham.

Seddon, R., Winter, M. G. and Nettleton, I. M. 2018. Innovative geotechnical repair techniques: effectiveness of fibre reinforced soil. PPR 873. TRL, Wokingham.

Winter, M. G., Nettleton, I. M. and Seddon, R. 2018. Innovative geotechnical repair techniques: recommendations and guidance for management of future Highways England trials with innovative techniques. PPR 891. TRL, Wokingham.

## Estimation of the sediment yield in earth-fill dams with the use of the Revised Universal Soil Loss Equation

Maria Michalopoulou<sup>1</sup>, Nikolaos Depountis<sup>1</sup>, Katerina Kavoura<sup>1</sup>, Nikolaos Sabatakakis<sup>1</sup>

<sup>1</sup>Department of Geology, University of Patras, Greece, [geo12088@upnet.gr](mailto:geo12088@upnet.gr)

### Introduction

Soil erosion has always been a worldwide environmental concern because its effects are evident in the natural and anthropogenic environment. One of the most significant outcomes of soil erosion in dam water reservoir's is the deposition of sediment which may lead to an increased aggradation rate and a reduced water storage capacity of the dam. In the current study the Revised Universal Soil Loss Equation (RUSLE) adopted in a Geographical Information System (GIS) framework is used for estimating the soil erosion rate and the sediment yield in the water reservoir of the Pinios earth-fill dam, which is located in Western Greece and has been affected by a severe wildfire that hit Greece in August 2007 (Figure 1).

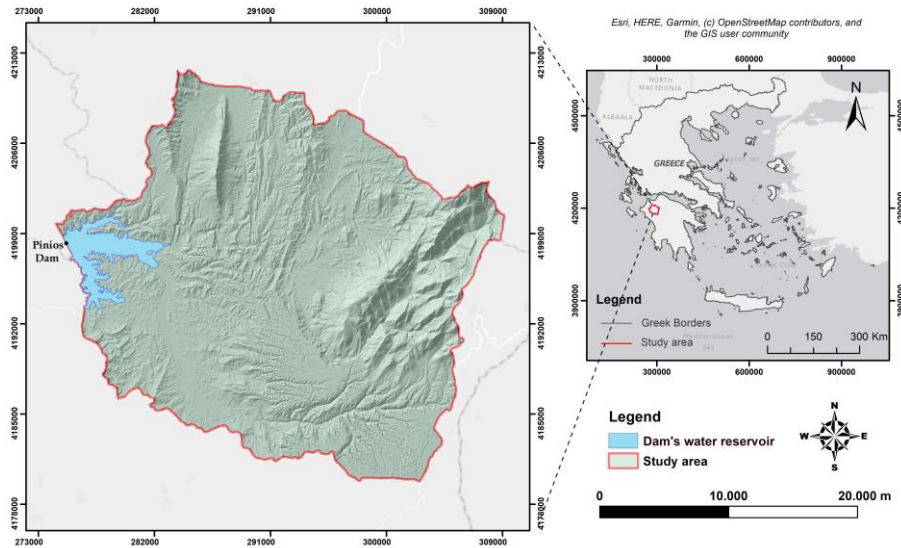


**Figure 2: Study area.**

### Methodology

The soil erosion rate (SE) for the last fifty years, which is the operational time of the dam, is calculated with the import of the following RUSLE equation (Renard et al., 1997), in the GIS framework:

$$SE = R * K * L * S * C * P \quad (1)$$

where SE is the computed average soil loss per unit area expressed in tones/ha/year, R is the rainfall-runoff erosivity factor, K is the soil erodibility factor, LS are the slope length and steepness factors, C is the cover management factor and P is the erosion control practice factor.

With this methodology soil erosion rate maps are produced, and the soil loss is estimated for the catchment area upstream of the dam's water reservoir. A significant amount of this soil loss is deposited in the dam's reservoir. Therefore, by using Maner's equation (1958), the average annual sediment yield (SY) is estimated by multiplying the Sediment Delivery Ratio (SDR) with the computed average soil loss (SE) per unit area:

$$SY = SDR * SE \quad (2)$$



SDR is estimated by using the weighted average of Renfro's equations (1975):

$$\log(SDR1) = 1.7935 - 0.14191 * \log(A) \quad (3)$$

$$\log(SDR2) = 2.94259 + 0.82362 * \log(R/L) \quad (4)$$

where A is the dam's catchment area, L is the length of the longest stream and R is the altitude difference between the beginning and the end of this stream.

### **Results**

The computed average soil loss (SE) per unit area in the research area is equal to SE(1)=69 t/ha/year for the pre-fire period, SE(2)=94 t/ha/year for the post-fire period and SE(3)=64 t/ha/year for the last two years. Therefore, the average soil loss in the dam's catchment area for the last fifty (50) years, which corresponds to the dam's operational life is calculated with the following equation:

$$SE50 = (SE38 + SE10 + SE2)/50 = 73.80 \text{ t/ha/year}$$

The Sediment Delivery Ratio (SDR) is calculated with the use of equations (3) and (4), with SDR(1)=24.53% and SDR(2)= 39.2% and the weighted average of both is applied in equation (2) for estimating the average annual sediment yield of the dam's reservoir, which is SY=824,378 m<sup>3</sup>/year.

Based on the above results and the fact that the reservoir of the dam occupies an area of E = 19.87 Km<sup>2</sup>, the average sediment deposition in m/year is SY=0,04m/year, which means that a 2m thick load-bearing materials have been deposited in the dam's reservoir the last fifty years.

### **Conclusions**

The methodology applied in this research for estimating sediment yield in earth-field dams seems to work very efficiently, since all the mathematical calculations are close to the real measurements that have been made in the dam's reservoir. The sediments that have been deposited at the deepest point of the reservoir are lying between the absolute altitudes of +52 and +56, so an average of 2m sediment thickness deposited in the reservoir's basin seems to be reasonable.

### **Acknowledgment**

This research has been partially financed by the Water Union of Pinios located in the Ilia regional Unit, Greece

### **REFERENCES**

- Renard, K.G., Foster, G.R., Weesies, G.A., McCool, D.K., Yoder, D.C., 1997, Predicting soil erosion by water: a guide to conservation planning with the Revised Universal Soil Loss Equation (RUSLE), Agriculture Handbook, No.703, USDA-ARS. United States Department of Agriculture, Washington, D.C., USA. pp.384
- Renfro, G.W., 1975, Use of erosion equations and sediment delivery ratios for predicting sediment yield. In Present and Prospective technology for predicting sediment yields and sources, Agricultural Resources Services, ARS-S-40, 33- 45. US Dept. Agric., Washington, D.C.
- Maner, S.B., 1958, Factors affecting sediment delivery rates in the Red Hills physiographic area. Trans AGU 39(4): 669-675.

## Rock material reutilization from tunnel excavation with reference to long tunnel structures

Klaus Voit<sup>1</sup>, Erik Kuschel<sup>1</sup>, Christian Zangerl<sup>1</sup>

<sup>1</sup>*Institute of Applied Geology, University of Natural Resources and Life Sciences, Austria,*

[klaus.voit@boku.ac.at](mailto:klaus.voit@boku.ac.at)

During tunnel construction, large quantities of excavated rock material are generated from the in-situ rock mass. Thereby, type and quality of the excavation material is depending on the geomechanical characteristics of the surrounding rock mass, including i) rock type and mineral composition, ii) discontinuity type and network (e.g. stratification, schistosity, joints) iii) major tectonic stresses, iv) groundwater conditions, and v) excavation methods (i.e. blasting or tunnel drilling machine). However, excavation material – if showing suitable aggregate characteristics and being appropriate for further processing – can be processed and used as a substitute for conventional mineral aggregates. Since there is a considerable need for construction material – at least locally on the construction site itself –, this approach makes sense from an economic and ecologic point of view. Due its nature it can be assumed that excavated rock is not a standard material in terms of geometric, physical and chemical characteristics and is subject to quality deviations during tunnel driving, meaning each tunnel construction site, even each tunnel section is different. Therefore, intensive research and testing are necessary to optimize selection, processing and type of utilization of the rock material.

Examples in Switzerland at the Lötschberg and Gotthard base tunnel showed that a strategy of extensive material recycling can lead to the reduction of costs regarding material procurement, storage and transport as well as a decreased demand for landfill volume. At the Lötschberg base tunnel, mainly rocks composed of gneisses, schists and amphibolites excavated from die Aar Massif as well as limestones were used for aggregate production, while sandstones and marlstones from extended Helvetic Units were discarded. In the case of the Gotthard base tunnel, excavation material composed of gneisses, migmatites, schists and granodioritic intrusions from the Aar and Gotthard Massif as well as granitic gneisses from the Penninic Gneiss Zone were processed and recycled, sediments made of Anhydrite and Dolomite were discarded.

The aim of the current research is to investigate the rock characteristics and to explore the optimum processing and recycling possibilities demonstrated with the example of the currently ongoing tunnel construction of the Brenner Base Tunnel between Austria and Italy. The Brenner Base Tunnel crosses the complex tectonic transition zone between the Northern and Southern Alps cutting through the Brenner massif with all major tectonic units of the Alps. In doing so, particularly for the Austrian tunnel section mainly the metamorphic units of the Quartz Phyllites of Innsbruck (Austroalpine bedrock) and the Bündner Schists (Subpenninic in the antiformal structure of the Tauern Window) were crossed. Both rock types belong to metamorphic rocks, containing large amounts of sheet silicates and therefore showing a penetrative foliation (Figure 1).

Physical and chemical rock properties of both rock types, Bündner Schists as well as Quartz Phyllites of Innsbruck, were evaluated regarding their recycling potentials. Tests regarding water absorption, rock strength (compressive strength as well as tensile strength), Young's modulus, resistance against impact and abrasive loads, abrasiveness, as well as chemical and petrological testing were performed.

In a next step, large-scale processing experiments were conducted performing a wide range of rock investigation concerning the geometrical, physical and chemical properties after processing (crushing, screening and washing) as well as intensive concrete testing using the recycled aggregates for concrete production. After developing a processing concept, a processing plant was installed using a three-stage rock



crushing system as well as a high performing wet-processing (washing and sieving) at the tunnel construction site (Figure 2).



**Figure 1: Calcareous Schists from Bündner Schist Unit used for aggregate production during tunnel driving;**



**Figure 2: Pre-crushing and screening (0/150 mm) in tunnel**

Rock material obtained of the Bündner Schists showed adequate properties in terms of grain size distribution, grain shape and content of fines regarding the utilization as aggregate for concrete, while rocks from the Quartz Phyllites of Innsbruck only reached poor quality. According to this, the produced aggregates from the Bündner Schists were used for concrete production, but making identity tests necessary during concrete production as well as the in-situ examination of hardened concrete through the extraction of drill cores from structures and precast concrete components.

Finally, by using a three-stage rock crushing system and a high performing wet-processing for Bündner Schist rock material processing, the production of about 600 tons per day of aggregate for concrete was possible, manufacturing ca. 100 m<sup>3</sup> shotcrete per day as well as the required quantity of structural and inner lining concrete. Through this approach, natural resources could be preserved, costs for material procurement, storage and transport be reduced and the demand for landfill volume be decreased. In this research project it could be shown, that even for rock types with a moderate rock characteristics recycling is well realizable, ecologically and economically viable and thus will also be applied for future construction projects.

## REFERENCES

Voit, K., and Kuschel, E., 2020, Rock Material Recycling in Tunnel Engineering. MDPI Appl. Sci. 2020, 10(8), 2722; <https://doi.org/10.3390/app10082722>

## Numerical assessment of groundwater flow and transport in fractured rocks: Benchmark cases for concepts of DFN, ECPM, and Hybrid approaches

Yun-Chen Yu<sup>1,2</sup>, I-Hsien Lee<sup>3,4</sup>, Chuen-Fa Ni<sup>5</sup>

<sup>1</sup>*Institute of Nuclear Energy Research, Atomic Energy Council, Executive Yuan, Taiwan(ROC),*

[yuyc@iner.gov.tw](mailto:yuyc@iner.gov.tw)

<sup>2</sup>*Graduate Institute of Applied Geology, National Central University, Taiwan(ROC),* [yuyc@iner.gov.tw](mailto:yuyc@iner.gov.tw)

<sup>3</sup>*Center for Environmental Studies, National Central University, Taiwan(ROC),* [ihsienlee@ncu.edu.tw](mailto:ihsienlee@ncu.edu.tw)

<sup>4</sup>*Graduate Institute of Applied Geology, National Central University, Taiwan(ROC),* [ihsienlee@ncu.edu.tw](mailto:ihsienlee@ncu.edu.tw)

<sup>5</sup>*Graduate Institute of Applied Geology, National Central University, Taiwan(ROC),*

[nichuenfa@geo.ncu.edu.tw](mailto:nichuenfa@geo.ncu.edu.tw)

Modeling groundwater flow and solute transport in fractured rocks are crucial issues in the fields of environmental engineering geology. With the large discrepancy of hydraulic properties between fractures and matrix in rocks, the simulations of flow, transport, and chemical reactions in fractured rocks are challenging tasks (Hyman et al., 2014; Hyman et al., 2015). Numerous models have been developed and implemented for practical problems. The general concepts involved in the models are either discrete fracture network (DFN)(Hyman et al., 2014; Hyman et al., 2015; Kalbacher et al., 2005; Makedonska et al., 2015-p1137; Zhang, 2015) or equivalent continuum porous medium (ECPM) (Chen et al., 2001, p440-p450; Jing, 2003, p283-p353; Rutqvist et al., 2013, p20-p24), depending on the site-specific conditions. The accuracy of simulation results highly relies on selecting a suitable DFN or ECPM modeling concept. However, practical problems might involve complex mechanisms, which require resolving the detailed interactions between fractures and rock matrix.

Recently, investigations have focused on developing complex numerical models, which enable the separation of the computational domain into fracture and rock matrix domains (Berre et al., 2018). More accuracy was obtained to benefit the computational costs for simulating complex fracture and matrix interactions. The study developed a hybrid domain model, which is flexible in considering the concepts of DFN, ECPM, or both. Specifically, the hybrid model uses the 2D triangular mesh for fractures and tetrahedron mesh for 3D rock matrix and solve the system of equations simultaneously (Figure 1). We proposed a benchmark study to assess and quantify the differences in flow and transport in a simple fracture connection using the concepts of DFN, ECPM, and Hybrid approaches. More complex DFN realizations were considered in the study. The simulation of DFN used the software FracMAN, and the simulation of ECPM used DarcyTools. The systematic comparison was conducted to quantify the differences in heads and particle paths obtained from three modeling concepts.

Figure 2 shows the groundwater flow in a fractured rock for three different conceptual approaches. Results have indicated that the solutions from the Hybrid model can match well with those obtained from DarcyTools (Figures 2a and b) and FracMAN (Figures 2c and d) models. Additionally, the flux and the interactions between fractures and matrix are available for the proposed Hybrid model. The study has shown the flexibility of the developed Hybrid model that enables the simulation of flow and transport interactions in fractured rocks. Considerable differences of interactions in high fracture intensity zones were obtained and quantified based on the generations of multiple DFN realizations.

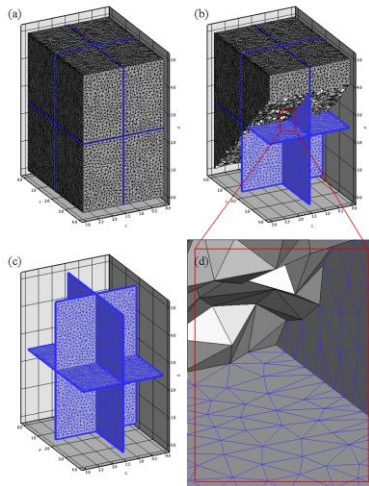


**Figure 1. The computational mesh for the proposed Hybrid domain model.**

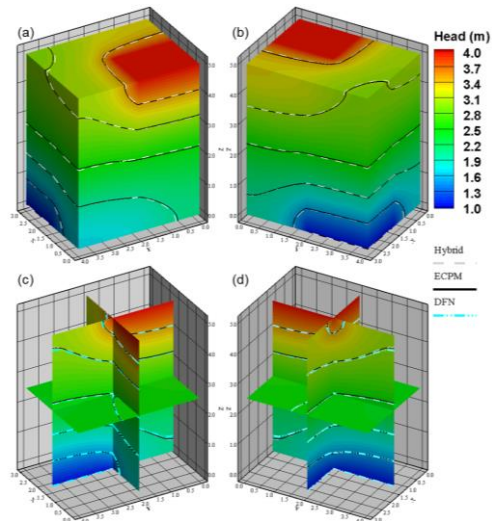


**Figure 2. The heads obtained from the concepts of Hybrid domain, DFN, and ECPM approaches.**

**Acknowledgments**

This research is supported by the Ministry of Science and Technology (MOST), Taiwan ROC (Contracts MOST 107-2116-M-008-003-MY2, 108-2625-M-008-007-, and 108-2116-M-008-004-).

**REFERENCES**

Berre, I., Boon, W., Flemisch, B., Fumagalli, A., Glaser, D., Keilegavlen, E., Scotti, A., Stefansson, I., and Tatomir, A., 2018, Call for participation: Verification benchmarks for single-phase flow in three-dimensional fractured porous media, pp. 1-17.

Chen, R. H., Lee, C. H., and Chen, C. S., 2001, Evaluation of transport of radioactive contaminant in fractured rock. *Environmental Geology*, v. 41, pp. 440-450.

Hyman, J. D., Gable, C. W., Painter, S. L., and Makedonska, N., 2014, Conforming delaunay triangulation of stochastically generated three dimensional discrete fracture networks: A feature rejection algorithm for meshing strategy. *SIAM Journal on Scientific Computing*, v. 36, pp. A1871-A1894.

Hyman, J. D., Karra, S., Makedonska, N., Gable, C. W., Painter, S.L., and Viswanathan, H. S., 2015, dfnWorks: A discrete fracture network framework for modeling subsurface flow and transport. *Computers & Geosciences*, v. 84, pp. 10-19.

Jing, L., 2003, A review of techniques, advances and outstanding issues in numerical modelling for rock mechanics and rock engineering. *International Journal of Rock Mechanics and Mining Sciences*, v. 40, pp. 283-353.

Kalbacher, T., Wang, W., McDermott, C., Kolditz, O., and Taniguchi, T., 2005, Development and application of a CAD interface for fractured rock. *Environmental Geology*, v. 47, pp. 1017-1027.

Makedonska, N., Painter, S., Bui, Q., Gable, C., and Karra, S., 2015, Particle tracking approach for transport in three-dimensional discrete fracture networks. *Computational Geosciences*, v. 19, pp. 1123-1137.

Rutqvist, J., Leung, C., Hoch, A., Wang, Y., and Wang, Z., 2013, Linked multicontinuum and crack tensor approach for modeling of coupled geomechanics, fluid flow and transport in fractured rock. *Journal of Rock Mechanics and Geotechnical Engineering*, v. 5, pp. 18-31.

Zhang, Q. H., 2015, Finite element generation of arbitrary 3-D fracture networks for flow analysis in complicated discrete fracture networks. *Journal of Hydrology*, v. 529(3), pp. 890-908.

## Decadal change in land use and land cover pattern and river dynamics in Indrawati River, Central Nepal

Kumud Raj Kafle<sup>1</sup>, Kevin Bajracharya<sup>1</sup>, Simrik Bhandari<sup>1</sup>, Benju Shrestha<sup>1</sup>

<sup>1</sup>*Department of Environmental Science and Engineering, Kathmandu University, Nepal, [krkafle@ku.edu.np](mailto:krkafle@ku.edu.np)*

### **Background-**

The study of river dynamics is essential for the development of environmentally acceptable and sustainable river based projects. In these regards, the Indrawati river including 4 watersheds from Banskharka to Dolalghat has been chosen because of its over exploitation as sand and gravel extraction as construction material over a decade.

The study area is a combined watershed area consisting of 4 sub-watersheds. Taking into account the diverse topography and climate of the basin, it is of symbolic national importance in view of its high probability for cultivation of high-value crops, livestock and water diversion project to meet the growing urban drinking water needs, hydroelectricity generation, and ecotourism.

### **Methods**

Study area was clipped from satellite images of Landsat 4-5 TM, OLI/TIRS C1 for the decadal period of 1999, 2008 and 2018 and re-projected to WGS\_84 datum and UTM Zone 45 N. NDVI (Normalized Difference Vegetation Index) map was prepared using corresponding bands for the red channel and near infrared channel.

The river was divided into 10 strips from Banskharka to Dolalghat, reference cross-sections were also drawn at the boundary of each strip. The river centerlines were created from the river shapefile polygon. Sinuosity index was calculated as the ratio channel length to the air length.

### **Results**

After analysis it was found that the forest area markedly increased (14%) and bare land markedly decreased (-46%) compared to other LULC classes between the time period of 1999 to 2018 which was directly and indirectly linked to various driving factors. Besides environmental factors (topography, climatic factors, precipitation), anthropogenic activities have significantly influenced LULC shift.

The planform morphometric parameter, including sinuosity and channel migration, of the Indrawati River was observed during the period of 1999-2008. The study was analyzed by dividing the river into 10 sections. The sinuosity index of Indrawati River ranges from 1.07 to 1.26 in the period 1999-2018. Sinuosity exhibited different characteristics in different sections.

### **Conclusion**

The study shows the increasing trend of the forest in the recent years which indicates the efficiency of the community forest programs. The overall average sinuosity was calculated as 1.13 that shows the channel is sinuous. Channel migration exhibited a generally decreasing trend. The total decrease rate was 22%. The total migration area to the left bank was approximately two times that of the right bank. The centerline in the Indrawati River exhibited a visible tendency to migrate to the left bank in the past 19 years because of anthropogenic activities as sand and gravel over extraction from river bank deposits as source of construction materials.





## **An experimental study to improve permeability and cleaning efficiency of oil contaminated soil by plasma blasting**

Bo-An Jang<sup>1</sup>, Hyun-Sic Jang<sup>2</sup>, Ahhyeon Kim<sup>3</sup>, Injoon Baek<sup>4</sup>

<sup>1</sup>*Department of Geophysics, Kangwon national University, Republic of Korea, [bajang@kangwon.ac.kr](mailto:bajang@kangwon.ac.kr)*

<sup>2</sup>*Department of Geophysics, Kangwon national University, Republic of Korea, [whitenull@kangwon.ac.kr](mailto:whitenull@kangwon.ac.kr)*

<sup>3</sup>*Department of Geophysics, Kangwon national University, Republic of Korea, [kah97@naver.com](mailto:kah97@naver.com)*

<sup>4</sup>*Department of Geophysics, Kangwon national University, Republic of Korea, [dlswns520@naver.com](mailto:dlswns520@naver.com)*

Plasma blasting which is generated by high voltage arc discharge of electricity is applied to soil mass to improve permeability of soil and cleaning efficiency of oil contamination. A new high voltage generator was manufactured and three types of soil including silty sand, silty sand mixed with lime and silty sand mixed with cement were prepared. Small and large soil columns were produced using these types of soil and plasma blasting was performed within soil columns to investigate the variation of soil volume penetrated by fluid and permeability. Fluid penetration volumes by plasma blasting increased by 11-71%, compared with those by pressure. Although plasma blasting with low electricity voltage induced horizontal fracture and fluid penetrated along this weak plane, plasma blasting with high voltage induced spherical penetration of fluid. Plasma blasting increased the permeability of soil. Permeability of soils mixed with lime and cement increased by 450-1,052% with plasma blasting. Permeability of soil increased as discharge voltage increased when plasma blasting was applied once. However, several blasting with the same discharge voltage increase or decrease permeability of soil. Oil contaminated soil was prepared by adding diesel into soil artificially and plasma blasting was performed in these oil contaminated soil. Cleaning efficiency increased by average of 393% for soil located nearby the blasting and by average of 239% for soil located far from the blasting. Cleaning efficiency did not show any correlation with discharge voltage. All these results indicated that plasma blasting might be used for in-situ cleaning of oil contaminated soil because plasma blasting increased permeability of soil and cleaning efficiency.





## **THEME 3 - ADVANCES IN SITE INVESTIGATION FOR ENGINEERING GEOLOGY**



## Layer interpolation with tomographic aid

Juan Chavez-Olalla<sup>1</sup>

<sup>1</sup>*Delft University of Technology, Department of Geoscience & Engineering, the Netherlands,*

[j.f.chavezolalla@tudelft.nl](mailto:j.f.chavezolalla@tudelft.nl)

### **Background**

Geological schematization is of paramount importance in safety assessment of existing dikes. In particular when the risk of internal erosion of clay-over-sand dikes is assessed. In that case, the upper clay layer in the hinterland generates resistance against erosion (Sellmeijer, 1991). Thus, the geometrical variability of the upper layer has a direct impact in structural safety. Characterizing geometrical variability proves challenging with conventional site investigation methods. Methods such as the Cone Penetration Test (CPT) provide only one-dimensional information. In most cases the scale of variability is shorter than the distance between data points. Lack of information in geotechnical models is accounted for by safety factors. However, large safety factors lead to uneconomical designs or unnecessary reinforcement of existing structures. Therefore, there is a need for horizontally-continuous characterization of geometrical variability. For this purpose, geophysical tomograms have become increasingly popular. A method to objectively incorporate tomographic and one-dimensional data is proposed. The method consists in retrieving layer orientations from tomograms and interface locations from one-dimensional data.

### **Methods**

Layer orientations are retrieved from tomographic data. First, geological interfaces are found in the tomogram via Laplacian edge detection. This technique finds interfaces at the zero crossings of the Laplacian operator applied to the tomographic grid. Due to the biased nature of tomograms, interface locations do not coincide with the interfaces derived from one-dimensional data. Thus, the orientation of the tomographic interfaces are used instead which are assumed to represent the true orientation of the geological layers. The true location of the interfaces is obtained from the interpretation of one-dimensional data, in this case CPT data. The final interfaces are obtained via implicit geological modeling. Specifically, the potential-field method was used as implemented in the python package GemPy (De La Varga, 2019). The final interface geometry is an unbiased estimation which uses objectively two distinct data sets.

### **Results**

The method was applied to data collected in the flood plain of the Spui river in the Netherlands. Figure 1 shows CPT data at two locations of the survey line. Interface locations are indicated by the horizontal dashed lines. The laplacian edge-detection technique was applied to a direct-current electrical resistivity tomogram (Figure 2). Tomographic layer orientations and interfaces are indicated in Figure 2. The final interface is also shown in Figure 2. It preserves the original orientation while fitting the CPT points.

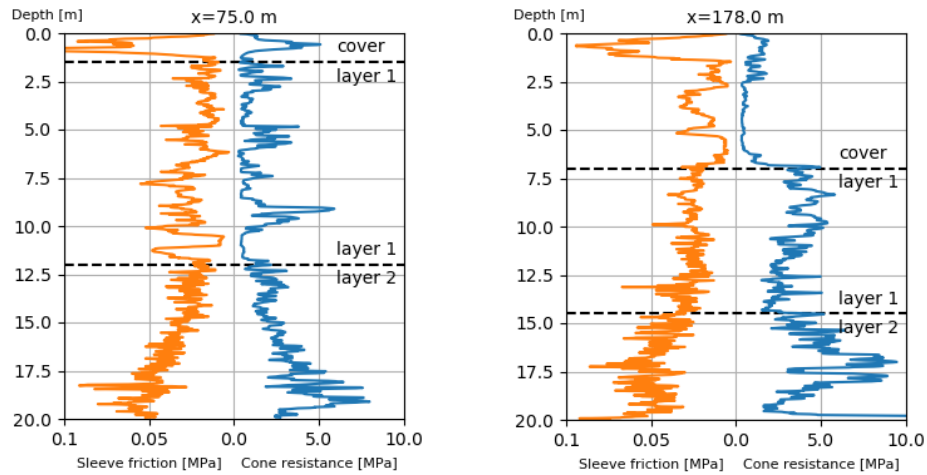


Figure 1. CPT data.

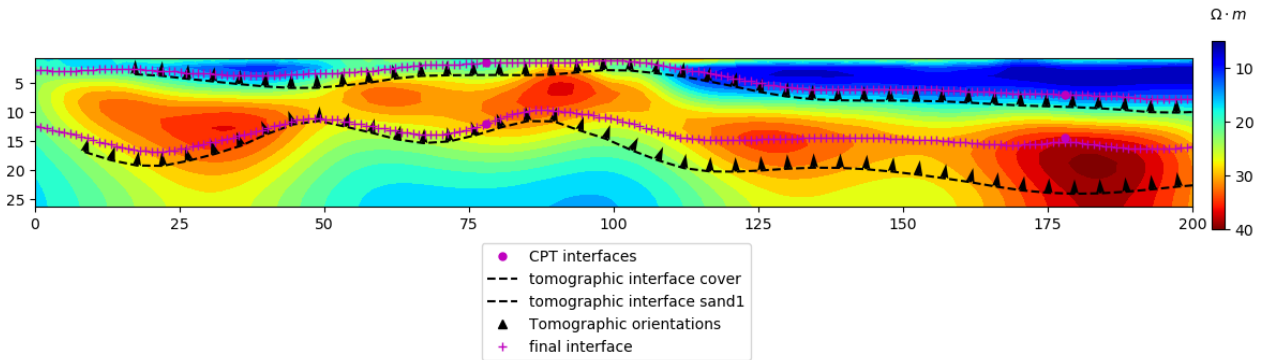


Figure 2. Tomographic data with estimated interfaces and orientations.

**Conclusions**

A method was presented to objectively estimate interface geometry with tomographic aid. The final interface is an unbiased estimation which incorporates objectively the data. The method is a first step into reducing geological uncertainty for the safety assessments of dikes. The next step is to use geophysical for testing geological hypothesis within a probabilistic framework.

**REFERENCES**

De La Varga, M., Schaaf, A., & Wellmann, F., 2019. GemPy 1.0: Open-source stochastic geological modeling and inversion. *Geoscientific Model Development*, 12(1), 1–32. <https://doi.org/10.5194/gmd-12-1-2019>

Mlsna, P. A., & Rodríguez, J. J., 2009. Gradient and Laplacian Edge Detection. In *The Essential Guide to Image Processing* (pp. 495–524). Elsevier. <https://doi.org/10.1016/B978-0-12-374457-9.00019-6>

Sellmeijer, J. B., & Koenders, M. A., 1991. A mathematical model for piping. *Applied Mathematical Modelling*, 15(11–12), 646–651. [https://doi.org/10.1016/S0307-904X\(09\)81011-1](https://doi.org/10.1016/S0307-904X(09)81011-1)



## Project, site and deliverables management systems integration for ground investigation projects

Alkis Gkouvailas<sup>1</sup>, Michael Blakely<sup>2</sup>, Emmanouil Zervas<sup>3</sup>, Tania Santiapillai<sup>4</sup>, Maryse Buot<sup>5</sup>

<sup>1</sup>AECOM, United Kingdom, [alkiviadis.gkouvailas@aecom.com](mailto:alkiviadis.gkouvailas@aecom.com)

<sup>2</sup>AECOM, United Kingdom, [Michael.Blakely@aecom.com](mailto:Michael.Blakely@aecom.com)

<sup>3</sup>AECOM, United Kingdom, [Emmanouil.Zervas@aecom.com](mailto:Emmanouil.Zervas@aecom.com)

<sup>4</sup>AECOM, United Kingdom, [Tania.Santiapillai@aecom.com](mailto:Tania.Santiapillai@aecom.com)

<sup>5</sup>AECOM, United Kingdom, [Maryse.Buot@aecom.com](mailto:Maryse.Buot@aecom.com)

### Introduction

Large scale ground investigations (GI) present significant challenges with high volume and short deadlines for technical deliverables (logs, test results, etc.). Communication of progress is also a key challenge on large schemes. Many parties (Client, Principal designer, Principal contractor, etc.) are usually involved in such large schemes and readily available, real time information is essential to ensure timely project delivery.

Mainstream GI data management processes include significant amounts of paperwork, multiple sources of truth and sometimes exchange of information via emails. Based on experience from previous GIs, these processes were found to be time consuming and limited in providing quick, interrogatable information to a variety of end users. The data itself was not always consistent and in some cases was missing, when coming from different originators. Furthermore, lack of clear and easily accessible audit trail, for produced deliverables, has also been an issue in some cases.

Presented with the challenge of delivering quality factual investigation data on one of the United Kingdom's largest ground investigations in recent memory, the authors concluded a methodical and innovative approach to deliverables management would be required. The new approach was required to centralise collation of site and post-site deliverables, allow effective and timely Quality Control (QC), track progress against programme, and simplify reporting to managers with high level project progress and compliance. As a result, AECOM UK has produced an innovative, centralised information system, using familiar industry tools. This provides access to real time information to all the parties involved, through user customised dashboards.

### System development

A holistic, internal shared working space was built within ProjectWise and ArcGIS Online to streamline and centralise high volumes of GI data and progress information. Project team members are able to record/ import their data in a structured, consistent and controlled way. This information and associated metadata can then be accessed by anyone within the project team, with user privileges controlling editing and viewing rights based on role. Centralising and structuring these processes increased efficiency and significantly improved QC.

To enable these improvements, the following systems/ processes were developed:

Common file naming convention (BS 1192:2007+A2:2016 and BS 8574:2014) co-developed with Clients, and a name generator built into a custom ProjectWise implementation.

Traceability via metadata. Leverage inherent metadata created by digital data handling to assist QA at all stages and progress reporting.

Error prevention via logical functions.

Centralised site progress recording via mobile apps (ArcGIS Online).

Link between main database and approved/ revised programmes.

Connection between GI contractor’s and Client’s data platforms.

Both systems (ProjectWise and ArcGIS) feed directly into Power BI – the project reporting tool used for dashboards and data analytics. Power BI is utilized to read metadata to recognize the site progress, QC workflow status of deliverables, apply logical functions to investigate deviations from established processes and highlight errors. A simplified flowchart of these processes is shown in Figure 1.

In two major GI projects (Lower Thames Crossing and a confidential GI in Vietnam) Power BI was the centralised reporting tool whose dashboards comprised the main data analysis and metrics system, used by the Client and project management to monitor project progress and take corrective measures, when needed.

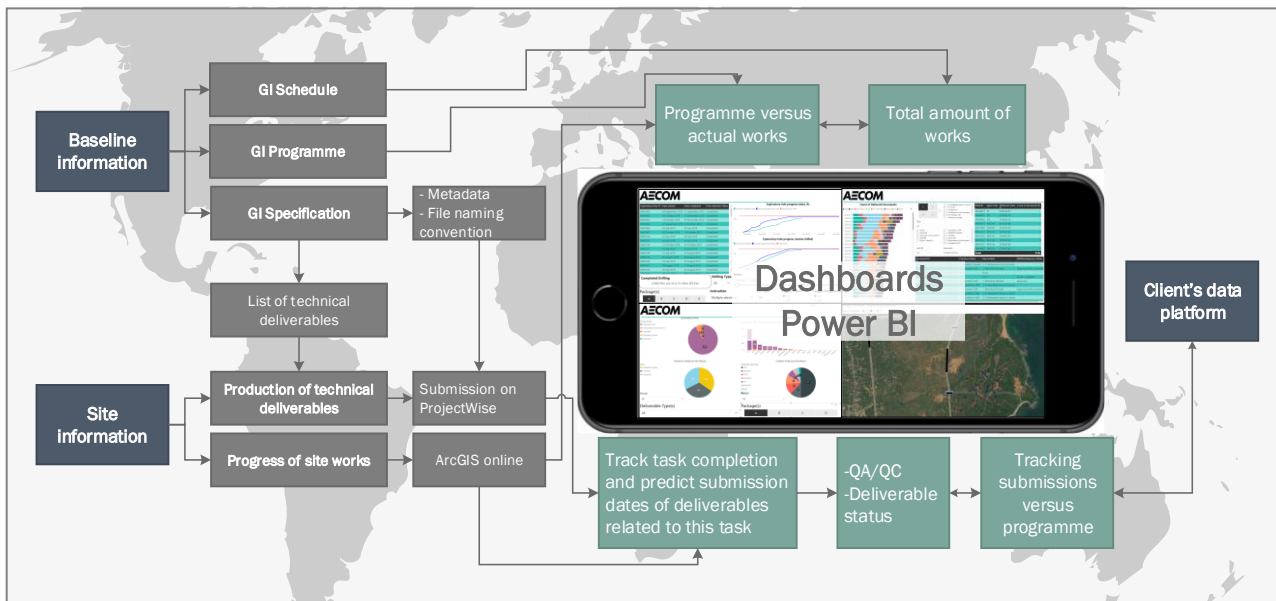


Figure 1. Data management system integration

**System’s benefits**

This systems’ integration can be easily adjusted to fit the specific needs of almost any GI project. The innovative digital tools developed for large-scale GIs are providing an improved service to the designers and the client; especially when it comes to deliverables turnaround times and identifying errors and inconsistencies. A small and flexible information management team can easily process this data and detect “bottlenecks” in the QC procedures and inform the senior management team.

The developed system redefines the future of data management for GI and is an excellent example of lean management that creates new efficiencies and most importantly gets the information to the designer on time and verified.

**Acknowledgments**

Highways England, Lower Thames Crossing, David Ridout, Aris Zourmpakis, Selena Pearce and Gareth McClimonds.

**REFERENCES**

British Standards Institution, 2016, BS 1192:2007+A2:2016: *Collaborative production of architectural, engineering and construction information. Code of practice*. Available at <https://identity.bsigroup.com/> (Accessed: 28 December 2018).  
 British Standards Institution, 2014, BS 8574:2014: *Code of practice for the management of geotechnical data for ground engineering projects*. Available at <https://identity.bsigroup.com/> (Accessed: 29 January 2019).



## Variability of penetration rates (PRs) during open-hole drilling for different geological formations in Doha, Qatar

Alkis P. Gkouvailas<sup>1</sup>, Dafni E. Sifnioti<sup>2</sup>, Julian Ashley<sup>3</sup>, Francesco Barbagli<sup>4</sup>, Maryse Buot<sup>5</sup>.

<sup>1</sup>AECOM, United Kingdom, [alkiviadis.gkouvailas@aecom.com](mailto:alkiviadis.gkouvailas@aecom.com)

<sup>2</sup>CEFAS, United Kingdom, [dafni.sifnioti@cefas.co.uk](mailto:dafni.sifnioti@cefas.co.uk)

<sup>3</sup>AECOM, United Kingdom, [julian.ashley@aecom.com](mailto:julian.ashley@aecom.com)

<sup>4</sup>AECOM, United Kingdom, [francesco.barbagli@aecom.com](mailto:francesco.barbagli@aecom.com)

<sup>5</sup>AECOM, United Kingdom, [maryse.buot@aecom.com](mailto:maryse.buot@aecom.com)

### Introduction

An extensive ground investigation campaign was carried out between 2013 and 2018, for the purposes of the Doha South Sewer Infrastructure Project (DSSIP), developed by Qatar Public Works Authority (ASHGHAL). This ground investigation consisted mainly of rotary core boreholes and Multi-channel Analysis of Surface Waves surveys (MASW).

After assessing the ground information, areas of geological/ geotechnical uncertainty, especially in the proximity of tunnel shafts, were identified and a series of supplementary intrusive ground investigation was decided. Due to temporal and spatial constraints, some of the additional geotechnical boreholes were constructed as open-holes (without sampling), in close proximity of previously completed rotary cored boreholes. Subsequently, a comparison between the open-hole recorded PRs (ISO 22476-15:2016) and the geological formations encountered in the rotary cored boreholes, was carried out.

### Geology – Geotechnical formations

The Qatar peninsula is part of the Arabian Gulf basin, formed by a more than 10 km thick succession of carbonate and evaporitic sediments (Fourniadis, 2010). An adapted summary of the geotechnical formations and their subunits, from Karagkounis et al. (2016), is listed below in chronological order (youngest to oldest):

- i. Simsima limestone formation (SL).
  - Weathered Simsima limestone (WSL) subunit.
  - Karstified Simsima limestone (KSL) subunit.
- ii. Midra shale formation (MSH).
- iii. Midra shale – Fahail Velates limestone (MSH Imst).
- iv. Rus limestone formation (RUS).
  - Karstified Rus formation (KRUS) subunit

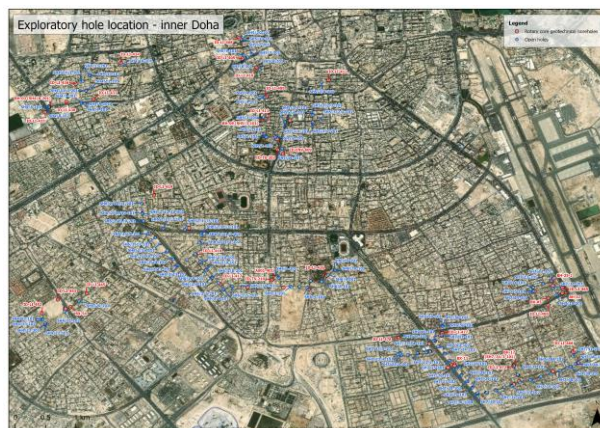


Figure 3 Exploratory hole (open and rotary cored)

### Methodology

A detailed geological model was produced based on ground information from more than 500 rotary core geotechnical boreholes and 60 MASW lines. Open-holes located less than 150 m away from the closest rotary cored geotechnical borehole (Figure 1) were selected and plotted on the geological model. The recorded PRs were compared with and assigned to the geological formations indicated by the geological model. Overall, 1,447 PR values were related to the 7 aforementioned geotechnical formations.

The same drilling rig type (Mobile B-48) was used for all open-holes considered in this assessment.

### Results

A high variability of PRs was observed for most of the geotechnical formations and their subunits (Figure 2). Formations with inherited inhomogeneity (different lithologies within the same formation, variable weathering grade, strength, etc.), such as WSL and KSL, exhibited higher variability. The average PRs corresponding to the main geotechnical formations (SL, MSH, MSH Imst and RUS) were found to vary between 3.1 and 6.2 m/h, whilst the three additional, less competent formations (WSL, KSL and KRUS), showed higher PRs. PR values above 20 m/h (refer to SL, WSL and KLS in Figure 2) indicated presence of karstic features and were validated by ground information from adjacent boreholes.

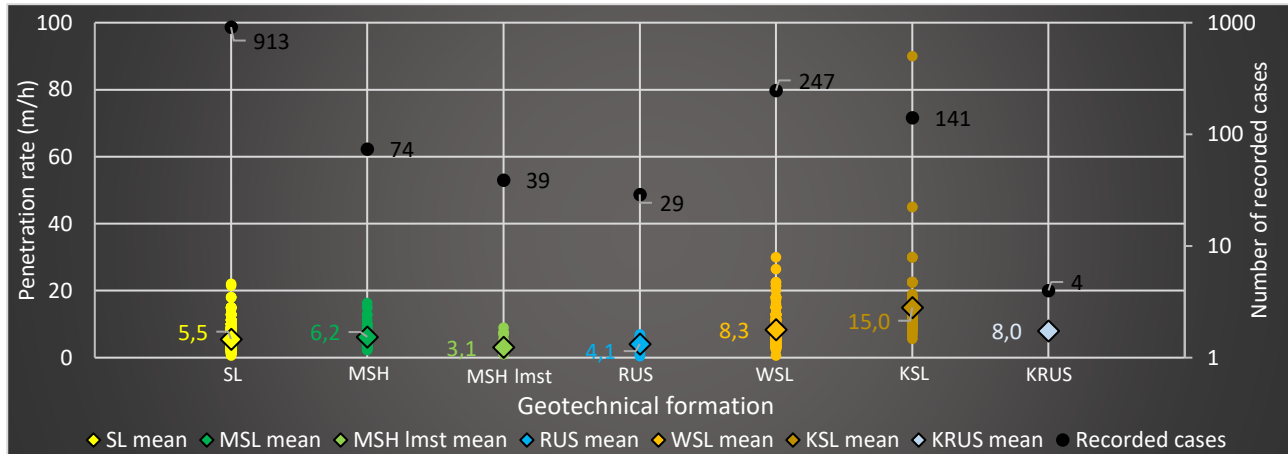


**Figure 2** Plot showing the average penetration rates, recorded in 115 open-holes, for different geotechnical formations. The secondary y- axis shows the total number of PR recorded cases per geotechnical formation.

**Conclusions**

It becomes apparent that the PRs cannot be used as a standalone tool to distinguish between these different geotechnical units even though, in some cases PRs can assist in detecting transitions between units. Moreover, PRs seem to correlate well with lithologies, even within the same geological unit, as in the case of MSH and MSH Imst. The contrast in the mechanical properties between shale and limestone allow PRs to reflect this change by a drop of PRs when drilling through more competent materials, such as limestone. Additionally, PRs can assist in identifying highly weathered, karstified zones and in general zones of weaker, less competent geomaterials. A further analysis correlating PRs with lithology, Unconfined Compressive Strength, RQD and GSI, for these geotechnical units, is in progress.

**Acknowledgments**

ASHGHAL, Ian Hosking, Avinash Shrivastava, Sandeep Shetty, Aishwarya Sinha and Cathy Coldrey

**REFERENCES**

British Standards Institution, 2016, BS EN ISO 22476-15: Geotechnical investigation and testing – Field testing – Part 15: Measuring while drilling. Available at <https://identity.bsigroup.com/> (Accessed: 14 February 2018)

Fourniadis I., 2010, Geotechnical characterization of the Simsima Limestone (Doha, Qatar). In *Geoenvironmental Engineering and Geotechnics: Progress in Modeling and Applications – GeoShanghai 2010* (He Q and Shen SL (eds)). American Society of Civil Engineers, Reston, VA, USA, Geotechnical Special Publication no. 204, pp. 273–278.

Karagkounis N., Latapie B., Sayers K. and Mulinti S. R., 2016, Geology and geotechnical evaluation of Doha rock formations, ICE, Geotechnical research Volume 3 Issue 3.



## Temperature and rock slope stability: a multi-sensor site monitoring network

Ondřej Racek<sup>1,2</sup>, Jan Blahůt<sup>1</sup>, Filip Hartvich<sup>1,2</sup>

<sup>1</sup>*Department of Engineering Geology, Institute of Rock Structure and Mechanics, Czech Academy of Sciences, Czechia, [racek@irms.cas.cz](mailto:racek@irms.cas.cz)*

<sup>2</sup>*Department of Physical geography and Geoecology, Faculty of Science, Charles University, Czechia*

Both exogenous factors and endogenous rock properties have crucial influence on the rock slope stability (D'Amato et al., 2016). One of frequently discussed exogenous factors, that strongly affects rock stability, is the temperature and its changes. Acting through thermal expansion, which causes rapid changes in the rock stress field, it can eventually trigger a rockfall (Gunzburger et al., 2005). To assess the contribution of rock properties, temperature changes and other exogenous factors to rock stability, we have developed a complex in situ monitoring system. Nowadays complex monitoring systems are primary used for first warning (Loew et al., 2017; Jaboyedoff et al., 2011). Resulted rock slope dynamic from site specifically designed monitoring systems, cannot be directly compared.

We have constructed this innovative monitoring system so far at four different sites, using the same instrumentation. The sites were deliberately selected according to following criteria: various rock types; steep rock faces; various slope aspect; and possible endangering of lives, infrastructure or other society asset.

The monitoring system is composed of several elements: automatic induction dilatometers measuring relative block displacement, environmental monitoring station with a set of sensors measuring various exogenous factors: temperature in a depth profile (3 m borehole with 12 sensors at various depths), air temperature, humidity and pressure, and radiation balance of rock face using pair of pyranometers. To expand the data from point measuring to the whole rock face we have additionally performed several 24 h campaigns of continuous measuring the rock surface temperature using a thermal camera.

Each site rock face is characterized using traditional field geological, geomorphological and geotechnical methods, such as measuring geometrical properties of joints and fault planes, surface hardness estimation using a Schmidt hammer, discontinuity roughness measuring, or stability estimation by geotechnical classifications. Mechanical properties of rock were determined by laboratory tests, using in situ collected representative samples. These traditional methods are supplemented with state-of-the-art methods of rock slope analysis, including analyses of 3D point clouds and derived mesh surface, based on SfM processing using UAVs or TLS (terrestrial laser scanner). The obtained detailed rock surface models are then analyzed using Cloud compare and DSE software (Riquelme et al., 2014; Thiele et al., 2017) to derive the joint and fault planes and measure their properties.

Based on approx. year and half of continuous measuring, we are able to partly determine the influence of the exogeneous factors on rock blocks thermal behavior. In longer period, we expect to be able to observe the process of long-term rock slope destabilization represented by crack opening.

First results show perceptible differences between sites. Temperature in depth profile of rock mass temporally differs for each site. This effect is very likely caused by different rock type which forms each rock slope, moreover by unmatched aspect. By further monitoring and data processing, using advanced modelling approaches, should be more of variability between sites explained.

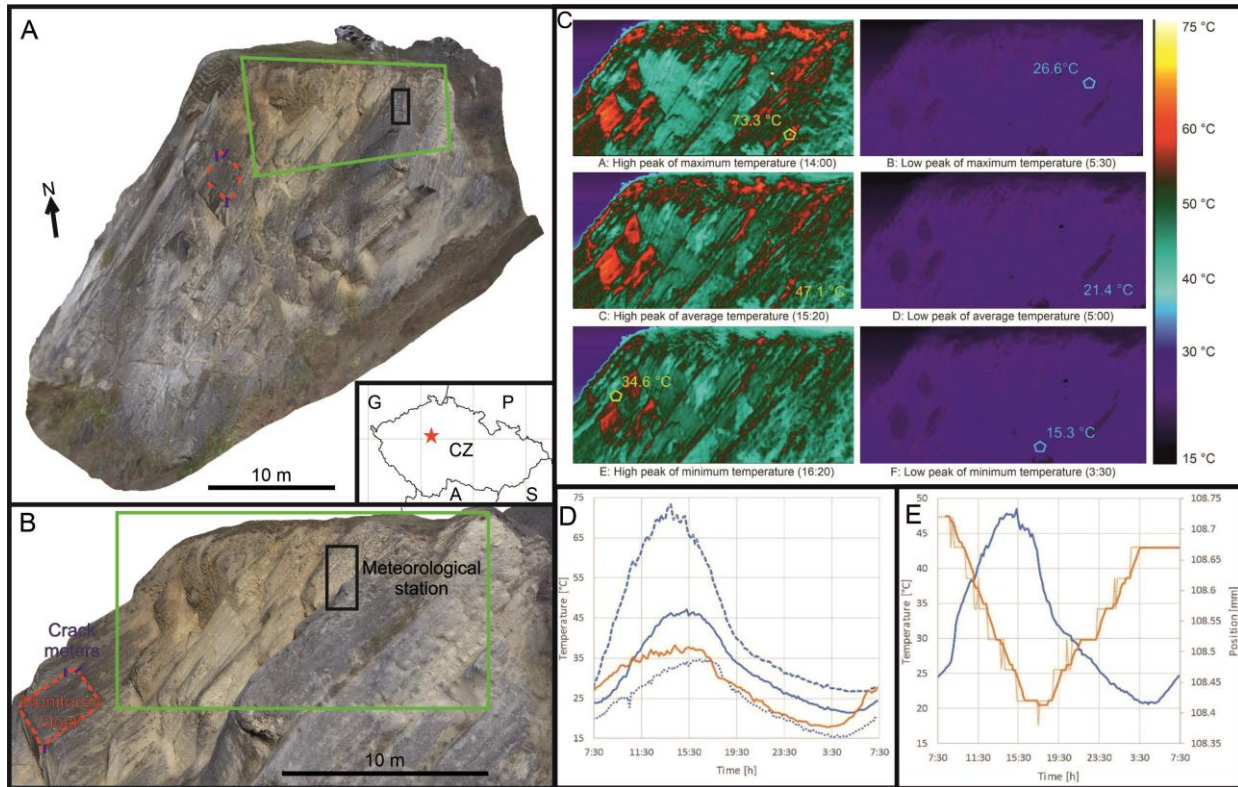


**Figure 1: Example of monitoring system and preliminary results. A: Overview of the rock mass monitoring system; inset figure shows the location with a red star (CZ: Czechia, G: Germany, P: Poland, A: Austria, S: Slovakia)., B: Detailed view of the IR camera monitoring site (green rectangle). C: Partial results from 24-hour thermal camera monitoring campaign. D: Temperature graph for rock face: Orange: Air temperature; Blue: rock surface temperatures derived from IR camera; dashed line: maximum temperatures; bold line: average temperatures; dotted line minimum temperatures. E: Graph of the movements recorded on the crack meters. Blue: air temperature at the datalogger; dotted orange: measured movements; bold orange: 1-hour moving average**

**REFERENCES**

D'Amato, J., Hantz, D., Guerin, A., Jaboyedoff, M., Baillet, L., Mariscal, A.M., 2016. Influence of meteorological factors on rockfall occurrence in a middle mountain limestone cliff. *Natural hazards and earth system sciences* 16, 719-735..

Gunzburger, Y., Merrien-Soukatchoff, V., Guglielmi, Y., 2005. Influence of daily surface temperature fluctuations on rock slope stability: case study of the Rochers de Valabres slope (France). *International journal of rock mechanics and mining sciences* (1997) 42, 331-349..

Jaboyedoff, M., Oppikofer, T., Derron, M.H., Blikra, L.H., Böhme, M., Saintot, A., 2011. Complex landslide behaviour and structural control: a three-dimensional conceptual model of Åknes rockslide, Norway. Geological Society, London, Special Publications 351.

Loew, S., Gschwind, S., Gischig, V., Keller-Signer, A., Valenti, G., 2017. Monitoring and early warning of the 2012 Preonzo catastrophic rockslope failure. *Landslides* 14, 141-154.

Riquelme, A., Abelian, A., Tomas, R., Jaboyedoff, M., 2014. A new approach for semi-automatic rock mass joints recognition from 3D point clouds. *Computers & geosciences* 68, 38-52.

Thiele, S., Grose, L., Samsu, A., Mickelthwaite, S., Vollgger, S.A., Cruden, A.R., 2017. Rapid, semi-automatic fracture and contact mapping for point clouds, images and geophysical data. *Solid Earth* 8, 1241-1253.



## Subsoil litho-technical reconstruction via multivariate geostatistical tools

Giovanna Vessia<sup>1</sup>, Diego Di Curzio<sup>2</sup>

<sup>1</sup>Assistant Professor, University "G. d' Annunzio" of Chieti-Pescara, Chieti, Italy, [g.vessia@unich.it](mailto:g.vessia@unich.it)

<sup>2</sup>Assistant Researcher, University "G. d' Annunzio" of Chieti-Pescara, Chieti, Italy, [diego.dicurzio@unich.it](mailto:diego.dicurzio@unich.it)

Subsoil characterization through direct in situ investigations, such as electrical cone penetration tests (CPTu), is commonly used in those quaternary sediments that are often characterized by mixtures of sand, silt, and clay. Although this type of point testing gives almost continuous measures along with depth, they are not able to catch the volumetric variations (both horizontal and vertical ones) of litho-technical properties of subsoil.

In the present study, a 3D litho-technical model of an area of about 900 km<sup>2</sup> (and up to 30 m depth) located in the Eastern part of Bologna district (Italy) has been reconstructed, through 182 CPTu profiles consisting of tip resistance  $q_c$ , sleeve friction  $f_s$ , and pore pressure  $u_2$  measurements (Figure 1a). This model has been carried out by the Partially Heterotopic Co-Kriging technique (PHCK), a multivariate geostatistical method (Matheron, 1973) enabling to read the spatial variability of a measurement setting and to include it in the spatial estimations and the associated uncertainties of the studied variables. This technique enables describing a continuous 3D model of both measured parameters and derived design variables, considering the spatial variability structures of a specific site.

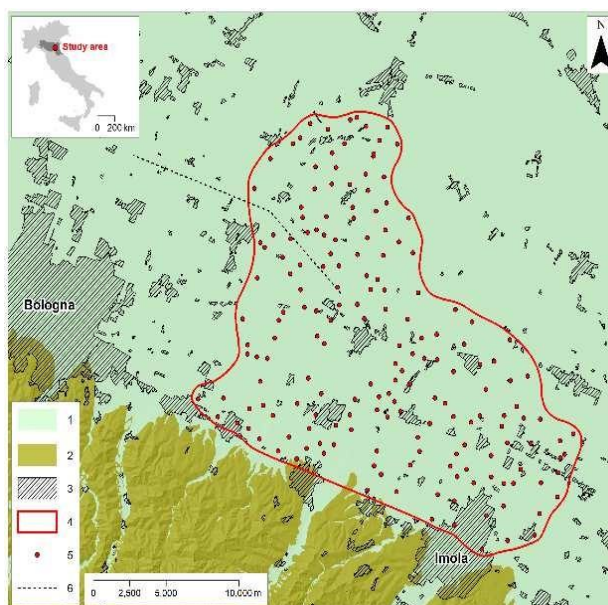


**Figure 1. (a) Schematic geological map with the 182 CPT locations. In legend: 1) alluvial deposits, 2) undifferentiated bedrock, 3) urban areas, 4) the study area, 5) CPTu locations.**

Besides the 3D models of  $q_c$ ,  $f_s$ , and  $u_2$ , the Soil Behavior Type Index ( $I_{SBT}$ ) has been calculated, describing the lithological characters of soils. The most recent formulation of  $I_{SBT}$  by Robertson (2009) has been considered, allowing to recursively calculate the  $I_{SBTn}$  through the old  $I_c$  value that is related only to the raw  $q_c$  and  $f_s$  profiles.

Tab. 1 shows the  $I_{SBTn}$  classes, identifying the corresponding Soil Behavior Type, (i.e. the soil lithotype).



**Table 1. Normalized CPT Soil Behavior Type (SBT<sub>n</sub>)**

Soil behavior type	ISBT <sub>n</sub>
Organic soils – clay	>3.6
Clays – silty clay to clay	2.95-3.6
Silt mixtures – clayey silt to silty clay	2.60-2.95
Sand mixtures – silty sand to sandy silt	2.05-2.60
Sands – clean sand to silty sand	1.31-2.05
Gravelly sand to dense sand	<1.31

Figure 2 shows, from the excavated 3D model of ISBT<sub>n</sub>, silt mixtures with inclusions of gravels and sands. The continuous 3D model of ISBT<sub>n</sub> enables to clearly outline the geometry of paleochannel-shaped coarse soil inclusions (red circle in Figure 2) and evidence the spatial continuity of soil types from fine to coarse soils, pointing out the extreme heterogeneity of these soils.

The results showed that multivariate geostatistical tools represent a powerful means for administrators and technicians to manage the use of the territory with informed knowledge and quantitative insights into the subsoil's physical and mechanical properties as well as associated uncertainty. The increased awareness of the subsoil characters will promote more effective land use, monitoring and protection activities within vulnerable areas especially set in urbanized territories.

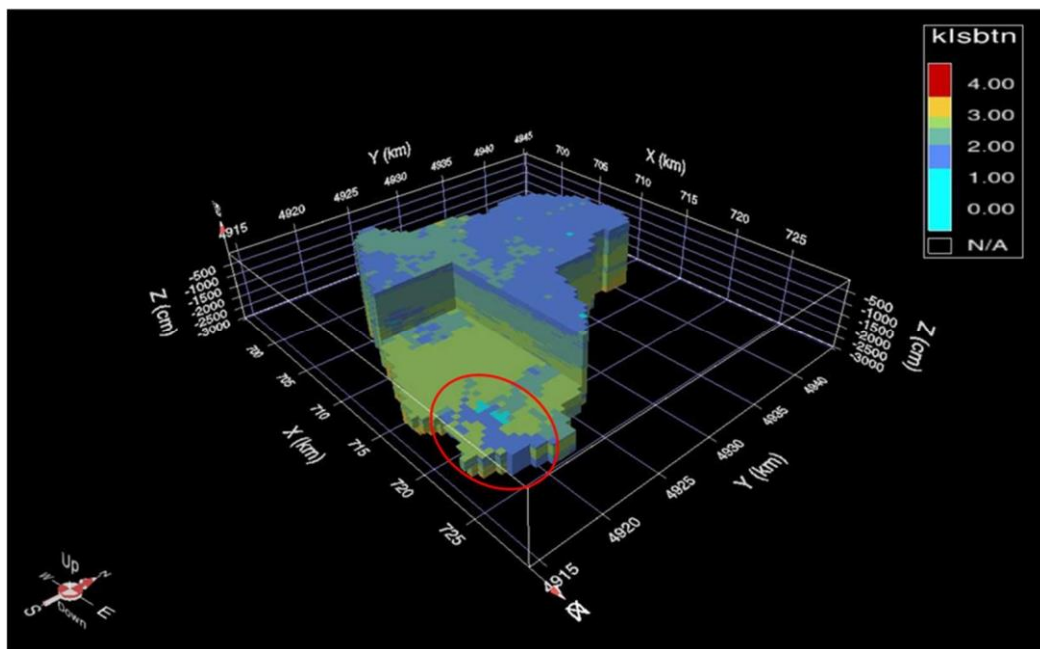


**Figure 2. 3D models of the ISBT<sub>n</sub> index derived from the qc, fs, and u2 profiles of the 182 CPTus from the case study.**

**REFERENCES**

Matheron, G., 1973, The intrinsic random functions and their applications. *Advances in Applied Probability*, v. 5, pp 439–468

Robertson, P. K., 2009, CPT interpretation – a unified approach. *Journal of Geotechnical and Geological engineering*, v. 46, pp 1–19



## Geomechanical evaluation of an abandoned chalk mine using in-situ measurements

Temenuga Georgieva<sup>1</sup>, Fanny Descamps<sup>2</sup>, Sara Vandyccke<sup>3</sup>, George Ajdanlijsky<sup>4</sup>, Jean-Pierre Tshibangu<sup>5</sup>

<sup>1</sup>Faculty of Engineering, UMONS, Belgium, [TemenugaDimova.GEORGIEVA@umons.ac.be](mailto:TemenugaDimova.GEORGIEVA@umons.ac.be)

<sup>2</sup>Faculty of Engineering, UMONS, Belgium, [Fanny.DESCAMPS@umons.ac.be](mailto:Fanny.DESCAMPS@umons.ac.be)

<sup>3</sup>Faculty of Engineering, UMONS, Belgium, [Sara.VANDYCKE@umons.ac.be](mailto:Sara.VANDYCKE@umons.ac.be)

<sup>4</sup>Faculty of Geology, University of Mining and Geology, Bulgaria, [g.ajdanlijsky@mgu.bg](mailto:g.ajdanlijsky@mgu.bg)

<sup>5</sup>Faculty of Engineering, UMONS, Belgium, [Katshidikaya.TSHIBANGU@umons.ac.be](mailto:Katshidikaya.TSHIBANGU@umons.ac.be)

The Malogne site is an abandoned underground phosphatic chalk quarry located in the Mons Basin (Belgium) mined out at shallow depth by the room-and-pillar method. With its 67 ha total area the site is situated very close to important surface infrastructure and residential houses. During and after its exploitation several significant ground collapses were registered. The last one from 2015, with an area of 1.2 ha and a maximum amplitude of 3 m, occurred close to the railway Brussels-Paris affecting agricultural land.

To characterize the geomechanical conditions of the underground openings in the central part of the quarry the Geological Strength Index (GSI) (Hoek et al., 1995; Marinos et al., 2005) and Rock Mass Rating (RMR<sub>89</sub>) (Bieniawski, 1989) classification systems were applied. The discontinuities characterization is based on a structural survey (293 measurements). The geomechanical evaluation of the massif is realized by a set of parameters as the Joint Roughness Coefficient (in 39 profiles), the Rock Quality Designation (in 8 locations) and the Intact Rock Strength (in 356 points).

Due to the seasonal groundwater level fluctuation in the studied area three zones are differentiated - dry, transitional and water-saturated which is not accessible for observations. As a result, of the annual variations some of the pillars are exposed to cycles of water saturation and drying.

Considering the most unfavorable rock mass conditions three geomechanical zones were identified in the studied area (Figure 1). Those connected with Good to Fair rock mass (classes II and III) are typical for the dry parts of the quarry while the Poor one (class IV) is mainly related to the transitional zone. An exception of that is a narrow elongated area of rock mass class IV in the western part of the site that follows the faulted zone. The rock mass next to the collapsed sector was also classified as Poor.

**Table 1. Rating for computing RMR<sub>89</sub> values for dry and transitional zones in the central part of the Malogne quarry**

Parameter	Dry zone			Transitional zone		
	min.	avg.	max.	min.	avg.	max.
Strength of the intact rock mass	1	2	2	1	1	1
RQD	17	20	20	17	17	20
Spacing of discontinuities	6	10	15	5	8	10
Conditions of discontinuities	5	15	20	0	10	15
Groundwater	10	13	15	0	4	7
RMR <sub>89</sub>	39	60	72	23	40	53
Rock mass classes	IV Poor	III Fair	II Good	IV Poor	IV Poor	III Good

Based on the GSI estimation, two geomechanical zones were distinguished - such with GSI values in the range of 55-60 that mostly corresponds to the dry part of the site, and another one with lower levels (GSI=45-50) that is more related to the transitional zone but also identified in the Very Blocky dry zone. Regarding the RMR<sub>89</sub> assessment (Tab. 1) three different zones were defined: (1) with higher values of RMR<sub>89</sub> corresponding to Good and Fair rock mass quality, associated to the dry zone, and (2) with Good and Poor rock mass quality

that are mainly related to the transitional zone.

The in situ observations confirmed the obtained results for the geomechanical conditions in the studied part of the site. The presented data could be used as indicative for the possible geomechanical risk that could be expected in the Malogne quarry as well as for conducting preventive monitoring if necessary.

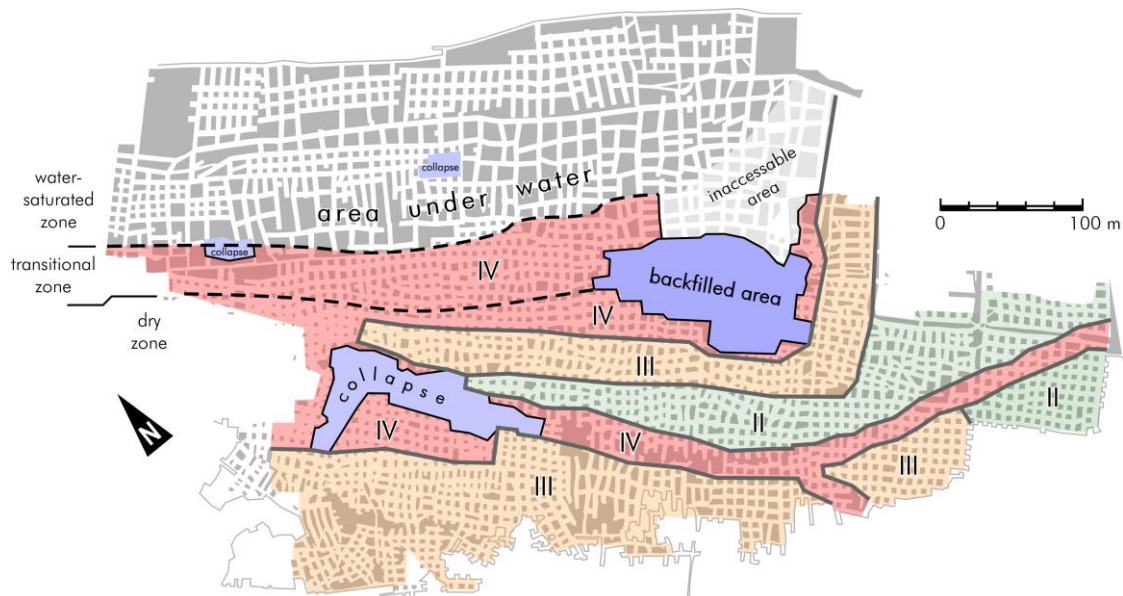


**Figure 1. Geomechanical zonation of the central part of the Malogne quarry indicating the level of the possible geomechanical risk.**

### **Acknowledgments**

This research is financially supported by the European Funds for Regional Development in the framework of the Interreg «RISSC» project. The authors thanks SPW for the provided map materials for the studied part of the Malogne quarry, and to the team of L'ASBL Project Malogne for their support during the fieldwork.

### **REFERENCES**

- Bieniawski, Z. T., 1989, Engineering rock mass classifications. A Complete Manual for Engineers and Geologists in Mining, Civil, and Petroleum Engineering. J. Wiley, New York, 251 p.
- Hoek E., Kaiser, P.K., and Bawden, W.F., 1995, Support of Underground Excavations in Hard Rock. Rotterdam, Balkema, 215 p.
- Marinos V., Marinos, P., and Hoek, E., 2005, The geological strength index: Applications and limitations. Bull. Eng. Geol. Environ., vol. 64, n ° 1, pp. 55-65.



## THEME 4 - ENGINEERING GEOLOGY FOR ENGINEERING WORKS



## The effectiveness of willow poles for shallow slope failure stabilisation

Mike G Winter<sup>1</sup>, Ian M Nettleton<sup>2</sup>, Richard Seddon<sup>3</sup>, Jan Marsden<sup>4</sup>

<sup>1</sup>Formerly TRL Limited now Winter Associates, United Kingdom, [mwinter@winterassociates.co.uk](mailto:mwinter@winterassociates.co.uk)

<sup>2</sup>Coffey Geotechnics, United Kingdom, [ian.nettleton@coffey.com](mailto:ian.nettleton@coffey.com)

<sup>3</sup>Formerly Coffey Geotechnics now Jacobs, United Kingdom, [richard.seddon@jacobs.com](mailto:richard.seddon@jacobs.com)

<sup>4</sup>Formerly Highways England, United Kingdom, [geotechnicsteam@highwaysengland.co.uk](mailto:geotechnicsteam@highwaysengland.co.uk)

Work to evaluate the effectiveness of innovative geotechnical repair techniques for slopes was commissioned by Highways England. The techniques are the planting of live willow poles, Fibre Reinforced Soil (FRS) and Electrokinetic Geosynthetics (EKG). These techniques were used in place of conventional approaches in order to reduce the overall impact of various challenges including environmental constraints (habitat and visual), access and utility constraints, and the need to reduce the scale and/or cost of traffic management and delays.

Trials of these techniques have been undertaken over the last 20 years or so, but monitoring was generally limited to just a few years post-construction. Longer term evaluation has not generally been undertaken. This work assesses the effectiveness of live willow poles as an aid to increased stability.

The use of vegetation as an aid to slope stability has been widely written about and the associated benefits are often described as follows:

- Root reinforcement as the root structure develops, which will enhance the initial reinforcement provided by the willow poles.
- Canopy interception of rainfall and subsequent evaporation.
- Increased root water uptake of the water that does infiltrate into the soil and subsequent transpiration via the leaf cover.

Trials at the A10 Hoddesdon, M1 J12 Toddington, A5 Milton Keynes and M23 Gatwick have been assessed. It seems clear that, although monitoring was undertaken only in the relatively short-term, the planting of live willow poles has been beneficial in terms of promoting the type of changes and behaviours in the soil that would be expected and that would be beneficial from the point of view of reducing instability.

In addition to the trial sites a practical application of willow poles to stabilise a slope was examined at the M6 South of J40 (Figure 1). At this site inclinometer readings were taken before, during and after the willow poles were installed. Progressive downslope movements of up to around 50mm were evident during a period of around 570 days before and during construction. In the 540 days post-construction these movements largely stopped and/or were reversed.

The success of both the trials and the practical application of willow poles led directly to the development of design guidance and specification information which can be found along with a much more expansive treatment of this work by Winter et al. (2018a). Lessons learned from the trials and practical application will be incorporated into that design guidance and specification in due course.





**Figure 1. General view of the M6 south of J40 from the B5320 overbridge looking south-east: Left, March 2017 (installation was between November 2105 and February 2016); Right, August 2018 showing growth.**

Specific challenges related to willow pole trials and the future use of willow poles include:

- the selection of appropriate willow species including in the light of climate change and in consultation with statutory bodies and appropriate professionals,
- construction issues related to the installation of the poles and the fitment of appropriate tree guards,
- design and construction costs,
- the types of monitoring that have proven to be useful,
- maintenance issues, particularly the need to ensure that the willows are appropriately coppiced, and that competing vegetation is eradicated during the period of establishment,
- future uses for willow pole coppicing products, and
- the need for a long-term end-of-life strategy for willows to allow for, for example, succession planting.

More generic lessons learnt from the trials and the practical application are reported and these were combined with those from the work on FRS (Seddon et al. 2018) and EKG (Nettleton et al. 2018) to produce guidance for future Highways England trials of innovative geotechnical repair techniques (Winter et al. 2018b).

**REFERENCES**

Nettleton, I. M., Seddon, R.and Winter, M. G. 2018. Innovative geotechnical repair techniques: effectiveness of electrokinetic geosynthetics. PPR 890. TRL, Wokingham.

Seddon, R., Winter, M. G.and Nettleton, I. M. 2018. Innovative geotechnical repair techniques: effectiveness of fibre reinforced soil. PPR 873. TRL, Wokingham.

Winter, M. G., Nettleton, I. M.and Seddon, R. 2018a. Innovative geotechnical repair techniques: recommendations and guidance for management of future Highways England trials with innovative techniques. PPR 891. TRL, Wokingham.

Winter, M. G., Nettleton, I. M.and Seddon, R. 2018b. Innovative geotechnical repair techniques: recommendations and guidance for management of future Highways England trials with innovative techniques. PPR 891. TRL, Wokingham.



## The effectiveness of electrokinetic geosynthetics for shallow slope failure stabilization

Ian M Nettleton<sup>1</sup>, Richard Seddon<sup>2</sup>, Mike G Winter<sup>3</sup>, Jan Marsden<sup>4</sup>

<sup>1</sup>*Coffey Geotechnics, United Kingdom, [ian.nettleton@coffey.com](mailto:ian.nettleton@coffey.com)*

<sup>2</sup>*Formerly Coffey Geotechnics now Jacobs, United Kingdom, [richard.seddon@jacobs.com](mailto:richard.seddon@jacobs.com)*

<sup>3</sup>*Formerly TRL Limited now Winter Associates, United Kingdom, [mwinter@winterassociates.co.uk](mailto:mwinter@winterassociates.co.uk)*

<sup>4</sup>*Formerly Highways England, United Kingdom, [geotechnicsteam@highwaysengland.co.uk](mailto:geotechnicsteam@highwaysengland.co.uk)*

Work to evaluate the effectiveness of innovative geotechnical repair techniques for slopes has been commissioned by Highways England (HE). The techniques are the planting of live willow poles, Fibre Reinforced Soil (FRS) and Electrokinetic Geosynthetics (EKG). These techniques were used in place of conventional approaches in order to reduce the overall impact of various challenges including environmental constraints (habitat and visual), access and utility constraints, and to address the need to reduce the scale and/or cost of traffic management and traffic delays.

Trials of the EKG techniques on the Highways England network have been undertaken over the last eight years or so, but post-trial ground investigations and monitoring was generally very limited, or in some cases absent. Post-EKG trial determination of soil parameters is generally not available and longer-term evaluation and verification of EKG treatment has not generally been undertaken. This work assesses the effectiveness of EKG treatment to increase the stability of highway earthworks.

The use of EKG treatment to aid slope stability has been widely written about and the associated benefits are often described as follows:

- Electroosmotic active dewatering, leading to a reduction in water content, pore water pressures, consolidation and an increase in shear strength.
- Physio-chemical changes in the soil, such as cementation, precipitation, ion exchange and flocculation, which can lead to increases in shear strength, stiffness and a reduction in plasticity.
- Temporary active EKG drainage and permanent passive drainage provided by the EKG cathodes.
- Soil nail reinforcement provided by the EKG anodes with an enhanced soil/nail bond.

Three of the four EKG trials (A21 Stocks Green, M5 Junction 7 and A419 Rat Trap) were undertaken as practical remedial works for known relatively shallow (1m to 2m deep) earthwork embankment instability issues. The fourth EKG trial (A56 Woodcliffe) was undertaken to demonstrate, on a small scale, the effectiveness of EKG primarily for active dewatering of fine grained soils, but also ground improvement.

The lack of adequate post-EKG trial ground investigation, testing and monitoring prevent any clear assessment of the contribution of the various elements of EKG slope stabilisation to be made. A lack of longer term monitoring and verification also hinders the adoption of the EKG treatment to be recommended at the current stage. It was concluded that further EKG trials, building on the lessons learnt, should be undertaken and documented to enable the technique to be taken into more regular use.

Lessons learned from the trials and practical application will need to be incorporated into design guidance and specification in due course, building on the tentative guidance on design and specification issues presented along with a much more expansive treatment of this work by Nettleton et al. (2018).



**Figure 1. A21 Stocks Green site 12 months after construction (left), the EKG anodes and cathodes were installed amongst the trees maintaining the character of the site. Cathode at the M5 J7 site (right).**

Specific issues related to the EKG trials include:

- that there is currently there is only one supplier of the EKG system,
- the need for more robust and effective system components and monitoring systems (electrical and water discharge),
- the need for early assessment of likely current draw coupled with discrete EKG panels with monitored and controlled current supply, and
- the need for post-trial ground investigation, in situ testing, laboratory testing and monitoring to determine effectiveness and the longevity, and thus the design life, of the EKG processes.

More generic lessons learnt from the trials and the practical application are reported and these are combined with those from the work on Willow Poles (Winter et al. 2018a) and FRS (Seddon et al. 2018) to produce guidance for future Highways England trials of innovative geotechnical repair techniques (Winter et al. 2018b).

**REFERENCES**

Nettleton, I. M., Seddon, R. and Winter, M. G. 2018. Innovative geotechnical repair techniques: effectiveness of electrokinetic geosynthetics. PPR 890. TRL, Wokingham.

Seddon, R., Winter, M. G. and Nettleton, I. M. 2018. Innovative geotechnical repair techniques: effectiveness of fibre reinforced soil. PPR 873. TRL, Wokingham.

Winter, M. G., Nettleton, I. M. and Seddon, R. 2018a. Innovative geotechnical repair techniques: recommendations and guidance for management of future Highways England trials with innovative techniques. PPR 891. TRL, Wokingham.

Winter, M. G., Nettleton, I. M. and Seddon, R. 2018b. Innovative geotechnical repair techniques: recommendations and guidance for management of future Highways England trials with innovative techniques. PPR 891. TRL, Wokingham.



## The effectiveness of fibre reinforced soil for shallow slope failure stabilization

Richard Seddon<sup>1</sup>, Mike G Winter<sup>2</sup>, Ian M Nettleton<sup>3</sup>, Jan Marsden<sup>4</sup>

<sup>1</sup>Formerly Coffey Geotechnics now Jacobs, United Kingdom, [richard.seddon@jacobs.com](mailto:richard.seddon@jacobs.com)

<sup>2</sup>Formerly TRL Limited now Winter Associates, United Kingdom, [mwinter@winterassociates.co.uk](mailto:mwinter@winterassociates.co.uk)

<sup>3</sup>Coffey Geotechnics, United Kingdom, [ian.nettleton@coffey.com](mailto:ian.nettleton@coffey.com)

<sup>4</sup>Formerly Highways England, United Kingdom, [geotechnicsteam@highwaysengland.co.uk](mailto:geotechnicsteam@highwaysengland.co.uk)

Work to evaluate the effectiveness of innovative geotechnical repair techniques for slopes has been commissioned by Highways England. The techniques are the planting of live willow poles, Fibre Reinforced Soil (FRS) and Electrokinetic Geosynthetics (EKG). These techniques were trialled to assess the overall impact of various challenges including environmental constraints (habitat and visual), access and utility constraints, and the need to reduce the scale and/or cost of traffic management and traffic delays.

Trials of these techniques have been undertaken over the last 20 years or so but monitoring was generally limited to just a few years post-construction. Longer term evaluation has not generally been undertaken.

This assesses the effectiveness of FRS as a long-term slope repair technique and is one of a series for this project.

The addition of discrete randomly orientated fibres to improve the physical properties of soil is a technique that is more widely used in other countries such as the USA. The use of FRS has been reported to have benefits over other more commonly used slope repair techniques. In general, it allows the reuse of site-won material through the addition of a relatively small proportion of fibres to the soil fill.

Three trials using FRS as a slope repair technique, undertaken in the past nine years, have been assessed. An initial trial was constructed on a cutting at the A1(M) Junction 1 in 2009, two slope failures on a combined embankment and acoustic bund were repaired at the A27 at Polegate in 2010 and 2011, and in 2014 an FRS trial on a cutting on the M20 near Smeeth was constructed.

The assessment of the trials was undertaken by reviewing the information contained in geotechnical reports and site inspections. The knowledge and understanding of the trials was augmented through discussions with technical staff from the Maintaining Agents and Highways England.

Difficulties in accurately determining the improvement to the geotechnical properties of the soils at the trial sites were reported at both the design and construction stage. For instance, at design stage, a 25% increase in the effective angle of shearing resistance was generally adopted. However, post-construction testing at the A1(M) site and slope instability at A27 Polegate suggest that the increase in effective angle of shearing resistance is much less.

Construction of the FRS trials was frequently during wet weather. This result in some FRS being placed wet of optimum. This potentially has reduced or masked the effectiveness of the FRS. At A27 Polegate trafficability of the ground, softened as result the extremely wet weather, was improved by the addition of fibres. This demonstrated a potential application of FRS for temporary works.

The use of FRS to repair failing slopes has been partly successful in the short-term on two of the sites: i.e. A1(M) Junction 1 and M20 Smeeth. At the A27 Polegate, the use of FRS to repair the slope was not successful (Figure 1). Overall, it is considered that the three trials have not demonstrated effectiveness of the FRS as a long-term slope repair technique.



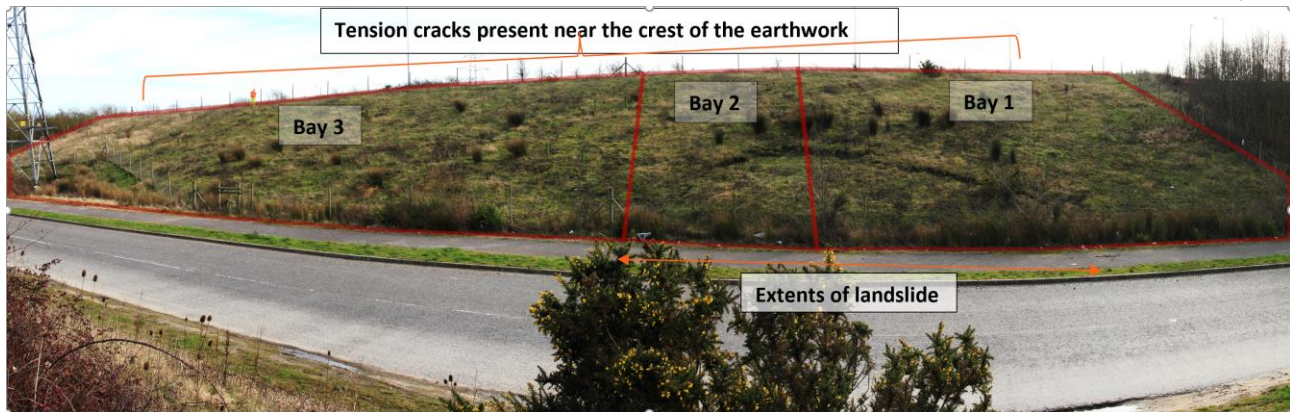


**Figure 1. Photomontage of the A27 Polegate/Bay Tree Lane FRS trial. Note arcuate back scar indicating slope failure.**

In addition to the carbon impacts, the long-term sustainability of FRS, when using non-biodegradable fibres, may be questioned. The reuse of a soil-plastic mix, such as FRS, poses waste management, environment and geotechnical challenges which would need to be resolved before it could comply with Highways England's ambition for a circular approach to managing resources. Resolving these end-of-life issues is considered to be key to the adoption of FRS as a slope repair technique in the future.

Given these issues it was considered that FRS technology and the knowledge for its use were not sufficiently developed for it to be adopted as a long-term slope repair technique. Nevertheless, the trials have demonstrated the potential for FRS to be used to improve trafficability of soils. It is recommended that further research is undertaken to assess the use of FRS, created with sustainable natural fibres, for temporary ground improvement and the construction of temporary roads and tracks. A much more expansive treatment of this work by Seddon et al. (2018).

More generic lessons learnt from the trials and the practical application are reported and these were combined with those from the work on willow poles (Winter et al. 2018a) and EKG (Nettleton et al. 2018) to produce guidance for future Highways England trials of innovative geotechnical repair techniques (Winter et al. 2018b).

## REFERENCES

- Nettleton, I. M., Seddon, R. and Winter, M. G. 2018. Innovative geotechnical repair techniques: effectiveness of electrokinetic geosynthetics. PPR 890. TRL, Wokingham.
- Seddon, R., Winter, M. G. and Nettleton, I. M. 2018. Innovative geotechnical repair techniques: effectiveness of fibre reinforced soil. PPR 873. TRL, Wokingham.
- Winter, M. G., Nettleton, I. M. and Seddon, R. 2018a. Innovative geotechnical repair techniques: recommendations and guidance for management of future Highways England trials with innovative techniques. PPR 891. TRL, Wokingham.
- Winter, M. G., Nettleton, I. M. and Seddon, R. 2018b. Innovative geotechnical repair techniques: recommendations and guidance for management of future Highways England trials with innovative techniques. PPR 891. TRL, Wokingham.





## Forensic examination of critical special geotechnical measures

Mike G Winter<sup>1</sup>, Ian M Nettleton<sup>2</sup>, Michelle Duffy-Turner<sup>3</sup>, Gillian Butler<sup>4</sup>, Philip Liew<sup>5</sup>

<sup>1</sup>Winter Associates, United Kingdom, [mwinter@winterassociates.co.uk](mailto:mwinter@winterassociates.co.uk)

<sup>2</sup>Coffey Geotechnics, United Kingdom, [ian.nettleton@coffey.com](mailto:ian.nettleton@coffey.com)

<sup>3</sup>Coffey Geotechnics, United Kingdom, [michelle.duffyturner@coffey.com](mailto:michelle.duffyturner@coffey.com)

<sup>4</sup>Coffey Geotechnics, United Kingdom, [gillian.butler@coffey.com](mailto:gillian.butler@coffey.com)

<sup>5</sup>Highways England, United Kingdom, [philip.liew@highwaysengland.co.uk](mailto:philip.liew@highwaysengland.co.uk)

The Highways England Strategic Road Network (SRN) relies upon a wide range of Special Geotechnical Measures (SGMs) to strengthen or enhance the natural geological materials or engineering materials derived from them to form earthworks. There are currently almost 100 SGM techniques, and the design, specification and application of many of these techniques is based on limited studies. Many of these techniques have been in service for periods approaching their predicted design lives (typically 60 years) and it is considered timely to validate the predicted long-term performance of these SGMs.

SGMs are defined as "... measures over and above general earthworks construction required to; mitigate geotechnical risk associated with ground related hazards or remediate geotechnical defects that may have resulted from the presence of geo-hazards. Similar techniques implemented to facilitate widening or other improvements are, for the purposes of this task, also classified as Special Geotechnical Measures."

Planned SRN major projects and operational renewals present a significant and innovative opportunity to undertake forensic examination, including exhumation of elements, to determine the validity of the existing design, specification and application guidance. This presents a unique opportunity to determine their in-service performance against that predicted and relied upon in terms of design life. A number of cases, both on and off the SRN, have come to light where the selection, design, specification or application of some SGMs have had issues that affect their performance and design life.

Given the SRN's required performance in terms of resilience, reliability, redundancy and recovery it is essential that SGMs are themselves reliable in terms of performance and life; resilient to external conditions such as earthworks deterioration and extraordinary conditions (e.g. climate change). This phase of the project will:

- Identify SGMs on which the SRN is/or has the potential to become critically reliant in the following categories: extent of application; criticality of location; insufficient guidance / understanding in the industry; and emerging techniques.
- Assess for these categories where forensic checks/challenges would be warranted in future project phases, to compare design with the performance that is achieved for prioritised SGMs.
- Evaluate the adequacy of design, specification and construction guidance available.
- Develop a system to prioritise the selected SGMs for further investigation and assessment as opportunities arise for forensic exhumation and examination.

A 'long list' of SGMs was identified from responses to a questionnaire sent to Highways England Geotechnical Advisors, Geotechnical Maintenance Liaison Engineers and Designer's Geotechnical Advisors for both Smart Motorway Projects and Complex Infrastructure Projects. This was corroborated using SGM statistics produced from a project delivered by Atkins on Geotechnical Asset Performance – Whole Life Assessment. Other asset owners including Network Rail and transport Scotland were also consulted. The survey specifically sought information on SGMs that were viewed to be problematic and could be evidenced as such.



This list was the subject of discussion with Highways England and was reduced to the following SGMs that are considered to be of paramount importance:

- Counterfort drains.
- Soil Nails.
- Gabion and Block Walls.
- Geogrids and Metallic Reinforcement.
- Regrades.

Geogrids and Metallic Reinforcement as components of reinforced earth were not rated as being problematic based on the questionnaire results; however, these two SGMs have been highlighted by Highways England as being of particular concern to the network by the Geotechnical Advisors and therefore they have been included as SGMs to consider for further consideration.

Regrades were highlighted in the questionnaire results as being of interest, making up 15% of the 52 examples of SGM given; however, these had not been flagged as a major problem within work on whole life cost and they are not perceived to be an issue internally within Highway England. Discussions with Highways England are ongoing as to whether this SGM should also be included.

This first phase of the project is due to report by the end of 2019/20 and subsequent phases will be targeted at the exhumation and examination of the pre-selected SGMs to determine the Technology Readiness Level (TRL), to assess whether reliance on particular SGMs is justified and to attempt to validate (or otherwise) design assumptions.

It is anticipated that outcomes could follow a wide range of possibilities including that some SGMs have the potential to maintain or transition towards DMRB/MCHW status; others may need further work in terms of the development of specification and/or design guidance before that transition becomes a possibility. Other SGMs may need to have that status further reviewed, including those that have limited to no potential for future use on the SRN (e.g. for technical, environmental, safety reasons), and/or existing applications may need to be reviewed with a view as to their longer-term suitability. In the latter case, advice will be provided on the potential need for decommissioning of SGMs, the performance of which has been found to be inadequate relative to the assumptions made at the design stage.

The work will enable Highways England to appropriately employ (or otherwise) the selected SGMs on the SRN and to assess the future budget requirements for upgrading or replacing SGMs nearing their end of life. The work will help innovation, aligning with Highways England KPIs and will also benefit external stakeholders.

## Assessment of slope stability by monitoring change of tensile force of anchor

Oil Kwon<sup>1</sup>, Jonghyun Lee<sup>2</sup>, Byungsuk Park<sup>3</sup>, Jahe Jung<sup>4</sup>

<sup>1</sup>*Regional Cooperation Center, Korea Institute of Civil Engineering and Building Technology, Republic of Korea, [kwonoil@kict.re.kr](mailto:kwonoil@kict.re.kr)*

<sup>2</sup>*Multi Disaster Countermeasures Research Center, Korea Institute of Civil Engineering and Building Technology, Republic of Korea, [jhrhee@kict.re.kr](mailto:jhrhee@kict.re.kr)*

<sup>3</sup>*Integrated Road Management Research Center, Korea Institute of Civil Engineering and Building Technology, Republic of Korea, [parkbyungsukl@kict.re.kr](mailto:parkbyungsukl@kict.re.kr)*

<sup>4</sup>*Underground Space Safety Research Center, Korea Institute of Civil Engineering and Building Technology, Republic of Korea, [jhjung@kict.re.kr](mailto:jhjung@kict.re.kr)*

The purpose of this study is to present criteria for evaluating stability by monitoring changes in tensile force of anchor in the event of collapse on the slope reinforced by anchors. In the event of collapse on a slope, shear and bending stresses are applied in the section of the shear plane along the activity surface. And as the shear displacement increases, deformation occurs on the anchor installed on the slope. Anchor increases the axial force as deformation occurs. For the behavior of anchors due to such slope collapse, large-scale model experiments were conducted with variables such as location and lateral pressure conditions of the anchor and the results were analyzed. The large-scale model experiment confirmed the phenomenon in which the shear force is applied to the anchor as the shear deformation occurs and the tension of the anchor increases if the deformation above a certain displacement persists.

The trend of change in shear and axial force acting on anchors was analyzed. As a result of conducting the experiment with different application of the location and lateral pressure conditions of the anchor, which is a variable of the experiment, it was analyzed that the changes in shear and axial force acting on the anchor were correlated. Next, the numerical analysis analyzed the increasing tendency of the axial force acting on the anchor. The increasing tendency of axial forces acting on anchors according to the variables in the experiment was found to be similar compared to the results of the larger model experiment. However, the results of the large-scale model experiment and the results analyzed in the numerical analysis differed quantitatively. To overcome these differences, it is believed that studies will be needed to develop new analytical models for failure criteria and boundary interface.

The increase in the axial force acting on the anchor was measured up to 48.19 kN. The increase in the axial force was not relatively large, but the grout body of the anchor was transformed to the level at which the destruction occurred despite the change in the small axial force. As the axial force of the anchor tends to increase linearly, it is expected that the tendon of the anchor can be broken if the shear deformation continues to increase. Therefore, if the axial force increase of the anchor is confirmed during slope maintenance, the cause must be determined. It is also necessary to promptly establish stabilization measures if it is deemed that the movement of the slope will continue.

In this study, the shear behavior of anchors is analyzed by installing anchors within the model ground and conducting large-scale model experiments. And the experiment was carried out with minimal variables. Therefore, the results may differ from the actual ones depending on the type and condition of the ground and the conditions of the lateral pressure. Therefore, it is necessary to conduct additional experiments that apply various conditions as variables to obtain and analyze a lot of data. In addition, it is deemed necessary to study various conditions that are difficult to implement in experiments through numerical analysis methods.

## A Soil Improvement Methodology for a Shallow Tunnel Excavated in Extremely Weak Clay: A case study from Turkey

Arif Emre Kaan Gündoğdu<sup>1</sup>, Aslı Can<sup>1</sup>, Kemal Acar<sup>1</sup>, Candan Gökçeoğlu<sup>2</sup>

<sup>1</sup>Progeo Project Company, Ankara, Turkey, {[e.gundogdu](mailto:e.gundogdu), [a.can](mailto:a.can), [k.acar](mailto:k.acar@progeo.com.tr)}@progeo.com.tr

<sup>2</sup>Hacettepe University, Geological Engineering Department, Ankara, Turkey, [cgokce@hacettepe.edu.tr](mailto:cgokce@hacettepe.edu.tr)

Shallow tunnels excavated in weak ground conditions have serious engineering problems because excavations in weak ground conditions result in high deformations. These deformations occurring in shallow tunnels also cause serious settlements on surface. In this study, the problems encountered in a railway tunnel are described and the proposed engineering measures are presented. The length of T2 tunnel of Karaman – Ulukisla Railway Project (south of Turkey) is about 2.5 km and the exit parts of the tunnel is rather shallow because the overburden in this part varies between 15-25 m. The tunnel is excavated in clay having low to high plasticity (CL-CH). Groundwater level is about 4.5 to 9 m. Another important problem is the presence of an oil pipeline passing through the tunnel. Oil pipelines are very sensitive to ground settlements, and the damage to the pipe creates serious problems.

Due to these difficulties, this part of the tunnel must be excavated with no or minimum deformation and without any failure. However, if a tunnel is excavated in weak ground conditions with New Austrian Tunneling Method, high deformations can be expected. To avoid these deformations, a soil improvement method, deep soil mix (DSM), is proposed to improve the ground conditions before excavation. DSM columns improve the ground, increase the NATM class and decrease deformations. The proposed improvement methodology is evaluated with numerical analyses. The DSM method is a widely used technique in geotechnical engineering applications. Performance of this method mainly depends on increasing the stiffness of natural soil by adding a strengthening admixture material such as water/cement injection by mechanical mixing. By using DSM columns, it is aimed to increase the soft soil properties to soft rock class, thus the improved ground of the tunnel section can be classified as B2 NATM Class. The DSM columns are designed with a dimension of 1 m and with 0.85 to 0.90 m of spacing per column at the center and at the sides of the tunnel, respectively. Additionally, the stability of the B2 Class tunnel is needed to support system. For this class, Store Norfors (SN) type bolts with 6 m length and shotcrete with 0.20 cm thickness were selected as the support system of the tunnel (Figure 1).

Consequently, to verify and check the validity of the suggested support systems with the improved ground four different critical tunnel sections were analyzed numerically by Plaxis 2D software which is a finite element analysis (FEA) program. In the Plaxis 2D analysis the deformations, the shear and axial forces, and the bending moments were applied on the tunnel excavation were determined. The results of the FEA (Figure 2) show that the maximum deformation in natural ground conditions is 608 mm while that in the improved ground is obtained as 40 mm. It is concluded that the suggested improvement methodology, excavation and support systems are found satisfactory. This study is significant as it is one of the first examples of a NATM project with ground improvement by using DSM columns.

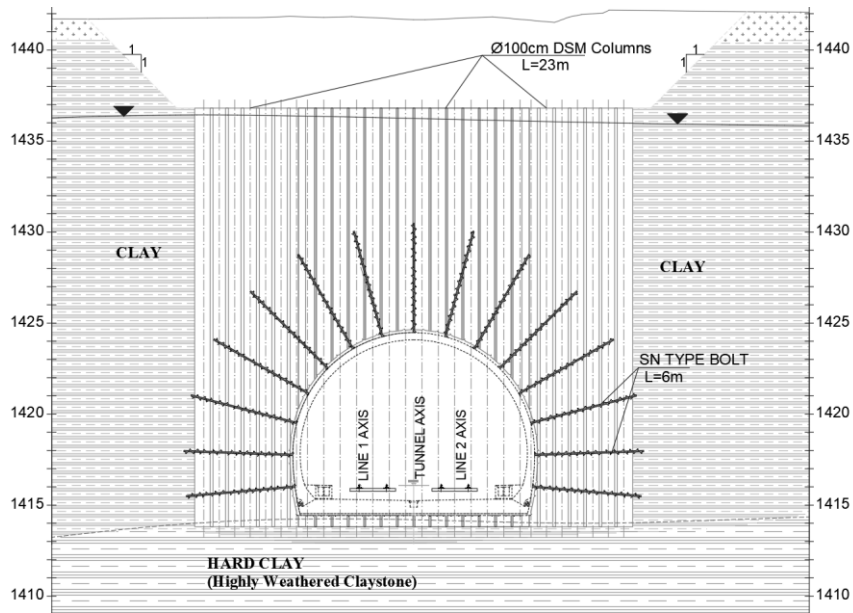


Figure 1. The proposed support system of the tunnel excavated in improved ground.

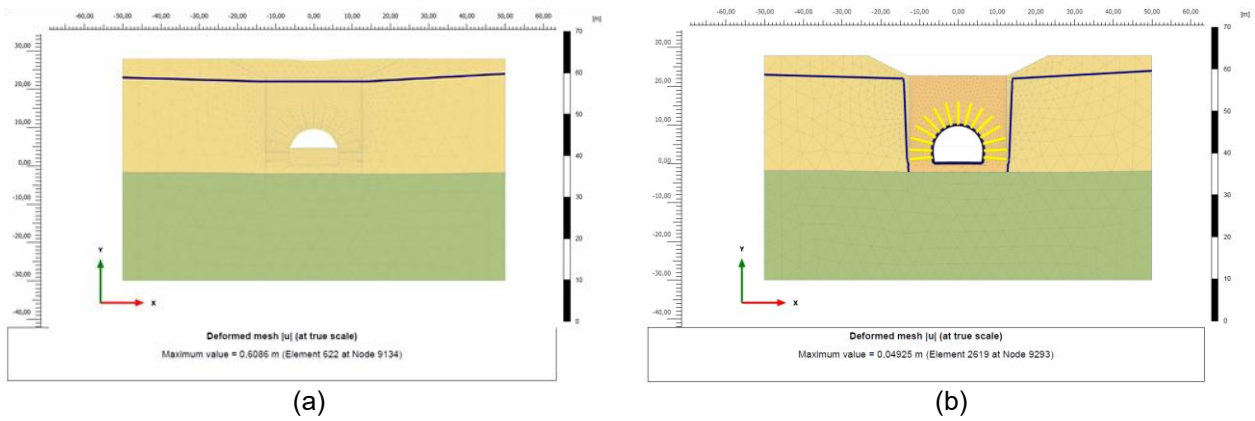


Figure 2. Finite element analysis results of the tunnel section (a) Total displacements of the ground without improvement (b) Total displacements of the improved ground by the DSM columns.



## Proposed Engineering Measures and Analysis of Tunnel Portal Excavated in Paleo-Landslide Deposits (Bahce – Nurdag Tunnel, Turkey)

Yunus Emre Özyürek<sup>1</sup>, Aslı Can<sup>1</sup>, Kemal Acar<sup>1</sup>, Candan Gökçeoğlu<sup>2</sup>

<sup>1</sup>*Progeo Project Company, Ankara, Turkey, {a.can, e.ozyurek, k.acar}@progeo.com.tr*

<sup>2</sup>*Hacettepe University, Geological Engineering Department, Ankara, Turkey, cgokce@hacettepe.edu.tr*

Due to geometrical restrictions of high-speed railways, excavation is mandatory under adverse geological and geotechnical conditions. The Bahce – Nurdag tunnel with an approximate length of 10 km is the longest among the railway tunnels of Turkey. The study area locates in Eastern Anatolian Fault Zone (EAFZ) and as the consequences of the active tectonism, the topography is steep and there are several paleo and active landslides. When selecting the portal locations, active landslide areas were avoided, but the paleo-landslide mass could not be avoided at the Bahce portal. For this reason, to the safety of the tunnel and the Bahce portal, extra engineering measures had to be taken. This study describes the problems sourced from the geological conditions of the Bahce portal, the extra engineering measures and the analysis of the measures to understand of the performance of the proposed measures. Before excavation, a retaining system with 1 m-diameter piles was constructed and the excavations were started. When the last stage of the excavation was reached, deformations up to 46 mm were detected in inclinometers. Upon this, the excavation was stopped and was backfilled immediately, thus the movements were stopped before it spreads to the buildings at close vicinity of the portal. Subsequently, a new site investigation program including boreholes was applied to understand the mechanism of failure. The paleo-landslide material in the portal region was 15 to 27 m thick sliding mass underlain by highly weathered schist. The groundwater level was measured approximately as 13 m in the new boreholes. Inclinometers were also installed in the new boreholes but all inclinometers were damaged in a short time due to movement. Consequently, the cross-section of the failure was prepared by analyzing a combination of topographic maps, in-situ observations and data obtained from the boreholes. To provide safety of tunnel and portal construction, a new retaining system with diaphragm walls with a dimension of 1.2 x 2.8 m was proposed and designed. Additionally, to support the retaining system against the loads sourced from the triggered paleo-landslide mass, barrette piles with a dimension of 1.2 x 2.8 m and with 2.6m of spacing per pile and steel struts with a dimension of approximately 1400 mm were selected as the support system (Figure 1).

Consequently, the finite element analysis (FEA) of the slope stabilization was analyzed through Plaxis 2D software (Figure 2). The shear and axial forces and the bending moments were applied on the support system units and the analyses were performed for the static and dynamic cases because the area has a very high seismic activity. The factor of safety (k) in the slope stability analysis of the final stage of the works was also checked and the stability conditions were provided. In September 2017, the construction of the retaining walls, the support system, and the tunnel excavation were started again. The deformations of the system were monitored continuously by inclinometers which were placed in the diaphragm walls. The construction works with the suggested support system against active landslide loads were successfully completed in January 2019. No significant displacements in inclinometers have been recorded over the 15-months period. In this respect, it can be concluded that barrette piles can be effectively used to prevent further landslides. This study was able to conclude that finite element analysis is a useful tool for simulating the mechanism of slope failure; the success of the project and the reliability of FEA are found satisfactory.

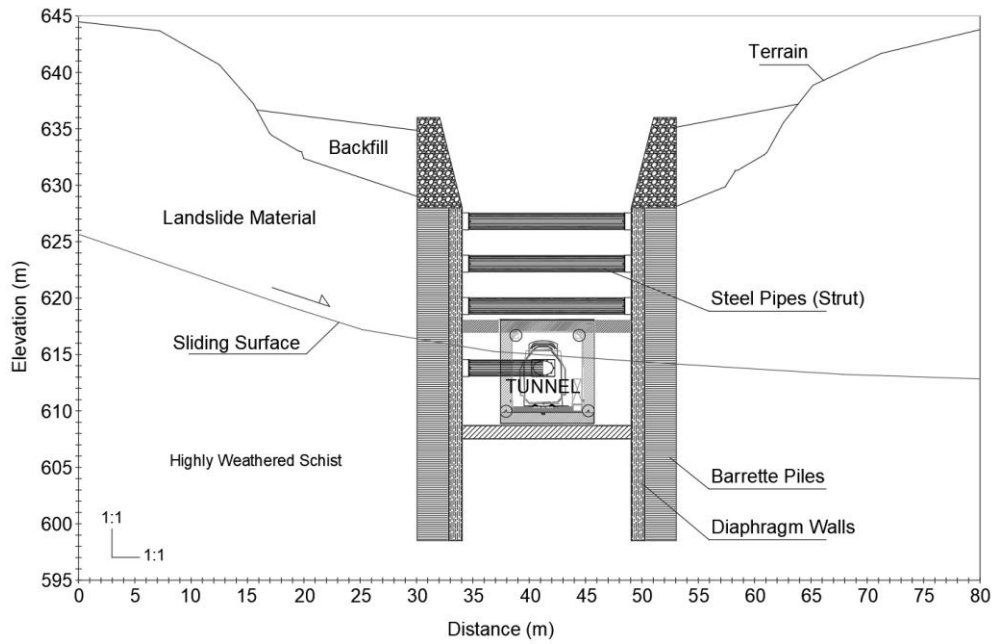


Figure 1. The retaining and support system of the tunnel for landslide stabilization.

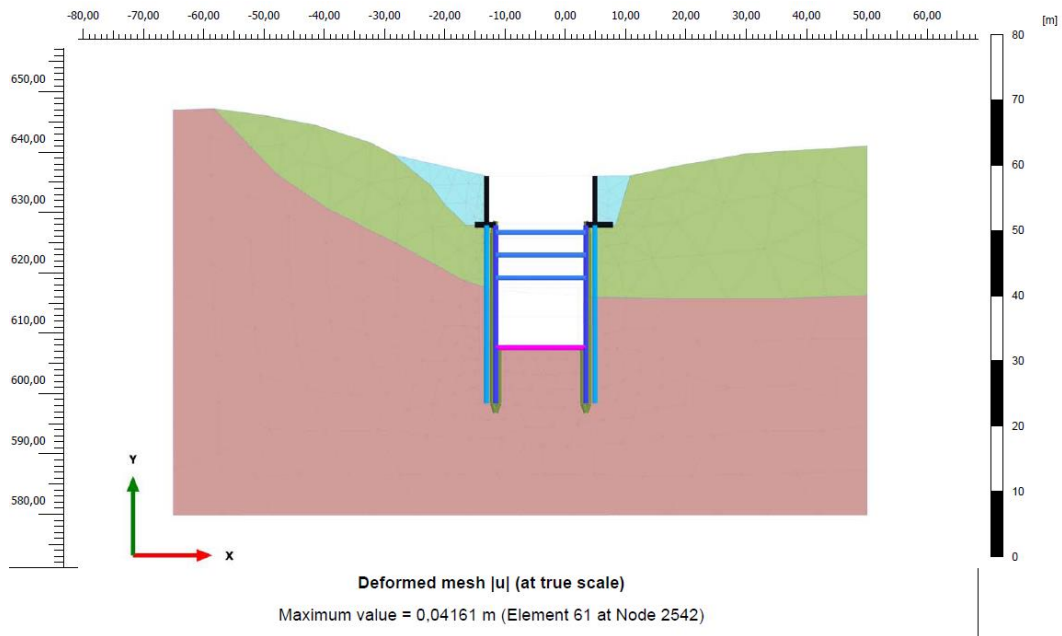


Figure 2. Finite element model of the retaining and support system of the tunnel

## A probabilistic approach to deal with uncertainty in tunneling

Antonios Skolidis<sup>1</sup>, Dr. Chrysothemis Paraskevopoulou<sup>2</sup>, Dr. Vassilis Marinos<sup>3</sup>

<sup>1</sup>MSc Graduate, University of Leeds, Leeds, UK, [mlecko\\_sko@hotmail.gr](mailto:mlecko_sko@hotmail.gr)

<sup>2</sup>Assistant Professor, University of Leeds, Leeds, UK, [c.paraskevopoulou@leeds.ac.uk](mailto:c.paraskevopoulou@leeds.ac.uk)

<sup>3</sup>Associate Professor, Aristotle University, Thessaloniki, Greece, [marinosv@geo.auth.gr](mailto:marinosv@geo.auth.gr)

Uncertainty is prevalent in the ground due to constant modifications throughout its geological history, which results in temporal and spatial variability of its properties and stress regime (Yau et al. 2020). In tunnelling, uncertainty has the tendency to propagate through the different project stages, e.g. from geotechnical parameters to rock mass type behaviour and insufficient support tunnel measures, increasing the likelihood of unsound designs that can result to cost and time overruns (Paraskevopoulou and Benardos, 2013). Probabilistic approach refers to simply a mathematical tool that can be used to quantify and deal with uncertainties consistently (Baecher and Christian, 2003). In this regard, the engineer can identify the risks and define every failure scenario but can also quantify the response of the design using the probability of failure of the expected scenarios.

The presented work aims at discerning sources of uncertainty in tunnelling evaluating its effect on the output design parameters by utilizing a simple systematic probabilistic approach initially proposed by Schubert and Goricki (2004) and has been further developed herein using an example tunnel alignment for the Egnatia Odos Highway, in Northern Greece, the Agnantero tunnel. The tunnel was excavated in a heterogeneous molassic formation (Figure 1), which generally consists of alternations of sandstones, siltstones, conglomerates and possibly claystones and/or marls (Marinos, 2007). The engineering geological particularities of this formation is characterized by: a) the heterogeneity, due to the alternate strengths of the persistent rocks and/ or the change in bedding stratification, b) the weathering of the weak silty-clayey members that are highly prone to slaking (Figure 1.a). Hence, we have two “blocks” of structure-competence along these masses: i) the weathered structures with severe stratification or even schistose forms, found close to surface and ii) the compact, continuous and tight rock masses with very few joints, possibly composed of different lithologies, found after 10-15m in depth.

Particularly in this case study, uncertainty in the design outputs (displacements) stems from uncertainty in the rockmass parameters, which in turn stems from uncertainty in the strength properties of the intact rock, but most importantly from the uncertainty in the structure of the molasse at depth, since structure is key in determining its expected behaviour. The proposed methodology, presented in Figure 1, is based after Schubert (2004) and Marinos (2012). In this particular study, it begins with the determination of the statistical moments of every lithology's intact rock strength properties, namely elastic modulus ( $E_i$ ) and unconfined compressive strength ( $\sigma_{ci}$ ) (Figure 1.a. and b). The distributions of the rockmass strength parameters for every lithological unit type are assessed, together with other influencing factors such as GSI ratings, as well as bedding and joint orientations classifying the lithological units into Rock Mass Types or RMTs (Figure 1.c), considering the expected failure mechanisms, defining the Rock Mass Behaviour Types RMBTs (Figure 1.d). Stress and stability analyses are carried out, using UnWedge and RS2 and the numerical results allow the categorization of the variable rockmass behaviours/failure modes into the pre-defined RMBTs (Figure 1.e), subsequently leading to the preliminary design of the respective support sections (Figure 1.f). Finally, this research work shows that accounting for the variability in the design inputs, enables the distinction of a variety of potential failure modes and the assessment of the most probable ones under the project specific geological conditions.

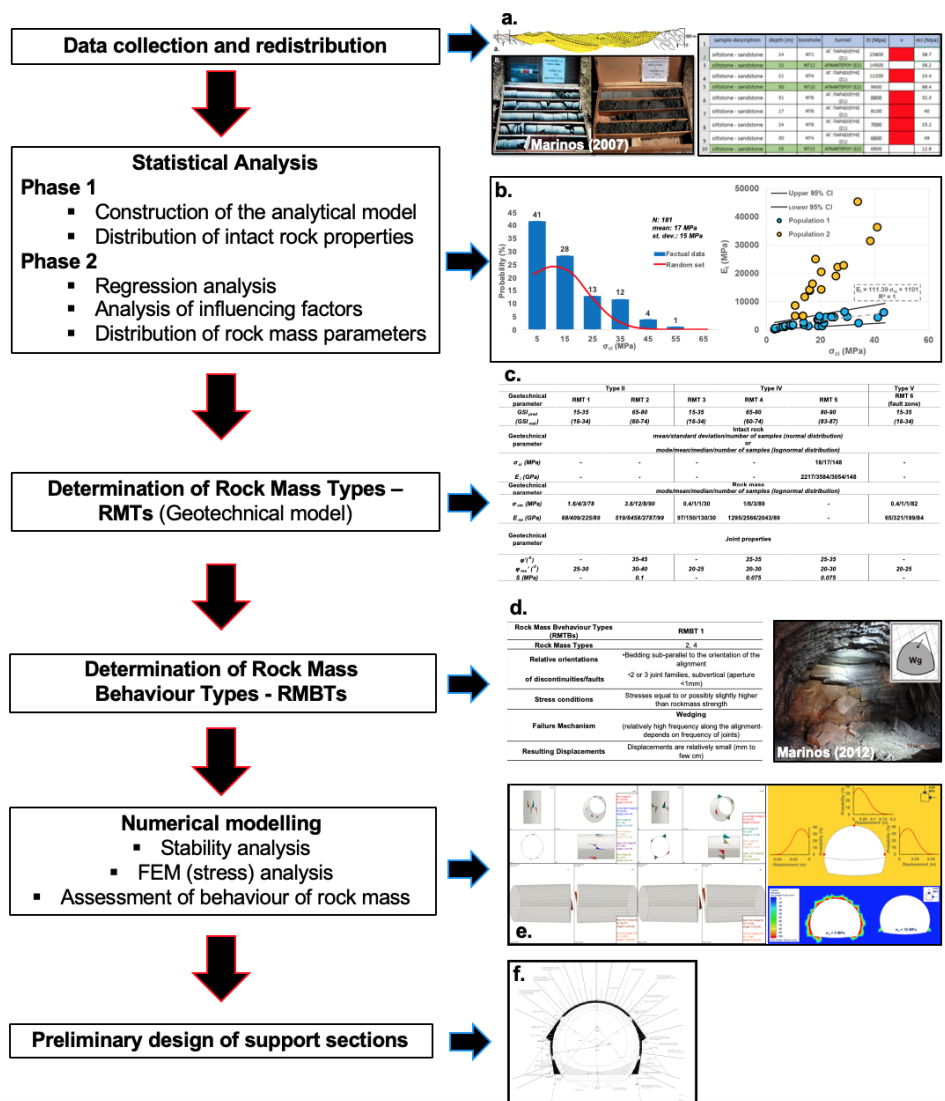


Figure 1. Illustration of the proposed methodology, applied here for our particular study of Agnantero tunnel (of Egnatia Odos S.A in Northern Greece), modified from Schubert, 2004 and Marinos, 2012.

**REFERENCES**

Baecher, G.B., Christian, J.T. 2003. *Reliability and Statistics in Geotechnical Engineering*. Wiley. New York.

Marinos, V. 2007. *The geotechnical classification and behaviour of weak and complex geomaterials during tunnel excavation*. PhD Thesis. National Technical University of Athens (NTUA). Athens, Greece.

Marinos V. 2012. Assessing rock mass behaviour for tunneling. *Envi. and Eng. Geoscience*; 18(4): 327–41.

Paraskevopoulou C. Benardos, A. 2013. Assessing the construction cost of tunnel projects. *TUST J.*, 38(2013), 497–505.

Schubert W. 2004. Basics and application of the austrian guideline for the geomechanical design of underground structures. In: *EUROCK2004 and 53th Geomechanics Colloquium*. VGE.

Schubert, W., Goricki, A. 2004. Probabilistic assessment of rock mass behaviour as basis for stability analyses of tunnels. *Proceedings Rock Mechanics Day 2004*. pp.1-20.

Yau, K., Paraskevopoulou, C., Konstantis, S. 2020. Spatial variability of karst and effect on tunnel lining and water inflow. A probabilistic approach. *TUST J.I.*, 97(2020), 103248, 13 pages.

## Evaluation of Collapsed Zone in T24 Tunnel (Ankara-Istanbul High Speed Railway Project, Turkey)

Ebu Bekir Aygar<sup>1</sup>, Candan Gokceoglu<sup>2</sup>

<sup>1</sup>Fugro Sial Geosciences Consulting and Engineering, Turkey, [e.aygar@fugro.com](mailto:e.aygar@fugro.com)

<sup>2</sup>Hacettepe University, Department of Geological Engineering, Turkey, [cgokce@hacettepe.edu.tr](mailto:cgokce@hacettepe.edu.tr)

T24 tunnel constructed within the scope of Ankara-Istanbul High Speed Train Railway Project locates between km: 213 + 969 - 216 + 176 and has a total length of 2207 m. The T24 tunnel excavated in heavily weathered graphitic schists and the overburden in the collapsed zone is around 100 m. This part of the tunnel has very weak rock mass conditions and shows swelling and squeezing ground properties. Tunnel excavation was completed in the form of top heading, bench and invert sections. The tunnel was excavated in B2 (very friable rock class), B3 (ravelling rock class), C2 (squeezing rock conditions), and C3 (heavily squeezing) rock classes according to the NATM classes.

After completing the tunnel excavation and outer support, the deformation was stabilizing in a period of 6 months between September 2010 and February 2011 (Figure 1).

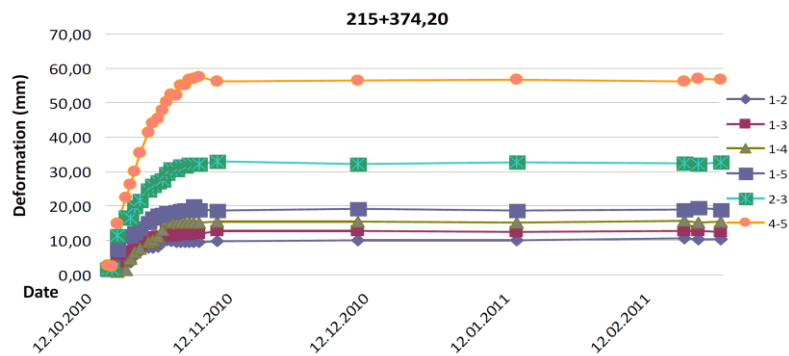


Figure 1. Invert buckling and yielding in shotcrete at Km:215+415

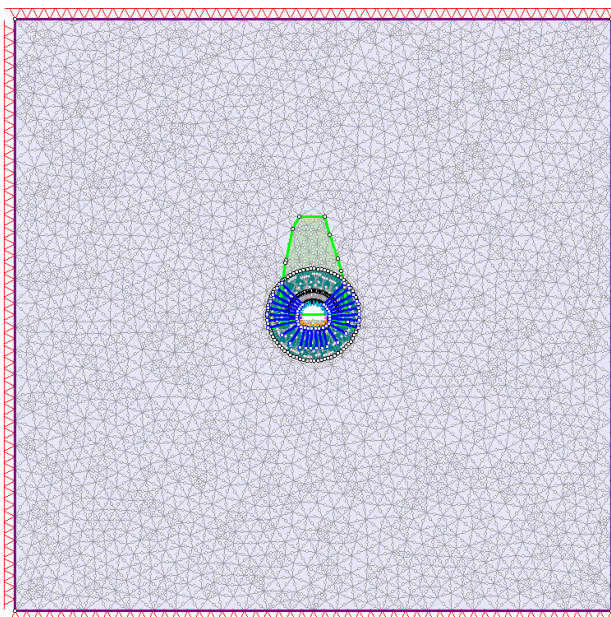
After this stage, inner lining concrete has started. During this period, a sudden increase in deformations was observed in May 2011, and this rapid increase caused buckling in the invert concrete and failure in shotcrete (Figure 2). As soon as these problems were observed, between the Km:215+370 - 215+500, all the tunnel works were stopped, and this part of the tunnel collapsed completely. Extreme deformations developed in this was sourced from the squeezing of the ground. This type of collapse would not have been encountered if the inner lining concrete had been made immediately following the damping of deformations.



Figure 2. Invert buckling and yielding in shotcrete at Km:215+415 (Figure 2)



The purpose of this study is to explain the mechanism of the failure and the approaches used for rebuilding the collapsed zone. The collapsed zone filled with the backfill material and covered with shotcrete and wire mesh. Thus, tunnel face stability was provided. Following that, the injection process from the tunnel face was performed with 1x1 m patterned and 3m, 6m and 9m lengths. After the termination of improvement of the collapsed zone, the excavation was started. During this stage, excavations were carried out using a 2-layer 3.5" diameter, 12 m length umbrella system in the top heading. The first layer umbrella was installed approximately 5 degree and the second layer umbrella was installed 15 to 20 degree. For the numerical analyses, Phase2d program was used to determine appropriate support systems (Figure 3). Back-analyses were performed to determine the rock mass parameters, and finally new support systems were proposed and analysed. Consequently, the collapsed mechanism in the tunnel is explained and the necessary revisions in the support systems are given for the re-excavation of the collapsed area.



**Figure 3. Phase 2d v8.0 tunnel model**

## Tunnel Collapse Due to the Insufficient Umbrella System: A Case Study from Turkey

Ebu Bekir Aygar<sup>1</sup>, Candan Gökçeoğlu<sup>2</sup>

<sup>1</sup>Fugro Sial Geosciences Consulting and Engineering, Turkey, [e.aygar@fugro.com](mailto:e.aygar@fugro.com)

<sup>2</sup>Hacettepe University, Department of Geological Engineering, Turkey, [cgokce@hacettepe.edu.tr](mailto:cgokce@hacettepe.edu.tr)

T1 tunnel (L=2140 m) which locates between Km:3+360 –5+500of Güvem – Çerkeş State Highway (Ankara-İstanbul Junction) under the governance of Ministry of Transport and Infrastructure of Turkish Republic, General Directorate of Highways. A collapse occurred during top heading excavation at Km:3+785.50 bringing along material discharge towards the tunnel face that in turn blocked the tunnel, completely (Figure 1). Afterwards, excavation work inside the tunnel was interrupted. This section of the tunnel was being excavated through completely weathered, heavily jointed and fractured basalt with clay and sand content. The NATM classes of the ground was B3 (ravelling rock class).



**Figure 1. Views from the collapse of the T1 tunnel**

It was obviously seen that this section of the tunnel was not be excavated with the existing support system and, a revision of the support system was required. In addition, an additional problem was encountered because the stability deficiency in the ceiling of the top heading occurred. The collapse developed as a material discharge resulting from inadequacy of forepoling application at the tunnel ceiling. As a result, this material discharged in the tunnel ceiling caused loose material to be accumulated in front of the tunnel face, thus stability of tunnel ceiling was entirely deteriorated. The numerical analysis was performed with Phase2d-finite element analyses program and the model used in the analyses is given in the Figure 2.

A series of back analyses were performed to obtain the rock mass parameters when the tunnel collapsed. In the back analyses, different cohesion and internal friction angle and different deformation modulus values were analyzed using the existing support systems. Employing the parameters obtained from the back analyses, the proposed support systems were analyzed.

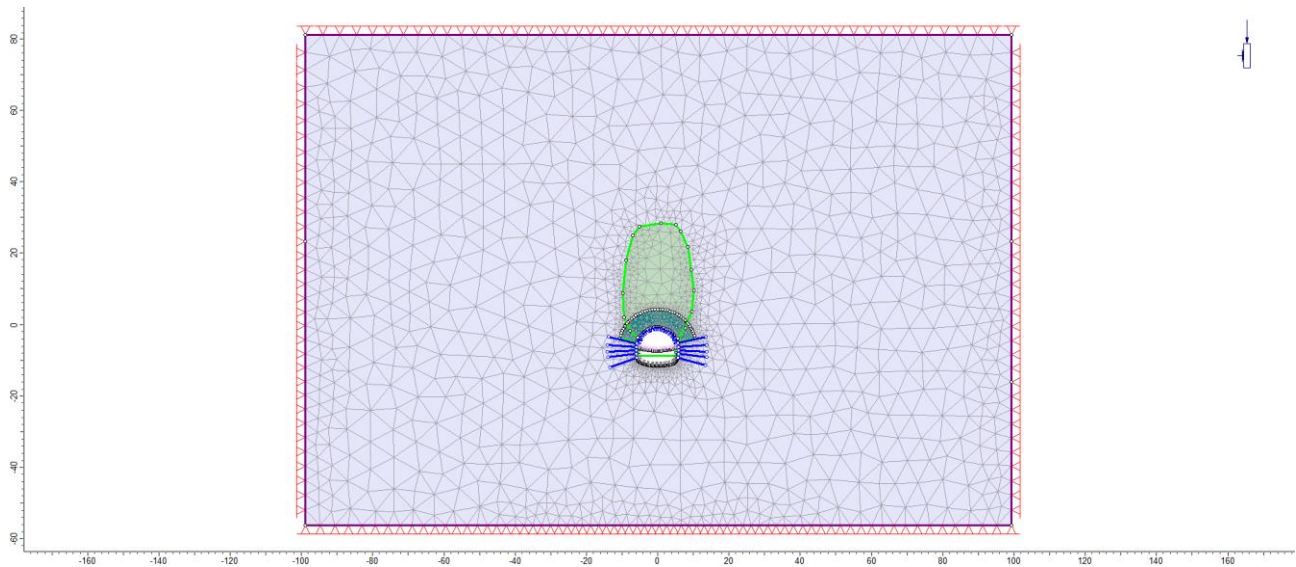


**Figure 2. Phase2d model**

In order to re-excavate the collapsed tunnel section, the collapsed zone was improved with injection. For this purpose, the tunnel face was fully improved by injection with IBO bolts having 1.5x1.5 m pattern, then the tunnel excavation was started again. During the tunnel excavation, two layers of umbrellas were used to strengthen the ceiling stability and collapsed area. The umbrellas are 9 m long, 3.5” in diameter with 4.5 m overlap. The first layer umbrella was installed approximately 5-6 degrees above the steel ribs, while the second-layer umbrella was installed with a 15 to 20 degree angle in order to fill the gap on the tunnel. The tunnel collapsed zone was excavated successfully with the new support systems. Within the scope of this study, improvement methods of the displaced material emerged because of the collapse and determination of appropriate support system are explained and discussed.

## Predicting uniaxial compressive strength of evaporitic rocks from Abu Dhabi, United Arab Emirates-Phase I with unit weight values

Hasan Arman<sup>1</sup>, Osman Abdelghany<sup>2</sup>, Ala Aldahan<sup>3</sup>

<sup>1</sup>United Arab Emirates University, Geology Department, United Arab Emirates, [harman@uaeu.ac.ae](mailto:harman@uaeu.ac.ae)

<sup>2</sup>United Arab Emirates University, Geology Department, United Arab Emirates,  
[osman.abdelghany@uaeu.ac.ae](mailto:osman.abdelghany@uaeu.ac.ae)

<sup>3</sup>United Arab Emirates University, Geology Department, United Arab Emirates, [aaldahan@uaeu.ac.ae](mailto:aaldahan@uaeu.ac.ae)

Precise estimating uniaxial compressive strength (UCS) of rock material is an essential concern in engineering practices in or on rock material. Such an attempt requires concentrated field and laboratory work of rock sampling, test sample preparation, test results reporting etc. All works must be done according to one of the commonly recognized standards, which are the International Society of Rock Mechanics (ISRM) and the American Society for Testing Material (ASTM). In addition, the UCS test takes substantial time, requires carefully sample handling and testing process, and of course is one of the expensive test in rock engineering applications. Moreover, different physical characteristics of rock material like rock type, density, porosity, grain size, water content etc. has significant influences on rock material UCS. In fact, the UCS of rock material can be effectively predicted through simple, hand, inexpensive density tests, then calculated natural ( $\gamma_n$ ), dry ( $\gamma_d$ ), and saturated ( $\gamma_s$ ) unit weight of rock material.

This study was mainly focused on evaporitic rocks, which are mostly available in Arabian Peninsula, occur at the surface or at depth about 10 m and may be found in foundations of buildings and infrastructure levels. Despite the common occurrence of evaporitic rocks in Abu Dhabi city and surroundings, no published data are available for evaporitic rocks properties of Abu Dhabi city and even the United Arab Emirates(UAE) in general. Due to the variable textures, structures and chemical composition of the evaporitic rocks, changes in the surrounding conditions because of watering and dewatering can change their properties. The first phase of study, Phase I, was carried out on representative eight-seven rock blocks, which were collected from various locations of Abu Dhabi city and its surrounding areas (Figure. 1) (Geological Map of Abu Dhabi, 2006).

In addition, the textural and compositional features of selected rock samples were characterized through a polarized light microscope, scanning electron microscope (SEM), X-ray fluorescence (XRF) and X-ray diffraction (XRD). In general, gypsum crystals were found in many forms of mega-meso – microcrystalline. Their texture varied from xenotopic to idiotopic, but usually poikilotopic and porphyrotopic textures are clear. In few cases, it was observed that anhydrite was replacing gypsum. The, the relationships between UCS and  $\gamma_n$ ,  $\gamma_d$  and  $\gamma_s$  were intensively investigated in term of number of experimental work of one hundred fourth-four UCS tests, about five hundred fifty  $\gamma_n$  tests, around two hundred fifty  $\gamma_d$  and  $\gamma_s$  tests on core samples. The correlation coefficient values (R) ranging 0.64-0.75 indicate that there is strong relationships between UCS and  $\gamma_n$ ,  $\gamma_d$  and  $\gamma_s$  for the evaporitic rocks (Figure 2). These results provide better understanding of the evaporites especially in preliminary design stage in the study area and elsewhere, and it will help to reduce expenses associated with engineering problems in evaporites terrain.



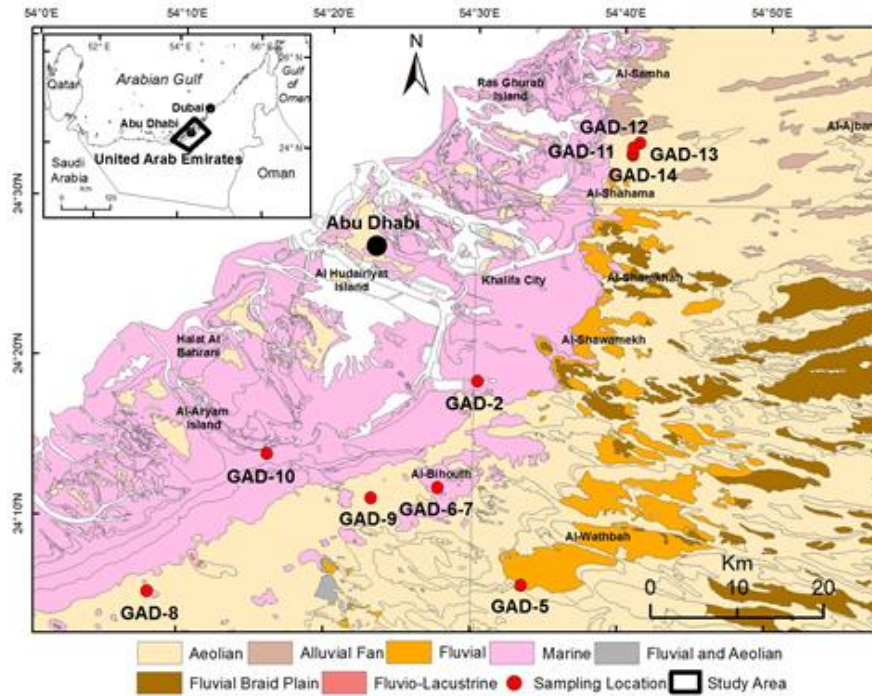


Figure 1. Map of the study and sampling locations (modified from Geological Map of Abu Dhabi, 2006).

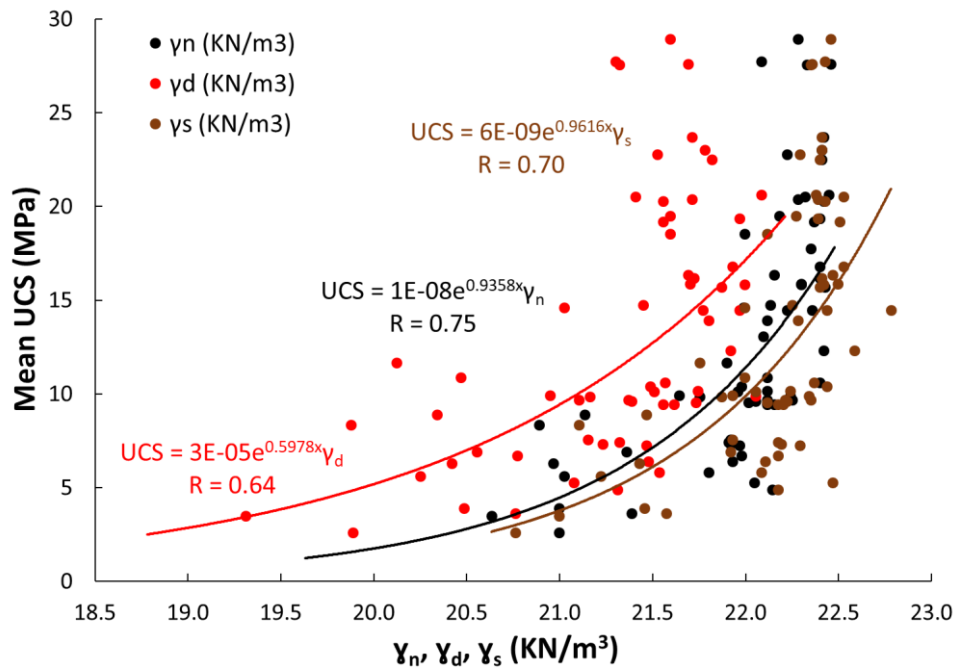


Figure 2. Mean UCS versus  $\gamma_n$ ,  $\gamma_d$  and  $\gamma_s$ .

REFERENCE

Geological Map of Abu Dhabi, 2006. Digital Map, 1:100 000, United Arab Emirates, United Arab Emirates Ministry of Energy, Department of Geology and Mineral Resources.





## Some empirical equations for estimating grout take amount: A case study from Turkey

Ali Kayabasi<sup>1</sup>, Candan Gokceoglu<sup>2</sup>

<sup>1</sup>Eskişehir Osmangazi University, Turkey, [akayabasi@ogu.edu.tr](mailto:akayabasi@ogu.edu.tr)

<sup>2</sup>Hacettepe University, Turkey, [cgokce@hacettepe.edu.tr](mailto:cgokce@hacettepe.edu.tr)

Grouting is widely used method to prevent water leakage from reservoirs. Grouting is very expensive process and hence engineer needs to make pilot grouting before constructing stage of projects. Equilateral angle type pilot grouting is commonly performed at dam sites to estimate grouting amount. The Lugeon tests after and before grouting is correlated. In the present study, permeability of lithologies outcropping at Mut dam site was studied with a pilot grouting. Seven boreholes were opened. RQD, Q system classification, GSI, joint spacing, joint aperture, the secondary permeability index (SPI) and permeability of lithologies were determined in pilot grouting. The dam site that the focus of this study is located near the Derinçay village of Mut district of Mersin city. Mut district locates at 178 km north of Mersin city. Derinçay village locates at 18 km northwest of the Mut district. Mut dam is at the 8 km northwest of the Derinçay village. The generalized description and the depth of the units drilled at boreholes could be summarized as: 0.00-16.00 m Slope debris, 16.00-72.50 m Karstic limestone (Belveren limestone block), 72.50-147.45m Sandstone-siltstone-claystone alternations (Derinçay Formation), 147.45-170.00 m clayey limestone (Fakırca Formation).

Total injected material was 669321 kg during pilot grouting. Majority of solid material was injected in karstified limestone block levels. 90.72 % of (607230 kg) total injected material was injected in karstified limestone. The solid material injection was increased at the depth between 25.00 and 60.00 m depth. 558799 kg solid material was injected between 25.00 m and 60.00 m depth. The depth of karstic limestone block grouting was not achieved even though 84.49 % of the total injected solid material injected between 25.00 m and 60.00 m depth of the karstic limestone block. Karstic limestone block is permeable due to karstification and heavy discontinuities. The impermeability of discontinuities could be provided by injecting 650-700 kg/m solid material per meter, but the impermeability of karstified zones weren't achieved with respect to 15966 kg/m solid material injection between the depth of 25.00 m and 60.00 m karstic limestone block. Average values of rock mass properties of karstic limestone block Q value, rock quality designation (RQD), geologic strength index (GSI), Joint spacing (JSP), joint aperture (Ap), lugeon (Lu), secondary permeability index (SPI), permeability constant (k) and average grout take (Gt) were calculated. Gt and average values of RQD, Q, GSI, JSP, Ap, Lu, and SPI were correlated with simple regression analyses. Equations 1–8 are the derived empirical equations from simple regression analyses (Table 1) while Q class, GSI, RQD, Lugeon, SPI, and aperture were used as input parameters for multiple nonlinear regression analysis. Derived equations are given in Table 2.

**Table 1 The values of the root mean square errors (RMSE), values account for (VAF) and mean absolute percentage error (MAPE) estimated grout take.**

Eq.No	Empirical equations	R <sup>2</sup>	RMSE	VAF	MAPE
1	$Gt(\text{prdct})=14690e^{-0.046RQD}$	0.72	1.93	41.19	37.31
2	$Gt(\text{prdct})=-1984\ln(Q)+1107.3$	0.64	1.51	64.04	65.12
3	$Gt(\text{prdct})=309291e^{-0.116GSI}$	0.36	2.48	5.96	69.36
4	$Gt(\text{prdct})=5 \times 10^6 JSP^{-1.784}$	0.78	1.48	65.62	34.92
5	$Gt(\text{prdct})=5 \times 10^6 Ap^{1.772}$	0.69	1.71	56.10	38.55
6	$Gt(\text{prdct})=658.71(Lu)-8959.9$	0.63	1.53	63.02	63,23
7	$Gt(\text{prdct})=5030\ln(SPI)-1880.7$	0.85	0.97	85.08	42,66
8	$Gt(\text{prdct})=541907k^{1.576}$	0.63	1.77	50.17	45.93



**Table 2 The values of the root mean square errors (RMSE), values account for (VAF) and mean absolute percentage error (MAPE) estimated grout take.**

Eq.No	Empirical equations	R <sup>2</sup>	RMSE	VAF	MAPE
12	Gt(prdct)=1078LN(Q)+448(Lu)-2576	0.755	1,24	75,50	33,76
13	Gt(prdct)=-596,283LN(Q)+446.607(Lu)-97920.747(Ap)-1653.2	0.773	1,14	79,32	29,63
14	Gt(prdct)=216LN(Q)+5429LN(SPI)+159712	0.853	0,96	85,29	45,99
15	Gt(prdct)=-163LN(Q)+5492LN(SPI)+(15405Ap)+161333)	0.853	0,10	85,17	37,41
16	Gt(prdct)=5693.334LN(GSI)+557.859Lu-27546.85	0.686	1,41	68,63	58,36
17	Gt(prdct)=886.849LN(GSI)+497.875Lu-180552.328(Ap)+898.436	0.758	1,19	77,58	35,84
18	Gt(prdct)=-2572.757LN(GSI)+5483.395LN(SPI)+171007.586	0.858	0,94	85,83	41,14
19	Gt(prdct)=-2688LN(GSI)+5452LN(SPI)-(4918Ap)+170643.231	0.858	0,94	86,04	41,21
20	Gt(prdct)=1931.584LN(RQD)+409.128(Lu)-10077.57	0.755	1,24	75,51	42,51
21	Gt(prdct)=1001.774LN(RQD)+436.383(Lu)-94995.23(Ap)-5876.032	0.797	1,17	78,18	36,51
22	Gt(prdct)=-937.386LN(RQD)+6132.818LN(SPI)+183306.319	0.861	0,94	86,06	45,58
23	Gt(prdct)=-1164.606LN(RQD)+6139.639LN(SPI)-25131.793(Ap)+184701.957	0.871	0,90	87,09	43,94

Prediction performance of the empirical equations derived in this study are mainly satisfactory. Even so, all empirical equations rely on the number and quality of the data used. Hence, for design purposes, the empirical equations should be controlled. This study must also be supported by another studies because the main result obtained from the study is that the empirical equations for Gt predictions have serious uncertainties. Especially, karstic environments are extremely complex, and it is too difficult to predict the amount of Gt from the rock mass parameters. For this reason, the empirical equations for Gt prediction is open to discussion. However, this study is an example for investigation of karstic limestone rock masses and the estimation of amount of grout material from rock mass properties. Estimation of amount of grout material is extremely important for dam construction because the amount of grout material directly affects the feasibility of dams.

## Engineering Geological Assessment of the Louziki dam site suitability, Chalkidiki, Greece

Antriana Gkorani<sup>1</sup>, Thomas Makedon<sup>1</sup>, Vassilis Marinos<sup>1</sup>, Vasileios Christaras<sup>1</sup>

<sup>1</sup>Department of Geology, Aristotle University of Thessaloniki, 54124, Thessaloniki, Greece,  
[andrianagorani@hotmail.com](mailto:andrianagorani@hotmail.com), [thomas@geo.auth.gr](mailto:thomas@geo.auth.gr), [marinosv@geo.auth.gr](mailto:marinosv@geo.auth.gr), [christar@geo.auth.gr](mailto:christar@geo.auth.gr)

Dams constitute major construction projects for the accumulation of water for various purposes. The construction of a dam demands meticulous and thorough investigation, since it constitutes a multi-factor discipline, aiming to the safe and efficient construction. A dam site suitability investigation includes hydrological, geological and engineering geological investigation in the dam and reservoir area.

Louziki dam site is in Chalkidiki peninsula and more specifically on Vatonias (Olynthios) river. It is an earth fill dam with a design height of 72 m, crest length 210 m and crest width 10 m. The main supplementary structures for the dam are the spillway, the diversion tunnel and the coffer dam.

The geological bedrock of the area consists of metamorphic rock alternations, of Lower-Middle Jurassic age, comprising the "Svoula flysch formation", (Mountrakis D., 2010), as well as Neogene and Quaternary sediments encountered close to the riverbed.

For the assessment of the engineering geological conditions, several index and mechanical properties were considered, namely RQD, GSI, degree of weathering, rock mass permeability and intact rock compressive strength. These parameters were introduced in the definition of engineering geological units to further estimate the rock mass behavior. The estimation of the rock mass behavior includes slope stability via kinematic analysis, evaluation of strength and deformability as well as groundwater and piezometric data.

The uncertainties relating to the suitability of the dam site are associated with the heterogeneity and erodibility of the formations, the presence of faults, the tectonic disturbance of the rock-mass and the estimated water losses.

The site assessment is summarized in the conceptual model shown in Figure1. In the foundation zone of the dam, stability problems can arise due to the heterogeneous formations, the erodibility of graphitic schist and the water pressure conditions. The right abutment is not expected to present stability problems, but wedge failures may occur in the left abutment. Based on the in-situ permeability tests in the area of the dam axis no significant leakages are expected, hence the depth of the grout curtain is evaluated to be close to the surface. In the reservoir area two landslides were identified, one of them in a close distance from the dam's axis (500m), as well as some rockfalls phenomena (wedge failures). In respect to the water losses, the presence of conglomerates at the northern limit of the reservoir poses a hazard. The earthfill dam appears as the optimal option based on the weak nature of the rock masses and the heterogeneity of the foundation's formations.

### REFERENCES

Geotechnologiki T.S.A., Mixalopoulou K., Spiliopoulos K. Geotechnical investigation and presentation of results of Olynthios dam (Louziki site), complementary investigation of projects regarding the utilization of water resources in Chalkidiki - Olynthios dam, 2008.

ISRM Rock characterization, testing and monitoring. In: Brown ET (ed) ISRM suggested methods. Pergamon Press, Oxford, p 211, 1981.

Marinos V (2017) A revised, geotechnical classification GSI system for tectonically disturbed heterogeneous rock masses, such as flysch, Bulletin of Engineering Geology and the Environment, <https://doi.org/10.1007/s10064-017-1151-z>.

Mountrakis D.: Geology and geotectonic evolution of Greece. University Studio Press, Thessaloniki (2010).

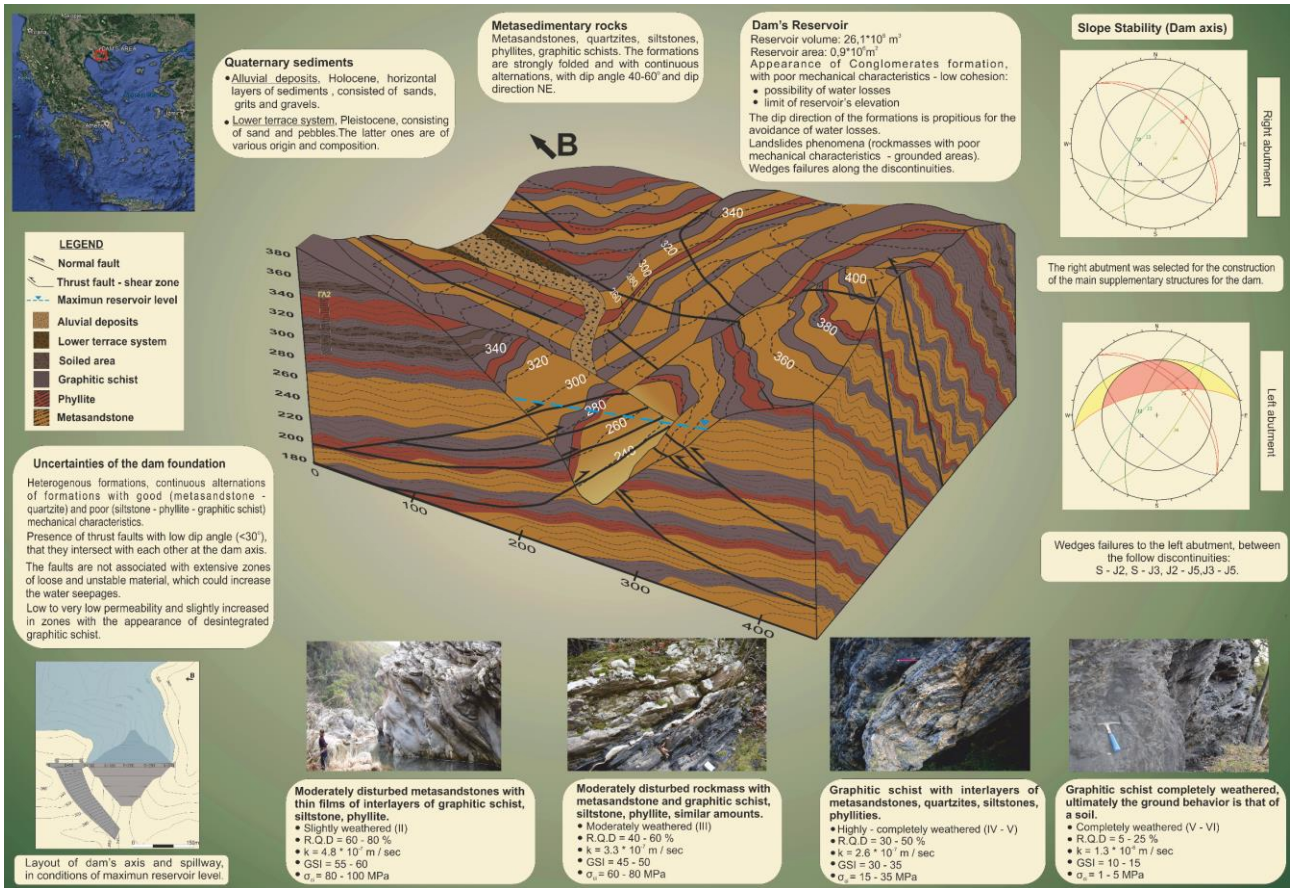


Figure 1. Engineering geological conceptual model of Louziki Dam, Northern Greece.

## Site evaluation for the tunneling with an approach of engineering Geomorphology in Nepal

Ranjan Kumar Dahal<sup>1</sup>, Manita Timilsina<sup>2</sup>, Shuichi Hasegawa<sup>3</sup>

<sup>1</sup>Central Department of Geology, Tribhuvan University, Kirtipur, Kathmandu, Nepal, [rkdahal@gmail.com](mailto:rkdahal@gmail.com)

<sup>2</sup>Geotech Solutions International Pvt. Ltd., Kalika Marga, Sanepa, Lalitpur, Nepal,  
[manitatimilsina@gmail.com](mailto:manitatimilsina@gmail.com)

<sup>3</sup>Faculty of Engineering and Design, Kagawa University, Hayashi Cho, Takamatsu, Kagawa, Japan,  
[hasegawa@eng.kagawa-u.ac.jp](mailto:hasegawa@eng.kagawa-u.ac.jp)

### **Background**

Geomorphological evaluation of engineering project sites is a recently developed science and it is called engineering geomorphology. Many construction projects in mountainous regions need a comprehensive evaluation of geomorphological evolution of site to understand possible engineering geological issues of soil and rock inside the mountain. In mountainous region, role played by the Deep-seated Gravitational Slope Deformations (DGSD) for the evolution of relief and hillock are fundamental issues of engineering geomorphology and they have been well pointed out by several authors who analysed typology and distribution of deep-seated slope deformations in different geological and geomorphological conditions since 1930s. Being a geologically young and active Himalayan belt, the Nepal Himalaya is also having similar issues where deep-seated slope deformations have been favoured by the noteworthy relief, the complex geological structure, seismic activities, and the frequency of extreme rainfall. Deep-seated gravitational slope deformations and related large-scale landslides are complex phenomena taking place through a wide variety of mechanisms whose genesis and evolution are controlled by several factors, among which structure, relief, and tectonic and seismic activities have a particular importance. The deep-seated slope deformations related large-scale landslides have typical morphological elements which help to recognize them in topographical maps and satellite images along with field data.

### **Method**

Observations of various hydropower tunnel construction sites in Nepal have been done to evaluate relation of DSGDs. Detail mappings of the selected tunnels have been done to understand the DGGDs. Rock mass analysis of topography around the tunnel sites is also evaluated. Few sites having hummocky mountain slope was also mapped to characterize rock mass in the slope.

### **Conclusion**

The surface extension of deformation is generally more than 1 square km with thickness of deformed mass ranges around several tens to hundreds of meters. These deformations related large-scale landslides lack a continuous slip or shear surface delimiting the deformed mass. The rate of movement of deformation is very slow, happening in past geologic times with long periods of inactivity. But sometimes they might be active after a consequence of earthquakes or extreme rainfall. In many cases, the deformational mechanism is continuous creep, with accelerations and creep ruptures. The deformed slopes are often involved in many shallow-seated landslides and have less drainage density. Many shear zones and highly jointed rock masses along with extreme groundwater flow encountered during tunnelling are typical signs of deep-seated slope deformations. In Nepal, site investigations for tunnel do not comply engineering geomorphology and they are limited to rock mass characterization along with geological and engineering geological mapping only. Engineering





geomorphological evaluation of tunnelling site before the project commencement can help to reduce project cost and unnecessary delay of the projects using a blaming phrase: “the Geological Issues”. Nepal is now working with not only hydropower tunnels, but road and railway tunnels also. Therefore, this paper highlights the importance of engineering geomorphological evaluation of tunnel project site emphasizing DSGDs in Nepal with few examples

## Rock mass excavatability assessment in tunnelling based on GSI. The case of Tempi tunnels in Greece

Athina Tsirogianni<sup>1</sup>, Charalampos Saroglou<sup>2</sup>

<sup>1</sup>Civil Engineer M.Sc., [athinatsiro@hotmail.com](mailto:athinatsiro@hotmail.com)

<sup>2</sup>Geotechnical Engineering Department, School of Civil Engineering, National Technical University of Athens, Greece, [saroglou@central.ntua.gr](mailto:saroglou@central.ntua.gr)

The aim of this paper is to propose an excavatability classification method tailored to conventional tunnelling, based on the Geological Strength Index (GSI) classification.

The case study area involves the Tempi tunnels, which are three twin tunnels across Maliakos-Kleidi section of the Patras-Athens-Thessaloniki-Evzonoï (PATHE) highway, in the Tempi-Platamonas area. The tunnels were excavated through mica-amphibole schists, amphibolites-amphibole schists, prasinites, crystalline limestones-marbles, phyllites and serpentized peridotites. The excavation methods applied were mechanical means, blasting, and combined use of the above, that is, blasting over 80% of the tunnel section and completing excavation with mechanical means.

A total of 1681 tunnel face mapping logs were examined and a database was then formed where certain data as recorded at the tunnel face were stored, including lithologic description, GSI, overburden depth, spacing of the main joint set and the applied excavation method. Moreover, 22 boreholes were taken into account with the associated laboratory data. In order to allow for the effect of intact rock strength on the selection of the appropriate excavation method, the intact point load strength,  $I_s(50)$ , and the uniaxial compressive strength of intact rock,  $\sigma_{ci}$ , for a given rock type were correlated with GSI and the applied excavation method.

Representative rock masses from all the encountered geological formations were projected in the GSI chart (Marinos & Hoek, 2000) in the form of data points referring to the relevant applied excavation method. According to the scatter plot and co-estimating the overall findings of the study, the GSI chart was divided into three distinct zones, each representing the range of application of a specific excavation method: mechanical means, blasting and combined use of these two methods. According to the proposed excavatability classification, the following conclusions can be drawn:

- Mechanical means can be used for rock masses with very blocky to laminated/sheared structure classified with  $GSI \leq 35$ .
- Blasting in combination with mechanical means (combined method) is required for the following cases:
  - a) rock masses with blocky/disturbed/seamy to disintegrated structure classified within the range  $35 \leq GSI < 65$
  - b) rock masses with very blocky structure rated within the range  $35 \leq GSI \leq 50$  and
  - c) rock masses with blocky structure classified with  $GSI \leq 50$ .
- Blasting is the only feasible excavation method for rock masses with an intact/massive to very blocky structure classified with  $GSI \geq 50$ .



## Geotechnical Block Model (GBM) of Olympias Mine Using Q Classification System

N. Grendas<sup>1</sup>, E. Vagkli<sup>2</sup>, M. Yumlu<sup>3</sup>, G. Gkekas<sup>4</sup>, D. Bogas<sup>5</sup>

<sup>1</sup>Hellas Gold S.A. (Eldoradogold S.A. Subsidiary), Olympiada, Greece,

[Nikolaos.Grendas@gr.eldoradogold.com](mailto:Nikolaos.Grendas@gr.eldoradogold.com)

<sup>2</sup>Hellas Gold S.A. (Eldoradogold S.A. Subsidiary), Olympiada, Greece,

[eleutheria.vagli@gr.eldoradogold.com](mailto:eleutheria.vagli@gr.eldoradogold.com)

<sup>3</sup>Backfill Geotechnical Mining Consultants Pty Ltd, PO BOX 296, Balwyn North, VIC 3104, Australia,

[myumlu@bgmconsultants.com.au](mailto:myumlu@bgmconsultants.com.au)

<sup>4</sup>Hellas Gold S.A. (Eldoradogold S.A. Subsidiary), Olympiada, Greece,

[Georgios.Gkekas@gr.eldoradogold.com](mailto:Georgios.Gkekas@gr.eldoradogold.com)

<sup>5</sup>Hellas Gold S.A. (Eldoradogold S.A. Subsidiary), Olympiada, Greece,

[Dimitris.Bogas@gr.eldoradogold.com](mailto:Dimitris.Bogas@gr.eldoradogold.com)

### **Background**

Core of the current project consists Olympias Mine's internal desire to apply interpreted Geotechnical Data on the current and future Mine's design. Gathering of Geotechnical data initiated from early 2015 and constitutes daily routine for Mine Production Geologists. Q (Barton et al., 1974) and RMR (Beniawski, 1989) are the foundational systems based on which, collection of the geotechnical data occurred. Subsequently to gathering and interpreting of Geotechnical Data, construction of a Geotechnical Block Model (GBM) followed, with intention of qualitative and quantitative application of the geotechnical interpretation.

### **Methods**

Crucial factors for GBM's construction possess vital role for its final model structure. The major three factors are as followed: a) Estimation method for Block Modelling, b) Composed geotechnical domains' length derived from borehole logging and c) The size of each block. Nearest Neighbor (NN) is the estimation method used for the current GBM and is described as a non-spatial statistical method in global literature (Sankey et al, 2017). Nevertheless, utilizing descriptive statistics builds an efficient 3D trend model for data representation (Coombes, 2008). Decision on compositing lengths for geotechnical domains was built upon mean values' ( $\mu$ ), standard deviation's (SD) and coefficient's of variation (CV) comparison, for composite lengths of 1 up to 5 meters. The referred comparison stated that composite lengths above 3m produce significant decrease of CV whereas  $\mu$  and SD increased. Conclusively, 1m composite length resulted from the above comparison. Regarding the block size, this should not be smaller than the half the drill spacing of the ore body (Coombes, 2008). Based on Olympias designed and actual drilling space grid, a minimum of 3(m)x3(m)x3(m) (m<sup>3</sup>) block size was applied, with intention the block size to be aligned with the above mentioned rule of thumb. Leapfrog Edge (Seequent) consists the Software for GBM's entire estimation process.

### **Results**

The area of coverage for Geotechnical Block Model (GBM), extends in a future designed mining zone, with an elevation buffer of 10 m above and below the zone (Figure 1). For GBM's validation purposes two methods were applied. Visual validation and validation via Swath Plots. Visual validation was achieved through cross and plan sections which indicated an efficient distribution of block values compared to the actual ones. Swath plot comprises a common validation process for block models while their analysis could prevent over and under estimation

regarding the actual values. For Olympias GBM, swath plots verify an acceptable produced model based on the factors used for the estimation (Figure 2).

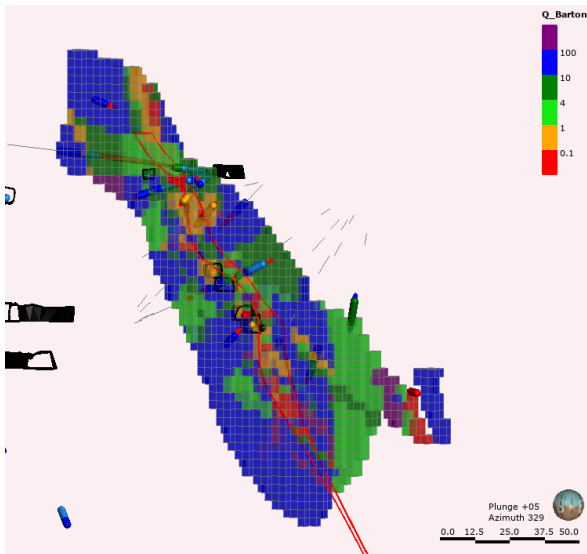


**Figure 1. Cross section (W-E) that presents the block model with Q (Barton, 1974) classification. The major fault (red line) has a good correlation with the low quality rock mass (red-orange blocks). The tunnels are presented with black color.**

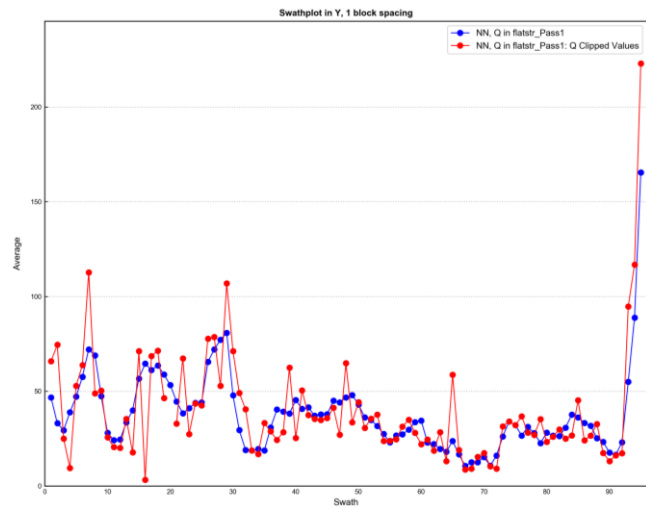


**Figure 2. Block model validation with Swath plots. The red line presents the actual Q values in every section and the blue line presents the Q values produced by the Nearest Neighbor estimation. The estimated values are as they expected: Inside actual values and smoother.**

## Conclusion

It is important to underline that the present geotechnical block model was not formed to predict ground failure hazards inside the mine. Fall of grounds is a combination of a variety of factors –such as opening size, blast rounds, support time and type, unexpected water inflow– including geotechnical rockmass quality description i.e. Q-system. The major role for block model is to predict low quality rock mass in future mined areas and achieve proactive measures for ground support prior to blasting. Fall of grounds –from Mine’s current experience–, is correlated with ore production stopes, causes valuable time waste and financial loss. As a matter of fact, a combination of pre-defined support classes via geotechnical block model and in situ decision when the blasting happens, is the key to sustainable life of mine.

## **REFERENCES**

- Barton, N., R. Lien and J. Lunde, 1974, Engineering classification of rock masses for the design of tunnel support. *Rock Mechanics and Rock Engineering* 6(4) , pp. 189-236.
- Bieniawski, Z.T., 1989. *Engineering rock mass classifications*. New York: Wiley
- Coombes J., 2008, *The art and science of resource estimation*. Coombes Capability, PO Box 1708, Subiaco, W.A., Australia, 6904. ISBN: 9780980490800
- Sankey T. ,2017, *Statistical Descriptions of Spatial Patterns*. In: Shekhar S., Xiong H., Zhou X. (eds) *Encyclopedia of GIS*. Springer, Cham

## A study of biocementation implementation methods for embankment foundation soil

Muhammad U. Safdar<sup>1</sup>, Maria Mavroulidou<sup>1\*</sup>, Mike J. Gunn<sup>1</sup>, D. Purchase<sup>2</sup>, Ian Payne<sup>3</sup>, Jonathan Garelick<sup>3</sup>

<sup>1</sup>London South Bank University, UK, [mavroum@lsbu.ac.uk](mailto:mavroum@lsbu.ac.uk) (corresponding author)

<sup>2</sup>School of Natural Sciences, Faculty of Science and Technology, Middlesex University, UK

<sup>3</sup>Network Rail, UK

Due to the growing urbanisation and the scarcity of urban space, new infrastructure works in urbanised areas will be increasingly constructed on inferior ground i.e. weak natural on man-made geomaterials (e.g. in waste disposal sites) with increased hazards and impacts of catastrophic failures. Existing infrastructure facilities will also need to be upgraded to meet future needs and changing environmental loads due to climate change. These include ageing transport earthworks in many European countries suffering from serviceability problems and requiring costly maintenance/remediation. Current policies require infrastructure to be provided in an economical and environmentally responsible manner (reducing material use, embedded carbon and other impacts on the natural environment and ecosystems). Improving rather than replacing and landfilling inferior ground or geomaterials (including wastes) for civil infrastructure uses, will thus become critically important in future engineering practice towards low-carbon, sustainable solutions. In line with this, an emerging ground improvement technique, which has recently attracted the interest of researchers worldwide, is soil biocementation. It utilises the natural biological process of biomineralisation (the biological production of minerals through the metabolic processes of different types of microorganisms/ plants) as a soil stabilisation method. The technique was claimed to be environmentally superior to conventional grouts or other common soil stabilisers e.g. cement or lime (linked to high CO<sub>2</sub> emissions) and potentially more sustainable overall, since the non-pathogenic micro-organisms used are natural, readily available and renewable (DeJong et al, 2013). A major challenge is however finding suitable ways to implement treatments under existing infrastructure, as pressure injection can often lead to non-uniform mineral precipitation.

Recent work funded by Network Rail (under research contract NR-ANG-00164), proved biocementation of a problematic organic foundation soil of UK railway embankments, using non-pathogenic, indigenous ureolytic bacterial strains extracted from the *in situ* soil (Mavroulidou et al, 2019; Safdar et al, 2020). This paper focuses on the effect of different treatment implementation techniques in successfully biocementing the soil.

The soil used in this study came from two boreholes at an East Anglian railway site. It was dark grayish brown, had a 50.8% organic matter content, 55.5% natural water content (consistent with a humified/decomposed organic soil), quasi-neutral pH (7.15) and Liquid Limit and Plastic Limit of 101% and 63% respectively. The soil was identified as amorphous peat. Following a microbiological study (Safdar et al, 2020) four ureolytic indigenous strains were identified as possible candidates for biocementation of the soil, through microbially induced calcite precipitation, of which *Bacillus licheniformis* performed the best for the bacterial populations and cementing agent solution concentrations studied. Five different treatment implementation methods were used, i.e. biostimulation (with nutrients added in the soil to stimulate native micro-organism growth) and four bioaugmentation methods (i.e. supplying precultured microorganisms into the soil to enhance favourable microorganism populations, here *Bacillus licheniformis*). These were (a) mixing with soil of both the nutrients+bacteria solution and the cementing agent solution (urea and calcium chloride); (b) implementation of cementing solution through a flow column under light pressure (nutrients+bacteria were premixed in the soil); (c) Electrokinetic (EK) injection of cementing agents with nutrients+bacteria premixed in the soil; (d) full treatment injected electrokinetically (i.e. nutrients+bacteria and





cementing agents). Bacteria were initially premixed to prove biocementation for this soil, circumventing bacteria delivery complications. Mixing is however unfeasible under existing infrastructure unless deep mixing is used.

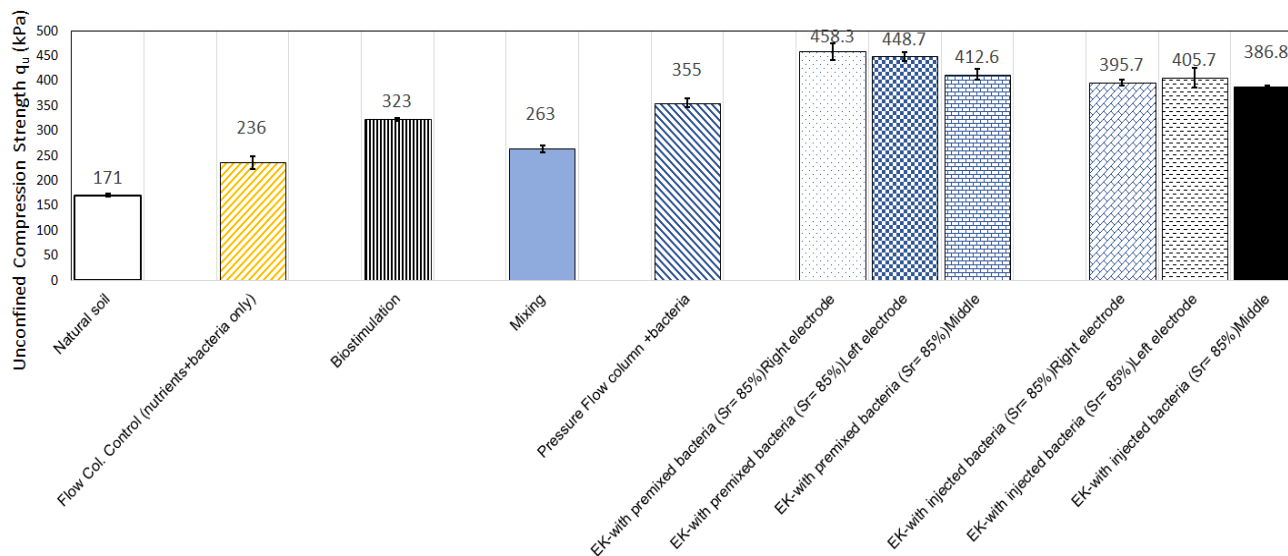


Figure 1. Indicative results

From Figure 1 it can be seen that EK injection (with polarity reversal) was the most successful implementation method; the method was proven for degrees of saturation  $S_r=75-95\%$  with the latter giving the best results (not shown here for brevity). Implementation in wetter periods of the year would therefore be recommended for better success of the treatment. Consistently, the highest  $\text{CaCO}_3$  contents in the soil (not shown here) were detected for the EK method. Pressure flow did lead to strength improvement (and increased  $\text{CaCO}_3$  contents) but to a lesser extent than EK, whilst mixing was not successful. There was obviously a combined effect of biocementation and electrokinetics (which is an improvement method per se) as EK control samples (not shown here) had higher strengths than the respective pressure flow ones; however  $\text{CaCO}_3$  contents and increased strengths compared to EK control when bacteria were used in the EK tests, support the conclusion that the strength increase was due to biocementation. Whilst treatment non-uniformity (when bacteria were injected rather than premixed) still needs to be addressed, there is promise that EK could be a viable technique for treating foundation soil under existing infrastructure, which is a major challenge for engineers.

REFERENCES

DeJong J. T., Soga K., Kavazanjian E. et al., 2013, Biogeochemical processes and geotechnical applications: progress, opportunities and challenges. *Géotechnique* **63**(4), pp. 287–301

Mavroulidou M., Safdar MU, Gunn MJ, Payne I., Garelick J., Purchase D. ,2019, Innovative methods of ground improvement for problematic transport earthwork materials 16<sup>th</sup> Int. Conference on Environmental Science and Technology CEST2019, Rhodes 4-7 September 2019 Safdar, M.U., Mavroulidou, M., Gunn, M.J. et al, 2020, Innovative methods of ground improvement for railway embankment Peat Fens foundation soil. *Géotechnique* (online eprint) DOI: 10.1680/jgeot.19.sip.030

## **D8 motorway landslide: largest construction accident in recent Czech history**

Jan Blahút<sup>1</sup>, Josef Stemberk<sup>1</sup>, David Mašín<sup>2</sup>, Jan Klimeš<sup>1</sup>, Filip Hartvich<sup>1</sup>, Josef Rott<sup>2</sup>, Jan Balek<sup>1</sup>,  
Petr Tábořík<sup>3</sup>, Michal Kusák<sup>1</sup>

<sup>1</sup>*Department Of Engineering Geology, Institute of Rock Structure and Mechanics, Czech Academy of Sciences, Czechia, [blahut@irsm.cas.cz](mailto:blahut@irsm.cas.cz)*

<sup>2</sup>*Institute of Hydrogeology, Engineering Geology and Applied Geophysics, Faculty of Sciences, Charles University in Prague, Czechia*

<sup>3</sup>*Department of Neotectonics and Thermochronology, Institute of Rock Structure and Mechanics, Czech Academy of Sciences, Czechia*

On 6th June 2013 a considerable landslide with a volume of approximately 500,000 m<sup>3</sup> partially destroyed the construction site of the D8 motorway near Dobkovičky, N Czechia. An extensive analysis made for the Ministry of Transport (Stemberk and Mašín 2016) determined the causes of this landslide. The analysis included field geophysical and hydrogeological surveys, geological-geomorphological mapping, 2D and 3D slope stability modelling and remote sensing analysis. It has been documented that the construction area has been known as landslide-susceptible since 1960s. It is composed of Tertiary basaltic rocks overlying Jurassic claystone rocks, which form very favorable conditions for landslide initiation, as the brittle permeable rocks overlay plastic impermeable strata (Matula and Pašek, 1986).

It has been proved that the landslide started to develop already in summer 2010 when intense rainfall hit the area (with total precipitation reaching 204.3 mm in August, which is more than 1/3 of mean annual precipitation in the area – 550-600 mm) and when the middle part of the slope was already undercut by the motorway construction. As it was later documented by the inclinometric monitoring on the site, the sliding plane started to develop already at that time and the residual strength on the sliding plane started to evolve. Further deterioration of the stability was caused by a large open quarry upslope the area, which allowed the rainfall water infiltrate easily and thus significantly raising the groundwater water level.

Additional overloading of the upper part of the slope by a gravel depot and another intense rainfall in May/June 2013 significantly contributed to the landslide triggering. The resulting landslide was about 500 m long and 200 m wide, and consisted of shallow colluvium (up to 6-8 m deep).

The analysis also showed that despite favorable conditions, the landslide was essentially of anthropogenic origin. A combination of landslide-prone area, without sufficient mitigation and stabilization measures and, importantly, insufficient communication between the construction company, the investor and the owner of the quarry led to a sequence of events, which ended in an inevitable construction accident.

### **REFERENCES**

Matula, M., and Pašek, J., 1986, Regional engineering geology of Czechoslovakia. Prague, SNTL.

Stemberk, J., and Mašín, D. (eds.), 2016, Analysis of the causes of landslide on the D8 motorway near Dobkovičky. Prague, IRSM CAS.

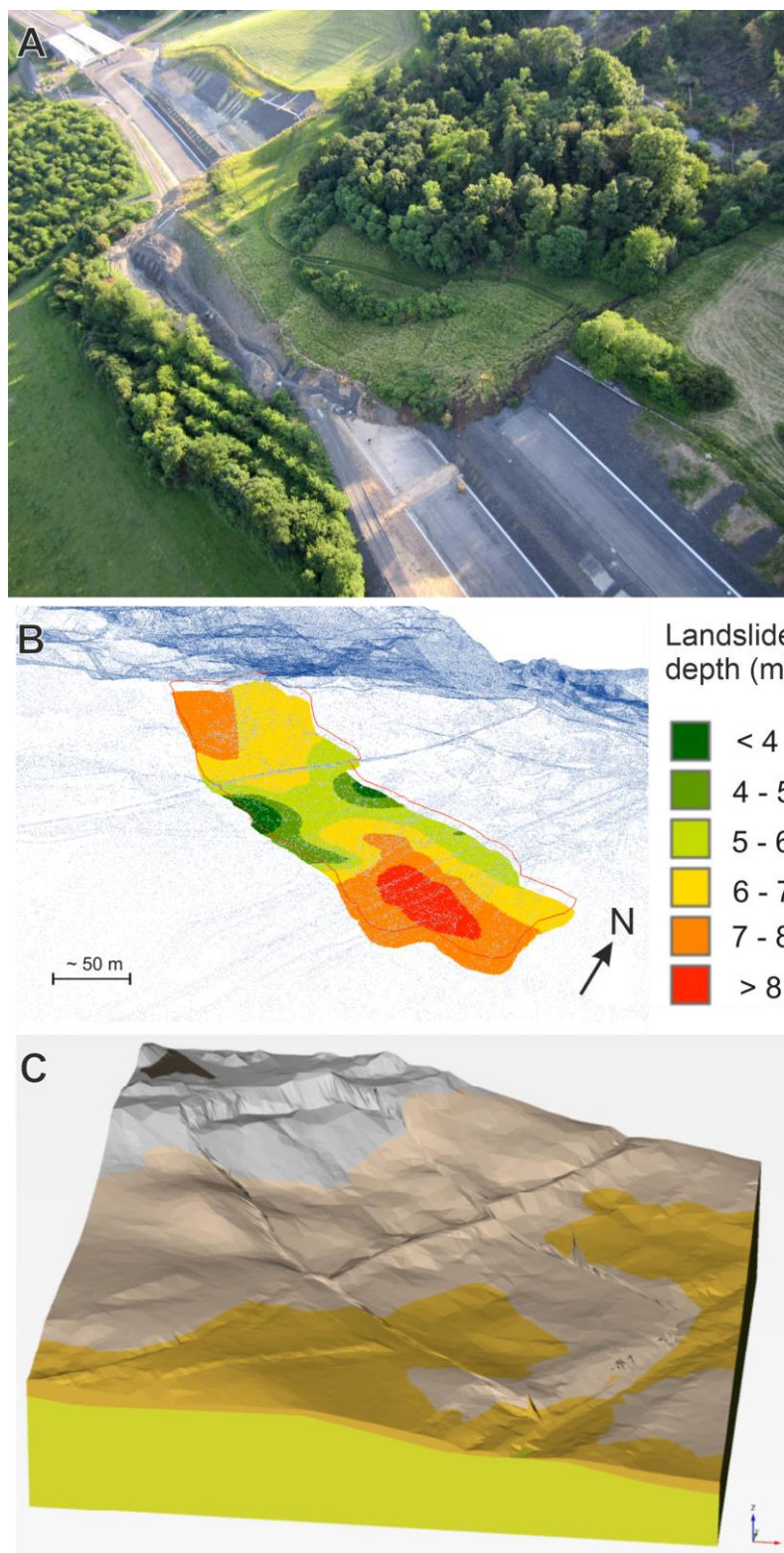


Figure 1. A: Aerial photograph showing the frontal part of the landslide, photo V. Kulić; B: 3D model of the landslide showing the depth of the sliding plane; C: Results of 3D geotechnical modelling in Plaxis software.

## Compactability and permeability of clay-gravel composites: a laboratory evaluation

Yang Lu<sup>1\*,2</sup>, Sihong Liu<sup>1</sup>, Yonggan Zhang<sup>1</sup>

<sup>1</sup>College of Water Conservancy and Hydropower, Hohai University, China, [luy@hhu.edu.cn](mailto:luy@hhu.edu.cn)

<sup>2</sup>Key Laboratory of Ministry of Education for Geomechanics and Embankment Engineering, Hohai University, China

Clay-gravel composite is a geological and engineering material mixed with cohesive clayey soils and coarse granular gravels, which is not only widely distributed in glacial tills, mudflows, landslides and colluvial soil deposits but also usually used for the construction of subgrade filling, landfill cover barrier and core wall of high earth-rockfill dams. Behaviours of compactability and permeability are the two most fundamental aspects of such soil composites from whether practical or academic perspective. In this study, a series of modified Proctor compaction tests were firstly conducted on the clay-gravel composites with different gravel contents ranging from 0% to 90%. The effects of gravel content ( $C_g$ ) on the evaluation of compaction curves, compaction parameters as well as the particle breakage of gravel particles were discussed. A comparison of global void ratio and clay matrix void ratio for the composite soils was also made, and then the inter-relationships between them were explored based on the meso-structural distribution of clay aggregates-gravel particles. Further, composite soils were compacted into cylindrical samples to determine the variation in hydraulic conductivity with gravel content, confining stress and gravel particle size distribution. It is found that: 1) Compaction behaviour of clay-gravel composite changes significantly with  $C_g$ . A peak maximum dry density of the global composites can generally be achieved when  $C_g$  is around 70%, beyond which the dry density decreases considerably. Besides, the fine clay matrix can be compacted to its densest state when the gravel content is below about 30%, beyond which the maximum dry density of the total composite continues to increase while the percent compaction of the clay matrix decreases; 2) Permeability will reach a lowest value for the samples with  $C_g$  of 30%. It can be interpreted from a conceptual perspective of preferential flow paths considering gravel content effects. Due to the effect of the clay bridge, the larger the particle size is, the smaller the permeability coefficient will become; 3) The meso-structural distribution of inner particles inside compacted clay-gravel composites, controlled by gravel content, can be classified into different structures. The permeability, as a good indication of meso-structure in soil composites, is significantly dominated by gravel content as well as the clay matrix void ratio.

### REFERENCES

- Vallejo, L. E., Lobo-Guerrero, S., 2005, The elastic moduli of clays with dispersed oversized particles. *Engineering geology*, v. 78(1-2), pp. 163-171.
- Monkul, M. M., Ozden, G., 2007, Compressional behavior of clayey sand and transition fines content. *Engineering Geology*, v. 89(3-4), pp. 195-205.
- Tarantino, A., De Col, E., 2008, Compaction behaviour of clay. *Géotechnique*, v. 58(3), pp. 199-213.
- Fei, K., 2016, Experimental study of the mechanical behavior of clay-aggregate mixtures. *Engineering geology*, v. 210, 1-9.

## Engineering Geological in-situ Investigation of the Tanahu HPP Powerhouse Cavern, Nepal

M. R. Pokharel<sup>1</sup>, E. Schnäcker<sup>1</sup>

<sup>1</sup>Tractebel Engineering GmbH, Germany, [eckhard.schnaecker@tractebel.engie.com](mailto:eckhard.schnaecker@tractebel.engie.com)

Tanahu Hydropower Project (THPP) is located in Tanahun District of Gandaki Provenance in the Western Region of Nepal. The project site is being developed by Tanahu Hydropower Limited (THL) established for the purpose of construction and operation of the project by Nepal Electricity Authority (NEA), the public power utility of the Government of Nepal. The Tanahu Hydropower Project (THPP) is located on the Seti River, a major tributary of the Trishuli River in the Gandaki Basin in central Nepal. The dam site is located about 2 km upstream of the confluence of the Madi and Seti rivers.

The headworks of the Tanahu HPP include a 140 m high concrete gravity arch dam with a deep grout curtain, a spillway integrated into the dam, an auxiliary dam downstream, two river diversion tunnels and the power intake. From there an approx. 1.39 km long headrace tunnel combined with a 97 m high headrace surge tank and a penstock leads to an underground powerhouse which will accommodate two Francis type turbines with an installed capacity of 140 MW. A 213.77 m long tailrace tunnel then conveys the tail water through the tailrace outlet structure at the right bank into the Seti River again.

Typically, the powerhouse cavern (PHC) is the largest underground opening of a hydropower project. The aim of the investigations was to adapt and optimise the location and orientation of the cavern to the prevailing engineering geological conditions in order to keep the costs for the required rock support to a minimum. From a geological point of view, the project area is situated in the Lesser Himalayan zone. Prevailing slates exposed in test adit AP-2 represent parts of the Benighat Slate presumably of Upper Palaeozoic age. The PH cavern area is planned in moderately strong, thinly foliated slates (UCS: 5 MPa to 80 MPa, average 30 MPa) with minor intercalations of dolomitic and calcareous slates. At places, dolomitic and/or quartz veins with thicknesses in mm- to cm, rarely dm-range are increasingly present. Obviously, the veins utilised the pre-existing foliation striking sub-perpendicular to the cavern axis

With respect to the Tanahu HPP powerhouse cavern, in-situ tests including plate loading tests, direct block shear tests as well as hydraulic fracturing tests were conducted already at an earlier stage of the investigations inside an exploratory adit (AP-1) some 100 m above the initial cavern location. As a result of these tests, the initial powerhouse location was discarded, and the PHC ( $w/h/l = 22/□□54.3/89$ ) was moved some 100 m towards the river to reduce the overburden load.

In order to verify the revised PHC location additional engineering geological in-situ tests were requested inside the new test adit AP-2, excavated directly above the future powerhouse roof. In addition to detailed engineering geological mapping and a discontinuity survey of the AP-2 walls, direct block shear tests as well as drilling of 6 exploratory boreholes was carried out. Various borehole tests such as packer tests (Lugeon methods), flexible dilatometer tests as well as in-situ stress measurements were conducted.

Stress measurements to determine the principle directions and amount of in-situ stress were carried out with the borehole slotter. All borehole walls were inspected and examined by means of a borehole digital optical televiewer (scanner).

The orientation of the discontinuity fabric inside the rock mass controls the kinematic potential of rock blocks in underground openings, and thus its stability. Various discontinuity surveys and analyses conducted inside





test adit AP-2 unveiled the relevant discontinuity fabric of the PH cavern area consisting of three major joint sets. Two of which are forming favourite angles with the AP-2 or PH cavern axis. A third joint set is striking almost parallel to the cavern axis. However, due to the steep dip and its low frequency, this joint set will play a minor role on the cavern stability.

In-situ stress measurements conducted by the borehole slotter under unfavourable rock and rock mass conditions confirmed the in-situ stress state already determined by hydraulic fracturing and DCDA rock core analysis in AP-1. The trend of the principle axis of maximum stress  $\sigma_1$  lies between  $210^\circ$  (NNW – SSE) and  $190^\circ$  (N – S).  $\sigma_1$  is almost horizontal ( $0^\circ$  to  $7^\circ$ ).

In case of the proposed Tanahu PH cavern with a bearing of  $210^\circ$ , the horizontal component of  $\sigma_1$  would act more or less parallel to the long cavern walls which is favourable in terms of the required rock support. However, the smaller walls at the end of the PH cavern would take the entire maximum stress. The actual orientation of the PH cavern axis can be considered as optimum already regarding both discontinuity fabric, as well as primary in-situ stresses. A re-orientation of the cavern alignment is not considered necessary.

## The Effect of the Horizontal-Vertical Stress Ratio on the Deformations at the T3 Tunnel (Çorum, Turkey) Entrance Section

Anıl Atakan<sup>1,2</sup>, Murat Yılmaz<sup>1</sup>, Atiye Tuğrul<sup>1</sup>, Bora Arslan<sup>2</sup>, Cemal Samur<sup>2</sup>

<sup>1</sup>Istanbul University-Cerrahpasa, Geological Engineering Dep, 34500, İstanbul, Turkey

[anil.atakaan@ogr.iuc.edu.tr](mailto:anil.atakaan@ogr.iuc.edu.tr)

<sup>2</sup>ARS Geotechnical Eng. Consultancy LLC, 34752 İstanbul, Turkey, [b.arslan@arsgeo.com](mailto:b.arslan@arsgeo.com)

In this study, the examined tunnel is located in the northern part of Turkey, Çorum province. The project site is placed in a tectonically active region and near to study area, approximately 40 km, the North Anatolian fault (Ketin, 1948) which is right lateral strike-slip characterised and its branches.

The geology of tunnel route is composed of Triassic aged Karakaya formation weak greenschist (Bingöl, 1973; Özcan et al., 1980) and JuraCretaceous aged recrystallized deep-sea Bilecik limestone (Altınlı, 1973; Altıner et al., 1991). High deformation values were determined by convergence measurements in the tunnel at the transition zone of geological units (Figure 1). Within the scope of this study, it is aimed to determine the horizontal-vertical stress ratio ( $K_0$ ), which is thought to cause deformations, by 3D numerical back analysis.



**Figure 1. Appearance of tectonic boundary between the geological units at the tunnel face**

The geotechnical input parameters (Hoek-Brown etc.) were specified according to field observations and laboratory test results of samples which obtained from horizontal-vertical drillings in the scope of field works. Within the context, uniaxial compressive strength's mean value calculated as  $\sigma_{ci} = 40.0$  MPa,  $E_i = 27.0$  GPa for modulus of elasticity,  $\gamma = 28.3$  kN/m<sup>3</sup> for unit weight were determined according to test results, also the suggested material constant ( $m_i$ ) value by Rocdata (v5.009) was used as  $m_i = 12$  for limestone. GSI value was selected 56 for peak parameters, 26 was specified for residual parameters.

All derived rock mass parameters determined with same methodology for greenschist as well. The uniaxial compressive strength's mean value calculated as  $\sigma_{ci} = 15.0$  MPa,  $E_i = 10.0$  GPa for modulus of elasticity,  $\gamma = 27.0$  kN/m<sup>3</sup> for unit weight were determined according to test results, also the suggested material constant ( $m_i$ ) value by Rocdata (v5.009) was used as  $m_i = 9$  for greenschist. GSI value was selected 30 for peak parameters, 20 was specified for residual parameters. Moreover, disturbance factor was taken 0,5 due to conventional

excavation. Rock mass were derived by Rocdata (v5.009) software for 85 meter cover thickness both units (Table 1 ). Project site and tunnel model were created by Midas GTS NX software with determined parameters.

**Table 1 : Determined rock mass parameters for geological units**

	Unit	Disturbance factor	Cohesion	Friction angle	Deformation modulus	Hoek – Brown failure criterion		
		<i>D</i>	<i>c</i> [kPa]	$\phi$ [°]	<i>E<sub>m</sub></i> [GPa]	<i>mb</i>	<i>s</i>	<i>a</i>
Peak parameters	Greenschist	0	220	34	0.810	0.739	0.0004	0.522
		0.5	159	27	0.440	0.321	0.0001	0.522
	Limestone	0	577	49	8.29	2.012	0.0039	0.506
		0.5	443	45	3.97	1.110	0.0013	0.506
Residual parameters	Greenschist	0	168	30	0,450	0,517	0,0001	0,544
		0,5	114	22	0,300	0,199	0,000002	0,544
	Limestone	0	323	42	1,71	0,854	0,0003	0,529
		0,5	232	34	0,995	0,354	0,0001	0,529

The ideal K0 ratio was determined by 3D back-analyses which seen close deformation to convergence measurements with different K0 ratios. As a result of the analyses, the ideal K0 value was found to be 1.90. Moreover, ideal K0 value was compared with the values obtained from empirical equations present in the literature (Zhang, L., 2017). A new support system was proposed to supply the high displacement at the tunnel entrance and numerical analyses which applied proposed support system performed to with ideal K0 ratio. proposed support system. Numerical analyses were recreated and performed to the proposed support system and specified ideal K0 ratio. Consequently, when deformations measurements were investigated during and after the application it is seen to reach out to displacements close to field measurements and stability was achieved.

As a result, the approach of estimating K0 ratio, which is an important parameter on tunnel safety and stability, was performed 3D back-analyses by Midas GTS NX software. The reliability of the approach should be compared with the results obtained from the in-situ stress tests recommended by ISRM (Stephansson, O. et al., 2012).

## REFERENCES

- Altıner, D., Koçyiğit, A., Farinacci, A., Nicosia, U.Q., Conti, M.A., 1991 , Jurassic-Lower Cretaceous stratigraphy and paleogeographic evolution of the southern part of North-western Anatolia, *Geologica Romana*, 27, pp. 13-80.
- Altınlı, İ., 1973, Orta Sakarya Jeolojisi, Cumhuriyetin 50. yılı Yer Bilimleri Kongresi, MTA Enstitüsü, Ankara, pp 151 -191.
- Bingöl, E., Akyürek, B. ve Korkmaz, B., 1973, Biga yarımadasının jeolojisi ve Karakaya formasyonunun bazı özellikleri, Yılı Yer Bilimleri Kongresi Tebliğler, pp 70-76.
- Ketin, İ., 1948, Ü ber die tektonisch-mechanischen Folgerungen aus den grossen anadoluischen Erdbeben des letzten Dezenniums. *Geol. Rund.* 36:77–83.
- Özcan, A., Erkan, A., Keskin, E., Oral, A., Özer, S., Sümengen, M. ve Tekeli, O., 1980, Kuzey Anadolu Fayı-Kırşehir Masifi arasının temel jeolojisi, MTA Rapor no:6722 (yayınlanmamış).
- Stephansson, O., Arno, Z., 2012, Rock Mechanics and Rock Engineering, ISRM Suggested Methods for Rocks Stress Estimation – Part 5: Establishing a Model for the In Situ stress at a Given Site, (DOI: 10.1007/s00603-012-0270-x).
- Zhang, L., 2017, Engineering Properties of Rocks, Chapter-2: In situ Stresses, 2nd edition, pp 19-38.

## Water level variation and slope stability analysis in a pit lake

Emmanouil Steiakakis<sup>1</sup>, G. Syllignakis<sup>2</sup>, M. Galetakis<sup>3</sup>, D.Vavadakis<sup>4</sup>

<sup>1</sup>*Department of Mineral Resources Engineering, Technical University of Crete, 73 100 Chania, Greece,*  
[stiakaki@mred.tuc.gr](mailto:stiakaki@mred.tuc.gr)

<sup>2</sup>*Department of Mineral Resources Engineering, Technical University of Crete, 73 100 Chania, Greece,*  
[georgesillign@gmail.com](mailto:georgesillign@gmail.com)

<sup>3</sup>*Department of Mineral Resources Engineering, Technical University of Crete, 73 100 Chania, Greece,*  
[galetaki@mred.tuc.gr](mailto:galetaki@mred.tuc.gr)

<sup>4</sup>*Department of Mineral Resources Engineering, Technical University of Crete, 73 100 Chania, Greece,*  
[vavadaki@mred.tuc.gr](mailto:vavadaki@mred.tuc.gr)

The formation of a pit lake by flooding the remaining voids after the mine closure has become an increasingly important topic to mine owners, environmental groups and local communities.

The slope stability of the reservoir that is largely affected by water-related changes in the soil mass, often needs to be addressed in the planning or in the early stages of pit lake formation.

In order to capture the effects of water-level variation on slopes stability in Most pit lake, investigation was performed using advanced modelling approaches.

The modelling was performed by using the PLAXIS 2D Version 2016.01 software, allowing for fully coupled flow - deformation analyses. For the fully coupled approach Bishop's effective-stress equation was used, and for description of hydraulic behavior in the soil van Genuchten's model was applied.

Parameter-influence analysis was performed with respect to stability factor, using the strength reduction approach.

The results suggest that the slope of the reservoir is stable under the considered water-level fluctuation conditions. The analyses revealed that the most critical surface where failure potentially may occur, approximates a composite failure passing through the clayey layer at the base of the slope.

Analysis of slope stability associated with reservoir water level variations, revealed that the stability factor is related to the hydraulic conductivity of the soil formations and water level variations.

Under the assumed rates of decrease in reservoir water level, the slope stability decreases as the water level drops up to five meters (5 m) below the initial level of the reservoir; the stability factor is also positively related to the rate of lowering the water level.

The stability of the slope is getting weaker when the water-level drops ten meters (10 m) below the initial water level, and the reservoir slope becomes unstable.

When the slope is exposed to a series of water level fluctuations around the initial water level, with a range  $\pm 60$  cm, the slope stability is improved.

During the process of filling the reservoir up to 5m over the initial level, at a rate less than the hydraulic conductivity of the soil, the slope stability increases.

Based on the aforementioned analysis it is concluded that the stability factor is related to the hydraulic conductivity of the soil mass and the rate of variation in the water level.



Although the results obtained are reflecting effects occurred under the specified conditions of the site, they can be used as a reference for stability evaluation of the slopes in pit lakes.

### **Acknowledgments**

The research presented in this paper has been conducted within the RAFF project (Risk Assessment of Final Pits During Flooding) co-financed by the Research Fund for Coal and Steel (RFCS) under the Grant Agreement No-847299-RAFF.

### **REFERENCES**

- Johansson J. M. A and Edeskär T., 2014, Modelling Approaches Considering Impacts of Water-level Fluctuations on Slope Stability. *Journal of Earth Sciences and Geotechnical Engineering*, v. 4, no. 4, 2014, pp. 17-34. ISSN: 1792-9040 (print), 1792-9660 (online)
- Mao J-Z., Guo J., Fu Y., Zhang W-P., Ding Y-N., 2019, Effects of Rapid Water-Level Fluctuations on the Stability of an Unsaturated Reservoir Bank Slope. *Advances in Civil Engineering Volume 2020*, Article ID 2360947, p. 10.
- PLAXIS, "PLAXIS 2D, 2012, Available at: <http://www.plaxis.nl/>, Delft, Netherlands, 2012.
- Xia, Min & Ren, Guang & Zhu, Shao & Ma, Xin, 2014, Relationship between landslide stability and reservoir water level variation. *Bulletin of Engineering Geology and the Environment*, v. 74. 10.1007/s10064-014-0654-0.
- Xia, M., Ren, G.M., Zhu, S.S., & Ma, X.L., 2015, Relationship between landslide stability and reservoir water level variation. *Bulletin of Engineering Geology and the Environment*, v. 74(3), pp. 909–17. <https://doi.org/10.1007/s10064-014-0654-0>



## Stability Assessment of Fractured Dolomite and Marl Rock Masses in a Tunnel

Ákos Török<sup>1</sup>, Péter Görög<sup>2</sup>, László Rózsa<sup>3</sup>

<sup>1</sup>*Dept. of Engineering Geology and Geotechnics, Budapest University of Technology and Economics, Hungary, [torok.akos@emk.bme.hu](mailto:torok.akos@emk.bme.hu)*

<sup>2</sup>*Dept. of Engineering Geology and Geotechnics, Budapest University of Technology and Economics, Hungary, [gorog.peter@emk.bme.hu](mailto:gorog.peter@emk.bme.hu)*

<sup>3</sup>*Hungarian State Railways, Geotechnical Division, Hungary, [rozsa.laszlo@mav.hu](mailto:rozsa.laszlo@mav.hu)*

Engineering geological and rock mechanical condition assessment of fractured rock masses is challenging, especially when the structure is located underground. The current study presents a case study where fractured dolomite and marl are found in an existing railway tunnel. The challenge is related to the extension of the existing tunnel system of the city centre of Budapest (Hungary). The tunnel is currently used as one of the main rail links to the capital of Hungary. The engineering geological properties and stability of the enlarged tunnel are outlined here, focusing on the condition assessment of the rock masses and the description of difficult ground conditions and provide long-term safety. The study site is located on the hilly side of Buda in Budapest. The current lining of the tunnel is made from porous limestone ashlar (Figure 1). The engineering geology of the area is complex, and it reflects the structural geological evolution of Buda Mountains. Several major fault zones intersect the tunnel. Fractured Triassic dolomite and Eocene marl are in tectonic contact along with one of the major faults. The stability assessment of the existing structure and the new extended tunnel is based on various data sources obtained from the field and from the laboratory. 8 core drillings from the tunnel wall and 10 exploration pits in the tunnel allowed us to understand the stratigraphy and geological conditions of the tunnel interior. Field surveys of existing outcrops and laboratory analysis of core samples provide data on the mechanical properties of dolomite and marl. The laboratory tests were performed according to EN and ISRM guidelines. Uniaxial compressive strength tests, indirect tensile strength tests, point load tests and the determination of modulus of elasticity were the main mechanical parameters. Rock masses were characterized using GSI system of fractured rock and heterogeneous rock masses. Stability calculations were made using Rocscience Phase2. The conditions and displacements of both the initial stage and the new extended tunnel were analyzed. Our calculations suggest that there are minor displacements at present, but when the tunnel is extended, additional reinforcement is necessary, especially at the fractured dolomitic zones.

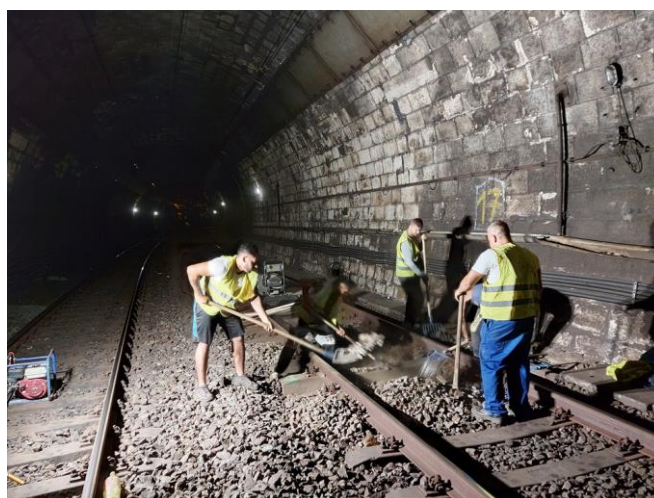


Figure 1. Railway tunnel with porous limestone ashlar lining

## A visual and laboratory estimation of the Hoek-Brown constant $m_i$ for two marbles

Anastasios Tsirikis<sup>1</sup>, Trevor G. Carter<sup>2</sup>, Vassilis Marinov<sup>3</sup>

<sup>1</sup>Department of Geology, Aristotle University of Thessaloniki, Greece, [tsirikika@geo.auth.gr](mailto:tsirikika@geo.auth.gr)

<sup>2</sup>TGCGeoSolutions, Oakville, Ontario, Canada, [tcarter@tgcgeosolutions.com](mailto:tcarter@tgcgeosolutions.com)

<sup>3</sup>School of Civil Engineering, National Technical University of Athens, Greece, [marinosv@civil.ntua.gr](mailto:marinosv@civil.ntua.gr)

### **Background**

The Hoek-Brown (H-B) failure criterion, which is used worldwide in rock engineering design, relies on accurate assessment of two intact rock material parameters, the constant  $m_i$  and the unconfined compressive strength  $\sigma_{ci}$ . Both exert significant influence on rock strength determined utilizing the H-B criterion (Carter and Marinov, 2020) and obviously this has impacts for numerical modelling by potentially allowing incorrect prediction of rock behaviour. In fact, quite significantly erroneous results can occur if  $m_i$  values are wrongly selected for a modelled rock type (Carter, 2021). For most engineering projects generally only UCS values are available, as typically triaxial and tensile tests are not routinely conducted. Practitioners are thus forced to determine  $m_i$  values empirically from published tables of typical values.

This paper utilizes detailed triaxial testing of two rock types to undertake validation and verification checks on a new methodology introduced by Carter (2019) for visually assessing  $m_i$  based on simple rocktype textural characterization of fabric, grain size and interlock, (as can be readily conducted as part of a field core logging or laboratory testing program). The results of best-fit H-B envelope regression determinations of the constant  $m_i$  experimentally determined through comprehensive laboratory rock strength testing (uniaxial, triaxial, and tensile) are specifically compared in this study with the results of  $m_i$  determinations made with the visual approach

### **Experimental Procedure**

Two marbles, namely "Tranovaltos Marble" (TM) and "Thasos marble-commercial name Krystallina of Thasos" (KTM) were tested in triaxial compression, according to ASTM D7012 - 14A, using a 4000kN INSTRON servo-controlled compression testing machine. 18 cylindrical samples 54 mm x 108 mm were tested dry, at a constant displacement rate of  $5 \times 10^{-5} \text{ s}^{-1}$  in a conventional NX Hoek triaxial cell at room temperature and confining pressures ranging from 5 to 50 MPa. Seven additional samples were tested in uniaxial compression. The execution of laboratory tests on intact rock material, as well as the determination of physical (Porosity) and mechanical parameters (Point load and Brazilian tests) needed for inclusion in the visual determination controlling expression were carried out in accordance with ASTM (D3967, D5731) and ISRM (1979) suggested methods. For the detailed fabric observations, thin sections were obtained from key locations selected within the rock samples and microstructural observations ( $d$  - the rock grain particle size,  $\xi$  - the degree of interlock and angularity of the crystal grains,  $kG\phi$  - the graphic kurtosis) were then performed using a transmitted polarized light microscope.

### **Results**

The values of the Hoek-Brown criterion constant  $m_i$ , determined from the uniaxial and triaxial data sets in the range of confining pressure between zero and the brittle-ductile transition (Hoek and Brown, 2018), as determined using the RSdata software (Rocscience Inc.) are listed in Table 1 below the parameters determined from the visual observations applied in the visual approach equation.



**Table 1: Petrographical, physical and mechanical properties of investigated rocks**

Parameter	Units	Rocktype	
		Tranovaltos Marble	Thasos Marble (Krystallina)
$\xi$	(%)	5	60
d	(mm)	0.146	1.433
$\varphi$	(%)	0.15	0.32
$\psi$	(%)	14	30
$\sigma_c$	(MPa)	93	56
$\sigma_T$	(MPa)	8,5	5,2
kG	$\varphi$	0,9	0,96
Visual $m_i$		8.4	13.6
$m_i$ (Triaxial & UCS tests)		8.7	14.3

**Conclusion**

The experimental results from this present study suggest that  $m_i$  estimations made for the investigated marbles using the visual  $m_i$  equation are in reasonable accordance with results determined by conventional regression analysis of laboratory triaxial test data. The methodology thus appears to show promise for providing a better first estimate of appropriate  $m_i$  values before laboratory test data is available, than merely utilizing published tabulations. Although thin section procedures have been employed in these validation checks, evaluation of parallel experimental testing data on other rock types (Ganye et al, 2020, Carter, 2021) suggests that application of a scaling relationship may allow direct visual use of hand specimens, outcrops and core or hand specimen lump samples rather than always requiring thin sections to be cut from rock samples in order to determine the values needed for visual  $m_i$  estimation. Further analyses of other rock types data and further laboratory testing to critically compare laboratory-based  $m_i$  values with those determined from Carter’s, 2019 expression are under investigation.

**REFERENCES**

ASTM Standard D3967, 5371, 7012 (2014, 2016) “Standard Test Methods for Compressive Strength and Elastic Moduli of Intact Rock Core Specimens under Varying States of Stress and Temperatures”, “Test Method for Splitting Tensile Strength of Intact Rock Core Specimens”, “Standard Test Method for Determination of the Point Load Strength Index of Rock and Application to Rock Strength Classifications” ASTM International, West Conshohocken, PA, [www.astm.org](http://www.astm.org)

Carter, T.G. (2019). A suggested visual approach for estimating Hoek-Brown  $m_i$  for different rock types. In proc. 14th ISRM Congress on Rock Mech and Rock Eng, Paper # 14356 , pp. 13, Foz do Iguassu, Brazil.

Carter T.G. & Marinos, V., 2020, Putting Geological Focus back into Rock Engineering Design. Rock Mechanics & Rock Eng. V 53, pp.4487–4508. <https://doi.org/10.1007/s00603-020-02177-1>

Carter T.G. ,2021, Towards Improved Definition of the Hoek-Brown constant  $m_i$  for Numerical Modelling, Paper RICAB84, Rocscience International Conference 2021, 20-21 April 2021,pp. 8

Ganye, J., Vasileiou, A. Perras, M.A & Carter, T.G., 2020, Influence of grain size and interlock on intact rock properties. Proc. 54th US Rock Mechanics Conf, Golden, Colorado. Paper ARMA 20–2097,pp. 7

Hoek E., Brown E.T., 2018, The Hoek–Brown failure criterion and GSI – 2018 edition. Journal of Rock Mechanics and Geotechnical Engineering, 11, 445-463.<https://doi.org/10.1016/j.jrmge.2018.08.001>

## The Application of Advanced Numerical Models in Capturing Complex Rockmass Behaviour

Ioannis Vazaios<sup>1</sup>, Anastasios Stavrou<sup>2</sup>

<sup>1</sup>Ove Arup & Partners Ltd., London, UK, [Yannis.Vazaios@arup.com](mailto:Yannis.Vazaios@arup.com)

<sup>2</sup>Ove Arup & Partners Ltd., London, UK, [Tasos.Stavrou@arup.com](mailto:Tasos.Stavrou@arup.com)

### Background

Ground behaviour during underground excavations in highly anisotropic, blocky rockmasses due to the presence of highly pervasive discontinuities, such as bedding planes, foliation, banding etc. are difficult to capture by using conventional analytical approaches and continuum numerical modelling. In such conditions, the rockmass modelling is imperative to include explicitly the discontinuity presence. This can be achieved by applying advanced discontinuum methods e.g. the Distinct Element Method (DEM) and constitutive models e.g. Ubiquitous Joint Model (UJM). For the purposes of this research, we used Itasca’s UDEC and 3DEC to demonstrate the value of advanced numerical modelling to capture the rockmass behaviour.

### Method

Due to the increased complexity of the rock structure system geometry, a certain number of discontinuities can only be included in the model explicitly. This includes larger scale structures that cut the medium into discrete blocks, hence forming a block assembly. However, smaller scale discontinuities need to be excluded from being explicitly simulated in the model to maintain a balance between achieving a representative rock mass behaviour and computational cost. However, their influence may be significant and needs to be considered. The impact of this closed closely spaced structure is captured indirectly by using the UJM model allowing the introduction of anisotropy in continuum blocks of the discontinuum assembly.

### Analysis and Results

The development calibration of the UJM parameters is performed by using an Unconfined Compressive Strength (UCS) laboratory configuration except that the model size is adjusted to reflect the response of a specimen of 1-2 m<sup>3</sup> rock block volumes which form the basis of the discontinuum modelling in UDEC and 3DEC for the tunnel/cavern scale excavation (Figure 1).

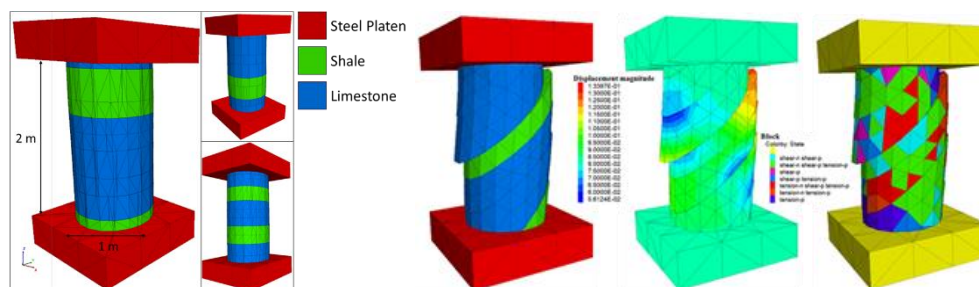


**Figure 1: 3DEC UCS model representing rock block scale for the calibration of the UJM model parameters and resulting failure mechanism due to the presence of discontinuous planes.**

The calibrated UJM parameters are implemented to tunnel scale models at the rock block scale hence accounting for both large-scale and small-scale discontinuities impacting the excavation and the associated support design. Displacement analysis results for the same large-scale discontinuity pattern but by adopting the UJM model for the continuum blocks against the conventional Hoek-Brown criterion reveal differences in

the expected displacement magnitude, hence directly impacting the excavation response and as such the design for an appropriate support system (Figure 2).

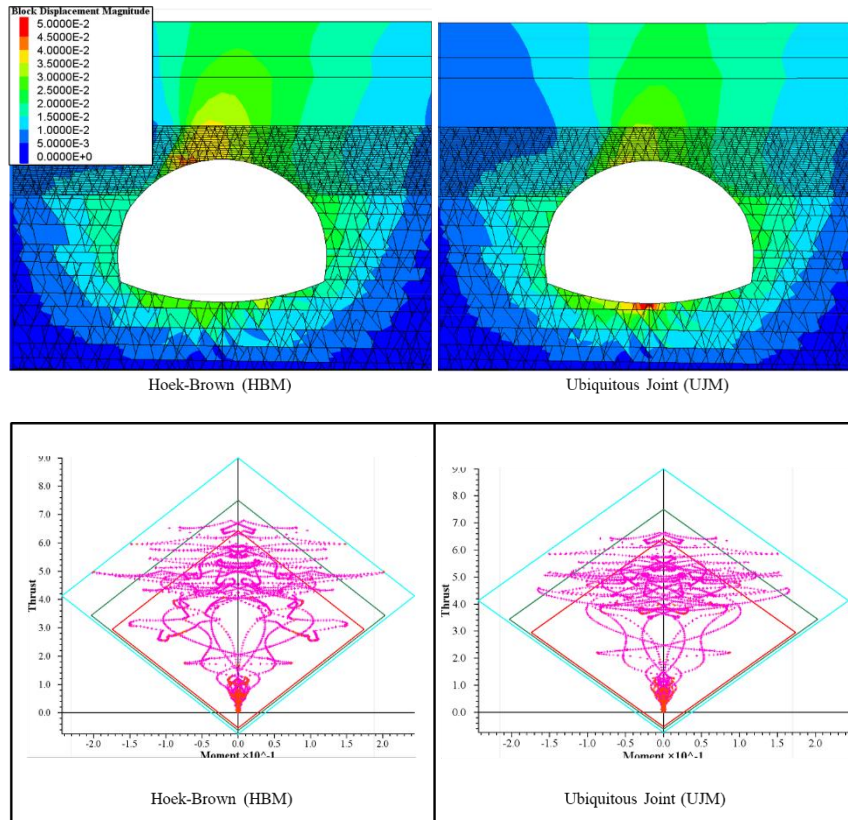


**Figure 2: Top-Displacement magnitude contours (in meters) for a cavern excavation using the Hoek-Brown and UJM constitutive models for the continuum blocks, and Bottom-Sprayed Concrete Liner (SCL) internal forces at the end of excavation.**

**Conclusions**

Application of advanced numerical modelling has been proven to be a valuable tool in understanding complex rockmass behaviour and adopting appropriate support strategies during design. Use of the UJM model within discontinuum assemblies provides further insights on the role of small-scale structure in underground excavations and their influence on the anticipated support response. An important step, however, is to appropriately calibrate the UJM parameters to reflect the site-specific conditions and corresponding rock block sizes for implementation in the discontinuum assembly. Unless properly calibrated, the coupling of the UJM constitutive model with discontinuum models may yield results that are not representative for the examined rockmass and its response during excavation, hence resulting in not appropriate support measures for the intended underground works with significant consequences on site in terms of health and safety, programme etc.



## Engineering Geological detailed aspects impacting on the foundation and watertightness of the Julius Nyerere HPP Main RCC Dam, in Tanzania

Nikolaos Kazilis<sup>1</sup>, Maria Kazili<sup>2</sup>

<sup>1</sup>Project and Design Manager, Geodata Engineering SpA, Italy, [nka@geodata.it](mailto:nka@geodata.it)

<sup>2</sup>Engineering Geologist, formerly Geodata Engineering SpA, Italy, currently AECOM, England, [kazili.maria@gmail.com](mailto:kazili.maria@gmail.com)

The Julius Nyerere Hydropower Project (JNHPP) is being developed on the Rufiji River in the southeast part of the United Republic of Tanzania. The project is located at about 350 km, south-west of Dar Es Salaam, Tanzania's largest city, situated on the coast. The project is one of the largest development project proposed in the Rufiji River Basin, the largest in Tanzania, covering an area of 177000 km<sup>2</sup> and extending 700 km between Mbeya in the west, to the Indian Ocean coast in the east. The mean annual flow of the dam site is 887.6 m<sup>3</sup>/s, and the mean annual runoff is 27.9 billion m<sup>3</sup>. The JNHPP is developed for power generation, flood control and environmental flow, with a total installed capacity of 2115 MW and annual power generation is 6 307 GWh. The water retaining structures consist of, a Main Dam (RCC type, 131m high and 4 saddle dams at the right bank of the river.

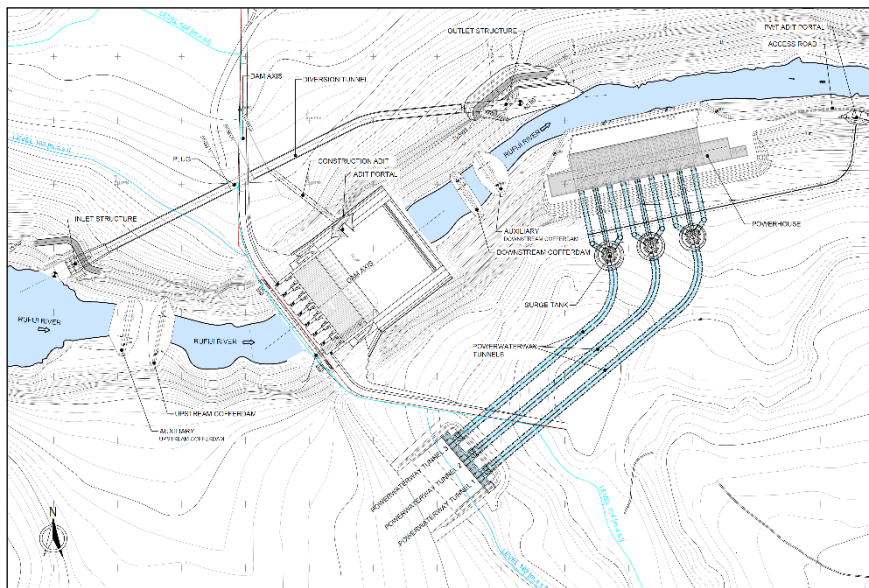
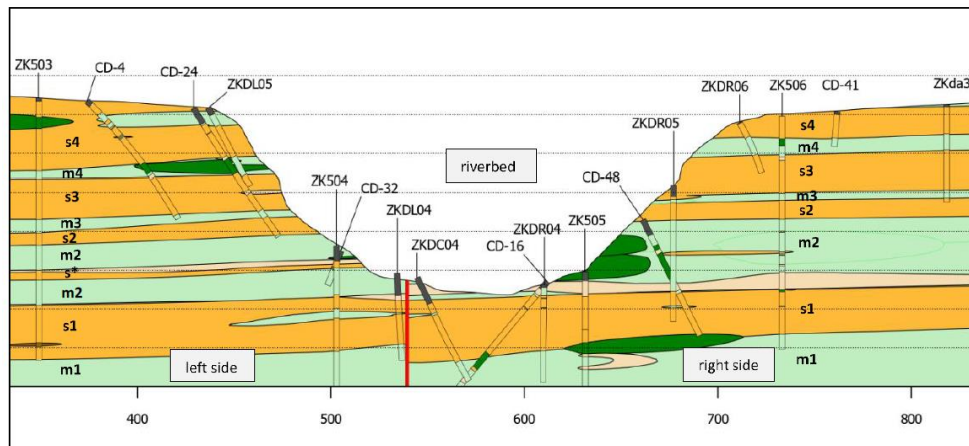


Figure 1. General layout of the Main dam and the appurtenant structures of the JNHPP.

The main dam site is developed over Stiegler's Gorge, a typical gorge with steep slopes. The geological sedimentary sequence under the body of the main dam is composed of a series of alternating strata of mudstone (four individual layers) and sandstone (four individual layers), as shown in following figure. Two main Sub-vertical fault families (oriented NW-SE and NE-SW, respectively) cut the wider dam area. The rock-masses are characterised by the presence of typical two sub-vertical joint sets (with similar orientation of the faults) and the sub-horizontal bedding. Geohydrologically, the ground water is fairly deep in both abutments, a fact indicating a deep drainage, while the permeability is generally high in the sandstones and moderate to low in the mudstones, with higher values along the sub-vertical faults.



**Figure 2. General longitudinal section along the axis of the main dam showing the geological sequence.**

The examined engineering geological aspects that potentially impact on the foundation and the water-tightness conditions of the main RCC dam, are the following: (i) stress relief deformations occurring over the upper parts of both abutments have produced the “relief” of the rock mass, leaving open, or filled with clay cracks, which offer paths to rain water to percolate easily down to the contact with the underlying mudstone layer, leading to serious weathering and fully softening of the upper mudstone limited thickness layer close to the contact, (ii) The stress relief deformations from one side in the upper part of both dam abutments and the extensive tectonic fracturing and shearing, in the sandstones layers along the influence zones of the faults, offer preferential potential water leakage paths affecting the requirements and thus the design of the water-tightness grouting curtain below and to the wider sides of the dam, (iii) the presence of faults with limited, of even small deformations, of the NW-SE orientation, offer “shear keying” conditions in the potential sliding tendency of the dam body along sub-horizontal bedding planes towards downstream and (iv) the confinement of the low area of the bottom of the gorge and thus the main dam foundation, offers in general, comparatively adequate shear strength conditions, badly needed for the stability of the dam body against sliding in a sub-horizontal sedimentary sequence involving hard sandstones and locally weathered, softened mudstones. All the above engineering geological characteristics and the potential impacts, are thoroughly demonstrated and discussed in the oral presentation.

## REFERENCES

- GDE Technical Note No-10 (N. Kazilis) which is an un-published internal Technical Note within the Design-Built Sub-Contractor organization (2020): On the potential presence of weak argillaceous layers in both upper abutments of the main dam.
- GDE Technical Note No-12 (N. Kazilis) which is an un-published internal Technical Note within the Design-Built Sub-Contractor organization (2020): On the needs to re-examine the Basic Design of the grout curtain below and to the sides of the main dam



**THEME 5 - ENGINEERING GEOLOGY FOR URBAN ENVIRONMENT**

## Engineering geological mapping of Moscow megacity area: from geological maps to georisk maps

Olga Eremina<sup>1</sup>, Irina Kozliakova<sup>1</sup>

<sup>1</sup>*Sergeev Institute of Environmental Geoscience RAS, Moscow, Russia, [o\\_eremina@mail.ru](mailto:o_eremina@mail.ru)*

The report gives a brief overview on the progress in engineering geological mapping of Moscow area by the example of the studies performed at IEG RAS for several decades on the basis of processing a huge amount of borehole data on Moscow subsurface.

Compilation of the first geological maps for the Moscow area date back to the second half of the 19th century. Three generations of river valleys as the main factor controlling the variability of geological and hydrogeological conditions in Moscow have been revealed and mapped in the first half of the 20th century. Since then, the geological maps were recurrently updated and the mapping area was broadening. Engineering geologists usually get a general view on the geological structure at the particular construction site by addressing the following geological maps: (1) the map of Carboniferous deposits subcrop topography, for the distribution of preJurassic river valleys; (2) the map of preQuaternary deposits, for the preQuaternary valleys; and (3) the map of Quaternary deposits, for the modern river valleys.

The next stage of mapping Moscow subsurface was focused on the distribution of exogenous geological processes (EGP) in Moscow, i.e., karst and karst-related suffosion, landslides, and waterlogging. The EGP maps were compiled in the second half of the 20th century, when a vast database has been accumulated on geohazard manifestation in the city. The EGP maps are of estimative purpose, and they show the comparative categories of geohazard impact on urban infrastructure. The integral map of geoecological conditions of Moscow, compiled at IEG RAS distinguishes favorability categories for urban construction depending on EGP combination in the certain area. It was included in the General Plan of Moscow urban development.

At the threshold of the 21st century, engineering geological assessment of urban areas started using the term "geological risk". It became clear that geohazards in urban areas should be investigated in conjunction to urban infrastructure vulnerability. On one hand, in densely built-up areas, EGPs would inevitably affect buildings and subsurface engineering structures; and on the other hand, running engineering structures in cities induces the intensification of geological processes and their undesirable manifestation on the surface and in ground bases of buildings. At present, the map of geological risk has been compiled for the Moscow territory to a scale 1 : 50 000. The spatial subdivision in this map is based on the qualitative assessment of value and probability of economic damage caused by EGPs. The damage is measured by the possibility of deformations and ruining of buildings and engineering structures, disturbance of sustainable operation of urban infrastructure units, need for their repair during the warranty period, etc.

The next research step appears to consist in the assessment of urban area sustainability on the basis of the analysis of exogenous geohazards and relevant risk, on one hand, and the complexity of subsurface development.

### Acknowledgments

This study was financially supported by the Russian Science Foundation, project no. 16-17-00125.

## Engineering geological evaluation for urban land use planning and engineering construction within a database environment, a case study for the city of Thessaloniki, Northern Greece

Aliki Kokkala<sup>1</sup>, Vassilis Marinos<sup>1</sup>, Vasileios Christaras<sup>1</sup>, Konstantinos Voudouris<sup>1</sup>

<sup>1</sup> Department of Geology, Aristotle University of Thessaloniki, Thessaloniki, Greece, [kokkalaa@geo.auth.gr](mailto:kokkalaa@geo.auth.gr), [marinosv@geo.auth.gr](mailto:marinosv@geo.auth.gr), [christar@geo.auth.gr](mailto:christar@geo.auth.gr), [kvoudour@geo.auth.gr](mailto:kvoudour@geo.auth.gr)

The urbanization process is influenced by many factors and faces several challenges. The identification and definition of the engineering geological conditions in an urban area are crucial factors for planning and designing geotechnical works. A valuable tool is a well-organized database (Marinos et al. 2013) capable of storing, navigating, correlating and presenting all the required geoengineering properties of the geomaterials on which or within which engineering structures are to be created, whether it is a tunnel, a foundation or a slope cut. In this study, the engineering geological conditions of the city of Thessaloniki in northern Greece are analyzed. A large amount of geological and geotechnical data are stored in a georeferenced database that was created for this study. The data that are processed are mainly based on borehole geological information, laboratory testing, geotechnical characterization and in situ field tests collected from soils of Quaternary and Neogene deposits of Thessaloniki's urban area.

Specific value ranges for several physical and mechanical properties are proposed by the assessment and correlation of the information originating from the database (Kokkala A. and Marinos V. 2018). Thematic maps, 2-D profiles and 3-D models, and references to geological and geotechnical factors are constructed to provide stored and organized information that serve multiple purposes such as new construction works, seismic hazard zoning and management of other natural hazards. In addition, the purpose of this work is to examine the behavior of the formations in relation to mechanized tunneling and Tunnel Boring Machine (TBM) selection (Marinos et al. 2008), understanding particular geotechnical problems and identifying certain geological hazardous zones (Mufida el May et al. 2010). The work focuses on the engineering geological characterisation of the various ground types that are extended in the city area, but also on their behavior in an engineering structure, be it a tunnel, a foundation or a slope. The paper points out the need for future prospective studies by exploring the importance of underground and surface development for urban sustainability (Price S. J. et al. 2013). The approach tested in the research area provides the basis for a future methodology on which to assess and visualise the suitability of the ground for proposed uses during spatial development planning.

### REFERENCES

- Kokkala A., Marinos V., 2018, Assessment on the Engineering Geological Conditions of the Eastern Urban Area of Thessaloniki Basin, in Northern Greece, Using a Geotechnical Database, IAEG/AEG Annual Meeting Proceedings, San Francisco, California, Volume 6 [https://doi.org/10.1007/978-3-319-93142-5\\_15](https://doi.org/10.1007/978-3-319-93142-5_15)
- Marinos P., Novack M., Benissi M., Panteliadou M., Papouli D., Stoumpos G., Marinos V. and Korkaris, K., 2008, Ground Information and Selection of TBM for the Thessaloniki Metro in Greece: Environmental and Engineering Geoscience, Vol XIV, no 1, pp. 17–30. <https://doi.org/10.2113/gseegeosci.14.1.17>



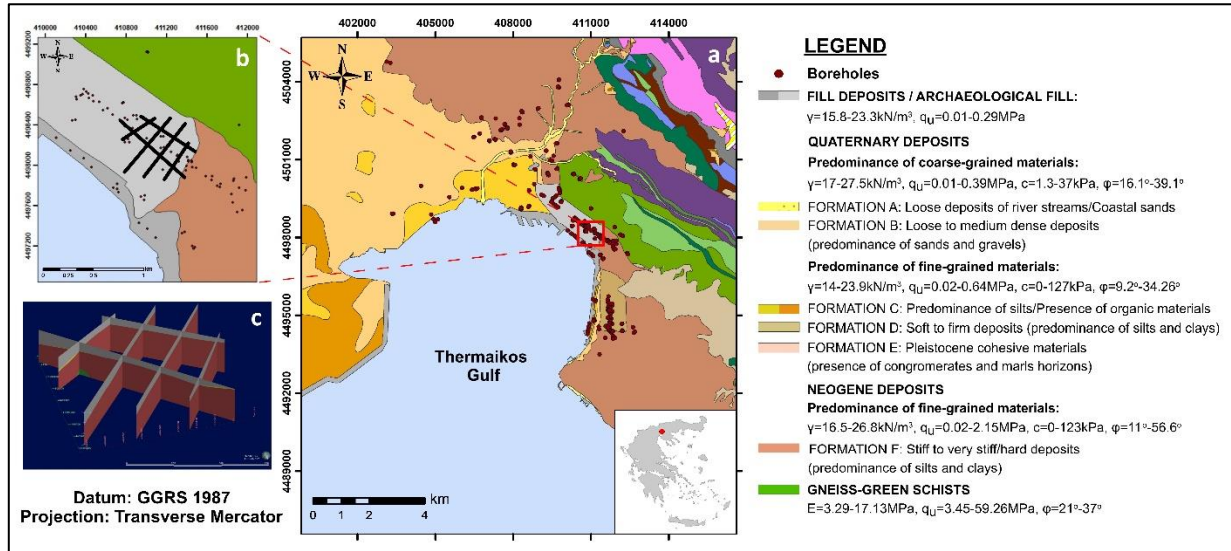
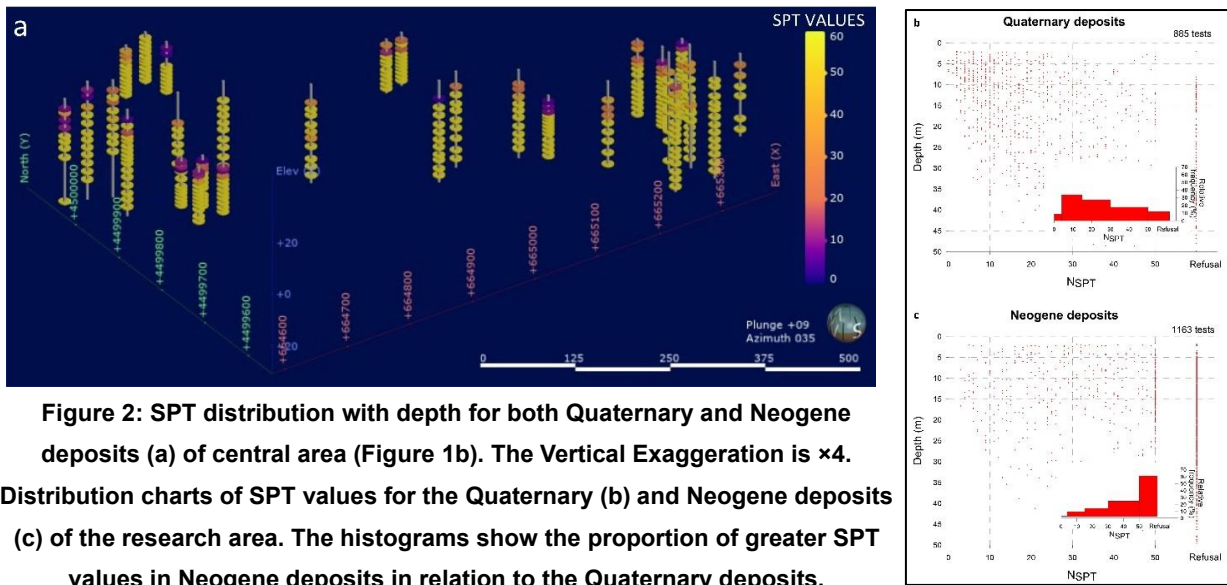


Figure 1: Engineering geological map of Thessaloniki city (a) illustrating the spatial distribution of formations in the research area (modified by the authors from Rozos et al. 1998). 3-D fence diagram (c) of generated cross-sections for the central region (b). The Vertical Exaggeration is  $\times 4$ . Neogene deposits prevail in depth and length instead of Quaternary deposits.



Marinos V., Proutzopoulos G., Fortsakis P., Koumoutsakos D., Korkaris K. and Papouli D., 2013, Tunnel Information and Analysis System: A Geotechnical Database for Tunnels: Geotechnical and Geological Engineering, Vol 31, no 3, pp. 891-910 <https://doi.org/10.1007/s10706-012-9570-x>

Mufida el May, Mahmoud Dlala, Ismail Chenini, 2010, Urban geological mapping Geotechnical data analysis for rational development planning, Engineering Geology, Vol 116, pp. 129-138 <https://doi.org/10.1016/j.enggeo.2010.08.002>

Price S. J., Terrington R. L., Busby J., Bricker S., Berry T., 2018, 3D ground-use optimisation for sustainable urban development planning: A case-study from Earls Court, London, UK, Tunnelling and Underground Space Technology, Volume 81, pp. 144-164 <https://doi.org/10.1016/j.tust.2018.06.025>

Rozos, D.; Apostolidis, E. and Hadzinakos, I. (HSGME), 1998, Engineering-geological map of Thessaloniki wider area, Scale 1:25.000

## **I.S.G.E.: An Integrated Spatial Geophysical & Geotechnical Evaluation tool based on fuzzy logic**

Christos Orfanos<sup>1</sup>, Konstantinos Leontarakis<sup>1</sup>, George Apostolopoulos<sup>1</sup>, Ioannis E. Zevgolis<sup>1</sup>

<sup>1</sup>National Technical University of Athens, Greece, [orf@metal.ntua.gr](mailto:orf@metal.ntua.gr)

<sup>1</sup>National Technical University of Athens, Greece, [leon@metal.ntua.gr](mailto:leon@metal.ntua.gr)

<sup>1</sup>National Technical University of Athens, Greece, [gapo@metal.ntua.gr](mailto:gapo@metal.ntua.gr)

<sup>1</sup>National Technical University of Athens, Greece, [izevgolis@metal.ntua.gr](mailto:izevgolis@metal.ntua.gr)

### **Introduction**

This study aims to provide more insight into the inherent uncertainty related to spatial variability of engineering properties of the subsurface. A novel multiparameter algorithm has been developed for the estimation of spatial distribution of geotechnical parameters by utilizing both geotechnical and geophysical methods. The proposed algorithm is based on fuzzy logic and the final output is the prediction of the 2D or 3D distribution of a geotechnical parameter in a survey area.

### **The I.S.G.E. algorithm**

The main advantage of the newly developed Integrated Spatial Geophysical & Geotechnical evaluation (I.S.G.E) tool is the incorporation of available geotechnical information in the multiparameter analysis process. In this way, the propagation of the geotechnical sparse or even point information can be achieved from 1D to 2D or even 3D space, without the need for predefined equations linking the measured geophysical to the desired geotechnical parameter.

When borehole information exists, a data-driven approach is followed by structurally integrate different geophysical models achieved by individual tomographic inversion and transforming them into fuzzy sets (Paashe 2017). In a post inversion analysis, systems of linear equations are then set up and solved linking the fuzzy sets and the sparse information about the target parameter.

In the case that there is no borehole information, a multiparameter analysis using Fuzzy c-means clustering technique is performed for the creation of a Unified Geophysical Model (Orfanos & Apostolopoulos 2013) and the calculation of fuzzy updated geophysical models. Then, with a deterministic approach, a prediction of a desired geotechnical parameter can be assessed using predefined empirical relationships linking the measured geophysical methods with a specific geotechnical parameter.

### **Evaluation at a controlled Test site**

An integrated 3D geophysical study has been applied at a controlled Test site, in order to evaluate the effectiveness of the I.S.G.E. algorithm. The input data consists of the 3D geophysical tomographic models (P-wave velocity, Shear wave velocity & Resistivity models) and the 1D geotechnical model assessed by borehole data in the context of a previous geotechnical study (Figure 1). The output for two different geotechnical parameters (SPT, Cohesion) is presented as an example in Figure 1. As it can be observed in both cases, it is possible to assess their 3D distribution by exploiting the point information (1D) of the borehole. The predicted values are in very good agreement with the given values in the borehole, with correlation coefficients for the SPT and Cohesion values 95% and 88%, respectively.

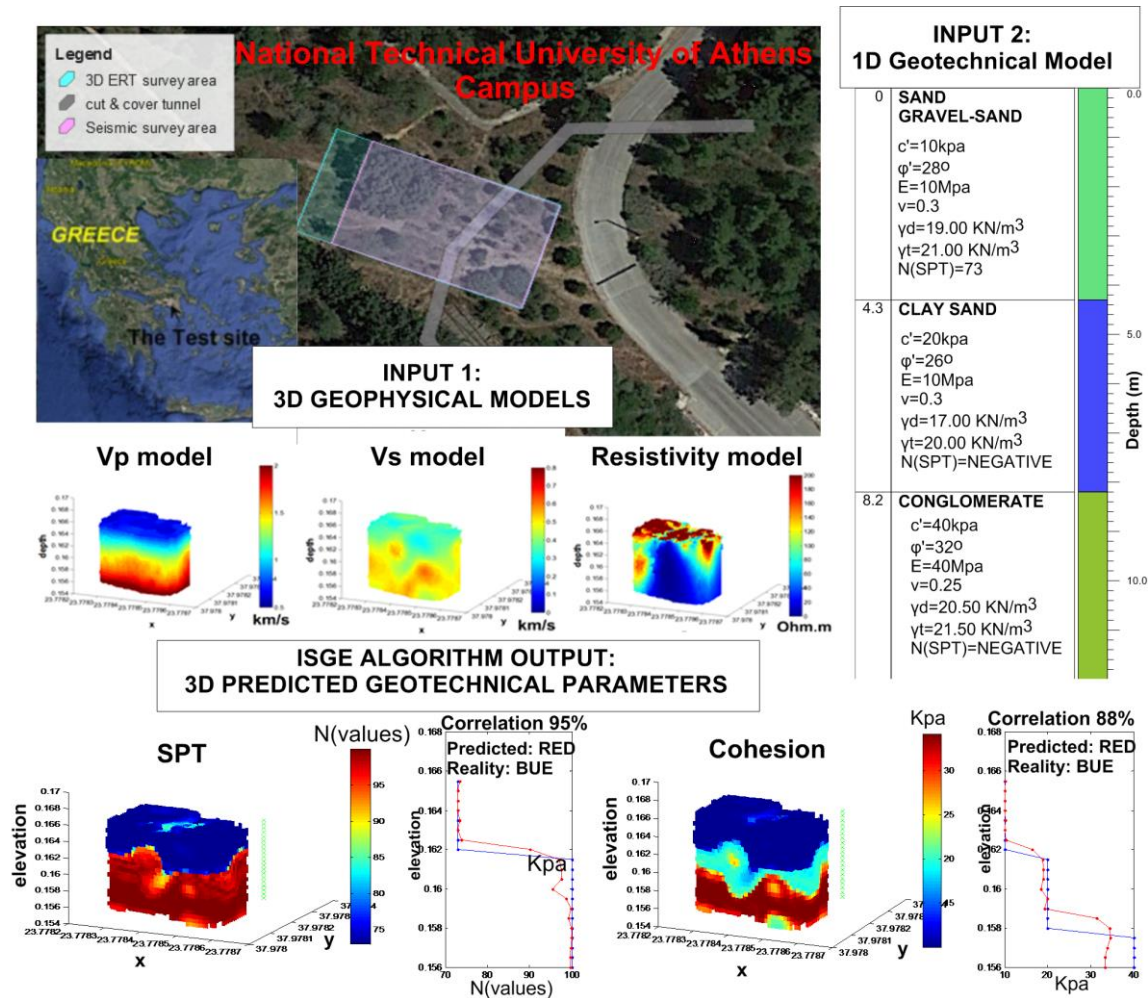


Figure 1. Input and Output data of I.S.G.E. algorithm at the Test site of National Technical University of Athens

**Conclusions**

A new multiparameter algorithm has been developed, providing engineers with an additional interpretation tool in geotechnical investigations. The main advantage is that geotechnical sparse or even point information can be propagated from 1D to 3D space without the need for predefined equations linking the measured geophysical to the predicted geotechnical one. The implementation of the proposed method at a controlled test site presents very promising results, regarding the prediction of the spatial distribution of various geotechnical parameters in the survey area.

**Acknowledgments**

This project has received funding from the Hellenic Foundation for Research and Innovation (HFRI) and the General Secretariat for Research and Technology (GSRT), under grant agreement No [2465].

**REFERENCES**

Orfanos, C., and Apostolopoulos G., 2013. Multiparameter analysis of geophysical methods for target detection: The unified geophysical model approach. *Geophysics*, 78(6)

Paasche, H, 2017. Translating tomographic ambiguity into the probabilistic inference of hydrologic and engineering target parameter. *Geophysics*, 82.



## Assessment of Earthquake Induced Liquefaction Risks in the Hills of The Rohingya Refugee Camp Area, Cox's Bazar, Bangladesh for Sustainable Development

A.T.M. Shakhawat Hossain<sup>1</sup>, T. Dutta<sup>1</sup>, M.E. Haque<sup>1</sup>, M.H. Sayem<sup>1</sup>, H. Imam<sup>1</sup>, M. Khatun<sup>1</sup>, S.J. Jafrin<sup>1</sup>, P.A. Khan<sup>1</sup>, M. Hasan<sup>1</sup>

<sup>1</sup>EGG Research Group, Dept. of Geological Sciences, Jahangirnagar University, Dhaka, Bangladesh, [shakhawathos2004@yahoo.com](mailto:shakhawathos2004@yahoo.com)

This research has evaluated the liquefaction potential of some granular soils of the Rohingya Refugee camp area of Ukhia & Teknaf region of Cox's Bazar district, Bangladesh. Standard Penetration Test (SPT) data have been used to evaluate the Liquefaction potential of the soils of the investigated area. Different liquefaction potential parameters including Cyclic Resistance Ratio (CRR), Cyclic Stress Ratio (CSR) and settlement amount at different depths have been calculated and the corresponding Factor of safety (Fs) values were identified using empirical relationship commonly used in Geotechnical Engineering. Different earthquake magnitude values (M = 5.5 to 7.5) have been applied to see the impacts of different earthquake magnitudes on the granular soils of the Rohingya refugee camp area of Cox's Bazar district, Bangladesh.

Corrected SPT and recommended maximum peak ground acceleration (PGA) values according to Bangladesh National Building Code (2015) for earthquake zonation in the eastern folded part of Bangladesh have been used to calculate the liquefaction potential and factor of safety values. It is established from this research that these soils are mainly very loose to loose sandy soils on the top with areal and vertical depth variations. In some areas, some silty shales are associated with sands at the lower part in the Rohingya camp hills. During wet seasons these soils are almost saturated and the water level is very close to the surface at depth of 1 m to 3 m. It is also established that these soils are mainly sand dominated up to a depth of 15 m with a size range lie in between 0.05 to 1 mm, uniformly graded and have high potential to liquefy. Liquefaction potential values have been calculated using LiquePro (2005) software for recommended maximum peak ground acceleration (PGA) at M = 5.5 & 7.5. It is observed that at lower earthquake magnitudes these soils are not liquefiable but at higher magnitudes (M= 5 or above) these soils are susceptible to liquefy up to a depth equivalent to 15 m. However, at greater depths these soils are less susceptible to liquefy even at higher magnitudes. The obtained CSR, CRR and Fs value in addition to the grain size results and change in pore water pressure values are also consistent with the criteria of liquefiable soils. Findings from this research will help planners, engineers and policy makers to construct engineering infrastructures and ensure sustainable housing and development for improving the quality of life for the local inhabitants and more than 1 million Rohingya refugees living in the Rohingya camp areas of Cox's Bazar district Bangladesh.



## THEME 6 - ANALYSIS AND MITIGATION OF GEO-HAZARDS



## The Kosova landslide in Bosnia and Herzegovina

Mike G Winter<sup>1</sup>, Sarah J Reeves<sup>2</sup>, Senad Smajlović<sup>3</sup>, Gurmel Ghataora<sup>4</sup>, Dželila Šehić<sup>3</sup>, Haris Zejnić<sup>3</sup>

<sup>1</sup>Formerly TRL Limited now Winter Associates, United Kingdom, [mwinter@winterassociates.co.uk](mailto:mwinter@winterassociates.co.uk)

<sup>2</sup>Formerly TRL Limited, United Kingdom, [sjr1002@btinternet.com](mailto:sjr1002@btinternet.com)

<sup>3</sup>PC Main Roads (JP Ceste), Bosnia and Herzegovina [ssenad@jpcfbih.ba](mailto:ssenad@jpcfbih.ba),  
[sdzelila@jpcfbih.ba](mailto:sdzelila@jpcfbih.ba), [haris.zejnic@jpcfbih.ba](mailto:haris.zejnic@jpcfbih.ba)

<sup>4</sup>University of Birmingham, United Kingdom, [g.s.ghataora@bham.ac.uk](mailto:g.s.ghataora@bham.ac.uk)

The Kosova landslide is a large translational landslide and caused significant damage to the main road, in the toe area, and to buildings on the slide mass during a major movement on 19 May 2014. This movement followed a period of prolonged heavy rain and flooding that caused significant disruption in Bosnia and Herzegovina (BiH) and the Balkans. As of 20 May, an estimated 24 lives had been lost in BiH as a direct result of the floods, with seven people missing. The rainfall was the highest in 120 years of recorded measurements.

Kosova is in the Federation of Bosnia and Herzegovina (FBiH) around 90km NNE of the capital Sarajevo. The landslide affected part of of Kosova village, in the northern part of the Maglaj Municipality, above and to the west of the main road M17 (E73), S of Doboj. Many buildings were destroyed and left uninhabitable (Figure 1) while the road required significant repair, including the construction of a retaining wall, prior to reopening.



**Figure 1. Scarp features at the northern lateral margin of the landslide (the red line indicates the most evident parts of the scarp features but is not intended to reflect the full complexity of the landslide). Damaged buildings are also evident.**

The site is close to the border between the FBiH and Republika Srpska (RS), which entities, along with the District of Brčko, form the country of BiH. The River Bosna forms the border at this location. The authors investigation of the landslide in March 2018 was in weather conditions that very clearly delimited the mass movement and they estimated a landslide plan area of around 115,000m<sup>2</sup> (Winter et al. 2020) some two to four times that returned from earlier investigations. In addition to the damage to the road significant damage to a number of buildings is evident (Figures 1 and 2), rendering them uninhabitable.

It seems clear that the landslide has the potential to dam the Bosna River and to create significant risk associated with the hazards of flooding and subsequent landslide dam burst. As the river forms the border

between FBiH and RS the governance of the landslide risk management process is also a major issue that will need to be resolved.



**Figure 2. Panoramic image showing (1) the northerly lateral margin scarps (red lines indicate the clearest scarp features do not reflect the full complexity of the landslide) with (2) significantly damaged buildings, (3) buildings with relatively less damage in the central portion of the landslide, (4) tree demonstrating the lifting of the frontal lobe, (5) at the extreme right the roofs of buildings at the southern lateral margin of the landslides are evident.**

The Kosova landslide clearly presents a major operational risk for the M17 (E73) road and thus to PC Roads. However, given the risk to houses on the flood plain there is a case to be made that the Municipality and/or the Canton should be involved. In addition, the potential for damming the Bosna River also brings both the Sava River Basin Agency and the Civil Protection Agency into that forum. However, given that the Bosna River forms the border between the FBiH and the RS at this location, any flooding (both upstream and downstream) would affect both the FBiH and the RS; it thus seems appropriate that the relevant agencies from the latter should also be involved. In this context consideration should be given to a national, BiH, effort to monitor the landslide and to effect remediation risk reduction where necessary.

The damage observed is significant but relatively slight compared to the potential for future damage. This highlights the need for a joined-up multi-entity and/or national approach to the investigation, monitoring, governance and, ultimately, to the subsequent management and mitigation of the Kosova landslide.

Acknowledgement: PC Roads, TRL and the University of Birmingham collaborated under a technical assistance project to PC Roads funded by the Global Facility for Disaster Reduction and Recovery and implemented by the World Bank. The findings, interpretations, and conclusions expressed in this paper do not necessarily reflect the views of the World Bank, the Executive Directors of the World Bank or the governments they represent. The World Bank does not guarantee the accuracy of the data included in this work.

## REFERENCES

Winter, M. G., Reeves, S. J., Smajlović, S., Ghataora, G., Šehić, D. and Zejnić, H., 2020, The Kosova landslide, Bosnia and Herzegovina. *Quarterly Journal of Engineering Geology & Hydrogeology*, 53(4). <https://doi.org/10.1144/qjegh2019-097>.



## Probabilistic rainfall thresholds for debris flow warning in Scotland

Mike G Winter<sup>1</sup>, Flora Ognissanto<sup>2</sup>, Luke A Martin<sup>3</sup>

<sup>1</sup>Formerly TRL Limited now Winter Associates, United Kingdom, [mwinter@winterassociates.co.uk](mailto:mwinter@winterassociates.co.uk)

<sup>2</sup>TRL Limited, United Kingdom, United Kingdom, [fognissanto@trl.co.uk](mailto:fognissanto@trl.co.uk)

<sup>3</sup>Formerly TRL Limited now WSP, United Kingdom, [lukemartin74@hotmail.co.uk](mailto:lukemartin74@hotmail.co.uk)

The link between rainfall and debris flow is well-established in Scotland and in this short contribution we reflect the past and ongoing state of early warning for debris flow in Scotland. A tentative threshold to describe the relation between rainfall and debris flow has been developed (Winter et al. 2010) and is closely-related to the Met Office heavy rainfall warning used to switch wig-wag warning signs on during periods of heavy rainfall and to thus indicate higher debris flow hazard and risk to road users (Winter et al. 2020).

This tentative, deterministic threshold is, however, limited by the lack of data proximal to debris flow events and underestimates the rainfall required to trigger an event. Consequently, two rain gauges were installed at the A83 Rest and be Thankful (RabT), to acquire data at this remote, high elevation debris flow site.

This threshold is also limited by its deterministic nature, predating techniques for probabilistic thresholds. Like all deterministic thresholds it simply divides the rainfall duration-intensity plane into two regions: one in which debris flow occurs and one in which debris flow does not occur. This binary approach is not well-matched to reality, which is significantly more complex and, in reality, the two regions represent undefined, but greater and lesser, likelihoods of event occurrence. A probabilistic approach provides a more realistic, reliable and defensible rainfall trigger threshold for debris flow that is, additionally, based on similar principles to rainfall forecasts.

The approach potentially yields a suite of rainfall thresholds, or rainfall states, that correspond to differing probabilities of debris flow occurrence given different rainfall duration-intensity pairings. The deterministic approach relies on cause and effect, with a set amount of rainfall in a defined period leading to a landslide, while the probabilistic approach uses Bayes' theorem. This allows that a degree of randomness is present and that it is not possible to trace a unique path linking an event and a single outcome. In this way an evaluation of the likelihood is given that a result occurs as an outcome of certain inputs; that is, a probability is associated with its occurrence.

The probabilistic approach debris flow forecast has been developed, primarily for the RabT site, but with the potential to be adapted for application more widely (Winter et al. 2019). The probabilistic analyses used the prior probability of landslide occurrence and the posterior probability associated with recent rainfall and landslides to develop one-dimensional analyses for conditional landslide probability based on rainfall duration, rainfall intensity and total rainfall. This was then extended to encompass a two-dimensional analysis to derive the conditional probability of landslide occurrence dependent upon paired values of rainfall duration and intensity.

Probabilistic thresholds for the conditional probability of landslide occurrence ( $L$ ) dependent on rainfall duration ( $D$ ) and intensity ( $I$ ),  $P(L|D,I)$  are derived in the range 0.05 (5%) to 0.3 (30%) (Figure 1). This is considered to be a significant improvement on the deterministic approach to the forecast of periods during which landslide hazard and risk are elevated due to rainfall conditions.

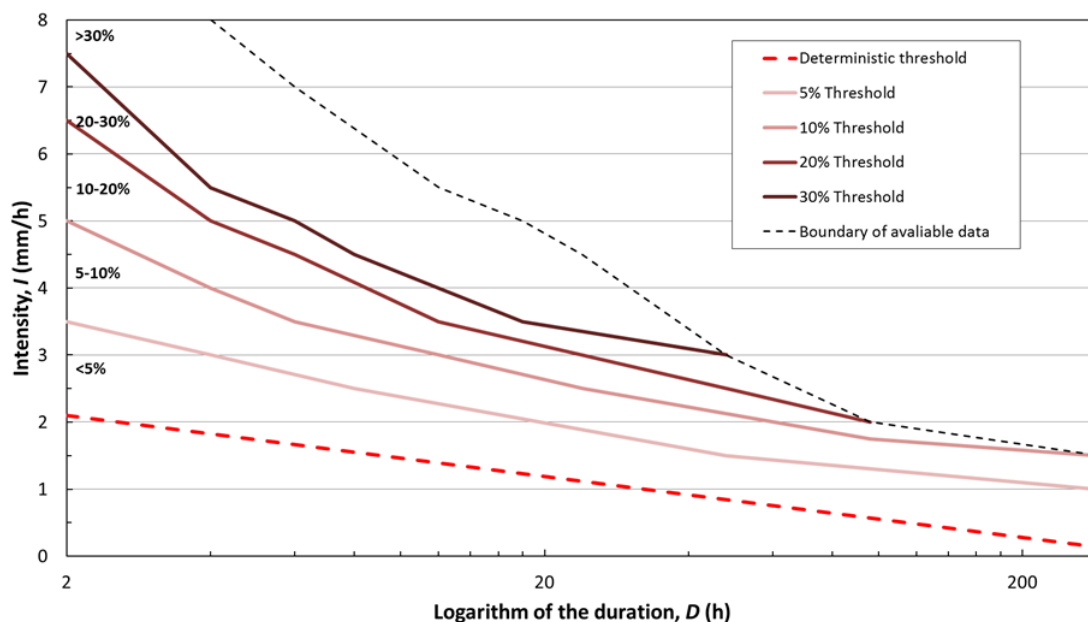


**Figure 1. Conditional probability threshold of landslides given a rainfall event of Intensity (*I*) and Duration (*D*).  
The red dashed line represents the deterministic threshold developed by Winter et al. (2010).**

In order to implement the probabilistic threshold to practice a process of ‘shadow’ trial and refinement will be needed in order to, for example, specific landslide risk reduction measures such as the wig-wag warning signs that are used at the site.

In the longer-term a tiered, multi-criteria threshold approach to the warning of debris flow events is planned with rainfall simply being the first stage of that process. This will encompass rainfall, groundwater spatial and temporal distribution as well as slope-wide slope landslide pre-cursory movement detection using optical and near-infrared imagery. This will allow warnings ranging from ‘more likely’, through ‘imminent’, to ‘event occurrence’ and provide a much more robust system of warning.

**REFERENCES**

Winter, M. G. and Wong, J. C. F. 2020. The assessment of quantitative risk to road users from debris flow. *Geoenvironmental Disasters*, 7(4), 1-19. DOI: <https://doi.org/10.1186/s40677-019-0140-x>.

Winter, M. G., Dent, J., Macgregor, F., Dempsey, P., Motion, A. and Shackman, L. 2010. Debris flow, rainfall and climate change in Scotland. *Quarterly Journal of Engineering Geology & Hydrogeology*, 43(4), 429-446.

Winter, M. G., Kinnear, N. and Helman, S. 2020. A technical and perceptual evaluation of a novel landslide early warning system. *Proceedings, Institution of Civil Engineers (Transport)*. DOI: 10.1680/jtran.19.00138.

Winter, M. G., Ognissanto, F., and Martin, L. A. 2019. Rainfall thresholds for landslides: deterministic and probabilistic approaches. PPR 991. TRL, Wokingham.



## Investigation of land subsidence due to the overexploitation of the aquifer at the Amyntaio basin, Greece

Ploutarchos Tzampoglou<sup>1</sup>, Constantinos Loupasakis<sup>2</sup>

<sup>1</sup>*Department of Civil and Environmental Engineering, University of Cyprus, Nicosia, CYPRUS,*  
[tzampoglou.ploutarchos@ucy.ac.cy](mailto:tzampoglou.ploutarchos@ucy.ac.cy)

<sup>2</sup>*School of Mining and Metallurgical Engineering, National Technical University of Athens, Greece,*  
[cloupasakis@metal.ntua.gr](mailto:cloupasakis@metal.ntua.gr)

The main objective of this study was to investigate the mechanism of the land subsidence due to overexploitation of the aquifer. The study area is located at the Amyntaio basin, West Macedonia, Greece, where the systematic overexploitation of the aquifer led to the emergence of extensive land subsidence. In this direction, all the factors that affect this phenomenon were investigated and all the data were collected at first. Then, a comprehensive methodology for the construction of both susceptibility and risk maps in land subsidence was created.

The necessary primary data have been collected through the classical geotechnical research. To this direction ,6 field campaigns have been conducted, during which all the geological and tectonic data wererecorded. In addition, 60 soil samples have been selected for laboratory soil and crystallographic analysis tests. Also, all visible surface ruptures have been mapped. In detail, the following maps were constructed: A) Four isopiezometrics contour lines maps (based on ground water level measurements conducted in October 2014, May 2015, October 2015, May 2016); B) Two equal drawdown contour lines maps (drawn by subtracting the piezometric surfaces from May 1992 to May 2015 and from May 1992 to May 2016); C) The geotechnicalmap of the Amyntaio basin; D) The distribution of the surface ruptures.

The combination of the geotechnical conditions with the tectonics and hydrogeological data of the study area eliminated the uncertainty about the mechanism of the phenomenon and highlighted the factors that play an active role (Tzampoglou and Loupasakis 2017a).

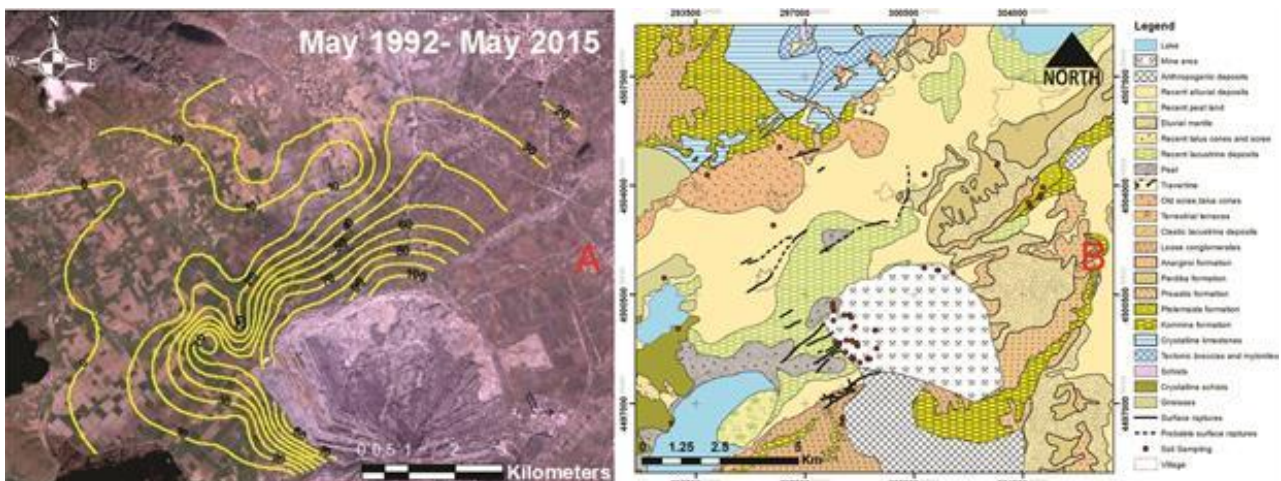


**Figure 1. A. Drawdown contour lines map drawn by subtracting the piezometric surfaces from May 1992 (Dimitrakopoulos 2001) to May 2015 (Tzampoglou and Loupasakis 2016); B. Geotechnical map of the Amyntaio basin.**



In order to determine the degree of influence of the above factors, 50 parametric analyses were carried out by using the Plaxis 3D (2016) finite element code. Taking into account the results of this analysis, it seems that the factors affecting this phenomenon (from the most dangerous to the less dangerous) are the groundwater drawdown, the geotechnical behavior of the study area, the tectonic structure and the offset of the faults (Tzampoglou and Loupasakis 2019).

The methodology applied for the production of the susceptibility and a risk map in land subsidence was based on the semi-quantitative method WLC (Weighted Linear Combination). The excellent agreement between the produced maps and the findings of the field survey, proved that the WLC method, although depending on the knowledge of experts, in cases where the quality of the available data is high and of course the expert provides the right class rating and weighting of the thematic layer, the results can be rewarding (Tzampoglou and Loupasakis 2017b; Tzampoglou and Loupasakis 2017c). The produced maps can be used by decision-making authorities for the assessment of the mining risk, the management and the mitigation of the environmental impacts.

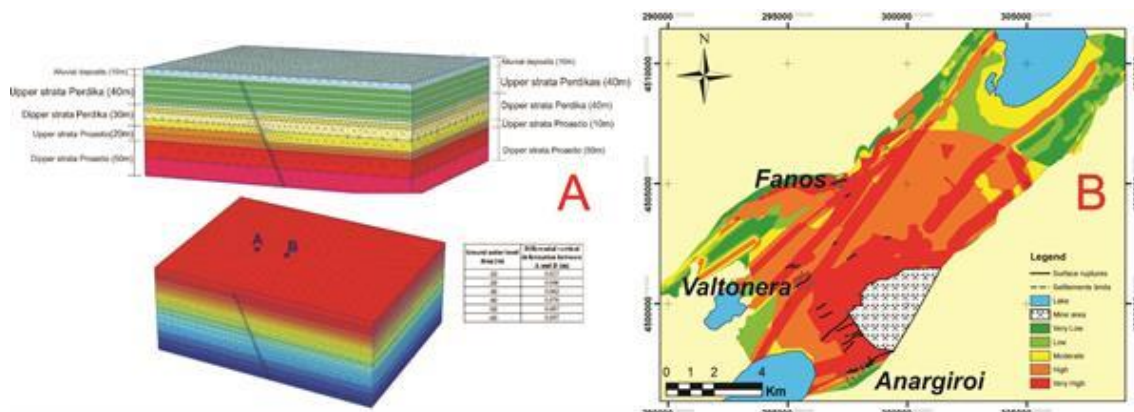


**Figure 2. A. 3D simulation model at the Valtонера village; B. Land subsidence susceptibility map in combination with the recorded surfaces ruptures**

**REFERENCES**

Dimitrakopoulos, D., 2001, Hydrogeological conditioning of Amyndeon mine. Problems during exploitation and overcoming them. Phd thesis, NTUA

Tzampoglou, P., and Loupasakis C., 2016, New data regarding the ground water level changes at the Amyntaio basin-Florina Prefecture, Greece. Bulletin of the Geological Society of Greece 50:1006-1015

Tzampoglou, P., and Loupasakis C., 2017a, Evaluating geological and geotechnical data for the study of land subsidence phenomena at the perimeter of the Amyntaio coalmine, Greece. International Journal of Mining Science and Technology 28:61-612 doi:https://doi.org/10.1016/j.ijmst.2017.11.002

Tzampoglou, P., and Loupasakis C., 2017b, Land subsidence susceptibility and hazard mapping: the case of Amyntaio Basin, Greece. In: Fifth International Conference on Remote Sensing and Geoinformation of the Environment (RSCy2017), 2017b. International Society for Optics and Photonics, pp. 104441L

Tzampoglou, P., and Loupasakis C., 2017c, Mining geohazards susceptibility and risk mapping: The case of the Amyntaio open-pit coal mine, West Macedonia, Greece. Environmental Earth Sciences 76:542

Tzampoglou P., and Loupasakis, C., 2019, Numerical simulation of the factors causing land subsidence due to overexploitation of the aquifer in the Amyntaio open coal mine. Greece HydroResearch 1:8-24

## Prehistoric rock slides in Dagestan (Caucasus, Russia): Justification of their seismic triggering by slopes' stability back analysis

Alexander Strom<sup>1</sup>, Igor Fomenko<sup>2</sup>, Vladislav Tarabukin<sup>2</sup>, Oleg Zerkal<sup>3</sup>

<sup>1</sup>Geodynamics Research Center LCC, Moscow, Russia, [strom.alexandr@yandex.ru](mailto:strom.alexandr@yandex.ru)

<sup>2</sup>Ordzhonikidze Russian State Geological Prospecting University, Moscow, Russia, [ifolga@gmail.com](mailto:ifolga@gmail.com),  
[tarabukin.vladislav@yandex.ru](mailto:tarabukin.vladislav@yandex.ru)

<sup>3</sup>Moscow State University, Moscow, Russia, [igzov@mail.ru](mailto:igzov@mail.ru)

The Dagestan Republic (Russia) is located at the North-East of the Greater Caucasus and its mountainous part is composed of thick Jurassic, Cretaceous and Cenozoic deposits folded in large brachiform folds with anticlines up to several tens of kilometers long and 5 to 9 km wide divided by narrower synclines. Lower and Middle Jurassic strata are rather ductile shale and siltstone, while Upper Jurassic to Lower Barremian unit is represented by alternating thick-bedded carbonate rocks (competent limestone and dolostone beds from ca. 50 to more than 100 m thick) and much softer terrigenous thin-bedded layers between them up to several tens meter thick. This unit is overlaid by the terrigenous upper part of the Lower Cretaceous Epoch, that in turn, is overlaid by thin-bedded carbonate Upper Cretaceous and Paleogene sediments (limestone and marl) (Brod, 1958). The competent carbonate-terrigenous unit armors anticlinal mountain ridges from ca. 500 m to more than 1200 m high (Figure 1).



**Figure 1. Overview of the anticlinal ridge with armoring limestone layer (K<sub>1</sub>br<sub>1</sub>) affected by the planar Kakh rockslide (boundary of its source zone is marked by red dashed line).**

Analysis of high-resolution space images revealed more than 15 sites where one or two armoring limestone layers had slid downslope from these anticline limbs (see Figure 1). Each of these planar slides had affected area from several hectares and up to more than square kilometer and is up to ca.  $100 \times 10^6$  m<sup>3</sup> in volume, rarely more. Exact age of these slope failures is unknown, though from the geomorphic position of their bodies and lacustrine deposits that have been found at some localities upstream, it can be assumed as Late Pleistocene, may be Early Holocene. It can be hypothesized that such rock slope failures could be triggered by strong earthquakes, moreover, this part of Dagestan, as well as the entire Greater Caucasus Range, is considered as seismically active region. Its seismicity, according to the State seismic zoning map is 8 to 9 points of the MSK-64 scale, depending on the recurrence interval.

However, strongest historical or instrumentally recorded earthquakes occurred outside this part of Dagestan, either at the northern foothills of the Greater Caucasus (1830, 1970) or at its southern slope (1668). Thus, determination of the real origin of these rockslides can provide information that will be critically important for both long-term landslide and seismic hazard assessment. It has been done by back analysis of the slope

stability. The important advantage of such modeling in this region is the possibility to restore the pre-slide topography with high accuracy, since thickness and shape of the  $K_1br_1$  limestone layer or  $K_1br_1 + K_1g$  layers that slid down can be considered as constant at each particular site.

The following back analysis of the reconstructed slopes' stability for the Kakh rockslide about 40 Mm<sup>3</sup> in volume was performed by use of the Rocscience Slide 2 software and considering linear anisotropic streaboutngth model based on the Coulomb-Mohr model. This model was selected not coincidentally. One of the main factors responsible for rockslides formation is rock massif fracturing, bedding or other discontinuities, and the linear anisotropic model assumes that minimal shear strength is along the fracture or bedding plane ( $C=20$  kPa,  $\varphi=25^\circ$ ). The quantitative slope stability assessment performed by use of the limit equilibrium method (Morgenstern, Price, 1965) showed that without seismic loading slope is safe since its Factor of Safety exceeds 1.5 regardless the exact computation method (Figure 2). It was demonstrated that this slope was destabilized by an earthquake with intensity not less than 7.5 points of the MSK-64 scale ( $PGA>0.15$  g) so that the limestone layer ca. 40 m thick slid down (Figure 3). The comparable results were obtained for several other past rockslides in this region.

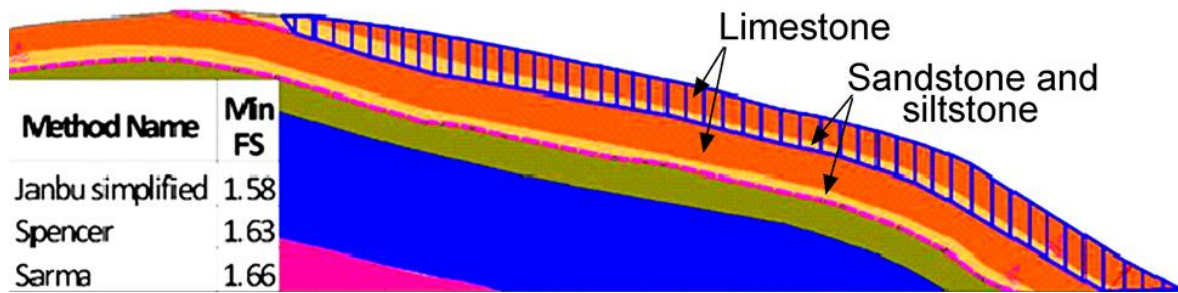


Figure 2. The geomechanical model and results of slope stability model without seismic loading. Blue hatched area – block that slid down.

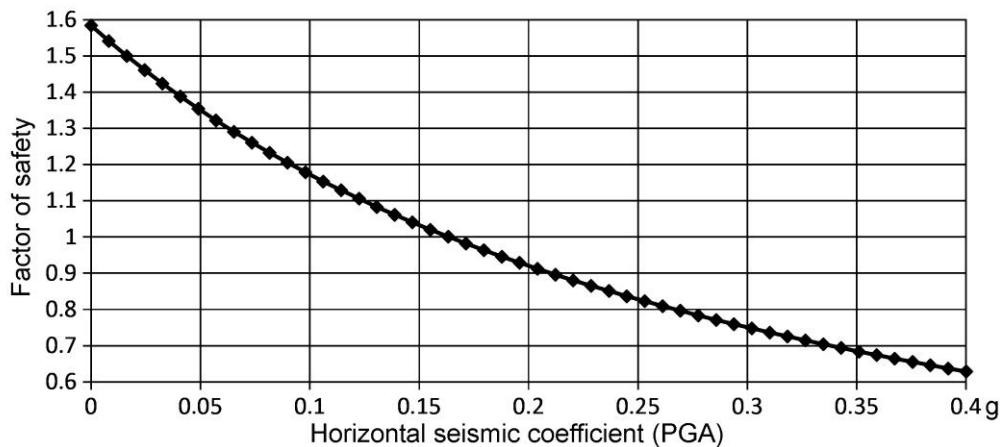


Figure 3. Dependence of safety factor from PGA at Kakh site

**REFERENCES**

Brod, I.O. (ed). 1958. Geology and oil-and-gas-bearing capacity of the Eastern Ciscaucasia. Proc. Of the Complex Southern Geological Company, Issue 1, Leningrad, Gostoptekhizdat, 621 p. (in Russian).  
 Morgenstern N.R., Price V.E. 1965. The analysis of the stability of general slip surface. Geotechnique, 15, No 1. 70-93.

## Assessing land subsidence phenomena with SAR Interferometry techniques and hydrogeological data in the Thriassio plain

Agavni Kaitantzian<sup>1</sup>, Constantinos Loupasakis<sup>1</sup>, Issak Parcharidis<sup>2</sup>

<sup>1</sup>*School of Mining and Metallurgical Engineering, National Technical University of Athens,*

[ankait@metal.ntua.gr](mailto:ankait@metal.ntua.gr), [cloupasakis@metal.ntua.gr](mailto:cloupasakis@metal.ntua.gr)

<sup>2</sup>*Department of Geography, Harokopio University of Athens, [parchar@hua.gr](mailto:parchar@hua.gr)*

Land subsidence induced by the overpumping of aquifers is an important geohazard that affects several areas worldwide subjected to intensive urban growth, industrial development and intensification of agricultural activity. In Greece, the Thessaly Plain (Ilia et al., 2016; Rozos et al., 2010), Kalochori village in the east sector of Thessaloniki plain (Costantini et. al., 2016; Raspini et. al., 2014), the Amyntaio basin of Florina Prefecture (Tzampoglou & Loupasakis, 2016; Loupasakis et al., 2014) are few examples of areas where land subsidence phenomena has been identified and monitored. The current study focuses on Thriassio plain, located 25km west of Athens city and covering an area of approximately 100km<sup>2</sup>. The geological formations constituting the Thriassio basin can be distinguished on the Mesozoic alpine formations, occupying the bordering mountains and the post-alpine deposits occupying the plain area. Considering the aquifers two systems can be distinguished at the area: a) the phreatic aquifers system occupying the coarse-grained Quaternary deposits and b) the deeper karstic at the underling karstified carbonate formations.

The knowledge of the piezometric conditions, the geotechnical characteristics and the space born radar measurements data are essential for the interpretation of the land subsidence phenomenon. For the purpose of this study, available records of piezometric level measurements have been evaluated for the comparison of groundwater level contour maps between 2000 and 2016. From the comparison of the two aforementioned piezometric surfaces, a ground water drawdown, reaching 16m northwest of the study area was observed. Furthermore, the isopiezometric curves of April 2016 and September 2016 indicate a drawdown cone in Kato Fousa, probably caused by the exploitation applied for irrigation purposes.

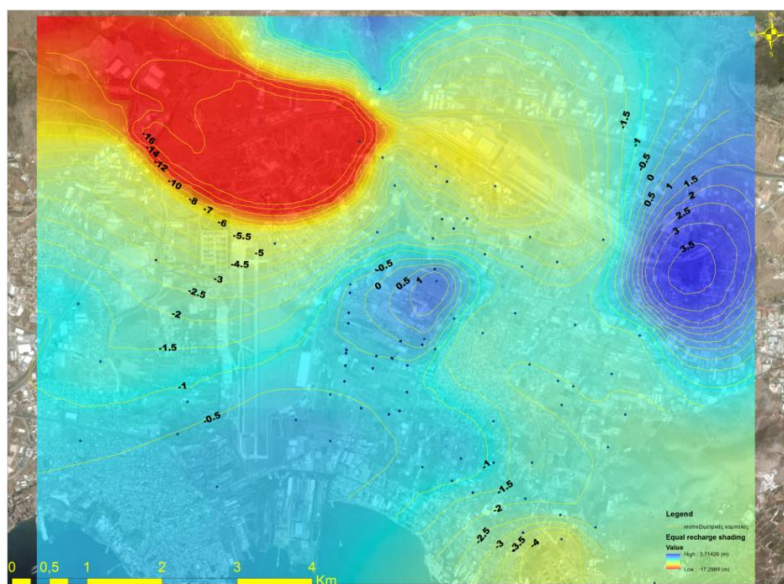
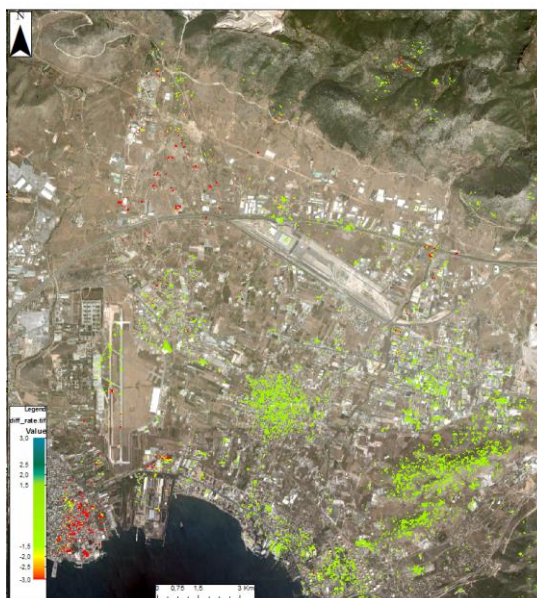


Figure 1. Equal drawdown contours between April 2016 and March 2000



The spatial distribution and the deformation rates of the land subsidence phenomena were attributed by the evaluation of PSI and SVD data. The PSI results of ERS 1&2 data from 1992 to 2001 indicate that the entire area extending northwest of the Aspropyrgos town exhibits displacements ranging between -3 and -10 mm/yr, along the Line of Sight (LOS). On the contrary, the SVD results of ENVISAT data from 2002 to 2010 indicate that the Elefsis town and the northern west part of the Thriassio plain have been exhibiting deformations of -3mm/yr along the LOS. The outcomes of the present study indicated that the land subsidence phenomena must be attributed primarily to the exploitation of groundwater reservoir resulting to the compaction fine-grain Quaternary formations.



**Figure 2. Deformation rates for the period 2002-2010, according to the SVD dataset**

## REFERENCES

- Costantini F., Mouratidis A., Schiavon G., and Sarti F., 2016. Advanced InSAR techniques for deformation studies and for simulating the PS-assisted calibration procedure of Sentinel-1 data: Case study from Thessaloniki (Greece), based on the Envisat / ASAR archive, *International Journal of Remote Sensing*, v.37, pp. 729-744.
- Iliá I., Loupasakis C. and Tsangaratos P., 2016. Assessing ground subsidence phenomena with persistent scatterer interferometry data in western Thessaly, Greece, *Proceedings of the 14th International Congress of the Geological Society of Greece*, *Bulletin of the Geological Society of Greece*, v. L, 3.
- Loupasakis C., Agelitsa B., Rozos D., Spanou N., 2014. Mining geohazards—land subsidence caused by the dewatering of opencast coal mines: The case study of the Amyntaio coal mine, Florina, Greece. *Natural Hazards*, Springer, v.70, pp. 675–691.
- Raspini, F., Loupasakis, C., Rozos, D., and Moretti, S., 2014. Advanced interpretation of land subsidence by validating multi-interferometric SAR data: the case study of the Anthemountas basin (northern Greece), *Nat. Hazards Earth Syst. Sci. Discuss.*, v.1, pp. 1213–1256.
- Rozos, D., Sideri, D., Loupasakis, C., and Apostolidis, E., 2010. Land subsidence due to excessive groundwater withdrawal, a case study from Stavros-Farsala site, west Thessaly Greece, *Proc. of the 12th International Congress, Patras, Bull. Geol. Soc. Greece*, v. 4, pp. 1850–1857.
- Tzampoglou P., Loupasakis C., 2016. New data regarding the ground water level changes at the Amyntaio basin- Florina Prefecture, Greece, Athens, Greece. *Proceedings of the 14th International Congress of the Geological Society of Greece*, *Bulletin of the Geological Society of Greece*, v. L, 2, pp.1006-1015.



## Rainfall thresholds for forecasting shallow rainfall-induced landslides in western Greece

Spyridon Lainas<sup>1</sup>, Nikolaos Depountis<sup>2</sup>, Nikolaos Sabatakakis<sup>3</sup>

<sup>1</sup>*Dr Engineering Geologist, University of Patras, Greece, [splainas@upatras.gr](mailto:splainas@upatras.gr)*

<sup>2</sup>*Assistant Professor of Engineering Geology, University of Patras, Greece, [ndepountis@upatras.gr](mailto:ndepountis@upatras.gr)*

<sup>3</sup>*Professor of Engineering Geology, University of Patras, Greece, [sabatak@upatras.gr](mailto:sabatak@upatras.gr)*

Empirical rainfall thresholds and combination between landslides triggering and rainfall can be a useful tool for landslide forecasting. Indeed, the establishment of the quantitative relationship between rainfall conditions and landslide trigger are an important element during the design of a landslide warning system for use in urban planning and design, transportation networks and main infrastructures. In the frame of Climate change, the corresponding observed changes in the frequency and pattern of extreme meteorological events (e.g. high temperatures, droughts and rainfall regime), as well as in the human environment, there is a strong confidence that the current status in related natural disaster, as for example landslide activity, will also change. So, the comprehensive study of the correlation between landslides and rainfall can, doubtless, aid to the better understanding of the influence of rainfall in landslide triggering in specific geological and climatic conditions by providing a tool towards landslide hazard, prediction and mitigation.

The aim of this paper is to use recently published empirical rainfall thresholds in western Greece towards shallow landslide forecasting by means of exceedance statistics and probability estimates. Study area is located within affected areas by the wildfires of August 2007, one of the most devastating wildfires that have ever happened on European level. During the 4-year period post-fire period soil erosion and shallow landslide phenomena triggered by seasonal heavy rainfall were triggered, mainly in Neogene fine sediments and Flysch formations, causing severe social-economic damage. Throughout comprehensive methodology for detailed landslide recording and daily rainfall data connections relationships between observed landslide events and associated rainfalls were established in order to define the conditions that favor landslide trigger. Through this work, cumulative event rainfall – duration (ED) and Rainfall Intensity – Duration (ID) empirical rainfall thresholds for possible landslide initiation for both pre- and post-fire conditions were proposed.

The jointed analysis of landslide activation, rainfall data and exceedance probability statistics helped to analyse the frequency of the critical rainfall thresholds values. This process helped to determine the annual exceedance probability of a shallow landslide under specific geological and rainfall conditions, given rainfall events of known cumulative rainfall and duration, also separating analysis for pre- and post-fire conditions. As a final result, annual probability rates for rainfall-induced landslides trigger were estimated.

This approach can provide key data for regional landslide data analyses aiming to distinguish between different probability levels for the manifestation of a landslide event in a specific region, under certain climatic and engineering geological conditions. It can contribute towards landslide hazard and risk analyses and has exceptional interest in the concept of Climate Change and its direct or indirect impact on human and physical environment.

### REFERENCES

- Brunetti, M.t., Peruccacci, S., Rossi, M., Luciani, S., Valigi, D. and Guzzetti, f., 2010, Rainfall thresholds for the possible occurrence of landslides in Italy. *Nat. Hazards Earth Syst. Sci.*:pp447-458.
- Chleborad, A.F., Baum, R.L., Godt J.W., 2006, Rainfall thresholds for forecasting landslides in the Seattle, Washington,



Area – Exceedance and Probability. USGS Open-File Report 1064, pp30.

Depountis, N., Lainas, S., Koulouris, S., Pyrgakis, D., Sabatakakis, N and Koukis, G., 2010, Engineering geological and geotechnical investigation of landslide events in wildfire affected areas of Ilia Prefecture, Western Greece. Bulletin of the Geological Society of Greece vol. XLIII, 2010, Proceedings of the 12th International Congress, Patras, May, 2010, Part 3, pp.1138-1148.

Gariano, S.L. and Guzzetti, F. ,2016, Landslides in a changing climate. Invited Review, Earth-Science Reviews, 162, pp. 227–252.

Gostelow, T.P. ,1991, Rainfall and landslides. Engineering geology research group. British Geological Survey pp. 139-161.

Guzzetti, F., Peruccacci, S., Rossi, M., Stark, C.P., 2007, Rainfall thresholds for the initiation of landslides in central and southern Europe. Meteorol Atmos Phys 98, pp 239-267.

Lainas, S., Sabatakakis, N., Koukis G., 2016, Rainfall thresholds for possible landslide initiation in wildfire-affected areas of western Greece. Bulletin of Engineering Geology and the Environment, v75, pp. 883-896,

Sabatakakis, N., Koukis, G., Vassiliades, E., Lainas, S., 2013, Landslide susceptibility zonation in Greece. Natural Hazards, v65,1, pp.523-543.

## Investigation of tectonized limestones in western Lefkada Island with field and laboratory testing and back-analyses of co-seismic landslides

Vasilis Kallimogiannis<sup>1</sup>, Charalampos Saroglou<sup>2</sup>, G. Palantzas<sup>3</sup>

<sup>1</sup>Ph.D. student, School of Civil Engineering, NTUA, Greece, e-mail: [vkallim@hotmail.com](mailto:vkallim@hotmail.com)

<sup>2</sup>Teaching & Research Associate, School of Civil Engineering, NTUA, Greece, e-mail: [saroglou@central.ntua.gr](mailto:saroglou@central.ntua.gr)

<sup>3</sup>MSc student, School of Civil Engineering, NTUA, Greece, e-mail: [georgios.palantzas@hotmail.com](mailto:georgios.palantzas@hotmail.com)

### **Background**

Lefkada Island consists of carbonate rock masses of the Ionian Zone, limestones of the Paxos Zone and sporadic developments of Ionian flysch, sandstones and marls (Bornovas, 1964; Rondoyanni-Tsiambaou 1997). The presence of NE-SW to NNE-SSW trending fault systems along the western part of Lefkada Island has resulted in intense tectonization of the limestone rock masses. As the coastal area is inaccessible and steep, the mechanical behavior of these weak rock masses has not been adequately studied. Additionally, laboratory testing in these materials is very challenging as sampling is almost impossible due to its completely disintegrated nature.

### **Methodology**

An in-situ investigation was conducted along the west coast of Lefkada Island to characterize these weak rock masses and perform point load and schmidt hammer tests. Moreover, samples of intact limestone and limestone breccia were collected to investigate the mechanical properties of the intact rock in the laboratory.

To assess the response of the entire geological formations during seismic loading, 3D limit equilibrium back-analyses in three co-seismic landslides that occurred in 2015 in Egremnoi beach were also conducted. The pre- and post-earthquake landslides' surface were determined using data from the Hellenic National Cadastre and field mapping with Unmanned Aerial Vehicles (UAVs) that generated a 3D Point Cloud model using the Structure-From-Motion (SfM) technique (Zekkos et al. 2018). The backanalyses results were evaluated using the Mohr-Coulomb failure criterion (Kallimogiannis et al., 2019).

### **Results and Conclusions**

The limestones in the study area are tectonised and are either characterized as limestone breccia or brecciated limestone depending on the degree of brecciation. A detailed map presenting the sites visited and the rock mass characterization in each one is shown in Figure 1. The locations where intact rock blocks were collected to perform laboratory tests are included. Laboratory testing is underway in both intact and brecciated samples, consisting of uniaxial and triaxial testing, determination of wave velocity and acoustic emission testing.

Based on point load and schmidt hammer tests in the field, a histogram of the derived  $I_{s50}$  and the correspondent UCS in various study locations is presented in Figure 2. The average uniaxial compressive strength was 76.5 MPa.

The back-calculations conducted in Egremnoi site for the three co-seismic landslides showed that the actual strength of the in-situ material is highly reduced. Weathering and tectonic processes have deteriorated its mechanical properties. As a result, the material can be characterized as a weak rock-hard soil. A typical cohesion-friction angle curve of a back analysis is presented in Figure 2 (Kallimogiannis et al., 2019).

The uniaxial compressive strength of the intact rock determined in the laboratory for the limestone and the

limestone breccia was 86,2 MPa and 105 MPa respectively, providing significant data about the upper strength of the material.



Figure 1: Rock mass characterization of the sites visited in western Lefkada

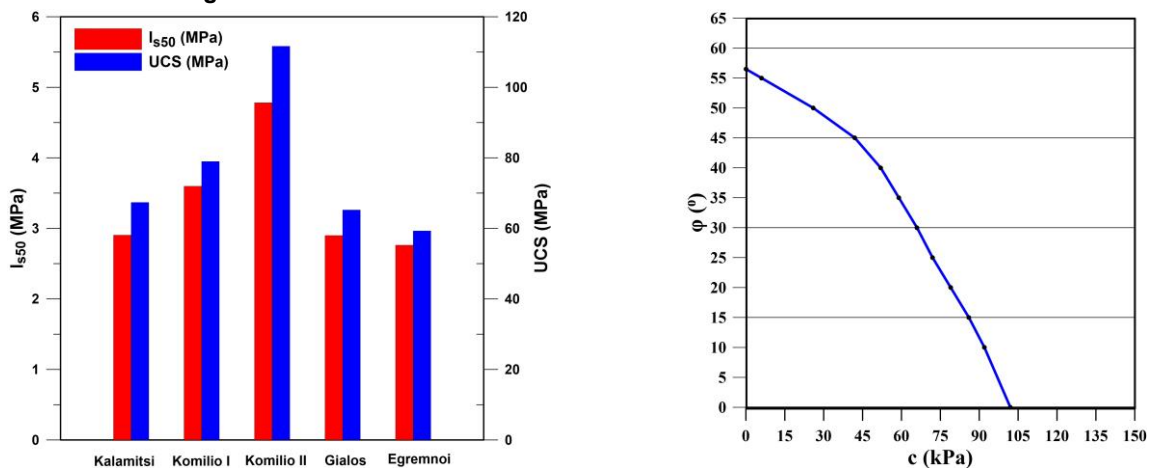


Figure 2: a) Histogram of spatial distribution of  $I_{s50}$  indices and the derived Uniaxial Compressive Strength obtained from point load tests in Western Lefkada and b) C- $\phi$  envelope of a 3D limit equilibrium back analysis for a co-seismic landslide in Egremnoi, Lefkada Island

### References

Bornovas J., (1964). Géologie de l'île de Lefkade, vol 1, 10th edn, Geological geophysique research (IGSR). Geological Geophysique Research, Athens.

Kallimogiannis V., Saroglou H., Zekkos D., Manousakis J. (2019). Back-analysis of landslide in Egremnoi caused by the 2015 Lefkada earthquake. Proc. of 2nd Int. Conference on Natural Hazards & Infrastructure, 2019; Chania, Greece.

Rondoyanni-Tsiambaou, Th., (1997). Les seismes et l'environnement geologique de l'île de Lefkade, Grece: Passe et Futur. In: Marinos, et al., (Eds.), Engineering Geology and the Environment. Balkema, 1469– 1474.

Zekkos, D, Greenwood, W., Lynch J., Manousakis, J., Zekkos, A., Clark, M., Cook, K. & Saroglou, H. (2018). Lessons Learned from The Application of UAV-Enabled Structure-From-Motion Photogrammetry in Geotechnical Engineering. 4. 254. 10.4417/IJGCH-04-04-03.



## Geohazard evaluation in central Nepal Himalaya with focus on landslide

Prem Bahadur Thapa<sup>1</sup>

<sup>1</sup>*Department of Geology, Tri-Chandra Multiple Campus, Tribhuvan University, Kathmandu, Nepal,*  
[geoscithapa@yahoo.com](mailto:geoscithapa@yahoo.com)

Nepal lies in the central part of the seismo-tectonically active Himalayan belt and it is prone to various kinds of geohazards which are causing serious threats to human lives, property, and infrastructures. Among the various types of geohazards, landslide is one of most significant and pervasive geohazard in central Nepal Himalaya. Earthquakes are often considered the most important geohazards but much of the damage may be caused by the secondary hazards such as landslides and large mass-flows triggered by them. The landslides present a widely distributed geohazard and pose a risk to many developments. Occurrences of landslides are almost every year during the rainy season, therefore landslides are always the biggest challenge for resettling displaced peoples and important for any reconstruction strategies after the great earthquake or extreme weather events. Various types of landslides are occurring in the central Nepal Himalaya due to variable topography, diverse geology and frequent extreme events. Rainfall and earthquake play the critical role to cause the mountain hill-slopes vulnerable to landslides and other mass movements. Spatial distribution of landslides are found in steep slopes of river valleys, close proximity to thrust/faults or boundary between competent and incompetent geological units. Daylight conditions in dip-slopes are the main cause of landslides when excavations are made with inclined strata. Landslides are frequently initiating as planar slides and that converted into debris slide to flow and usually moves in down-slope with high speed.

The geohazard evaluation with focus on landslide has been carried out through extracting the relevant information from satellite images in addition to the use of available secondary information as well as field study. A GIS database has been developed with the required information, which was used to prepare various thematic layers (like geology, drainage proximity, slope, aspect, rainfall or peak ground acceleration), followed by further analysis. Statistical modeling is considered to be useful for landslide hazard modeling due to the large spatial variability of the mechanical, hydrological, and geometrical parameters in different geo-environmental settings. Modeling of landslide hazard in typical area of central Nepal Lesser Himalaya has indicated the maximum occurrence of landslides in highly susceptible zones and computed success and prediction rates also showed the area under curve (AUC) varied from 0.91 to 0.94 within prediction accuracy of 0.5 to 1. It is concluded that geohazard caused by landslide in central Nepal Himalaya is because of the interplay of various factors such as geology, geological structures, slope geometry, and rainfall or earthquake.



## Long-term rockslope monitoring and rockfall prediction

Miloš Marjanović<sup>1</sup>, Biljana Abolmasov<sup>1</sup>, Marko Pejić<sup>2</sup>, Jelka Krušić<sup>1</sup>

<sup>1</sup>University of Belgrade, Faculty of Mining and Geology, Serbia, [milos.marjanovic@rgf.bg.ac.rs](mailto:milos.marjanovic@rgf.bg.ac.rs),

[biljana.abolmasov@rgf.bg.ac.rs](mailto:biljana.abolmasov@rgf.bg.ac.rs), [jelka.krusic@rgf.bg.ac.rs](mailto:jelka.krusic@rgf.bg.ac.rs)

<sup>2</sup>University of Belgrade, Faculty of Civil Engineering, Serbia, [mpejic@grf.bg.ac.rs](mailto:mpejic@grf.bg.ac.rs)

### Background

Many rockfalls are unpleasant reminders of the damage they can inflict, including human casualties; traffic interruption; property damage; river damming and secondary floods and landslides. Dealing with rockfalls is a major topic for decision-makers and engineers, targeted at answering where and when will rockfalls occur and what preventive and remediation measures should be undertaken to neutralize them. Rock faces can be monitored for longer periods, using multiple monitoring systems (geodetic, geotechnical, etc.), annually, seasonally or in real-time, which provides the data needed for better understanding of the (pre)failure stages, leading to their efficient prediction.

### Methods

Terrestrial Laser Scanning (TLS) revolutionized the rockslope monitoring and proved to be one of the most efficient and most robust approaches. It is based on change detection of point clouds, collected in sequences, annually or more frequently, depending on the slope's dynamics. Each new point cloud can be compared against any of the previous, and all detectable changes can be calculated, commonly by Cloud-to-Cloud distance method, thereby delineating areas of detachment or volume loss, and areas of accumulation or volume gain.

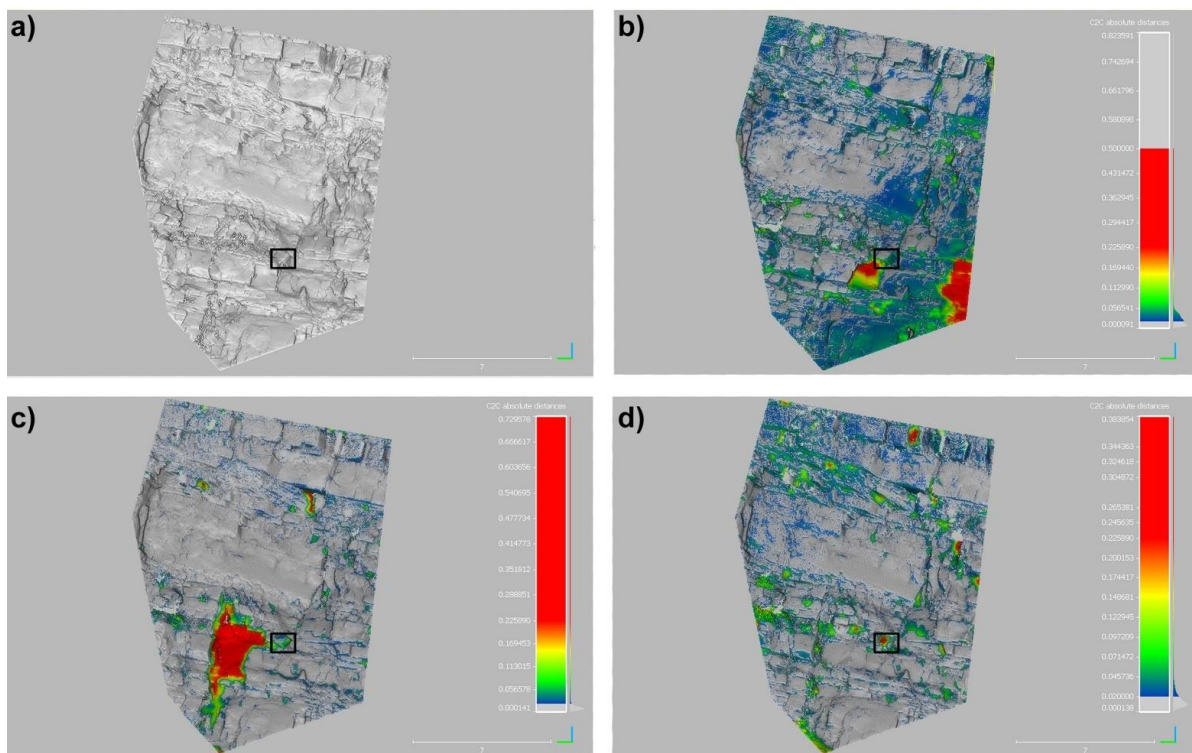


Figure 1. Example of differential displacement change detection: a) Initial point cloud from 2012 sequence; b) Sequence 2013 vs. 2012; c) Sequence 2014 vs. 2013; d) Sequence 2016 vs. 2014.



### **Case Study: A Rockslope near LJIG**

The road cut near Ljig is one of those threatening rockfall cases. It was monitored by using TLS, sequentially at least once a year, since 2012. The site was investigated for various slope features, such as, kinematic analysis, joint densities, block sizes, detached volumes and rockfall simulations (Bogdanović et al. 2015, Marjanović et al. 2017). Several rockfalls have been identified throughout the years (Figure 1). Long-term monitoring provided evidence of precursory deformation captured by the Cloud-to-Cloud change detection. A small volume (approximately half a cubic meter, outlined in a black frame in Figure 1) was affected by adjacent large detachment from 2013 (Figure 1b), which expectedly, progressed in time. From initial differential change vector of approximately 0.01 m (Figure 1c), through further progression with significant displacement of approximately 0.07 m, this small block was clearly detached in 2016 (Figure 1d). Precursory deformations of blocks that have high probability to detach can be mapped across the entire rockslope (Figure 1d).

### **Conclusions**

TLS-based rockslope monitoring is an advancing field in Geotechnics. Conventional practice remains accountable, but TLS extends monitoring possibilities further. It does not only diagnose rockfalls post festum (back-analysis), but also enables prediction of new events by identifying their precursor deformations.

### **REFERENCES**

- Bogdanović, S., Marjanović, M., Abolmasov, B., Đurić, U., Basarić, I., 2015, Rockfall monitoring based on surface models. In: Surface Models for Geosciences. Růžičková, Inspector (eds). Springer International Publishing, pp. 37–44.
- Marjanović, M., Abolmasov, B., Pejić, M., Bogdanović, S., Samardžić -Petrović, M., 2017, Rockfall monitoring and simulation on a rock slope near Ljig in Serbia. Proceedings of the 3rd Regional Symposium on Landslides in the Adriatic Balkan Region. 11–13 October 2017. Slovenia, Ljubljana, pp. 83–88.



## Fault influence zones assessment and its accounting in site investigations

Olga Barykina<sup>1</sup>, Oleg Zerkal<sup>2</sup>, Ernest Kalinin<sup>3</sup>

<sup>1</sup>Senior research scientist, Faculty of Geology, Lomonosov Moscow State University, Russia,  
[ol.barykina2011@yandex.ru](mailto:ol.barykina2011@yandex.ru)

<sup>2</sup>Chief of Engineering Geodynamics Lab, Faculty of Geology, Lomonosov Moscow State University, Russia,  
[igzov@mail.ru](mailto:igzov@mail.ru)

<sup>3</sup>Professor, Faculty of Geology, Lomonosov Moscow State University, Russia, [kalinin@sumail.ru](mailto:kalinin@sumail.ru)

The problem of fault estimation in engineering surveys is rather complicated and bad studied. Fault zones, where modern movements are fixed, can be a place of intensive surface movements during earthquakes. Active movements of the Earth's crust cause changes in strength, deformation and filtration properties of rocks in the massif. Movements in tectonic faults can lead to redistribution of stresses in the rocks of high slopes, to occurrence of stresses exceeding strength of rocks and dangerous for slope stability. The zones of fault influence cannot be clearly and fully fixed at the construction site without proper research. Abstract touches on the question of potential hazardous zone estimation within which the development of dangerous geological processes is possible.

With the help of numerical modeling the criteria for assessment of the potential size of the dynamic influence area has been developed. Also the questions of correspondence of observed changes in massif - real fault zone geometry, location of stress concentration areas, movement of free surface, change of these parameters as a result of change of any condition were discussed. The purpose of the modeling was to estimate the size of fault area, to identify the peculiarities of stress distribution within this area and how it affects the stability of the landslide slopes.

### Geology

The construction site of Rogun dam was chosen as the object of research. The Rogun dam site is located within the joint zone of two major structural regions of Central Asia - South-Western Tien Shan and Tajik Depression. Seismic activity of the territory is very high, up to 9. Located in the upper Vakhsh River in Tajikistan, the dam, about 350 m high, is located in a single tectonic block, bounded by sub-parallel Ionakhsh and Gulizindan regional faults (second order).

The canyon sides of the Vakhsh River are composed of sediments of Cretaceous age and represent a thickness of unevenly interspersed sandstones and siltstones with interlayers of argillites. The territory of Rogun dam site is broken up by numerous faults of different orders.

The site of the Rogun HPP is located directly in Ionakhsh Fault influence zone, which crosses the river at the upper wedge of the dam. Here, the fault falls to the southeast at an angle of 75-80°, stretching parallel to the stretch of rocks.

The results of complex inclinometric-deformographic observations at the site has shown that all faults are tectonically active. Vertical displacements of the Ionakhsh Fault edges, in 1-3 mm per year, have been recorded.



## **Methods**

The calculation scheme was based on the geological materials of "Hydroproject" Institute, Russia. The width of the Ionakhsh Fault together with the crushing zone on the surface was taken as 20 m. In the calculation scheme for all rocks it was accepted: deformation module - 30 MPa; Poisson's coefficient - 0.3; density - 2.6 g/cm<sup>3</sup>. Horizontal compressive tectonic force was given equal to 12 MPa.

For this, firstly, the stress-strain state of fault zone under the action of gravitational force was studied; secondly, the same under the action of gravity and tectonic force; and thirdly, the direction and magnitude of free surface displacements (from stresses) under the action of gravity and tectonic. This was done with the help of calculations based on the method of boundary elements. Calculations were performed using a computational program for 2D method of discontinuous displacements, developed by researchers of the geological faculty of Lomonosov Moscow State University. The rock massif was considered as an isotropic linear-elastic environment, taking into account the influence of the following factors: terrain features; disturbance of the massif by the fault; gravity; horizontal compression force simulating the tectonic force.

## **Results**

Simulation results have shown that the dynamic influence zone is limited to 200 m on the side of the lying block and 70 m on the side of the hanging block. The stress concentration zones are located at the mouth and in the middle part of the fault on the side of the lying block and between the hanging side of the fault and the bottom of the valley.

According to engineering and geological surveys, the width of tectonic breccia zone of the Ionakhsh Fault is equal up to 80 m, and with the zone of cracking the influence of the fault may increase up to 120 m. However, according to the calculations, this zone is about 270 m. Thus, the numerical calculations have shown that the zone of stress-strain state change exceeds the zone of changed rocks observed in the massif. Moreover, on the side of the lying block zone of stress-strain state is more than twice as much as that of the hanging block. Accordingly, the real zone of fault influence exceeds directly measured more than twice.

## **Conclusions**

1. The method of boundary elements makes it possible to characterize stresses in the rock massifs and free surface movement near the fault.
2. This method can be used to predict the location of areas of stress concentration in the fault dynamic zone.
3. By means of numerical modeling the area of near-fault changes can be estimated experimentally, and thus the width of the dynamic influence zone can be determined.
4. The width of the zone of elastic transformations caused by the fault and obtained with the help of calculations is 2.17 times more than the width of the zone we can see in nature.
5. On the basis of comparison of dynamic influence zone width, received at calculations, with the "nature" width we can observed on the site, it is possible to assert, that the zone of dynamic influence of fault includes not only observed changes of rocks (crushing and cracking), but also area of the stress state changes.
6. The presented results are just a preliminary estimation of the potential zone size that can be unfavorable within construction site.
7. Within this area, during construction and operation, dangerous geological processes, such as landslides, debris flows, rock impacts, rock avalanches and others may occur.

## Bayesian probabilistic back-analysis and run-out prediction of landslides: a case study in the Heifangtai, Gansu Province, China

Peng Zeng<sup>1</sup>, Xiaoping Sun<sup>1</sup>, Tianbin Li<sup>1</sup>, Rafael Jimenez<sup>2</sup>

<sup>1</sup>State Key Laboratory of Geo-hazard Prevention and Geo-environment Protection  
(Chengdu University of Technology), Chengdu, China, [zengpeng15@cdut.edu.cn](mailto:zengpeng15@cdut.edu.cn),  
[sunxiaoping1996@gmail.com](mailto:sunxiaoping1996@gmail.com), [ltb@cdut.edu.cn](mailto:ltb@cdut.edu.cn)

<sup>2</sup>Technical University of Madrid, Madrid, Spain, [rafael.jimenez@upm.es](mailto:rafael.jimenez@upm.es)

Input parameters of dynamic numerical models for landslide run-out distance simulation cannot be measured accurately, resulting in large uncertainties existed in these models (Hung and McDougall 2009; Luna 2012; van Westen et al. 2006). In order to quantify these uncertainties, this paper proposes a new methodology for landslide run-out distance modelling from probabilistic back-analysis to probabilistic run-out prediction. A continuum mechanics concept-based dynamic numerical model namely Massflow (Ouyang et al. 2013), is used herein to conduct run-out analysis. Model input parameters —i.e., effective friction angle and pore pressure ratio— are modeled as random variables, and their distributions are efficiently improved using Markov Chain Monte Carlo-based Bayesian inference with observed run-out distance of a past event. With the improved posterior distributions, the probabilistic run-out prediction is carried out using Monte Carlo Simulation to produce a run-out distance exceedance probability curve of a potential landslide similar to the past event. In order to improve the computational efficiency of the proposed methodology, a Kriging-based surrogate model is employed to approximate the dynamic numerical model, and following probabilistic back analysis and probabilistic run-out prediction can be performed based on the surrogate model. Two sequential landslides, DC2# landslide occurred in 2015 and DC3# landslide occurred in 2016, located in the Heifangtai, Gansu, China, are employed to demonstrate performance of the proposed methodology.

Prior distributions are updated using Bayesian inference with the observed run-out distance of DC2# landslide (780 m), and the results are presented in Figure 1. It is observed that the updating degree of the pore pressure ratio is greater than the effective friction angle, reflecting that the pore water pressure has a greater influence on the run-out distance; and that the standard deviations of both random variables are decreasing after the updating, indicating that uncertainties of input parameters can be reduced through the back-analysis. With the updated posterior distributions, the run-out distance exceedance probability curve of DC3# landslide is produced using the surrogate model coupling with Monte Carlo Simulation. Based on the landslide run-out distance-exceedance probability curve, with the given probability classification (50%, 10%, 1%, and 0.1%), the potentially affected area of DC3# landslide is classified into five categories (i.e., extremely high, high, medium, low, and extremely low), as shown in Figure 2. Several conclusions can be drawn from this study: (i) probabilistic back-analysis provides information about the uncertainties in the calibrated input parameters, which is useful for probabilistic run-out forward prediction; (ii) with the results of probabilistic back-analysis of DC2# landslide, the hazard zoning of DC3# landslide is conducted based on the exceedance probability of run-out distance for points at different locations along the landslide path, which may provide a new perspective for landslide hazard mapping; (iii) accuracy check of Kriging-based surrogate model shows that the model trained with 300 training data (i.e., 300 dynamic numerical simulations) has sufficient accuracy, which greatly improves the computational efficiency compared to direct Monte Carlo Simulation.



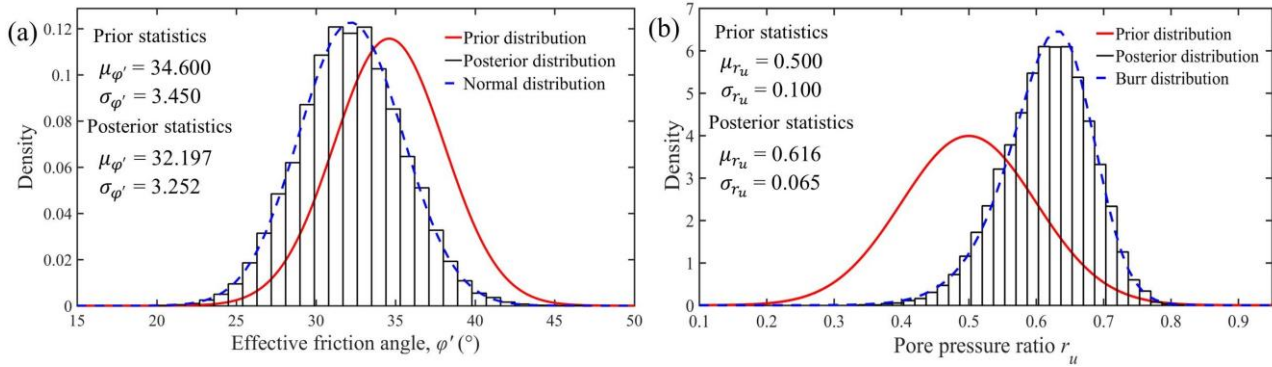


Figure 1. Prior and posterior distributions of the effective friction angle (a) and the pore pressure ratio (b)

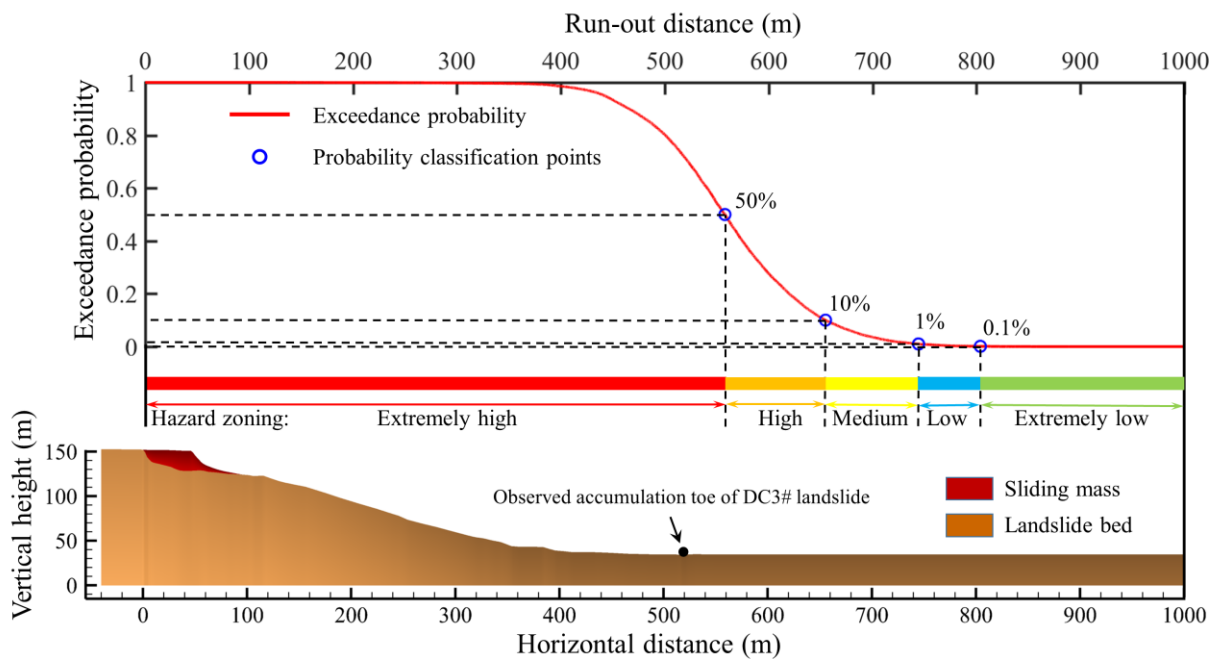


Figure 2. Run-out hazard zoning of DC3# landslide based on the run-out distance-exceedance probability curve

REFERENCES

Hungr, O. & McDougall, S., 2009, Two numerical models for landslide dynamic analysis. *Computers & Geosciences*, 35, 978-992

Luna, B.Q. 2012, Dynamic numerical run-out modeling for quantitative landslide risk assessment. Thesis of University of Twente, ITC, 206, 1-237

Ouyang, C., He, S., Xu, Q., Luo, Y. & Zhang, W., 2013, A MacCormack-TVD finite difference method to simulate the mass flow in mountainous terrain with variable computational domain. *Computers & Geosciences*, 52, 1-10

van Westen, C.J., van Asch, T.W.J. & Soeters, R., 2006, Landslide hazard and risk zonation—why is it still so difficult? *Bulletin of Engineering Geology and the Environment*, 65, 167-184

## Soil Liquefaction evidences during the November 26th 2019 Durres Earthquake, Albania

Shkëlqim Daja<sup>1</sup>, Besnik Ago<sup>1</sup>, Çerçis Durmishi<sup>1</sup>, Shaqir Nazaj<sup>1</sup>, Arjol Lule<sup>1</sup>, Neritan Shkodrani<sup>2</sup>

<sup>1</sup> Polytechnic University of Tirana, Faculty of Geology and Mining, Albania, [shkelqim.daja@fgjm.edu.al](mailto:shkelqim.daja@fgjm.edu.al), [besnik.ago@fgjm.edu.al](mailto:besnik.ago@fgjm.edu.al), [cecodurmishi@yahoo.com](mailto:cecodurmishi@yahoo.com), [shaqir.nazaj@fgjm.edu.al](mailto:shaqir.nazaj@fgjm.edu.al), [arjol.lule@fgjm.edu.al](mailto:arjol.lule@fgjm.edu.al)

<sup>2</sup> Polytechnic University of Tirana, Faculty of Civil Engineering, Albania, [neritans@yahoo.com](mailto:neritans@yahoo.com)

On November 26, 2019 at 01:54 GMT, a 6.3 Magnitude earthquake having a focal depth of 38 km (according to IGEWE, Institute of GeoSciences, Energy, Water and Environment) shook Albania. Its epicenter was located in Lalëzi Bay area, 15 km in the North of Durres city. The earthquake was associated with significant structural damages in the cities of Durres, Vore, Thumane, Shijak, Tirana, and in all the epicentral areas.

Ground failures, consisting in line-arranged sand boils, lateral spreads, damages to road pavements and building foundations occurred, caused by soil liquefaction.

During the period from 26/11/2019 to 05/12/2019 field surveys, mainly focused on identifying and mapping the liquefaction evidences, were carried out in Durres and Lalëzi Bays, covering an area of about 75 km<sup>2</sup>. The purpose of this campaign was to identify all superficial evidences of the phenomenon aiming not only to understand its spatial distribution but, also to collect data for further analysis based on geotechnical measurements, such as geotechnical boreholes, CPTU profiling etc.

Series of line-arranged sand boils along cracks of different lengths and directions, lateral spreading cracks, differentiated settlements between the buildings and their sidewalks, deformation of the boundary walls and road pavements, are identified and mapped. At each site, the location, the main orientation and crack extension, the diameter of the sand volcanoes, the distance between them, and where possible, the volume of the ejected sand were estimated. Differentiated settlements between the buildings and their sidewalks as well as the dimensions of road cracks are measured.

The results of the field observations are represented in a georeferenced map accompanied by an adequate legend.

A continuous coring borehole accompanied by SPT (Standard Penetration Test) was performed. Samples of ejected sand from the sand boils and from the borehole were collected and analyzed in laboratory regarding their grain size distribution as well as their mineralogical composition.

Based on the spatial distribution of the phenomenon, the results of field surveys and laboratory analysis some preliminary conclusions have been drafted regarding the stratigraphy of the liquefied soils, their geological characteristics as well as their stress history.

## Roadmap to an early warning system in a large landslide near Tbilisi, Georgia

Klaus Keilig<sup>1,2</sup>, Markus Bauer<sup>2</sup>, Peter Neumann<sup>2</sup>, Kurosch Thuro<sup>1</sup>







<sup>1</sup>Technical University of Munich, Chair for Engineering Geology, Germany, [kp.keilig@tum.de](mailto:kp.keilig@tum.de)

<sup>2</sup>Baugeologisches Büro Bauer GmbH, Germany, [mail@baugeologie.de](mailto:mail@baugeologie.de)

In June 2015 a flash flood caused by a failure of a natural dam originated by a hazardous debris flow in the Vere valley hit Georgias capital Tbilisi. The landslide mass temporarily blocked the Vere river and a flash flood impacted in Tbilisi after failing of the dam (UNDP 2015, Gaprindashvili et al. 2016). More than 700 citizens were directly affected, direct physical damage was estimated to be at least USD 24 mio and most tragically it caused 23 fatalities (UNDP 2015). The catchment area is a region of high landslide susceptibility with a range of active and expectable processes with differing intensities and volumes. The event of 2015 must be seen as megaevent with a recurrence period of several 1000s of years or even more. However, the landslide has created even more unstable conditions and weakened an already semi-stable system. As conclusion, the likelihood for medium to large subsequent events has risen significantly.



### Legend:

	Meteo station and central data acquisition system		Multi-piezometer string		Crackmeter, automatic
	Combined inclinometer and TDR monitoring location		Tape-extensometer, manual		Crackmeter, manual

**Figure 1. Upper part of the landslide area with one of the reconstructed roads crossing. Installed sensors are indicated.**

Along with the planning of the reconstruction of two destroyed roads an early warning system shall be developed and implemented for the safe use of the new roads. Therefore, some detailed geological investigations were carried out. This includes detailed engineering-geological mapping, hazard and risk mapping, geophysical measurements as well as planning and execution of exploration boreholes (Neumann et al. 2018). Furthermore, a setup of a multi-sensor network was designed and is already installed in large parts (Figure 1). The monitoring network consists of a variety of both automatic and manual sensors. Naturally, focus is laid on deformation with two inclinometers, five automatic and eleven manual crackmeters and six digital tape extensometer sections. Additionally, piezometers measure the pore water pressure and precipitation is measured at a meteo station.

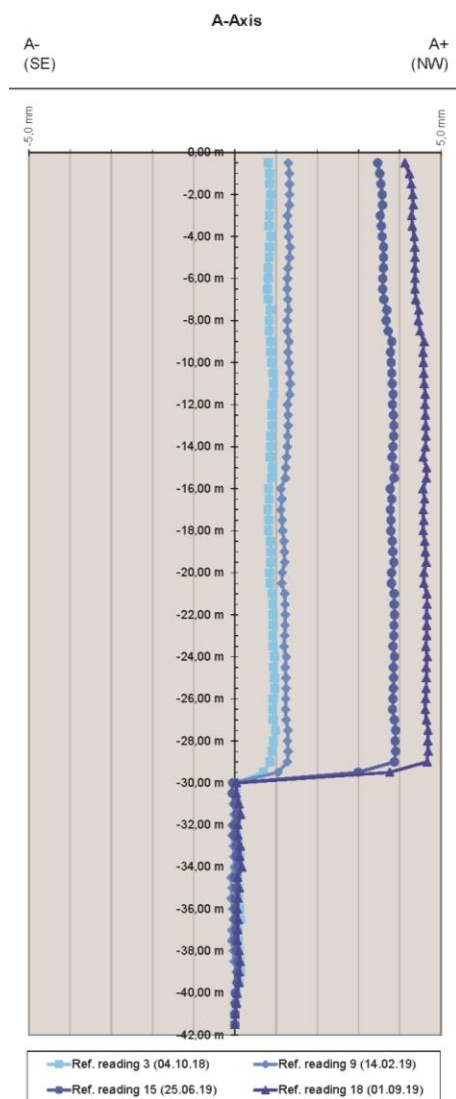


**Figure 2. Exemplary inclinometer measurements in one of the inclinometer boreholes.**

First measurement results show active movements in multiple sensors. Figure 2 shows parts of the inclinometer measurements monitoring a large cliff near the main scarp (right inclinometer in Figure 1). A very defined translational shear movement in about 30 m depth can be detected and quantified. The results prove the ongoing deformation of the slope and provide vital information about the activity, velocity and intensity of the rockslide at the cliff. Tape extensometer measurements have detected a high acceleration of a shallow slide directly next to the road west of the main landslide. Based on this data the slide was stabilized by a simple wall construction and damage to the road was avoided successfully.

To develop a true local EWS, thresholds must be defined that are able to trigger the closure of the affected roads in case of hazard. In this project we aim for a multi-level threshold consisting of a threshold for precipitation, pore water pressure and deformation rate. Between each step is a certain time lag, which provides the possibility to both review the data and have a timely and early warning in its true meaning.

The most important task for the near future will be to complement and refine the geological model. This includes e.g. the ongoing laboratory tests of geotechnical parameters, further drilling and their equipment to new measurement locations or the implementation and evaluation of planned geophysical measurements like ERT electrical resistivity tomography and ongoing hydrogeological studies.

**REFERENCES**

Gaprindashvili G., Gaprindashvili M. and Tsereteli E., 2016, Natural Disaster in Tbilisi City (Riv. Vere Basin) in the Year 2015. International Journal of Geosciences. 7(9), pp. 1074-1087.

Neumann, P., Bauer, M., Haidn, M., Keilig, K., Menabde, Z. and Dumbadze, D., 2018, Geological and geotechnical findings of the catastrophic debris flow near Tskneti, Georgia, June 2015. 5<sup>th</sup> International Conference on Debris Flows, 01.-05.10.2018, Tbilisi, Georgia, pp. 158-165.

UNDP-United Nations Development Programme. 2015, Tbilisi Disaster Needs Assessment 2015. Part 1 (Final draft), 59 p.



## Earthquake - induced landslides in the island of Lefkada triggered by the November 17, 2015 event and assessment of landslide susceptibility

Aglaia Matsakou<sup>1</sup>, Vassilis Marinos<sup>1</sup>, George Papathanassiou<sup>2</sup>, Sotirios Valkaniotis<sup>3</sup>, Athanasios Ganas<sup>4</sup>

<sup>1</sup>*Department of Geology, Aristotle University of Thessaloniki, 54124, Thessaloniki, Greece, [matsakoulia@hotmail.com](mailto:matsakoulia@hotmail.com), [marinosv@geo.auth.gr](mailto:marinosv@geo.auth.gr)*

<sup>2</sup>*Department of Civil Engineering, Democritus University of Xanthi, Kimmeria, Greece, [gpapatha@civil.duth.gr](mailto:gpapatha@civil.duth.gr)*

<sup>3</sup>*Koronidos Str., 42100, Trikala, Greece, [valkaniotis@yahoo.com](mailto:valkaniotis@yahoo.com)*

<sup>4</sup>*Institute of Geodynamics, National Observatory of Athens, Athens, Greece, [aganas@noa.gr](mailto:aganas@noa.gr)*

Landslides and earthquake induced landslides consist one of the most important and widespread natural hazard worldwide. The compilation of landslide inventory and susceptibility maps play an important role in the design of technical projects, in the development of urban design, and in the proper selection of land use. The aim of this project is to study the earthquake-induced landslides triggered by the 2015 earthquake in the island of Lefkada and to develop a susceptibility model in order to predict slope failure locations in a future earthquake. In order to achieve this, information regarding the spatial distribution of slope failures generated by the 2015 inventory (Papathanassiou et al. 2017) was analyzed (596 landslides) in ArcGIS. The developed inventory map indicates that the density of landslides increases from east to west, while a recently published research (Grendas et al. 2018), focused on the correlation of the severity of slope failures with the classification (GSI) of the rock mass, highlighted the importance of engineering geological mapping for developing a reliable and detailed landslide hazard map.

Furthermore, the spatial distribution of landslides was statistically analyzed in relation to the causal factors of geology (provided by Cushing, 1985) and topography (classified at classes), in order to investigate their influence in landsliding phenomena, (Guzzetti et al. 1997, Van Westen 1997). Moreover, values such as densclass (the percentage of landslides within each class) and densmap (the density of landslides throughout the map), were evaluated, in order to calculate the weighted factors. Subsequently, all these factors were overlaid as thematic layers and the resulted map was classified at 10 susceptibility classes (natural breaks method). The 1st class represents very low susceptibility, whereas the 10th class represents very high susceptibility. As an outcome, a landslide susceptibility map of pixel size 10x10m was compiled (Figure 1a). Afterwards, this model was further analyzed by calculating frequency values in order to estimate the success rate. Consequently, the success rate was made taking into account the landslide inventory of 2015 earthquake. The outcome of the analysis shows that 61,58% of the 596 landslides corresponds to the 10th susceptibility class, (in classes 8,9,10 the rate is 88,93%).

Concerning the prediction rate, we took into account the landslide inventory of 2003 earthquake (302 landslides), following the same procedure, (Papathanassiou et al. 2013). The susceptibility map indicates that 51,99% of the 302 landslides corresponds to the 10th susceptibility class, (in classes 8,9,10 the rate is 88,74%). These two cumulative curves, success rate & prediction rate curves, that are shown in Figure 1b, present the percentage of the susceptibility map and the percentage of landslides. Regarding the success rate, the 10% of the susceptibility map includes almost the 80% of landslides, while almost the 80% of the landslides could be predicted in the 10% of the susceptibility map (based on the prediction rate curve). Finally, for both curves, 25% of the susceptibility map verifies and predicts more than 90% of landslides, proving the reliability of model.



As an outcome, this study presents the earthquake-induced landslide susceptibility map of the island of Lefkada. It is highlighted that the inventories that were used for the development of this map (training and validation dataset) are based on data provided by earthquakes occurred on the northern part (14/8/2003) and on the southern part (17/11/2015 event) of the island. Thus, it is stated that this map is considered as the final susceptibility map for the whole island and can be used by public agencies and civil protection authorities in order to forecast slope failures triggered by future earthquakes.

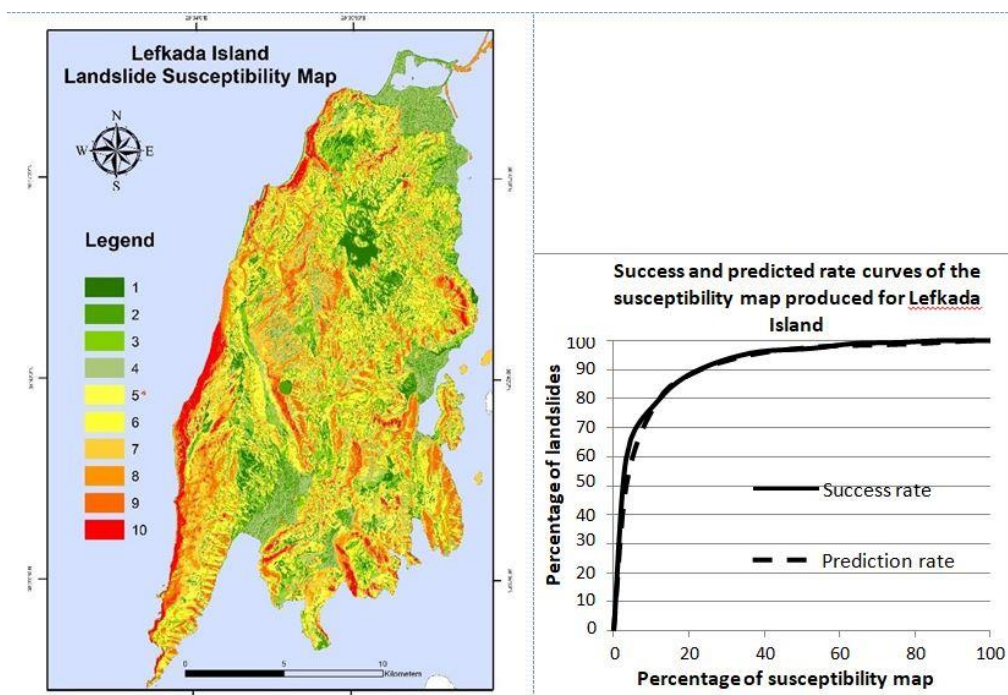


**Figure 1a. Lefkada Island landslide susceptibility map. The pixel size is 10x10m. From 1 to 10 are the landslide susceptibility classes. The 1<sup>st</sup> class represents very low susceptibility, whereas the 10<sup>th</sup> class represents very high susceptibility. Figure 1b. Success and prediction rate curves of the susceptibility map produced for Lefkada.**

## REFERENCES

- Cushing, (1985) Evolution structurale de la marge nord-ouest hellénique dans l'île de Levkas et ses environs (Grèce nord-occidentale), Université de Paris-Sud. Faculté des sciences d'Orsay (Essonne).
- Grendas N, Marinos V, Papathanassiou G, Ganas A, Valkaniotis S, (2018) Engineering geological mapping of earthquake-induced landslides in South Lefkada Island, Greece: evaluation of the type and characteristics of the slope failures. *Environmental Earth Sciences*, 77:425, <https://doi.org/10.1007/s12665-018-7598-9>.
- Guzzetti F, Carrara AI, Cardinalia M, Reichenbach P, (1997) Landslide hazard evaluation: a review of current techniques and their application in a multi-scale study, Central Italy. *Elsevier*, 181–216, PII: S0169-555X9900078 – 1.
- Papathanassiou G, Valkaniotis S, Ganas A, Pavlides Sp, (2013) GIS-based statistical analysis of the spatial distribution of earthquake-induced landslides in the island of Lefkada, Ionian islands, Greece. *Landslides* 10, 771-783.
- Papathanassiou G, Valkaniotis S, Ganas A, Grendas N, Kollia EI (2017) The November 17th, 2015 Lefkada (Greece) strike-slip earthquake: Field mapping of generated failures and assessment of macroseismic intensity ESI-07, *Engineering Geology*, Vol. 220, Pages 13–30 <http://dx.doi.org/10.1016/j.enggeo.2017.01.019>.
- Van Westen CJ (1997) Statistical landslide hazard analysis. ILWIS 2.1 for windows application guide. ITC Publication, Enschede, pp 73–84.

## Locating-allocating emergency response services facilities considering landslide susceptibility assessments

Anastasios Balampanis<sup>1</sup>, Paraskevas Tsangaratos<sup>1</sup>, Constantinos Loupasakis<sup>1</sup>, Constantinos Athanassas<sup>1</sup>

<sup>1</sup>NTUA, School of Mining and Metallurgical Engineering, Greece, [tasosblbns@gmail.com](mailto:tasosblbns@gmail.com),  
[ptsag@metal.ntua.gr](mailto:ptsag@metal.ntua.gr), [cloupasakis@metal.ntua.gr](mailto:cloupasakis@metal.ntua.gr), [constathanassas@metal.ntua.gr](mailto:constathanassas@metal.ntua.gr)

In cases of road blockage caused by landslides, the assistance needs to be at place as soon as possible. In the extend of a municipality, the main objective is to allocate the optimal sites for emergency response service (ERS) facilities so as to make it possible for assistance to reach the most of the susceptible areas within a defined time frame (Casagli et al., 2016). In this context, the main objective of the present study was to develop a landslide susceptibility model by using the Frequency Ratio (FR) method and the Analytic Hierarchy Process (AHP) and later define the optimal location of ERS by using a Network Analyst model developed within a Geographic Information System (GIS) (ESRI, 2011). The water basin of the Arachthos river, located in the Perfection of Epirus, Greece, was selected as a test site to evaluate the predictive capability of the developed methodology. The developed methodology involved two phases. During the first phase 204 landslide incidents and nine variables related to landslide phenomena were selected, namely elevation, slope angle, aspect, distance from the river network, profile curvature, stream transportation index (STI), land cover and lithology. By implementing the Frequency Ratio (FR) and the Analytical Hierarchy Process (AHP) each variable was weighted and the landslide susceptibility map was designed. The evaluation of the performance of the FR-AHP model was based on the calculation of the area under the success and predictive curve (AUC). The second phase involved the implementation of a Network Analyst model and an algorithm that maximizes attendance with the assumption that all facilities are equally attractive and service to landslide sites will be offered by nearby ERS facilities. The very high susceptible areas were considered as areas that need assistance (demand points), whereas seven towns within the area of the water basin were considered as candidate locations for the ERS facilities. Based on the results of the FR-AHP model, around 16.30% of the study area was characterized as high and very high susceptible as shown in Figure 1. The AUC value for the training data was calculated to be 0.8162 and the AUC value for the validation data was calculated to be 0.7884 indicating a very good performance for the FR-AHP model. The Network Analyst model, based on the landslide susceptible values, showed that the two optimal ERS facility sites should be placed in the towns of Kalentzi and Tristeno as these two could serve the most landslide prone areas in the shortest time (figure 1). The developed approach could benefit landslide susceptibility assessments and provide valuable knowledge during emergency response operations, the analysis of risks and decision making.

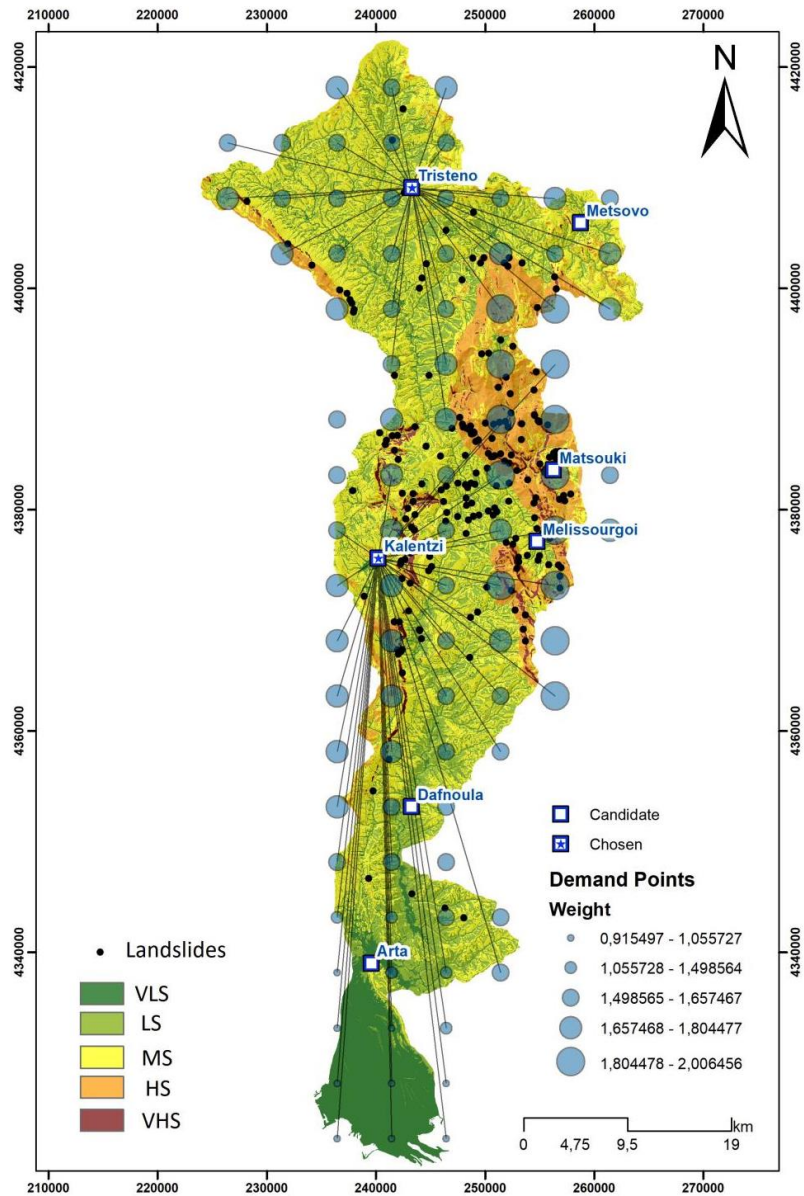


Figure 1. Landslide susceptibility and Optimal Location for ERS facilities

## REFERENCES

- Casagli, N., Cigna, F., Bianchini, S., Hobling, D., Fureder, P., Righini, G., Del Conte, S., Friedl, B., Scheiderbauer, Lasio, C., Vicko, J., Greif, V., Proske, H., Granica, K., Falco, S., Lozzi, S., Mora, O., Arnaud, A., Novali, F., Bianchi, M., 2016. Landslide mapping and monitoring by using radar and optical remote sensing: Examples from the EC-FP7 project SAFER. Remote Sensing Applications: Society and Environment. 4, 92-108.
- ESRI 2011. ArcGIS Desktop: Release 10. Redlands, CA: Environmental Systems Research Institute.

## Implementing a novel ANN ensemble model based on machine learning models for landslide susceptibility mapping

Paraskevas Tsangaratos<sup>1</sup>, Anastasios Balampanis<sup>1</sup>, Constantinou Loupasakis<sup>1</sup>

<sup>1</sup>NTUA, School of Mining and Metallurgical Engineering, Greece,

[ptsag@metal.ntua.gr](mailto:ptsag@metal.ntua.gr), [tasosblbns@gmail.com](mailto:tasosblbns@gmail.com), [cloupasakis@metal.ntua.gr](mailto:cloupasakis@metal.ntua.gr)

Landslide susceptibility assessment is considered as the main investigation tool capable of providing valuable geo-information concerning the relation between landslides and landslide related variables (Pourghasemi et al., 2018). Nowadays, it is common practice to apply Machine learning (ML) models along with Geographic Information Systems (GIS) so as to develop landslide susceptibility models (Chen et al., 2019). From the long list of ML models especial attention have been given to ensemble models which are capable to boost the prediction accuracy of a set of base models. In this context, the main objective of the present study was to develop a novel supervisor model based on stacking method for the estimation of landslide susceptibility by using the prediction of a set of ML models. In our case, an Artificial Neural Network (ANN) model was used as the supervisor model, whereas Linear Discriminate Analysis (LDA), Classification and Regression Trees (CART), Logistic Regression, k-Nearest Neighbors (kNN) and Support Vector Machine (SVM) were used as the base models. The water basin of the Arachthos river located in the Perfection of Epirous, Greece was selected as a test site to evaluate the predictive performance of the developed methodology. Nine landslide-related variables (elevation, slope angle, aspect, distance from the river network, profile curvature, stream transportation index (STI), land cover and lithology) and a data set of 204 landslide events were analyzed. Each variable was classified and weighted according to the results obtained by the Frequency Ration method and a normalization process. By the implementation of the Learning Vector Quantization (LVQ) algorithm, the predictive ability of the variables was estimated. Finally, based on the predictions of the 5 ML models, the novel ensemble ANN model produced the landslide susceptibility map (Figure 1). The accuracy and kappa index and also the area under the predictive curve (AUC) were used so as to evaluate the performance of the base learners and ANN model. Based on the LVQ algorithm the most important and critical variable was the STI, followed by slope angle, lithology, profile and land cover. The implementation of the 5 models indicated that the SVM model had the highest accuracy (0.8034) and kappa (0.6168) values among the other models. The novel ensemble ANN model, showed an accuracy and kappa value of 0.8334 and 0.6665, respectively. Both metrics indicate that the ensemble ANN model had a quite significant predictive ability concerning the identification of landslide prone areas. The outcome of the study clearly demonstrated that the ensemble ANN model provided more reliable and consistent results compared to the base ML methods. As a stand-alone product the developed novel approach could assist in landslide susceptibility assessments since it provides crucial geo-information and knowledge concerning the mechanism responsible for landslide phenomena.

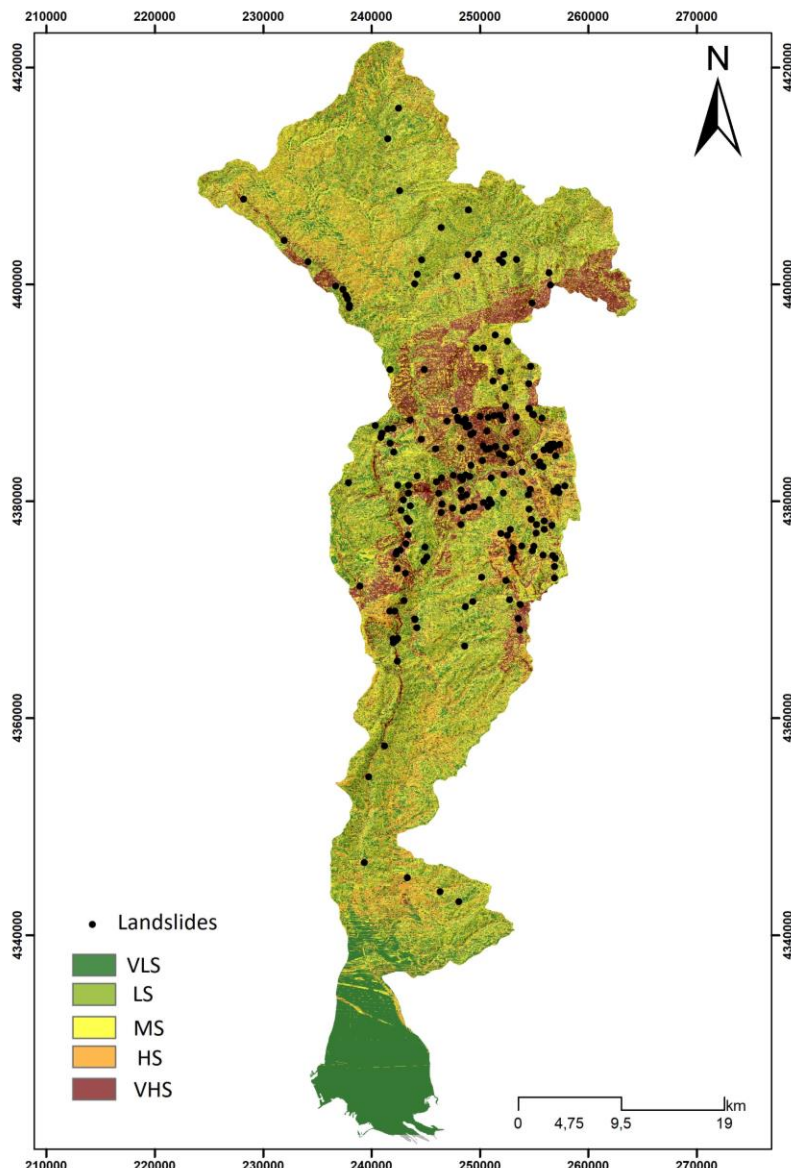


**Figure 1. Landslide susceptibility map based on the ensemble ANN model.**

**REFERENCES**

Chen, W., Panahi, M., Tsangaratos, P., Shahabi, H., Ilija, I., Panahi, S., Li, S., Jaafari, A., Ahmad B.B., 2019. Applying population-based evolutionary algorithms and a neuro fuzzy system for modeling landslide susceptibility. *Catena* 172, 212-231.

Pourghasemi, H.R., Yansari, Z.T., Panagos, P., Pradhan, B., 2018. Analysis and evaluation of landslide susceptibility: a review on articles published during 2005–2016 (periods of 2005–2012 and 2013–2016). *Arab. J. Geosci.* 11, 193. <https://doi.org/10.1007/s12517-018-3531-5>.





## Assessing the shrink swell potential of Highways England's geotechnical assets

Jack Randall<sup>1</sup>, Dr Christopher Power<sup>1</sup>, James Codd<sup>2</sup>

<sup>1</sup>*Mott MacDonald, United Kingdom, [Jack.Randall@mottmac.com](mailto:Jack.Randall@mottmac.com), [Christopher.Power@mottmac.com](mailto:Christopher.Power@mottmac.com)*

<sup>2</sup>*Highways England, United Kingdom, [James.Codd@highwaysengland.co.uk](mailto:James.Codd@highwaysengland.co.uk)*

The Strategic Road Network of England, managed and operated by Highways England, is a vitally important national transport asset. It comprises 2% of England's roads but carries approximately a third of all traffic. Improving understanding of the geotechnical assets that the road network lies on or runs through has been an important focus over the last 20 years, allowing for developments in asset management practice and research into their performance. This presentation will focus on work undertaken to better understand the potential for shrink swell behaviour to impact upon geotechnical asset performance. The work has included a detailed review of the geological composition of each geotechnical asset and an in depth review of the organisation's inspection records, AGS data and other reports, alongside published literature resulting in a comprehensive database of geotechnical properties. The development of a Highways England specific hazard map for shrink-swell potential, from new datasets, will be described, and examples of the final output shown. The scope for further improving this dataset will be discussed, and the implications of climate change for asset performance considered.

## Investigation of the Kafireas Mountain landslide, in Evia Island, Greece

Vasilis Perleros<sup>1</sup>, A. Kalos<sup>2</sup>, D. Georgiou<sup>3</sup>, Paul Marinou<sup>4</sup>

<sup>1</sup>Consultant Geologist, Greece, [perlerosv@gmail.com](mailto:perlerosv@gmail.com)

<sup>2</sup>PhD Civil Engineer, National Technical University of Athens, Greece, [alkalos@central.ntua.gr](mailto:alkalos@central.ntua.gr)

<sup>3</sup>MSc Mining Engineer, National Technical University of Athens, Greece, [dgeorgiou@mail.ntua.gr](mailto:dgeorgiou@mail.ntua.gr)

<sup>4</sup>Emeritus Professor, National Technical University of Athens, Greece, [marinos@central.ntua.gr](mailto:marinos@central.ntua.gr)

This paper studies the landslide sustained at the Kafireas area, at the South of Evia Island, Greece, on 2018. The landslide occurred after the construction of the access road to the Wind Park and probably because of it. The landslide is located approximately 220m to the southwest of the closest wind turbine. This area is mountainous, for the most part, as the altitude ranges to 1,398 m at the Ochi mountain peak. Forestation covers the northern slopes, while most of the remaining mountain area is covered with grassland and bushes affected in the past by fires. This paper focuses on the landslide triggering agents and mitigation measures, by mainly studying the principles and techniques working towards the stabilization of the mobilized mass and drainage of the uphill geomaterial.

The geological profile of the region consists of : (a) marbles and cipolins mainly thin-bedded micro to medium crystalline marbles (chlorite is also encountered on occasion), and (b) mica- schist characterized by strongly schistose and microfolds rock masses arranged into various stratigraphic intercalations and (c) greater masses of quartzites and quartz schists. The area is being disrupted by two fault systems, apart from the characteristic main thrust faults present. A fault with direction N-S is observed at the southern part of the landslide and has created a steep almost vertical slope in marbles.

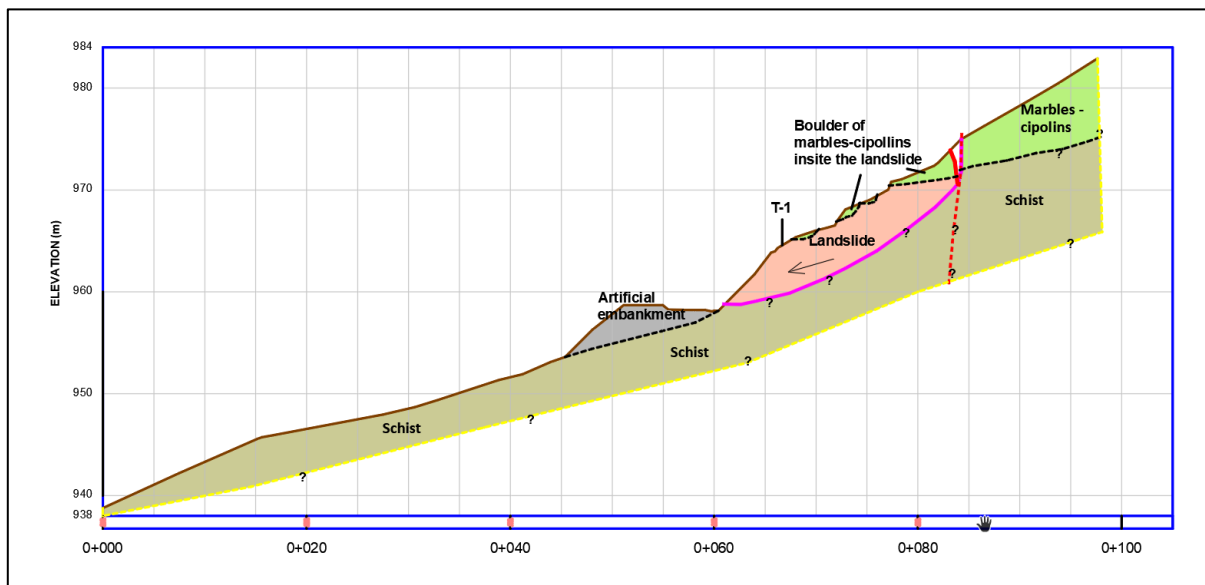
The landslide occurred during the excavation of the access road to the wind park, as shown in Figure 1.



Figure 1. General view of the landslide.

The landslide develops as the outcome of the downward rock-mass movement of an already destabilized mass at the western edges of an elongated ridge of about north - south direction. In this area, the access road runs close to the contact between the underlying shists and the overlying marbles and cipolins.

The landslide is manifested in different modes from place to place (Figure 2). In the uphill section, where the large landslide volume movement is detected, the mass is separated and moved away from the pre-existing fault that crosses the uphill area. The detachment (scarp) surface follows the fault surface deep down to the contact (between the marbles-cipolins and the underlying schist). Subsequently, the surface follows a contact of beds, until the landslide toe emerges at the access road side. Hence, the contact between the layers works as a low-strength zone from the one geomaterial to the next, posing a kinematic constrain to the onset and full activation of the failure surface.



**Figure 2. Typical geological cross-section of the landslide.**

The landslide mitigation measures address the risk of slope instability by working on the safety factor. The landslide mitigation measures include a series of procedures, techniques and measures to be applied which ensure the stability of the area and sustainability of the project with an eye towards minimizing the financial cost.

Based on analysis, the safety factor increases by means of : (a) placing a gabion wall at the landslide toe; (b) removing part of the uphill geomaterial; (c) slope geometry reshaping to include a bench in the formation of the final reformed slope; (d) excavation of transverse trenches filled with well graded gravel to ensure drainage of the weathered mantle and mobilized rock-mass; (e) backfilling behind the gabion wall and the open chasm with well graded gravel which could be covered with geomembrane to avoid cloaking, while still permitting the drainage of the destabilized volume. Piling or a heavy retaining wall seem not to be the optimum mitigation approach in this case, both scientifically and economically.

**REFERENCES**

Geological Map 1:50.000 of the Karystos – Platanistos, Institute of Geology and Mineral Exploration (Geological mapping: Ch.Latsoudas & M.Triantaphyllis,1989-1991 - Publication 1997)  
 Geometrisi: Wind park spilia. wind turbine foundation design - geotechnical investigation report. june 2018  
 Geometrisi: Geophysical investigation at landslide area on the access road of spilia wind park, karystos region project: kafiareas project. june 2018

## Forest Fires' impact on Landslide Susceptibility Assessment

Constantinos Nefros<sup>1</sup>, Constantinos Loupasakis<sup>1</sup>, Gianna Kitsara<sup>2</sup>

<sup>1</sup>Laboratory of Engineering Geology and Hydrogeology, School of Mining and Metallurgical Engineering, Greece, [kostasnefros@central.ntua.gr](mailto:kostasnefros@central.ntua.gr), [cloupasakis@metal.ntua.gr](mailto:cloupasakis@metal.ntua.gr)

<sup>2</sup>Institute for Environmental Research and Sustainable Development, National Observatory of Athens [gkitsara@noa.gr](mailto:gkitsara@noa.gr)

Forest fires are natural disasters that change dramatically a region's landscape and ecosystem, which in turn can cause terrain's instability and eventually lead to landslides. Over the last few years, climate change has altered the way that wildfires are spreading, affecting even more the landslides' occurrence. In this research the relative literature has been reviewed and useful conclusions have been extracted.

High burn severity areas are more prone to instability and soil erosion problems (Rozos et al. 2010). As Calcaterra et al. (2007) points out burned watersheds are rather susceptible to debris flows. About 200 landslides were triggered in Naples, Italy four (4) months after forest fires (July 27, 1996) and extreme rainfall events occurred in the same area (fire was a predisposing factor and rainfall events were the triggering). Rozos et al. (2010) have also found out that after the devastating forest fires of 2007 near Zacharo/Greece, the area's susceptibility to landslides had increased about 27%. Depountis et al. (2010) also verified that the primary reasons for these landslide events, were the fire's devastating results on vegetation and forestry structure.

Large trees usually have deep seated roots which work like "soil nails", stabilizing the earth slopes, making them less susceptible to landslides (Ruff et Czurda 2008, Guerra et al 2017). In many cases after a wildfire, the big trees' roots remain alive, retaining soil in place for the next years, while after their decomposition their contribution to the slope's stability is almost insignificant (Sprague – Wheeler 2003).

The wildfires can be generally divided in surface and crown fires. Surface fires remove the protective litter layer from the forest's floor, increasing the water's surface runoff and destabilizing the slope (Sprague -Wheeler 2003), while crown fires spread mostly across the forest canopy and do not affect significantly the forest understory vegetation and trees' roots.

The 23/07/2018 Attica wildfire (Greece), was a typical crown fire (Lekkas et al. 2018 and Xantopoulos and Athanasiou 2019). In that case, the Normalized Difference Vegetation Index (NDVI) was clearly low (Figure 1) although trees' trunks and roots remained relative steady (Figure 2). Thus, if the NDVI is selected as a factor for the Landslide Susceptibility Assessment (LSA) of an area recently affected by a crown wildfire, it would probably provide a false indication about the slope's stability. Particularly, it is expected to show a significant alteration, falsely implying that the landslide's susceptibility has also significantly increased. It is also possible that climate parameters such as evapotranspiration, could provide satisfactory results for representing the understory vegetation's condition after a wildfire. McKean et al. (1991) used Landsat Thematic Mapper (TM) and proved that root strength and evapotranspiration are important variables in the occurrence of shallow landslides.

Nitschke, et al. (2006), predicted that forest fires are expected to be more frequent and with higher severity over the next 70 years due to the climate change. Therefore, a relative effect on the landslide phenomenon, is also expected.

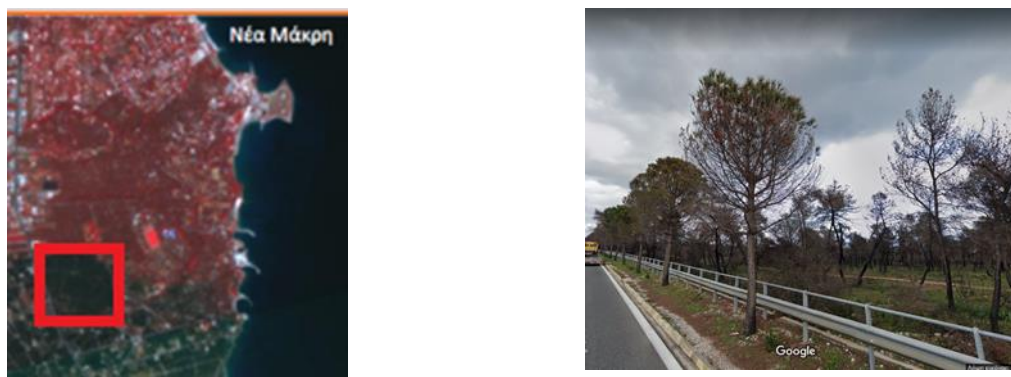


**Figure1. NDVI,27/7/18, After Wildfire (Lekkas et al. 2018)-Figure 2, Photo after(Feb 19)Wildfire (Google Street View)**

As it was revealed during this research a wildfire in a landslide prone area, accelerates significantly the landslides' occurrence. Crown fires seem to have lower impact, as the crown foliage is been burned but the "understory vegetation cover" and trees' roots retain soil's coherence. Thus, parameters such as the NDVI, do not provide satisfactory results, and other parameters, such as Evapotranspiration, must be further examined.

## REFERENCES

- Calcaterra, D. & Parise, M. & S, Strumia & E, Mazzella., 2007, Relations between fire, vegetation and landslides in the heavily populated metropolitan area of Naples, Italy.
- Depountis, N., Lainas, S., Pyrgakis, D., Sabatakakis, N., & Koukis, G., 2010, Engineering Geological and Geotechnical Investigation of Landslide Events in Wildfire Affected Areas of Ilia Prefecture, Western Greece. Bulletin of the Geological Society of Greece.
- Guerra, A.J.T. & Fullen, M.A., Jorge, M.C.O., Bezerra, J.F.R., 2017, Slope Processes, Mass Movements and Soil Erosion: A Review. *Pedosphere*. 10.1016/S1002-0160(15)600
- Lekkas, E., Carydis, P., Lagouvardos, K., Mavroulis, S., Diakakis, M., Andreadakis, Emm., Gogou, M.E., Spyrou, N.I., Athanassiou, M., Kapourani, E., Arianoutsou, M., Vassilakis, M., Parcharidis P. Kotsi, E., Speis, P.D., Delakouridis, J., Milios, D., Kotroni, V., Giannaros, T., Dafis, S., Kargiannidis, A., Papagiannaki, K., 2018, The July 2018 Attica (Central Greece) Wildfires – Scientific Report (Version 1.0). Newsletter of Environmental, Disaster, and Crisis Management Strategies, 8, ISSN 2653-9454.
- McKean, J., Buechel, S., and Gaydos, L., 1991, Remote Sensing and Landslide Hazard Assessment: Photogrammetric Engineering and Remote Sensing, v. 57, no. 9, p. 1185-1193.
- Nitschke, Cr & Innes, J., 2006, Interactions between fire, climate change and forest biodiversity. *CAB Reviews Perspectives in Agriculture Veterinary Science Nutrition and Natural Resources*. 1. 10.1079/PAVSNNR20061060.
- Rozos, D & Bathrellos, G & Skilodimou, H, 2010, Landslide susceptibility mapping of the northeastern part of Achaia Prefecture using Analytical Hierarchical Process and GIS techniques.
- Ruff, M. & Czurda, K., 2008, Landslide susceptibility analysis with a heuristic approach in the Eastern Alps (Vorarlberg, Austria). *Geomorphology*. 94. 314-324. 10.1016/j.geomorph.2006.10.032.
- Sprague-Wheeler, D.K., 2003, The use of remote sensing imagery for evaluation of post-wildfire susceptibility to landslide and erosion hazards in the Salmon Challis National Forest, Lemhi County, Idaho: Pocatello ID, Idaho State University.



## 2D and 3D dynamic numerical modelling of seismically induced rock slope failure

Anne-Sophie Mreyen<sup>1</sup>, Emilie Lemaire<sup>1</sup>, Hans-Balder Havenith<sup>1</sup>

<sup>1</sup>UR Geology, Liege University, Belgium, [as.mreyen@uliege.be](mailto:as.mreyen@uliege.be), [HB.Havenith@uliege.be](mailto:HB.Havenith@uliege.be)

### **Background**

The stability of rock slopes is often guided by the structural geology of the rocks composing the slope. Especially, discontinuities can significantly influence slope stability according to their orientation with respect to the one of general slope. Here, we will focus on the triggering of giant rockslides. The final goal is to identify failure characteristics allowing us to distinguish seismic trigger modes from climatic ones, notably on the basis of the source zone rock structures. This study is supported by dynamic numerical modelling. More specifically, we will present results based on a parametric numerical study, using distinct element codes designed for 2D and 3D dynamic analysis. This study was applied to the Balta rockslide in the SE Carpathian Mountains (Romania) that has been extensively studied by Mreyen et al. (2019) during the last years.

### **Methods**

For the numerical modelling, we chose the distinct element codes UDEC and 3DEC (2D and 3D, respectively) developed by Itasca® (2016). This method allows us to quantify the effects of loads and external stresses applied to discontinuous media, such as jointed rock material, taking also into account dynamically changing groundwater pressures.

Both 2D and 3D models consider the 'observed morphological-structural case' as well as slopes with lower or steeper inclination and with variously dipping joint orientations. One of the scenarios representing the most realistic slope conditions (jointed anti-dip rock slope) was simulated with 3DEC, accounting for seismic effects, and changing groundwater pressures.

### **Results**

Two results of this back-analysis and parametric study are presented below in terms of along-slope displacements, respectively for the close-to-observed scenarios simulated with UDEC in 2D (Figure 1) and for the one in 3D (Figure 2). For both dynamic numerical models, a Ricker wavelet (with energy between 0.5 – 8 Hz) was used as seismic input. Both confirm that the slope modelled with the close-to-observed structure is highly stable in static conditions and affected by minor deformation after seismic loading. Note, the 2D model only includes one bedrock material. Here, dynamic effects are purely influenced by the structure and the topography (with larger shaking in the convex upper part of the slope), while the 2-layer 3D model also produces some material-dependent site amplification.

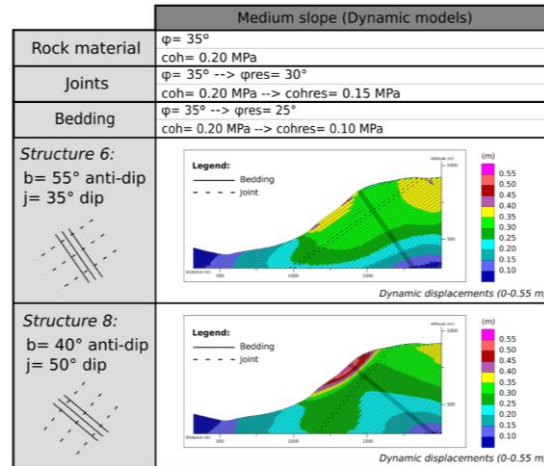


Figure 1. 2D Dynamic modelling results (in terms of displacements, with maximum values close to 0.5 m) for the rock slope conditions closest to the Balta case, with anti-dip slope bedding structure.

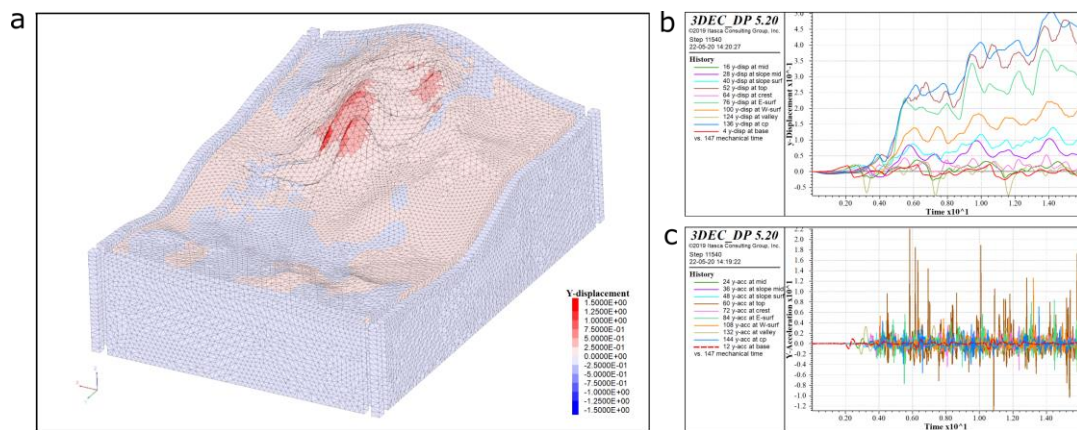


Figure 2. 3D Dynamic loading of the Balta rock slope with 3DEC: a) 3D block model quantifying displacement in y-direction (positive towards the slope foot), y-Displacement (b) and y-Acceleration records (c) for defined history points.

**Conclusions**

2D and 3D results both confirm that anti-di slope bedding structures are always stable in static conditions. Significant along-slope displacements only occur after simulation of severe shaking (PGA>0.2g). An interesting result was obtained for a bedding structure steeply dipping (> 70° dip) into the slope – actually, this structure revealed to be the most unstable on as affected by flexural toppling (also in the static domain) – even a model with a gentle slope (<15°) presented some displacements of almost 0.5 m after seismic input (while only elastic non-permanent deformation was modelled for all other bedding structures within a gentle slope).

**REFERENCES**

Itasca., 2016, 2- and 3-Dimensional Distinct Element Code Manuals (UDEC version 6.0; 3DEC version 5.2). Minneapolis, Minnesota: Itasca Consulting Group, Inc.

Mreyen A.-S., Cauchie L., Micu M., Cerfontaine P., Havenith H.-B., 2019, Multi-technique approach to characterize ancient deep-seated landslides in seismic regions. American Geophysical Union Fall Meeting, 9-13 December, 2019, San Francisco, USA.

## Development of a web-based landslide inventory map of Attica Region, Greece

Nikolaos Tavoularis<sup>1</sup>, Panagiotis Argyrakis<sup>2</sup>, George Papathanassiou<sup>3</sup>, Athanasios Ganas<sup>4</sup>

<sup>1</sup>*Dr. Engineering Geologist NTUA, Attica Regional Authority, Greece, [ntavoularis@patt.gov.gr](mailto:ntavoularis@patt.gov.gr)*

<sup>2</sup>*PhD candidate Electronics Engineer, University of Peloponnese, Greece, [pargyrak@noa.gr](mailto:pargyrak@noa.gr)*

<sup>3</sup>*Assistant Professor, Democritus University of Thrace, Greece, [gpapatha@civil.duth.gr](mailto:gpapatha@civil.duth.gr)*

<sup>4</sup>*Research Director, Institute of Geodynamics, National Observatory of Athens, Greece, [aganas@gein.noa.gr](mailto:aganas@gein.noa.gr)*

Landslide disasters are the result of the impacts of hazardous movement of soil and rocks that threaten vulnerable human settlements and infrastructure in cities, coasts, islands and mountains. In those areas, developments such as roads, railways, expansion of urban areas increase exposure to the hazards of landslides (Kyoto, 2020 Commitment). In Greece, and particularly in the Attica region, many prone to landslides areas exist. Attica is a county of 3810 km<sup>2</sup>, concentrating almost half of the Greek population, more than 60% of the industrial production in Greece and high value properties and infrastructure.

In the current study, a web-based landslide inventory for the entire area of the Attica regional Authority will be generated for the first time under the terms of the research project named "Landslide Risk Resilience of Attica region", co-financed by the EU. The initial goal of this project is to develop a database of slope failures that will be used as core data by the public agencies in the Attica Region for producing relevant maps of risk and hazard for the whole area. Afterwards, having compiled the landslide inventory map, studies focusing on spatial planning, risk assessment, and development (design and construction of infrastructure projects) can be realized in relation to earthquakes and floods.

### **Methods**

The compilation of a reliable landslide inventory map is mandatory for an accurate assessment of landslide susceptibility, hazard and risk (Van Westen et al., 2008 Tavoularis, 2017). Regarding the Attica Region, information on landslide occurrence is dispersed in more than one agency and mainly focuses on landslides documented along the road network and residential areas, while only few cases are georeferenced.

In this study, the generated inventory map, and the landslide geodatabase, cover a chronological period from 1961 up to present (2020). The methods that are used for the generation of the inventory can be classified into the following main groups:

- Collection of technical reports from public authorities and from newspaper articles
- Field surveys and review of previously mapped landslides
- Airborne and satellite Image analysis and interpretation: a) using multi-temporal images from Google Earth Pro, b) hillshading images (as well as slope and aspect map) derived from LiDAR Digital Elevation Model with pixel size of 5 m, which turned out to be very useful for mapping older landslide features and furthermore to identify new potential ones. The landslides areas that have been mapped, were delineated based on the guidelines recommended by the protocol (Special Paper 42, Oregon Department of Geology and Mineral Industries (Burns and Madin, 2009). The identified slope failures were employed in the ArcGIS database as: 1) spatial data (mapped as points and polygons) and 2) tabular (descriptive) data in text or numeric form, stored in rows and columns in a database and linked to spatial data (Burns and Madin, 2009). In addition, the following information per slope failure is presented based on Working Party on World Landslide Inventory (1990) findings: (i) geographic details: prefecture, municipality, locality, (ii) geotectonic unit, (iii) geological formation, lithological composition, (iv) seismic risk zone, (v) meteorological data, (vi) older activation, (vii) slope gradient and aspect, (viii) mass movement date - field survey date, (ix) type of movement,

(x) geometry, (xi) triggering factor, (xii) landslide causes, (xiii) consequences, (xiv) proposed remedial measures, (xv) confidence of landslide identification, (xvi) structural geological conditions and (xvii) hydrogeological behaviour. The preliminary landslide inventory map is shown in Figure 1, where slope failures are interpreted as points, assigning a unique identifier and a number of attributes to each landslide.

**Acknowledgments**

This work is supported by the Action “Supporting new researchers” of the Operational Program “Education and Lifelong Learning” of the Greek Ministry of Education (co-financed by the European Social Fund and the Greek State). The authors are grateful to the Ministry of Environment, Region of Attica, and HSGME for providing valuable technical landslide reports as well as crucial digital geodata records.

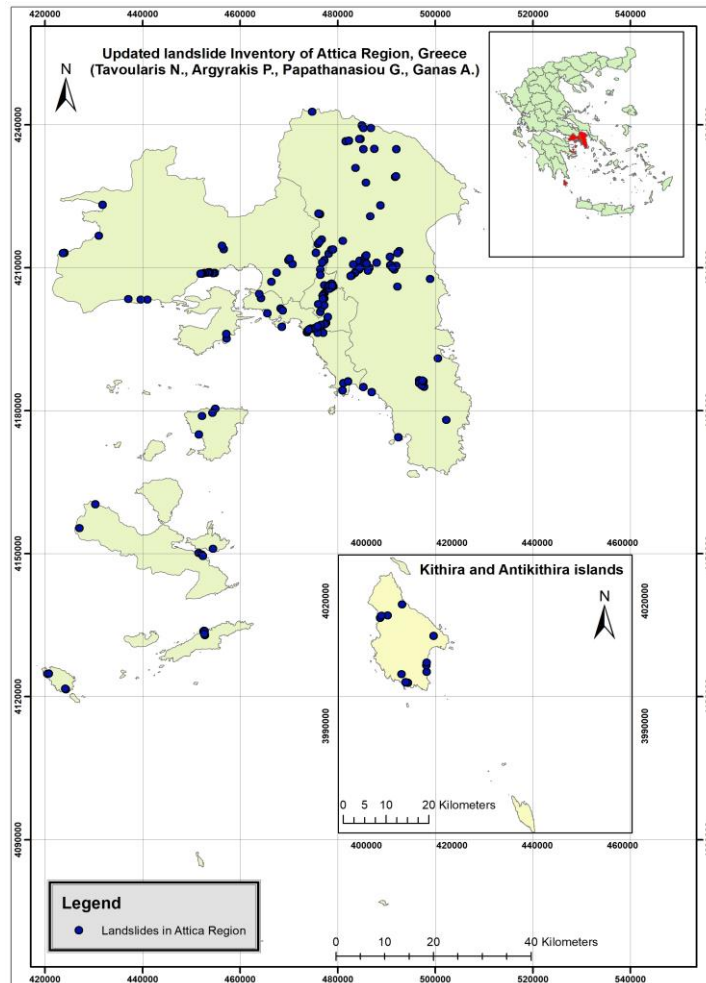


**Figure 1. Updated landslide inventory map of Attica region (scale 1:700.000) for the period 1961-2020. Solid circles depict occurrence of landslide phenomena.**

**REFERENCES**

Burns, W., and Madin, I., 2009, Protocol for inventory mapping of landslide deposits from light detection and ranging (LiDAR) imagery. Special paper 42, Oregon Department of Geology and Mineral Industries.

Kyoto, 2020, Commitment for Global Promotion of Understanding and Reducing Landslide Disaster Risk (Final draft)

Tavoularis, N., 2017. The contribution of landslide parameters to the prognosis of slope failures. PhD thesis, School of Mining and Metallurgical Engineering, National Technical University of Athens (Greece).

Van Westen, C.J., Castelannos, Abella, E.A. and Sekhar, L.K., 2008, Spatial data for landslide susceptibility, hazards and vulnerability assessment: an overview, in *Engineering Geology*, 102 (2008), 3-4, pp 112-131.

WP/WLI, (International Geotechnical Societies' UNESCO Working Party on World Landslide Inventory), 1990, A suggested method for reporting a landslide, *Bulletin International Association of Engineering Geology*, 41, 5-12.



## **A Probabilistic Approach for Mapping the Hazards Posed by Coseismic Landslides**

Mingdong Zang<sup>1</sup>, Shengwen Qi<sup>2</sup>

<sup>1</sup>*School of Engineering and Technology, China University of Geosciences (Beijing), China,*

[mingdong.zang@hotmail.com](mailto:mingdong.zang@hotmail.com)

<sup>2</sup>*Key Laboratory of Shale Gas and Geoengineering, Institute of Geology and Geophysics, Chinese Academy of Sciences, China, [qishengwen@mail.iggcas.ac.cn](mailto:qishengwen@mail.iggcas.ac.cn)*

Coseismic landslides can destroy buildings and cause tens of thousands of deaths. Occurrences of earthquakes are random and difficult to predict accurately. Therefore, before an earthquake occurred, predicting the spatial distribution of coseismic landslides is one of key scientific issues needing to be solved. This paper proposes a new approach for mapping the hazards of coseismic landslides by considering the probability of potential earthquakes. Newmark's method is employed to assess the permanent displacements due to the 2014 Ludian earthquake. The predicted displacements are compared with a comprehensive inventory of landslides triggered by the Ludian earthquake to produce a regression curve relating the predicted displacement and the probability of coseismic landslides. This probability function can be applied to predict the hazards of coseismic landslides for any seismic scenario of interest. The potential coseismic landslide displacements are then estimated in each grid cell from a probabilistic framework through calculating a seismic hazard level of 10% probability of exceedance in 50 years. The probability of coseismic landslides with this seismic hazard level are predicted through the probability function, and the coseismic landslide hazard map is then generated based on the classification of the probability of failures. This mapping procedure can be used to predict coseismic landslides posed by potential earthquakes and provide guidelines for decisions regarding the development of infrastructure and pre-earthquake construction.





## A landslide in bentonitic clays in Paphos, Cyprus

Michael Bardanis<sup>1</sup>, Evagelia Ioannou<sup>2</sup>

<sup>1</sup>*Neapolis University Paphos, Cyprus & EDAFOS Engineering Consultants S.A., Greece,*  
[mbardanis@edafos.gr](mailto:mbardanis@edafos.gr)

<sup>2</sup>*Neapolis University Paphos, Cyprus*

Paphos region in west Cyprus is a region notorious for its landslide susceptibility. Bentonitic clays of very high plasticity are found from the ground surface to considerable depth. These materials have very low peak and residual shear strength with angles of residual shear strength as low as 6-7°. Combining this very low strength with high precipitation dictated by the Mediterranean Sea to the west of the region leads to frequent slope stability problems even in very mild slopes.

The paper presents one such case near Armou village close to the city of Paphos. The landslide is approximately 300m long and 150m wide affecting a number of properties close to the crest. The average slope angle toe to crest is 7°. The landslide's lateral boundaries are streams eroding its sides and contributing to the pore pressure regime in the landslide mass. Pore pressure increase and duration is aggravated by local small earth dams created for agricultural purposes on these streams. The landslide is a combination of circular and translational landslide with evidence indicating it is retrogressive in nature. Marine terrace layers lie above the bentonitic clays and are currently found turned due to rotation of the lowest part before the upstream one followed and so forth. Adding to this, between autumn 2018 and spring 2020 the crest of the landslide has advanced further upstream in a fashion similar to that found in the downstream parts of the landslide. Evident accumulated movements of the landslide mass make it a palaeolandslide with the material along the sliding surface having strength practically close to residual.

Due to the proximity of the area to Neapolis University, Paphos, the landslide serves as the subject of a site visit for the students of Engineering Geology and Soil Mechanics of the university. During these visits surface samples from around the landslide were collected and tested. These tests indicate the presence of a bentonitic clay with liquid limit in the order of 120-130% and a plasticity index of 100%. Peak shear strength values correspond to cohesion between 10 and 20 kPa and an angle of shearing resistance in the order of 20°, while the angle of residual shear strength ranges between 6 and 10°. Topographical data were collected from the Land Registry and Mapping Department of Cyprus and longitudinal and lateral sections were drafted in order to carry out slope stability back analyses using the limit equilibrium method. Pore pressures were modelled using the pore pressure coefficient  $r_u$ , and values were sought after so that the angle of residual shear strength from the back analyses was 1-2° higher than those obtained in the laboratory tests. Sliding surfaces along the longitudinal sections were cross-checked so as they correspond to a convex surface from their depths plotted along the lateral sections.

This work is presented in the paper as an initial study of the Armou landslide contributing to the geological and engineering identification and classification of this landslide and serving even further to the educational material provided to the students of Neapolis University during their site visits to the area.

## Development of a low cost geosensor network for detection and monitoring of rainfall induced landslides in soil

Dr. John Singer<sup>1</sup>, Prof. Dr. Kurosch Thuro<sup>2</sup>, Moritz Gamperl<sup>2</sup>, Tamara Breuninger<sup>2</sup>, Dr. Bettina Menschik<sup>2</sup>

<sup>1</sup>AlpGeorisk, Germany, [singer@alpgeorisk.de](mailto:singer@alpgeorisk.de)

<sup>2</sup>Chair of Engineering Geology, Technical University of Munich, [thuro@tum.de](mailto:thuro@tum.de)

Although great advances in the recognition, prediction and mitigation of landslides have been made in the last decades, landslide events still claim a high social and economic tribute worldwide. For example, Froude & Petley (2018) have collected and analyzed records of 4862 fatal landslide events around the globe in the years 2004 to 2016 in which in total nearly 56000 people were killed. Of these events the majority (79 %) were triggered by rainfall. At the same time fatal landslide events cluster around cities and occur most frequently in countries with lower gross national income, which often is linked to the existence of low-income informal settlements around cities in these countries.

While the high disposition especially of soil slopes to develop landslides often is known, municipalities and administrations with limited resources are often overwhelmed by the task of preventing settlement in these endangered areas, implementing necessary mitigation measures or the controlled resettlement of existing population to safer areas. Due to this, for example in the metropolitan area of Medellin, Colombia, which has a total population of about 3,9 Million, it is estimated that about 250'000 people live in medium to high landslide risk areas.

As an intermediate measure, until final long-term risk reduction solutions are found, landslide early warning systems (LEWS) can be a valuable element of landslide risk management, especially for the most endangered areas. Additionally, if implemented in a socially integrative way, LEWS can increase the awareness and resilience of the population concerning landslide risk, positively influencing areas far beyond the monitored area.

In course of the Infom@Risk research project, which is funded by the German federal ministry of education and research, currently a LEWS is being developed for informal settlements in the city of Medellin. For this a cost-effective geosensor network has been designed based on modern IoT technologies as e.g. MEMS sensors and the LoRa (LongRange) communication standard (Figure 1). The system, which in large parts is developed as open source and in future can be replicated freely, consists of versatile LoRa sensor nodes which have a set of MEMS sensors (e.g. tilt sensor) on board and can be connected to various different sensors including a new easy to install subsurface sensor probe. This allows to monitor important parameters concerning landslides as e.g. the deformation and groundwater levels. Complemented with further innovative measurement systems as e.g. the Continuous Shear Monitor (CSM), a flexible data management and analysis system and a risk based strategy for sensor deployment, the newly developed LEWS offers an outstanding cost to benefit ratio and hopefully will find widespread application throughout the world.

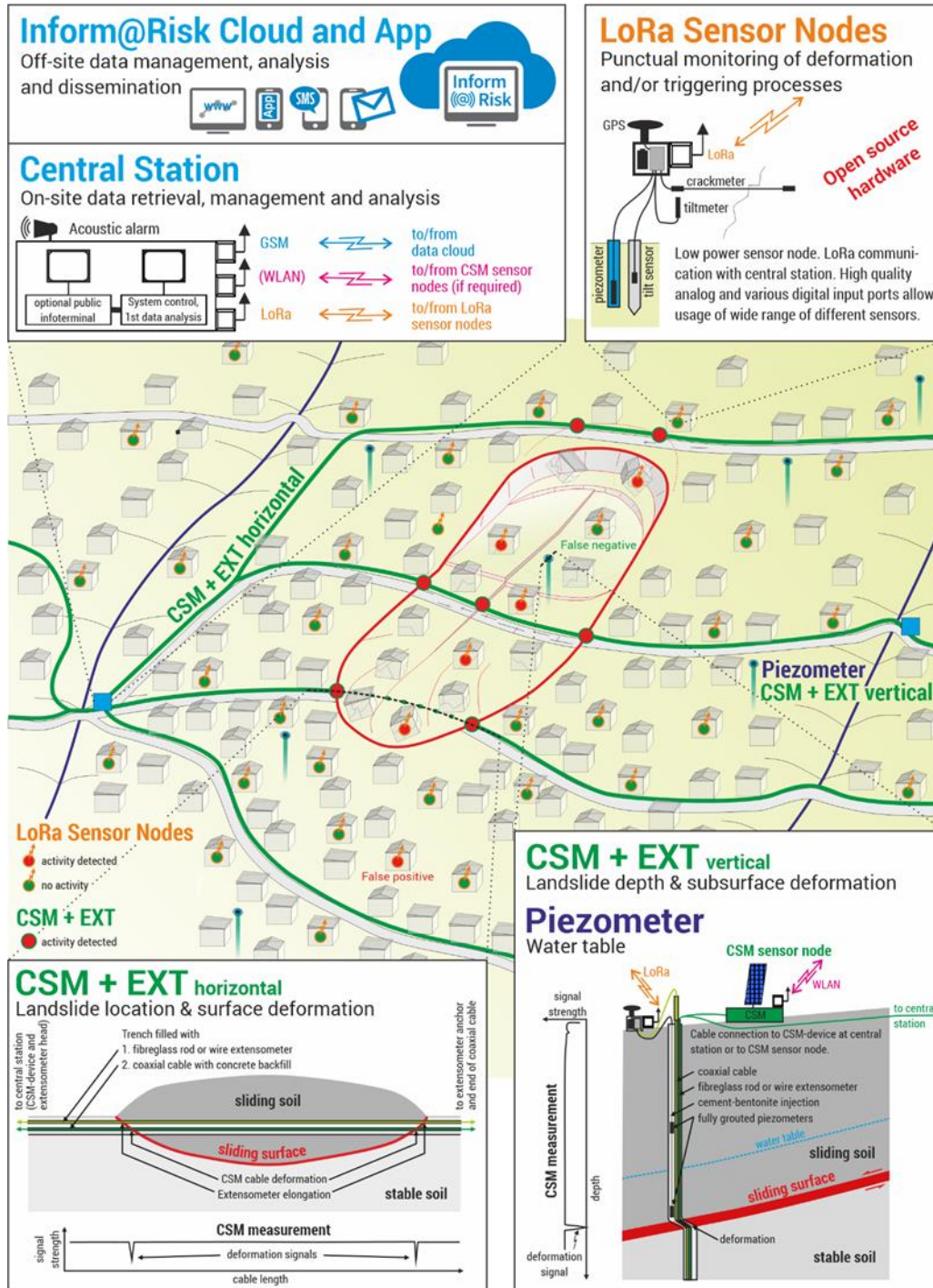


Figure 1. Schematic layout of the proposed landslide early warning system (Thuro et al. 2020).

**REFERENCES**

Froude M. J., Petley D. N., 2018, Global fatal landslide occurrence from 2004 to 2016. Nat. Haz. Earth Syst. Sci. 18: 2161–2181.

Thuro K., Singer J., Menschik B., Breuninger T., Gamperl M., 2020, Development of an early warning system for landslides in the tropical Andes (Medellin; Colombia). Geomechanics and tunneling: 13,1: 103-115.

## **Vulnerability of road infrastructure exposed to earthquake-induced landslides: a case study from Lefkada island, Greece**

Sotirios A. Argyroudis<sup>1</sup>, George Papathanassiou<sup>2</sup>, Sotiris Valkaniotis<sup>3</sup>, Vassilis Marinos<sup>4</sup>, Mike G Winter<sup>5</sup>

<sup>1</sup>*Department of Civil Engineering, Aristotle University, Thessaloniki, Greece & Department of Civil & Environmental Engineering, University of Surrey, UK, [sarg@civil.auth.gr](mailto:sarg@civil.auth.gr)*

<sup>2</sup>*Department of Civil Engineering, Democritus University of Thrace, Greece, [gpapatha@civil.duth.gr](mailto:gpapatha@civil.duth.gr)*

<sup>3</sup>*Koronidos 9, Trikala, Greece, [valkaniotis@yahoo.com](mailto:valkaniotis@yahoo.com)*

<sup>4</sup>*Department of Geology, Aristotle University, Thessaloniki, Greece, [marinosv@geo.auth.gr](mailto:marinosv@geo.auth.gr)*

<sup>5</sup>*Winter Associates Limited, UK, [mwinter@winterassociates.co.uk](mailto:mwinter@winterassociates.co.uk)*

Earthquake-induced landslides and ground failures often cause damage to road infrastructure resulting in disruption to traffic and social and economic consequences, as well as safety-related risks. The analysis of the geohazard risk associated with road networks is important to determine appropriate risk management and mitigation (Winter et al., 2019; Winter & Wong, 2020).

On November 17, 2015 a Mw 6.5 earthquake occurred on the island of Lefkada, in West Greece, triggering geohazard and environmental effects that were reported mainly in the western part of the island. The major earthquake-related phenomena included rock falls, rockslides, landslides and road-fill failures. The epicentral intensity was assessed based on the definitions of the Environment Seismic Intensity scale equal to VIII ESI-07, and the macroseismic epicenter (VIII up to IX) was located at the area of Egremnoi (west of Athani village, south Lefkada). The detailed field surveys conducted on November 2015, April 2016 and July 2016 by Papathanassiou et al. (2017) and Grendas et al. (2018) revealed that slope failures of high severity occurred at Egremnoi and Gialos areas. These areas were investigated in detail by Grendas et al. (2018) aiming to correlate the engineering geological characterization of rock mass, assigned based on the Geological Strength Index (GSI) classification (Marinos, 2010), with the type and size of the earthquake induced landslides. The impact of the slope failures on the road network, classified as very low, low, moderate, high and very high severity, was correlated with the engineering geological classification of the rock mass and landslide severity maps were compiled. Closures of the road network resulted in direct, direct consequential and indirect consequential socio-economic impacts (Winter & Bromhead, 2012), with particularly significant impacts on tourism to the island; the road access to Egremnoi beach, for example, has not been restored as of mid-2020.

The degree to which a road exposed to a geohazard can be damaged is commonly assessed through the damage functions that correlate the severity of the hazard with the level of the expected damage (Argyroudis et al., 2019). The most common types of damage functions used in risk analysis are the fragility and vulnerability functions that relate the hazard intensity (e.g. debris volume or ground displacement) to damage probabilities and losses (Winter et al. 2014). In this paper we investigate, for the first time in the literature, the correlation between the GSI classification of the rock mass and the impact to the road infrastructure, based on the damage data reported after the 2015 Lefkada earthquake. These correlations aim to provide essential input for making reasonable predictions of losses for road infrastructure in future events toward enhancing the resilience of transport networks and minimizing socio-economic impacts and safety risks.



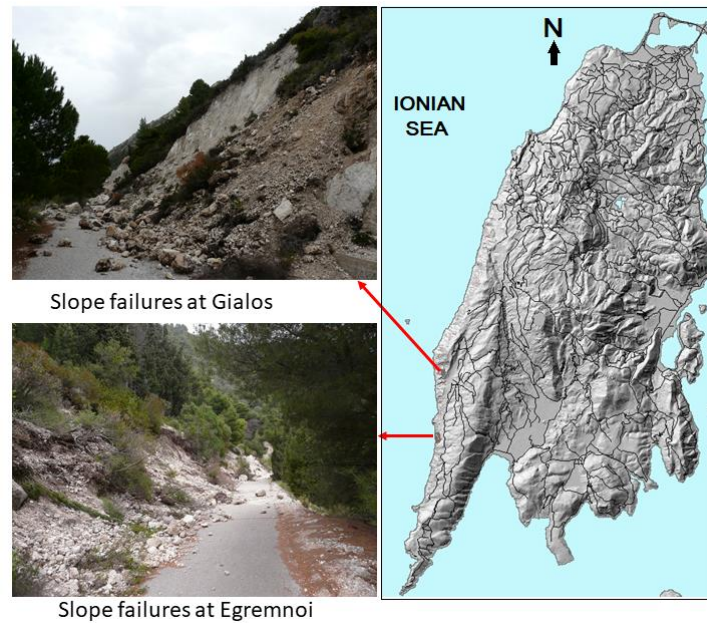


**Figure 1. Map of Lefkada island, representative photos showing road closures due to debris flows**

## REFERENCES

- Argyroudis, S., Mitoulis, S.A., Winter, M., Kaynia, A.M., 2019, Fragility of Transport Assets Exposed to Multiple Hazards: State-of-the-art Review toward Infrastructural Resilience. *Reliability Engineering and System Safety*, 191, 106567.
- Grendas, N., Marinos, V., Papathanassiou, G., Ganas, Ath., Valkaniotis, S., 2018, Engineering Geological Mapping of Earthquake-Induced Landslides in South Lefkada Island, Greece: evaluation of the type and characteristics of the slope failures. *Environmental Earth Sciences*, v. 77(12), 425.
- Marinos, V., 2010, New Proposed GSI Classification Charts for Weak or Complex Rock Masses. *Bulletin of the Geological Society of Greece*, v. 43(3), pp. 1248-1258.
- Papathanassiou, G., Valkaniotis S., Ganas Ath., Grendas, N., Kollia, El., 2017, The November 17th, 2015 Lefkada (Greece) Strike-Slip Earthquake: Field Mapping of Generated Failures and Assessment of Macroseismic Intensity ESI-07, *Engineering Geology*, v. 220, pp. 13-30.
- Winter, M.G., Bromhead, E.N., 2012, Landslide Risk: Some Issues that Determine Societal Acceptance. *Natural Hazards*, v. 62(2), pp. 169-187.
- Winter, M.G., Smith, J.T., Fotopoulou, S., Pitolakis, K., Mavrouli, O., Corominas, J., Argyroudis, S., 2014, An Expert Judgement Approach to Determining the Physical Vulnerability of Roads to Debris Flow. *Bulletin of Engineering Geology and the Environment*, v. 73(2), pp. 291-305.
- Winter, M.G., Peeling, D., Palmer, D., Peeling, J., 2019, Economic Impacts of Landslides and Floods on a Road Network. *AUC Geographica*, v. 54(2), pp. 207-220.
- Winter, M.G., Wong, J.C.F., 2020, The Assessment of Quantitative Risk to Road Users from Debris Flow. *Geoenvironmental Disasters*, v. 7(4), pp. 1-19.





## Projecting landslide susceptibility under Climate Change. The case of Eastern Pelion, Greece

Aikaterini-Alexandra Chrysafi<sup>1</sup>, Ioanna Ili<sup>2</sup>, Paraskevas Tsangaratos<sup>2</sup>

<sup>1</sup>*School of Science & Technology, Hellenic Open University, Patra, Greece, [std112294@ac.eap.gr](mailto:std112294@ac.eap.gr)*

<sup>2</sup>*NTUA, School of Mining and Metallurgical Engineering, Athens, Greece,*

*[gilia@metal.ntua.gr](mailto:gilia@metal.ntua.gr), [ptsag@metal.ntua.gr](mailto:ptsag@metal.ntua.gr)*

According to the Intergovernmental Panel on Climate Change (IPCC) special report “Managing the Risks of Extreme Events and Disasters to Advance Climate Change Adaptation” among other issues it is documented that there is high confidence that changes in heavy precipitation will affect landslides in some regions of the world (Seneviratne et al., 2012). In this context, the main objective of the present study was to assess the impact of the projected climate change on the occurrence of landslides in Eastern Pelion, Greece, an area with significant history of landslide and tourism development. The developed methodology involved two phases: The first phase involved assessing the landslide susceptibility, which expresses the likelihood of a landslide occurring in an area on the basis of local terrain conditions (Brabb, 1984). Logistic Regression Model (LRM) was used as the predictive model, whereas elevation, slope angle, aspect, distance from the river network, profile curvature, stream transportation index (STI), stream power index (SPI) and lithology were the variables identified as most important and relevant to the landslide phenomena recorded in the research area. Also, 187 landslide events were analyzed and along with 187 non-landslide events, identified following certain criteria (Tsangaratos et al., 2017), consisted the original database. For the purpose of validation procedures the original database was separated into a training and validation database, whereas the evaluation of the learning and predictive performance of the developed methodology was made by the calculation of the area under the success and predictive curve (AUC) concerning the final landslide susceptibility map. The second phase involved the estimation of the difference of the Modified Fourier Index (MFI), which represents the ratio between average monthly rainfall and average annual rainfall, a strong indicator of rainfall aggressiveness, for two time periods, at the present and in 2050. For the present study, the climate model HadGEM2-ES from the Coupled Model Intercomparison project was used. The HadGEM2-ES projection was driven by the representative concentration pathways 8.5, the most worst scenario. From the conducted analysis and for the first phase, the landslide susceptibility map was classified into 5 levels, namely: very low susceptibility, low susceptibility, medium susceptibility, high susceptibility and very high susceptibility (Figure1a). The eastern part of the area exhibits the largest landslide prone area, that is mainly covered by metamorphic rocks (schists, gneisses, phyllites, quartzites), with elevations ranging between 400 – 600 meters and slopes between 16-25 degrees. The LRM, based on the training and validation data showed a 50.61 % and 43.67 % relative landslide density for the very high susceptible zone, respectively. The AUC for the training data was calculated to be 0.7181 and the AUC value for the validation data 0.7118. Both indicate that the LRM had a quite significant learning and predictive ability concerning identifying landslide prone areas. Concerning the second phase, a 13 to 18 % increase in the MFI values was observed, covering the whole study area, which will affect the evolution of landslides. Specifically, the south parts of the study area, are likely to exhibit the highest increase, whereas the areas of high and very high susceptibility will have an increase of approximately, above 16% (Figure1b). Having in mind the special report of IPCC, mentioned earlier, those areas will experience an increase probability of slope failure. The results of the present study could assist in landslide susceptibility assessments that have an additional focus in climate change providing significant spatial information and knowledge to local and regional authorities.

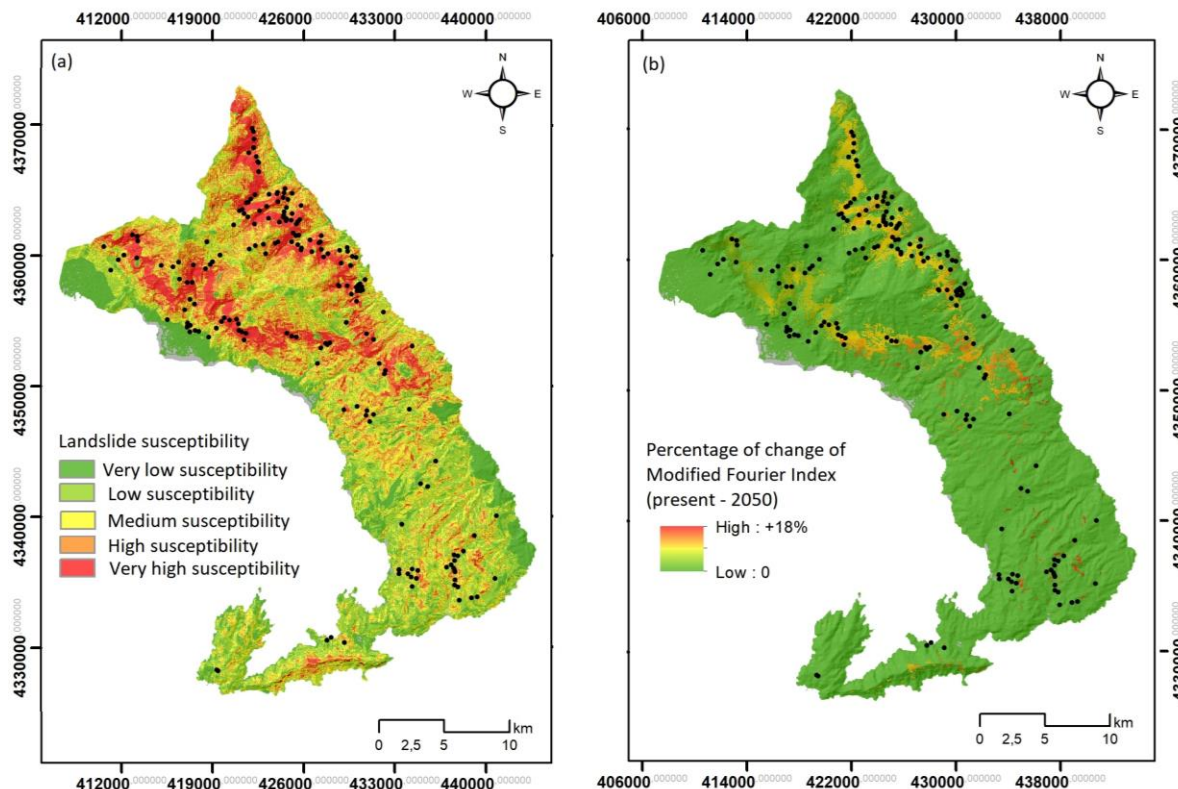


Figure 1. a. Landslide susceptibility map, b. Changes of Modified Fourier Index (present-2050)

**REFERENCES**

Brabb, E.E., 1984, Innovative approaches to landslide hazard mapping. Proc IV ISL, Toronto 1: 307 - 324.

Hong, H., Ilia, I., Tsangaratos, P., Chen, W., Xu., C., 2017, A hybrid fuzzy weight of evidence method in landslide susceptibility analysis on the Wuyuan area, China. *Geomorphology* 290, 1-16.

Seneviratne, S.I., Nicholls, N., Easterling, D., Goodess, C.M., Kanae, S., Kossin, J., Luo, Y., Marengo, J., McInnes, K., Rahimi, M., Reichstein, M., Sorteberg, A., Vera, C., Zhang, X., 2012, Changes in climate extremes and their impacts on the natural physical environment. C.B. Field, V. Barros, T.F. Stocker, D. Qin, D.J. Dokken, K.L. Ebi, M.D. Mastrandrea, K.J. Mach, G.-K. Plattner, S.K. Allen, M. Tignor, P.M. Midgley (Eds.), *Managing the Risks of Extreme Events and Disasters to Advance Climate Change Adaptation. A Special Report of Working Groups I and II of the Intergovernmental Panel on Climate Change (IPCC)*, Cambridge University Press, Cambridge, UK, and New York, NY, USA (2012), pp. 109-230.

## The tsunami component of the Hellenic Plate Observing System (HELPOS) research infrastructure

Marinos Charalampakis<sup>1</sup>, Nikos Kalligeris<sup>1</sup>, George Drakatos<sup>1</sup>, Akis Tselentis<sup>1</sup>

<sup>1</sup>*Institute of Geodynamics, National Observatory of Athens, Greece, [cmarinos@noa.gr](mailto:cmarinos@noa.gr), [nkalligeris@noa.gr](mailto:nkalligeris@noa.gr), [g.drakat@noa.gr](mailto:g.drakat@noa.gr), [tselenti@noa.gr](mailto:tselenti@noa.gr)*

Amongst the most devastating marine disasters that can occur in areas prone to seismic and volcanic activity, are earthquakes, volcanic eruptions and submarine slides, all of which can lead to tsunamis. Tsunami waves pose a serious threat, especially in densely populated coastal areas (CIESM. 2011). Advancing tsunami science and assessing tsunami hazard requires the long-term availability of high-quality field data. The Hellenic Plate Observing System (HELPOS) is a distributed network of geosciences and earthquake engineering observatories, run by Greek Research Institutions and Universities.

The tsunami component of the project foresees the installation of 3 new tide gauge stations. They will be integrated into the tide gauge network of the Hellenic National Tsunami Warning Center (HL-NTWC), which operates in the Institute of Geodynamics of the National Observatory of Athens (NOA-IG). The tide gauge network currently consists of 18 real-time stations (radar and/or pressure type) with a 30 sec sampling rate or less, suitable to record tsunami waves and support tsunami warning operations. The three new installation sites are the city of Kos (Dodecanese Islands), Plomari (Lesvos) and Preveza (western Greece) (fig. 1). Besides the new installations, an upgrade is planned for the existing tide gauge infrastructure. The upgrade includes maintenance of almost all the stations, as well as the installation of advanced equipment that will allow to remotely control and monitor the instruments. In order to fulfill the needs of the network, the computational facility will also be upgraded with the utilization of new dedicated hardware, i.e. a powerful workstation with peripherals, a large storage disk array and finally geospatial processing software, i.e. ESRI GIS mapping products.



**Figure 1: Two out of the three tide gauge stations that have been installed in Kos (left) and Plomari, Lesvos (right).**

The improvement of the infrastructure is also accompanied by an upgrade of the services provided by the HL-NTWC. The center provides a 24/7 tsunami monitoring service for Greece and the eastern Mediterranean Sea, issuing warning messages sent to the General Secretariat for Civil Protection in Greece. It is also an accredited Tsunami Service Provider in the framework of the North-Eastern Atlantic, the Mediterranean and connected seas Tsunami Warning System (NEAMTWS) of IOC/UNESCO, broadcasting tsunami warning messages to a

large number of subscribers. The messages are planned to include new enhanced products such as geographical maps that have been designed according to the needs of the end users, i.e. the national CPA and foreign subscribers.

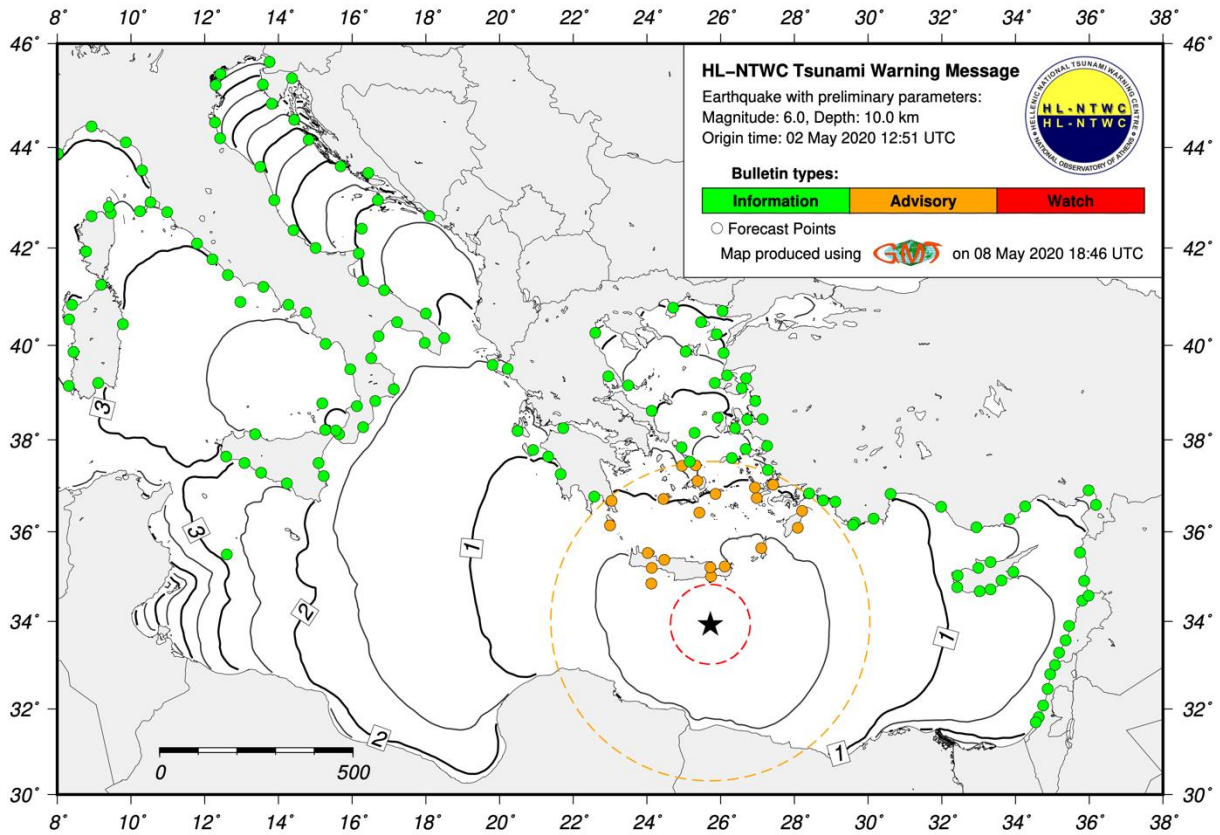


Figure 2: “Tsunami enhanced products” designed to be incorporated in the warning messages.

This research is supported by HELPOS ("Hellenic Plate Observing System" - MIS5002697) which is implemented under the Action "Reinforcement of the Research and Innovation Infrastructure", funded by the Operational Programme "Competitiveness, Entrepreneurship and Innovation" (NSRF 2014-2020) and co-financed by Greece and the European Union (European Regional Development Fund).

**REFERENCES**

CIESM Workshop Monographs, no. 42. Marine geo-hazards in the Mediterranean. Nicosia (Cyprus), 2-5 February 2011. Available from: <http://www.ciesm.org/online/monographs/Nicosia.html>.



## Tsunami risk assessment in the framework of the GEORISK project

Marinos Charalampakis<sup>1</sup>, Akis Tselentis<sup>1</sup>, George Drakatos<sup>1</sup>

<sup>1</sup>*Institute of Geodynamics, National Observatory of Athens, Greece, [cmarinos@noa.gr](mailto:cmarinos@noa.gr), [tselenti@noa.gr](mailto:tselenti@noa.gr), [g.drakat@noa.gr](mailto:g.drakat@noa.gr)*

Tsunami hazard assessment is traditionally based on events that could occur in the future (scenario-based), with poorly constrained probabilities of occurrence or return periods (e.g. Løvholt et al., 2006, Lorito et al., 2008; Okal and Synolakis, 2008). Another methodology that has been developed and put to use is the Probabilistic Tsunami Hazard Analysis (PTHA) (e.g. Geist and Parsons, 2006; Annaka et al., 2007; Thio et al., 2007). Although, researchers (e.g. Nadim and Gladem, 2006) suggest that the scenario based approach is best suited for tsunami hazard and risk assessment, it is scientifically and operationally very useful to know the probability of a tsunami of a certain severity in a certain coastal zone over a period of time.

The GEORISK project (<http://georisk.gein.noa.gr/intro/>), amongst other goals, aims to assess tsunami hazard and risk, in selected vulnerable regions of Greece. With the method of scenarios, an attempt is made to calculate the severity of the wave from credible worst-case tsunamis. The risk, which refers to the expected consequence of the tsunami, i.e. estimation of fatalities, damage to buildings, economic consequences, etc., is also estimated for the selected case studies.

In the framework of the project, three main actions were carried out. A new updated catalogue of the tsunamis in the Mediterranean has been developed. Following that, a set of maps has been prepared, illustrating both the tsunami events from antiquity to present, as well as the tsunamigenic sources in the entire Mediterranean region.

As regards tsunami hazard and risk assessment, two vulnerable areas at the eastern part of the Hellenic arc, Rhodes and Kos Islands, have been selected for the application of numerical simulations, based on credible worst case tsunami scenarios. The maximum tsunami height has been estimated, as well as the consequent extent of the flooded area (figure 1). The inundation zone for the town of Faliraki (Rhodes Island) extends up to 300m, with a flow depth ranging from 2 to 3m, while the run-up reaches up to 7m. For the town of Kos, the flow depth is about 3 m and the inundation zone extends up to 150m inland, reaching a topographic height of 4m. Most of the buildings in both study areas are expected to suffer light to moderate damages. An attempt has been made to estimate the repairing cost, which showed that even if the damage is expected to be low to medium, the cost for the city of Faliraki is about 4M€, while for the city of Kos it is expected to be three times bigger, i.e. ~13M€.

Tsunami awareness activities for the general public, like the development of an educational platform, the design of a leaflet (figure 2), the participation in events regarding research, technology & innovation, had been also planned and carried out during the project.

This work is supported by the project GEORISK (MIS-5002541) which is implemented under the Action "Strategic Development for Research and Technological Institutes" funded by the Operational Program "Competitiveness, Entrepreneurship and Innovation" (NSRF 2014-2020) and co-financed by Greece and the EU.



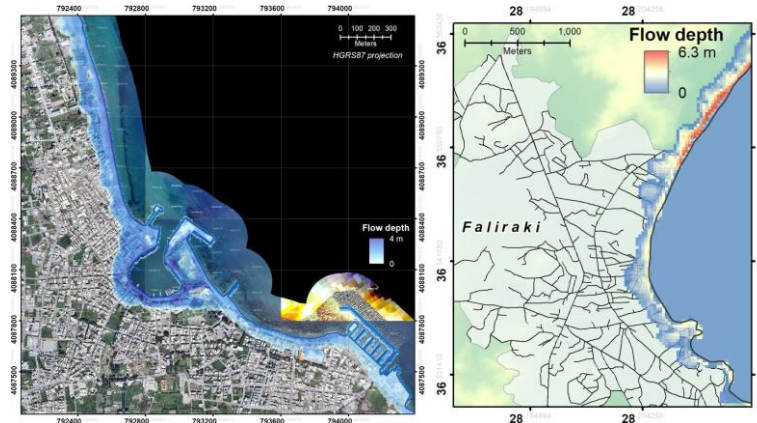


Figure 1: Maps illustrating the extent of the inundation zone for the cities of Kos (left) and Faliraki, Rhodes island (right).

Figure 2: Outreach material designed and disseminated as part of the GEORISK project.

REFERENCES

Annaka, T., Satake, K., Sakakiyama, T., Yanagisawa, K., and Shuto, N., 2007, Logic-tree approach for probabilistic tsunami hazard analysis and its applications to the Japanese coasts Pure and Applied Geophysics, 164, pp. 577-592.

Geist, E., and Parsons, T., 2006, Probabilistic analysis of tsunami hazards Natural Hazards, 37, pp. 277-314.

Lorito, S., Tiberti, M.M., Basili, R., Piatanesi, A., and Valensise, G., 2008, Earthquake-generated tsunamis in the Mediterranean Sea: scenarios of potential threats to Southern Italy Journal of Geophysical Research, 113 (B1), pp. B01301-B.

Løvholt, F., Bungum, H., Harbitz, C.B., Glimsdal, S., Lindholm, C.D., and Pedersen, G., 2006, Earthquake related tsunami hazard along the western coast of Thailand Natural Hazards and Earth Systems Sciences, 6, pp. 1-19.

Okal, E., and Synloakis, C.E., 2008, Far-field tsunami hazard from mega-thrust earthquakes in the Indian Ocean Geophysical Journal International, 172, pp. 995-1015.

Nadim, F., and Glade, T., 2006, On tsunami risk assessment for the west coast of Thailand F. Nadim, R. Pöttler, H. Einstein, H. Klapperich, S. Kramer (Eds.), ECI Symposium Series, 7.

Thio, H.K., Sommerville, P., and Ichinose, G., 2007. Probabilistic analysis of strong ground motion and tsunami hazards in Southeast Asia Proc. from 2007 NUS-TMSI Workshop, National University of Singapore, Singapore, 7–9 March 2007.



## Earthquake-generated tsunami hazard assessment for the Ionian Islands

Marinos Charalampakis<sup>1</sup>, George Drakatos<sup>1</sup>, Christos Evangelidis<sup>1</sup>

<sup>1</sup>*Institute of Geodynamics, National Observatory of Athens, Greece, [cmarinos@noa.gr](mailto:cmarinos@noa.gr), [g.drakat@noa.gr](mailto:g.drakat@noa.gr), [cevan@noa.gr](mailto:cevan@noa.gr)*

Tsunami events in the last 20 years alarmed coastal residents and resulted in researchers reassessing tsunami hazard exposure. In 2017, the Bodrum-Kos earthquake (Aegean Sea), in the Mediterranean, with a magnitude of 6.6, generated a local tsunami with ~2m run-up (Heidarzadeh et al., 2017). Despite the relatively small earthquake magnitude, this event was a reminder of the existing threat of tsunamis in the region. Similarly, in the Ionian Islands, laying in the western part of the Hellenic arc, one of the most seismically active areas in Greece and the entire Mediterranean region, small to moderate tsunamis may occur (e.g. England et al., 2015). The economic and touristic growth of the whole region during the past decades has led to an increase in coastal population and to the development of large leisure areas, close to shore, making them prospective targets for a large-scale disaster, even if for moderate tsunami waves.

This study aims to assess tsunami hazard in the region, by exploring the tsunamigenic potential of known seismic sources in the area. To this end, following the evaluation of the various sources in the broader Ionian Sea, we selected three credible scenarios and performed numerical simulations using the NAMI-DANCE code, a high level computational tsunami modeling tool. Further analysis of the results and preparation of thematic map products was held using the ArcGIS suite. Besides the estimation of the maximum tsunami height along the coast, we estimated the inundation zone in designated areas. The The selected scenarios were the AD 365 earthquake in western Crete, and two other fault ruptures, southwest of Zakynthos and west of Corfu.

For the AD 365 case, the highest simulated waves reach about 3m. This particular event produces the highest simulated waves observed at almost all islands. Exceptions are the islands of the northern Ionian, Corfu and Paxos, where the maximum wave heights are observed for the western Corfu scenario, although with lower absolute values, ~1.5m. Areas located in the eastern part of the islands are generally more protected from tsunami waves. These waves, although smaller in amplitude, ranging between 0.1 to 0.5m, still have significant size and are capable of causing human loss, and potentially cause damage to coastal infrastructure.

In terms of the range of wave arrival times, this varies depending on the distance of the site of interest from the seismic source. In general, the times in most cases are satisfactory enough, so that there can be a limited time window for early warning, as they usually exceed 15 to 20 min. It is worth noting that in all cases the first wave is not the largest. In Zakynthos, the largest wave reaches the coast 58 min after the arrival of the first wave. As regards the estimation of the inundation zones, this was feasible only for specific areas (e.g. figure 1). The extent of the inundation zone varies between 200 and 500m, while the run-up reaches up to 5m.

This work is supported by the project TELEMACHUS (MIS-5007986) which is implemented under the Action "Environmental Protection and Sustainable Development" funded by the Region of Ionian Islands and co-financed by Greece and the EU.

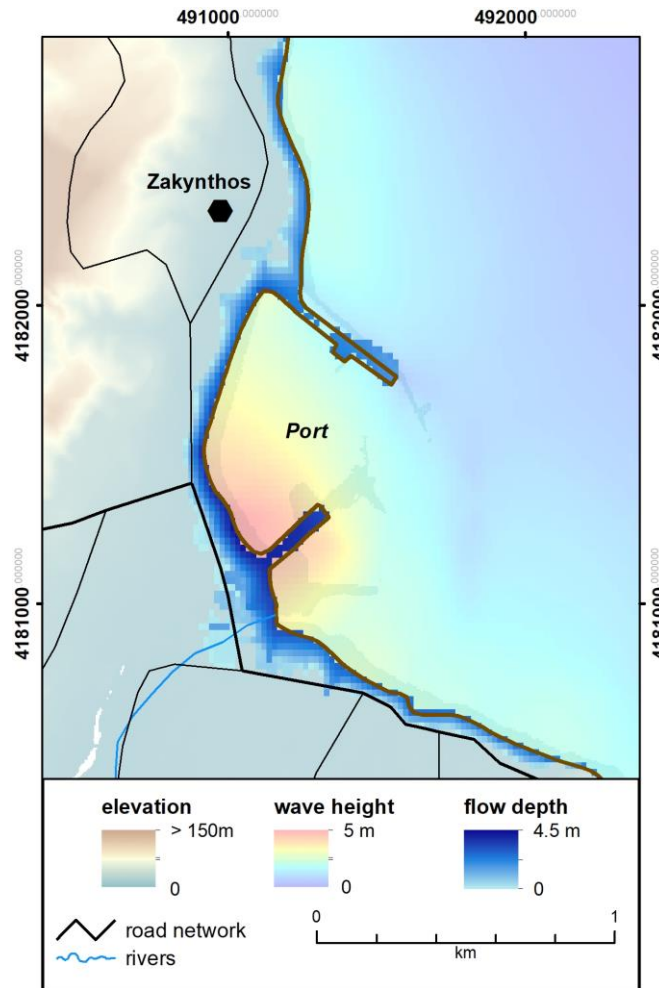


**Figure 1: Inundation zone in the area of the city of Zakynthos and distribution of maximum wave height.**

## REFERENCES

- England, P., Howell, A., Jackson, J., and Synolakis, C., 2015, Palaeotsunamis and tsunami hazards in the Eastern Mediterranean. *Philosophical Transactions of the Royal Society A*, 373(2053), 20140374.
- Heidarzadeh, M., Necmioglu, O., Ishibe, T., and Yalciner, A. C., 2017, Bodrum–Kos (Turkey–Greece) Mw 6.6 earthquake and tsunami of 20 July 2017: A test for the Mediterranean tsunami warning system. *Geoscience Letters*, 4, 31. <https://doi.org/10.1186/s40562-017-0097-0>.

## Spatial characteristics of a deep-seated gravitational slope deformation case in Taiwan: insights from long-term, multiple types of geodetic surveys

Pai Chiao Lo<sup>1</sup>, Ya Chu Chiu<sup>2</sup>, Tai Tien Wang<sup>3</sup>, Wei Lo<sup>1</sup>

<sup>1</sup>*Institute of Mineral Resources Engineering, National Taipei University of Technology, Taiwan,*  
[www90251@gmail.com](mailto:www90251@gmail.com), [lowei93@ntut.edu.tw](mailto:lowei93@ntut.edu.tw)

<sup>2</sup>*Department of Soil and Water Conservation, National Chung Hsing University, Taiwan,*  
[clarice.chiou@gmail.com](mailto:clarice.chiou@gmail.com)

<sup>3</sup>*Department of Civil Engineering, National Taiwan University, Taiwan, [ttwang@ntu.edu.tw](mailto:ttwang@ntu.edu.tw)*

One of the iconic features of deep-seated gravitational slope deformation (DSGSD) is its slow moving. As DSGSDs may be observable over long-term ( $\geq 10^2$  years) or short-term ( $< 10^2$  years) (Pánek and Klimeš, 2016), their qualitative variations may be deduced from geomorphological features, but their quantitative evolutions are generally achieved by numerical modeling with few points as verification. The study case, having a remarkable surface displacement rate of 0.1 m/year in the past 30 years, already has some local areas with deformations accumulated approximately 3 m. In the aid of such significant deformation rate and persistent geodetic monitoring throughout the study slope started from 1999, this study is able to resolve a detailed temporal development of the DSGSD.

The DSGSD case is a highway slope in southeastern Taiwan dipping to northeast. The highway passes the slope at about west-northwest to east-southeast direction, and goes through a mountain ridge in a double-lane tunnel. Ever since the highway is completed in 1972, there are always collapses, developing gullies, road settlement, cracked retaining structures, and cracked tunnel lining found within the case slope. Therefore, this study utilizes remote-sensing images interpretation, field investigation, geodetic surveys aboveground, underground, and in the tunnel, to examine the slope movement. First, the boundaries of moving masses were identified from remote-sensing images, and then modified according to the locations of scarps, road settlements, artificial structure damages and the features of rock mass outcrops. Rock core images and inclinometer displacements confirmed that the slope contains one large moving mass, mass A in the figure 1, and two smaller moving masses, mass B and C. The depths to mass A, B and C are around 90 m, 50 m and 50 m. The thirty-years geodetic monitoring results were catalogued in years. Two-dimensional information was input in ArcGIS to correlate with each other. While three-dimensional information, such as the displacement of control points set along monitoring profiles in highway tunnel, can be shown in three-dimension to compare with inclinometer displacement manually, or deduced to produce two-dimensional vectors. Forty-two ground points were measured by global positioning system in 2011-2013. A total number of twenty boreholes with depths ranging from 50 to 120 m served with inclinometers in 1999-2007 and 2013-2014. The monitoring profiles inside the tunnel were set in every 5 m, each profile with 43 monitoring points, in depths 0 to 75 m. Rock masses in the slope are mostly quartz-mica schist, but there is a mica schist belt close to the slope toe.

It is found that displacements differ in every moving masses. Take 2011-2013 for example, mass C has the largest ground surface displacement rate of about 75 mm/year, the eastern part of mass A comes next for around 38 mm/year, and then mass B of only 15 mm/year or so. Besides, mass C moves consistently to the slope dipping direction, when the eastern part of mass A is not. Therefore, zoning should be encouraged in the further investigation of every DSGSD cases.



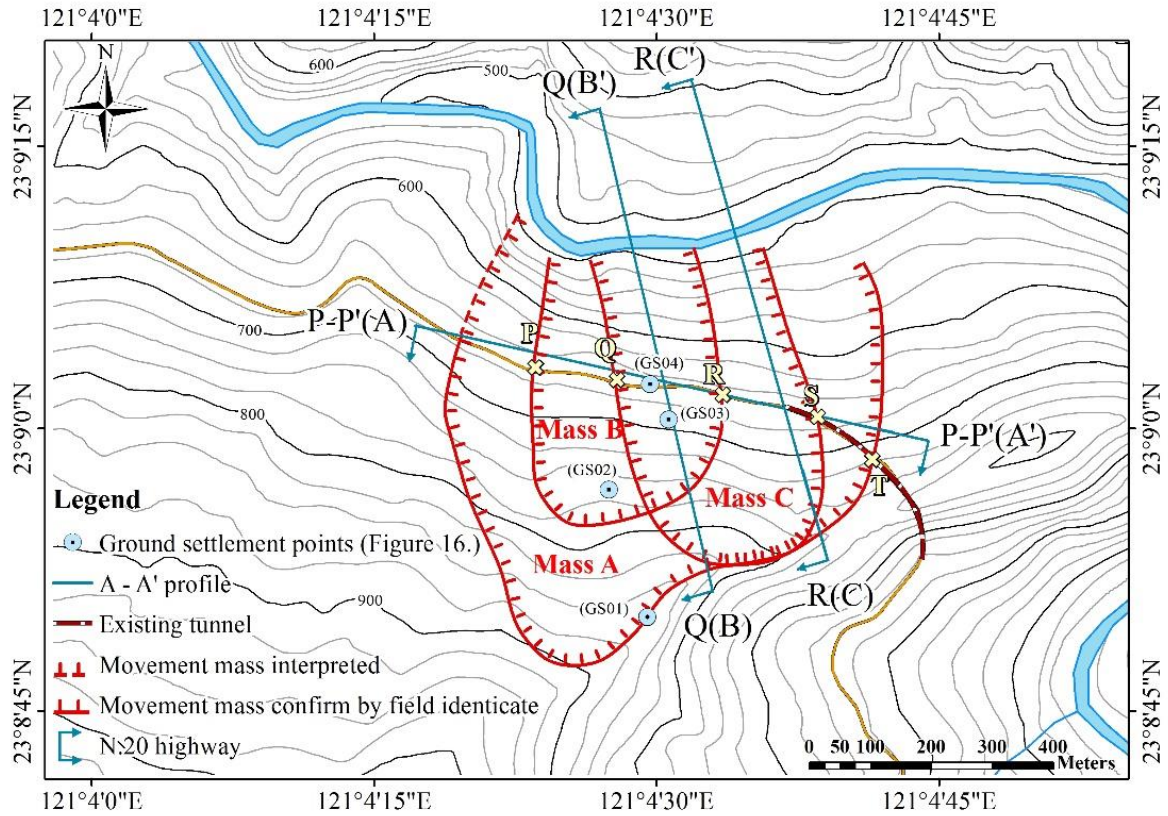


Figure 1. Plan view of slope

**REFERENCES**

Pánek, T, and Klimeš J., 2016, Temporal behavior of deep-seated gravitational slope deformations: A review. Earth-Science Reviews, 156, 14-38.





## Engineering geological study of rockfall phenomena and instability analysis in Proussos Dipotama site, Central Greece, using terrestrial LIDAR and UAV platforms

Maria Dandika<sup>1</sup>, Vassilis Marinos<sup>1</sup>, Efstratios Karantanellis<sup>1</sup>, George Papathanassiou<sup>2</sup>, Thomas Makedon<sup>1</sup>

<sup>1</sup>*Department of Geology, Aristotle University of Thessaloniki, 54124 Thessaloniki, Greece, [dandikamaria@hotmail.com](mailto:dandikamaria@hotmail.com), [skarantanellis@gmail.com](mailto:skarantanellis@gmail.com)*

<sup>2</sup>*Department of Civil Engineering, Democritus University of Xanthi, Greece, [gpapatha@civil.duth.gr](mailto:gpapatha@civil.duth.gr)*

Rockfalls undoubtedly constitute a serious and frequent geological hazard and can often have catastrophic consequences on the anthropogenic environment. In order to determine the failure mechanism as well as the triggering factors is important to determine the rock mass characteristics in detail. In cases where geological mapping is limited by morphology or accessibility, field observations can be significantly enhanced by a combination of Lidar scanners (Light Detection and Ranging) and Unmanned Aerial Vehicle platforms (UAV).

The research area is located in the district of Dipotama – Prouso, Evritania on a limestone slope, where several rockfalls have occurred (Karantanellis, 2019). The slope's elevation is around 90m, the slide is approximately 70° steep and facing north-east (NE). It is about a characteristic area that has presented multiple rockfalls in the last decade, with partial to complete destruction of the road, with the most recent and catastrophic rockfall occurring five years ago (February 2015). So, the scope of this paper is the geotechnical evaluation of the slope, the determination of failure mechanism, the detection of geomorphological changes in recent years and the qualitative hazard assessment.

The predominant geological formation in the area is the Pindos limestone, with marl alternations forming angular blocks, dipping at approximately 82°. The limestones are thin bedded and slightly weathered. The area is also affected by thrust fault zones, dipping at a low dip angle (30°), with the same dip direction as the slope. In order to determine the failure mechanism, we used point clouds from terrestrial laser scanner (TLS) and UAV. However, all these data cannot solely support the engineering geological appreciation of the rock falls. Hence, the field work incorporated geotechnical rock mass classification with the GSI system (Marinos, 2010; Farmakis et al., 2019) along the whole slope and measurements considering the geometry and strength of the principle structural elements of the slope.

In conclusion, two geological units were classified regarding the engineering geological conditions. In the current case there are flexural topplings with joints (J2). As for the rockfalls' failure mechanism, it is the planar sliding along the fault zones. The failure mechanism is triggered, because these zones have poor mechanical characteristics and planar slide is geometrically favored, due to the structure of the formations in the slope. Finally, change detection based on 3D point cloud analysis was performed along the slope in order to detect the prominent recent hazardous zones.

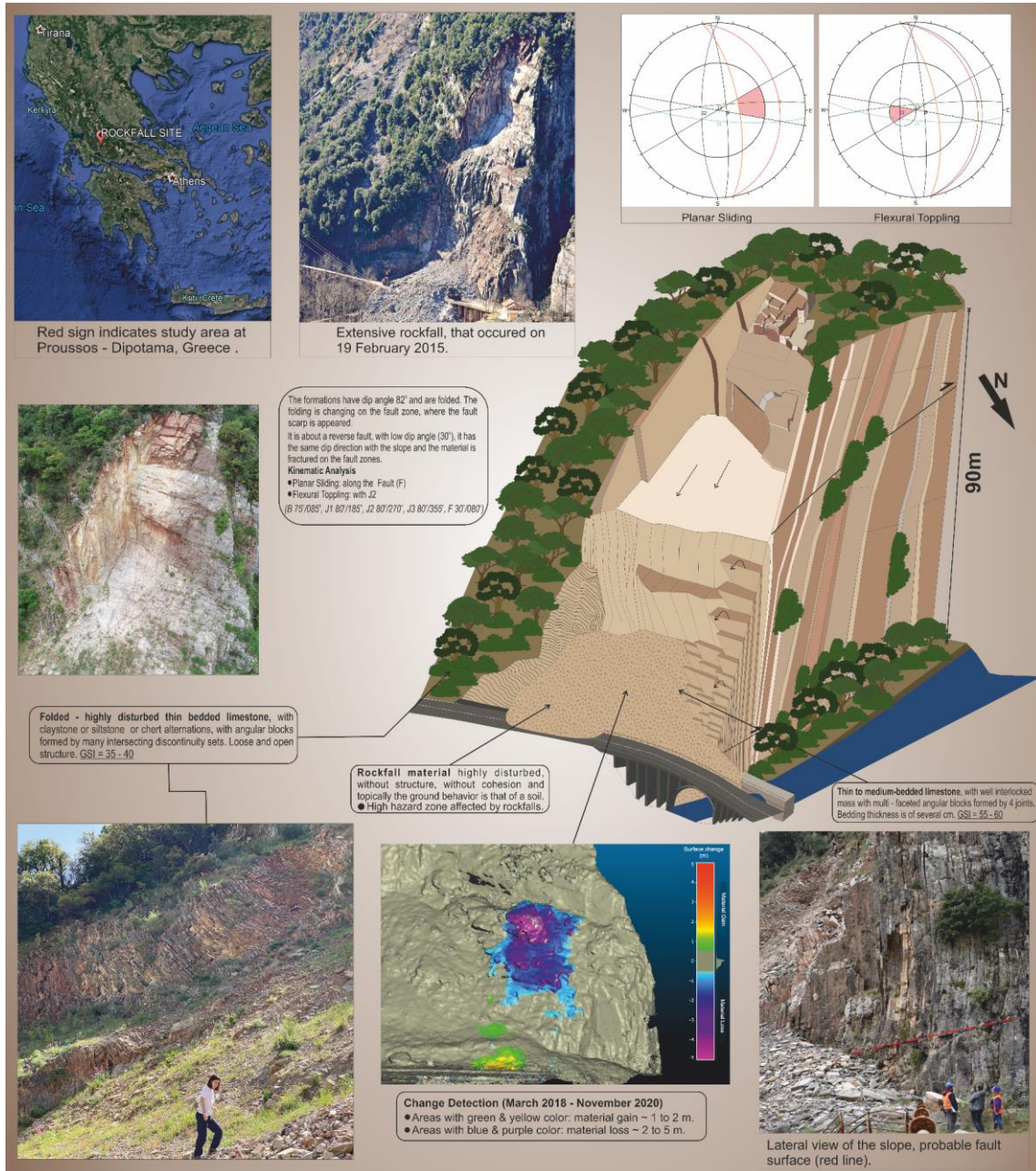


Figure 1: Engineering geological conceptual model of Proussos Dipotama rockfall site, Central Greece.

**REFERENCES**

Farmakis I, Marinos V, Vlachopoulos N., 2019, Assessment of the GSI along rock slopes based on LiDAR and photogrammetry point clouds. In: 53rd US rock mechanics/geomechanics symposium held in New York, NY, USA, 23–26 June

Karantanellis, E., Marinos, V., Vassilakis, E., 2019, “3D hazard analysis and object-based characterization of landslide motion mechanism using UAV imagery”, Int. Arch. Photogram. Remote Sens. Spatial Inf. Sci., XLII-2/W13, 425–430, <https://doi.org/10.5194/isprs-archives-XLII-2-W13-425-2019>.

Marinos, V., 2010, "New proposed GSI classification charts for weak or complex rock masses. Bull Geol Soc Greece 4(3):1248-1258.

## Study on mechanism of loess landslide induced by train vibration combined with water

Yuanjun Xu<sup>1</sup>, Jiading Wang<sup>1</sup>, Tianfeng Gu<sup>1</sup>

<sup>1</sup>State Key Laboratory of Continental Dynamics, Department of Geology, Northwest University, China,  
[graceyxu@163.com](mailto:graceyxu@163.com), [wangjiading029@163.com](mailto:wangjiading029@163.com), [gutf@nwu.edu.cn](mailto:gutf@nwu.edu.cn)

With the continuous development of the global economy and the deepening of the interconnection between the global economies, railway as an economic and environmentally friendly transportation mode will continue to develop. But at the same time, landslides, collapses and other geological hazards along the railway have also attracted more and more attention. This paper focuses on the loess landslides along the railway in the Loess Plateau of China, and analyzes the loess landslide pattern under the combined action of train vibration and water using on-site monitoring and indoor test methods to provide scientific guidance for the safe operation of the railway. In the loess mountains and plains, field monitoring was conducted along the railway to learn the propagation of train vibrations in the loess. The monitoring results show that the vibration acceleration decays exponentially with the increase of the distance from the rail. And the vibration attenuation rate in mountain areas is significantly greater than that in the plains due to the greater depth. Based on the improved indoor saturated loess vibration penetration test and one-dimensional vertical soil column infiltration test under vibration, the saturated vibration penetration test results show that the penetration rate of the loess accelerates with the increase of vibration amplitude, and the saturation increases after the seepage stabilizes. So, the effect of vibration combined with water on the permeability of loess is the most obvious. The results of the soil column test show that under the action of external vibration, the closed bubbles inside the loess escape, and then the gas phase escape rate increases, the infiltration resistance decreases, finally the penetration rate is accelerated. Based on the results of field investigation and indoor experiments, the mechanism of the combined action of train vibration and water to induce loess landslides mainly includes three stages. The first stage is the cracking stage. The long-term train vibration causes cracks in the surface soil layer based on Photos of on-site investigation along the railway. The second stage of the combined action of train vibration and water, the summer short-time heavy rainfall in the Loess Plateau combined with the train vibration formed a dominant channel at the original fissure, accelerated the infiltration of surface water, and caused the rapid saturation of the soil layer near the potential sliding surface of the slope. Vibration accelerates the infiltration of rainwater, makes the surface water quickly saturated, softens, and reduces the strength of the soil, especially the vibration frequency of a train is just close to the natural frequency of the soil layer in the area, the stability of the slope is further reduced. In the third stage of the landslide sliding phase, as the effect of the long-term train vibration and water, the soil strength of the potential sliding surface is further reduced, and then induced loess landslides.

## The effect of suction on differential weathering and stability of soft rock cliffs on the example of Zenta Bay cliff (Split, Croatia)

Ana Raič<sup>1</sup>, Nataša Štambuk Cvitanović<sup>1</sup>, Goran Vlastelica<sup>1</sup>

<sup>1</sup>Faculty of Civil Engineering, Architecture and Geodesy, University of Split, Croatia, [ana.raic@gradst.hr](mailto:ana.raic@gradst.hr),  
[nstambuk@gradst.hr](mailto:nstambuk@gradst.hr), [goran.vlastelica@gradst.hr](mailto:goran.vlastelica@gradst.hr)

The coastline of the Split area (Croatia) is characterized by soft rock cliffs, as the Split area lies on Eocene flysch formations. The shape of a rock coast is usually a result of local tectonic, geological and climatic conditions. Seasonal and daily temperature changes, precipitation, relative humidity, frequency of high wave storms and many other climatic variables influence the development of coastal processes. Although marine erosion (i.e. the influence of waves and tides) is the most common recession factor, the recession of soft rock cliffs is dominated by the weathering. Flysch formations in the greater Split area are characterized by a layered structure in which the lithological components of the layers alternate between hard clays/soft rocks and hard rocks. The stratification results in differential weathering between the layers, which causes undercutting of hard rocks and ultimately leads to slope instabilities and rockfalls. The dominant soft rock lithotype in the Split region is marl, which varies from clayey marls to calcareous marls. These materials are extremely susceptible to a change in properties due to weathering processes (physical and chemical) that transform the material with soft rock properties into a fine-grained material (Miščević & Roje-Bonacci, 2001). Physical weathering in this area is usually caused by the process of wetting, and drying and it can be assumed that this process is highly related to the unsaturated state of the material, i.e. the development of suction in the pores. The weathering process of Dalmatian marls and its influence on slope stability has been extensively studied (Miščević & Roje-Bonacci, 2001; Miščević & Vlastelica, 2014; Vlastelica et al., 2018a; Vlastelica et al., 2019, etc.).

The problem of differential weathering and cliff instability is observed on the example of Zenta Bay cliff in Split, located on the southern coast of the Split peninsula. The observed cliff is a 14-meter-high steep slope with a landscaped promenade at the cliff toe. The geological structure of the cliff consists of highly weathered clayey marl layers intertwined with calcareous sandstone layers. In March 2019, a geotechnical survey was carried out to evaluate the slope stability. Global stability control of the slope is performed assuming a solid sliding body according to one of the available limit boundary methods using computer program Slide (Rocscience) and in accordance with Eurocode 7, design approach 3 (methodology presented in Vlastelica et al., 2018b). As the slope surface is highly weathered, the surface material is prone to shallow landslides. Consequently, the slope is quasi stable and does not comply to EC7 requirements (i.e. for one profile safety factor of 0.91). If EC7 is dismissed, a safety factor of 1.14 is obtained for the same profile. However, in the case of an extreme situation such as heavy rainfall or earthquake, it can be lower than 1 and thus lead to landslide. In April 2019, heavy rainfall, preceded by dry March and February, caused a large rockfall. Improper cliff reconstruction and stabilisation led to a second rockfall in November 2019, caused by similar weather conditions. Based on the above-mentioned events, where heavy rainfall after long dry periods caused slope movements, suction differential was analysed as an instability trigger and weathering agent for soft rock cliffs and slopes.

Namely, significant changes in suction can occur during the year (monthly and seasonal) or a specific month in the surface zone of marly cliff materials interacting with the environment/atmosphere. This causes significant suction gradients and differential suction (also towards the deeper layers), as well as the process of induced differential swelling and consequently further development of the weathering (through development of the tensile and shear stresses, slaking, decomposition of the binder and loss of resistance). Suction changes were calculated according to the Kelvin's equation (1) for total suction and analysed using the climate data from the



$$\text{meteorological station Marjan-Split. } s = - \frac{RT}{v_{w0}\omega_v} \ln(RH) \quad (1)$$

where:  $s$  – total suction (kPa),  $R$  – universal gas constant ( $\text{J mol}^{-1} \text{K}^{-1}$ ),  $T$  – absolute temperature (K),  $M_w$  – molecular mass of water ( $\text{kg/kmol}$ ),  $\rho_w$  – density of pure water ( $\text{kg/m}^3$ ),  $RH$  – relative humidity.

The analysis conducted shows that changes in suction for different annual and monthly periods are significant considering the retention curves for marl. Furthermore, the specific climatic conditions during the year of rockfalls affected the suction changes in such a way that the differences are more pronounced compared to the reference average suction values over longer time periods. The RH on the days of the rockfalls reaches monthly and annual maximum (89%), temperatures are in a decreasing trend and close to the lowest value (about  $13^\circ\text{C}$ ), precipitation increases significantly after the previous dry period (cumulative precipitation above the 98th and 90th percentile for the period 1961-2000, for the 1st and 2nd rockfall, respectively) and consequently suction is at a minimum (15 MPa). The maximum and minimum values of suction and their differences are given in Table 1.

In summary, monitoring of weather conditions and trends with emphasis on relative humidity and temperature changes prior to the rainfall occurrence and the associated suction changes may contribute to the understanding of rockfall triggering mechanisms and the prediction of rockfall events.

**Table 1. Suction differences in the surface zone of marly cliff materials**

Period / data source	Type of analysis	Maximum suction $s_{MAX}$ (MPa)	Minimum suction $s_{MIN}$ (MPa)	Difference $\Delta s = s_{MAX} - s_{MIN}$ (MPa)	Remarks
1961-1990 (CHMC)	1	97.0	58.9	38.1	difference July-November
	2	88.3	65.1	23.2	difference summer-winter
1971-2000 (CHMC)	1	97.3	60.7	36.6	difference July-November
	2	89.7	65.1	24.6	difference summer-autumn
2019 (CHMC, WeatherOnline)	1	103.9	44.1	59.8	difference August-November
	2	99.8	65.7	34.1	difference summer-autumn
April 2019 (WeatherOnline)	3	153.5	15.38	138.1	$s_{MIN}$ obtained on the day of the 1 <sup>st</sup> rockfall 10.4.2019
November 2019 (WeatherOnline)	3	101.1	15.37	85.7	$s_{MIN}$ obtained on the day of the 2 <sup>nd</sup> rockfall 20.11.2019 (almost the same conditions)

CHMC – Croatian Meteorological and Hydrological Service/ WeatherOnline – <https://www.weatheronline.co.uk/weather/maps/city/>

1 – analysis by months in a year, 2 – analysis by seasons in a year, 3 – analysis by days in a month

### Acknowledgements

This work has been supported in part by the Croatian Science Foundation under the project number UIP-2017-05-3429.

### REFERENCES

- Miščević, P., Roje-Bonacci, T., 2001, Weathering process in Eocene flysch in region of Split (Croatia). *Rudarsko-geološko-naftni zbornik*, v. 13, pp. 47-55.
- Miščević, P., Vlastelica, G., 2014, Impact of weathering on slope stability in soft rock mass. *Journal of Rock Mechanics and Geotechnical Engineering*, v. 6 (2014), pp. 240-250. <https://doi.org/10.1016/j.jrmge.2014.03.006>
- Vlastelica, G., Miščević, P., Štambuk Cvitanović, N., 2018a, Durability of soft rocks in Eocene flysch formation (Dalmatia, Croatia). *Engineering Geology*, v. 245 (2018), pp. 207-217. <https://doi.org/10.1016/j.enggeo.2018.08.015>
- Vlastelica, G., Miščević, P., Štambuk Cvitanović, N., Glibota, A., 2018b, Geomechanical aspects of remediation of quarries in the flysch: case study of abandoned quarry in Majdan, Croatia. In: Litvinenko, V. (ed.) *Geomechanics and Geodynamics of Rock Masses - Selected Papers from the 2018. European Rock Mechanics Symposium*, 1st ed., CRC Press, London, UK, 2018, pp. 679–684. <https://doi.org/10.1201/9780429449222>
- Vlastelica, G., Štambuk Cvitanović, N., Miščević, P., Nikolić, M., Raić, A., 2019, The role of unsaturated condition & suction in weathering mechanisms in flysch marls. In: Sigursteinsson, H., Erlingsson, S., Bessason, B. *Geotechnical Engineering foundation of the future- Proceedings of XVII ECSMGE-2019*, Reykjavik: Icelandic Geotechnical Society, 2019, 0878, 8 doi:10.32075/17ECSMGE-2019-0878



## Investigation of deep geohazard sites with seismic and ambient noise methods, combined with 3D Geomodelling

Hans-Balder Havenith<sup>1</sup>, Lena Cauchie<sup>1</sup>, Anne-Sophie Mreyen<sup>1</sup>

<sup>1</sup>UR Geology, Liege University, Belgium, [hb.havenith@uliege.be](mailto:hb.havenith@uliege.be)

[as.mreyen@uliege.be](mailto:as.mreyen@uliege.be)

### **Background**

During the last years our group has studied a series of massive slope failures as well as deep geo-sites for engineering projects (dam and possible tunnel construction sites) located in various geohazard contexts. Therefore, we tested various combinations of active seismic and ambient noise methods and representation of related outputs in complex 3D Geomodels. Investigated sites include massive, likely seismically landslides in the Romanian Carpathian Mountains, slopes near the Rogun Dam construction site in Tajikistan, a very large active landslide in the Swiss Alps, an incipient volcanic flank collapse on El Hierro Canary Island and a site selected for the possible installation of an Einstein Telescope in the BE-NL-DE border region.

### **Methods**

Our active seismic prospection includes seismic refraction tomography (SRT) and multi-channel analysis of surface waves (MASW) while ambient noise investigation methods cover the single station H/V and multi-station array techniques. Field data were collected during multiple geophysical campaigns (2015-2020) on the aforementioned sites. The geological, geophysical, and seismological analysis outputs were integrated in a 3D geomodel (most of them supported by 3D surface models constructed on the basis of UAV imagery) that was used as tool to assess basic elements of the slope stability, in terms of morphology and deeper internal structure, possible sliding horizons (basal and lateral) as well as elastic material properties, or in order to identify karst phenomena, and fault structures that may represent a problematic zone for tunnel construction projects. Some of those sites were later also analysed by applying a numerical modelling analysis, as for the Rogun site presented in Havenith et al. (2018), or for a massive landslide in the Romanian Carpathian Mountains described in detail in Mreyen et al. (2021).

### **Results**

Results of the active seismic (SRT, MASW) are represented in terms of P-wave velocity ( $V_p$ ) sections and S-wave velocity ( $V_s$ ) logs; the ambient noise H/V noise data were first interpreted in terms of fundamental or higher resonance frequencies of the ground, which are in a second process, involving seismic velocity information, used to provide depth information on the resonant layers. Figure 1 presents an example for the Balta site in Romania, investigated by those seismic and ambient noise methods, with compilation of analysis outputs and interpreted structures in a 3D geomodel.

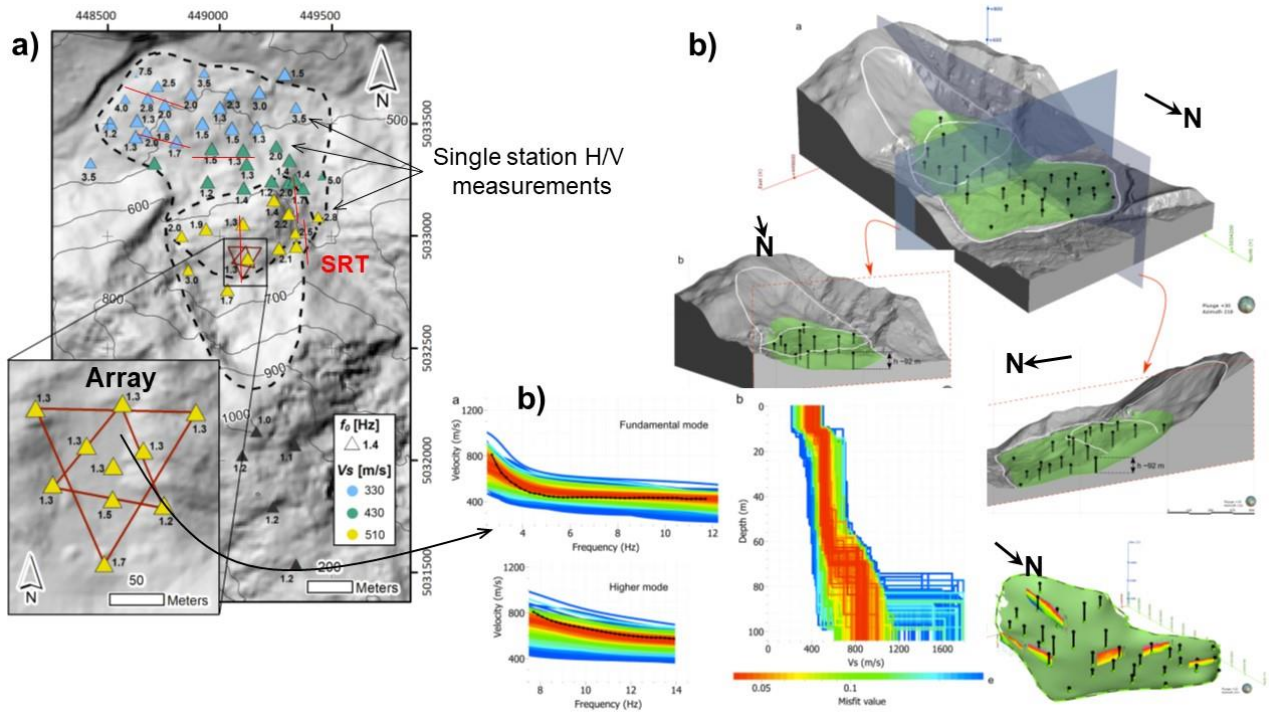


**Figure 1. a) Survey map with active and passive seismic measurements on the massive Balta rockslide in the Romanian Carpathians, with location of H/V and array measurements, as well as seismic profiles, mainly used in this case for SRT analysis (some also used for MASW analysis); see also average  $V_s$  estimates for different parts of the landslide. b) Dispersion curves and  $V_s$  models derived from the seismological array measurement. c) 3D geomodel views of the site with H/V data transformed into depth-logs of the resonant landslide body, the green surface representing the sliding surface; see also SRT sections together with H/V logs in lower right corner.**

### Conclusions

We combined the seismic and ambient noise survey techniques to get the best information on the elastic properties of the subsurface (here, we do not consider the electrical resistivity measurements that were performed on most of the investigated sites as well – also to get information on the groundwater level depth). 3D geomodels allow us to represent different types of topographic data together with the geophysical outputs and inferred subsurface information. We estimate that this type of proceeding and representation will define the new state-of-the-art in landslide investigation, especially in seismic regions where the information on the  $V_s$  of the underground is essential to model dynamic effects caused by earthquakes.

### REFERENCES

Havenith, H.-B., Torgoev, I., & Ischuk, A., 2018, Integrated geophysical-geological 3D model of the right-bank slope downstream from the Rogun Dam construction site, Tajikistan. *International Journal of Geophysics*, 16 p.

Mreyen A.-S., Cauchie L., Micu M., Onaca A.L., Havenith H.-B., 2021, Multiple geophysical investigations to characterize massive slope failure deposits: application to the Balta rockslide, Carpathians. *Geophysical Journal International*, in press.

## Detecting early landslide phenomena after wildfires through UAV-photogrammetric mapping

Aggelos Pallikarakis<sup>1</sup>, Georgios Deligiannakis<sup>1</sup>, Ioannis Papanikolaou<sup>1</sup>

<sup>1</sup>Laboratory Mineralogy-Geology Department of Natural Resources Management and Agricultural Engineering Agricultural University of Athens, Greece, [agpall@aua.gr](mailto:agpall@aua.gr), [gdeligian@aua.gr](mailto:gdeligian@aua.gr), [ipap@aua.gr](mailto:ipap@aua.gr)

### Introduction

Wildfires are among the most critical factors controlling landslides and debris flow, especially in severely burned areas (e.g., Cannon et al., 2001). Wildfires alter vegetation and soil properties, rendering the burned area susceptible to rapid geomorphological changes (e.g., Swanson, 1981, Cannon et al., 2001). Detailed mapping of such areas can reveal cracks at the top of landslide-prone slopes and small displacements at existing landslide head scarps. The use of UAV based photogrammetry provides a new tool that offers high spatial resolution, assisting traditional field mapping techniques (e.g., Colomina & Molina, 2014).

### Methods

A southeast-facing slope in Kechries, Greece, with a mean gradient of 30° was selected as a pilot area, after it suffered a severe wildfire on 22/07/2020. The burned slope was scanned twice within a month, using a DJI Phantom 4 drone with a 12mp camera sensor. In every flight, more than 400 photos were taken, with an 80% overlap on average. 12 GCPs were surveyed using RTK GNSS, with a range of <1cm in the horizontal plane and 1,7cm in the vertical. The photogrammetric process resulted in 2 high-resolution DSMs.

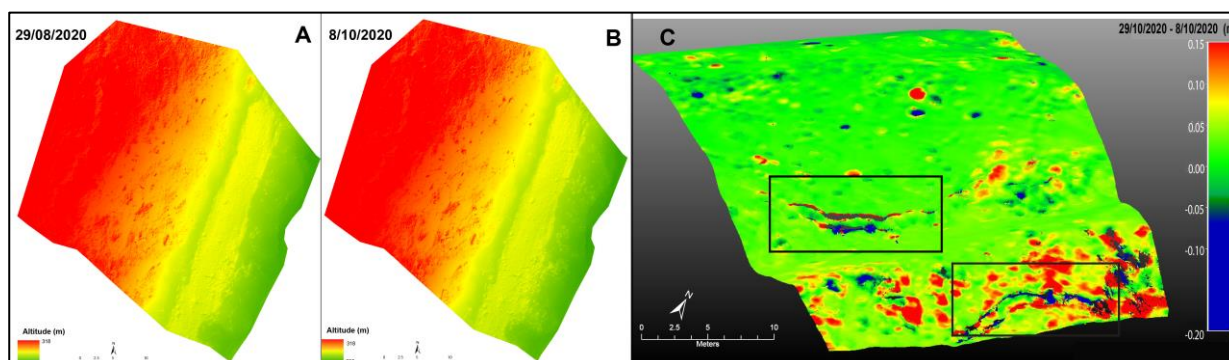


Figure 1. The correlation of the two DSMs (A-B) revealed minor scarps in two locations a few cm high (highlighted in black boxes in C), indicating early sliding phenomena.

### Results

The comparison of the DSMs revealed slight differences in the examined area, in forms of sediment transportation over the surface and accumulation towards the slope's foot. Also, minor scarps were traced, indicating the initiation of landslide phenomena (Figure 1).

### Conclusions

The methodology followed in this study appears to be highly efficient for detecting early landslide phenomena in postfire settings due to the high spatial resolution provided. Notable, it is impossible to describe any significant changes to the topography based only on surface observations, considering that the presented DSM extracted by both scans has minor differences. Only after correlating the two DSMs, it is possible to detect early landslide scarps.



## **Acknowledgments**

Cofinanced by Greece and the E.U. (European Social Fund) through the Operational Program «Human Resources Development, Education and Lifelong Learning 2014-2020» and the Program encoded EDBM103, titled “Support for researchers with an emphasis on young researchers-cycle B ”, in the context of the project “Detect and describe small landslides through t-LIDAR and UAV scanning techniques” (MIS 5048452).

## **REFERENCES**

- Cannon, S., Kirkham, R., Parise, M., 2001, Wildfire-related debris-flow initiation processes, Storm King Mountain, Colorado. *Geomorphology* 39 (3–4), pp. 171–188.
- Colomina, I., Molina, P. 2014, Unmanned aerial systems for photogrammetry and remote sensing: A review. *ISPRS J. Photogramm. Remote Sens.* 92, pp. 79–97.
- Swanson, F.J., 1981, Fire and geomorphic processes. In: Mooney, H.A., Bonnicksen, T.M., Christensen, N.L., Lotan, J.E., Reiners, W.A. Eds., *Fire Regimes and Ecosystem Properties*. USDA For. Serv. Gen. Tech. Rep. WO, vol. 26, pp. 401–420.

## Prediction of Karst susceptibility combining GIS based modeling and Remote Sensing data analysis

Mirko Vendramini<sup>1</sup>, Walter Giulietto<sup>1</sup>, Fabrizio Peruzzo<sup>1</sup>, Attilio Eusebio<sup>1</sup>

<sup>1</sup>Geodata Engineering SpA, Italy, [mve@geodata.it](mailto:mve@geodata.it), [wgi@geodata.it](mailto:wgi@geodata.it), [fpe@geodata.it](mailto:fpe@geodata.it), [aeu@geodata.it](mailto:aeu@geodata.it)

Karst phenomena are considered among the most important geological hazards affecting the railways and motorways design and construction. The prediction of their characteristics, occurrence and impacts on the environment is often difficult to define because of the complex interaction of the geo related factors and the parameters which trigger the karst processes. The quality and quantity of the available data can influence the accuracy of the karst susceptibility assessment; thus a sensitive analysis of the input data is required before validating the results. The aim of this paper is to present the methodology applied to the geomorphological study of a karst susceptible area based on the combination of different techniques and data. The study was performed over an area more than 650 km<sup>2</sup> wide within the Russian Nizhegorodskaya region, which is deeply affected by karst processes. The karst processes affect the shallowest part of the Permian bedrock (limestone, dolomite, gypsum) and can develop up to the surfaces creating large voids and sinkhole. The analysis was performed using a GIS based modeling of spatial data and combining the Fuzzy Logic method with the Analytic Hierarchy Process (AHP). It was applied following different steps: 1) all the principal karst - related “factors” (karst forms distribution, ground elevation, depth of the bedrock and groundwater table, distance to the river valleys and fault zones, etc..) were identified and mapped. Comparing these factors with the existing karst forms occurrence, the fuzzy membership values were calculated getting the Frequency Ratio. 2) the “importance” of each factor in the karst occurrence was also defined. A pairwise comparison matrix was implemented following the AHP criteria and the weight of each factor determined. 3) The fuzzy membership values were evaluated in accordance with the values (weights) given by the AHP process and a karst susceptibility map of the area was obtained combining the factors.

The final susceptibility map was finally checked with the existing karst forms distribution, as detected by field surveys and remote sensing analysis. Additionally, a satellite monitoring with SqueeSAR method was carried out over a 5-year period both to validate results and assess the potential active sectors. The obtained results are generally consistent with the local geological layout and the characteristics of the observed karst processes surveyed in the region. The most susceptible sectors are related to the structural uplifts and river valleys, where the Permian bedrock is close to the surface and the connection between the rainfalls infiltrations and the ground water circulation can trigger or accelerate the karst processes. This pattern seems also confirmed by the results of SqueeSAR analysis which provide interesting information about the potential active karst deformation zones occurring in the area. This method can be considered a suitable tool to be used especially during the preliminary geological studies and the road alignments selection. The prediction reliability is overall good as confirmed by the different sources of data. Furthermore, the uncertainty related to the input data and the modeling is also acceptable if related to the scale of the study area.



## **A multi-instrument and multidisciplinary landslide assessment: The case of Monesi Landslide, Ligurian Alps (NW Italy)**

Davide Notti<sup>1</sup>, Aleksandra Wrzesniak<sup>1</sup>, Niccolò Dematteis<sup>1</sup>, Piernicola Lollino<sup>2</sup>, Nunzio Luciano Fazio<sup>2</sup>, Francesco Zucca<sup>3</sup>, Daniele Giordan<sup>1</sup>

<sup>1</sup> CNR-IRPI, Strada delle Cacce 73, 10135 Torino, Italy, [davide.notti@irpi.cnr.it](mailto:davide.notti@irpi.cnr.it), [daniele.giordan@irpi.cnr.it](mailto:daniele.giordan@irpi.cnr.it)

<sup>2</sup>CNR-IRPI, Bari Italy,

<sup>3</sup>Department of Earth and Environmental Science, University of Pavia, Italy,

### **Study objectives.**

Many landslides that reactivate after an extreme rainfall event are not monitored by in-situ measuring systems. Consequently, the pre- and catastrophic phases cannot be directly registered, limiting the understanding of landslide behaviour. This problem can be overcome by using a multidisciplinary and multi-instrument approach that combines traditional and innovative elements (Tomas et al., 2018). We applied such approach to characterise two landslides that affected the village of Monesi di Mendatica in the Ligurian Alps after the extreme rainfall event of November 2016: the failure of a rotational landslide (L1) and the reactivation of a deep-seated planar landslide (L2) (Figure 1a) (Notti et al., 2021).

### **Methodology.**

To characterise these two landslides, several actions were carried out. We analysed the 2016 rainfall records and their correlation with the landslide catastrophic phase evolution. This evolution was defined through photographs and technical reports. We also analysed other historical rainfall datasets to find similar events. We applied a Digital Image Correlation (DIC) technique (Fienup 1997, Dematteis and Giordan 2021) to Sentinel-2 and Planet Scope satellite images to obtain a co-event displacement map. The Persistent Scatterer InSAR data from Radarsat and Sentinel-1 satellites were used to assess the pre-event (2003-2016) and post-event (2017-2019) landslides kinematic. Moreover, after the 2016 event, several ground-monitoring instruments were installed: piezometers, GNSS benchmarks, topographic network and crackmeters. We used the data from these instruments to define post-event landslide behaviour and its correlation with rainfall and groundwater level.

We performed numerical modelling of the slope, based on the finite element method to estimate slope conditions at the time of failure in terms of strength parameters, pore water pressure and failure mechanisms. We performed field surveys to assess structure damages and for geomorphological mapping purposes.

### **Results and conclusion.**

The 2016 event resulted as one the most severe in the last 70 years, with a cumulative rainfall of 700 mm in five days. The co-event displacements, estimated from the DIC technique, showed that the whole mass of L2 moved from 2 to 4 m NNW (Figure 1b). From reports and rainfall analysis, we estimated that the main movement occurred within a few days from the extreme event. The geomorphological effects and the structural damages mapped during the field surveys (Figure 1d) correspond to the co-event displacement results.

The post-event monitoring based on InSAR data, GNSS and topographic measurements (Figure 1c) showed higher velocities (up to 25 mm/yr) for L2 compared to the pre-event period (< 10 mm/yr from InSAR data) (Figure 1e). The rainfall and piezometric data analysis and their correlation with landslide velocity suggest that the landslide responds to the groundwater level increase caused by intense rainfall event (Figure 1e).

The numerical model results, even if qualitative, are realistic as they show strain and displacement concentration at the toe (the collapsed L1) and at the crown of the landslide (Figure. 1f). These results are also coherent with field observations and DIC results.

This multidisciplinary approach allowed for an almost complete understanding of the landslide behaviour and its triggering causes.

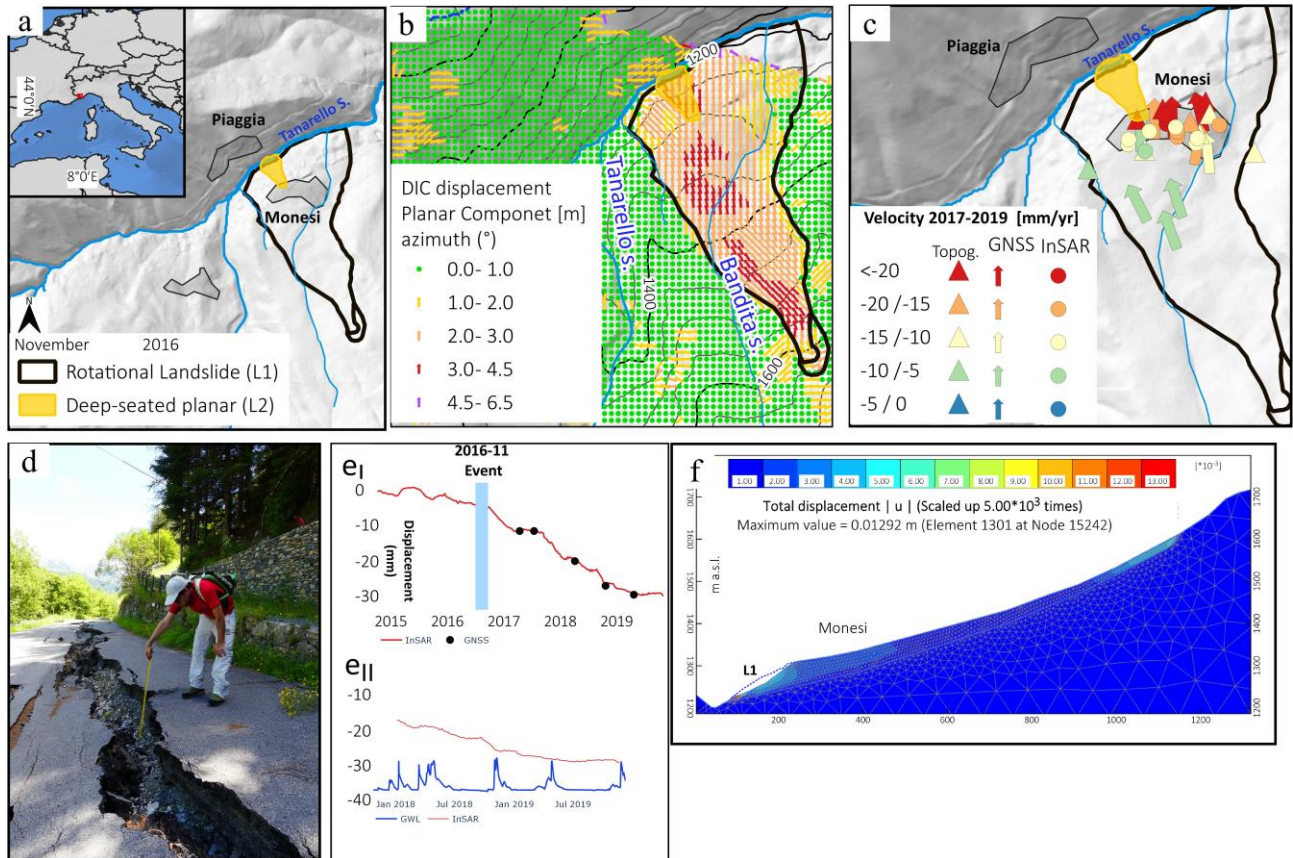


**Figure 1. a) Location of L1 and L2 Monesi landslides; b) Co-event displacement map derived from DIC; c) Post-event velocity obtained from different monitoring instruments; d) field surveys damages assessment; e) Time series of displacement (2014-2019) from InSA and GNSS data (e<sub>i</sub>) and comparison with groundwater level (e<sub>ii</sub>); f) Numerical modelling output: pre-failure displacement.**

**REFERENCES**

Dematteis, N., Giordan, D., 2021, Comparison of Digital Image Correlation Methods and the Impact of Noise in Geoscience Applications. *Remote Sensing* 13:327.

Fienup JR, 1997, Invariant error metrics for image reconstruction. *Applied optics* 36:8352–8357

Notti, D., Wrzesniak, A., Dematteis, N., Lollino, P. Fazio. N.L, Zucca F, and Giordan, D., 2021, A multidisciplinary investigation of deep-seated landslide reactivation triggered by an extreme rainfall event: A case study of the Monesi di Mendatica landslide, Ligurian Alps. *Landslides* (2021). <https://doi.org/10.1007/s10346-021-01651-3>

Tomás, R., Abellán, A., Cano, M., Riquelme, A., Tenza-Abril, A.J., Baeza-Brotons, F., Saval, J.M. and Jaboyedoff, M., 2018, A multidisciplinary approach for the investigation of a rock spreading on an urban slope. *Landslides*, 15(2), pp.199-217.



## Geological Control on Large-scale Landslide in the Central Nepal Himalaya

Bikash Phuyal<sup>1</sup>, Prem Bahadur Thapa<sup>2</sup>

<sup>1</sup>Central Department of Geology, Tribhuvan University, Kirtipur, Kathmandu, Nepal

[bikashphuyal2071@gmail.com](mailto:bikashphuyal2071@gmail.com)

<sup>2</sup>Department of Geology, Tri-Chandra Multiple Campus, Tribhuvan University, Kathmandu, Nepal

[geoscithapa@yahoo.com](mailto:geoscithapa@yahoo.com)

It is an effort to evaluate the geological influence for the initiation of large-scale landslide in heterogeneous geo-environment setting. Complex geology due to continuous deformation history of rock strata in central Nepal are causing the number of large-scale landslides. Most of the triggered large-scale landslides were the result of torrential rainfalls and litho-tectonic characteristics. Many landslides were extracted from satellite imageries and prepared the landslide inventories that occurred due to earthquake or rainfall or both events in different time periods which were also verified from field observations. Based on the conditions of geo-tectonic setup and characteristics of large-scale landslide, relationship was computed. The events of occurrence have shown the significance effect due to control of geological factors (i.e. relation of hill-slope with respect to orientation of rock strata geometry). Analysis showed that spatial distribution pattern of landslides are found to be in close proximity of major thrust/faults or boundary between competent and incompetent strata. The distribution of large-scale landslide indicated that 42% of them observed in close to regional and local fault/thrust sequence. 18% of large-scale landslide were occurred in the Siwalik Zone comprising the inter-bedding of shale, siltstone, mudstone with sandstone, conglomerate and 34% of them belongs to the Lesser Himalayan rock sequences that are mostly confined to phyllite and schist rock with high degree of weathering and fracturing. Midland Zone of Lesser Himalaya is more prone to landslides due to extensive human activities and periodic cycle of monsoon rainfall. 8% landslides are found to be located in Ulleri gneiss or Lesser Himalayan gneiss due to deep weathering and coarse-grained constituting minerals which exhibiting the low rock mass strength. Large-scale landslide are also noticeable in the Higher Himalayan rock sequences in which Proterozoic Higher Himalayan Crystalline rocks are characterized by presence of several events. In terms of large geological structures, Kathmandu Nappe and Okhaldhunga Window have 13% and 18% landslides respectively. The dipping of rock strata have shown the close relationship of geological influence on occurrence of large-scale landslides. Presence of discontinuities in the rock mass have also shown the influence for the extent of landslide size in moderate hill-slope consisting of competent nature of surrounding rocks. Thus, the major factor for the initiation and occurrence of large-scale landslide in the central Nepal Himalaya is mainly by the geological control. Furthermore, the depth understanding of local and regional geological controls are found to be useful for the establishing the relationship of large-scale landslide and geological factors in the Himalayan region.

## Stochastic approach for karst risk assessment of a motorway project

Fabrizio Peruzzo<sup>1</sup>, Walter Giulietto<sup>2</sup>, Mirko Vendramini<sup>2</sup>, Attilio Eusebio<sup>2</sup>

<sup>1</sup>Geodata Engineering Spa Italy, ISRM, ISSMGE, AGI-IGS, [fpe@geodata.it](mailto:fpe@geodata.it)

<sup>2</sup>Geodata Engineering Spa Italy, [wgi@geodata.it](mailto:wgi@geodata.it), [mve@geodata.it](mailto:mve@geodata.it), [aeu@geodata.it](mailto:aeu@geodata.it)

Sinkholes and subsidence in motorway project developed in karst areas disrupt transportation route serviceability causing significant direct and indirect economic losses. A stochastic approach has been used to evaluate different scenarios of risks.

The process involves an initial phase, where karst related information is collected, based on ground evidence, aerial and satellite data.

Based on this data we reconstruct a ground level statistical model of karst occurrence and successively a rock bed karst spatial stochastic model by means of python PYMC3 package.

The latter is used to build elaborate a stochastic model of surface sinkholes and subsidence occurrence based on literature analytical formulations. Each stochastic run is a scenario, and the sum of all scenarios can be used to statistically define the rate of occurrence, which represent a measure of the risk, and successively identify the applicable countermeasure used to reduce the risk.

This article presents a concrete application of the methodology for a motorway project in karst areas, whereas the versatility of the method allows for a waste field of applicability.

The results are presented in form of tables and graphs showing many scenarios, optimistic, baseline, pessimistic and extremely pessimistic, representing the 25th, 50th, 75th and 95th quantiles of the stochastic analysis. The karst mitigation countermeasures are presented as tables and their publication is inserted in the project drawings.



**Figure 1.** left image shows the karst position derived from the stochastic analysis plotted on the motorway project the right figure shows the kernel density distribution of karsts intercepting the project site for a particular sector

## Rockfalls occurrence administration along with the road network: an operative methodology for local standardized management in alpine territory

Daniele Giordan<sup>1</sup>, Martina Cignetti<sup>1</sup>, Danilo Godone<sup>1</sup>, Davide Bertolo<sup>2</sup>, Marco Paganone<sup>2</sup>

<sup>1</sup>National Research Council of Italy, Research Institute for Geo-Hydrological Protection (CNR-IRPI), Italy, [daniele.giordan@irpi.cnr.it](mailto:daniele.giordan@irpi.cnr.it), [martina.cignetti@irpi.cnr.it](mailto:martina.cignetti@irpi.cnr.it), [daniilo.godone@irpi.cnr.it](mailto:daniilo.godone@irpi.cnr.it).

<sup>2</sup>Strutture Attività Geologiche, Regione Autonoma Valle d'Aosta, Italy, [d.bertolo@regione.vda.it](mailto:d.bertolo@regione.vda.it), [m.paganone@regione.vda.it](mailto:m.paganone@regione.vda.it).

In mountainous territories, the road networks are usually located along steep slopes highly prone to rockfalls. Due to the unpredictable occurrence of these type of slope instabilities, their high energy and long runout, rockfalls are often cause of casualties and damage (Guzzetti, 2000; Spizzichino et al., 2013). The management of this hazardous process poses major challenge, in term of emergency administration and motorist’s safety (Guzzetti et al., 2004; Carlà et al., 2019). Nowadays, a codified procedure for the delineation of the operative actions to be undertaken during a rockfall event occurrence along with the road, is becoming a growing need for regional and local authorities and administrators (Michoud et al., 2012; Macciotta et al., 2016). By exploiting an alpine territory highly affected by rockfalls like the Aosta Valley Region (AVR) (NW Italy), a procedure activatable each time a rockfall event occurs has been implemented. Firstly, a detailed analysis of the data and information collected in the regional landslide inventory, *i.e.* the “*Catasto Dissesti*”, was carried out.

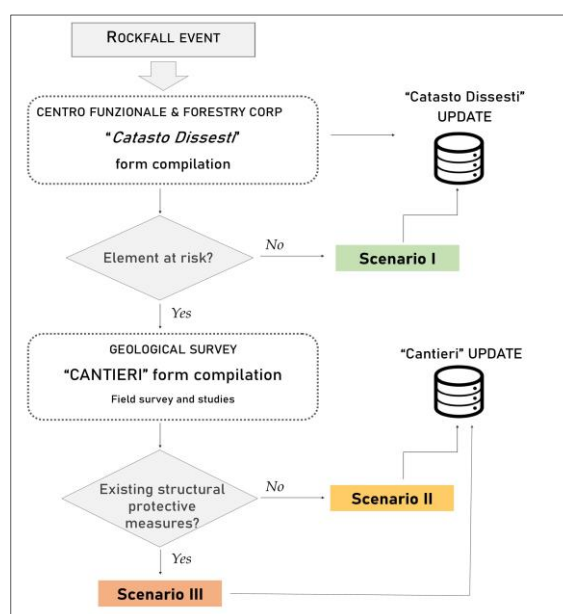
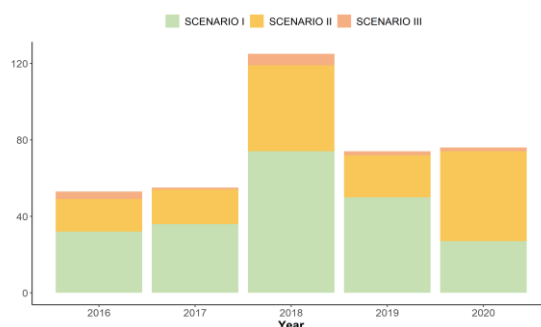


Figure 1. Scheme of the operative methodology implemented for rockfall occurrence management at local scale.

An existing regional practice, handled by the “*Centro Funzionale*” with the regional Forestry Corp, guarantees a constant update of the regional inventory, actually associated with a web-service, *i.e.* “*Cantieri*”, implemented with additional technical information. The analysis of the available data of the “*Catasto Dissesti*” and “*Cantieri*” poses the basis suitable to define a spatial-temporal distribution of the rockfalls, leading to a preliminary characterization at regional scale of the AVR. Starting from these consolidate information, a new local scale operative methodology was designed and three distinct scenarios were implemented (Figure 1). This codified procedure starts immediately after the occurrence of a rockfall, ending with remedial works activities definition and/or activation. For each scenario, the procedure defines an incremental sequence of the actions, choices and priorities to be undertaken in a pre-defined timeline, mainly based on the presence or absence of elements



at risk and protective measures. The activation of the subsequent action take place if the results of the previous one does not obtain the required level of risk mitigation. The distinct results associated to each action are managed and organized leveraging on the Operative Monographies (OMs) tools (Giordan et al., 2018; Giordan et al., 2020). Moreover, actions and products are compliant with the actual norms of the Italian Institution of Standardization UNI (Ente Italiano di Normazione, 2019) and the international standard ISO (ISO Norms, 2018). Considering the last five years of data available in “*Catasto Dissesti*” and “*Cantier*”, an overall framework of the distribution in the three scenarios of the inventoried rockfalls was outlined for the AVR, examining a case in point for each of expected scenario (Figure 2).



**Figure 2. Rockfall evens of the “*Catasto Dissesti*” distribution, in the period 2016-2020, in the three provided scenarios**

The proposed operative methodology represents a standardized protocol aimed at multi-user exploitation, providing a well-defined management of the diverse phases of an emergency along with the road networks, also in term of funds allocations. This codified procedure provides an effective tool for local and regional authorities of mountain areas all over the World, allowing for immediate screening of the emergency, by scheduling the appropriate risk management measures to guarantee safeguard of both road infrastructure and motorists safety.

## REFERENCES

- Carlà, T., Nolesini, T., Solari, L., Rivolta, C., Dei Cas, L., Casagli, N., 2019. Rockfall forecasting and risk management along a major transportation corridor in the Alps through ground-based radar interferometry. *Landslides* 16, 1425–1435.
- Giordan, D., Cignetti, M., Godone, D., Peruccacci, S., Raso, E., Pepe, G., Calcaterra, D., Cevasco, A., Firpo, M., Scarpellini, P., Gnone, M., 2020. A New Procedure for an Effective Management of Geo-Hydrological Risks across the “Sentiero Verde-Azzurro” Trail, Cinque Terre National Park, Liguria (North-Western Italy). *Sustainability* 12, 561.
- Giordan, D., Cignetti, M., Wrzesniak, A., Allasia, P., Bertolo, D., 2018. Operative Monographies: Development of a New Tool for the Effective Management of Landslide Risks. *Geosciences* 8, 485.
- Guzzetti, F., 2000. Landslide fatalities and the evaluation of landslide risk in Italy. *Eng. Geol.* 58, 89–107.
- Guzzetti, F., Reichenbach, P., Ghigi, S., 2004. Rockfall hazard and risk assessment along a transportation corridor in the Nera valley, central Italy. *Environ. Manage.* 34, 191–208.
- ISO Norms, 2018. ISO 31000 - Risk management - Guidelines.
- Macciotta, R., Martin, C.D., Morgenstern, N.R., Cruden, D.M., 2016. Quantitative risk assessment of slope hazards along a section of railway in the Canadian Cordillera—a methodology considering the uncertainty in the results. *Landslides* 13, 115–127.
- Michoud, C., Derron, M.H., Horton, P., Jaboyedoff, M., Baillifard, F.J., Loye, A., Nicolet, P., Pedrazzini, A., Queyrel, A., 2012. Rockfall hazard and risk assessments along roads at a regional scale: example in Swiss Alps. *Nat. Hazards Earth Syst. Sci.* 12.
- Spizzichino, D., Margottini, C., Trigila, A., Iadanza, C., 2013. Landslide Impacts in Europe: Weaknesses and Strengths of Databases Available at European and National Scale, in: *Landslide Science and Practice*. Springer Berlin Heidelberg, Berlin, Heidelberg, pp. 73–80.
- Ente Italiano di Normazione, 2020. UNI Norms. Web-site URL <http://store.uni.com> (accessed 12.10.20).

## State of knowledge delineation of Deep-seated Gravitational Slope Deformation impact on anthropic elements: the Western Italian Alps case

Martina Cignetti<sup>1</sup>, Danilo Godone<sup>1</sup>, Francesco Zucca<sup>2</sup>, Davide Bertolo<sup>3</sup>, Daniele Giordan<sup>1</sup>

<sup>1</sup>National Research Council of Italy, Research Institute for Geo-Hydrological Protection (CNR-IRPI), Italy, [martina.cignetti@irpi.cnr.it](mailto:martina.cignetti@irpi.cnr.it), [daniilo.godone@irpi.cnr.it](mailto:daniilo.godone@irpi.cnr.it), [daniele.giordan@irpi.cnr.it](mailto:daniele.giordan@irpi.cnr.it)

<sup>2</sup>Department of Earth and Environmental Sciences, University of Pavia, Italy, [francesco.zucca@unipv.it](mailto:francesco.zucca@unipv.it)

<sup>3</sup>Strutture Attività Geologiche, Regione Autonoma Valle d'Aosta, Italy, [d.bertolo@regione.vda.it](mailto:d.bertolo@regione.vda.it)

The definition of an overall framework of slope instabilities impact is a key element in the context of urban planning and damage assessment. In literature, many efforts have been made to provide an overview of the existing landslide inventories (Spizzichino et al. 2013; Herrera et al., 2018) and landslide hazard definition into urban planning (Van Den Eeckhaut et al., 2012; Mateos et al., 2020). However, unlike other landslides, classically characterized by high rates of deformation and high intensity, Deep-seated Gravitational Slope Deformation represent a still open issue in terms of land use planning and impact characterization. These phenomena are large-slope gravitational deformation, affecting entire valley flanks and extended for hundreds of meters in depth. Featured by very slow deformation (*i.e.* mm/year up few cm/year) that may last for long period through a progressive failure (Pánek and Klimeš, 2016), the DsGSDs are largely well distinguished from all other types of landslide. The effect of the large cumulative displacement recorded by these huge phenomena can affect anthropic structures and infrastructures, causing relevant damage. Actually, this aspect is poorly described both in scientific community and by policy-makers in land use planning management.

By exploiting a territory highly affected by DsGSDs as the Italian Western Alps, a multi-source investigation to delineate the overall framework of the impact of DsGSDs on anthropic activities was implemented on a large-scale mountain region. The main goals are represented by: i. examination of the state-of-the-art of knowledge about DsGSDs, in terms of extension, state of activities, geological and geomorphological characteristics, drawing on the existing institutional sources online available; ii. establishment of a comprehensive analysis of the potential interactions existing between DsGSDs and the main anthropic elements spread around the area of interest, operating in a Geographic Information System; iii. establish a damage inventory due to the large cumulative displacement of these huge phenomena, actually missing. The executed investigation highlights that about 8% of the Italian Western Alps territory is affected by DsGSDs, mainly distributed in the Aosta Valley Region (13% of regional territory) and the Turin Province (10.5%). Considering the existing regional inventories (*i.e.* "Catasto Dissesti" for Aosta Valley Region, and "SiFraP" for Piemonte Region), analyzing and, for the AVR, integrating with SAR data the information about the state of activity, resulted that of 799 phenomena 17% are classified as active, 14% quiescent and the rest undetermined (69%). Subdividing the anthropic elements in four main group, *i.e.* i. buildings, ii. road, iii. railway, and iv. other linear elements as penstock, waterworks, dams, we observed that the 59% of the DsGSDs interfere with one or more of the considered groups of structures and infrastructures (Figure 1).

The obtained results revealed the need for a new consideration of DsGSDs in terms of characterization of their behavior over time and related impact on anthropic elements, for a more effective land use planning and a functional review of the current legislation framework in mountainous territory.

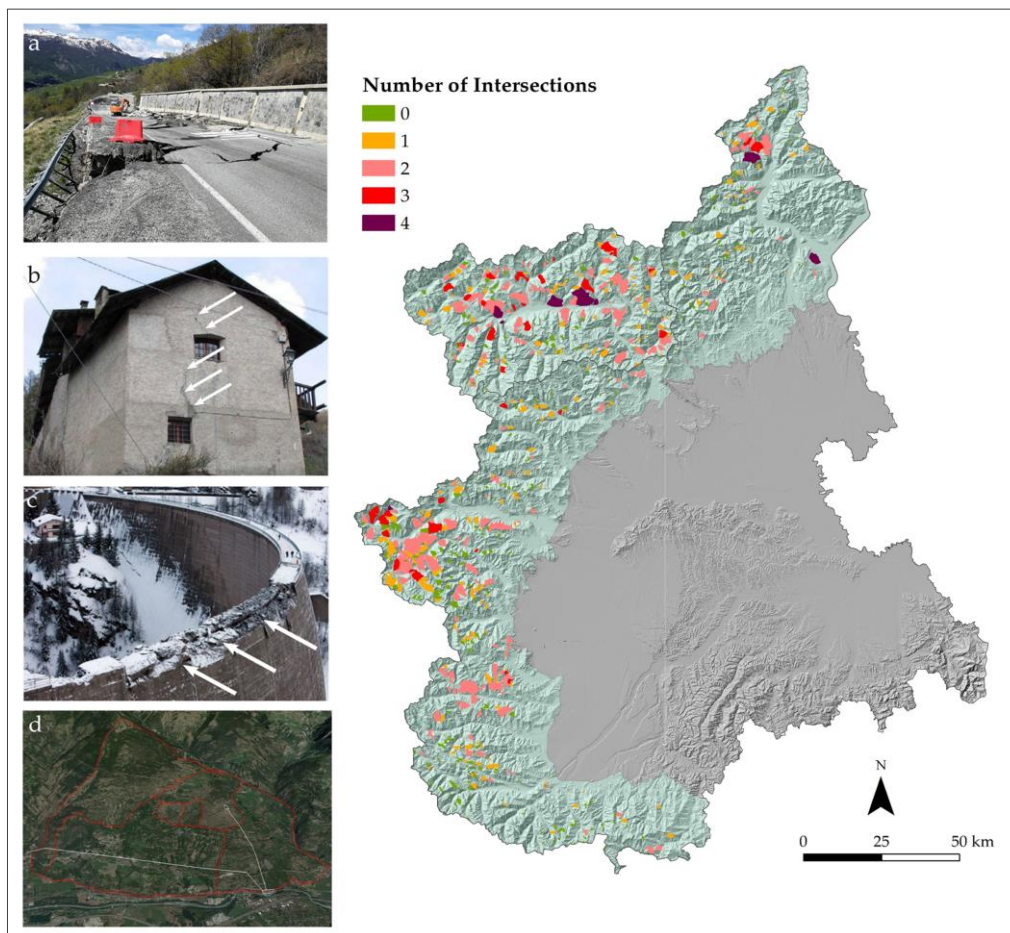


**Figure 1. Classification of the DsGSDs of the Western Italian Alps territory, based on the number of intersections with the main group of anthropic elements, referring to the four groups identified “buildings”, “road network”, “railway” and “other linear elements”. Some renowned damage to anthropic structures and infrastructure are shown in a) road interruption close to the Champlas du Col village, b) fractured wall in Grange Sises village; c) relevant damage to the Beaugard Dam, d) repeated damage to the hydroelectric bypass tunnel of Croix-de-Fana DsGSD.**

## REFERENCES

- Spizzichino, D., Margottini, C., Trigila, A., Iadanza, C., 2013. Landslide Impacts in Europe: Weaknesses and Strengths of Databases Available at European and National Scale, in: *Landslide Science and Practice*. Springer Berlin Heidelberg, Berlin, Heidelberg, pp. 73–80.
- Herrera, G., Mateos, R.M., García-Davalillo, J.C., Grandjean, G., Poyiadji, E., Maftai, R., Filipciuc, T.-C., Jemec Auflič, M., Jež, J., Podolszki, L., Trigila, A., Iadanza, C., Raetz, H., Kociu, A., Przyłucka, M., Kułak, M., Sheehy, M., Pellicer, X.M., McKeown, C., Ryan, G., Kopačková, V., Frei, M., Kuhn, D., Hermanns, R.L., Koulermou, N., Smith, C.A., Engdahl, M., Buxó, P., Gonzalez, M., Dashwood, C., Reeves, H., Cigna, F., Liščák, P., Pauditš, P., Mikulénas, V., Demir, V., Raha, M., Quental, L., Sandić, C., Fusi, B., Jensen, O.A., 2018. Landslide databases in the Geological Surveys of Europe. *Landslides* 15, 359–379.
- Van Den Eeckhaut, M., Hervás, J., Jaedicke, C., Malet, J.-P., Montanarella, L., Nadim, F., 2012. Statistical modelling of Europe-wide landslide susceptibility using limited landslide inventory data. *Landslides* 9, 357–369.
- Mateos, R.M., López-Vinielles, J., Poyiadji, E., Tsagkas, D., Sheehy, M., Hadjicharalambous, K., Liščák, P., Podolski, L., Laskowicz, I., Iadanza, C., Gauert, C., Todorović, S., Auflič, M.J., Maftai, R., Hermanns, R.L., Kociu, A., Sandić, C., Mauter, R., Sarro, R., Béjar, M., Herrera, G., 2020. Integration of landslide hazard into urban planning across Europe. *Landsc. Urban Plan.* 196.
- Pánek, T., Klimeš, J., 2016. Temporal behavior of deep-seated gravitational slope deformations: A review. *Earth-Science rev.* 156, 14–38.

## Slope protection respectful of natural resources and landscape thanks to earth retaining system

Steve Gruslin<sup>1</sup>, Domenico Nola<sup>1</sup>

<sup>1</sup>GEOCONSEILS S.A., Luxembourg, [steve.gruslin@geoconseils.lu](mailto:steve.gruslin@geoconseils.lu), [Domenico.nola@geoconseils.lu](mailto:Domenico.nola@geoconseils.lu)

During the night of June 1st, 2018, the Mullerthal region in Luxembourg was severely affected by violent thunderstorms. The road linking Echternach to Berdorf (CR364) was particularly affected.

Due to heavy rains (up to 90 liters per square meter), several landslides occurred. The flood of the river underneath caused considerable damages to the embankments and protective structures of the roadway.

The geotechnical investigations carried out encountered under the road stony gravelly backfills and slope screes consisting of sand and gravel over thicknesses of up to 7 m, then layers of the Triassic (Rhaetian and Middle Keuper).

Rhaetian layers, made of clay and clayey marls, have a high consistency in the dry state, but they are very sensitive to water, with the consequence that they soften very quickly, thus playing the role of a "soap layer" which, in combination with the inclination of the layer, constitute a sliding surface for overlying non cohesive materials.

The heavy rains caused significant erosion on the surface of the embankment. The water which penetrated under the road crossed the permeable layers (backfills and scree) and mobilized the sliding surface constituted by the Rhaetian, so that all the embankments and scree slipped (around 10,000 m<sup>3</sup> of material).

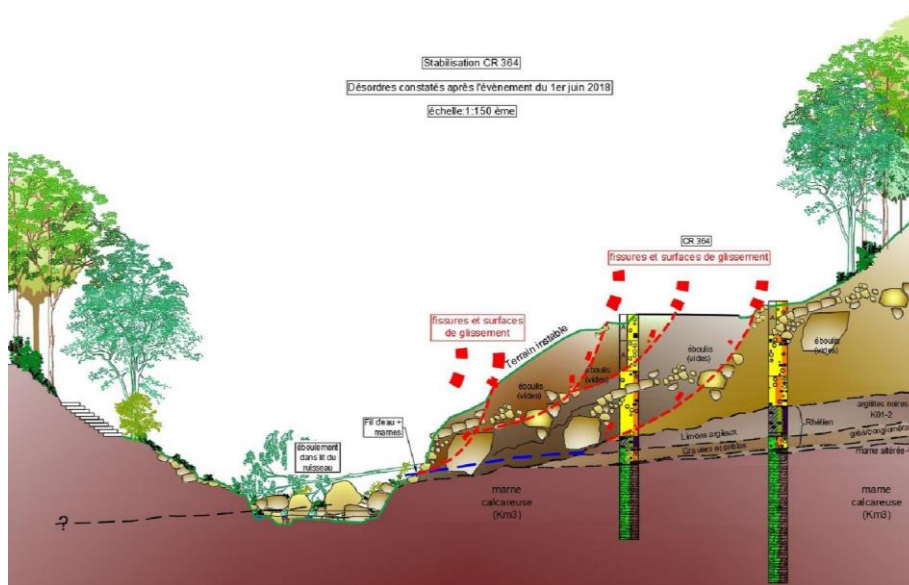


Figure 1. Interpretation of the situation

The damaged existing embankment was replaced by a steep embankment made of natural materials reinforced by geogrids that fits perfectly into the landscape.

Extensive geotechnical studies and calculations have shown that landslides can reoccur in affected areas if only limited corrective measures are put in place near the surface. To avoid long-term instabilities, it was necessary to excavate the entire body of the slip over the entire width of the roadway and down to the layers of Rhaetian at risk of slipping.



From a sustainability standpoint, most of the excavated material could be reused for backfilling in a way that saved resources. The excavated material, which consisted of stones, boulders, sand, and gravel, was prepared on site to produce a backfill material with a grain size of 0/45 mm. In this way, about 70% of the required backfill material could be obtained, which also had a positive effect on the ecological balance.

To provide the support structure for the earth retaining system fill sections, the steep slope system “Tensor Tech Green Slope” was chosen, which allows creating slopes up to 70 °. This system chosen for reinforcement is made up of steel grid elements in the front and horizontally laid geogrids, so that the backfill material results in a composite load-bearing body with a high degree of ductility.

For the protection against erosion and revegetation, a mat has been placed behind the face of the steel grid element. To consider the topography, the reinforced earth construction was built to heights of between 3 m and 9 m.

Thanks to the combination of the green construction in reinforced earth, the section of road blends harmoniously into the landscape since the end of the works in summer 2019.

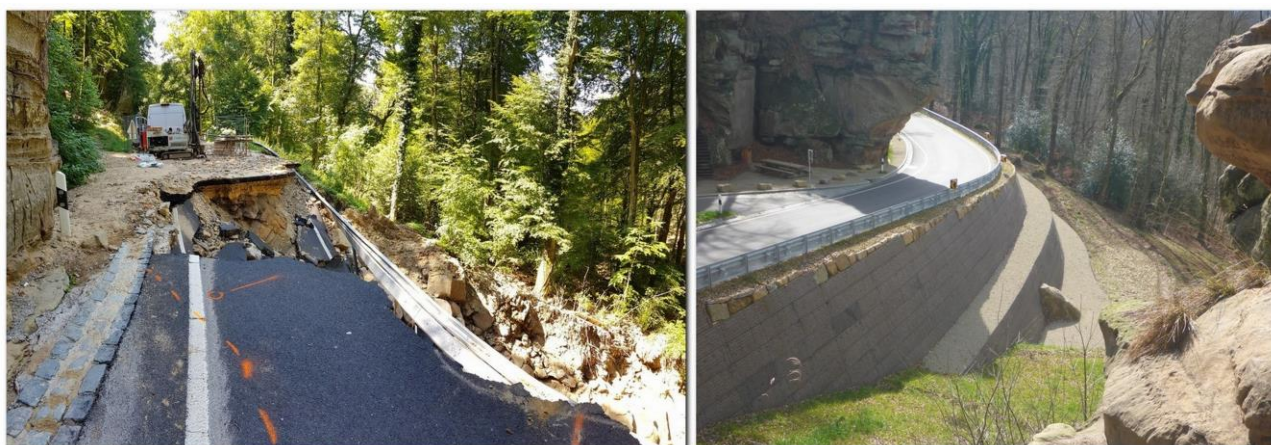


**Figure 2. Situation before and after stabilization**

## REFERENCES

- Meyer, N., Nola, D. and Scherbina, E., 2019, Ressourcen- und landschaftsschonende Hangsicherungen mit Kunststoff-Bewehrte-Erde (KBE)-Konstruktionen. Proceedings Fachsektionstage Geotechnik Würzburg, pp. 504-508
- Gruslin S., and Guillet A., 2018, Assainissement inondations CR364, Berdorf – SGP-218-009. Geotechnical study report Geoconseils S.A.
- Gruslin S., and Galibardy F., 2018, Assainissement inondations CR364, Beaufort – SGP-218-009. Geotechnical study report Geoconseils S.A.





## Slope Stability Hazards Evaluation of Dammam Formation West of Karbala Governorate-Middle of Iraq: Case study

A. Jaffar H.A. Al-Zubaydi<sup>1</sup>

<sup>1</sup>*Applied Geology Dept., College of science, Babylon University, [jafar\\_hussain68@yahoo.com](mailto:jafar_hussain68@yahoo.com)*

### **Abstract:**

Dammam Formation is exposed in the west and southwest of the Karbala Governorate, and is considered as an important aquifer in the Western Desert regions. It has unconformable contacts with both Euphrates and Rus Formations which lie above and beneath it respectively. In this study the stability of the rock have been evaluated to determine the most relevant factors affecting instability of slope and analyzed the discontinuity data collected from the field surveys using stereograph projection. (Sub horizontal-layer) slopes of limestone rocks in Dammam Formation, revealed the abundance of rock slope failures, the dominant types are rock fall, Secondary toppling, and rolling. The degree and nature of hazard risk depend on properties of the rock discontinuity. This study is recommended the rock instability is enhanced by barrier fences and scaling of rock faces to remove soft rocks.

### **Introduction**

1-1 Dammam Fn. (M. Up. Eocene): It extends along large distances in the Western and Southern Deserts. It is deposited in shallow neritic environments and mainly consists of carbonate rocks (Limestone and dolomite) with Nummulite species as index fossils (Al-Sayyab, et al., 1982). According to the stratigraphic sequence mentioned in the geological map of Najaf region (sheet NH-38-2 compiled by Barwary and Nasira, 1996), Dammam Formation can be subdivided into the following members (units) from top to bottom:

a- Upper member, mainly composed of marly, chalky limestone which is recrystallized in most parts. It contains voids and sinkholes resulted from permanent solution due to filtration of runoff water through the surface fractures.

b- Middle member, consisting of fossiliferous dolomite and dolomitic limestone with interbedded layers of marl and cherty nodules in some depths. This member is characteristic with fissures and paleokarst, so it became good groundwater bearing layers due to its secondary porosity resulting from the above features.

c- Lower member, constitutes a grayish green shale and marl with evaporates. This member occurs only in the core samples of the drilled wells at the eastern parts of the Iraqi Desert as in the studied area. Sometimes it is regarded as a part of Rus Fn. (Tamar Agha, et al., 1997).

Dammam Formation is exposed in the west and southwest of the studied area, and is considered as an important aquifer in the Western Desert regions as reported by the previous researchers. It has unconformable contacts with both Euphrates and Rus Formations which lie above and beneath it respectively. Its thickness may range between (150 -200m) at or near regions of the studied area as shown in the isopach of Figure 1.

### **Aims of the study**

This study aims at making an engineering geological evaluation of rock slope stability in the area by locating sites of past failures and those which are likely to occur in the future, its mechanism, types, and all factors influencing slope instability. This requires ;-

1-Locating unstable parts of the cliff and determining the modes of failure.

- 2-Proposing some treatment measures to stabilize the rock slopes.
- 3.Studying some geotechnical properties of the exposed rocks in the area
- 4.Preparing failure hazard map for the study area.

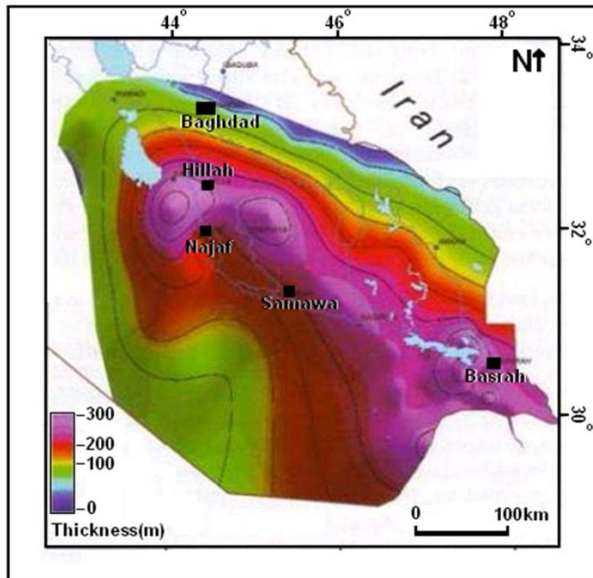


Figure 1. Isopach map of Dammam Formation within the stratigraphic column of Iraq from (Jassim and Goff, 2006)

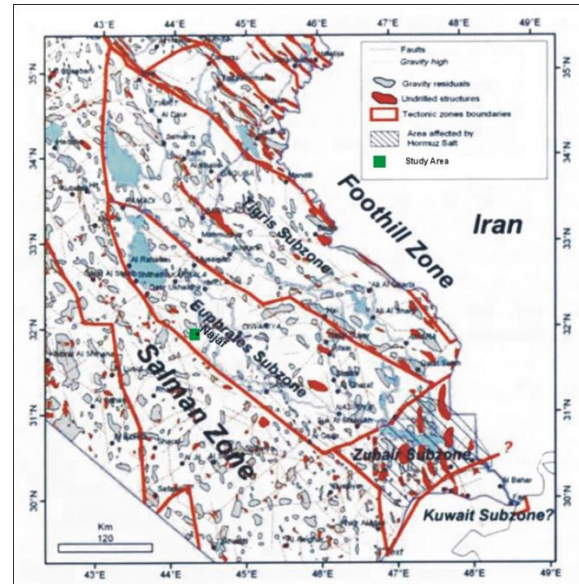


Figure 2. Location of the study area on the tectonic map (after Jassim and Goff, 2006).

### Tectonic and Structural Setting of the study area

Tectonically, the study area is located close to the boundary between the Stable shelf represented by the western desert territory and the Unstable shelf represented by Mesopotamia Zone and flood plain, at the Unstable Shelf within Euphrates subzone ( Al-Mashhdani ,1984) (Figure 2) . According to the tectonic map of Buday (1973), the fault direction is N-S corresponding with Abu Jir Fault which separates the Stable and Unstable shelves. Hassan and Al-Khateeb (2004), described the surface structure of the area and considered the outline of Abu Jir Fault Zone where most of the depressions and ridges are distributed along this fault developed by its effect. They described the surface structural features as follows :

1. Abu Jir Fault passes through the area as a fault zone responsible for the configuration of the ridges of Tar Al-Najaf which are higher both topographically and stratigraphically than the surrounding, (Hassan and Al-Khateeb ,2004)
2. The exposed uppermost layers of Injana and Dibdibba Formations show undulations development along the scarps of Tar Al-Najaf in some places (Hassan and Al-Khateeb, 2004). Such undulation havenot be seen.
3. The presence of a numerous Salifurous, Gaseous and Water seepages indicates fault area. (Hassan and Al-Khateeb, 2004).
4. By field observation the strata are horizontal to sub-horizontal.

## Comparing high accuracy tLiDAR and UAV-derived point clouds for change detection in two semi-mountainous Mediterranean catchments in Central Evia island, Greece

Simoni Alexiou<sup>1\*</sup>, Georgios Deligiannakis<sup>1</sup>, Aggelos Pallikarakis<sup>1</sup>, Ioannis Papanikolaou<sup>1</sup>,  
Emmanouil Psomiadis<sup>1</sup>, Klaus Reicherter<sup>2</sup>

<sup>1</sup>Laboratory of Mineralogy-Geology, Department of Natural Resources Management and Agricultural Engineering, Agricultural University of Athens, Greece, [gdeligian@aua.gr](mailto:gdeligian@aua.gr), [agpall@aua.gr](mailto:agpall@aua.gr), [i.pap@aua.gr](mailto:i.pap@aua.gr),  
[mpsomiadis@aua.gr](mailto:mpsomiadis@aua.gr), [sim.alexiou@aua.gr](mailto:sim.alexiou@aua.gr)

<sup>2</sup>Institute of Neotectonics and Natural Hazards, RWTH Aachen University, Aachen, Germany,  
[k.reicherter@nug.rwth-aachen.de](mailto:k.reicherter@nug.rwth-aachen.de)

Wildfires and soil erosion are among the most significant environmental issues resulting in soil degradation, therefore soil loss quantification is considered vital (Dregne 2002, Shakesby 2011). This study aims at soil erosion estimation following a severe wildfire event, focusing on the geomorphological change. Emerging tools such as Unmanned Aerial Vehicles (UAVs) in combination with well-established tools such as Terrestrial Laser Scanning (TLS) provide accurate results (Gulyaev et al. 2004, Niethammer et al. 2012, Rosca et al. 2018). Multitemporal analysis in two small semi-mountainous catchments in central Evia island, Greece, highlights the advantages of UAV and TLS- based change detection methods. TLS method leads to great accuracy, while the UAV method leads to detailed mapping at non-easily approachable sites. After a devastating wildfire of 2019, the study area was selected by applying the Difference Normalized Burn Ratio (Keeley 2009), in combination with extensive fieldwork. We used point clouds derived by both methods in two sites (S1 & S2), to estimate change detection at three different time periods within a year. Results indicate that topsoil's movements in the order of a few centimetres, occurring within a few months, can be estimated. Erosion at S2 is precisely delineated by both methods, yielding a mean value of 1.5 cm within four months. At S1, UAV-derived point clouds' comparison quantifies annual soil erosion more accurately, showing a maximum annual erosion rate of 48 cm. UAV-derived point clouds appear to be more accurate for channel erosion display and measurement, while the slope wash is more precisely estimated using TLS. Point Cloud analysis is a reliable and fast process for soil erosion assessment, especially in rapidly changing environments. The rising frequency of wildfire events results in soil erosion, highlighting the need for soil assessment tools and precaution measures. This study will contribute to proper georesource management by defining the best-suited methodology for soil erosion assessment after a wildfire in Mediterranean environments.

### REFERENCES

- Dregne, H.E., 2002, Land degradation in the drylands. *Arid Land Research and Management*. v. 16, pp. 99–132.
- Shakesby, R.A., 2011, Post-wildfire soil erosion in the Mediterranean: Review and future research directions. *Earth-Science Reviews*, v. 105, pp. 71–100.
- Gulyaev, S.A., Buckeridge, J.S., 2004, Terrestrial methods for monitoring cliff erosion in an urban environment. *Journal of Coastal Research*, v. 20(3), pp. 871-878.
- Niethammer, U., James, M.R., Rothmund, S., Travelletti, J., Joswig, M., 2012, UAV-based remote sensing of the Super-Sauze landslide: Evaluation and results, *Engineering Geology*, v. 128, pp. 2–11.
- Roşca, S., Suomalainen, J., Bartholomeus, H., Herold, M., 2018, Comparing terrestrial laser scanning and unmanned aerial vehicle structure from motion to assess top of canopy structure in tropical forests. *Interface Focus*, v. 8.
- Keeley, J.E., 2009, Fire intensity, fire severity and burn severity: A brief review and suggested usage, *International Journal of Wildland Fire*, v. 18, pp. 116–126.

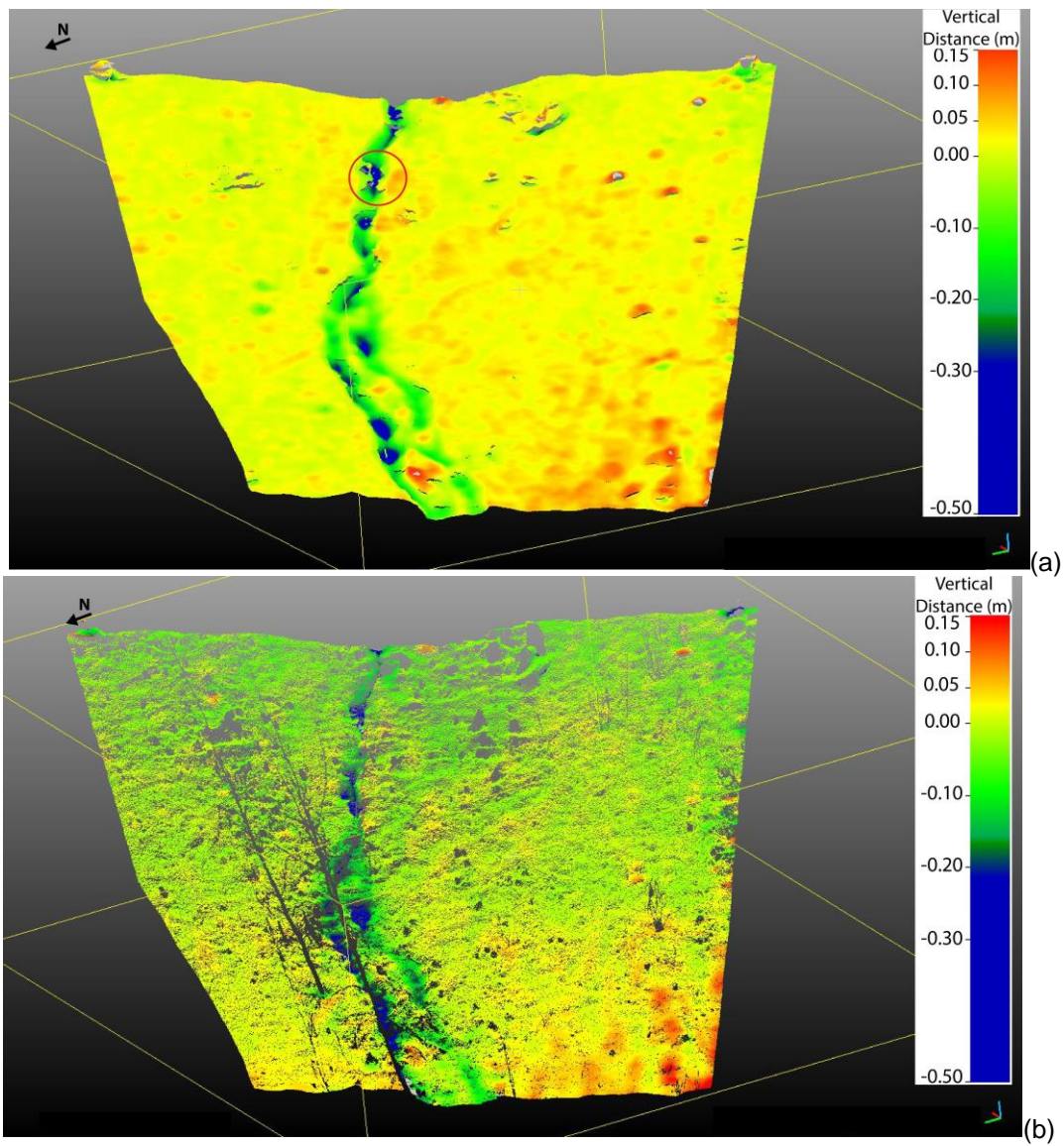


Figure 1. S1 total annual erosion (m) using (a) UAV and (b) TLS-derived data.



## Liquefaction phenomena triggered by the March 2021, Thessaly, Greece seismic sequence

George Papathanassiou<sup>1</sup>, Sotiris Valkaniotis<sup>1</sup>, Athanassios Ganas<sup>2</sup>, Riccardo Caputo<sup>3</sup>

<sup>1</sup>*Department of Civil Engineering, Democritus University of Thrace, Greece, [gpapatha@civil.duth.gr](mailto:gpapatha@civil.duth.gr), [svalkani@civil.duth.gr](mailto:svalkani@civil.duth.gr)*

<sup>2</sup>*Geodynamic Institute, National Observatory of Athens, Greece, [aganas@noa.gr](mailto:aganas@noa.gr)*

<sup>3</sup>*Department of Physics and Earth Sciences, University of Ferrara, Italy, [rcaputo@unife.it](mailto:rcaputo@unife.it)*

On March 3<sup>rd</sup>, 2021, a moderate earthquake of  $M_w=6.3$  occurred in the area between Tyrnavos and Ellassona (Thessaly, Greece) triggering numerous liquefaction phenomena e.g., sand craters, lateral spreading, etc. that are the dominant earthquake-induced secondary effects. Few hours after the mainshock, a strong aftershock of  $M_w=6.0$  occurred, followed by four other shocks of magnitude  $M>5$  (Valkaniotis et al. 2021). Applying the Environmental Seismic Intensity scale ESI-07, it was concluded that the highest intensity is assigned as VII-IX in Piniada Valley.

### **Method**

Starting on March 5<sup>th</sup>, 2021, a field survey took place within the floodplains of the Pinios and Titarissios rivers aiming to document the liquefaction manifestations. Though the fact that the latter area is located closer to the epicentre, the severity of liquefaction phenomena was less diffuse and intense with respect to the one reported along the Pinios. This oxymoron could be preliminary justified by the fact that the alluvial deposits mapped in the Titarissios flood plain are coarser comparing to the ones in the Piniada valley; this is a flood plain that is periodically covered by the flooding material of Pinios river (Caputo et al. 2021) classified as highly susceptible to liquefaction by Papathanassiou et al. (2010).

Our study started few hours after the mainshock by analyzing the satellite imageries for locating the most liquefied areas. Then a field survey, consisted of a set of drive-by, ground survey and UAV campaigns, performed to quantitatively document the liquefaction-induced ground disruption. In particular, the drive-by recon aimed to rapidly reporting the low- and high-density liquefaction zones as they have been delineated in advance based on data provided by satellite imagery. It is important to highlight that the preliminary map compiled based on data provided by remote sensing correctly delineated the location of liquefaction phenomena and their clustering as documented in the field. The ground and UAV-based surveys focused on high density areas aiming to measure their dimensions e.g., length, diameter and orientation.

### **Conclusions**

The length of the aligned sand craters was up to 26 m while the maximum diameter of sand craters, generated by the seismic sequence, was up to 3 m in the Piniada Valley. Considering the orientation of the aligned features, it was found that it is not unique for the whole area, but it follows the direction of the former channels and their associated ox-bow lakes inside the Piniada valley. The grain size analysis that was performed on collected samples from Piniada and Titarissios valleys indicated that the ejected material can be classified as SP and SW, respectively. In addition, lateral spreading phenomena were mapped both on inner and outer banks of Pinios and Titarissios rivers; the bridge at Mesochori is likely to have been damaged due to lateral spreading at the riverbanks of Titarissios River.





Finally, as it was shown by comparing the spatial distribution of liquefaction phenomena with the historical geomorphological maps showing the evolution of the Piniada Valley, the liquefaction clusters are clearly related to the presence of recently abandoned channels and palaeomeanders (ox-bow lakes).

## REFERENCES

Caputo R., Helly B., Rapti D., Valkaniotis S. 2021, Late Quaternary hydrographic evolution in Thessaly (Central Greece): The crucial role of the Piniada Valley. *Quaternary International*, <https://doi.org/10.1016/j.quaint.2021.02.013>

Papathanassiou G., Valkaniotis S., Chaztipetros Al., Pavlides S. 2010, Liquefaction susceptibility map of Greece, Proc. Of the 12th International Conference of Greek Geological Society, Bulletin of the Geological Society of Greece, vol. XLIII, No3, 1383-1392 <https://doi.org/10.12681/bgsg.11314>

Valkaniotis S., Papathanassiou G., Ganas Ath., Kremastas V., Caputo R. 2021, Preliminary report of liquefaction phenomena triggered by the March 2021 earthquakes in Central Thessaly, Greece. Zenodo. <http://doi.org/10.5281/zenodo.4608365>.

## Effect of temperature on the evolution of post-earthquake landslides

Marco Loche<sup>1\*</sup>, Luigi Lombardo<sup>2</sup>, Ali P. Yunus<sup>3</sup>, Filippo Catani<sup>4</sup>, Hakan Tanyaş<sup>2</sup>, William Frodella<sup>5</sup>, Xuanmei Fan<sup>3</sup>, Gianvito Scaringi<sup>1</sup>

<sup>1</sup>*Institute of Hydrogeology, Engineering Geology and Applied Geophysics, Faculty of Science, Charles University, Prague, Czech Republic, [marco.loche@natur.cuni.cz](mailto:marco.loche@natur.cuni.cz)*

<sup>2</sup>*Faculty of Geo Information Science and Earth Observation (ITC), University of Twente, Enschede, Netherlands*

<sup>3</sup>*State Key Laboratory of Geohazard Prevention and Geoenvironment Protection, Chengdu University of Technology, Chengdu, China*

<sup>4</sup>*Department of Geosciences, University of Padova, Padova, Italy*

<sup>5</sup>*Department of Earth Sciences, University of Florence, Florence, Italy*

The direct impact of temperature on landslide patterns and trends has not been investigated (Reichenbach et al., 2018). Identifying a suitable variable remains challenging. We suggest a possible covariate that can be used in landslide susceptibility analysis: Land Surface Temperature (LST). Indeed, it is a promising source available through Google Earth engine (Ermida et al., 2020), which can also be used in the context of co-seismic and post-seismic landscape evolution.

Geostatistical modelling is widely used to relate physical processes to spatial variables. Generalized Additive Models can explore landslides susceptibility through a nonparametric smoothing function (Petschko et al., 2014). We utilized this approach to develop a minimalistic slope unit-based (Alvioli et al., 2016) multitemporal susceptibility model for the epicentral region of the 2008 Wenchuan earthquake (Fan et al., 2019).

We evaluated a sharp decrease in susceptibility through time, consistent with a rapid stabilization of the landscape (Figure 1). More interestingly, looking at the individual covariates, we showed how the significance of both LST and Peak Ground Acceleration (PGA) changed in time, setting the basis for a discussion on the duration of the legacy effect of an earthquake and the reemerging of non-seismic variables (Figure 2).

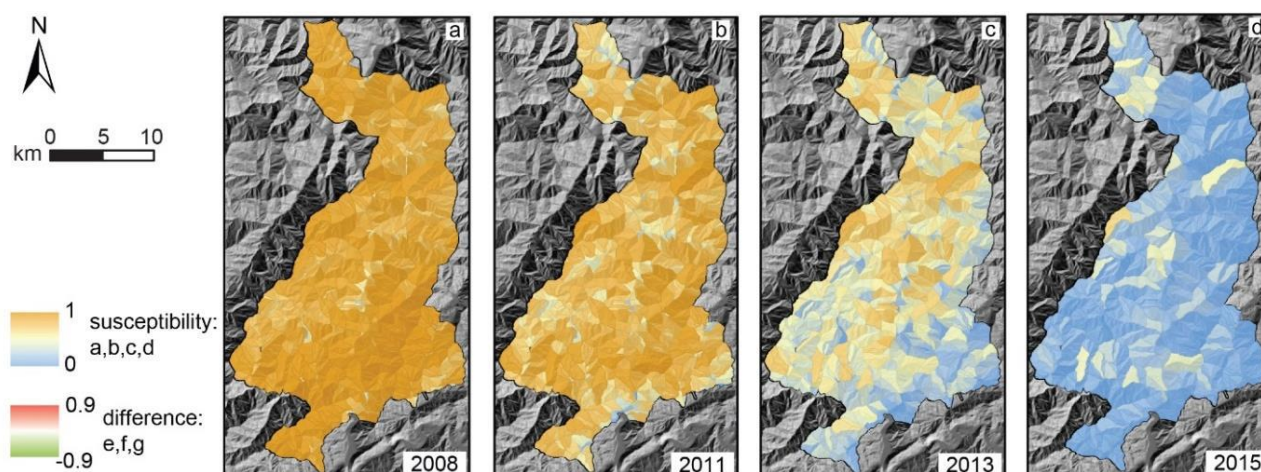
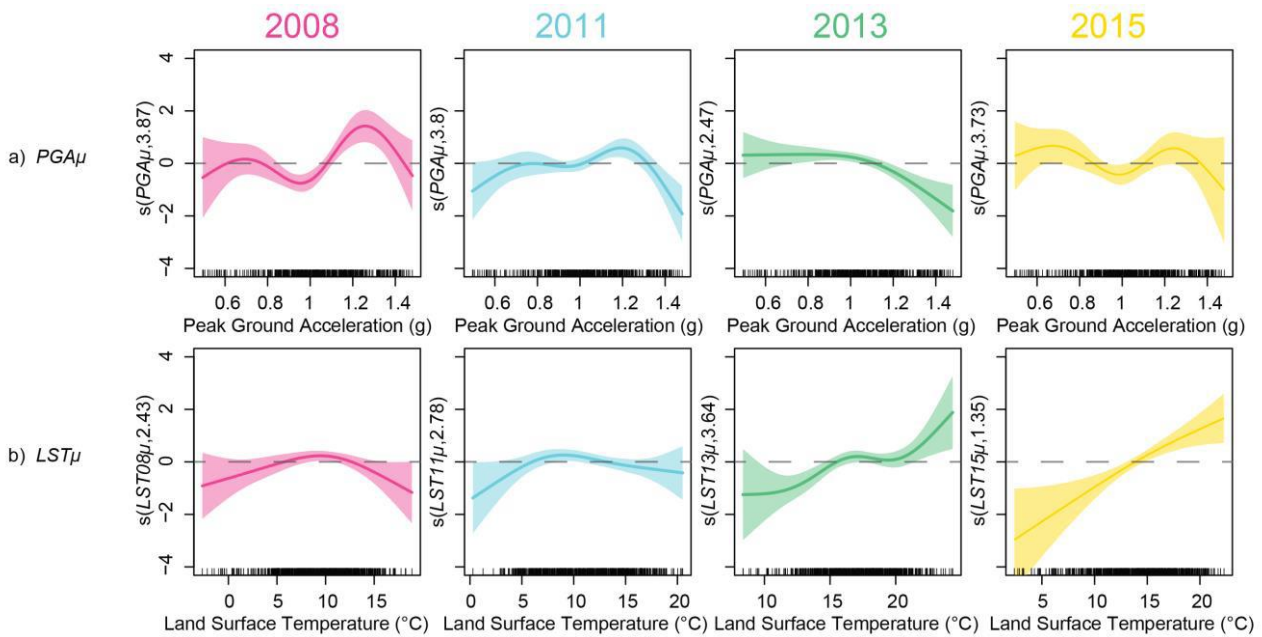


Figure 1. Landslide susceptibility maps across the years (a–d) in the Wenchuan earthquake epicentral area.



**Figure 2. Variable effects of (a) PGA and (b) LST displayed with confidence bands of 95% during the years.**

Using the LST, we were able to capture a possible effect of thermo-mechanical coupling in geomaterials. This coupling is well known in the literature in laboratory studies (Mitchell and Soga, 2005), but it has seldomly been applied to slope stability analysis, particularly at catchment scale. However, further studies are needed to confirm our observation in other climates, lithologies and landscapes (also in non-seismic regions).

**REFERENCES**

Alvioli, M., Marchesini, I., Reichenbach, P., Rossi, M., Ardizzone, F., Fiorucci, F. and Guzzetti, F., 2016. Automatic delineation of geomorphological slope units with r. slope units v1. 0 and their optimization for landslide susceptibility modeling. *Geoscientific Model Development*, 9(11), pp.3975-3991.

Ermida, S.L., Soares, P., Mantas, V., Göttsche, F.M. and Trigo, I.F., 2020. Google earth engine open-source code for land surface temperature estimation from the landsat series. *Remote Sensing*, 12(9), p.1471.

Fan, X., Scaringi, G., Domènech, G., Yang, F., Guo, X., Dai, L., He, C., Xu, Q. and Huang, R., 2019. Two multi-temporal datasets that track the enhanced landsliding after the 2008 Wenchuan earthquake. *Earth System Science Data*, 11(1), pp.35-55.

Mitchell, J.K. and Soga, K., 2005. *Fundamentals of soil behavior* (Vol. 3). New York: John Wiley & Sons.

Petschko, H., Brenning, A., Bell, R., Goetz, J. and Glade, T., 2014. Assessing the quality of landslide susceptibility maps—case study Lower Austria. *Natural Hazards and Earth System Sciences*, 14(1), pp.95-118.

Reichenbach, P., Rossi, M., Malamud, B.D., Mihir, M. and Guzzetti, F., 2018. A review of statistically-based landslide susceptibility models. *Earth-Science Reviews*, 180, pp.60-91.

## Real-time monitoring of landslides with the use of inclinometer and GNSS instrumentation

Nikolaos Depountis<sup>1</sup>, Katerina Kavoura<sup>1</sup>, Nikolaos Sabatakakis<sup>1</sup>, Panagiotis Argyrakis<sup>2</sup>, Kostas Chousianitis<sup>2</sup>, George Drakatos<sup>2</sup>

<sup>1</sup>Department of Geology, University of Patras, Greece, [ndepountis@upatras.gr](mailto:ndepountis@upatras.gr)

<sup>2</sup>National Observatory of Athens, Institute of Geodynamics, Greece

Slope inclinometers are widely used to determine the magnitude, rate, direction, depth, and type of landslide movement in several depths. This information is usually vitally important for understanding the cause, behavior, and remediation of a landslide. Additionally, to this, the rapid development of the Geodetic Navigation Satellite System (GNSS) receivers allowed landslide monitoring, especially on their surface with increasing accuracy. In this work, the first results of the combined use of slope inclinometers and GNSS receivers for landslide monitoring are presented, which can be further developed as a Landslide Early Warning System (LEWS). For this purpose, inclinometer and GNSS instrumentation has been installed in two pilot areas, the villages of Metsovo and Zotiko, which are located in the Region of Epirus in Western Greece (Figure 1).

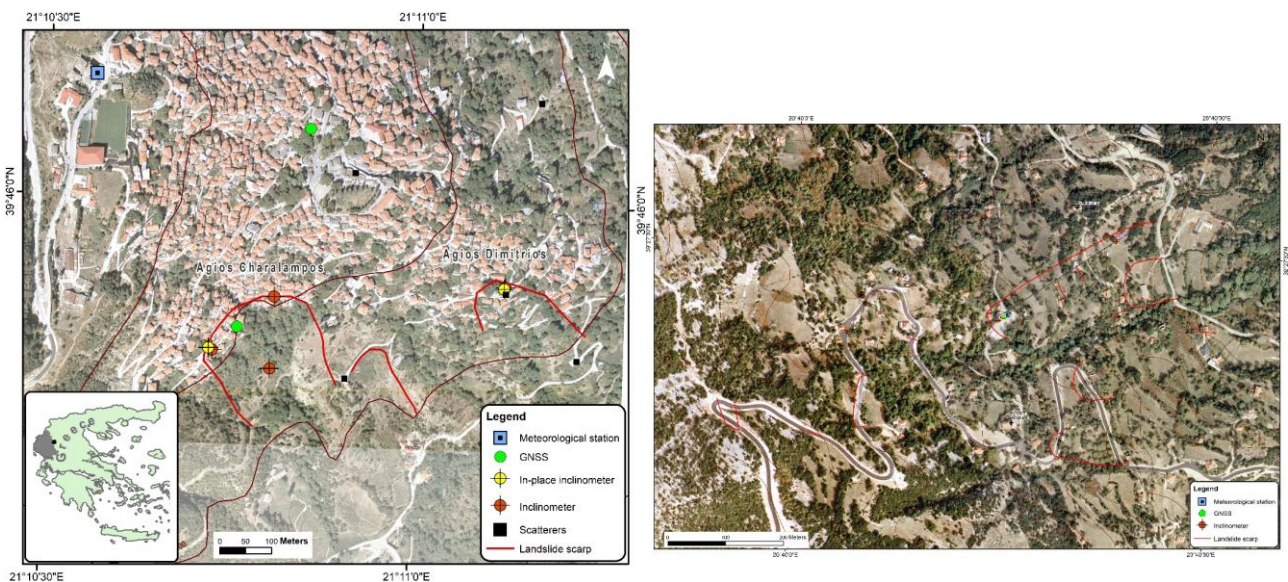


**Figure 1: The study areas of Metsovo (in the left) and Zotiko (in the right) with the installed instrumentation**

The presence of the tectonically highly sheared and weathered geological formations of the alpine basement (such as flysch) and the intense geomorphological relief of the Region of Epirus, strongly contribute to the periodically induced instability phenomena mainly triggered by heavy rainfalls and extreme meteorological events. The slide movements evolve very low velocity values at different depths; thus, the studied landslide cases can be characterized as complex and “extremely slow”. The real-time monitoring of the studied cases has been carried out by installing inclinometer casing that permit the detailed observation of subsurface displacements, for an extended period, with the use of in-place and portable gauges, as well as GNSS stations. All instrumentation has been installed in the wider area of the landslide zones, in both villages, and one of the main goals of this approach is to combine long and real time monitoring of the parameters connected to the landslide activity and kinematics.



The observation and analysis of such landslide characteristics on a large scale (site-scale, >1:500) takes into consideration some specific criteria (Corominas et al 2014; Soeters and van Westen 1996). The selection of Metsovo and Zotiko as pilot areas for the installation of a complete real-time monitoring system of landslides covers these criteria to a great extent, because: (a) both are residential areas with buildings and infrastructure works at risk, (b) the research areas are smaller than 0.1 km<sup>2</sup> and focus on periodically activated landslide zones, (c) a relatively sufficient knowledge of the engineering geological and geotechnical conditions of the subsoil and the geometry of the unstable areas is available and d) the geomaterials participating in the phenomenon belong to geological formations “prone to landslides”. The installed landslide monitoring system (inclinometers and GNSS receivers) basically provides insight into the evolution of surface and subsurface movements with a parallel real-time monitor of rainfall, as it seems that these landslides are directly connected with intense and extended rainfall phenomena.

Analyses in this research scale permit the development of a Landslide Early Warning System (LEWS) in the areas of interest, which is the first ever developed in Greece (Depountis et al 2021). The first results of the system appear in almost a real time and interactive way through a specially designed web-gis platform, accessible to the local authorities and the residents of the studied areas.

### **Acknowledgment**

This research has been financed by the Regional Development Programme of Epirus (NSRF 2014-2020).

### **REFERENCES**

- Corominas, J., Van Westen, C., Frattini, P., Cascini, L., Malet, J.P., Fotopoulou, S., Catani, F., Van Den Eeckhaut, M., Mavrouli, O., Agliardi, F., Pitilakis, K., Winter, M.G., Pastor, M., Ferlisi, S., Tofani, V., Hervás, J., Smith, J.T., 2014, Recommendations for the quantitative analysis of landslide risk. *Bulletin of Engineering Geology and the Environment*, 73 (2):209-263, DOI: 10.1007/s10064-013-0538-8.
- Depountis, N., Sabatakakis, N., Kavoura, K., Nikolakopoulos, K., Elias, P., Drakatos, G., 2021, Establishment of an integrated landslide early warning and monitoring system in populated areas”. In: Casagli N. et al. (eds), *Understanding and Reducing Landslide Disaster Risk, Volume 3 Monitoring and Early Warning*, pp. 189-194, ISBN 978-3-030-60311-3.
- Soeters, R., Van Westen, C.J., 1996, *Landslides, investigation and mitigation*. Transportation Research Board, National Research Council, Special Report, 247: 129-177.



## Assessing the effect of the coefficients of restitution on rockfall trajectory

Pavlos Asteriou<sup>1</sup>

<sup>1</sup>Adjunct Lecturer, University of West Attica, Greece, [pasteriou@uniwa.gr](mailto:pasteriou@uniwa.gr)

### **Rockfall Trajectory Modeling**

Rockfalls can have disastrous effects and constitute a significant natural hazard. To design effective protection measures, it is crucial to estimate the trajectory of the block, which highly depends on its response at impact. The response to the impact is described by the coefficients of restitution (CORs), which are overall parameters that take into account all the characteristics of the impact.

### **Analysis Methods And Assumptions**

The lump-mass model is most commonly used to analyze a rockfall due to its simplicity and is used in the majority of relevant software. Inevitably, there are some key limitations; the block is assumed as a rigid and dimensionless sphere. Therefore, the block's actual shape and its configuration at impact are neglected, even though both affect the resulting motion. In practice, COR values are obtained by suggested values, which depend solely on the slope material and are empirically derived.

Lately, some empirical models are proposed that originate from real rockfall incidents and experimental testing. Wyllie (2014) gathered literature data from field tests and studied the effect of impact angle ( $\alpha_i$ ) on  $n_{COR}$ , by classifying the results according to the slope material. He stated that  $n_{COR}$  is affected much more by the slope geometry than the material type and proposed the equation  $n_{COR}=19.5\alpha_i^{-1.03}$ . Giacomini et al. (2012) conducted field tests on a 50-m-high slope with an inclination of 70° and proposed the equation  $n_{COR}=0.92e^{-0.046\alpha_i}$ . Asteriou (2016) performed laboratory and small-scale field tests (over 3000 tests in total) and proposed an empirical model where  $n_{COR}$  is estimated according to the Schmidt hammer hardness (SHV) of both the block and the slope surface, the shape of the block and the intensity of the impact. The aforementioned methods for estimating CORs have been intergraded in a software developed in MatLab (Asteriou, 2019). In addition, a neural network algorithm has been included, trained with the aforementioned experimental data. The required input parameters are: slope's SHV and inclination, as well as block's SHV, mass, shape and impact velocity.

### **Case Study Demonstration**

In 2015 an earthquake-induced rockfall in Ponti - Lefkada resulted in one death. A block impacted a family residence, penetrated two brick walls and killed a person in the house (Saroglou et al., 2018). The rock path and the impact points on the slope were identified by a detailed field survey. The geological formations are limestones covered by moderately cemented talus materials (thickness 0.5-4.0m). The limestone block was detached at an elevation of 500m, rolled approximately for 250m, impacted 22 times on the slope and finally impacted the house that was at an elevation of 130m. The block traveled about 800m, its volume was approximately 2m<sup>3</sup> and was nearly cubical with 1.4-m-sides and the slope has an average inclination of ~35°.

The first analysis (Lump mass - suggested values) is performed according to the parameters proposed in literature; for scree those are:  $n_{COR}=0.35$  and  $t_{COR}=0.85$ . The block rests about 370m earlier compared to the documented trajectory. Then, a back-analysis is performed (Lump mass – Best fit), where the best set of parameters was found to be  $n_{COR}=0.75$  and  $t_{COR}=0.90$ . These values are much higher compared to those proposed and the rebounds are excessive: the second bounce is 50m long and 17.5m high.

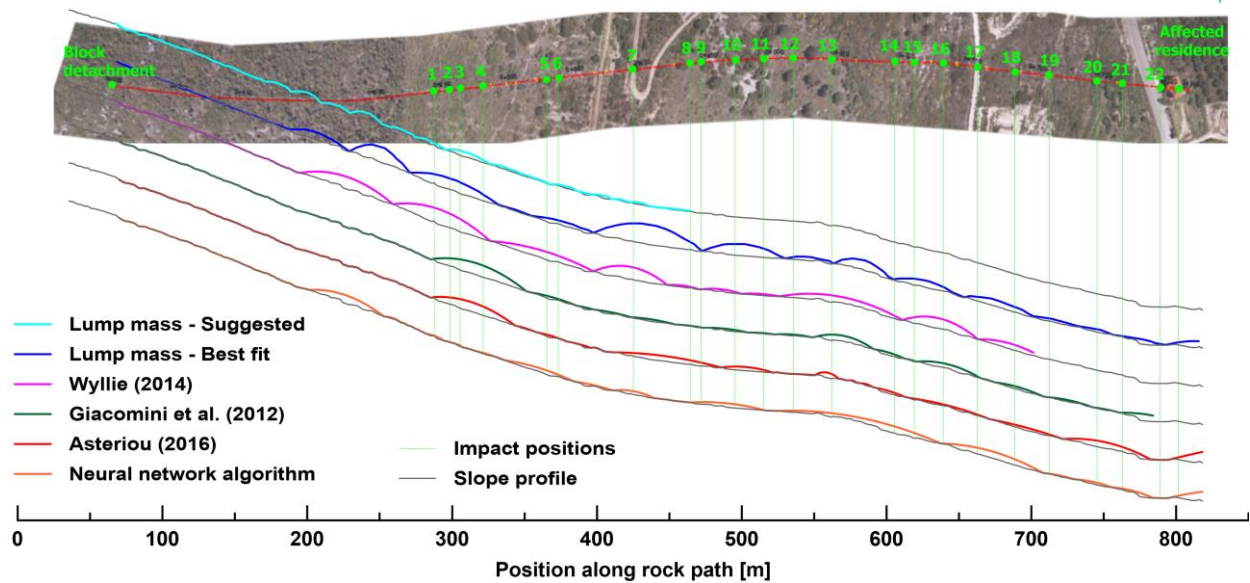


Figure 1.

The empirical models proposed by Wyllie (2014) and Giacomini et al. (2012) depend solely on impact angle. It is observed that both approach well and more rationally the documented trajectory. Wyllie (2014) correlation yields to just 7 bounces, with some being higher than anticipated. Giacomini et al. (2012) method results to 22 bounces with realistic rebound heights. Asteriou (2016) and the neural network algorithm (Asteriou, 2019) both depend on more parameters compared to the previous correlations and yield quite realistic trajectories consisting of a sequence of small bounces and sections in which the movement type becomes rolling/sliding.

### Conclusions

Regarding the analyses performed with the conventional approach, it is seen that the suggested COR values cannot replicate the trajectory that took place. Moreover, even by back analyzing the incident, the COR values obtained result to an unrealistic trajectory. Therefore, it appears that the assumption of COR values being material-based parameters is oversimplifying and may lead to false estimations and designs. The methods proposed by Wyllie (2014) and, especially, Giacomini et al. (2012) result to better trajectory estimates. Their major advantage is that selection of COR values requires no assumptions. Finally, the method proposed by Asteriou (2016) and the neural network algorithm (Asteriou, 2019) result to better trajectory estimates compared to the conventional approach, but require more input parameters that are easily measurable. Therefore, better methods for the estimation of CORs are available and their usage should be increased. This can only be achieved when these methods become available in relevant software.

### REFERENCES

Asteriou, P., 2016. Investigation of the geotechnical parameters which control rockfalls. PhD Thesis, NTUA, Athens  
 Asteriou, P., 2019. A new software tool for the analysis of rockfalls. 15th Int Congress of GSC, Athens.  
 Giacomini, AK., Thoeni, C., Lambert, S., Booth, Sloan, SW. 2012. Experimental study on rockfall drapery systems for open pit highwalls. *Int J Rock Mech Min Sci.*, 56, 171–181.  
 Saroglou, C., Asteriou, P., Zekkos, D., Tsiambaos, G., Clark, M., Manousakis, J., 2018. UAV-based mapping, back analysis and trajectory modeling of a coseismic rockfall in Lefkada island, Greece. *Nat. Hazards Earth Syst. Sci.*, 18, 321–333.  
 Wyllie, DC. 2014. Calibration of rock fall modeling parameters. *Int J Rock Mech Min Sci.*, 67, 170–180.



**THEME 7 - RECENT ADVANCES IN GEOMATICS AND REMOTE  
SENSING FOR USE IN ENGINEERING GEOLOGY**



## Investigation of the swelling/shrinkage phenomenon with the use of Earth Observation techniques in Nicosia, Cyprus

Ploutarchos Tzampoglou<sup>1</sup>, Dimitrios Loukidis<sup>1</sup>, Niki Koulermou<sup>2</sup>

<sup>1</sup>*Department of Civil and Environmental Engineering, University of Cyprus, Nicosia, CYPRUS,*

[tzampoglou.ploutarchos@ucy.ac.cy](mailto:tzampoglou.ploutarchos@ucy.ac.cy) ; [loukidis@ucy.ac.cy](mailto:loukidis@ucy.ac.cy)

<sup>2</sup>*Cyprus Geological Survey Department, Cyprus, [nkoulermou@gsd.moa.gov.cy](mailto:nkoulermou@gsd.moa.gov.cy)*

Expansive soils affect significantly many countries worldwide, damaging buildings and other infrastructure, causing economic losses in the scale of billions of dollars each year (Jones and Jefferson, 2012). In fact, the annual economic cost due to expansive soils surpasses that of other natural geohazards, such as earthquakes and landslides (Chen, 2012). The study area is the city of Nicosia, which suffers damages caused by the expansive soil called Nicosia Marl that is responsible for several millions of euros (Constantinou et al., 2002).

The main goal of the present study is to investigate the causative mechanisms of this phenomenon and highlight the factors that play major role in its occurrence. For this purpose, geological/geotechnical data were first collected from investigation reports, borehole logs and maps of the Cyprus Geological Survey Department, and thematic maps were constructed for the factors controlling ground swelling/shrinkage due to seasonal moisture changes (plasticity index, clay and montmorillonite content, expansive soil layer thickness and depth). Soil properties were averaged within an active zone assumed to extend down to 8m depth. Then, the ground movements in the area as inferred by Earth Observation (EO) techniques for the period between 16/11/2002–30/12/2006 (Zomeni & Koulermou, 2013) were processed.

In order to overcome the inherent weaknesses of EO techniques in the investigation of this phenomenon (i.e. repeated small amount of ground swelling/shrinkage without a characteristic monotonic trend; the vertical movements depend on the pressures applied by structures; each construction foundation type gives different deformation rates), instead of considering a velocity or an average movement rate, the amplitude of vertical movement, in the form of the difference between the maximum and minimum displacement observed in the given time period, was calculated for all the permanent scatterers (PS). This way, the severity of the vertical deformation fluctuations becomes evident. Furthermore, the PS points that did not belong to buildings were selected and treated separately as free field points that are not influenced by the loads or the rigidity of the structures.

The highest vertical displacements amplitudes, reaching 40 mm, were observed in the areas of Lykavitos and Aglantzia (Figure 1). It was found that the displacement amplitudes correlated quite well with the thematic layers of plasticity index (PI) and clay content. Similar trends were observed when considering only the free field PS points (Fig. 1b). Considering the statistical frequency of the vertical displacement amplitude as a function of each thematic layer, useful conclusions were drawn regarding the degree of influence of the factors governing the ground swelling/shrinkage phenomenon. More specifically, the strongest influence comes from the PI (Fig. 2). The correlations become even stronger when isolating the free field PS points (Fig. 2b). This fact demonstrates the necessity of special processing of PS data derived from EO techniques.

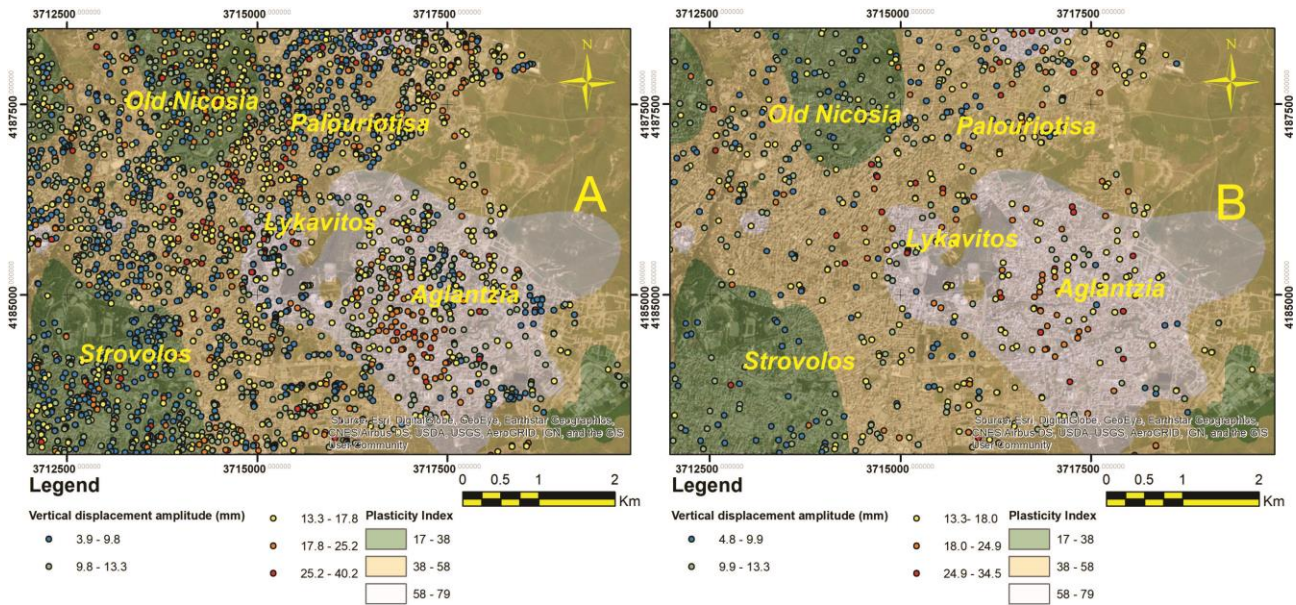


Figure 1. Spatial distribution of the vertical displacement amplitude for the period 16/11/02-30/12/06: A) all PS points, B) free field PS points, in combination with the plasticity index variation.

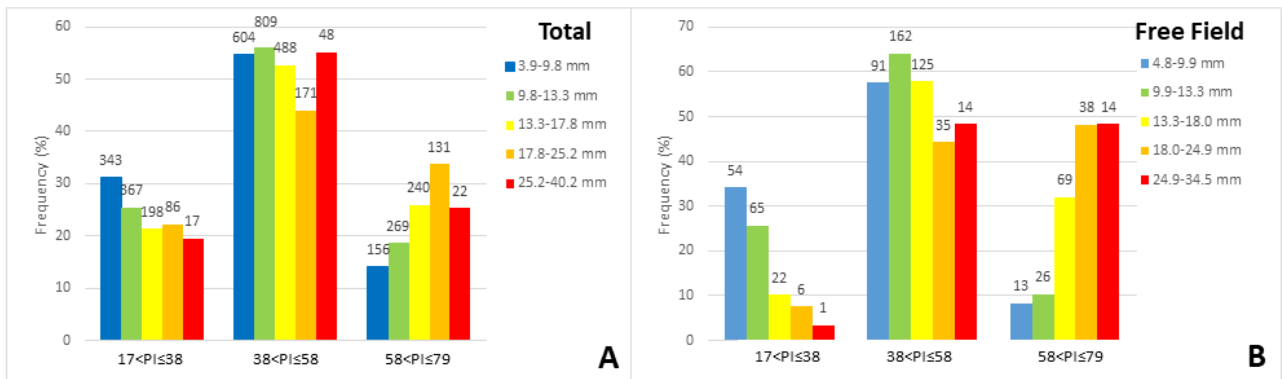


Figure 2. Statistical frequency of the vertical displacement amplitude as a function of the plasticity index: A) all PS points, B) free field PS points.

REFERENCES

Chen, F.H., 2012, Foundations on expansive soils, Elsevier.

Constantinou, G., Petrides, G., Kyrou, K., and Chrysostomou, C., 2002, Swelling Clays: A continuous Threat to the Built Environment of Cyprus. UNOPS Project Final Report, Scientific Technical Chamber of Cyprus, Nicosia, Cyprus.

Jones, L. D., and Jefferson, I., 2012, Expansive soils. In ICE Manual of Geotechnical Engineering, Institute of Civil Engineers, London, UK.

Zomeni, Z., and Koulermou, N., 2013, PanGeo D7.1.17 Geohazard Description for Lefkosia, Cyprus Geological Survey Department, Nicosia, Cyprus.



## **An Integrated Object-Based Analysis with UAV Imagery and Machine Learning for site-specific Mass Movement Assessment**

Efstratios Karantanellis<sup>1</sup>, Vassilis Marinos<sup>1</sup>, Emanuel Vassilakis<sup>2</sup>, Basile Christaras<sup>1</sup>

<sup>1</sup>*Faculty of Geology, Aristotle University of Thessaloniki, Thessaloniki, Greece, [skarantanellis@gmail.com](mailto:skarantanellis@gmail.com)*

<sup>2</sup>*Faculty of Geology & Geoenvironment, National and Kapodistrian University of Athens, Athens, Greece*

Landslide and rockfall accurate identification constitute an important aspect in landslide hazard assessment and risk management processes (Fell et al., 2008). Last years, remote sensing is increasingly used in engineering geology domain for exploiting and monitoring hazardous events. Consequently, the use of up-to-date technologies for landslide detection and monitoring is of paramount importance in reducing landslide risk. Mass movement events are mostly detected through visual assessment of remote sensing datasets (Xu, 2015). Although the visual assessment has high identification accuracy, the process is time-consuming and labor-intensive and most importantly it is subjective to expert's cognition. Thus, automated or semi-automated methods for precise and concrete landslide identification based on close range remote sensing techniques are highly sought. Current studies on site-specific landslide assessment are mainly hinge on high resolution satellite imagery or airborne based imagery or Light Detection and Ranging (LiDaR) surveys, or Digital Terrain Models (DTM) (Guzzetti et al., 2012) and lately with the use of Unmanned Aerial Vehicles (UAVs). UAV platforms have several advantages compared with traditional acquisition platforms, such as flexibility and lower operational costs, higher speed and safety. Moreover, UAVs are able to operate rather close to the object, which leads to ultra high resolution (cm to mm scale) imagery. In addition, they can be efficiently adopted for initial mass movement assessment in post-scenarios, in order to collect information on their magnitude, spatial extent, and temporal evolution, as well as provide imagery in unprecedented resolutions, in unreachable areas. As a result, the investigated scene provides significant details for identification and extraction of specific landslide and rockfall objects' parameters. Obtaining a good overview of individual objects' parameters such as spatial, spectral and contextual information and relate them with engineering geological and scene's morpho-dynamics can lead to a higher understanding of the natural processes of landslides and rockfalls (Figure 1).

In this study, we propose an integrated object-based framework based on fused UAV derivatives and machine learning operators to identify specific landslide and rockfall indicators. The overall process is represented as a pipeline consisting of an optimized UAV data acquisition phase, followed by the hierarchical segmentation phase of the fused RGB layers and the DSM derivatives such as slope aspect, curvature and hillshade and characterization of the extracted primitives in appropriate landslide and rockfall classes. Uniform homogeneity and semantic consistency have been taken into consideration for the segmentation stage. In order to evaluate the best-fitted machine learning procedure for the site-specific assessment different approaches have been tested. For this purpose, five advanced Artificial Intelligence (AI) models, namely, Naive Bayes (NB), KNN (K Nearest Neighbor), SVM (Support Vector Machine), Decision Tree and Random Trees, were applied and compared thoroughly in landslide and rockfall applications to evaluate their individual performance. By using machine learning and deep learning techniques, the proposed object-based mass movement detection and characterization method shows significant robustness and great potential in overcoming landslide cognitive subjectivity.

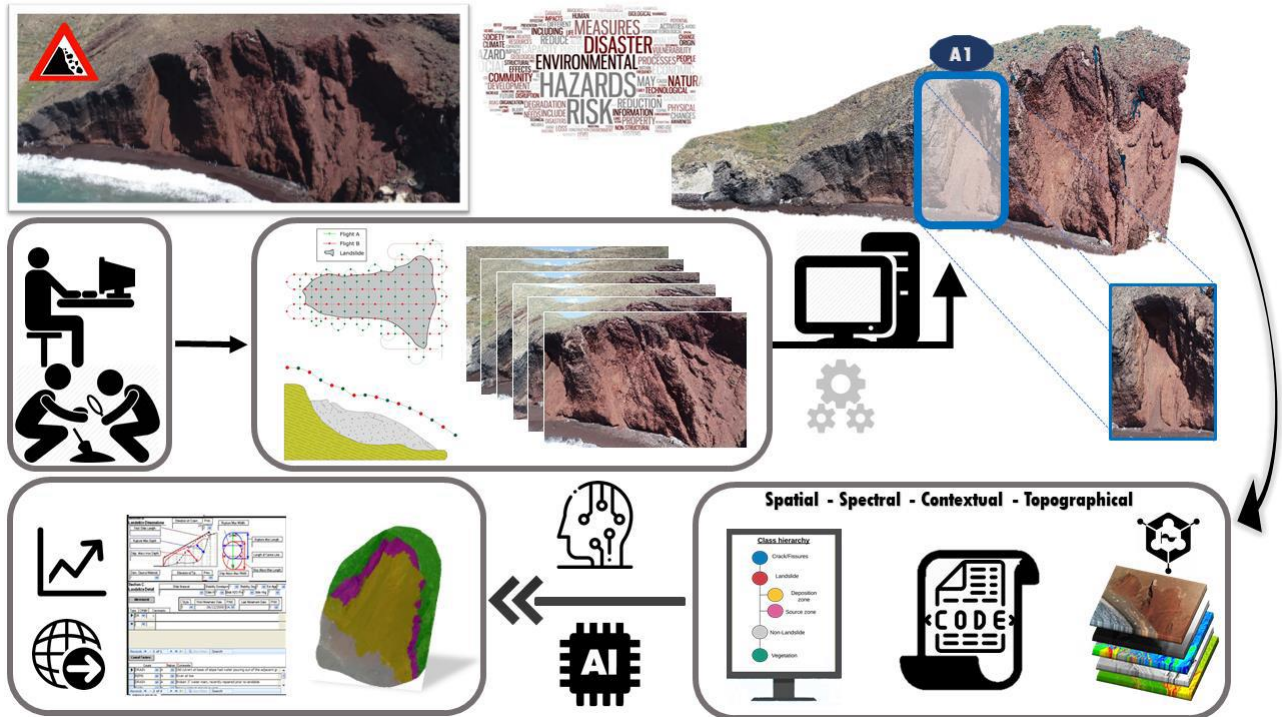


Figure 1. Schematic flowchart for the proposed object-based mass movement analysis.

**REFERENCES**

Fell, R., Corominas, J., Bonnard, C., Cascini, L., Leroi, E. and Savage, W.Z., on behalf of the JTC-1 Joint Technical Committee on Landslides and Engineered Slopes, 2008, Guidelines for landslide susceptibility, hazard and risk zoning for land use planning. Eng. Geol. 102, 85–98. <https://doi.org/10.1016/j.enggeo.2008.03.022>

Guzzetti F., Mondini A.C., Cardinali M., Fiorucci F., Santangelo M. and Chang K.T., 2012, Landslide inventory maps: new tools for an old problem, Earth-Sci. Rev., 112 (1), pp. 42-66, [10.1016/j.earscirev.2012.02.001](https://doi.org/10.1016/j.earscirev.2012.02.001).

Xu C., Xu X., Bruce J. and Shyu H., 2015, Database and spatial distribution of landslides triggered by the Lushan, China Mw 6.6 earthquake of 20 April 2013, Geomorphology, Volume 248, 2015, Pages 77-92, ISSN 0169-555X, <https://doi.org/10.1016/j.geomorph.2015.07.002>



## InSAR in monitoring of underground civil works in urban areas. Case of Glòries square, Barcelona

Joan Botey i Bassols<sup>1,2</sup>, Pierre Gerard<sup>2</sup>, Enric Vázquez-Suñé<sup>1</sup>, Michele Crosetto<sup>3</sup>, Anna Barra<sup>3</sup>

<sup>1</sup>*Institute of Environmental Assessment & Water Research (IDAEA), CSIC, Spain. [w.jbotey@gmail.com](mailto:w.jbotey@gmail.com) ; [enric.vazquez@idaea.csic.es](mailto:enric.vazquez@idaea.csic.es)*

<sup>2</sup>*Building, Architecture and Town Planning (BATir) department, Université libre de Bruxelles (ULB), Belgium. [piergera@ulb.ac.be](mailto:piergera@ulb.ac.be)*

<sup>3</sup>*Centre Tecnològic de Telecomunicacions de Catalunya (CTTC/CERCA), Division of Geomatics, Spain. [michele.crosetto@cttc.cat](mailto:michele.crosetto@cttc.cat) ; [abarra@cttc.cat](mailto:abarra@cttc.cat)*

### **Background**

Underground civil works in urban areas entail serious risks (i.e., settlements, modification of groundwater flows, etc.) that require a high control. In this context, SAR (Synthetic Aperture Radar) interferometry appears as a complement of great value to other common techniques such as levelling, as it provides a more complete view in space and time of the observed phenomena: the monitored area is larger, the spatial density of the data is greater and the acquisition frequency can be of the same order or higher (Karila et al., 2013). The construction works of two road tunnels under Glòries square in Barcelona might be the first case in which SAR interferometry is included in the continuous monitoring of the works performed by the Construction Management Office, and offers the opportunity to analyze its performance and compare it to levelling.

### **Methods**

The area of study is being monitored with SAR interferometry since 2015. The processed SAR dataset is composed of 97 descending IWS (Interferometric Wide Swath) SLC (Single Look Complex) Sentinel-1A images from 06/03/2015 to 28/09/2018. The applied SAR data treatment is a Persistent Scatterer Interferometry (PSI) technique. InSAR results have been analyzed using geological and hydrogeological field data (boreholes, pumping tests, etc.) and local numerical models, hydraulic and piezometric data (discharge rates, groundwater heads, etc.) and levelling surveying.

### **Results**

SAR interferometry has allowed to observe that the ground deformation is not centered around the construction site –as it could be expected– but concentrated in the east quadrant. This distribution agrees with both piezometry and hydrogeology. In addition, InSAR results have also allowed to observe that the largest settlements are not located in the works area but slightly to the southeast. The reason is that, although the temporal evolution of the deformation matches very much the evolution of the drainage and, therefore, confirms that the works dominate the dynamics of the deformation, several other groundwater pumpings have been and are still active south and eastward from the construction site. The area covered by the levelling network and its density would not have allowed such observations. In contrast, levelling seems to provide more accurate results, according to the analytical estimation (based on Cashman and Preene, 2001; Jacob, 1950; and Pujades et al., 2014a). InSAR results are 4 mm larger and measure maximum settlements in the works area of 8 mm –for a piezometric drawdown of 10 m.

### **Conclusion**

SAR interferometry has shown to be not only a technique suitable for quasi-real-time monitoring of deformation associated with civil works in urban environments, but also a highly valuable complement to usual monitoring techniques such as levelling, as it is able to provide a much more complete view of the observed deformation



phenomena. InSAR results have allowed to identify or confirm both the origin of the ground deformation and its controlling factors. Such observations would not have been possible with levelling due to the area and density of its monitoring network. In contrast, the weakness of SAR interferometry in this kind of applications, where a very high accuracy is required, remains the quantification of the deformation.

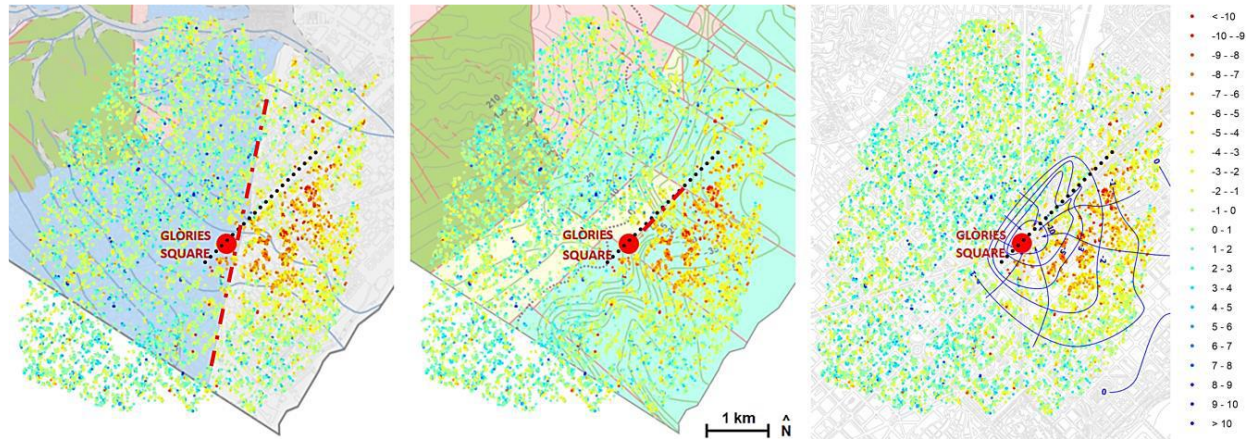


**Figure 1. InSAR vertical deformation (mm) accumulated between 03/04/2018 and 23/08/2018 over the Quaternary (left) and Tertiary (centre) geology and over the piezometry (right). Blue points represent uplifting (positive displacement) and red points, settlement (negative displacement). Red dashed lines highlight geological changes: stiffer cemented colluvial materials in the west and deltaic fine-grained materials in the east for the Quaternary strata; sands in the northwest and marls in the southeast for the Tertiary strata.**

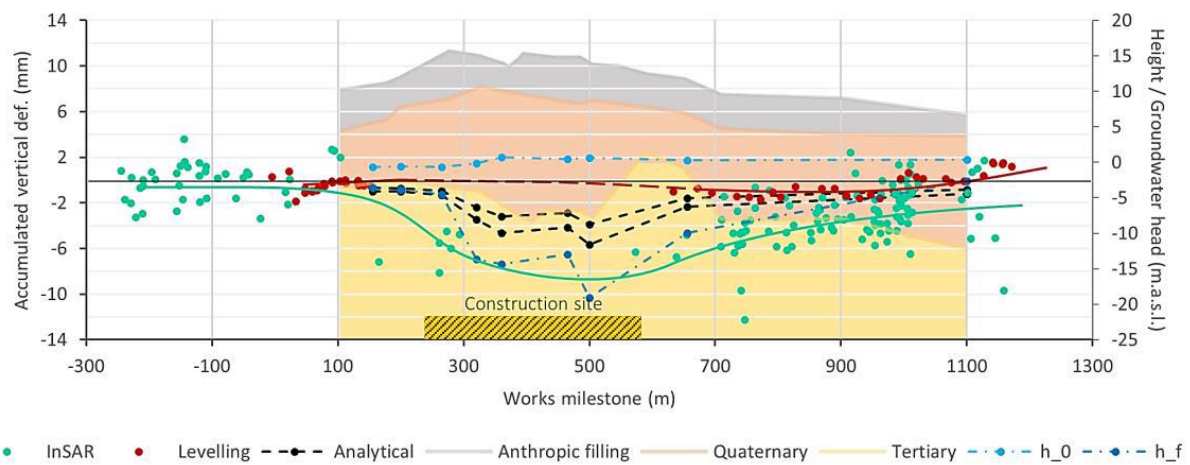


**Figure 2. SW-NE profiles of vertical deformation accumulated between 03/04/2018 and 23/08/2018 over the geological profile and the initial ( $h_0$ ) and final ( $h_f$ ) groundwater head. See location in Figure 1 (dashed black line).**

**REFERENCES**

Cashman, P.M. and Preene, M., 2001, Groundwater Lowering in Construction: A Practical Guide. CRC Press.  
 Jacob, C.E., 1950, Flow of ground water. In: Rouse, H. (ed.) Engineering Hydraulics. John Wiley, New York, 321-386.  
 Karila, K., Karjalainen, M., Hyyppa, J., Koskinen, J., Saaranen, V. and Rouhiainen, P., 2013, A Comparison of Precise Leveling and Persistent Scatterer SAR Interferometry for Building Subsidence Rate Measurement. *Isprs International Journal of Geo-Information*, 2, 797-816, doi: 10.3390/ijgi2030797.  
 Pujades, E., Vazquez-Sune, E., Carrera, J. and Jurado, A., 2014a, Dewatering of a deep excavation undertaken in a layered soil. *Engineering Geology*, 178, 15-27, doi:10.1016/j.enggeo.2014.06.007.

## Engineering Geological Appreciation and Monitoring of Rockfall's Dynamic, Based on Multi-Temporal UAV and LiDaR Surveys in "Apothikes" Area, Santorini Prefecture, Greece

Ioakeim Konstantinidis<sup>1</sup>, Efstratios Karantanellis<sup>1</sup>, Vassileios Marinos<sup>1</sup>, George Papathanassiou<sup>2</sup>

<sup>1</sup>Laboratory of Engineering Geology & Hydrogeology, School of Geology, Aristotle University of Thessaloniki, 54124, Thessaloniki, Greece, [ioakeimkk@geo.auth.gr](mailto:ioakeimkk@geo.auth.gr)

<sup>2</sup>Department of Civil Engineering, Democritus University of Thrace, Komotini, Greece

Lately, there has been an increasing demand in geo-engineering society for automatically monitored areas which are susceptible to landslide and catastrophic rockfall events. The implementation of this high-end technology such as Unmanned Aerial Vehicles (UAV) and Terrestrial Laser Scanners (TLS), combined with a solid geo-engineering investigation of the studied area, could lead to more accurate, precise and time-effective local scale modelling of the landslide or rockfall event. The current research demonstrates a powerful approach to precisely foresee potential rockfall hazards in the area of interest, based on a multi-temporal change detection procedure in time intervals in order to prevent any undesired consequence via the integration of innovative remote sensing tools and the suitable analysis of their results.

The investigated site ("Apothikes") is located across the road network that leads to the only beach that lays inside the caldera region, in Santorini Island, Greece. The area is geologically characterized by alternations of volcanic beds of strong ignimbrite and soft layers of pyroclastic tuffs. These different engineering properties of the materials combined with the very steep morphology ( $\leq 80^\circ$ ) and the vertical dip persistent discontinuities ( $76^\circ - 90^\circ$ ) constitute to differential erosion and undercut in the base of the slope. Tensile stresses developed and eventually lead to rock pillar detachment followed by toppling or planar sliding failure of the previously suspended blocks of ignimbrite from a notable height ( $\cong 20\text{m}$ ) (Marinos *et al.*, 2014). The significance of this specific region originates from the noteworthy human presence in the prone areas. Consequently, it is indispensable to provide precise precognitions of potential rockfall hazard via adequate visualization of the anticipated phenomena.

Analytically, in this particular case, multi-sensor fusion and multitemporal change detection techniques were performed among three different datasets derived from i) a TLS during summer of 2014 and ii) a UAV platform during summer of 2018 and spring of 2019 respectively. The aim of this procedure is to monitor and characterize topographical changes between different epochs for robust modelling of the rockfall's dynamics. The proposed approach of multi-sensor change detection was accomplished with the correlation of the 3 multi-epoch models in order to quantify the rockfall's displacements with computer-based methods.

At a subsequent step, in order to precisely predict potential rockfall hazards in the area, we proceed to a trajectometry simulation in the previously determined, prone sub-regions. The produced Digital Surface Model (DSM), from the latest acquired dataset, was converted to hillshade via QGIS3.4. The prone blocks, were analyzed and their potential trajectories were specified in both 3D and 2D display. This analysis provided us with the capability to estimate the outcome (energy, velocity, height and travel time) of any potential rockfall event pre and post the implementation of remedial measures. It gives us confidence that through this in-depth risk assessment we can mitigate potential miscarriages of the protection measurements that can be possibly applied in these certain sub-regions.

To conclude, during the 4-year period (2014-2018) significant rock displacements with notable magnitude ( $\leq 4\text{m}^3$ ), were observed. Furthermore, during the correlation of the latest datasets (2018-2019) important



shifting of rock pillars ( $\leq 0.37m$ ) was noted as a result of the extension of the tensile cracks (Figure 2). An essential point of our research was that the place where the main displacements occurred in the past seems stable now but new movements noticed in other sub-regions that were steady previously. Although the slopes under residences might have been considered as the main prone sub-regions (due to their commercial importance and the magnitude of the noticed displacements), the whole failure model is dynamic and constantly changing. These observations would have been unachievable without the holistic evaluation of the study area which has been achieved by the construction of a 3D Observational Model, via remote sensing technologies (Figure 1).

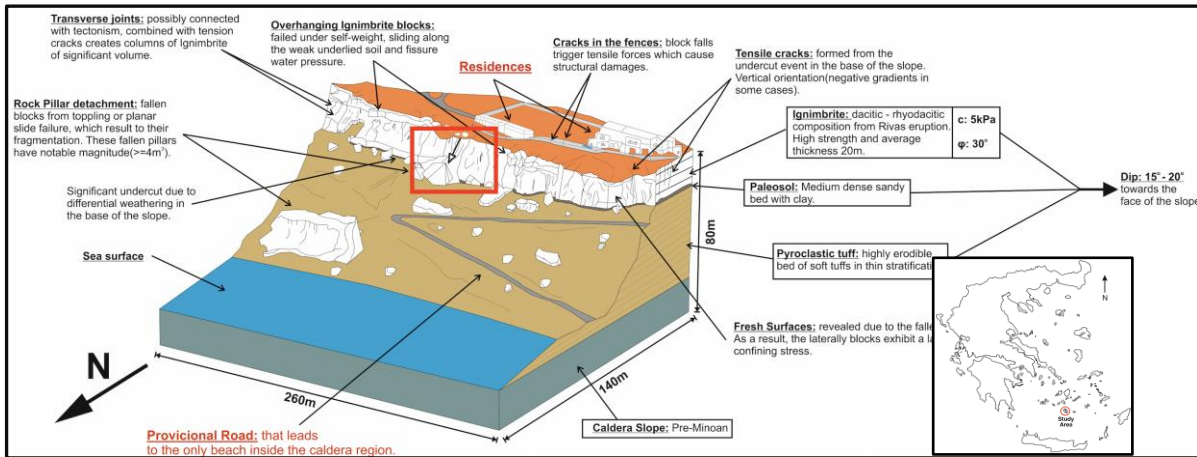


Figure 1. 3D Conceptual Model constructed from the latest UAV’s derived dataset. Marked area analyzed in Figure. 2.

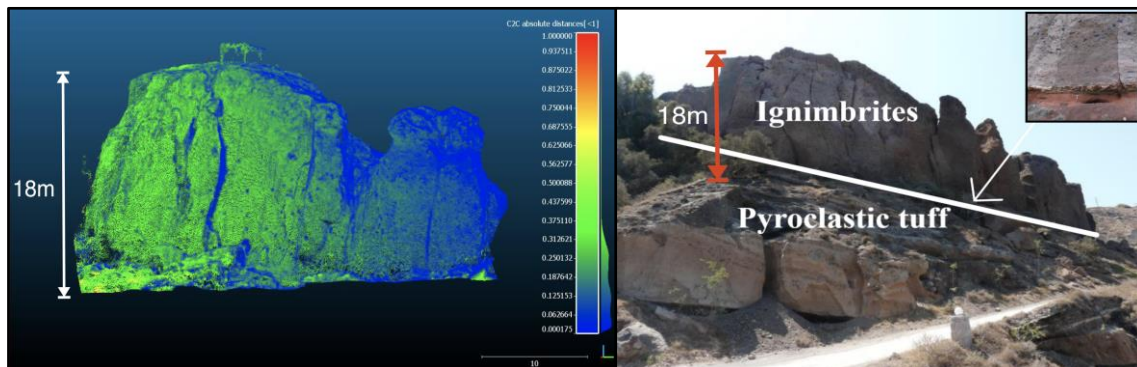


Figure 2. Change detection analysis in the prone sub-region with movement quantification output, showing the shifting of the Ignimbrite’s pillars towards the provisional road, due to the extension of tensile cracks.

## REFERENCES

D., Giordan, A., Manconi, A., Facello, M., Baldo, F., dell’Anese, P., Allasia, and F., Dutto, 2014, Brief Communication “The use of UAV in rock fall emergency scenario”. Natural Hazards Earth System Sciences Discussions, 2, pp 4011–4029.

A., Lucieer, S. M., de Jong and D., Turner, 2014, Mapping landslide displacements using Structure from Motion (SfM) and image correlation of multi-temporal UAV photography. Progress in Physical Geography, Vol. 38(1), pp 97–116.

V., Marinos, S., Paulidis, G., Pantazis, E., Lamprou, G., Prountzopoulos, P., Asteriou, G., Papathanassiou, T., Kakkis, 2014, Geological Research, Risk Estimation and Remedial Measures Suggestion for the Landslide Events in Kokkini Paralia and in the area of Apothikes, Municipality of Thira.

## Engineering geological appreciation on landslide and rockfall phenomena and monitoring using LiDAR and UAV platforms in a case site at Perivoli, Greece

Apostolos Azas<sup>1</sup>, Vassilis Marinos<sup>1</sup>, Efstratios Karantanellis<sup>1</sup>, George Papathanassiou<sup>2</sup>

<sup>1</sup>*Faculty of Geology, Aristotle University of Thessaloniki, Thessaloniki, Greece, [marinosv@geo.auth.gr](mailto:marinosv@geo.auth.gr), [skarantanellis@gmail.com](mailto:skarantanellis@gmail.com)*

<sup>2</sup>*Department of Civil Engineering, Democritus University of Thrace, 67100, Xanthi, Greece, [gpapatha@civil.duth.gr](mailto:gpapatha@civil.duth.gr)*

Landslides are natural phenomena that require early detection, research, quick response and continuous monitoring. Depending on their dynamics and kinematics, landslide results can lead to destruction of properties and even loss of human lives. In the last few years, landslide and rockfall phenomena appear in a road cut along the Grevena-Perivoli provincial road, at Perivoli village, causing continuous service disruptions and increased risk for the crossing vehicles. In this study, we carried out multiple field visits and we collected several data on the rock masses characteristics, their mode failure and we performed monitoring using terrestrial laser scanning (TLS LiDAR) and Unmanned Aerial Vehicle (UAV) platforms to accurately map and study the evolution of the landslide and rockfall phenomena.

The predominant geological formation in the wider region is compiled of a great tectonic mixture, well-known as "Avdella Melange", which includes, thin bedded limestones with chert intercallations, flysch layers of siltstones and sandstones (of Pindos geotectonic unit) and ophiolites. All these geological formations are highly tectonic disturbed, weathered and are eligible to landslide in this steep mountain terrain. Three consecutive visits have been executed, starting in 2017 and ending in 2019, where onsite engineering geological investigations of the area was carried out, such as rock mass classification with the GSI system and joint geometry and strength measurements. During the site visits, we performed a quadcopter UAV flight and a TLS LiDAR scanning, aiming on more accurate and precise data acquisition (Colomina I., Molina P., 2014). A change detection methodology was used to exploit these point clouds in pairs 2017-2018 and 2017-2019 (Giordan et al., 2018).

The structure of the rock masses is generally characterized by sub-vertical strata dipping inwards the slope (Figure 1), however the continuity of the rock masses in depth is questionable due to the nature of this tectonic mixture. The in-situ engineering geological investigations led to the estimation of GSI values for the different rock masses along the slope. Limestones, characterized by a GSI of 45-50, are only met in the corner of the slope rockmass, while thin-bedded interlayers of siltstones and sandstones, with some limestone floaters, are highly tectonised and weathered with a GSI of 20-30 (in Figure 1) (Marinos, 2010). The presence of the clayey zones, originated from the lensified flysch formations that have been taken from this melange, and the intense shearing along the whole rock mass, create unfavorable conditions for the overall stability of the slope. On the other hand, in the scale of this slope geometry, the most frequent instability problems are generated from structurally controlled instabilities. Toppling of the competent blocks, within this complex rock mass, is the principle mechanism of the rockfalls. The softer silty-clayey bands are easily weathered and eroded and can lead to the undermining of the competent limestone and sandstone blocks. Due to the steep nature of the slope, the rock blocks easily reach the road network.

Point cloud analysis has been performed on software for 3D modelling, leading to the creation of two-dimensional and three-dimensional digital map models. These models assisted to a better understanding of the landslide's failure mechanism, while monitoring the rock fall evolution along the slope. A total volume of

fallen debris and blocks, over the period 2017-2019, was calculated approximately 220m<sup>3</sup> (Figure 1).

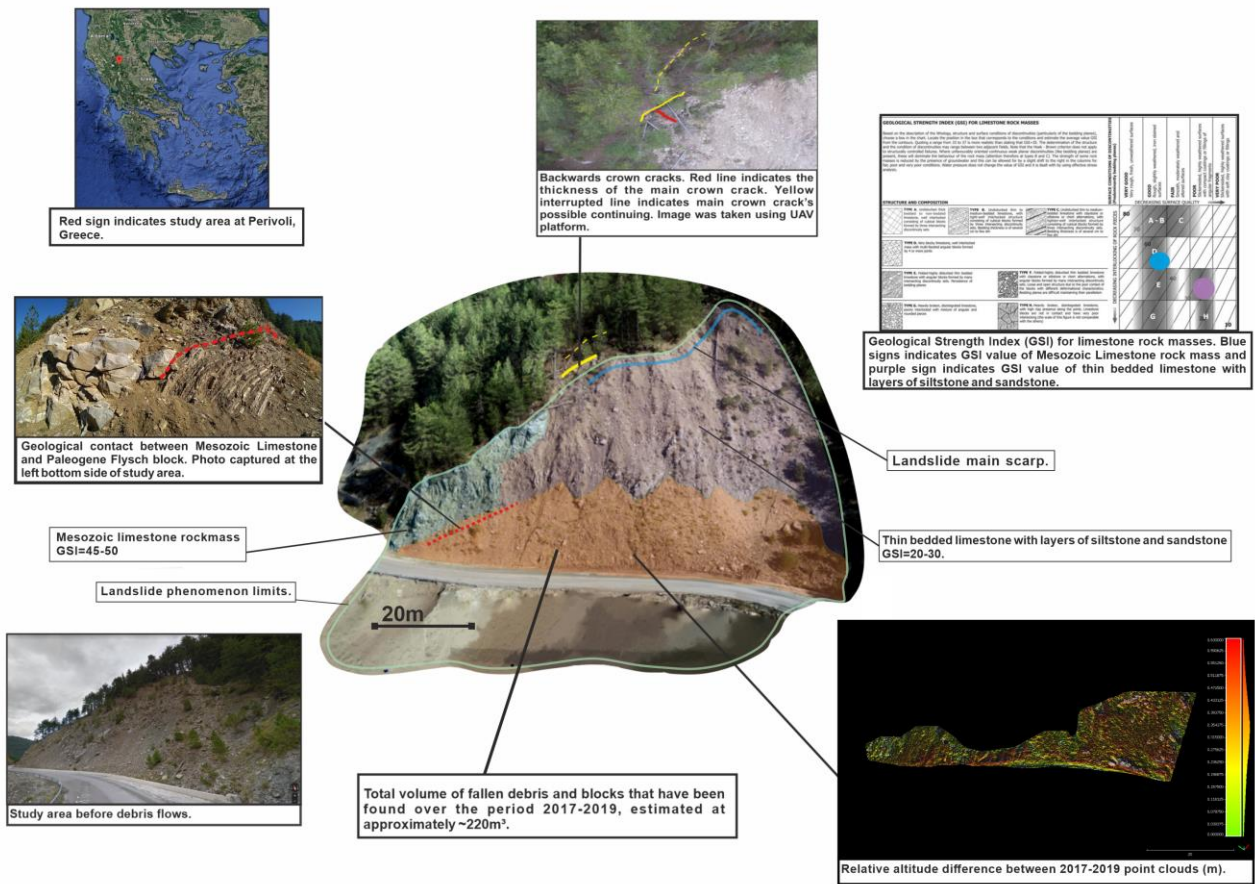


**Figure 1: Landslide and rockfall characteristics in the case site at Perivoli (Northern Greece). Data have derived from field engineering geological appreciation and change detection processed by point clouds of TLS LIDAR and UAV platform**

## REFERENCES

- Colomina, I. and Molina, P., 2014, Unmanned aerial systems for photogrammetry and remote sensing: A review - <https://doi.org/10.1016/j.isprsjprs.2014.02.013>
- Giordan, D., Hayakawa, Y., Nex, F., Remondino, F. and Tarolli, P., 2018, Review article: the use of remotely piloted aircraft systems (RPASs) for natural hazards monitoring and management - <https://doi.org/10.5194/nhess-18-1079-2018>
- Marinos, V., 2010, New proposed GSI classification charts for weak or complex rock masses. Proceedings of the 12th International Congress of Geological Society of Greece, Vol. III, Bulletin of the Geological Society of Greece XLIII, No3 1248-1259, Patra, Greece.

## Landslide Susceptibility Assessment under seismic motion surveys: A case in Melissoyrgoi, Epirus

Pinelopi Sotiriou<sup>1</sup>, Vassilis Marinos<sup>1</sup>, Efstratios Karantanellis<sup>1</sup>, George Papathanassiou<sup>2</sup>

<sup>1</sup>Laboratory of Engineering Geology & Hydrogeology, School of Geology, Aristotle University of Thessaloniki, Greece, [psotiriou@geo.auth.gr](mailto:psotiriou@geo.auth.gr)

<sup>2</sup>Department of Civil Engineering, Democritus University of Thrace, Greece

Various landslides incidents of significant magnitude have been recorded over the years, connected with various conditional and triggering factors. For years, landslides have been surveyed and analyzed using standard scientific approaches. Recently technological tools, though, have led to the greatest benefit of direct and rapid provision of high-precision geospatial data for structures and areas that are not readily detectable. Indeed, the use of Unmanned Aerial Vehicle (UAV) has led to a more reliable, effective and time-efficient localization modeling to scale of landslide.

The area under investigation is a steep slope within the Melissoyrgoi village in the mountains of Epirus prefecture, in Northern Greece. The research deals with the identification and analysis of possible landslides that may have occurred in the village Melissoyrgoi after the strong seismic motions on the 1<sup>st</sup> of May 1967. The studied area has been characterized as a possible old landslide due to, its distinct morphological indicators. This study was based in an engineering geological field mapping and point cloud processing derived an Unmanned Aerial Vehicle (UAV). Overall, the area is geologically characterized by flysch deposits (siltstone, sandstone) of the Ionian geotectonic zone, limestones of Pindus geotectonic zone and recent debris deposits. Tectonically the area has been affected from the overthrust of Pindos geotectonic zone above the Ionian geotectonic zone (Mountrakis, 2010). Specifically, in the area participate moderately disturbed sandstones and thin interlayers of siltstone (flysch formation) (GSI 50-55, type III) and disintegrated limestones (GSI 15-20, type H). The tectonic evolution affects the formations and more specific the stability of the village. Quite permeable areas can locally be detected after the brittle and disintegrate of limestone. These areas can feed with water the impermeable flysch formations and create increased water pore pressure. Consequently, we assume, that after the seismic motion the tectonically disturbed limestone has isotropically failed.

In this analysis, detailed imagery data were obtained using Unmanned Aerial Vehicles (UAVs). The processed Digital Elevation Models (DEM) provided high-precision and high-quality data which led to the mapping of potential landslides boundaries, even in regions that were not accessible during field work (Bemis, et al., 2014). The resulted models, in combination with the field observations and geological mapping of the ground quality and the sliding material guided to the delineation of the possible sliding mass. The possible sliding zone is expected along the possible old landslide materials and the stable bedrock of the flysch formations. A maximum of 15 m thickness of this layer is estimated, based on the morphology and data from other landslides in this environment. This sliding depth corresponds not only to high weathering profiles in flysch deposits but also to the tectonized nature of the material.

In order to investigate the slope stability of the sliding mass under seismic loading a numerical analysis has been performed with the geotechnical software Slide Rocsience Inc. The slope stability analysis was examined for circular and non- circular slides, for the following conditions a. static conditions (dry), b. seismic conditions (seismic acceleration 0.24g) and c. with groundwater pore pressure ( $r_u=0.1$ ,  $r_u=0.2$ ,  $r_u=0.3$ ). The stability analysis was performed with zero cohesion and friction angle of 15°. The current geometry with the studied



critical surface has a factor of safety less than 1 (F.S.<1) at seismic load conditions and pore pressure conditions (Bishop simplified Method was used).

In conclusion, the examined slope, assuming this unstable mass in 15m depth, is considered as stable under static conditions but unstable under seismic conditions seismic acceleration 0.24g and with groundwater pore pressure for each used value. It is noted though that the assigned geotechnical parameters are quite low and correspond to low residual strength.

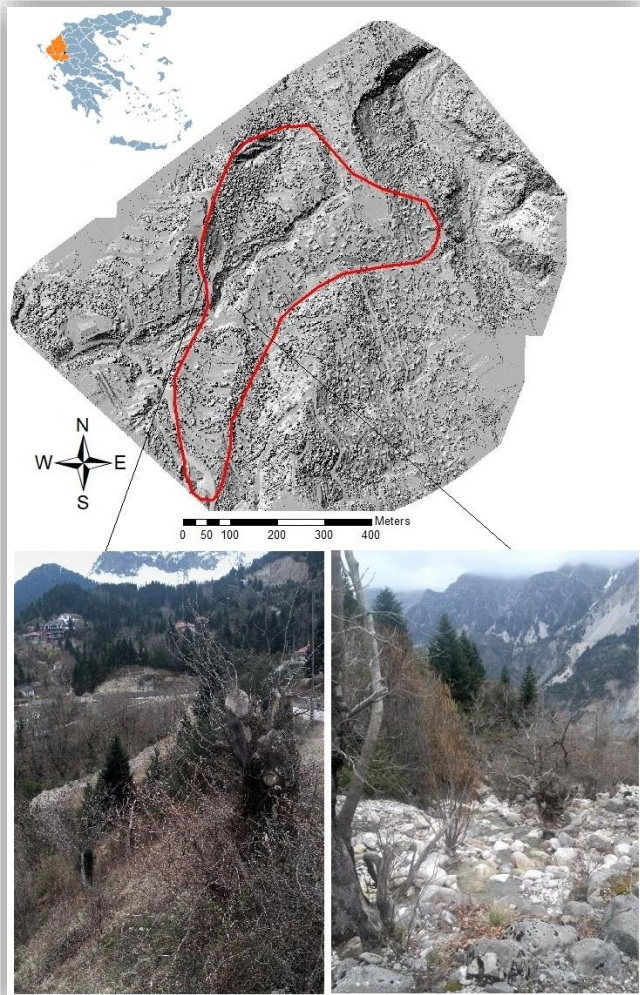


Figure 4: Landslide boundaries on DEM- Hillshade and feature image of the area

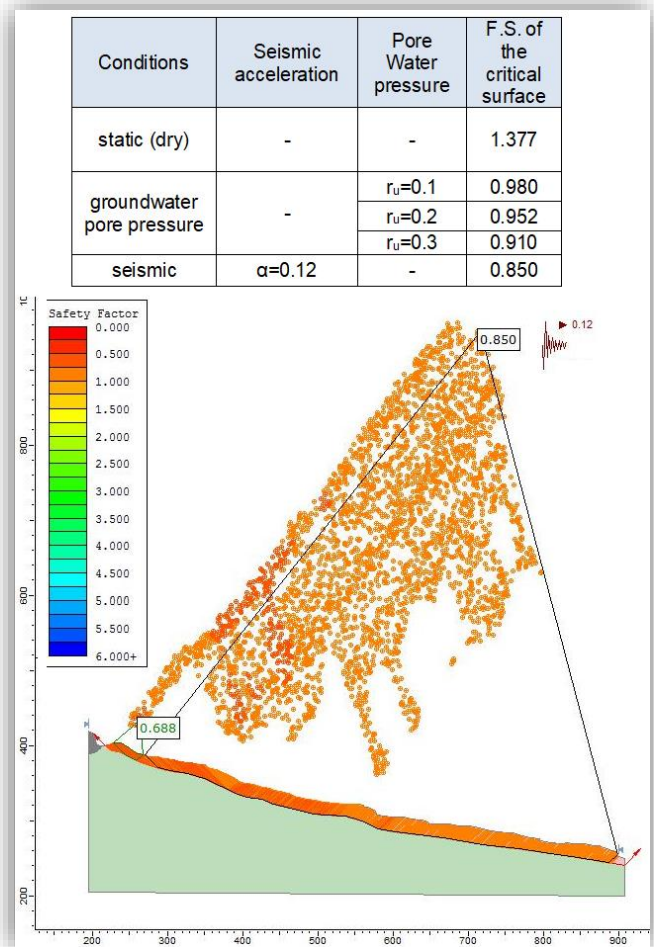


Figure 2: Stability analysis for no-circular circle

**REFERENCES**

Bemis S., Micklethwaite S., Turner D., James M., Akciz S., Thiele S. and Bangash H., 2014, Ground-based and UAV-Based photogrammetry: A multi-scale, high resolution mapping tool for structural geology and paleoseismology. Journal of Structural Geology v. 69, p. 163–178, doi: 10.1016/j.jsg.2014.10.007.

Harp, E. L., Keefer, D. K., Sato, H. P. and Yagi, H. 2011, Landslide inventories: the essential part of seismic landslide hazard analyses. Engineering Geology, 122(1-2), 9-21.

Mountrakis, D., 2010, Geology and Geo-tectonic Evolution of Greece, pp 132-143.



## Landslide Change Detection Based on Multi-Temporal Digital Elevation Models of Ropoto, Central Greece

Athanasia Vassou<sup>1</sup>, Vassilis Marinos<sup>1</sup>, Efstratios Karantanellis<sup>1</sup>, S. Valkaniotis<sup>3</sup>, George Papathanassiou<sup>2</sup>

<sup>1</sup> *Laboratory of Engineering Geology & Hydrogeology, Faculty of Geology, Aristotle University of Thessaloniki, Greece, [vassouna@gmail.com](mailto:vassouna@gmail.com)*

<sup>2</sup> *Department of Civil Engineering, Democritus University of Thrace, Greece*

<sup>3</sup> *Koronidos str, Trikala, Greece*

Landslides are one of the most destructive environmental hazards that can induce severe damages to manmade environment and generate considerable economic losses. The analysis of the landslide evolution based on multi-temporal studies can provide useful information in order to mitigate the risk and increase the resilience of the community. In order to achieve this collection of the appropriate geospatial data should be initially taken place. Considering the time-consuming field investigation combined with limited access, new methodologies and various remote sensing methods have been developed in order to provide useful topographic data. The present study focuses on the case history of a large landslide about 750 m long and 280 m wide) developed in 2012 in the Ropoto village area (Southwest Trikala, Greece), inducing severe structural damages to a large part of the community.

The area of interest consists of flysch formations that present a high heterogeneity (siltstones, conglomerates, sandstones, limestones, shales, marls) (GSI 35-40, Type VIII), transition beds consisted of thick-bedded limestones with sandstone and shale (GSI 35-40) and the thin-bedded limestone formation (GSI 30-35, Type F). The tectonic evolutions in the Ropoto area affects all the formations in particular the more clastic and ductile ones by developing intense folding, dense joint pattern, folds and thrust faults. Due to this tectonic disturbance, shear and fault zones have been developed in the site-specific area. Very permeable areas, can be locally encountered after the brittle limestone formations and their scree material where they can feed with water the impermeable flysch formations. Hence very high pore water pressure can be induced. As a consequence, in 2012 following 12 hours of heavy rainfall, the main landslide occurred in the heavily folded and weathered flysch and its transition beds deposits, resulting to the destruction of a large part of the main village infrastructure. In order to assess the landslide evolution within this area field investigation is needed for the identification of surface deformation due to landslides and usually include field mapping to identify geomorphological conditions.

Except the visual interpretation of the landslide detailed high-resolution imagery data recently acquired by Unmanned Aerial Vehicle (UAV), and relevant data provided by Greek Cadaster of 5m pixel were analyzed. UAVs are small aerial sensors that can be used to map landslides efficiently and at a high ground resolution based on 3D point cloud. Nowadays using UAV-oriented survey for assessing landslide risk in increasingly growing due to the fact that offers a secure way to investigate large-scale and difficult-to-access areas. Nevertheless, an engineering geological field survey is mandatory for collecting core data from the area and validate the outcome from the UAV-survey.

The aim of this analysis is to detect possible topographical changes in this large landslide area by using multi-temporal data. More specifically, digital elevation models (DEM) were developed showing the relevant surface on 2018 and 2007 based on the data provided by the UAV survey and the Greek Cadaster, respectively. Afterwards, a change detection approach was applied by comparing these multi-temporal digital elevation

models. As a result, a DEM of difference that quantifies volumetric change between these multi-temporal photogrammetric product was developed showing areas with gain of loss material (Figure 1).

Concluding, the Ropoto landslide is an active landslide that demonstrates progressive movements over the years. As an outcome of this study, it is proposed to continuously monitor the landslide in order to i) delineate the likely to landsliding zone, ii) determine the extent, magnitude and style of active landslide movement, iii) provide support for the design of possible mitigation measures in order to minimize the risk and iv) establish a near real-time prognosticate tool of future activation of mass movement.

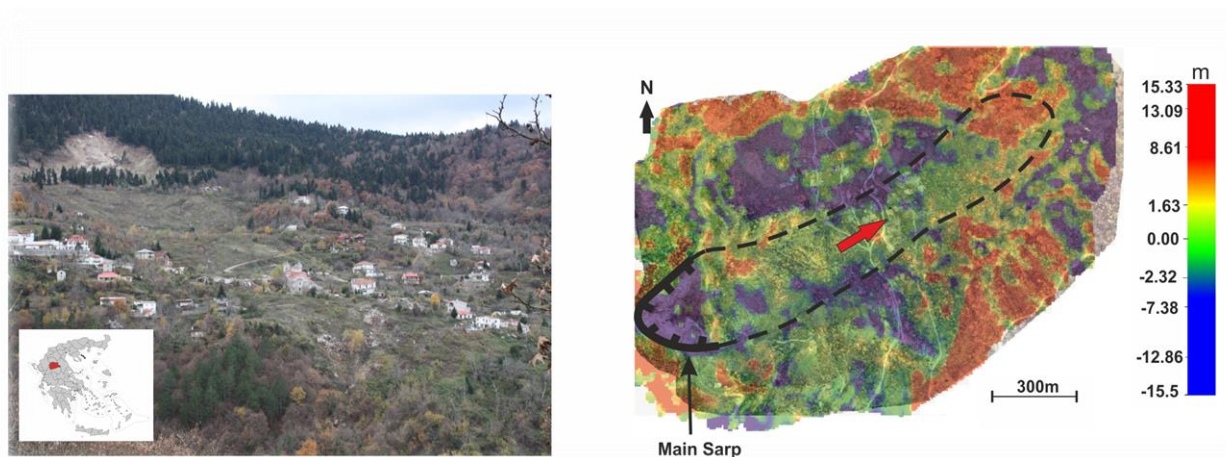


**Figure 1: a) Aspect of the landslide-Hillshade, b) DEM of Difference of Ropoto**

**REFERENCES**

Mountrakis, D.M., 2010. Geology and geotechnical evolution of Greece, 1st edition. University Studio Press, Thessaloniki

Williams, R.D. 2012. Section 2.3.2: DEMs of Difference. In: Cook, S.J., Clarke, L.E. & Nield, J.M. (Eds.) Geomorphological Techniques (Online Edition). British Society for Geomorphology; London, UK. ISSN: 2047-0371

Niethammer, U., Rothmund, S., James, M.R., Travelletti, J. and Joswing, M. 2010, UAV-Based Remote Sensing of Landslides. International Archives of Photogrammetry, Remote Sensing and Spatial Information Sciences, Vol. XXXVIII, Commission V Symposium, Newcastle upon Tyne, UK.

Jaukovic, I.C and Hunter, A.J., 2016. Unmanned Aerial Vehicle: A new tool for landslide risk assessment. Proceedings of the 11th ANZ Young Geotechnical Professionals Conference – 11YGPC Queenstown, New Zealand.

## Integrating 3D point clouds and machine learning for intelligent rock slope environments development

Ioannis Farmakis<sup>1</sup>, David Bonneau<sup>1</sup>, D. Jean Hutchinson<sup>1</sup>, Nicholas Vlachopoulos<sup>1</sup>

<sup>1</sup>*Dept. of Geological Science and Geological Engineering, Queen's University, Canada,*

[farmakisig@gmail.com](mailto:farmakisig@gmail.com)

Close-range 3D imaging technologies have become increasingly popular for visualization and monitoring within the field of engineering geology. Great advances in the utilization of 3D point clouds have occurred over the last fifteen years. These advances have predominantly focused on survey planning and optimization, pre-processing, and change detection among periodically acquired datasets providing very-high-resolution spatial information of rock slopes. Such information includes: the exact change positioning (Abellán et al. 2009; Kromer et al. 2015), change volume and shape (Bonneau et al. 2019), and motion kinematics (Oppikofer et al. 2009). These derivatives have proven useful for enriching landslide inventory building pipelines. In addition, a significant amount of the workflow from data acquisition to change detection has been automated. Another useful yet very time-consuming application includes the manual annotation of 3D scenes based on specific subjects of research. The assignment of semantic meaning to virtual natural scenes by means of ontologies such as the different geomaterials (rock, debris, soil, vegetation, etc.), landslide elements (i.e. scarp, deposition zone, toe, overhanging blocks, etc.), and other geomorphological features such as rock outcrops and debris channels is critical for an enhanced landslide susceptibility/hazard/risk assessment and management.

Automation in point cloud data processing is core in knowledge extraction within decision-making systems. 3D point cloud data describe the physical world spatially. Knowledge extraction procedures such as semantic segmentation and classification permit assignment of semantics to spatial information with specific analytic or domain knowledge. To keep a record of and use ontologies within landslide risk management analysis frameworks, the point cloud needs to be structured retaining spatial and relation information. It is also important to note that in point cloud classification, the appropriateness of descriptors should value quality over quantity (Weinmann et al. 2015). This highlights the need to prioritize and select the appropriate descriptors to address the great heterogeneity and shape irregularities observed in rock slopes.

In this study, we propose a supervoxel-based point cloud analysis framework that better defines point clusters and strongly supports both supervised and unsupervised classifications (Farmakis et al. 2020). The point cloud is characterized by means of geometric and topographic descriptors and represented at multiple hierarchical levels providing different scale organizations at the same time with interrelationships among the levels. Thus, every object within this semantic network knows its shape, size, and neighbors. One or more levels can be considered for analysis depending on the classes of interest and whether they are expected to appear at the same or different scales. The subsequent classification is performed based on expert-based knowledge expressed by geometric, topographic, spatial, and contextual rules. The methodology is presented step by step (Figure 1) and features such as debris channels, rock outcrops, and manmade structures are identified accurately, demonstrating success in first steps in development of intelligent geo-environments and deep automation.

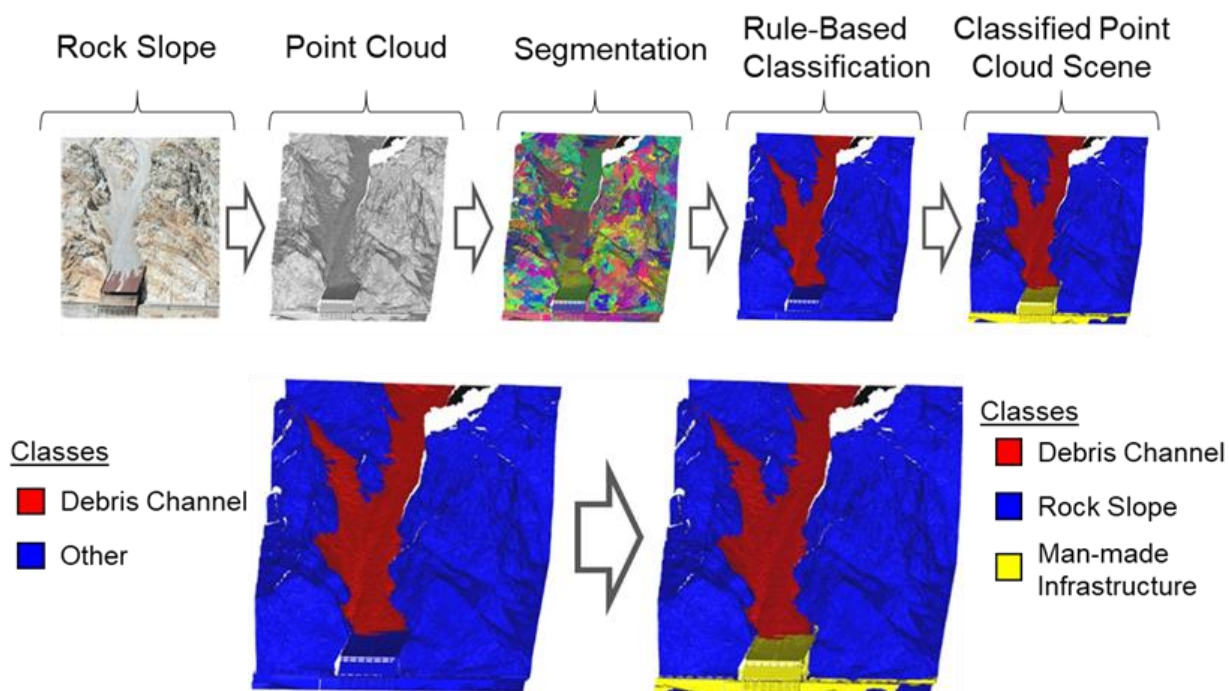


**Figure 1. Supervoxel-based point cloud semantic segmentation and classification for intelligent rock slope environments and cognitive decision systems**

## REFERENCES

- Abellán, A., Jaboyedoff, M., Oppikofer, T., and Vilaplana, J.M. 2009. Detection of millimetric deformation using a terrestrial laser scanner: Experiment and application to a rockfall event. *Natural Hazards and Earth System Science*, 9(2): 365–372. doi:10.5194/nhess-9-365-2009.
- Bonneau, D.A., Jean Hutchinson, D., DiFrancesco, P.M., Coombs, M., and Sala, Z. 2019. Three-dimensional rockfall shape back analysis: Methods and implications. *Natural Hazards and Earth System Sciences*, 19(12): 2745–2765. doi:10.5194/nhess-19-2745-2019.
- Farmakis, I., Bonneau, D., Hutchinson, D.J., and Vlachopoulos, N. 2020. Supervoxel-Based Multi-Scale Point Cloud Segmentation Using FNEA for Object-Oriented Rock Slope Classification Using TLS. *International Archives of the Photogrammetry, Remote Sensing and Spatial Information Sciences - ISPRS Archives*.
- Kromer, R.A., Hutchinson, D.J., Lato, M.J., Gauthier, D., and Edwards, T. 2015. Identifying rock slope failure precursors using LiDAR for transportation corridor hazard management. *Engineering Geology*, 195: 93–103. Elsevier B.V. doi:10.1016/j.enggeo.2015.05.012.
- Oppikofer, T., Jaboyedoff, M., Blikra, L., Derron, M.H., and Metzger, R. 2009. Characterization and monitoring of the Åknes rockslide using terrestrial laser scanning. *Natural Hazards and Earth System Science*, 9(3): 1003–1019. doi:10.5194/nhess-9-1003-2009.

## Automated 3D rock discontinuity surface mapping and characterization: Not a plane segmentation problem

Ioannis Farmakis<sup>1</sup>, Efstratios Karantanellis<sup>2</sup>, Nicholas Vlachopoulos<sup>1</sup>, Vassilis Marinov<sup>2</sup>

<sup>1</sup>*Dept. of Geological Sciences and Geological Engineering, Queen's University, Canada,*  
[farmakisig@gmail.com](mailto:farmakisig@gmail.com) - [vlachopoulos-n@rmc.ca](mailto:vlachopoulos-n@rmc.ca)

<sup>2</sup>*Dept. of Geology, Aristotle University of Thessaloniki, Greece, skarantanellis@gmail.com -*  
[marinosv@geo.auth.gr](mailto:marinosv@geo.auth.gr)

Discontinuity surface mapping and characterization is a crucial component of the preliminary slope stability assessment for efficient designing and operation of geotechnical site investigation phase in any structure-controlled environment. Discontinuity properties such as orientation, spacing, persistence, and roughness are directly related to the rock slope kinematics and factor of safety. Statistical analyses of a number of measurements taken along a rock slope are typically required for the definition of the representative input parameters in subsequent numerical modeling (Farmakis et al. 2020). Conventional methods are including manual collection of adequate and representative discontinuity measurements from excessive field mapping using compass, meter-scale, and profilometer. The latter application usually refers to extremely steep and harsh regions where human accessibility is limited.

Last years, the integration of close-range remote sensing techniques in engineering geological applications has been democratized. 3D point clouds have been proven significantly favorable to the acquisition of accurate and precise discontinuity measurements. Several methodologies regarding slope stability analysis have integrated manual discontinuity measurements using point clouds in the past. Although such methodologies resolve the inaccessibility issue, manual segmentation of vast point clouds is still a largely time-consuming process. However, various researchers proposed methodologies towards a more automated discontinuity surface extraction framework. Four different types of approaches have been considered. The three of them belong in the plane segmentation algorithms category and use either planarity-based region growing, Hough transform or model fitting algorithms (Dewez et al. 2016). The fourth type of approaches includes a clustering process of each point based on principal orientations defined by stereoplots consisted of poles corresponding to almost each point within the dataset (Riquelme et al. 2014; Liu et al. 2019). It is therefore systematically observed that such a stereoplot-based rock discontinuity segmentation leads to both large oversampling and noise due to the variation in surfaces size and shape irregularities, respectively. On the other hand, treating the rock discontinuity segmentation as a plane segmentation problem seems to be a quite optimistic assumption. As a result, segmentation routines following such a methodology are often observed to result in over- or under-sampled surfaces and not be able to take into account the heterogeneity in size and shape. Such an assumption may lead to stereoplot diagrams dominated by the orientation corresponding to the larger surfaces and systematically bias the final export (Farmakis and Hutchinson 2019).

In this study, an object-based rock discontinuity identification approach is proposed aiming to extract reliable rock discontinuity measurements by examining the local orientation heterogeneity in a supervoxel mode. The orientation of each voxel is expressed by means of dip and dip direction and homogenous areas are being merged until the required Degree of Homogenization (DoH) is achieved. In the current method the user should define two parameters: the resolution of the information that aims to perform the analysis at (voxel size) and the degree of homogenization (Farmakis et al. 2020). This comprises an advantage of the current method compared to the above-mentioned techniques where tuning a higher number of parameters is required. The



performance of the method is presented in different rock slopes and compared to existing available discontinuity extraction techniques by means of visualization (Figure 1) and produced stereonet diagrams.

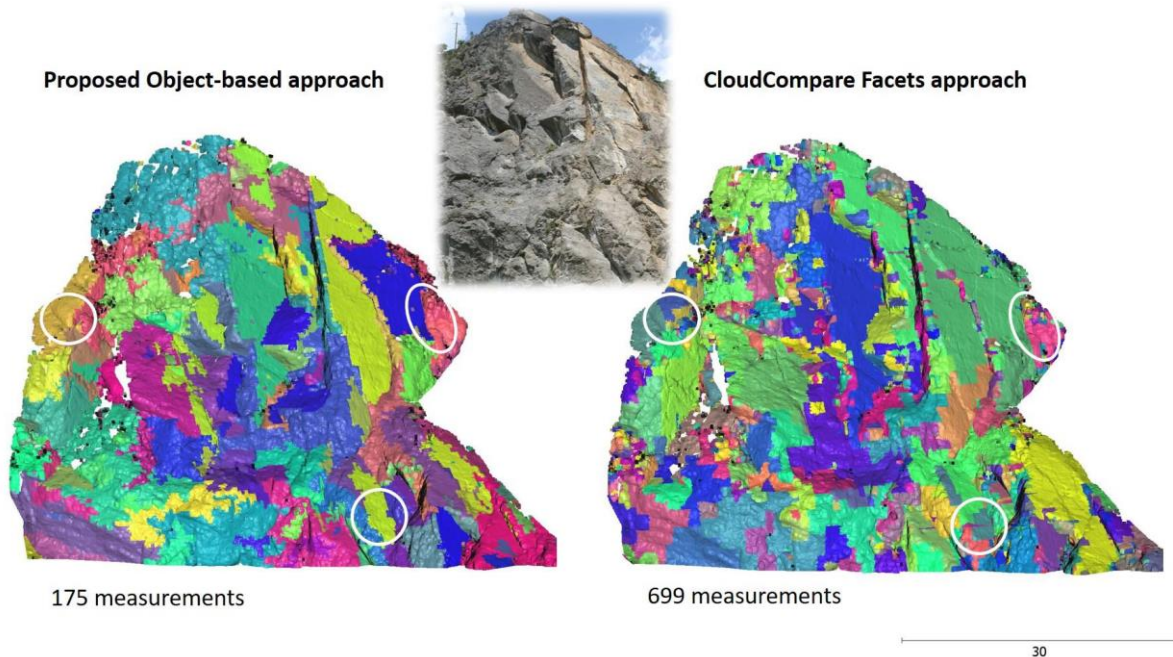


**Figure 1. Application highlighting the relative oversampling occurred by implementing the widely recognized Facets tool in CloudCompare software against the proposed object-based approach.**

## REFERENCES

- Dewez, T.J.B., Girardeau-Montaut, D., Allanic, C., and Rohmer, J., 2016, Facets : A cloudcompare plugin to extract geological planes from unstructured 3d point clouds. *International Archives of the Photogrammetry, Remote Sensing and Spatial Information Sciences - ISPRS Archives*, 41(July): 799–804. doi:10.5194/isprsarchives-XLI-B5-799-2016.
- Farmakis, I., Bonneau, D., Hutchinson, D.J., and Vlachopoulos, N., 2020a, Supervoxel-Based Multi-Scale Point Cloud Segmentation Using FNEA for Object-Oriented Rock Slope Classification Using TLS. *International Archives of the Photogrammetry, Remote Sensing and Spatial Information Sciences - ISPRS Archives* (in press).
- Farmakis, I., and Hutchinson, D.J., 2019, Semi-automated discontinuity orientation extraction in complex rock masses using single-scan LiDAR data . *EGU General Assembly 2019*, 21: 10853.
- Farmakis, I., Marinos, V., Papathanassiou, G., and Karantanellis, E., 2020b, Automated 3D Jointed Rock Mass Structural Analysis and Characterization Using LiDAR Terrestrial Laser Scanner for Rockfall Susceptibility Assessment: Perissa Area Case (Santorini). *Geotechnical and Geological Engineering*, 0123456789. Springer International Publishing. doi:10.1007/s10706-020-01203-x.
- Liu, L., Xiao, J., and Wang, Y., 2019, Major Orientation Estimation-Based Rock Surface Extraction for 3D Rock-Mass Point Clouds. *Remote Sensing*, 11(6): 635. doi:10.3390/rs11060635.
- Riquelme, A.J., Abellán, A., Tomás, R., and Jaboyedoff, M., 2014, A new approach for semi-automatic rock mass joints recognition from 3D point clouds. *Computers and Geosciences*, 68: 38–52. Elsevier. doi:10.1016/j.cageo.2014.03.014.

## Rockmass characterization and evaluation of rock fall potential based on traditional and SfM-based methods

George Papathanassiou<sup>1</sup>, Adrian Riquelme<sup>2</sup>, Theofilos Tzevelekis<sup>3</sup>, Evaggelos Evaggelou<sup>4</sup>

<sup>1</sup>Assistant Professor, Democritus University of Thrace, Xanthi, Greece, [gpapatha@civil.duth.gr](mailto:gpapatha@civil.duth.gr)

<sup>2</sup>Department of Civil Engineering, University of Alicante, Alicante, Spain, [ariquelme@ua.es](mailto:ariquelme@ua.es)

<sup>3</sup>Technical staff, Democritus University of Thrace, Xanthi, Greece, [tztzebel@civil.duth.gr](mailto:tztzebel@civil.duth.gr)

<sup>4</sup>Laboratory staff, Democritus University of Thrace, Xanthi, Greece, [eevange@civil.duth.gr](mailto:eevange@civil.duth.gr)

This study aims to characterise discontinuity sets of rock masses using conventional methods and by applying recently developed SfM-based methodologies on a rock slope located at the area of Nestos, Greece. In particular, the latter ones are focused on the development of a 3D model of the investigated area and the extraction of information regarding the orientation and spacing of discontinuities based on semi-automated and manually procedures.

### **Methodology**

Initially, traditional field survey methods have been applied at the lower part of the rock face (site 1 on Figure 1) aiming to define the geometrical characteristics of the joints and classified the rock mass based on the RMR system. It is pointed out that this area is affected by the blasting techniques applied during the construction of the rail network. For the same area, this information was additionally extracted based on open source software, i.e. Discontinuity Set Extractor (DSE) (Riquelme et al. 2014) and CloudCompare™. The DSE-based approach aids the discontinuity sets identification and gathers points in planar clusters. Once planes are identified and located on a slope face, then the normal spacing can be automatically estimated. On the other hand, the procedure required by CloudCompare™ for extracting the orientation of joints is totally subjective and can be influenced by the quality of the generated point cloud and the experience of the researcher. Furthermore, as an outcome of this study, it can be stated that at heavily fragmented areas the CloudCompare™ approach is considered as inappropriate due to the small size facets, while DSE approach is considered as more reliable.

At the second area (site 2 on Figure 1), this study shows that both DSE and CloudCompare™ extracted similar information regarding the orientation of discontinuity sets. This could be because this area is a zone free of human activities area and consequently not as much fragmented as the one at the lower part of the slope. Thus, the CloudCompare™-based identification of the joints and the extraction of the orientation could be more accurately extracted. Concerning the DSE approach, this study shows that that the semi-automatically procedure successfully define the clusters of the discontinuity sets, providing a useful 3D view of the possible failure mechanisms.

Finally, the most important advantage of a developed 3D model of a slope face is that can provide the opportunity to researchers to locate and estimate the volume of potentially unstable blocks. This procedure can be performed using the relevant tool on CloudCompare™ while the accuracy of the obtained block dimensions strongly depends on the quality of the point cloud.

### **Conclusions**

As a summary, this study shows that on heavily fragmented rock mass, the CloudCompare™ approach could not be considered as appropriate and is not recommended for the identification of joints' orientation. At these zones, it is required to initially perform a detailed field survey that can be used as core data and afterwards

conduct a point-cloud based structural analysis in order to define the discontinuity sets (DS) extracted by the DSE and to estimate the joint spacing. At the zones where the main DS can clearly be defined, CloudCompare™ can be additionally used for validating the orientation of joints. However, comparing to DSE, the extraction of this information is considered as time consuming. Thus, at this type of rock mass where conventional methods cannot be applied due to steep morphology, DSE is considered as a reliable tool.

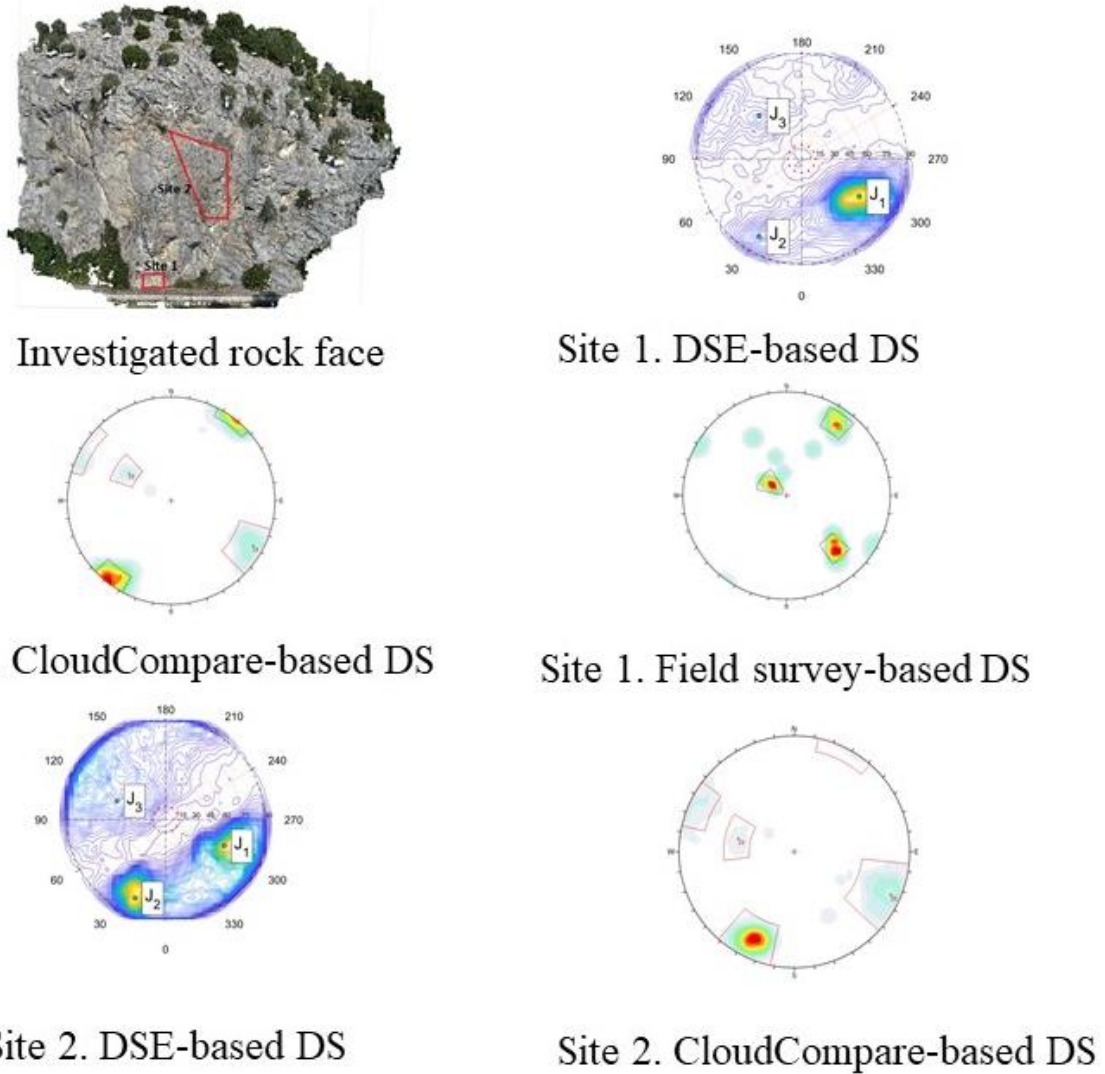


**Figure 1. Slope face and stereonet of the density of the normal vector's poles and its corresponding planes developed based on data provided by field survey, DSE and CloudCompare™**

**REFERENCES**

Riquelme, A. J., Abellán, A., Tomás, R., and Jaboyedoff, M., 2014, A new approach for semi-automatic rock mass joints recognition from 3D point clouds. Computers & Geosciences, 68, pp. 38-52

## Results of comprehensive monitoring activities on Umka landslide, Belgrade, Serbia

Biljana Abolmasov<sup>1</sup>, Uroš Đurić<sup>2</sup>

<sup>1</sup>University of Belgrade, Faculty of Mining and Geology, Serbia, [biljana.abolmasov@rgf.bg.ac.rs](mailto:biljana.abolmasov@rgf.bg.ac.rs)

<sup>2</sup>University of Belgrade, Faculty of Civil Engineering, Serbia, [udjuric@grf.bg.ac.rs](mailto:udjuric@grf.bg.ac.rs)

### **Background**

The Umka landslide is the deepest and biggest active landslide in the Republic of Serbia and has been investigated and monitored by different geotechnical techniques for decades. This paper will be focused on results and experience gained from automated Global Navigation Satellite System (GNSS) monitoring network data, PSInSAR data analysis from Sentinel1 radar satellite images, conventional geodetic monitoring network data and UAV imaging, processing and data analysis in the last six years.

### **Study area**

The Umka landslide is formed on the right Sava river bank, 22 km southwest from Belgrade, and occupies part of Belgrade suburban settlement Umka. Geometry, geological settings, mechanism and material properties of Umka landslide were well defined by previous geotechnical investigations (Ćorić et al. 2016; Abolmasov et al. 2012). This landslide is fan-shaped, with the length along the slope of 900 m, 1650 m wide in the toe, reaching maximum depth of sliding surface at 26 m, and average slope gradient of 9°. Previous geotechnical research has shown that Umka landslide can be described as complex landslide within the stiff fissured Miocene (M<sub>3</sub><sup>2</sup>) clayey marls. Landslide is active, with various phases of deceleration and acceleration, which are mostly in correlation with the Sava river level rise/drawdown, respectively, whereas landslide velocity is characterized as slow to very slow (Abolmasov et al. 2015).

### **Methods**

In the past decades many authors integrated monitoring data from different sources to reduce uncertainties. Monitoring activities are composed of several techniques introduced for landslide monitoring: automated GNSS monitoring network, geodetic benchmark survey monitoring, UAV imaging with photogrammetric processing and analysis, and PSInSAR data processing and analysis. Common to all implemented monitoring techniques is to measure displacement of the observed points ( $dx$ ,  $dy$ ,  $dz$ ) on the landslide surface. Results of all monitoring activities were analyzed according to the longest common survey period and then used for cross-correlation and for verification of monitoring results obtained using different techniques.

### **Results**

Displacement rates from GNSS indicate that object point Umka GNSS has moved 0.30 m towards the North and 0.50 m towards the West, while the vertical displacement was approximately -0.15 m for the 2014-2018 time span. Similar range of GNSS displacement rates were found in previously published results from GNSS monitoring activities realized from 2010-2014 (Abolmasov et al. 2015). PSInSAR data analysis showed very good correlation between nearest PS points and GNSS point for the same period of monitoring (2016-2018). Results from geodetic survey benchmarks (conventional monitoring) showed displacement rates in accordance to average displacement rates of GNSS object point. Results from UAV and geodetic benchmarks survey data analysis showed also very good correlation in vectors azimuth (for the period 2018-2019) (Figure 1).



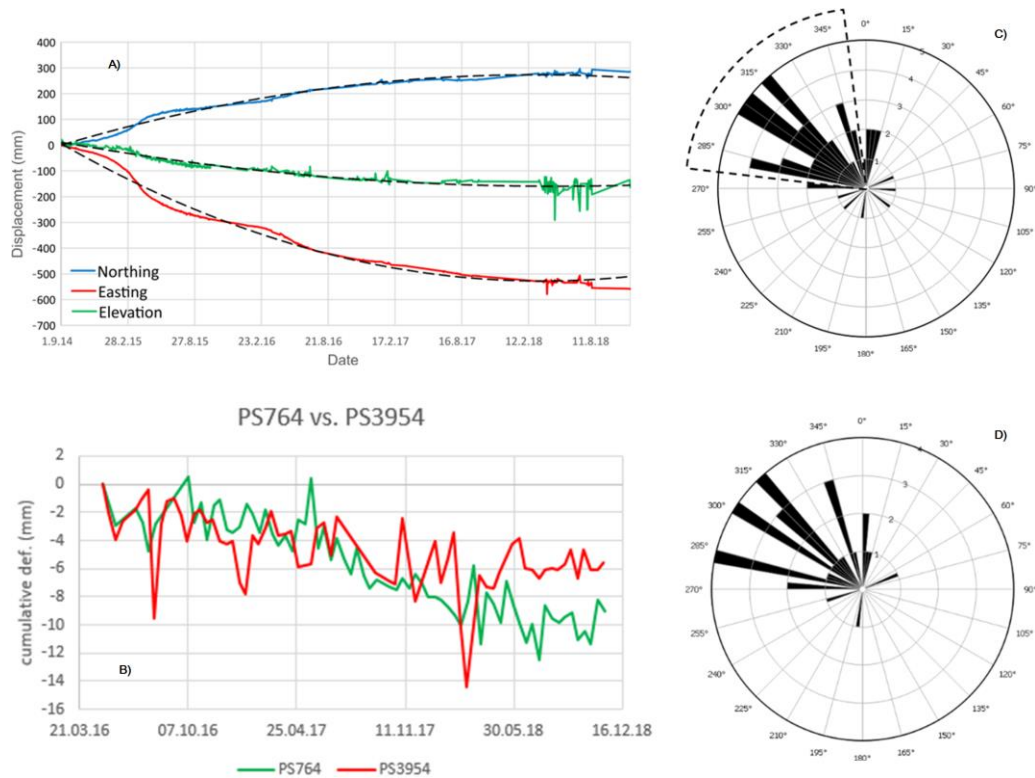


**Figure 1. A) GNSS monitoring data (2014-2018); B) PSInSAR monitoring data (2016-2019); Displacement vectors azimuth obtained from C) Geodetic benchmarks survey (2018-2019) and D) UAV imaging (2018-2019)**

## **Conclusion**

Comprehensive monitoring activities on the Umka landslide included several landslide monitoring techniques realized from 2014 to 2019. According to the analyzed data it could be concluded that all monitoring results are in compliance with previous published research and monitoring results, and confirm that the Umka is a slow to very slow moving landslide.

## **REFERENCES**

- Abolmasov B., Milenković S., Jelisavac B., Vujanić V., Pejić M. and Pejović M., 2012, Using GNSS sensors in real time monitoring of slow moving landslides-a case study. Proceedings of the 11th International and 2nd American Symposium on Landslides and Engineered Slopes, Banff, Canada, 3-8 June, 2012, Eds. Eberhardt E, Froese C, Turner K, Leroueil S, Taylor&Francis Group, London, Vol 2, pp. 1381-1385.
- Abolmasov B., Milenković, S., Marjanović M., Đurić U. and Jelisavac B., 2015, A geotechnical model of the Umka landslide with reference to landslides in weathered Neogene marls in Serbia. *Landslides* 12 (4): 689-702.
- Ćorić S., Božinović D., Vujanić V., Jotić M. and Jelisavac B., 1996, Geotechnical characteristics of old landslides in Belgrade area. In: Senneset K (ed) Proceedings of the 7th International Symposium on Landslides, 17–21 June 1996, Trondheim, Norway, Vol 2, Balkema, Rotterdam, pp 689–694



## New ground truth and space borne data for the verification of land subsidence occurring at the coastal zone of Athens, Greece

Agavni Kaitantzian<sup>1</sup>, Constantinos Loupasakis<sup>1</sup>, Ploutarchos Tzampoglou<sup>2</sup>, Issak Parcharidis<sup>3</sup>

<sup>1</sup>*School of Mining and Metallurgical Engineering, National Technical University of Athens,*

[ankait@metal.ntua.gr](mailto:ankait@metal.ntua.gr) , [cloupasakis@metal.ntua.gr](mailto:cloupasakis@metal.ntua.gr)

<sup>2</sup>*Department of Civil and Environmental Engineering, University of Cyprus,*

[tzampoglou.ploutarchos@ucy.ac.cy](mailto:tzampoglou.ploutarchos@ucy.ac.cy)

<sup>3</sup>*Department of Geography, Harokopio University of Athens, [parchar@hua.gr](mailto:parchar@hua.gr)*

Land subsidence phenomenon due to the overexploitation of the aquifers occurring in the coastal zone of the municipalities N.Faliro, Moschato and Kallithea, has been recorded since the mid 1960's. This phenomenon has been identified as one the most severe geological hazards affecting large plane areas, subject to rapid urban and industrial growth. Some examples include Italy (Stramondo et.al., 2008), USA (Galloway et.al., 1998) and China (Yang et.al., 2015). In Greece, this phenomenon has been observed in areas such as the Kalochori region (Svigkas et.al, 2016), the Thessaly plain (Iliia, et.al.2018), the Amyntaio basin (Tzampoglou & Loupasakis, 2017). SVD (Singular Value Decomposition) and IPTA (Interferometric Point Target Analysis) techniques are applied for the detection of surface deformation. The results of these DInSAR techniques are combined with geological, geotechnical and hydrogeological conditions of the study area in order to an interpretation of the land subsidence hazard mechanism.

The maximum displacement rates for the period 2002 - 2010 of ENVISAT data can be identified at the area extending between the riverbeds of Kiffisos and Ilissos River, at the south of the Tavros industrial zone. The SVD interferometric technique indicates LOS deformation rates, ranging between -1.5 and -3mm/yr, whereas the IPTA indicated higher deformation rates of -3 to -5mm/yr, along the LOS (Figure 1a & b).

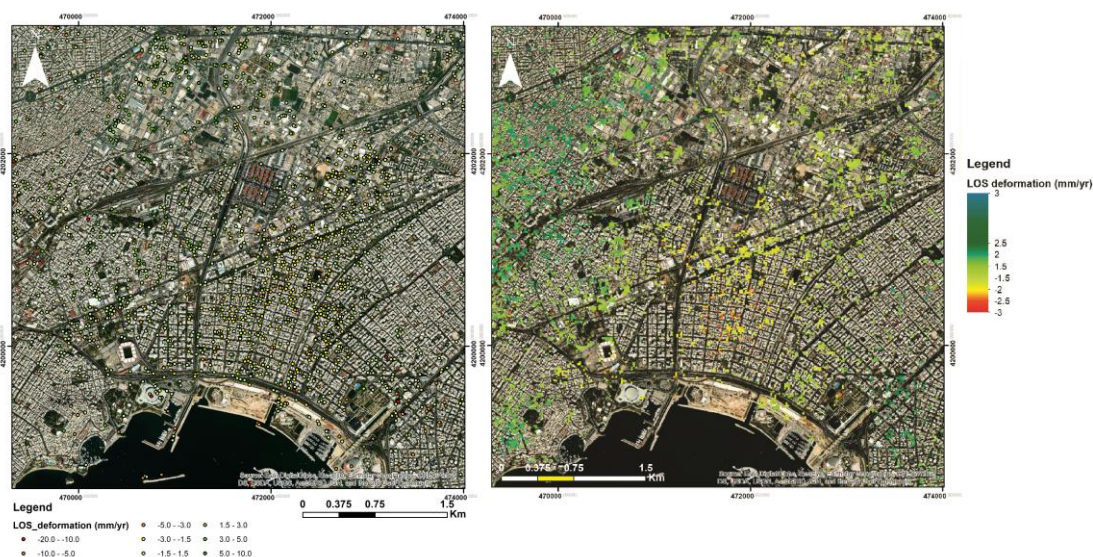


**Figure 1. LOS deformation rates from 2002 to 2010 as derived by the a) IPTA technique and b) SVD analysis**

The affected area is an area which is occupied by silty clay horizons of the coastal deposits with Compression Index (Cc) values between 0.2 and 0.8, indicating their high compressibility potential. Moreover, the oedometer tests revealed that the preconsolidation pressure values in some areas are slightly lower from the effective geostatic stresses, characterizing the coastal deposits as under-consolidated. Available records of piezometric

level measurements of July 1997 proved that the industrial activities have caused a depression cone extending from the Tavros industrial zone down to the coastline (Figure 2a). On the contrary, the isopiezometric contour lines based on the May 2015 measurement campaign indicated that the aquifers have recovered throughout the entire study area (Figure 2b). The aforementioned recovery is connected with the economic crisis that has led most of the industries of the Tavros industrial area to shut down, reducing the water consumption.

Finally, the holistic evaluation of the data proved that the occurring land subsidence phenomenon can be attributed to the over pumping of the aquifers for industrial purposes, without excluding the occurrence of some displacements due to the natural compaction of the slightly unconsolidated formations.

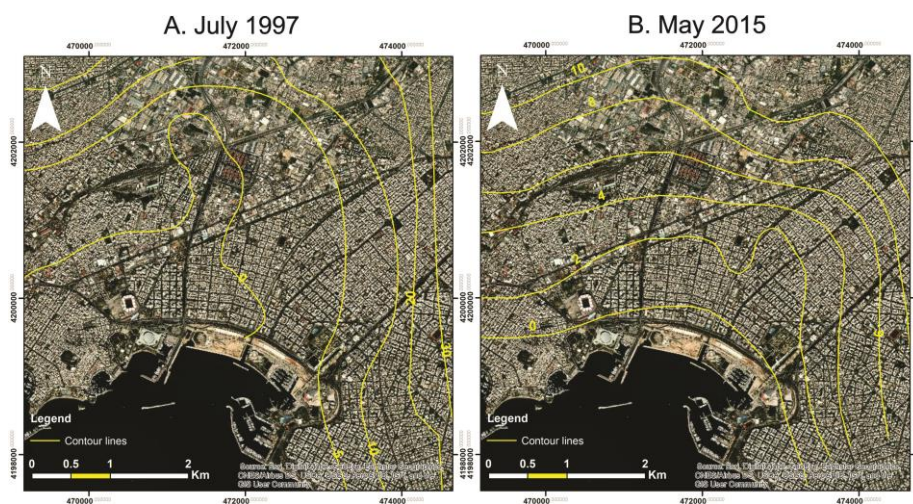


Figure 2. a) Piezometric contour lines of July 1997, b) Piezometric contour lines of May 2015

## REFERENCES

- Stramondo, S., Bozzano, F., Marra, F., Wegmuller, U., Cinti, F.R., Moro, M., and Saroli, M., 2008, Subsidence induced by urbanization in the city of Rome detected by advanced InSAR technique and geotechnical investigations. *Remote Sens. Environ.*, v. 112(6), pp. 3160–3172.
- Galloway, D.L., Hudnut, K.W., Ingebritsen, S.E., Phillips, S.P., Peltzer, G., Rogez, F., and Rosen P.A., 1998, Detection of aquifer system compaction and land subsidence using interferometric synthetic aperture radar, Antelope Valley, Mojave Desert, California. *Water Resour. Res.*, v. 34(10), pp. 2573–2585.
- Yang, H.L., Peng, J.H., Wang, B.C., Song, Y.Z., Zhang, D.X., and Li, L., 2015, Ground deformation monitoring of Zhengzhou city from 2012 to 2013 using an improved IPTA. *Nat. Hazards*, <http://doi:10.1007/s11069-0151953-x>.
- Svigkas, N., Papoutsis, I., Loupasakis, C., Tsangaratos, P., Kiratzi, A., and Kontoes, C., 2016, Land subsidence rebound detected via multi-temporal InSAR and ground truth data in Kalochoi and Sindos regions, Northern Greece. *Eng. Geol.*, v. 209, pp. 175–186.
- Iliá, I., Loupasakis, C., and Tsangaratos, P., 2018, Land subsidence phenomena investigated by spatiotemporal analysis of groundwater resources, remote sensing techniques, and random forest method: the case of Western Thessaly, Greece. *Environ Monit. Assess*, v. 190, pp. 623–642.
- Tzampoglou, P., and Loupasakis, C., 2017, Evaluating geological and geotechnical data for the study of land subsidence phenomena at the perimeter of the Amyntaio coalmine, Greece. *Int. J. of Mining Sci. Technology*, <https://doi.org/10.1016/j.ijmst.2017.11.002>.



## Rock strength of a rock cliff evaluated through infrared thermography

Marco Loche<sup>1\*</sup>, Gianvito Scaringi<sup>1</sup>, Jan Blahůt<sup>2</sup>, Maria Teresa Melis<sup>3</sup>, Antonio Funedda<sup>3</sup>, Stefania Da Pelo<sup>3</sup>, Ivan Erbi<sup>3</sup>, Giacomo Deiana<sup>3</sup>, Mattia Alessio Meloni<sup>3</sup>, Fabrizio Cocco<sup>3</sup>

<sup>1</sup>*Institute of Hydrogeology, Engineering Geology and Applied Geophysics, Faculty of Science, Charles University, Prague, Czech Republic*

<sup>2</sup>*Institute of Rock Structure and Mechanics, Czech Academy of Sciences, Prague, Czech Republic*

<sup>3</sup>*Department of Chemical and Geological Sciences, University of Cagliari, Monserrato (CA), Italy*

[marco.loche@natur.cuni.cz](mailto:marco.loche@natur.cuni.cz)

Rock strength is a fundamental characteristic of the mechanical behaviour of rock masses that can be used to empirically estimate a number of properties and predict the likelihood of instability phenomena (Bieniawski, 1989). The direct acquisition of mechanical information in the field is often hindered by the inaccessibility of the rock cliffs, particularly in coastal environments. For this reason, remote sensing approaches have become the object of extensive research. In particular, InfraRed Thermography (IRT) has been proven to be useful for the mechanical characterisation of geomaterials, including slope stability analysis (Melis et al., 2020).

We proposed a procedure for the evaluation of the rock strength through IRT by studying the cooling behaviour of rock blocks during a 24-hour period (Loche et al., 2021). We performed a detailed survey on naturally heated granitoids and phylonian rocks in a coastal cliff in SE Sardinia, Italy, characterised by different degrees of fracturing (Figure 1).

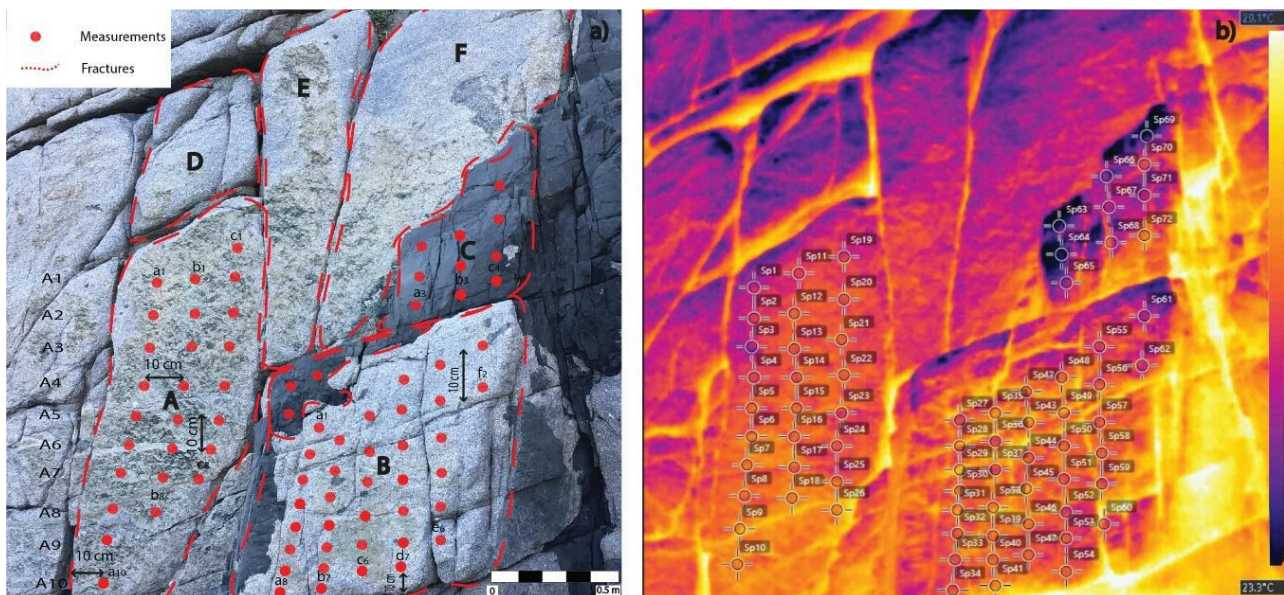


**Figure 1. (a) Acquisition scheme in the field where each point corresponds to 10 measurements; (b) in FLIR Tools software thermograms recorded at midnight where each point corresponds to a spot measurement (Loche et al., 2021).**

We showed that the cooling trend of the rock blocks can be related with rock strength values, and we define a cooling rate index (CRI) to obtain quantitative predictions through regression analysis (Pappalardo et al., 2016; Mineo and Pappalardo, 2016). The analysis pointed out a strong linear correlation between CRI, evaluated during the first five hours after the temperature peak (CRI5h), and the results of the Schmidt hammer test

(Figure 2). Different heating-cooling patterns were also observed in relation to the different lithology and structure of the rock blocks, and to the different size of the fractures (Loche et al., 2021).

IRT can be applied at various spatial scales: few repeated flights of a drone equipped with a thermal camera can be sufficient to characterise the strength of unreachable blocks after establishing an empirical correlation with a strength parameter. However, further validation is needed in different settings to explore multi-variate correlations applicable over larger areas and support the formulation of thermo-hydro-mechanical models of geomaterials.

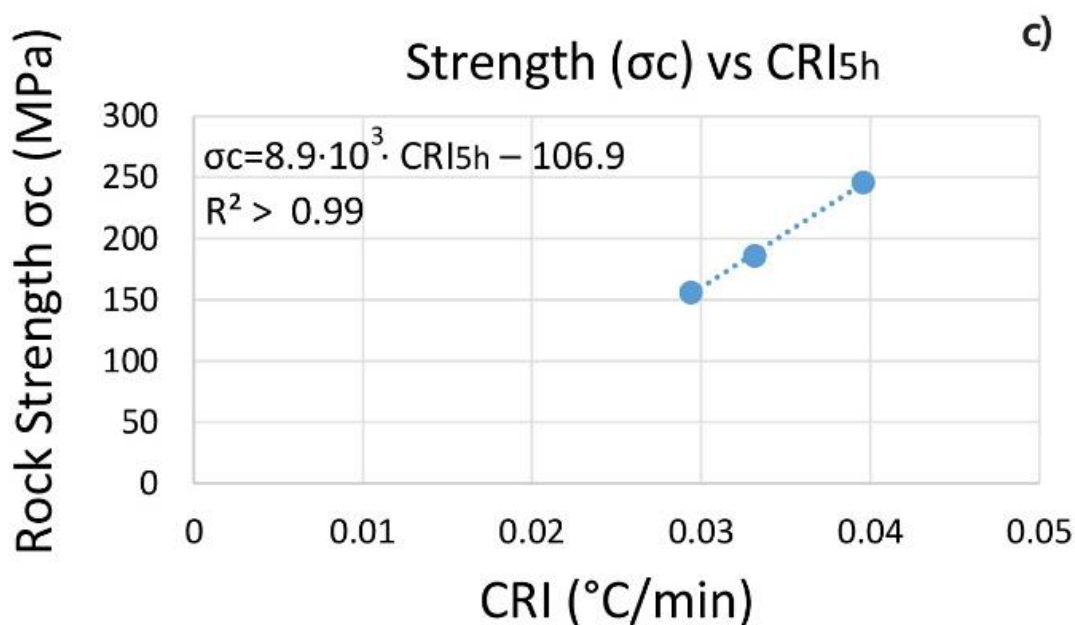


**Figure 2. Linear regression analysis between rock strength ( $\sigma_c$ ) and CRI5h. The three dots represent the different blocks A, B and C in Figure 1 (mod. from Loche et al., 2021).**

## REFERENCES

- Bieniawski, Z.T., 1989, Engineering Rock Mass Classifications: A Complete Manual for Engineers and Geologists in Mining, Civil, and Petroleum Engineering; Wiley: New York, ISBN 978-0-471-60172-2.
- Loche, M., Scaringi, G., Blahút, J., Melis, M.T.T., Funedda, A., Da Pelo, S.D., Erbi, I., Deiana, G., Meloni, M.A.A. and Cocco, F., 2021, An Infrared Thermography Approach to Evaluate the Strength of a Rock Cliff. *Remote Sensing*, 13(7), p.1265.
- Melis, M.T., Da Pelo, S., Erbi, I., Loche, M., Deiana, G., Demurtas, V., Meloni, M.A., Dessì, F., Funedda, A., Scaioni, M. and Scaringi, G., 2020, Thermal Remote Sensing from UAVs: A Review on Methods in Coastal Cliffs Prone to Landslides. *Remote Sensing*, 12(12), p.1971.
- Mineo, S. and Pappalardo, G., 2016, The Use of Infrared Thermography for Porosity Assessment of Intact Rock. *Rock Mech Rock Eng*, 49, 3027–3039.
- Pappalardo, G., Mineo, S., Zampelli, S.P., Cubito, A., Calcaterra, D., 2016, InfraRed Thermography Proposed for the Estimation of the Cooling Rate Index in the Remote Survey of Rock Masses. *Int J Rock Mech Min Sci*, 83, 182–196.

## Lithological discrimination using aster images in the coastal mountain chain of the Lampa sector, Santiago, Chile

Vidal V. Raúl<sup>1,5</sup>, Arriagada S. Hernán<sup>2,5</sup>, Péndola R. Daniel<sup>3,5</sup>, Arotaipe Q. Rosmery<sup>4,5</sup>.

<sup>1</sup>*Pontificia Universidad Católica del Perú, [ravidal@pucp.edu.pe](mailto:ravidal@pucp.edu.pe)*

<sup>2</sup>*Universidad de Concepción, [herarriagada@udec.cl](mailto:herarriagada@udec.cl)*

<sup>3</sup>*Universidad Central de Chile, [daniel.pendola@alumnos.uccentral.cl](mailto:daniel.pendola@alumnos.uccentral.cl)*

<sup>4</sup>*Universidad Nacional de San Agustín, [rarotaipeq@unsa.edu.pe](mailto:rarotaipeq@unsa.edu.pe)*

<sup>5</sup>*Consultora EGSCIENCES S.A. Chile.*

In the study area, units from the Cretaceous emerge, from the Berriasian to the Campanian (Charrier, 2007). The oldest rocks correspond to the Lo Prado formation that outcrops to the west of the study area, made up of oceanic volcanic-sedimentary sequences. It is consistently underlain by the andesites of the Veta Negra Formation, which is made up of the Purehue and Ocoe members respectively, ending with the continental volcano-sedimentary units of the Las Chilcas Formation (Wall et al., 1999). The Caleu-Alto de Lipangue multiplutonic complex, with a dioritic to monzogranitic composition, intrudes the Lo Prado, Veta Negra and the most basal units of Las Chilcas. The lithological units are forming a monocline in the Cordillera de la Costa, which was formed during a tectonic inversion event from rifting conditions (Lo Prado and Veta Negra) to compression (Las Chilcas), where the plutons of Caleu-Alto de Lipangue intruded at the turning point between both regimes and continued to cool during its exhumation caused by the formation of the mountain range (Parada et al., 2005; Boyce, 2015).

ASTER images were used from January 2001, they were processed with the ENVI 5.3 software, radiometric calibrations and atmospheric corrections were applied, the masking of shadows, clouds, urban areas and dense vegetation. With the corrected and masked ASTER images, ratios and combinations of bands more suitable for lithological discrimination of the units of the area are evaluated.

For the Veta Negra Formation, the 4, 6, 1 RGB combination of DiTomasso (2017) highlights it in greenish blue color and differentiates it from other units. The Las Chilcas Formation appears in cherry and orange color with the combination (2 + 4) / 3, (5 + 7) / 6, (7 + 9) / 8 RGB of Amer and others (2010). The Cordón Caleu Granitoids differ from the Veta Negra and Las Chilcas formations with the combinations 8/6, 8/7, 4/7 and 9/5, 1/3, 6/3 RGB respectively, both combinations of Gad and Raef (2012). The bluish hue of Veta Negra and the Caleu diorite facie show low absorption in bands 1 and 6 and almost zero in band 4 in rocks of andesitic composition that may be useful for their identification.

The geological map obtained has contacts that differ from previous publications. In the Lo Aguirre mine, the contact between Lo Prado and Veta Negra formations is located more to the W than is considered by the Tilttil-Santiago Sheet (Wall et al., 1999), this coincides with the proposals of Saric and Charrier that indicate that the roof of Lo Prado is actually part of the Purehue member of Veta Negra.

The Ocoe member outcrops in the entire eastern skirt of Cerro Macho Quemado in contrast to the outcrop of Las Chilcas to the north, in yellowish green, which is explained by the sintral displacement of the Bustamante fault (Saric, 2003) (Figure 1). In the map of Wall et al., (1999) to the southeast of Cerro Los Tres Morros there is an outcrop of the Las Chilcas formation with a dip of 22° that they explain with an abrupt thinning of the Ocoe member. A straight boundary between Veta Negra and Lo Prado to the east allowed the recognition of a dextral strike fault that explains the appearance of Las Chilcas in the area without affecting the thickness of Veta Negra (Figure 1).

To the southeast of the Cerro Blanco mine in Polpaico, according to Wall et al. (1999), the Caleu-Alto de Lipangue diorites emerge. However, the rocks in the area correspond to calcareous and volcanic facies corresponding to the upper part of Las Chilcas. With remote sensing, a clear difference is seen between this intrusive, in celestial color in RGB: 9 / 5.1 / 3.6 / 3 (Gad & Raef, 2012), and the supposedly equivalent dioritic units in the Cordillera de la Costa (in Pink color). In this study,



it is interpreted that the intrusive corresponds to a set of hypabyssal intrusives from the Oligocene, which intrude into the Lo Valle formation a short distance east of the study area (Figure 2).

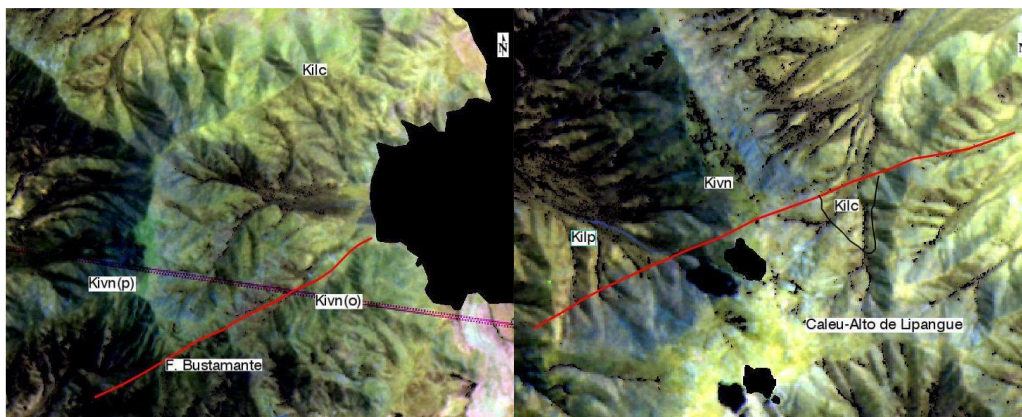


**Figure 1. RGB absorption image: 4,6,1 in the areas of the Macho Quemado and Bustamante hills (left) and the Los Tres Morros and Alto de Lipangue hills (right). Kilp = Lo Prado Formation, Kivn = Veta Negra Formation, Kivn (p) = Purehue Member, Kivn (o) = Ocoe Member, Kiloc = Las Chilcas Formation.**

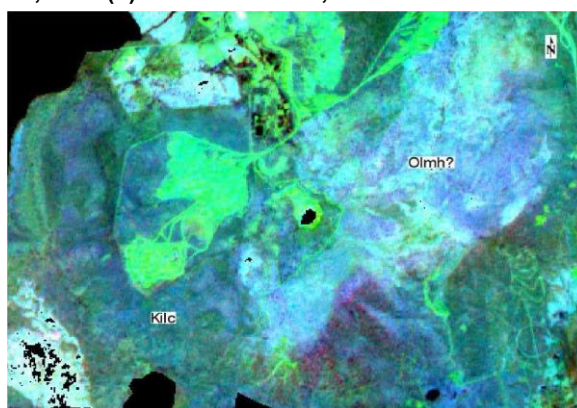


**Figure 2. Intrusive in Cerro Blanco de Polpaico in combination of RGB bands: 9 / 5,1 / 3,6 / 3 (Gad & Raef, 2012). Kiloc = Las Chilcas Formation, Olmh = Oligocene hypabyssal intrusives.**

**REFERENCES**

Amer, R., Kusky, T., and Ghulam, A., 2010, Lithological mapping in the Central Eastern Desert of Egypt using ASTER data. *Journal of African Earth Sciences*, 56 (2-3), 75-82.

Boyce Marto, D., 2015, Tectonic and palaeogeographic evolution model of the Andean margin in Central Chile during the mid-late Cretaceous: The structural and sedimentary record in the Las Chilcas formation (Master's thesis).

Charrier, R., Pinto, L., and Rodríguez, M.P. 2007, Tectonostratigraphic evolution of the Andean Orogen in Chile. In T. Moreno, & W. Gibbons *The Geology of Chile* (pp. 21–114). The Geological Society of London. doi: 10.1144 / goch.3

Di Tommaso, I., and Rubinstein, N., 2007, Hydrothermal alteration mapping using ASTER data in the Infiernillo porphyry deposit, Argentina. *Ore Geology Reviews*, 32 (1-2), 275-290.

Gad, S., and Raef, A. 2012, Factor analysis approach for composited ASTER band ratios and wavelet transform pixel-level image fusion: lithological mapping of the Neoproterozoic Wadi Kid area, Sinai, Egypt. *International journal of remote sensing*, 33 (5), 1488-1506.

Parada, MA, Féraud, G., Fuentes, F., Aguirre, L., Morata, D., and Larrondo, P., 2005, Ages and cooling history of the Early Cretaceous Caleu pluton: testimony of a switch from a rifted to a compressional continental margin in central Chile. *Journal of the Geological Society*, 162 (2), 273-287. Doi: 10.1144 / 0016-764903-173

Saric, N., Kreft, C., and Huete, C., 2003, Geology of the Lo Aguirre deposit, Chile. *Revista Geológica de Chile*, 30 (2), 317-331. doi: 10.4067 / S0716-02082003000200010

Wall, R., Sellés, D., and Gana, P. 1999, Tilttil-Santiago Area, Metropolitan Region. National Geology and Mining Service (Chile), Geological Maps, Santiago.



## **THEME 8 - ENGINEERING GEOLOGY AND CULTURAL HERITAGE PROTECTION**

## Structural analysis of Rock slopes, using UAV & LiDAR, in the Archaeological site of Delphi, Greece

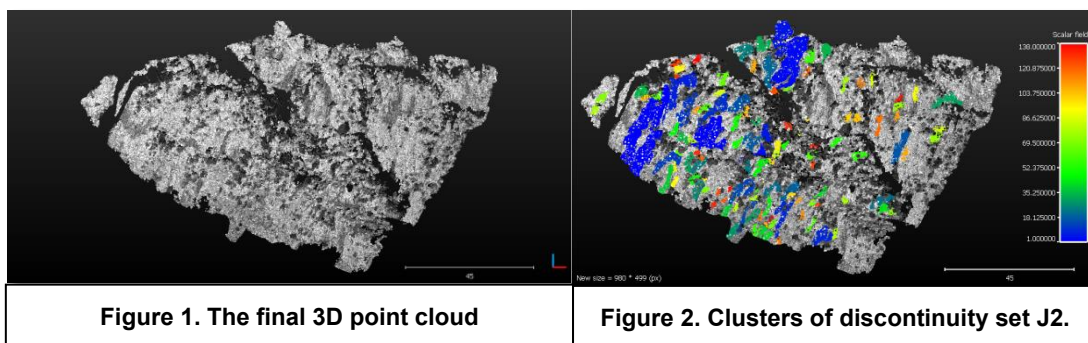
Kyriaki Devlioti<sup>1</sup>, Basile Christaras<sup>1</sup>, Vassilis Marinos<sup>1</sup>, Konstantinos Vouvalidis<sup>1,2</sup>, Silvana Fais<sup>2</sup>

<sup>1</sup>Department of Geology, Aristotle University of Thessaloniki, Greece, [kdevliot@geo.auth.gr](mailto:kdevliot@geo.auth.gr),  
[christar@geo.auth.gr](mailto:christar@geo.auth.gr), [marinosv@geo.auth.gr](mailto:marinosv@geo.auth.gr), [vouval@geo.auth.gr](mailto:vouval@geo.auth.gr)

<sup>2</sup>Department of Civil and Environmental Engineering and Architecture, University of Cagliari, Italy,  
[sfais@unica.it](mailto:sfais@unica.it)

Mapping of discontinuities in rock slopes is a very time-consuming and expensive process. The continual progress in 3D data acquisition techniques, such as drone photogrammetric ones and laser scanning revealed that it is likely for researchers to collect and generate accurate virtual 3D models, with analytical geotechnical features. Contrary to conventional methods (compass measurements), remote sensing techniques provide high resolution 3D surface models, which consist of million of points, with less than few millimeters distances, with accuracy, ease of use and high spatial resolution (Jaboyedoff et al., 2012). Since this information is classified and discontinuity sets are identified and extracted, then it is likely, mainly, for geotechnical researchers to analyze other geo-mechanical features, such as spacing and persistence of the examined rock face. Particularly, in this paper, a detailed discontinuity mapping and classification is presented, at the northern rock slope, overhanging the stadium, in the Archaeological site of Delphi, using Terrestrial Laser Scanning (LiDAR) and UAV (Devlioti, et. al., 2019). More specifically, a detailed, 3D geo-structural analysis of rock mass discontinuities, was made in order to collect accurate and dense 3D point cloud dataset of the rock slope to extract the precise number of discontinuity sets. Furthermore, the methodology that was followed, is separated in three steps. At the first one, UAV and LiDAR technologies were used, for precise and high resolution data acquisition of the research area (Figure 1). Subsequently, processing of the two recording techniques data performed, the results combined and compared, and the final number of discontinuity sets was demonstrated. For the identification and the extraction of the 3 discontinuity sets on the rock cliff, a semi-automatic process was followed, using several algorithms (Slob, S., et. al., 2004, Riquelme, A., et. al., 2017). At the last step, the orientation of discontinuities was determined, the normal spacing (Riquelme, A., et. al., 2015, Buyer, A. & Schubert, W., 2017) was computed (considering both persistent and non-persistent discontinuities) and their persistence was measured (Riquelme, A., et. al., 2018) (Figure 2), parameters which typically form slope geometry, the most important factor controlling rockfall trajectory.

This study consists part of a PhD Thesis, concerning the geotechnical risk, related to the safety of world's monumental areas. The Archaeological site of Delphi belongs in World's Cultured Heritage, which is protected by UNESCO, hosting thousands of visitors, from all over the world, every day. In recent past, rockfall events were noted, inside the archaeological site of Delphi, and also at the national highway, exposing visitors, drivers and employees to danger. Therefore, it is urgent to analytically record the current situation, so that contiguous rockfall phenomena will not occur in the future.



### **Acknowledgements**

We would like to thank the Archaeological Ephorate of Fokida and the Archaeological site of Delphi, for their permission, facilitation and willingness in order to fulfill the field work in the stadium of the archaeological site.

### **REFERENCES**

- Slob, S., Hack, H., R., Knapen, B., V. and Kemeny, J., 2004, Automated identification and characterisation of discontinuity sets in outcropping rock masses using 3D terrestrial laser scan survey techniques. In: Schubert, W. (Ed.) EUROCK 2004 & 53rd Geomechanics colloquy; Rock Engineering. Theory and Practice, Austrian Society for Geomechanics, ISBN: 978-3-7739-5995-9, pp. 439-443
- Jaboyedoff, M., Oppikofer, T., Abellán, A., Derron, M., H., Loye, A., Metzger, R. and Pedrazzini, A., 2012, Use of LIDAR in landslide investigations: a review. *Natural Hazards*, Springer, v. 61, pp. 5-28
- Riquelme, A., J., Abellán, A. and Tomás, R., 2015, Discontinuity spacing analysis in rock masses using 3D point clouds. *Engineering Geology*, Elsevier, doi: 10.1016/j.enggeo.2015.06.00
- Riquelme, A., Cano, M., Tomás, R. and Abellán A., 2017, Identification of Rock Slope Discontinuity Sets from Laser Scanner and Photogrammetric Point Clouds: a Comparative Analysis. *Symposium of the International Society for Rock Mechanics*, Elsevier, v. 191, pp. 838-845
- Buyer, A. and Schubert, W., 2017, Calculation the Spacing of Discontinuities from 3D Point Clouds. *Symposium of the International Society for Rock Mechanics*, Elsevier, v. 191, pp. 270-278
- Riquelme, A., Tomás, R., Cano, M., Pastor, J., L. and Abellán, A., 2018, Automatic Mapping of Discontinuity Persistence on Rock Masses Using 3D Point Clouds. *Rock Mechanics and Rock Engineering*, v. 51, pp. 3005-3028
- Devlioti, K., Christaras, V., Marinos, V., Vouvalidis, K. and Giannakopoulos, N., 2019, Kinematic Analysis of Rock Instability in the Archaeological Site of Delphi Using Innovative Techniques. *Communications in Computer and Information Science*, Springer, v. 962, pp. 407-418.



## Rehabilitation methods of Victorian Tunnels in the UK

Cameron Atkinson<sup>1</sup>, Dr. Chrysothemis Paraskevopoulou<sup>2</sup>, Richard Miller<sup>3</sup>

<sup>1</sup>MSc Engineering Geology Graduate, University of Leeds, Leeds, UK, [cameronatkinson1@hotmail.com](mailto:cameronatkinson1@hotmail.com)

<sup>2</sup>Assistant Professor, University of Leeds, Leeds, UK, [c.paraskevopoulou@leeds.ac.uk](mailto:c.paraskevopoulou@leeds.ac.uk)

<sup>3</sup>Director Ground Engineering and Tunnelling, Ramboll, Leeds, UK, [richard.miller@ramboll.co.uk](mailto:richard.miller@ramboll.co.uk)

Network rail oversees and maintains the UK's railway lines, around 20,000 miles of track, carrying around 4.7 million passengers a day. It also oversees all of the major infrastructure on the lines, including bridges and tunnels. Between the years 2014 and 2019 the total amount of money spent on maintenance was approximately £11 billion (Network Rail, 2018) mainly for the rail tunnels. Many of these tunnels were first constructed in Victorian times, broadly dated between 1837- 1901, during a rapid expansion of the railway network fuelled by the industrial revolution. Much of the UK's 335km tunnel network consists of old Victorian era tunnels, lined with several layers of concentric brick rings. Some of these are possibly 150 years old, and if left unchecked the brickwork will deteriorate over time. This can be very dangerous, causing ring failure, spalling or flaking. Large volumes of trains traveling through these tunnels can cause consistent vibration, increasing the rate of deterioration, putting in danger the passengers (Chiu, Wang and Huang, 2014). A standard course of action that Network Rail takes when failure in masonry tunnels occur is to close them, clear the hazard and repair the failed region. Unfortunately, nowadays these tunnels are becoming outdated, due to the increased need for faster, more efficient, larger trains, these tunnels need to be redeveloped, while preserving their heritage. modernization of the railways and they are lined with degrading brick.


The tunnels are too small facilitate Network Rail cannot afford to stop services running due to closures of the lines. One method of that could be used to solve these problems is potentially using a large Tunnel Enlargement Machine (TEM). The over-arching concept of this method involves installing a protective shield within the original lining of the tunnel, allowing for a service to continue, and then excavate material around the original tunnel and the original lining. This will leave behind a new enlarged tunnel profile. The TEM also facilitates installation of support, it does this while a train service remains operational. The actual procedure of this method is flexible, taking into account the purpose of the project and the geology. Excavation methods include either mechanical or drill and blast, dependent on the ground conditions. There are several examples of Tunnel Enlargement Machines (TEM) being utilized, to rehabilitate and expand tunnels, around world.

The aim of this project is to investigate the potential tunnel rehabilitation methods that could solve problems pertaining to failing masonry tunnels built in the Victorian era. The lining of these tunnels has been failing causing problems to the rail service, and the tunnels are often of an outdated size, stunting the modernization of the rail network. This technology can be used in both road and rail tunnels. Information derived from case studies and literature has been synthesized into a matrix (Table 1). This matrix includes 4 tunnel refurbishment methods, all of which have pros and cons. The process of selecting one of these methods depends on several things, but it is important to recognize that there is unlikely one standard method of refurbishing all tunnels, each of these methods will have to be adapted and modified in conjunction with the specific project and geology. The purpose of the matrix is to use the data in it and the circumstances of real world tunnels to hypothesize the best method of refurbishing any tunnel while the geological conditions have a huge influence on the method selected.





**Table 1. Tunnel refurbishment method matrix (after Atkinson et al. 2020)**

Method	Ground Conditions	Cost Considerations	Advantages (+)	Disadvantages (-)	Progression rate
<p><b>Ram Arch System</b></p> <p>Staged Tunnel rehabilitation, using Iron grids, shotcrete, and rockbolts</p> 	<p>Geology – N/A</p> <p>High water tables can be mitigated through installation of drains</p>	<p>Closure of line - £500,000/day</p> <p>Labour + materials + further maintenance</p>	<p>+ Standardised staged procedure.</p> <p>+ Effectively re-supports the areas of failing masonry.</p> <p>+ Drains can easily be installed to allow for some groundwater ingress.</p> <p>+ Can be mechanised, with the robotic shotcrete machines</p>	<p>- Will not increase the gauge of the original tunnel</p> <p>- Requires large amounts of possession time</p> <p>- Unable to run a train service while work is being carried out</p> <p>- Staged construction necessitates several closures</p>	<p>rate ranges</p>
<p><b>Tunnel re-boring</b></p> <p>In fill existing tunnel with light foam concrete, re-bore the tunnel either by conventional mechanical excavation or TBM</p> 	<p>Large variety of geological conditions, (weak – strong rock), will inform excavation method.</p> <p>Ground may need to be drained to mitigate ground water ingress.</p>	<p>Closure of line - £500,000/day</p> <p>TBM + support</p>	<p>+ Increase the gauge of the tunnel</p> <p>+ Can make adjustments to the alignment of the tunnel</p> <p>+ Relatively quick</p> <p>+ Precast lining can be installed, will require little maintenance</p>	<p>-Train service can no longer run through this tunnel</p> <p>-Large amounts of concrete infill needed and wasted in refilling and boring the tunnel.</p> <p>-Line closure cost network rail</p>	<p>4m / day</p>
<p><b>TEM (drill and blast)</b></p> <p>Rectangular shaped excavation machine, drill equipment mounted on the outer sections of the machine, while trains run through inner portion of the machine. Drill and blast the main method of excavation.</p> 	<p>Usually designed for hard rock (&gt;60-100 MPa), able to accommodate variable ground conditions</p> <p>Ground may need to be drained and grouted before excavation</p>	<p>TEM Machine + support</p> <p>(minimal maintenance cost for new lining)</p>	<p>+ Allows for the train line to be open and operational provided blasting happens at night, with protection from a steel lining</p> <p>+ Use of a modular versatile machine that facilitates all functions from excavation through to installation of the lining.</p> <p>+ Increase gauge of tunnel</p> <p>+ Reliable progression rates</p> <p>+ Allows for pre support of ground ahead</p> <p>+ Precast lining can be installed, will require little maintenance</p>	<p>-Fumes need to be flushed from the tunnel</p> <p>-Short closure of the line necessary for to lay down tracks for the TEM machine</p> <p>-Tight working environment</p> <p>-Vibrations</p> <p>-Potential damage intricate portals of historical significance</p>	<p>1-1.2 m / day (limited by blasting restrictions) – potentially around 3m</p>
<p><b>TEM (Mechanical)</b></p> <p>Rectangular shaped excavation machine, mechanical excavation equipment mounted on the outer sections of the machine, while trains run through inner portion of the machine.</p> 	<p>Soft rock and ground (&lt;60 MPa), able to accommodate variable ground conditions</p> <p>Ground may need to be drained and grouted before excavation</p>	<p>TEM Machine + support</p> <p>(minimal maintenance cost for new lining)</p>	<p>+ Allows for the train line to be open and operational throughout the period of excavation, with protection from a steel lining.</p> <p>+ Use of a modular versatile machine that facilitates all functions from excavation through to installation of the lining.</p> <p>+ Increase gauge of tunnel</p> <p>+ Little vibration in urban areas.</p> <p>+ Can be adaptable to changing ground conditions.</p> <p>+Reliable progression rates</p> <p>+Allows for pre support of ground ahead</p> <p>+ Precast lining can be installed, will require little maintenance</p>	<p>-Short closure of the line necessary for to lay down tracks for the TEM machine</p> <p>-Tight working environment</p> <p>-Some potential settling of the ground</p> <p>-Potential damage intricate portals of historical significance</p> <p>-Road headers may have difficulty excavating the multiple layers of brick lining</p>	<p>1m / day</p>

**REFERENCES**

Atkinson, C., Paraskevopoulou, C. and Miller, R., 2020, Investigation of rehabilitation methods of Victorian Tunnels. In: Proceedings of WTC 2020, September 2020, Kuala Lumpur, Malaysia. [Accepted for publication].

Network Rail (2018). Railway Upgrade Plan. Network rail.

Chiu, Y., Wang, T. and Huang, T., 2014, Investigating continual damage of a nineteenth century masonry tunnel. Proceedings of the Institution of Civil Engineers - Forensic Engineering, 167(3), pp.109-118.

## Parametric simulations on the stability conditions of the masonry wall of Chandakas

Nikolaos Antoniadis<sup>1</sup>, Michaela-Maria Karathanou-Nicholaidi<sup>2</sup>, Constantinos Loupasakis<sup>3</sup>

<sup>1</sup>Undergraduate student, School of Mining and Metallurgical Engineering, N.T.U.A, Greece,  
[antoniadis.nickolas@gmail.com](mailto:antoniadis.nickolas@gmail.com)

<sup>2</sup>PhD Candidate, School of Mining and Metallurgical Engineering, N.T.U.A., Greece,  
[karathanou@metal.ntua.gr](mailto:karathanou@metal.ntua.gr)

<sup>3</sup>Associate Professor, School of Mining and Metallurgical Engineering, N.T.U.A., Greece,  
[cloupasakis@metal.ntua.gr](mailto:cloupasakis@metal.ntua.gr)

The current research investigates, by means of parametric simulations, the stability conditions of the masonry wall of Chandakas in the city of Heraklion, Crete, Greece and proposes methods of support.

The construction of the wall began in 1462, by the Venice Candia, went through many phases and lasted more than two centuries before its completion (1669). It was built based on the Bastion fortification system (Fronte Bastionato), with a total of seven bastions connected with line-segments (cortine) and the rampart (cavaliere) as seen in the pictures below (Tzompanaki, 1996).



**Figure 1. Drone photograph of Chandakas (left) – The seven bastions of the wall (right)  
(Municipality of Heraklion, 2010)**

The wall acts as a gravity retaining wall, due to the existence of backfilling material. The analysis takes into consideration the different materials and dimensions for the mortar and the units of the masonry that were used during several phases of the construction of the wall. For the sections of the wall that will be evaluated in this paper, the lower segment is composed of calcareous sandstone and fossiliferous limestone connected with plaster, while the upper segment is mainly composed of dolomitized limestone (Xatzistergiou, 2010).

Various methods and models for the homogenization of the wall and the calculation of the Elastic modulus were used, such as Eurocode 6 (1996), P.B. Lourenco (1996), G. de Felice et al. (2010), A.J. Francis et al. (1971), D.M. Farshchi et al. (2008) and other. The results were implemented in Plaxis 2D, where a sheet piles wall was used to reduce the load caused by earth pressure.



**Figure 2. The line-segment Bembo - Saint Francis**

## REFERENCES

- Tzompanaki C., 1996, Chandakas. The city and the walls, Vikelaia Public Library, Heraklion
- Municipality of Heraklion, 2010, <https://www.heraklion.gr/municipality/press-releases-2010/25-06-10f.html>
- Municipality of Heraklion, 2010, <http://history.heraklion.gr>
- Xatzistergiou G.M., 2010, Restoration Study for the line-segment of St. Francis and oreccion Sampionara, Crete, Greece
- European Committee for Standardization, Eurocode 6, Brussels, Belgium, 1996.
- P.B. Lourenco, 1996, Computational Strategies for Masonry Structures, PhD thesis, Delft University, Delft, The Netherlands
- de Felice G., Amorosi A. and Malena M., 2010, Elasto-plastic analysis of block structures through a homogenization method. *Int. J. Numer. Analyt. Methods Geomech.* 34, No. 3, pp.221-247
- Francis A.J., Horman C.B. and Jerrems L.E., 1971, The effect of joint thickness and other factors on the compressive strength of brickwork, proceeding of the 2ed international brick masonry conference, H.W.H. west, ed, British Ceramic Association, Stoke on Trent, 31-37, UK
- Farshchi D.M., Motavali M. and Marefat M.R., 2008, A theoretical investigation on the seismic retrofitting of historical masonry buildings using FRP post-tensioned systems, PhD thesis, Tehran university



## THEME 9 - ENGINEERING GEOLOGY FOR THE SOCIETY



## Investigating the impact of Geological Uncertainty in Cost Overruns of Tunnelling Projects

Georgios Boutsis<sup>1</sup>, Dr. Chrysothemis Paraskevopoulou<sup>2</sup>

<sup>1</sup>MSc Engineering Geology Graduate, University of Leeds, UK, [georboutsis@yahoo.gr](mailto:georboutsis@yahoo.gr)

<sup>2</sup>Assistant Professor, University of Leeds, UK, [c.paraskevopoulou@leeds.ac.uk](mailto:c.paraskevopoulou@leeds.ac.uk)

Tunnelling construction is growing worldwide as a result of increasing population requiring a wider use of confined space as well as the upkeep of the existing one resulting in rising cost (Paraskevopoulou et al. 2019). The demand for these costly projects is being financed by both public and private sector assisting national economies being greatly benefited from the reduction of the cost. Tunnelling represents a unique category of infrastructure projects differentiate in a variety of ways from the rest of the construction projects. The main reason that tunnels differentiate from the rest of the infrastructure projects is the risk derived from the excavation in unknown ground conditions and the multiple cost related parameters contribute in the final cost. Geological uncertainties are considered as one of the main factors which impact on the cost and time of these kind of projects. Paraskevopoulou and Benardos (2013) articulate that in tunnelling projects price tag is the tool which reflects the complexity and size of projects. The main purpose of this study is to further investigate the impact of unforeseen geological conditions due to the limited geological investigation that may lead to poor and unsound design that subsequently results to project deliver delays increasing the overall cost by using as study case the Channel Tunnel Project, which experienced significant cost overruns. Although the tunnel has a long history during its multiple construction sequences, this paper focuses only during the period between 1987 – 1998.

The idea of building an English-French tunnel was initially proposed in 1802. In 1878, France started two shafts and a small tunnel (Warren and Mortimore, 2003). The tunnel was excavated mainly in the Chalk Marl formation (Figure 1.a.). Many geotechnical investigation campaigns took place during a hundred years (Figure 1.b) but according to Harris and Warren (1992) they: substantially underestimated the length of tunnel which was subject to over-break, they did not identify the area of consistently high-water inflow, the various structural zones along the tunnel route and the effect of minor folding on tunnel stability. The latter implies that geological and geotechnical uncertainty was present during the design and construction of Channel Tunnel.

Three types of costs are analysed herein: i) Tunnel Cost (TuC) – covers all tunneling and related equipment costs including TBM expenditure; ii) Construction Cost (CC) – covers the tunnel cost, the terminals, the rolling stock, bonuses/contingency and the direct cost, and, Total Cost (ToC) covers the construction cost plus the financial related cost, owners cost, finance fees, capital expenditure, net cash flow, inflation and interest reserves. In this work the cost figures for 1987, 1991, 1994 and 1998 (Figure 1.c) are further analysed. The main methodology used is shown in Figure 1.d. The price is adjusted in 2019, the total cost overrun plunges to 13% and the tunnelling cost overrun at 26% (Figure 1.e). The Geological Investigation (GI) cost is also compared for the two periods 1987 and 1994 (Figure 1.f). This covers 1.13% and 1% and of the Total Budget, 1.87% and 1.59% of the Tunnel Construction, and 4.4% and 3.5% Total Construction for 1987 and 1994 respectively. Adopting Clayton's (2001) approach on the impact of GI expenditure the optimum expenditure seems to be 5% to 6% that can lead to overruns of less than 10% (Figure 1.g). More specifically, the total construction cost overrun is 66% with GI contributing 1.87% (overall GI expenditure) as in the tender price of 1987. It is also observed that for an expenditure of 1.87% the average cost overrun is 22%. Finally, an additional expenditure in ground investigation would have impacted the construction cost presented herein.



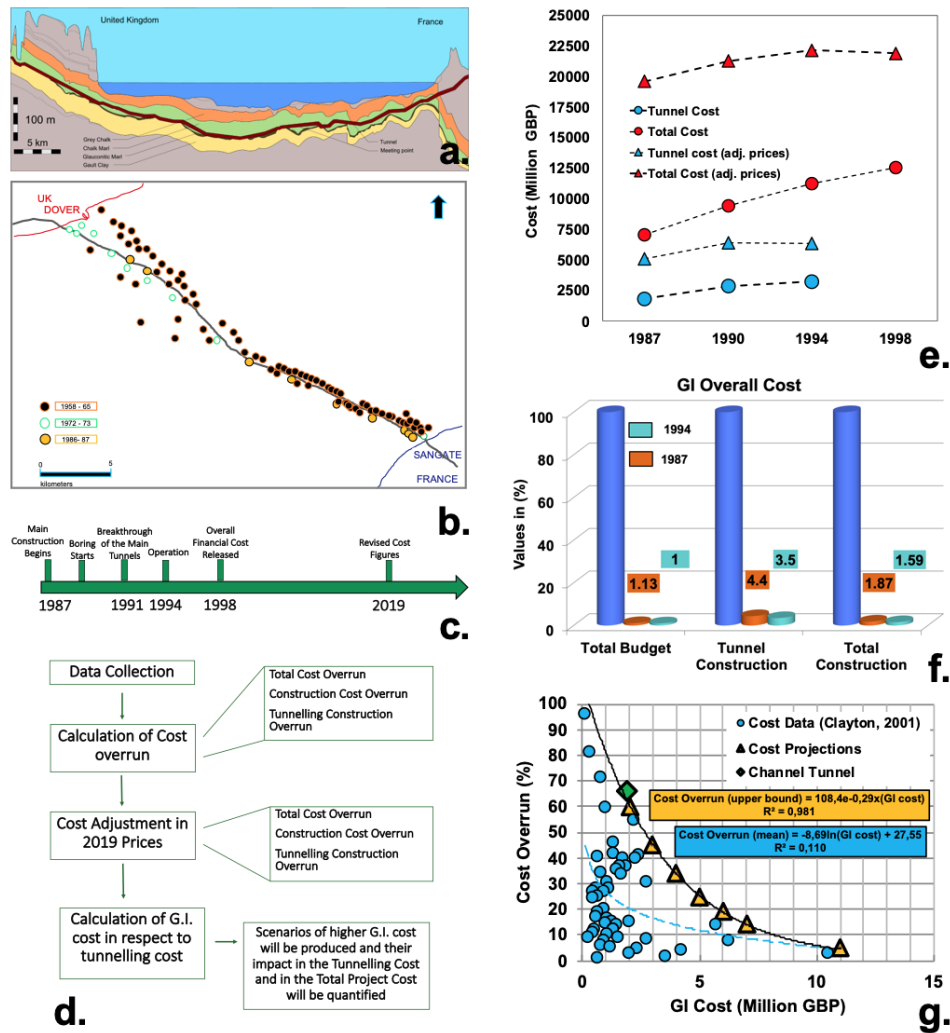


**Figure 1.** a. Cross section of the Channel Tunnel (<https://www.geolsoc.org.uk>); b. Locations of marine boreholes from 1958 to 1987(Birch et al., 1991); c. Timeline; d. Flowchart of the current methodology; e. Cost overruns included and excluded (adjusted price) inflation; f. Overall GI expenditure (%) cost for 1987 and 1994; and, g. Construction cost overrun in relation with the ground investigation expenditure from Clayton (2001).

**REFERENCES**

Birch, G., Rankin, W.J. and Warren, S. 1991. Geotechnical Aspects of the Design and Construction of the UK Crossover. Tunnelling '91, Inst. Min. Met., London, 143-159.

Clayton C. R. I., 2001. Managing geotechnical risk: time for change? Proceedings of the Institution of Civil Engineers, Geotechnical Engineering 149 (1), pp.3-11.

Harris, C.S. and Warren, ST. 1992. TML Deposition Report. TML Geotechnical Department Internal Report (unpublished).

Paraskevopoulou, C., Benardos, A. 2013. Assessing the construction cost of tunnel projects. Tunnelling and Underground Space Technology Journal, 38(2013), 497–505.

Paraskevopoulou, C., Cornaro, A., Admiraal, H., Paraskevopoulou, A., 2019. Underground space and urban sustainability: an integrated approach to the city of the future. Changing Cities IV, Crete, Greece.

Warren, C.D. and Mortimore, R.N., 2003. Chalk engineering geology–channel tunnel rail link and North Downs tunnel. Quarterly Journal of Engineering Geology and Hydrogeology, 36(1), pp.17-34.



## Socio-economic impacts of landslides in Pelion district, Greece

Garyfalia Konstantopoulou<sup>1</sup>

<sup>1</sup>*Hellenic Survey of Geology and Mineral Exploration, Greece, [kongar@igme.gr](mailto:kongar@igme.gr)*

### **Background**

Pelion district, located in the central-east part of Greece, exhibits a long history of landslides, affecting both residential areas and infrastructures. Landslides occur locally in Pelion almost every year, but periods of intensive rains, are followed by large scale ground mass movements. Over the last 35 years, two extreme precipitation events have been recorded: 1) 880mm in December 1986 and 2) 1155mm in February 2018, which is a new record for the area and one of the highest monthly levels in Greece. This extreme rainfall induced more than 100 landslides in an area of about 150 km<sup>2</sup>, causing significant damages within the 9 villages of the Municipality of Zagora – Mouresi, which had been declared in a state of emergency.

Northeastern Pelion area is mainly structured by a weak gneiss – schist geologic formation, easily weathered to form colluvial soil of various thickness and composition, depending on slope morphology and lithology. Rainwater infiltration increases shear stress induced soil weight and decreases the strength of the slope-forming material. The majority of slope failures occur in colluvial soils or at the colluvium-bedrock contact, facilitated by ground water circulation. Thus, physical conditions impose a high rate of landslide susceptibility of Pelion area [1]. However, the majority of landslides occur within the settlements, as well as along the road network, highlighting the effect of manmade interventions. The rapid urban and infrastructure development during the last decades, tremendously increased the likelihood, frequency and vulnerability of the area.

### **Methods**

Extensive field investigation and landslide mapping was done by HSGME within the Municipality of Zagora – Mouresi after the major landslide disaster of February 2018 [2]. The survey was mainly focused within settlements, in order to examine the extent of damage and evaluate the mechanism and dynamic for further evolution of every individual landslide.

### **Results**

Direct effects of landslides occurring in February 2018 include: 1) Damage to 103 houses, 3 public buildings and 2 hostels, some of which had been partially or totally collapsed. 2) Serious damage up to complete cutting of transportation in 35 sections of the municipal and provincial road network. 3) Destruction of farm land, with slope cuts and mass movements, making properties inaccessible and in some cases changing their boundaries. 4) Damage to local water and electricity networks. Indirect effects of landslides comprise the isolation of some settlements due to the destruction of the road network and the subsequent suspension of local schools for 2 weeks' time, as well as the inability of local people to be supplied with the necessary goods and health services. Furthermore, the landslides disaster extent has been created anxiety and insecurity feelings among residents.

Local authorities have so far implemented temporary remediation measures to ensure elementary road communication of the Municipality. Selection of the appropriate mitigation measures is a time consuming and expensive process since it depends on: a) engineering feasibility, b) economic feasibility, c) legal/regulatory conformity, d) social acceptability, and e) environmental acceptability [3]



**Figure 1. Typical aspects of landslide damage within northeastern Pelion area**

## **Conclusions**

The extent of landslide disasters occurring in Pelion shows that the mitigation measures taken over time are inadequate. Modern scientific and technical capabilities enable the reduction of socio-economic impacts of landslides. Detailed landslide mapping completed by HSGME and subsequent engineering geological and geotechnical investigation of both the main road network and the residential areas, provide the necessary information for proper planning, design and construction of safe and cost-effective remediation and mitigation measures, taking into account the possible reappearance of similar damages under the same or even more intensive precipitation events in the future.

## **REFERENCES**

- Koukis, G. Sabatakakis, N, Nikolaou, N. and Loupasakis C. 2005. Landslide zonation in Greece. In: Sassa K, Fukuoka H, Wang F, Wang G (eds) Landslides risk analysis and sustainable disaster management, part IV. Springer, Berlin. pp 291–296. doi: 10.1007/3-540-28680-2\_37.
- Konstantopoulou, G., Pyrgiotis, L., Poyiatzi El., Spanou, N., Nikolaou, N., Paschos, P., Exidaridi A. 2019. Mapping of landslide affected areas within the Municipality of Zagora-Mouresi from landslides of 2018. Int. HSGME report, 9 vol., 39 engineering geological maps (1:2000 scale), 79 damage delimitation maps (1:1000 scale).
- Popescu M.E., Sasahara K. 2009. Engineering Measures for Landslide Disaster Mitigation. In: Sassa K., Canuti P. (eds) Landslides – Disaster Risk Reduction. Springer, Berlin, Heidelberg.



## From post-disaster landslides inventory to open landslides data

Biljana Abolmasov<sup>1</sup>, Miloš Marjanović<sup>2</sup>, Uroš Đurić<sup>3</sup>, Jelka Krušić<sup>4</sup>

<sup>1</sup>University of Belgrade, Faculty of Mining and Geology, Serbia, [biljana.abolmasov@rgf.bg.ac.rs](mailto:biljana.abolmasov@rgf.bg.ac.rs)

<sup>2</sup>University of Belgrade, Faculty of Mining and Geology, Serbia, [milos.marjanovic@rgf.bg.ac.rs](mailto:milos.marjanovic@rgf.bg.ac.rs)

<sup>3</sup>University of Belgrade, Faculty of Civil Engineering, Serbia, [udjuric@grf.bg.ac.rs](mailto:udjuric@grf.bg.ac.rs)

<sup>4</sup>University of Belgrade, Faculty of Mining and Geology, Serbia, [jelka.krusic@rgf.bg.ac.rs](mailto:jelka.krusic@rgf.bg.ac.rs)

### **Background**

In the third week of May 2014, a massive low-pressure cyclone “Tamara” swept through Western Balkan resulting in extreme precipitation that caused floods, torrential floods and massive landsliding in the Republic of Serbia. The disaster affected more than 1.6 million people and caused 51 casualties. The total value of disaster effects was EUR 1.7 billion or over 4 % of the Serbian GDP. In the framework of the post-disaster recovery led by the UNDP Office in Serbia, the project “Beyond landslide aWAREness” (BEWARE) was implemented with the aim to support landslide risk assessment and management in the affected territory. This paper is presented basic results and main project deliverables.

### **Methodology**

Study area covered 11.840 km<sup>2</sup>, i.e. 24 most vulnerable municipalities affected by different type of landslides triggered by Cyclone Tamara in Western and Central part of the Republic of Serbia. Geological and geomorphological settings are very complex as well as other environmental conditions in such a wide area. Thus, attention was focused on developing a fast and efficient methodology for a post-event landslide inventory. Very High and High resolution Pléiades, SPOT6 and WorldView2 multispectral satellite images were used for visual landslide recognition and to build an inventory to support an extensive field landslide mapping during five months (Đurić et al. 2017). According to the Cruden and VanDine (2013) classification a harmonized landslide data report was prepared for field data inventory. BEWARE web portal was designed as a platform for interactive landslide event reporting and open landslide data records.

### **Results**

The total number of 1751 landslides were mapped as an open data file reports, as one of the BEWARE project deliverables (Abolmasov et al. 2017). Different type of movement and type of involved material, as well as other landslides data were registered during extensive field campaigns and analysis of remote sensing data (Table 1 and 2). According to the rainfall data analysis, landslide thresholds were identified for the Western Serbia (Marjanović et al. 2018). Improving land use planning documents was prepared for each municipality after SWOT analysis and landslide hazard, vulnerability and risk assessments. The crowd sourcing approach was used for improvement of governmental agencies/local authorities practice in building/updating national landslide database from BEWARE data itself. Additionally, mobile software application for tablets and android mobile phones was created for supporting local communities and governmental institution in effective landslide reporting. Also, identification of critical sites for landslide rehabilitation was done for every affected municipality.



**Table 1. Summary of landslides according to the types of movement and types of material involved**

Region	Type of movement	Type of material					Total
		Anthropogenic	Debris	Rock	Soil	Complex	
Western and Central Serbia	Slides	10	681	3	710	26	1430
	Slides/flows		92		40	3	135
	Rockfalls	2	18	9	1	6	36
	Rockfalls/slides	1	31	2	9	3	46
	Rockfalls/flows		5				5
	Flows	1	64		12	1	78
	Complex	2	6		12	1	21
Total		16	897	14	784	40	1751

**Table 2. Summary of landslides data is according to the types of movement and state of activity**

Region	Type of movement	State of activity					Abandoned	Total
		Active	Dormant	Reactivated	Stabilized	Suspended		
Western and Central Serbia	Slides	740	16	195	11	458	6	1426
	Slides/flows	43		15	5	72		135
	Rockfalls	13		7	2	13		35
	Rockfalls/slides	25	7	5		8		45
	Rockfalls/flows					5		5
	Flows	22	1	2	4	49		78
	Complex	12	1			6	8	27
Total		855	25	224	22	611	14	1751

**Conclusion**

BEWARE interactive GIS web portal was launched and hosts all project activities, including: participant and partner users data uploads, visualizing functionalities, transparency of the project to any beneficiary, disseminating project results, simple statistical analysis, SWOT analysis, rainfall data analysis, satellite data analysis, landslide susceptibility assessment for each municipality, news and information etc. All landslide data and landslide data analysis and results are available as an open access data. BEWARE project portal is available at <http://geoliss.mre.gov.rs/beware/>.

**REFERENCES**

Abolmasov B., Damjanović D., Marjanović M., Stanković R., Nikolić V., Nedeljković S., Petrović Ž. 2017. Project BEWARE - Landslides Post-disaster Relief Activities for Local Communities in Serbia. In: M. Mikoš et al. (eds.), *Advancing Culture of Living with Landslides*, Proceedings of 4th World Landslide Forum, Ljubljana 29 May-02 June 2017. Vol 3. pp. 413-422.

Cruden D.M., VanDine D.F. 2013. *Classification, Description, Causes And Indirect Effects-Canadian Technical Guidelines and Best Practices related to Landslides: a national initiative for loss reduction*, Geological Survey Of Canada Open File 7359.

Đurić D., Mladenović A., Pešić-Georgiadis M., Marjanović M., Abolmasov B. 2017. Using multiresolution and multitemporal satellite data for post disaster landslide inventory in the Republic of Serbia. *Landslides* 14 (4): 1467-1482.

Marjanović M., Krautblatter M., Abolmasov B., Đurić U., Sandić C., Nikolić V. 2018. The rainfall-induced landsliding in Western Serbia: A temporal prediction approach using Decision Tree technique. *Engineering Geology* 232: 147–159.



## **Landslide activity affected by sludge basin water: a 40-year history assessed by interdisciplinary research**

Filip Hartvich<sup>1</sup>, Petr Tábořík<sup>1</sup>, Jan Klimeš<sup>1</sup>, Jan Blahůt<sup>1</sup>, Ondřej Racek<sup>1</sup>, Josef Stemberk<sup>1</sup>, Jan Balek<sup>1</sup>

<sup>1</sup> *Dpt. of Engineering Geology, Institute of Rock Structure and Mechanics, Czech Academy of Sciences, Czech Republic, [hartvich@irsm.cas.cz](mailto:hartvich@irsm.cas.cz)*

In 1970ies, during the construction of the coal-powered power plant Tušimice, a sludge reservoir “Vysočany” was built as one of its auxiliary structures (70 km WNW from Prague, Czech Republic). The sludge pit, barred by 50 m high earthen dam filled fully a valley of Vysočany brook, left-side tributary of Hutná brook. The sludge pit was gradually filled up during the operation of the power plant (1980ies-2004). Since 2004, the recultivation works were performed to current state. In 2018, the recultivation of the sludge pit was finished and the activities of CEZ (owner of the power plant) terminated.

However, already since 1980ies, the activity of landslides at the N slopes of Hutná valley increased. Numerous springs and marshes developed on the slope, and repeated reactivations of the landslides damaged part of the nearby village, agricultural and transportation infrastructure. The persisting activity of the landslides was documented by numerous reports and papers (Rybář 1984, Rybář 1987, Nováková 1990, Zika et al. 1991, Rybář 2001).

Recently, the N slopes of Hutná valley property owners have contested the claim that the recultivation has fulfilled all its goals, namely the “assessment, stabilization, and/or mitigation of the active landslides in the affected area”. The team of dpt. of Engineering geology was encharged with performing a complex study on the site in question, and namely with answering following questions:

- Are there still active landslides?
- If so, what is the cause of the on-going slope processes?
- What technical or other measures should be taken to stop the activity of the landsliding?

The complex research was performed in the spring 2020, and the methods included geomorphological and engineering geological mapping, site documentation, vast geophysical survey, aerial photogrammetry using both visible spectrum and IR cameras, hydrological measurements and documentation, and study of borehole and geological documentation.

The mapping was aiming to observe the current activity of the landslide, document spatial changes of the individual landslides compared to previous research, locate the springs and swamps, using GPS devices to ascertain the position of the landforms. Geophysical survey consisted of 12 profiles across and along the slope, covering its whole extent. The aerial survey allowed construction of a detailed, actual DEM (though occasionally obscured by high vegetation) and orthophotomap, and the IR aerial photos were used for observing wetter areas on a special orthophotomap. Finally, the hydrological measurements of the discharge of Hutná brook were performed to observe water inflow from the studied slope.

The conclusions from the site study were following: The landslides on the studied slope are still active. They have obviously changed and developed since the last mapping in 2001, and numerous findings indicate persisting activity, including documented fresh scarps, inclined trees, broken and dislocated vertical drainage elements, evidences on historical aerial photographs etc.

The cause of the persisting activity of the slope processes is the combination of valley slope, structural-

lithological settings favorable to landslide initiation on the erosional slope of the Hutná brook, which were worsened by increased underground water input by seeping of sludge basin water through permeable sandy layers in the underlying sedimentary complex. As the underground water level increased with the filling of the dam, the water could reach the N slope of the Hutná valley (Figure 1). This was anticipated already before the operation of the sludge basin (Seyček and 1978) and confirmed during operation (Nováková 1990), which lead to construction of a drainage system in part of the slope. However, the drainage is slowly ceasing to work due to silting and deterioration, thus allowing the water seep into the slope again.

As concerns possible mitigation of the landsliding activity on the studied slope, first measure has to be the draining of the area. This can be achieved through combination of subhorizontal and vertical draining boreholes. Finally, stabilization elements and constructions can be proposed depending on the expected use of the properties. Generally, the measures that would achieve complete stabilization of the area are expected to be costly.

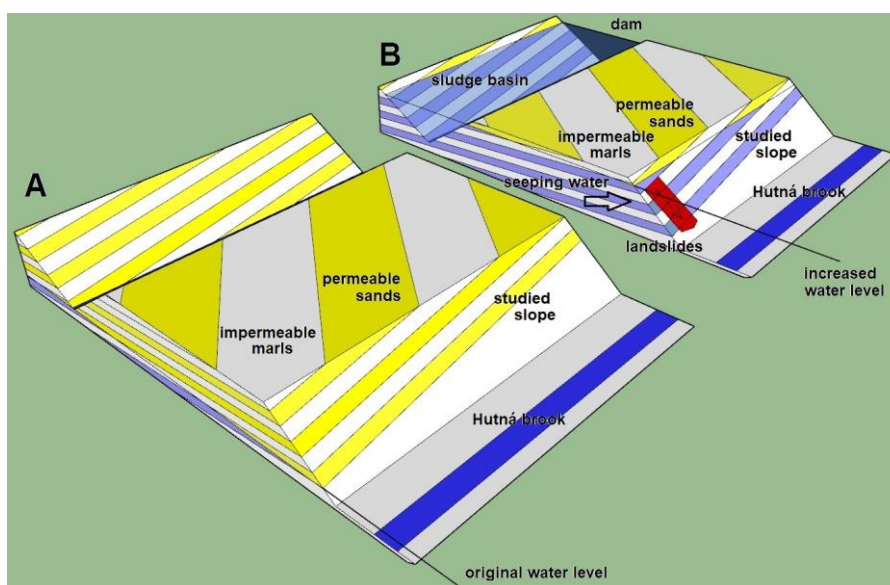


Figure 1. A - Situation before construction of the sludge basin. B - After construction.

## REFERENCES

- Rybář, J., 1984, Engineering-geological assessment of the causes of slope deformations in Hořetice village. MS, Institute of geotechnics CSAS, Prague, pp.17 (in Czech)
- Rybář, J., 1987, Engineering-geological assessment of potential sludge basins for Tušimice powerplant, MS, Institute of geotechnics CSAS, Prague, pp.13 (in Czech)
- Rybář, J., 2001, Engineering-geological assessment of the endangering of the road Hořetice – Hrušovany byl landsliding. MS, Institute of Rock Structure and Mechanics, CAS, pp 7. (in Czech)
- Nováková, J., 1990, Analysis of stability of the slopes of Hutná brook between Hořetice and Žiželice. MS/diploma thesis, Fac. of Science, Charles university in Prague. (in Czech)
- Seyček, J. and Čechová, E., 1982, A high dam on Tertiary clay. Journal of geological sciences - Hydrogeology, engineering geology, 16, ÚÚG Prague, 121-158 (in Czech)
- Zika P, Moravec J, Stemberk J, 1991, Evaluation of stability conditions of landslide area Hořetice. MS, Institute of geotechnics CSAS, Prague, pp. 39 (in Czech).



## THEME 11 - MARINE ENGINEERING GEOLOGY

## Investigation to soil-pile interaction in open-ended piles installed in soft soils

M.Sc. Moritz Anton Loreth<sup>1</sup>, Univ.-Prof. Dr.-Ing. habil. Sascha Henke<sup>1</sup>

<sup>1</sup>*Geotechnical Institute, Helmut-Schmidt-University / Universität der Bundeswehr Hamburg  
Campus Nord – Germany; [lorethm@hsu-hh.de](mailto:lorethm@hsu-hh.de)*

The soil-pile interaction of open ended pipe piles installed in cohesive soils, has only been discussed in isolated cases (Gavin et al., 2010). This leads to insufficient empirical data. Further the influence of static and dynamic installation on the effective stresses inside open-ended piles as an indicator of plug formation depends on the pore-water (compressibility, consistency, plasticity, viscosity) as well as stress-state (consolidation) related to soil mechanics of cohesive soils and is currently completely unconsidered in research. Considering these special properties, it is possible rearrangement of the cohesive soil particles in the pile base area can lead to soil plug formation inside the pipe pile. The rearrangement of cohesive soils depends from the effective lateral- and vertical stresses, as a result from total- and pore water pressures inside pipe piles (Doherty & Gavin, 2011). In particular, the water- and stress related soil mechanics in cohesive soils shows a special challenge to empirical results for both in-situ and laboratory conditions. However, the quality of such investigations is the basis for reliable material model formulation.

This study discusses the geological and soil mechanical conditions on the stress development of cohesive soils on the basis of empirical determined data from literature. Furthermore, the data was used for a numerical analysis with respect to open-ended piles in cohesive and additional granular soils using higher material models like *Hypoplasticity*, *Visko Hypoplasticity* and *Clay Hypoplasticity*. The calculations should be understood qualitatively, because a complete consideration of the influencing factors on the in-situ stress development of open-ended piles in cohesive soils has not yet been investigated. This will be in detail investigated in further research which is also discussed in this paper.

Finally, development of a new laboratory testing method called *Geo-Tribometer* for quantifying the soil-pile interaction during the rearrangement of cohesive soil particles in cohesive soils is presented.

### REFERENCES

- Gavin, K.; Gallagher, D.; Doherty, P.; McCabe, B. (2010): Field investigation of the effect of installation method on the shaft resistance of piles in clay. In: Canadian Geotechnical Journal 47 (7), pp. 730–741.
- Doherty, P.; Gavin, K. (2011): Shaft capacity of open-ended piles in clay. In: Journal of Geotechnical and Geoenvironmental Engineering 137 (11), pp. 1090–1102.

## Author Index

### A

Abdelghan O.	98
Abolmasov B.	150, 243, 263
Acar K.	88, 90
Ago B.	156
Ajdanlijsky G.	44, 76
Aldahan A.	98
Alexiou S.	212
Allasia P.	23
Al-Zubaydi J. H. A.	210
Anagnostopoulos C.	50
Antoniadis N.	256
Apostolopoulos G.	131
Argyrakis P.	172, 218
Argyroudis S. A.	178
Arman H.	98
Arslan B.	116
Ashley J.	70
Aslanoglou X.	53
Asteriou P.	220
Atakan A.	116
Athanassas C.	53, 161
Atkinson C.	254
Aygar E. B.	94, 96
Azas A.	231

### B

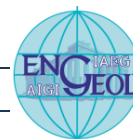
Baek I.	64
Bajracharya K.	63
Balampanis A.	161, 163
Baldo M.	23
Balek J.	111, 265
Barbagli F.	70
Bardanis M.	175
Barra A.	227
Barykina O.	152

Bassols J. B.	227
Bauer M.	157
Bergerat F.	45
Bertolo D.	204, 206
Bhandari S.	63
Blahūt J.	72, 111, 247, 265
Blakely M.	68
Bogas D.	107
Bonneau D.	237
Boumpoulis V.	48
Boutsis G.	259
Breuninger T.	9, 176
Bricker S.	8
Buot M.	68, 70
Butler G.	85

### C

Can A.	88, 90
Caputo R.	214
Carter T. G.	121
Catani F.	216
Cauchie L.	195
Charalampakis M.	182, 184, 186
Chatziangelou M.	50
Chavez-Olalla J.	66
Chiu Y. C.	188
Chousianitis K.	218
Christaras V.	102, 129, 225, 252
Chrysafi A.	180
Cignetti M.	204, 206
Cocco F.	247
Codd J.	165
Crosetto M.	227
Cui Y.	21
Curzio D. D.	74
Cvitanović N. Š.	193





## D

Da Pelo S.	247
Dahal R. K.	104
Daja S.	156
Dandika M.	190
Daniel P. R.	249
Deiana G.	247
Deligiannakis G.	197, 212
Dematteis N.	200
Depountis N.	48, 57, 145, 218
Descamps F.	44, 76
Devlioti K.	252
Dixon N.	15
Dong J. J.	39
Drakatos G.	182, 184, 186, 218
Duffy-Turner M.	85
Đurić U.	243, 263
Durmishi Ç.	156
Dutta T.	133

## E

Elter F. M.	23
Erbì I.	247
Eremina O.	128
Eusebio A.	199, 203
Evaggelou E.	241
Evangelidis C.	47, 186

## F

Faccini F.	23
Fais S.	252
Fan X.	216
Farmakis I.	237, 239
Fazio N. L.	200
Fey C.	4
Fomenko I.	141
Frodella W.	216
Funedda A.	247

## G

Galetakis M.	118
Gamperl M.	9, 176
Ganas A.	159, 172, 214
Garelick J.	109
Georgieva T.	44, 76
Georgiou D.	166
Gerard P.	227
Ghataora G.	135
Giordan D.	200, 204, 206
Giulietto W.	199, 203
Gkekas G.	107
Gkika F.	47
Gkorani A.	102
Gkouvailas A.	68, 70
Godone D.	23, 204, 206
Gökçeoğlu C.	88, 90, 94, 96, 100
Görög P.	120
Grendas N.	107
Gruslin S.	208
Gu T.	192
Gündoğdu A. E. K.	88
Gunn M. J.	109
Guo C.	21

## H

Haque M. E.	133
Hartvich F.	72, 111, 265
Hasan M.	133
Hasegawa S.	104
Havenith H. B.	170, 195
Henke S.	268
Hernán A. S.	249
Hossain A.T.M. S.	133
Hutchinson J.	6, 237

## I

Ilia I.	180
Imam H.	133
Ioannou E.	175



## J

Jafrin S.J.	133
Jang B-A.	64
Jang H.-S.	64
Jiang Y.	21
Jimenez R.	154
Jung J.	87

## K

Kafle K. R.	63
Kaitantzian A.	143, 245
Kalinin E.	152
Kalligeris N.	182
Kallimogiannis V.	147
Kalos A.	166
Kanavou K.V.	53
Karantanellis E.	190, 225, 229, 231, 233, 235, 239
Karathanou-Nicholaidi M.	256
Kavoura K.	57, 218
Kayabasi A.	100
Kazili M.	125
Kazilis N.	125
Keilig K.	157
Khan P.A.	133
Khatun M.	133
Kim A.	64
Kitsara G.	168
Klimeš J.	111, 265
Kokkala A.	129
Konstantinidis I.	229
Konstantopoulou G.	261
Kontopidis O.	48
Kotsanis D.	35, 37
Koulermou N.	223
Kovačević M. S.	19
Kozliakova I.	128
Krušić J.	150, 263
Ktenidou O. J	47

Kumar N.	43
Kusák M.	111
Kuschel E.	59
Kwon O.	87

## L

Lainas S.	145
Leal D.	55
Lee I-H.	31, 61
Lee J.	87
Lemaire E.	170
Leontarakis K.	131
Li W-Ci.	31
Li T.	154
Liang N.	17
Librić L.	19
Liew P.	85
Liouka A. X.	29
Liu X.	43
Liu S.	113
Lo P. C.	188
Lo W.	188
Loche M.	216, 247
Loew S.	2
Lollino G.	23
Lollino P.	200
Lombardo L.	216
Loreth M. A.	268
Loukidis D.	223
Loupasakis C.	139, 143, 161, 163, 168, 245, 256
Lu Y.	113
Lule A.	156

## M

Makedon T.	29, 102, 190
Mantovani F.	23
Marinos P.	166
Marinos V.	33, 92, 102, 121, 129, 159, 178, 190, 225, 229, 231, 233, 235, 239, 252



Marjanović M.	150, 263	Papathanassiou G.	159, 172, 178, 190, 214, 229, 231, 233, 235, 241
Marsden J.	55, 79, 81, 83	Paraskevopoulou C.	27, 41, 92, 254, 259
Martin L. A	137	Parcharidis I.	143, 245
Mašin D.	111	Park B.	87
Matsakou A.	159	Payne I.	109
Mavroulidou M.	109	Pejić M.	150
Melis M. T.	247	Perleros V.	166
Meloni M. A.	247	Peruzzo F.	199, 203
Menschik B.	9, 176	Phuyal B.	202
Michalopoulou M.	57	Poggi F.	23
Miller R.	254	Pokharel M. R.	114
Mohammad S.	45	Power C.	165
Mouslopoulou V.	53	Psomiadis E.	212
Mreyen A-S.	170, 195	Purchase D.	109

## N

Nazaj S.	156
Nefros C.	168
Nettleton I. M	55, 79, 81, 83, 85
Neumann P.	157
Ngan-Tillard D.	3
Ni C-F.	31, 61
Nola D.	208
Nomikos P.	35, 37
Notti D.	23, 200

## O

Ognissanto F.	137
Orfanos C.	131
Özyürek Y. E.	90

## P

Paganone M.	204
Palantzas G.	147
Pallikarakis A.	197, 212
Paolo L.	25
Papaliangas T.	33
Papanikolaou I.	197, 212
Papantonopoulos G	37

## Q

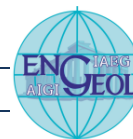
Qi S.	174
-------	-----

## R

Racek O.	72, 265
Raič A.	193
Randall J.	165
Raú V. V.	249
Rechberger C.	4
Reeves H.J.	8
Reeves S. J	135
Reicherter K.	212
Riquelme A.	241
Rosmery A. Q.	249
Rott J.	111
Rozos D.	35
Rózsa L.	120
Russo G.	25

## S

Sabatakakis N.	48, 57, 145, 218
Safdar M. U.	109
Samur C.	116



Santiapillai T.	68	Tsikrikis A.	29, 33, 121
Saroglou C.	106, 147	Tsirogianni A.	106
Sayem M. H.	133	Tuğrul A.	116
Scaringi G.	216, 247	Tzampoglou P.	139, 223, 245
Schnäcker E.	114	Tzevelekis T.	241
Seddon R.	55, 79, 81, 83	Tzilini M.	33
Šehić D.	135		
Shkodrani N.	156		
Shrestha B.	63	<b>U</b>	
Sifnioti D. E.	70	Ulusay R.	7
Singer J.	9, 176		
Sissins S.	27	<b>V</b>	
Sjöberg J.	13	Vagkli E.	107
Skolidis A.	92	Valkaniotis S.	159, 178, 214, 235
Smajlović S.	135	Vandycke S.	45, 76
Sotiriou P.	233	Vassilakis E.	225
Stamoulis K.	53	Vassou A.	235
Stavrou A.	123	Vavadakis D.	118
Steiakakis E.	118	Vazaios I.	123
Stemberk J.	111, 265	Vázquez-Suñé E.	227
Strom A.	141	Vendramini M.	199, 203
Sun X.	154	Vessia G.	74
Syllignakis G.	118	Vlachopoulos N.	237, 239
		Vlastelica G.	193
<b>T</b>		Voit K.	4, 59
Tábořík P.	111, 265	Voudouris K.	129
Tai P. L.	39	Vouvalidis K.	252
Tanyaş H.	216	Voznesensky E. A.	11
Tarabukin V.	141		
Tavoularis N.	172	<b>W</b>	
Thapa P. B.	149, 202	Wang T. T.	188
Thuro K.	9, 157, 176	Wang J.	192
Timilsina M.	104	Wasowski J.	14
Török Á.	120	Wattier M-L.	45
Tsangaratos P.	161, 163, 180	Wertz P.	45
Tselentis A.	182, 184	Wijaya I P. K.	4
Tshibangu J-P.	44, 45, 76	Winter M. G,	55, 79, 81, 83, 85, 135, 137, 178
		Wrzesniak A.	200
		Wu F.	17



## X

Xu Y.	192
-------	-----

## Y

Yilmaz M.	116
Yin Y.	21
Yu Y-C.	31, 61
Yumlu M.	107
Yunus A. P.	216

## Z

Zang M.	174
Zangerl C.	4, 59
Zejnić H.	135
Zeng P.	154
Zerkal O.	141, 152
Zervas E.	68
Zevgolis I. E.	131
Zhang Y.	113
Zucca F.	200, 206



# EUROENGEО ATHENS 2020

3<sup>RD</sup> EUROPEAN REGIONAL CONFERENCE OF THE INTERNATIONAL  
ASSOCIATION FOR ENGINEERING GEOLOGY & THE ENVIRONMENT  
Leading to Innovative Engineering Geology Practices



© National Group of Greece of IAEG